

Vehicle Weights and Dimensions Study

Volume 11

**Effects of Suspension Variations on the
Dynamic Wheel Loads of a Heavy
Articulated Highway Vehicle**

Copyright 1986 by:

Canroad Transportation
Research Corporation
1765 St. Laurent Blvd.
Ottawa, Canada K1G 3V4

ISBN: 0-919098-88-6

RTAC REPORT DOCUMENTATION FORM

Project No.	Report No.	Report Date July 25/86	IRRD No.
Project Manager J.R. Pearson			
Title and Subtitle Volume 11 -- Effects of Suspension Variations on the Dynamic Wheel Loads of a Heavy Articulated Highway Vehicle			
Author(s) J.H.F. Woodrooffe P.A. LeBlanc K.R. LePiane		Corporate Affiliation(s) National Research Council National Research Council University of Waterloo	
Sponsoring/Funding Agency and Address Canroad Transportation Research Corporation 1765 St. Laurent Blvd. Ottawa, Canada K1G 3V4		Performing Agency Name and Address Roads and Transportation Association of Canada 1765 St. Laurent Blvd. Ottawa, Canada K1G 3V4	
Abstract <p>The work reported here was supported jointly by Canroad and NRC Division of Mechanical Engineering, Vehicle Dynamics Laboratory, as part of the RTAC/CCMTA Heavy Truck Weights and Dimensions Study.</p> <p>This study has investigated the dynamic wheel load behaviour of various heavy highway vehicle suspension systems under a controlled experimental program. A 45 tonne tractor-trailer was modified to measure the dynamic axle loads of all major load carrying axles simultaneously. Suspension parameters such as suspension type, axle spread and axle load were investigated as functions of road roughness and vehicle speed.</p> <p>The effects of brake torque and suspension pitch attitude on the load equalization of the suspension were also investigated. Road tests were conducted at various speeds over variety of road roughness conditions. Findings relevant to the subject of dynamic road loading are highlighted.</p>		Keywords articulated vehicle axle load suspension (veh) variability evenness axle spacing road roughness	
No. of Pages	No. of Figures	Language English	Price
Supplementary Information			

DISCLAIMER

This publication is produced under the auspices of the Technical Steering Committee of the Vehicle Weights and Dimensions Study. The points of view expressed herein are exclusively those of the authors and do not necessarily reflect the opinions of the Technical Steering Committee, Canroad Transportation Research Corporation or its supporting agencies.

The test program discussed in this report was carried out using suspensions in common usage in the Canadian truck fleet. The suspensions and components used for testing were provided by the respective manufacturers, and were in brand new condition. The test results observed reflect the conditions of the equipment and test procedures used, and may be expected to vary with equipment which has been used in service, or under different test conditions.

This report has been published for the convenience of individuals or agencies with interests in the subject area. Readers are cautioned that the use and interpretation of the data, material and findings contained herein is done at their own risk. Conclusions drawn from this research, particularly as applied to regulation, should include consideration of the broader context of Vehicle Weights and Dimension issues, some of which have been examined in other elements of the research program and are reported on in other volumes in this series.

The Technical Steering Committee will be considering the findings of these research investigations in preparing its "Final Technical Report" (Volumes 1 & 2), scheduled for completion in December 1986.

PREFACE

The report which follows constitutes one volume in a series of sixteen which have been produced by contract researchers involved in the Vehicle Weights and Dimensions Study. The research procedures and findings contained herein address one or more specific technical objectives in the context of the development of a consistent knowledge base necessary to achieve the overall goal of the study; improved uniformity in interprovincial weight and dimension regulations.

The National Research Council of Canada undertook a program of testing to examine the dynamic loading characteristics of different tractor and trailer suspensions. Canroad Transportation Research Corporation gratefully acknowledges the contributions of the following companies in supplying equipment and components for testing:

Esso Petroleum Canada
Neway Canada
Reyco Industries
Chalmers Suspension International Ltd.
Hendrickson Manufacturing Canada Ltd.
Hayes-Dana Inc.

Funding to conduct the research was provided to Canroad Transportation Research Corporation by:

Alberta Transportation
British Columbia Ministry of Transportation and Highways
Manitoba Highways and Transportation
New Brunswick Department of Transportation
Newfoundland Department of Transportation
Nova Scotia Department of Transportation
Ontario Ministry of Transportation and Communications
Prince Edward Island Transportation and Public Works
Ministère des Transports du Québec
Saskatchewan Highways and Transportation
Transport Canada
Motor Vehicle Manufacturers Association
Canadian Trucking Association
Truck Trailer Manufacturers Association
Private Motor Truck Council

John Pearson, P.Eng.
Project Manager
Vehicle Weights and Dimensions Study

**VEHICLE WEIGHTS AND DIMENSIONS STUDY
TECHNICAL STEERING COMMITTEE**

Project Manager John R. Pearson, Senior Programs Manager, Roads and
Transportation Association of Canada

Chairman M.F. Clark, Associate Deputy Minister (Engineering),
Saskatchewan Highways and Transportation

Members

Dr. J.B.L. Robinson, Director of Technical Programs, Roads and Transportation
Association of Canada

M. Brenckmann, Director, Research Program Development, Transport Canada

M.W. Hattin, Manager, Vehicle Standards Office, Ontario Ministry of
Transportation and Communications

R.J. Lewis, Special Consultant, Canadian Trucking Association

M. Ouellette, Manager, Engineering, Mack Canada Inc.

R. Saddington, National Technical Advisor, Esso Petroleum Canada

W.A. Phang, Head, Pavement Research Division, Ontario Ministry of
Transportation and Communications

G. Tessier, Direction de la recherche, Ministère des Transports du Québec

E. Welbourne, Head, Vehicle Systems, Transport Canada

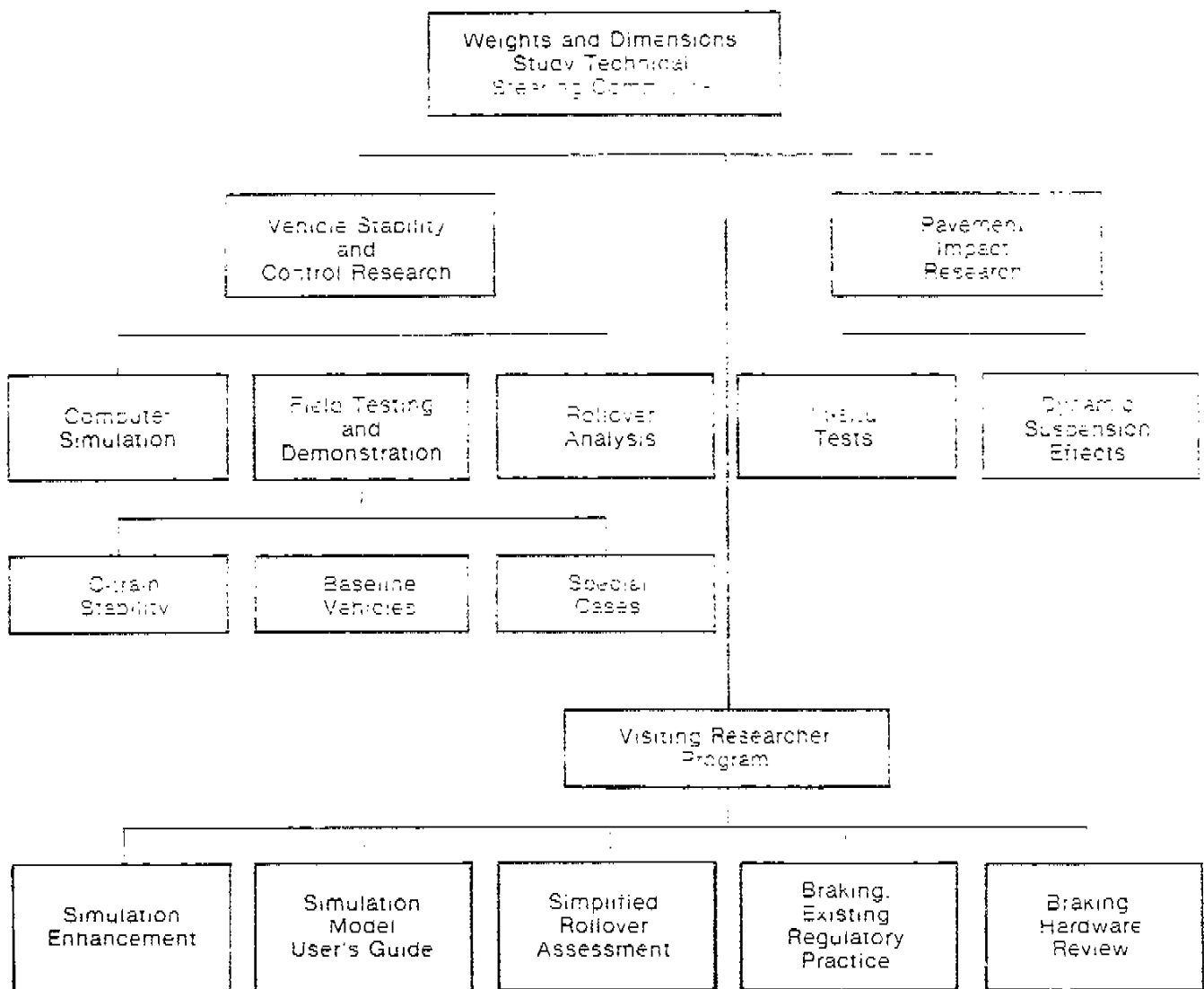
R. Zink, Chief Engineer, North Dakota State Highway Department (representing
AASHTO)

D.J. Kulash, Assistant Director, Special Projects, Transportation Research
Board



HEAVY VEHICLE WEIGHTS AND DIMENSIONS STUDY

TECHNICAL WORK ELEMENTS OVERVIEW



EFFECTS OF SUSPENSION VARIATIONS ON THE DYNAMIC WHEEL
LOADS OF A HEAVY ARTICULATED HIGHWAY VEHICLE

Rig Development, Experimental Program and Findings

J.H.F. Woodrooffe and P.A. LeBlanc
National Research Council
Division of Mechanical Engineering
Vehicle Dynamics Laboratory

K.R. LePiane
University of Waterloo
Mechanical Engineering
Co-Op Student

15 July 1986

DISCLAIMER NOTICE

The experimental results presented in this paper are pertinent to specific products which have been clearly identified by the manufacturer's product number. It should be emphasized that the experimental results should in no circumstances reflect the whole product line of an individual manufacturer, nor should the results be used to generalize on the performance of a generic suspension type. Subtle design variations in suspension components could, in some cases, lead to substantial changes in the performance of a suspension group. The objective of the study was not to endorse a product but rather to investigate the range of performance possible using these diverse systems.

ACKNOWLEDGEMENTS

The authors wish to extend their appreciation for the efforts and contributions of the following individuals and companies to this study.

We gratefully acknowledge Dr. R.E. Gagné of the Systems Laboratory, National Research Council of Canada, for his efforts in providing us with a suitable data acquisition system and related graphics software package.

Dr. P.F. Sweatman of the Australian Road Research Board provided us with valuable suggestions throughout the course of this research program. His contributions are gratefully appreciated.

The pavement response field experiments were conducted in cooperation with the Civil Engineering Department, National Resources Division, Alberta Research Council. We wish to acknowledge in particular the efforts of Dr. T. Christison and Mr. L.M. Chase. The assistance provided by the Gouvernement du Québec, Ministère des Transports, in providing services essential to the success of the field experiments was greatly appreciated.

The road roughness index was measured using a Mays-meter device from the Ministry of Transportation and Communications of Ontario (MTC). We extend our gratitude to Mr. T. Khan, Mr. F. Marciello and Mr. W.A. Phang of MTC and to Mr. A.T. Papagianakis and Professor R.C.G. Haas of the Department of Civil Engineering, University of Waterloo, for participating in the road roughness tests and for performing the data reduction and subsequent analysis of the results.

We are indebted to Chalmers Suspension International Ltd., Hayes-Dana Inc., Hendrickson Mfg. (Canada) Ltd., Neway (A Division of Lear Siegler Ltd.) and Reyco Canada Ltd. for supplying us with heavy duty truck suspensions and related hardware. Their cooperation and interest in the study are gratefully acknowledged.

ABSTRACT

The work reported here was supported jointly by Canroad and NRC Division of Mechanical Engineering, Vehicle Dynamics Laboratory, as part of the RTAC/CCMTA Heavy Truck Weights and Dimensions Study.

This study has investigated the dynamic wheel load behaviour of various heavy highway vehicle suspension systems under a controlled experimental program. A 45 tonne tractor-trailer was modified to measure the dynamic axle loads of all major load carrying axles simultaneously. Suspension parameters such as suspension type, axle spread and axle load were investigated as functions of road roughness and vehicle speed.

The effects of brake torque and suspension pitch attitude on the load equalization of the suspension were also investigated. Road tests were conducted at various speeds over variety of road roughness conditions. Findings relevant to the subject of dynamic road loading are highlighted.

TABLE OF CONTENTS

	Page
ACKNOWLEDGEMENTS	(ii)
ABSTRACT	(iii)
1.0 INTRODUCTION	1
1.1 Report Structure	2
1.2 Principles and Assumptions Governing the Choice of Hardware	2
2.0 THE TEST VEHICLE	6
2.1 Tractor	6
2.2 Trailer	7
3.0 INSTRUMENTATION AND CALIBRATION	8
4.0 TEST VARIABLES	10
4.1 Hardware Variables	10
4.2 Axle Load Variations	16
4.3 Road Roughness and Speed Variations	18
4.4 Single Bump Tests	20
4.5 Grade Level Railway Crossing Bump	21
4.6 Dynamic Bridge Loadings	22
4.7 Static Wheel Load Measurements	22
4.8 Static Pitch Test	23
4.9 Shake Test	23
5.0 ANALYSIS	24
5.1 Resolution of Dynamic Wheel Load	24
5.2 Shake Test	28
6.0 RESULTS	32
6.1 Special Cases	32
6.1.1 Impact Wheel Loads Associated with a Grade Level Railway Crossing	32
6.1.2 Dynamic Bridge Loading	33
6.1.3 Tire Scuffing in Turns as a Function of Axle Spread	33
6.1.4 Suspension Load Equalization Due to Variations in Trailer Pitch Angle	34

	Page	
6.2	Shake Tests	36
6.3	Road Tests	39
6.3.1	Dynamic Wheel Loads as a Function of Suspension Type	39
6.3.2	Dynamic Wheel Load as a Function of Trailer Suspension Spread	42
6.3.3	Dynamic Wheel Load as a Function of the Number of Axles in a Suspension Group	43
6.3.4	Axle to Axle Dynamics for Load Sharing Suspensions	48
6.3.5	Load Transfer Due to Braking	49
6.3.6	The Air Suspended Lift Axle	49
6.4	Pavement Deflection Due to Dynamic Wheel Loads	50
7.0	Concluding Remarks	54
7.1	Interpretation of Experimental Results	54
7.2	Relating Study Findings to Vehicle Weights and Dimensions Regulations	54
8.0	REFERENCES	62
APPENDICES		
A.	Mechanical Design Drawings of Hardware Fabricated for this Study	
B.	Vehicle Calibration and Instrumentation	
C.	Road Roughness Report	
D.	A Listing of Software Developed for the Analysis of Dynamic Data	
E.	Plots of Wheel Load vs Ride Comfort Rating for Various Suspension Combinations	
F.	Histograms of Digitized Wheel Load Data	
DOCUMENTATION PAGE		

EFFECTS OF SUSPENSION VARIATIONS ON THE DYNAMIC WHEEL
LOADS OF A HEAVY ARTICULATED HIGHWAY VEHICLE

1.0 INTRODUCTION

The purpose of this study is to provide the road regulatory authorities with factual data on the first order effects of suspension variations in terms of dynamic wheel loading as seen by the pavement. Simply put, the objective of this suspension study is to answer the following questions.

1. How well do multi-axle truck suspensions equalize load?
2. What are the dynamic wheel forces associated with typical suspension types?
3. How do variations in suspension axle spacing effect the dynamic wheel loads and the load equalization capabilities of a given suspension?
4. What is the effect of variations in vehicle speed and road roughness on dynamic wheel loads?

In addition to these four basic questions, typical examples of dynamic axle loads associated with discontinuities in the road structure will be provided. Included in this category are the following:

1. dynamic bridge loading associated with smooth and rough approaches.
2. dynamic road loading associated with a grade level railway crossing.

3. dynamic road loading associated with various pavement conditions such as:
- rigid pavement nearing the end of its acceptable life.
 - old flexible overlay on rigid pavement base with reflective cracking.
 - new smooth overlay on rigid pavement.
 - end of overlay transition bump.
 - rough and smooth flexible pavement.

Finally, the effect of vehicle braking and suspension equalization will be examined.

1.1 REPORT STRUCTURE

The main body of the report has been structured to be as concise as possible dealing with the first order results which are of primary interest to the overall study. Topics which serve to support the findings such as hardware development, instrumentation, theoretical analysis and calibration procedure are contained in the appendices.

1.2 PRINCIPLES AND ASSUMPTIONS GOVERNING THE CHOICE OF HARDWARE

In order to accurately measure the performance characteristics of heavy vehicle suspensions, as a function of road roughness variations and suspension parameter changes, considerable thought was required for the choice of vehicle to be used during the test program. It is well known that general vehicle characteristics such as vehicle mass, chassis compliance (both bending and torsion)

will effect the vertical dynamics and hence the dynamic axle loads of a vehicle. To accurately study the effects of suspension variations, these external influences must be held constant so that their contribution to vehicle response is not confused with those associated with a suspension parameter change.

Bearing in mind these concerns, the following points were used as guidelines in developing a vehicle suitable for these experiments.

- (1) The vehicle must be stiff in bending (beaming) and torsion so that structural compliance of the vehicle does not interfere with the response of the vehicle when a suspension parameter change is made.
- (2) The size and weight of the vehicle should be representative of large vehicles used in Canadian Interprovincial Trucking.
- (3) The weight of the vehicle must be controlled and must remain constant over time.
- (4) The modified chassis of the vehicle must permit rapid change out of suspensions and suspension components even when the vehicle is fully loaded.
- (5) Suspension components to be tested must cover the most common suspension types found on Canadian roads.
- (6) The suspensions must be fabricated in accordance with the manufacturers' instructions.
- (7) All suspensions must use the same make and model of axle, brake components and the same tires and rims.

- (8) The sensors used to measure force and torque cannot in any way effect the mechanical response of the suspension.
- (9) The vehicle's instrumentation system must continuously record all axle loads, brake torques and vertical accelerations simultaneously in analog form.
- (10) The sensors used must have minimum cross axis sensitivity and must be linear, with minimum hysteresis.

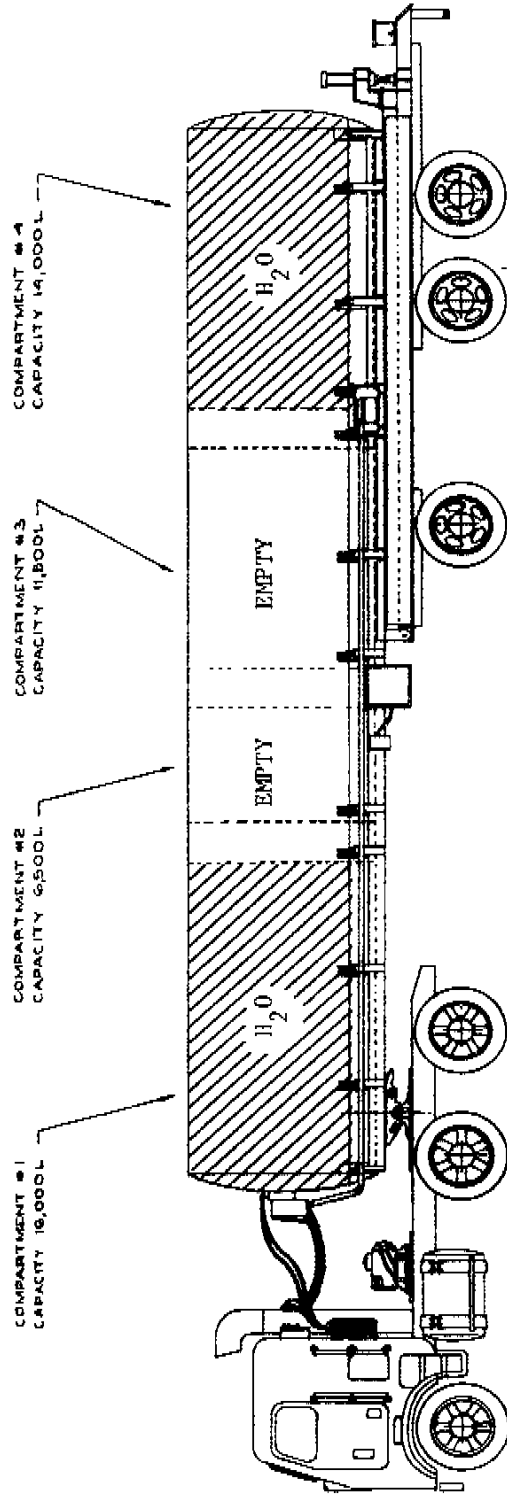


Figure 1. The NRC Test Vehicle

2.0 THE TEST VEHICLE

2.1 TRACTOR

A 1979 White Freightliner cab over tractor was refurbished to serve as the power unit for the study. Instrumentation recording systems were housed in the existing sleeper compartment which was fitted with a shock attenuating floating floor. All electronic data channels were routed through a connector junction box, a wiring harness and patch board were permanently fixed to the tractor. Electrical power was provided by an auxiliary power unit fixed to the tractor chassis.

The tractor was fitted with a new drive axle suspension. The suspension beams and drive axles were instrumented to yield vertical axle load, brake torque and vertical axle acceleration. A vertical accelerometer was also fitted to the steering axle of the tractor as a check on the relative road roughness between runs. Since the vertical response of the front axle is somewhat independent of the drive suspension, and since the static weight on the front axle is constant, the response of the front axle formed a reference from which runs of the vehicle over the same stretch of road could be compared with confidence. In short, if the front axle response characteristics were similar in energy content for two separate runs at the same speed over the same road but at different times of the year then one could be reasonably confident that the road roughness did not change significantly since the last time the test was run.

Finally, speed and distance were monitored by use of a trailing wheel.

2.2 TRAILER

A 1974 Fruehauf compartmentalized baffeled liquid tanker was refurbished for the study. The frame structure and original suspension were removed, scrapped and replaced by a new frame specifically designed for the purpose of this study.

The replacement frame was designed to accept different suspensions each mounted on its own sub frame. The sub frames could be moved to various positions on the main frame thereby permitting changes in axle position and spacing. Design drawings of the trailer frame, suspension sub frames and other mechanical components required for the study are found in Appendix A.

3.0 INSTRUMENTATION AND CALIBRATION

All dual-tire axles of the tractor and trailer were instrumented to measure vertical axle load, vertical acceleration and brake torque. Axle load measurement was achieved by the use of strain gauges on the axles which were sensitive to vertical bending of the axle. Brake torque was measured with strain gauges measuring strain in the axle along the torsional shear axis of the tube (i.e., 45° to the axle's axis.) Both of these measurement techniques provided linear results with no significant hysteresis. This was due in part to the choice of axle design used in these experiments. The axle was fabricated from steel tubing, and the axle spindles were friction welded to the tube without the use of a pilot shaft. This manufacturing technique eliminates the need for a pilot shaft on the end of the spindle, which is commonly pressed into the tube before welding. It was felt that the presence of a pilot shaft in the vicinity of the strain gauge section of the tube would detract from the linearity of the calibration curve.

The vertical acceleration of the axles was measured by strain gauge type accelerometers mounted on the same vertical axis as the load sensing strain gauges. The acceleration component is necessary to account for the vertical inertial effects of the tires, wheels and brake components outboard of the load sensing strain gauges. This inertial component is added to the vertical axle load to determine the impact load at the pavement.

Accelerometers were also fixed to both ends of the tank. By combining the outputs of these accelerometers, both pitch and bounce of the trailer were resolved.

Vehicle velocity and distance travelled were measured by an optically instrumented idler wheel mounted on the side of the trailer.

Quite by accident, it was observed that tire side forces in low speed turns could be resolved using the load sensing strain gauges on the axle. The side force induces a moment on the axle which, when calibrated, can be resolved into the magnitude of the side force. The prime limitation is that the cornering must be done at quasi-static speeds so that there is no roll induced load transfer to the axles.

Further details on the instrumentation and calibration procedures are found in Appendix B.

4.0 TEST VARIABLES

4.1 HARDWARE VARIABLES

The study examined three generic types of heavy vehicle suspension, the walking beam, the air suspension and the spring suspension. These represent the majority of suspension found on Canadian trucks. An explanation of each of these suspensions and their variations follows.

A. The Walking Beam Suspension

The two walking beam suspensions tested are illustrated in Figures 2 and 3. The axles are fixed to a rigid beam pivoted at its center or balance point thus facilitating ideal static load sharing. Two spring elements are used, one for each side of the chassis located between the frame rail and the walking beam. The specifications of the two walking beam suspensions are as follows:

Tractor Drive Suspension

Manufacturer - Hendrickson Mfg. (Canada) Ltd.

Model - RTE 440 (extended leaf tandem)

Combined Axle Rated Capacity - 20 tonnes

Axle spacing - 1.52 meters

Outer tire track width - 2.44 meters

Spring elements - steel leaf spring, 2 stage, Part Number
45322

Trailer Suspension

Manufacturer - Chalmers Suspensions International Ltd.

Model - 754-44-LW

Combined Axle Rated Capacity - 20 tonnes

Axle spacing - 1.37 meters

Outer tire track width - 2.59 meters

Spring element - rubber with restrictor can

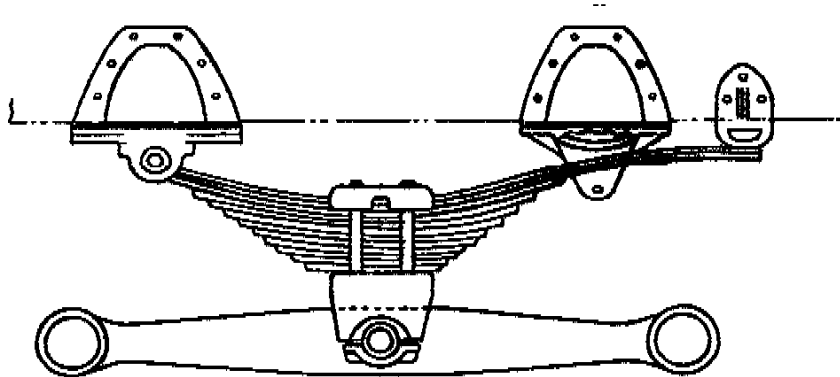


Figure 2 Tractor Drive Walking Beam Suspension

Hendrickson RTE 440

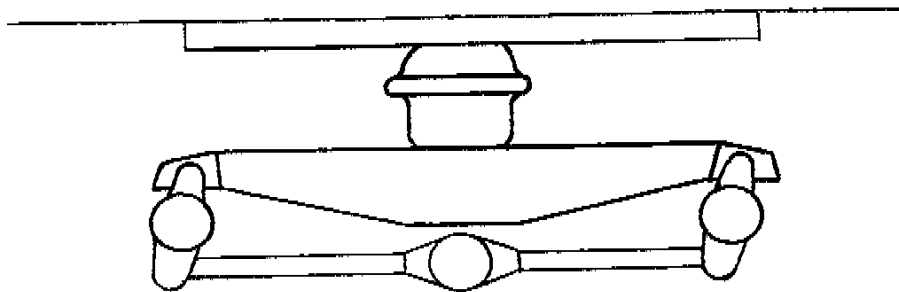


Figure 3 Trailer Walking Beam Suspension -

Chalmers 754-44-LW

B. The Air Suspension

Two tandem axle air suspensions were tested. The axles of both suspensions are mechanically independent of each other. The air supply to the air bags is regulated by two time delayed height sensing valves, one for each side of the vehicle. The air bags on each side of the vehicle are plumbed in parallel thus achieving load equalization

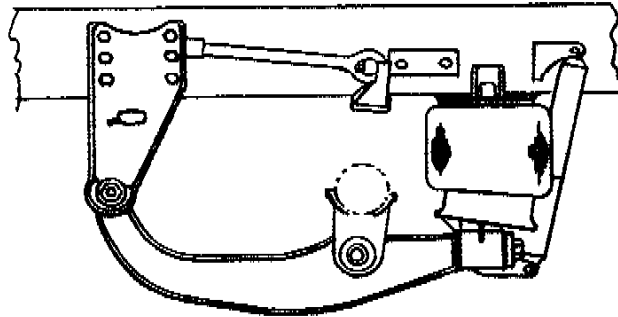


Figure 4a. Tractor Drive Air Suspension Neway ARD 244-6

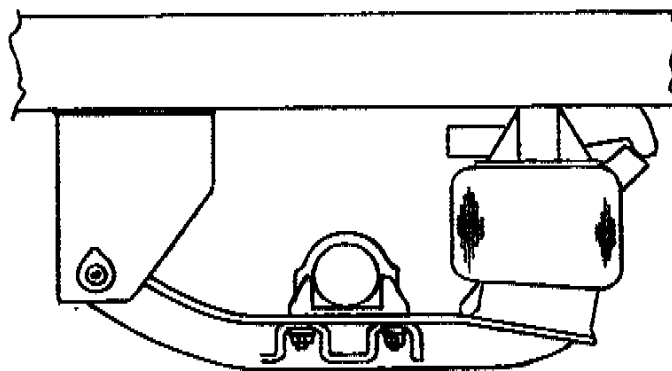


Figure 4b. Trailer Air Suspension Neway AR95-14

yet maintaining quasi-static vehicle roll resistance. Mechanical roll stiffness of the suspension is achieved by the use of trailing members semi rigidly fastened to the axle (trailer suspension) or a torsion tube (tractor suspension) to form an anti roll bar. This transfers roll moments of the vehicle to vertical forces at the wheels.

The lift axle was identical to the trailer tandem suspension unit except that the air pressure in the air bags was governed by a constant pressure regulator rather than a height sensing valve. It also had additional mechanical lifting members and air bags for the purpose of lifting the axle off the road surface. The lift axle therefore was fully independent of the tandem axle air suspension. The specifications of the air suspension axles tested are as follows:

Manufacturer - Neway (A Division of Lear Siegler Inc.)

Model - Tandem axle drive suspension ARD 244-6

Serial # C904157 EM

Combined Axle Rated Capacity - 20 tonnes

Spring Element - Air bag part number 905-57-031

Tandem Axle Spacing - 1.37 meters

Outer tire track width - 2.59 meters

Model - Tandem axle trailer suspension AR95-14

Serial # Lead - C9926210LK

Trailing - C9926211LK

Combined Axle Rated Capacity - 22.73 tonnes

Lift axle - AR95-14 (Lift)

Serial #C9926209LK

Rated Capacity per Axle - 11.36 tonnes

Spring Element - air bag Part Number 905-57-020

Tandem Axle Spacing Tested - 1.27 meters

- 1.83 meters

- 2.44 meters

Outer tire track width - 2.59 meters.

the suspensions are illustrated in Figures 4a, 4b and 5

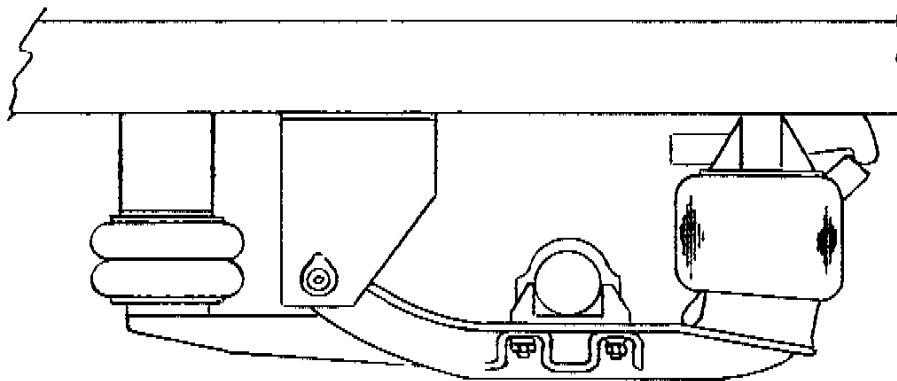


Figure 5 Trailer Lift Axle Neway AR95-14 (Lift)

C. Four Spring Suspension

A single tandem axle four spring trailer suspension was tested (see illustration Figure 6). As with the air suspension the four spring suspension was tested at three different axle spacings. The same springs and axles were used in all cases. The axle spacing variations were possible because of the design of the sub frame structure which accommodated various standard equalizing beams for this particular suspension. The specifications of the four spring suspensions tested are as follows:

Manufacturer - Reyco Canada Inc. (a subsidiary of Reyco Industries
Inc.)

Model - 2113-FAB-222-WB-14-C-50-3564

Combined Axle Rated Capacity - 20 tonnes

Tandem axle spacing tested - 1.27 meters

- 1.83 meters

- 2.44 meters

Outer tire track width - 2.59 meters

Spring elements - multi leaf spring - T-3564

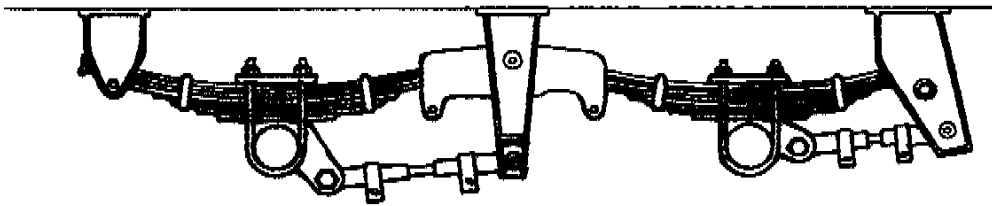


Figure 6a

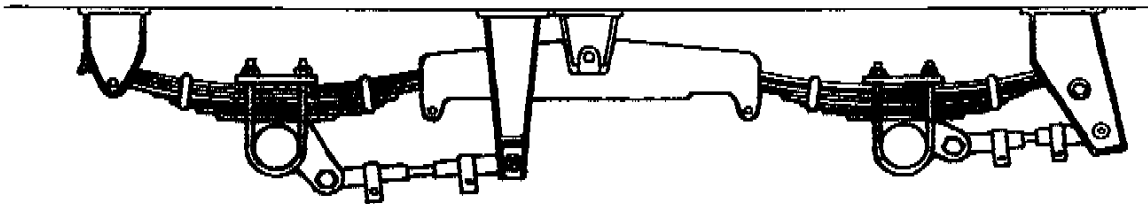


Figure 6b

Figure 6a, 6b The Trailer Four Spring Suspension Showing Support
Hardware Variations for 1.27, 1.83, 2.44 Meter
Spreads - Reyco 2113-FAB-222-WB-14-C-50-3564.

TYRES - When suspension changes were made the same tires were used.

Both the tractor and the trailer were fitted with dual tires. All

tires were inflated to 100 psi and checked before each run. The tires used are listed below.

Tractor - Steering axle - Uniroyal 14/80 R20

- Drive axles - Michelin 12R 22.5

Trailer - All axles - Michelin 11R 22.5

(The tires mentioned above are not tires which the NRC necessarily endorses.)

4.2 AXLE LOAD VARIATIONS

Vehicle mass and spring constants are the primary variables which have first order effects on vehicle vertical response. It was clear from the start of this study that control over the mass variable was considered to be of prime importance. To achieve constant mass, the fore and aft compartments of the trailer were completely filled with water and sealed for the duration of the test program. Changes in static axle load independent of vehicle mass variations were achieved through the use of an air suspended lift axle. The lift axle was located toward the longitudinal center of the trailer. The axle was controlled from the cab and could be raised clear of the road to increase the axle loads of the suspension being studied or lowered to decrease the axle loads.

This procedure allowed for constant control over the magnitude and the location of the suspended mass and its related properties such as pitch moment of inertia. Admittedly, the lift axle will have some influence on the vehicle response so care must be taken

in interpreting the data generated when the lift axle is down. (This task is helped by the fact that the air suspended lift axle has a linear response and a well defined spring stiffness and viscous damping characteristics.)

For example, when the lift axle is used in conjunction with the four spring trailer suspension, the spring constant and damping coefficient of the air suspension are much less than those of the four spring trailer suspension. Changes in the vehicle responses therefore may be attributed more to a reduction in static axle load of the four spring as opposed to the suspension effects of the air axle. This would be particularly true when considering the pitch dynamics of the trailer. By way of contrast, when the lift axle is used with the trailer air suspension, the spring constants and damping coefficients are nearly identical thereby playing a more dominant role in vehicle response variations.

The approximate static axle loads used during the test program are as follows:

TABLE 1

Condition	Tractor Drive Suspension Load Metric Tonnes Per Axle	Lift Axle Metric Tonnes	Trailer Suspension Load Metric Tonnes Per Axle
1	10	-	10
2	8.4	7.6	7.8

4.3 ROAD ROUGHNESS AND SPEED VARIATIONS

A range of road roughness conditions were selected to cover simple smooth, medium and rough categories. The test roads chosen were uniquely different from one another thus serving different purposes during the test program. All suspensions were tested over the same test sections at the same speeds. The road roughness was determined by the use of a Mays Meter. The Mays Meter measurements were then correlated with Ride Comfort Rating (RCR) by the following equations:

$$\text{RCR} = 9.63 - 0.02 \text{ Mays Meter measurement}$$

The RCR scale defines as Excellent, RCR Values 10-8

as Good,	"	"	8-6
as Fair,	"	"	6-4
as Poor,	"	"	4-2
as Very Poor,	"	"	less than 2

The vertical profile of two of the three roads was measured with a rod and chain. Full particulars pertaining to road roughness can be found in Appendix C.

What follows is a brief description of the test sites and the vehicle speeds used for each site.

A. Uplands Road North Bound Lane

- High Roughness Section 1 - Mays roughness 254 IPM (RCR 4.6)
Section 2 - Mays roughness 424 IPM (RCR 1.2)
- Test Speeds both sections 40, 60 km/hr

General Description - A two lane undivided road with badly deteriorating flexible pavement. There was excessive pavement cracking in a random pattern. Although the posted speed limit is 80 km/hr, the ride in the truck became unacceptable beyond 60 km/hr. For this particular road 60 km/hr is about the limit that most drivers would be prepared to push their equipment.

B. Woodroffe Ave. (Between CNR Tracks and Slack Rd.) North Bound

- Rough level railway crossing
- Smooth to medium rough roadway - Mays roughness 73 IPM (RCR 8.2)
- Test speeds - 40, 60, 80 km/hr

General Description - A two lane undivided road with flexible pavement in good condition. Three speeds were chosen for this roadway 40, 60, and 80 km/hr. The test section commenced with a grade level railway crossing which was impacted at full running speed. The analysis of the smooth road section commenced once the reaction of the vehicle to the railway crossing had dampened out. The dynamic wheel loads resulting from the railway crossing were analyzed separately.

C. Highway 417 (Between Maitland Ave. Overpass and Rochester Street Exit) East Bound

Three Sections

- smooth Mays roughness 59 IPM (RCR 8.5)
- medium Mays roughness 165 IPM (RCR 6.3)
- rough Mays roughness 217 IPM (RCR 5.3)
- several bridge structures
- test speed - 80 km/hr

General Description - A multi-lane divided highway through an urban area. The roadway is in the process of being reconstructed therefore there are three distinct surfaces present within the single test section. The smooth section (RCR 8.5) is new flexible overlay on a rigid pavement base. The medium surface (RCR 6.3) is an older overlay on the same rigid pavement. Reflective transverse cracking is evident. The rough surface (RCR 5.3) is the original rigid pavement in dire need of repair. These three surfaces were in close proximity to each other which allowed for continuous recording of all three surfaces during the same pass. The speed was held constant at 80 km/hr. This test section also contained several bridge structures with different approach roughnesses. Some approaches were undetectable by our instruments while some others gave very high reactions. These as well as the railway crossing data mentioned in the previous road description are presented under the section of special cases.

4.4 SINGLE BUMP TESTS

In addition to conducting tests on various roadways, there were a series of tests conducted with discrete bumps. These tests included both quasi-static or creeping over the bumps as well as dynamic impacts at various speeds.

The bumps were created by placing standard dimensional lumber across the road parallel to the axle axis of the vehicle.

The quasi-static or creep tests were used to measure quasi-static load equalization while the high speed runs were used to "pluck"

the suspension system so that the natural frequencies and apparent damping coefficient could be resolved. The ability of the suspensions to mitigate dynamic impact axle loads was also determined from the high speed runs. A listing of the bump arrangements and test speeds follows.

(a) Quasi-static creep tests (first gear deep reduction with engine idling).

- Two planks side by side 4 cm x 48 cm
- Three planks side by side 4 cm x 72 cm
- Two planks side by side with a third plank centered on top of the bottom two 8 cm x 48 cm.

(b) Dynamic Impacts

Speeds - Top end of first gear

- 18 km/hr
- 40 km/hr

All dynamic impacts were done at the above speeds over a single wooden plank fixed to the road surface having cross sectional dimensions of 4 cm x 24 cm.

Speed control during all tests was achieved by selecting the appropriate gear with the engine set against the maximum RPM governor.

4.5 GRADE LEVEL RAILWAY CROSSING BUMP

A single, grade level railway crossing was used in order to get a 'feel' for the dynamic axle loads that can be expected from such an input. The Mays meter roughness output for the 80 meter increment

of road containing the approaches and the crossing, was 252 IPM (RCR 4.6). Recognizing that this roughness figure is somewhat ambiguous, the general consensus was that in terms of roughness, the railway crossing could be considered to be typical.

The vehicle speeds used during the crossing were 40, 60 and 80 km/hr. The road roughness in the vicinity of the crossing was approximately 60 IPM (RCR 8.4).

4.6 DYNAMIC BRIDGE LOADINGS

A number of bridges were crossed during each of the tests conducted on Highway 417. The bridge approaches varied from smooth (undetectable) to very rough. One particular bridge on a recently repaved stretch of road produced quite a large vehicle response. The dynamic wheel loads associated with this bridge were included in this report, as a matter of interest.

4.7 STATIC WHEEL LOAD MEASUREMENTS

When a new suspension was installed on the vehicle or when the axle spacing was changed, the vehicle's static wheel load was measured on a flat level concrete floor.

The procedure used was to place jacks under the chassis of the fully loaded vehicle and then raise the vehicle until the wheels were off the ground. All load sensing strain gauge bridge circuits were balanced to zero and then the vehicle was lowered and the jacks removed. The voltage change across the bridge circuits was measured

using a digital voltmeter and the wheel load was then calculated using the appropriate calibration constants.

4.8 STATIC PITCH TEST

The static pitch test was used to determine the static load sharing characteristics of various suspensions as a function of trailer pitch angle. The intent is to explore the magnitude of the suspension equalization variations that can be expected when the tractor and trailer riding heights are mismatched. Heavy jacks were used to raise the fully loaded vehicle at the tractor's fifth wheel thereby inducing a pitch angle to the trailer's suspension.

4.9 SHAKE TEST

NRC's four post shaker rig was used to demonstrate the importance of considering inertial forces outboard of the strain gauge when evaluating dynamic wheel loads. The experiment consisted of lowering the air suspension lift axle on two load cells and exciting the wheels of the axle with two hydraulic actuators. The analysis of the spring mass system along with the experimental results are found in sections 5.2 and 6.2 respectively.

5.0 ANALYSIS

5.1 RESOLUTION OF DYNAMIC WHEEL LOAD

The resolution of vertical wheel loads at the pavement surface requires two data sources. One being the dynamic axle load as measured by the strain gauged axles and the other being the vertical inertial component of the mass outboard of the strain gauges. This mass is comprised of tires, rims, brake hardware and a portion of the axle. The inertial force is resolved by multiplying the measured vertical acceleration of the axle by the above mentioned mass. The sum of the vertical axle force and the vertical inertial force yields the force as seen at the tire/roadway interface.

In algebraic terms

$$\text{Total Dynamic Wheel Force at the Pavement Surface} = \text{Dynamic Axle Load} + \text{Vertical Acceleration of the Axle} \times \text{End of Axle Mass}$$

The following brief analysis proves the need to consider the vertical inertial forces.

The derivation of the equation of motion (1) makes use of the following assumptions. First, the axle is analysed as a simply supported beam, that is, the axle bending moments at points A and B in Figure 7 are zero and the member is free of axial load. The axle is considered to be a rigid body with two degrees of freedom, namely, bounce and roll, described respectively by x and α .

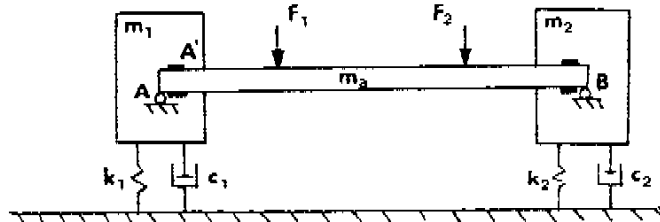


Figure 7

A free body diagram of the axle reveals that the reaction at point A, R_A , is a function of the forces transmitted by the leaf springs or air bags, F_1 and F_2 , and the inertial forces of the axle;

$$R_A = F_1 + (F_2 - F_1)a/l - \frac{1}{2} m_a \ddot{x} + I_a \ddot{\alpha}/l \quad (1)$$

The term m_a is the mass of the axle and I_a is the axle roll moment of inertia about its center of mass. The linear dimensions a and l are defined in Figure 8.

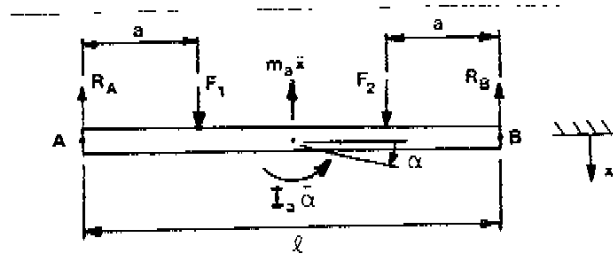


Figure 8

Assuming that the strain gauge at point A' accurately monitors the reaction R_A , one may proceed with the analysis of the free body diagram shown in Figure 9.

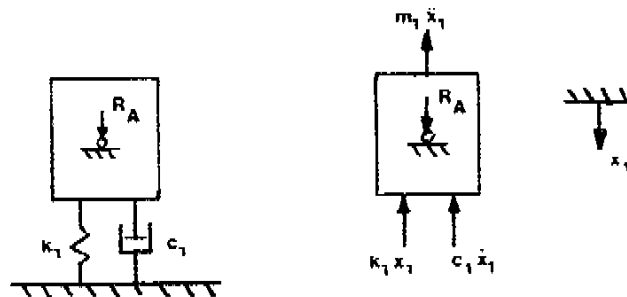


Figure 9

The equation of motion for the above figure is simply

$$m_1 \ddot{x}_1 + c_1 \dot{x}_1 + k_1 x_1 = R_A \quad (2)$$

The load transmitted to the pavement, T, is given by

$$T = k_1 x_1 + c_1 \dot{x}_1$$

By making use of equation (2), T can be expressed in the form,

$$T = R_A - m_1 \ddot{x}_1 \quad (3)$$

The variable m_1 represents the inertial mass outboard of the strain gauge and \ddot{x}_1 is the vertical acceleration of the inertial mass.

The breakdown of the inertial mass components is as follows:

Tires and Rims Qty 2	207.5 kg
Hub and Drum Qty 1	62.2 kg
Brake Shoes Qty 2	16.3 kg
Brake S Cam Shaft Qty (1)	3.1 kg
Wheel Studs and Nuts Qty 10	1.5 kg
Bare Axle Qty 1/10	10.6 kg
Total Inertial Mass	<u>301.2 kg</u>

The inertial mass was taken as 300 kg.

Summing of the axle forces and the inertial forces was done in the analogue state using operational summing amplifiers. Depending on the analysis technique required, the summed analogue signal was transferred to a strip chart recorder for direct interpretation of the data or it was digitized for numerical analysis.

The numerical analysis was performed with an IBM-AT personal computer. The computer was equipped with a four channel analogue to

digital converter, and the necessary software was developed to perform the numerical functions (see Appendix D).

The statistical functions of interest were:

- The mean
- First standard deviation
- 5th and 95th percentile and their corresponding histogram plots.

The sampling rate was 300 points/sec/channel.

The dynamic load coefficient was intended as the principle numerical quantity to be used for the analysis of continuous dynamic data. Known in statistics as the coefficient of variation, the DLC is defined as:

$$DLC = \frac{S}{Z}$$

S = standard deviation of the wheel forces
distribution (kN)

Z = overall mean wheel forces (kN)

The introduction of the DLC is based on the assumption that its numerical value is independent of the variation in the overall mean wheel force. Hence, the DLC allows one to compare different suspensions tested with different overall mean wheel loads. However, we find that a change in Z leads to a variation in the DLC.

Take for an example the test condition where the truck had a walking beam suspension as the drive axles and a four spring suspension as the trailer axles. A test was carried out where the drive axle wheel loads were decreased by 13%. The decrease in the standard

deviation was evaluated at 6% instead of the expected 13% decrease. By comparison, when the four spring trailer axle load was reduced by 24% there was a reduction in the standard deviation of 19%, which is within acceptable limits.

It is evident from this exercise that the relationship between S and Z may not be linear and, moreover, it may be dependent on the suspension type, that is

$$S = DLC \times Z$$

where

$$DLC = DLC(Z, \text{suspension type})$$

To eliminate possible confusion resulting from variations in the static wheel load, the DLC will not be used as the primary analysis term. It will be replaced by the standard deviation of the dynamic wheel force. This term will be examined as a function of vehicle speed, road roughness and suspension type. The DLC did prove useful however, during the final analysis with appropriate consideration.

5.2 SHAKE TESTS

To further explore the axle force and inertial force contributions of the vehicle measurement system, a vertical shake test was performed. The air lift suspension of the fully loaded vehicle was supported at the tires with two electro hydraulic vertical actuators. A low amplitude sinusoidal input, equal to the resonant frequency of the suspension, was applied. The configuration of the Vehicle Dynamics Laboratory required that the rear end of the trailer be supported by a

crane. The tractor, for its part, rested on the ground in its usual position. Figure 10 depicts a model of the spring mass system under study.

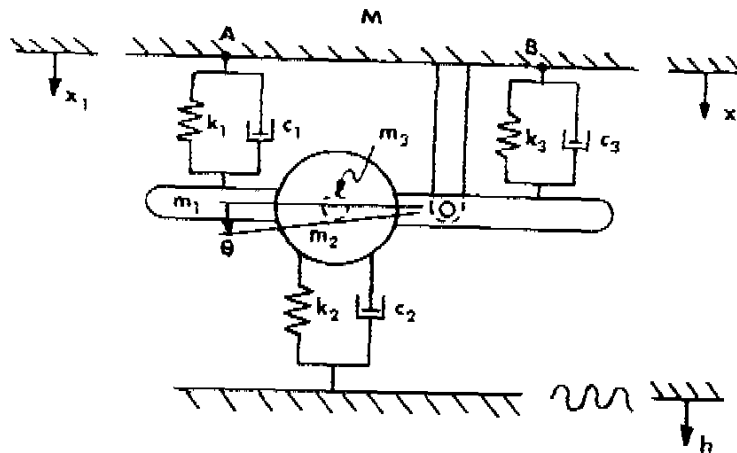


Figure 10

The span between points A and B is assumed to be small enough so that the displacement x_1 of the trailer mass, M, describes the motion of both points A and B, despite possible pitch of the trailer. The mass elements m_1 , m_2 and m_3 are assumed to be rigidly attached to one another. The quantity m_2 represents the mass outboard of the strain gauge, while m_1 and m_3 are the mass of the radius arm and axle respectively. A free body diagram of the system is shown in Figure 11.

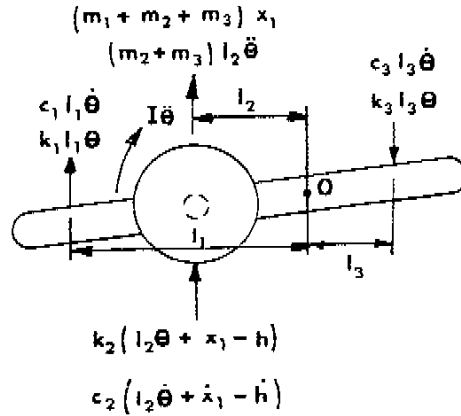


Figure 11

The sum of the moments about point O leads to

$$\begin{aligned}
 & k_2(l_2\theta + x_1 - h)l_2 + c_2(l_2\dot{\theta} + \dot{x}_1 - \dot{h})l_2 + k_1l_1^2\theta + c_1l_1^2\dot{\theta} \\
 & + k_3l_3^2\theta + c_3l_3^2\dot{\theta} + I\ddot{\theta} + m_3l_2^2\ddot{\theta} + m_1L_1\ddot{x}_1 + m_3l_2\ddot{x}_1 \\
 & + m_2l_2^2\ddot{\theta} + m_2l_2\ddot{x}_1 = 0
 \end{aligned} \tag{4}$$

The linear dimensions l_1 , l_2 and l_3 are as defined on Figure 11, I is the mass moment of inertia of m_1 about point O, L_1 is the distance of the mass center of m_1 from point O and k_1 , k_2 , k_3 and c_1 , c_2 , c_3 are stiffness and damping coefficients respectively.

The sign convention adopted for the axle strain gauge is the following: a downward force applied to the axle inboard of the strain gauge is considered positive and results in a positive voltage output. Hence the force F_S monitored by the strain gauge (that is the inertial and spring forces inboard of the strain gauge) takes the form

$$\begin{aligned}
 F_S = & - (k_1l_1^2\theta + c_1l_1^2\dot{\theta} + k_3l_3^2\theta + c_3l_3^2\dot{\theta} + I\ddot{\theta} \\
 & + m_3l_2^2\ddot{\theta} + m_1L_1\ddot{x}_1 + m_3l_2\ddot{x}_1) * l_2
 \end{aligned} \tag{5}$$

Defining the actuator force F_A as being positive in the upward direction leads to

$$F_A = c_2(1_2 \dot{\theta} + \dot{x}_1 - \dot{h}) + k_2(1_2 \theta + x_1 - h) \quad (6)$$

Equation (4) can therefore be written as

$$F_A = F_S - m_2 \ddot{x}_2 \quad (7)$$

where $\ddot{x}_2 = 1_2 \ddot{\theta} + \ddot{x}_1$ is the vertical acceleration of m_2 which is monitored by an accelerometer fastened to the axle right next to the wheel hub. The final result (Equation (7)) is identical to that obtained in Equation (3) on page 26.

6.0 RESULTS

6.1 SPECIAL CASES

The intent of the special cases section is to provide some typical measured values in the form of general interest material.

6.1.1 Impact Wheel Loads Associated With A Grade Level Railway

Crossing

As described earlier, this single track railway crossing was considered to be typical in terms of roughness. The Mays meter roughness output for the 80 meter increment of the road containing the crossing was 252 IPM (RCR 4.6). The road roughness in the vicinity of the crossing was approximately 60 IPM (RCR 8.4).

As would be expected, the dynamic wheel loads resulting from passing over a railway crossing are velocity dependent. The peak wheel load forces associated with the impact of the crossing, and the peak level after one cycle, are listed in the table below. The forces are expressed as a ratio of the total peak load/static load.

The peak level after one cycle occurred at points 10, 7.5, and 5 meters beyond the crossing for vehicle speeds of 80, 60 and 40 km/hr, respectively. The static axle load was 10 tonnes, 5 tonnes per dual wheel. (Five tonnes is equivalent to 49 kN.)

TABLE 2

Peak Dual Wheel Forces Associated with Crossing
a Grade Level Railway Crossing

Vehicle Speed km/hr	<u>Peak Dual Wheel Loads</u> Static Wheel Loads	
	At Crossing	1 Cycle After crossing
40	1.3	1.3
60	1.8	1.5
80	2.1	1.9

6.1.2 Dynamic Bridge Loading

As mentioned previously, a number of bridges were crossed during each of the tests conducted on Highway 417. The bridge approach varied from smooth (undetectable) to very rough. One particular bridge on a recently repaved section of road produced quite large vehicle responses. At a speed of 80 km/hr and a static axle load of 10 tonnes, the maximum wheel force experienced while crossing the bridge was 2.1 times the static load. The peak total wheel load associated with the roadway before and after the bridge was only 1.2 times the static load.

6.1.3 Tire Scuffing in Turns as a Function of Axle Spread

A typical intersection was used as our standard for these tests. In all cases, the vehicle negotiated the turn at the same creep speed, following the same wheel path. All tests were conducted on the same suspension at three different spreads, i.e. 1.27, 1.83 and 2.44 meters. The side force generated by the tires was measured continuously through the turn.

Findings show that because tire saturation occurred in all cases, there was no appreciable difference in the magnitude of the scuffing forces as a function of spread. There is, however, a significant difference in the duration of the scuffing for a given turn. Using the 1.27 meter axle spread as a baseline, the 1.83 meter spread increases the scuffing distance by approximately 17%, and the 2.44 meter axle spread increases the scuffing distance by 30%.

Increased trailer axle spread also increases the tractive forces and side forces on the tractor drive tires. The reason for this is that the tractor drive tires must overcome the yaw moment induced by the trailer axles while in a turn. An increase in the spread of these trailer axles will see a proportional increase in the yaw moment and thus an increase in the required tractive effort from the tractor. The increase in yaw moment of the trailer also means an increase in lateral bending moment in the frame structure of the trailer.

6.1.4 Suspension Load Equalization Due to Variations in Trailer Pitch Angle

Within the industry there are variations in the 5th wheel height of tractors and the coupling heights of trailers. Mismatching tractor and trailer coupling heights will result in variations in the pitch attitude of a trailer and its suspension. To gain an appreciation for the load equalization sensitivity to pitch attitude of the various suspensions, a static pitch test was performed. Since the study is interested in wheel loads, the experiment focused on wheel load variations rather than axle load variations.

The criteria used to assess the pitch load equalization characteristics of the suspension is in the form of percentage load transfer (PLT) recorded for pitch angles varying from 0.2 to 1.2°. PLT is defined as follows

$$\text{PLT} = \frac{\text{change in trailing wheel load} - \text{change in lead wheel load}}{\text{Total wheel load of the group}} \times \frac{100\%}{\text{degree}}$$

The results of the pitch test are as follows.

Both walking beam suspensions, Chalmers and Hendrickson had excellent PLT results of better than 3%.

The Neway air suspension results were the most difficult to interpret because it is an active suspension in that it utilizes height sensing control valves to maintain constant displacement from the axle to the trailer chassis. These control valves have a displacement lag feature which results in side to side differential wheel loading when the suspension is tested in a quasi-static manner. In some cases equalization was near perfect while in other cases there was a measurable difference. The highest PLT recorded with the air suspension was 6%.

The four spring suspension (Reyco) displayed the highest sensitivity to pitch variation of all suspensions examined by this study. PLT results of 14-17% were recorded depending on axle spread. 14% corresponded to the 1.27 meter spread while 17% corresponded to the 2.44 meter spread.

6.2 SHAKE TESTS

As indicated in section 5.2 the spring mass system from the shake test experiments could be modelled as a two degree of freedom system. However, to verify that the general properties of the mechanical system are properly monitored, it is less cumbersome to treat the axle-wheel combination as a one degree of freedom system with no damping. The following paragraphs justify such a simplification.

The shake tests were conducted without shock absorbers on the air suspension, thus considerably reducing the magnitude of the damping coefficients c_1 and c_3 of Equation (4) on page 30. Upon neglecting viscous forces associated with tires and air bags we obtain, for a sinusoidal forcing function, the following steady state solution for the strain gauge force;

$$F_S = [(k_1 l_1^2 + k_3 l_3^2) - \omega^2(I + m_3 l_2^2)] \ddot{x}_2 / l_2^2 \omega^2 + [\omega^2(I - m_1 L_1 l_2) - (k_1 l_1^2 + k_3 l_3^2)] \ddot{x}_1 / l_2^2 \omega^2$$

The factors multiplying \ddot{x}_1 and \ddot{x}_2 are of the same order of magnitude, however, video tape of the experiment clearly showed that the displacement x_1 was of second order in comparison with x_2 . Hence F_S may be approximated to

$$F_S = [k_1 l_1^2 + k_3 l_3^2 - (I + m_3 l_2^2) \omega^2] \ddot{x}_2 / l_2^2 \omega^2 \quad (8)$$

which is precisely the result obtained from a one degree of freedom analysis. By making use of the steady state solution for a one degree of freedom system we may rewrite the expression for the actuator force, Equation (6) on page 31, as

$$F_A = [k_1 l_1^2 + k_3 l_3^2 - (m_2 l_2^2 + I + m_3 l_2^2) \omega^2] \ddot{x}_2 / l_2^2 \omega^2 \quad (9)$$

Equations (8) and (9) reveal that for small driving frequencies ω the vertical acceleration \ddot{x}_2 is in phase with F_S and F_A . As we increase the driving frequency we can expect a 180° phase shift between \ddot{x}_2 and the signals F_S and F_A . If we define ω_A and ω_S as the frequencies at which a 180° shift occurs between F_A and \ddot{x}_2 , and F_S and \ddot{x}_2 , then the following results can be established from Equations (8) and (9):

$$\omega_A < \omega_n, \quad \omega_S > \omega_A$$

where the natural frequency for the system, ω_n , is

$$\omega_n^2 = (k_1 l_1^2 + k_2 l_2^2 + k_3 l_3^2) / (m_2 l_2^2 + I + m_3 l_2^2)$$

All of the above theoretical observations have been experimentally confirmed. The quantities ω_A , ω_S and ω_n were measured as

$$\omega_A \approx 4.5 \text{ Hz}$$

$$\omega_S \approx 6.5 \text{ Hz}$$

$$\omega_n \approx 11.0 \text{ Hz}$$

The simplifications which were made in the above discussion served only to insure that the instrumentation properly monitored the general mechanical behavior of the system. It must be emphasized that these simplifications are not required in the analysis of dynamic calibration. If the model described in section 5.2 is accurate then the strain gauge and load cell will monitor precisely every term in Equations (5) and (6). Hence Equation (7), on page 31, remains an exact relation.

Shake tests were performed at several different driving frequencies and amplitudes. Using Equation (7) the inertial mass outboard of the strain gauge was evaluated at 234 kg with a standard

deviation of 9 kg. This value is 22% lower than the actual mass outboard of the strain gauge.

A portion of the discrepancy between the outboard mass measured from dynamic calibration and the actual mass of the wheel could probably be attributed to the fact that the elements of the tires are not all accelerated at \ddot{x}_2 . The wheel could be modelled with say, one third of the mass of the two tires (38 kg) having a vertical acceleration of \ddot{h} while the remaining portion of the wheel be accelerated at \ddot{x}_2 . For cases where \ddot{h} is small this would account for 57% of the difference in the recorded mass.

Although dynamic calibration is in its preliminary stages of development the experiment confirmed the presence and the importance of measuring the inertial forces associated with the mass outboard of the strain gauge. For example, when excited at the resonant frequency of 11 Hz the inertial forces accounted for 58% of the force transmitted to the shaker's load cell.

The dynamic calibration experiment suggests that a 22% lower inertial mass should be used when evaluating the inertial forces. However, before the mass obtained from dynamic calibration can be confidently used we must develop a mathematical model of the wheel which will account for its entire static mass. Also the four post shaker is a complex apparatus for which the accuracy and limitations have yet to be fully assessed.

Any error associated with the simplified model used to determine the inertial forces applies equally to all suspensions tested. Although the actual wheel force may be in error by as much as

10% depending on road roughness, the accuracy of the system for unit to unit comparison is better than 5%.

6.3 ROAD TESTS

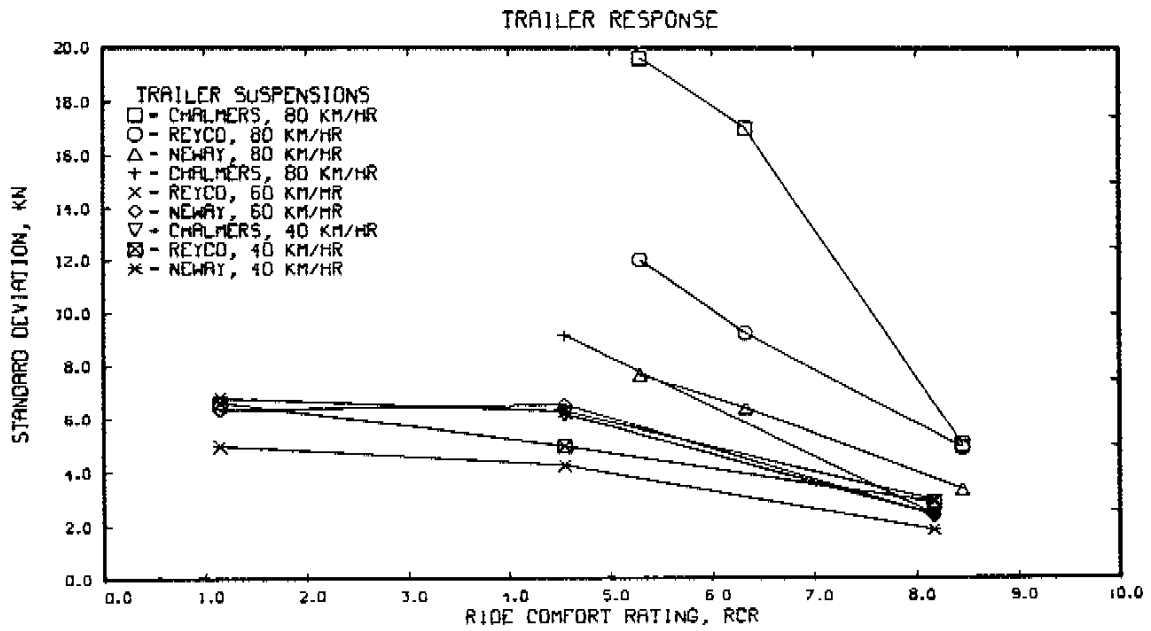
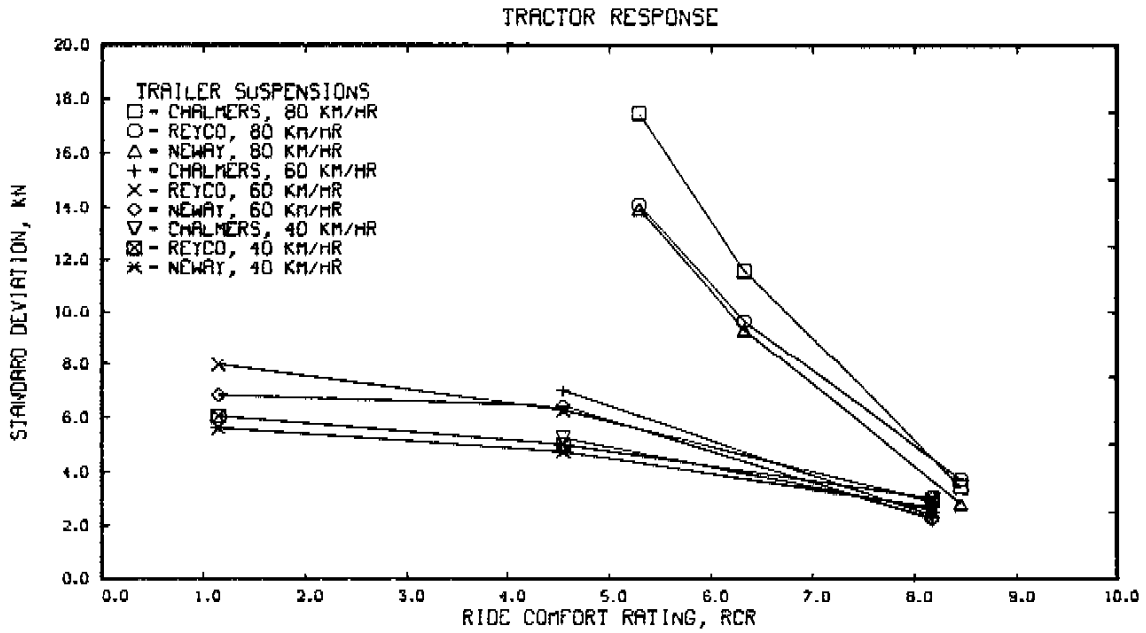
The results presented here were derived from the road tests outlined in Section 4.3. The data from these tests has been processed and is presented in graphical form in Appendix E. Selected graphs have been included in this section to illustrate points of discussion. All graphs are plotted in the form of standard deviation of dynamic dual wheel loads verses ride comfort rating (RCR). RCR classifies road roughness on a scale of 1 to 10 where 1 is rough and 10 is smooth.

6.3.1 Dynamic Wheel Loads as a Function of Suspension Type

Figures 12, 13, 14 and 15 illustrate how the different suspensions tested compare in terms of dynamic wheel load resulting from the same road input. The following observations can be made from these graphs.

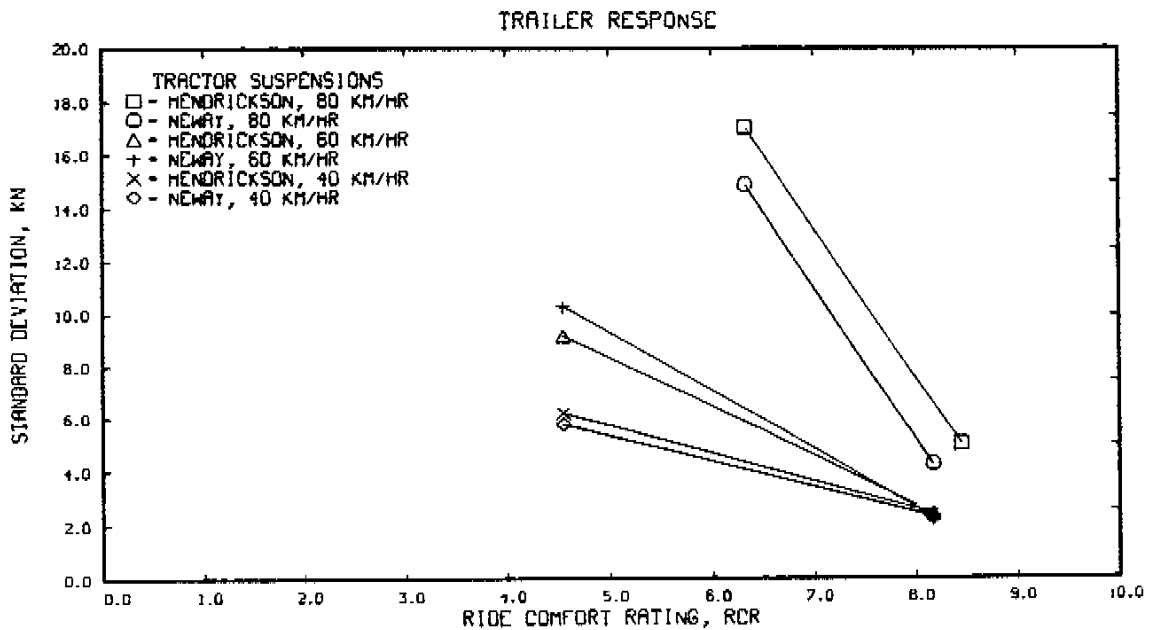
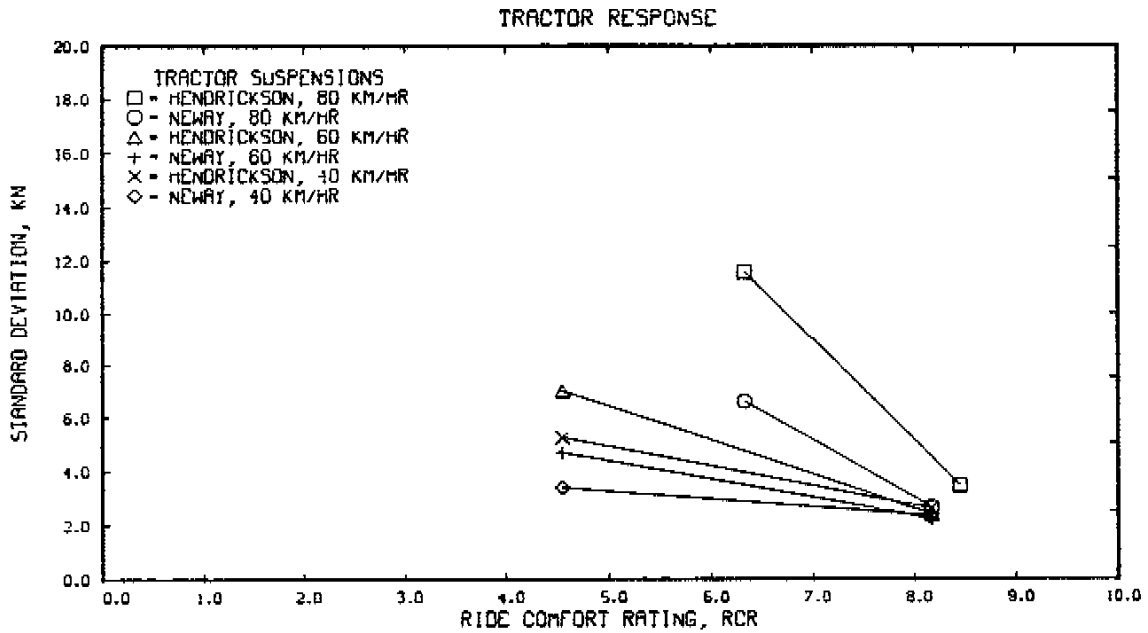
- a) It is clear that as the road becomes smoother the dynamic wheel loads diminish and tend to converge to small values independent of the suspension type.
- b) Dynamic wheel loads vary with vehicle speed in an exponential form. Consider for example the four spring suspension with a static dual wheel load of 50 kN (5 Tonnes) traveling over a road with a RCR of 5.2 at a speed of 80 km/hr. A marginal increase in dynamic wheel load of 20% is seen when the vehicle speed is increased from 40-60 km/hr. However, when the speed is increased from 60-80 km/hr a substantial increase in dynamic wheel load of 150% is seen.

VARIATION OF TRAILER SUSPENSION TYPE
TRACTOR SUSPENSION - HENDRICKSON
AIR AXLE UP - NOMINAL WHEEL LOAD OF 50 KN
NOMINAL TRAILER AXLE SPREAD OF 1.3 M



Figures 12 (upper), 13 (lower)

VARIATION OF TRACTOR SUSPENSION TYPE
TRAILER SUSPENSION - CHALMERS
AIR AXLE UP - NOMINAL WHEEL LOAD OF 50 KN
NOMINAL TRAILER AXLE SPREAD OF 1.3 M



Figures 14 (upper), 15 (lower)

c) Variations in dynamic wheel load are evident when comparing the different suspensions tested. The results presented in the following table are based on a vehicle speed of 80 km/hr and a RCR of 5.2, and expressed using a derivative of Sweatman's Dynamic Load coefficient

$$DLC = \frac{\text{Standard Deviation of wheel load}}{\text{Nominal Static Wheel Load (50 kN)}}$$

where nominal static wheel load is substituted for mean wheel load.

TABLE 3

SUSPENSION TYPE	DYNAMIC LOAD COEFFICIENT
Air Bag	16%
Four Spring	24%
Leaf Spring Walking Beam	28%
Rubber Spring Walking Beam	39%

6.3.2 Dynamic Wheel Load as a Function of Trailer Suspension Spread

Changes in dynamic wheel load associated with variations of trailer axle spread are generally small; expressed in terms of DLC they are less than 3%. See Figures 16, 17, 18 and 19. The only exception to this occurred with the four spring suspension. The largest variations occurred at 80 km/hr where changes in DLC as high as 8% were measured.

With the four spring suspension the order of preferred axle spread varies with road roughness. On rough roads at 80 km/hr, the order of suspension spread from most favorable to least favorable is 1.83, 1.27 and 2.44 meters. On smooth roads at 80 km/hr, the order is reversed, that is, 2.44, 1.27 and 1.83 meters.

Clearly, the results of Figures 16 to 19 reveal that the air suspension is only modestly sensitive to axle spread variations for all conditions of speed and roughness at which it was tested. On the other hand, at 80 km/hr the four spring suspension demonstrated acute sensitivity to changes in axle spread. The difference in axle spread sensitivity of the two suspensions is undoubtedly linked to the fact that the air suspension is mechanically independent whereas the four spring suspension is mechanically dependent. A change in axle spread on the four spring suspension does not only relocate the spring elements along the trailer but it also changes the mechanical properties of the suspension group. Hence, we may conclude that dynamic wheel load is insensitive to axle spread provided that changes in axle spread do not inherently alter the kinematic components of the tandem suspension.

6.3.3 Dynamic Wheel Load as a Function of the Number of Axles in a Suspension Group

As mentioned in section 4.2, adding an axle (air lift suspension) to a tandem axle suspension resulted in a 16% decrease of the tractor static wheel load and a 22% reduction of the trailer static wheel load. Figures 20, 21, 22 and 23 reveal that a reduction in static wheel load does not necessarily translate into a proportional decrease in dynamic wheel load. In general the percentage decrease in dynamic wheel load is less than the percentage decrease in static load.

VARIATION OF TRAILER AXLE SPREAD
TRACTOR SUSPENSION - HENDRICKSON
TRAILER SUSPENSION - NEWAY
AIR AXLE UP - NOMINAL WHEEL LOAD OF 50 KN

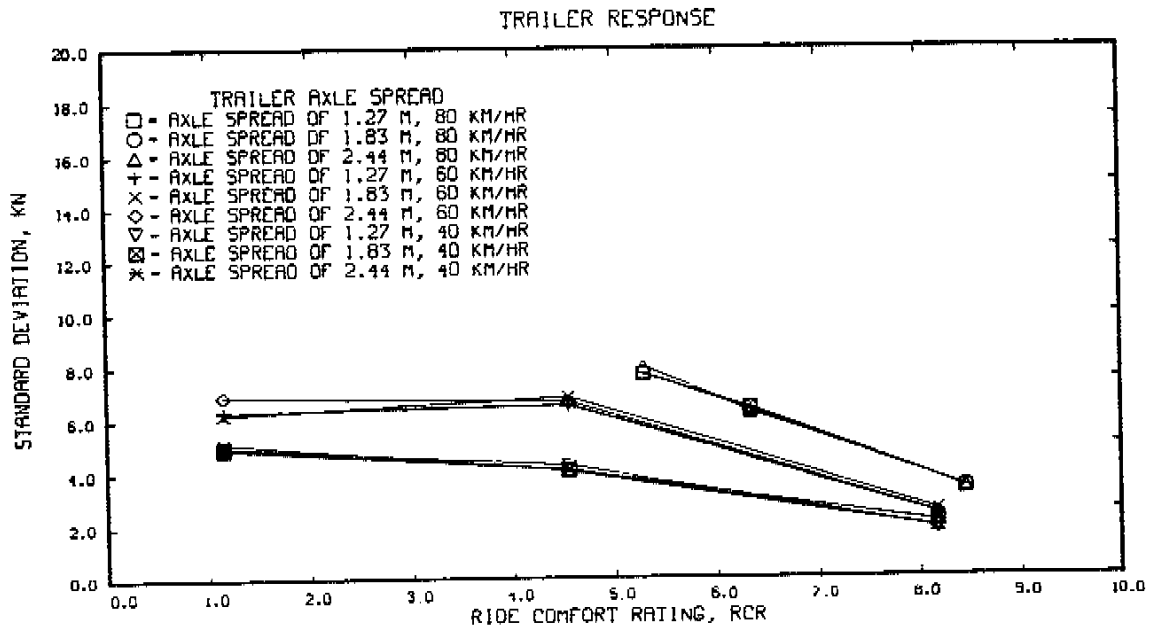
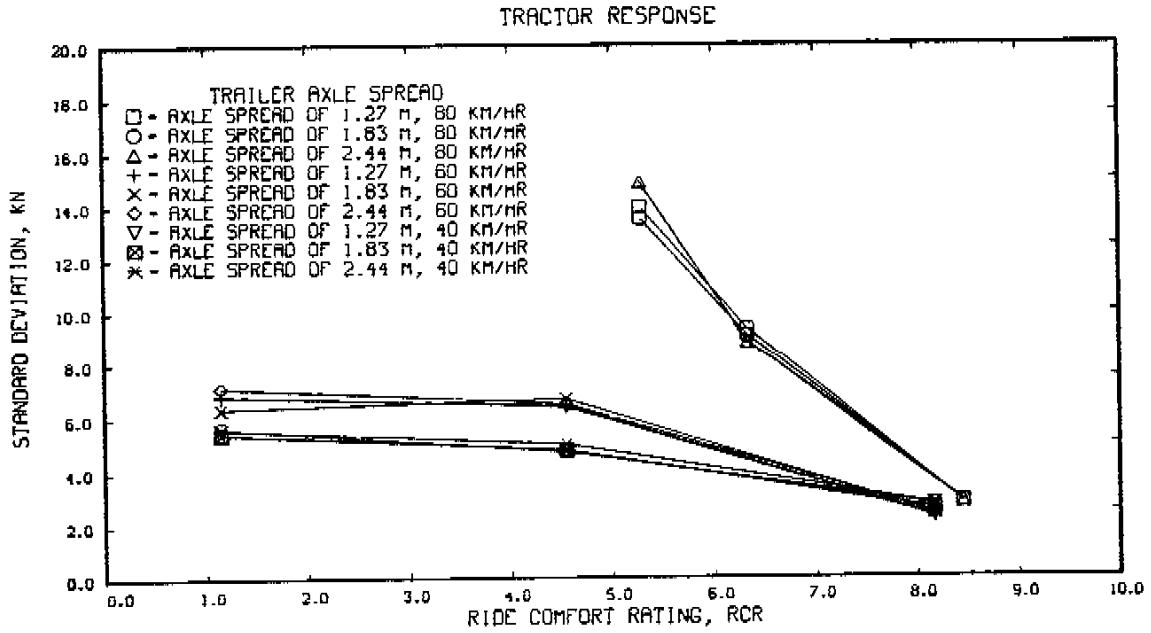


Figure 16 (upper), 17 (lower)

VARIATION OF TRAILER AXLE SPREAD
TRACTOR SUSPENSION - HENDRICKSON
TRAILER SUSPENSION - REYCO
AIR AXLE UP - NOMINAL WHEEL LOAD OF 50 KN

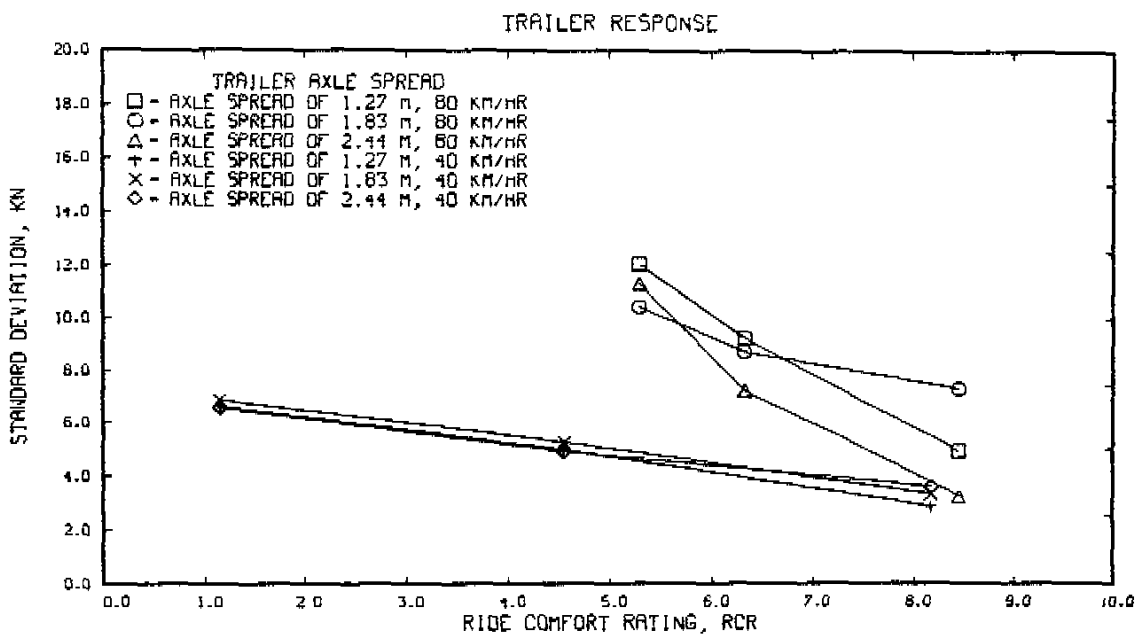
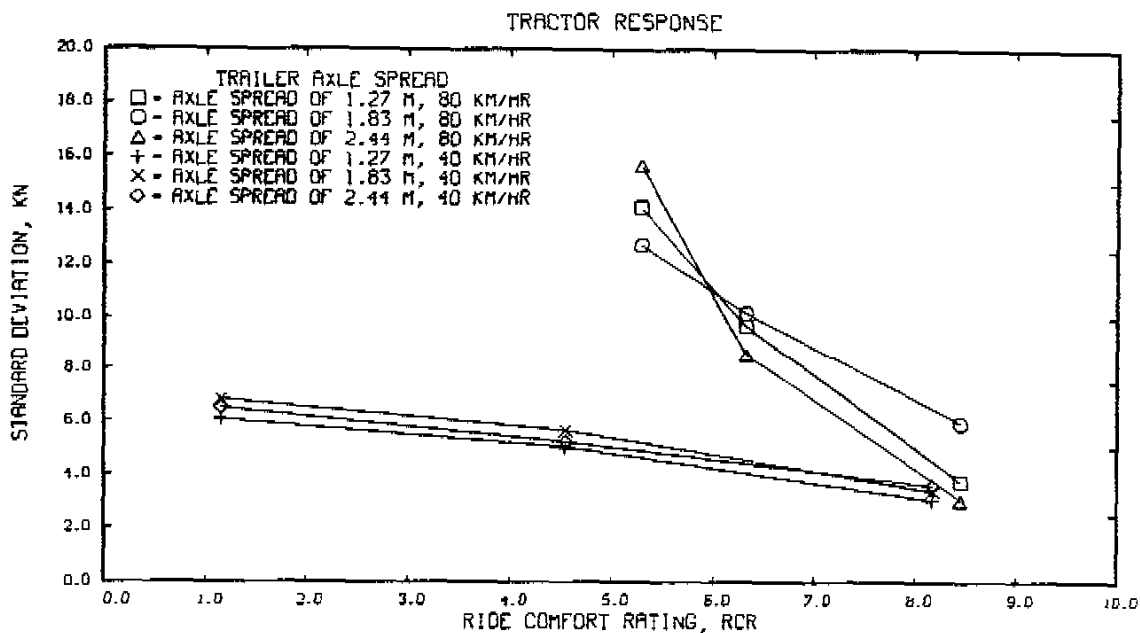


Figure 18 (upper), 19 (lower)

EFFECT OF AIR SUSPENSION LIFT AXLE
TRACTOR SUSPENSION - HENDRICKSON
TRAILER SUSPENSION - REYCO, AXLE SPREAD OF 1.27 M

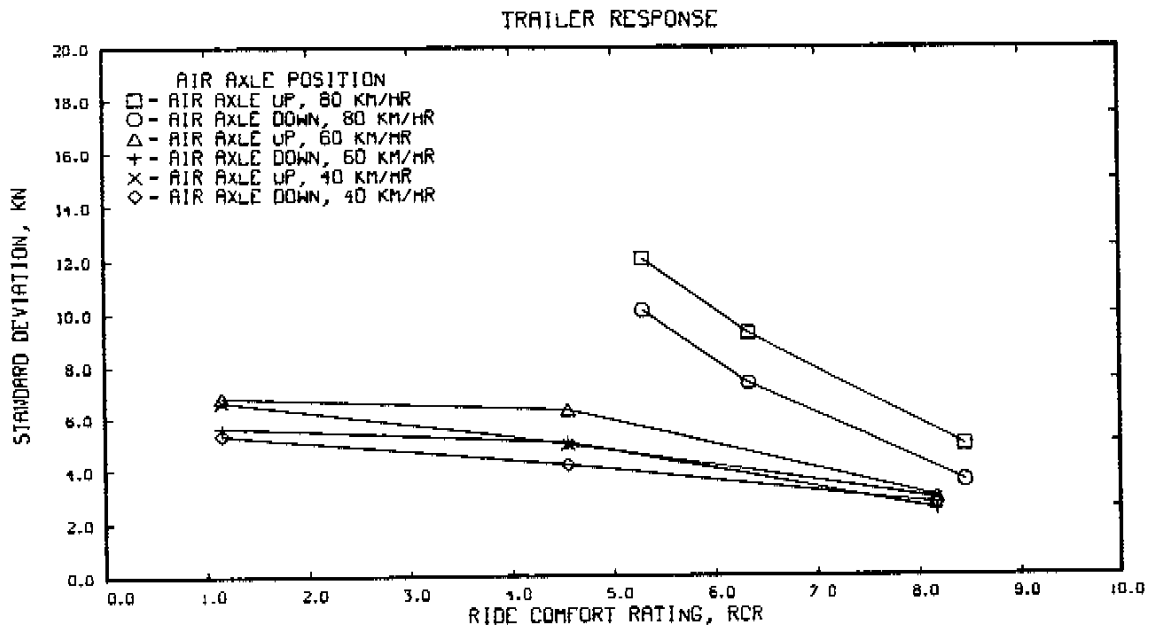
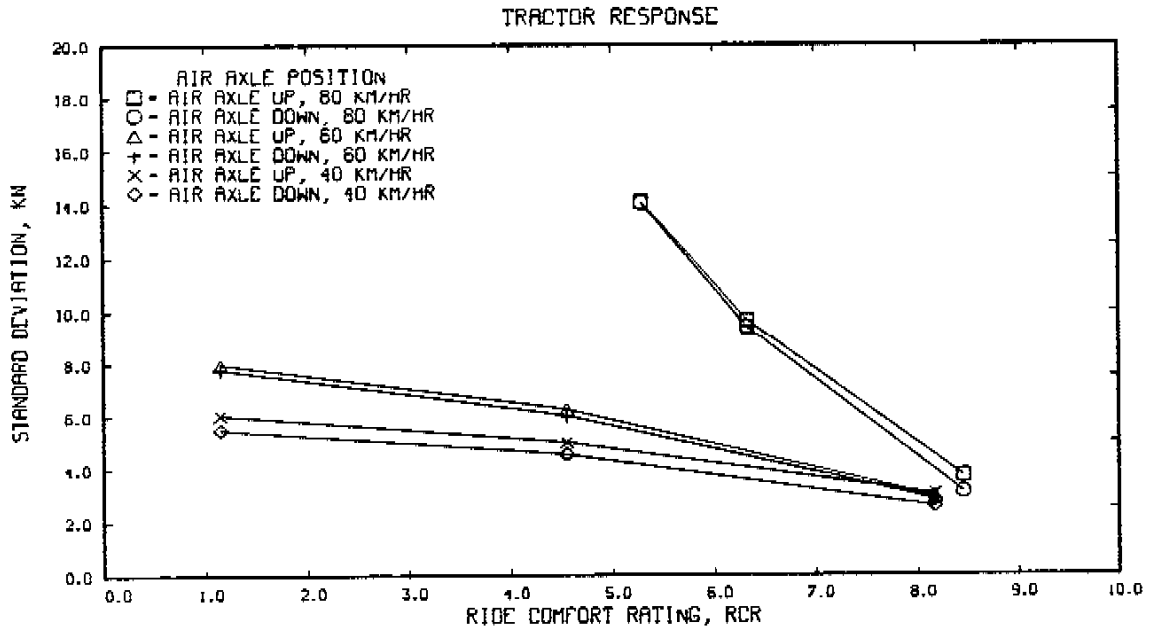


Figure 20 (upper), 21 (lower)

EFFECT OF AIR SUSPENSION LIFT AXLE
TRACTOR SUSPENSION - HENDRICKSON
TRAILER SUSPENSION - CHALMERS, AXLE SPREAD OF 1.37 M

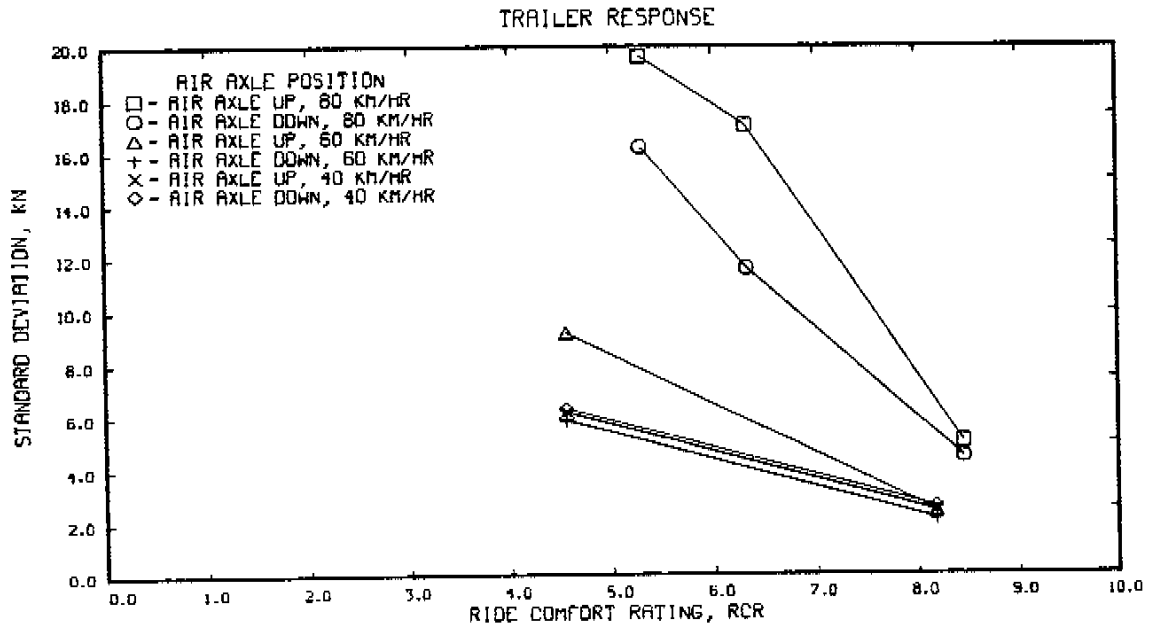
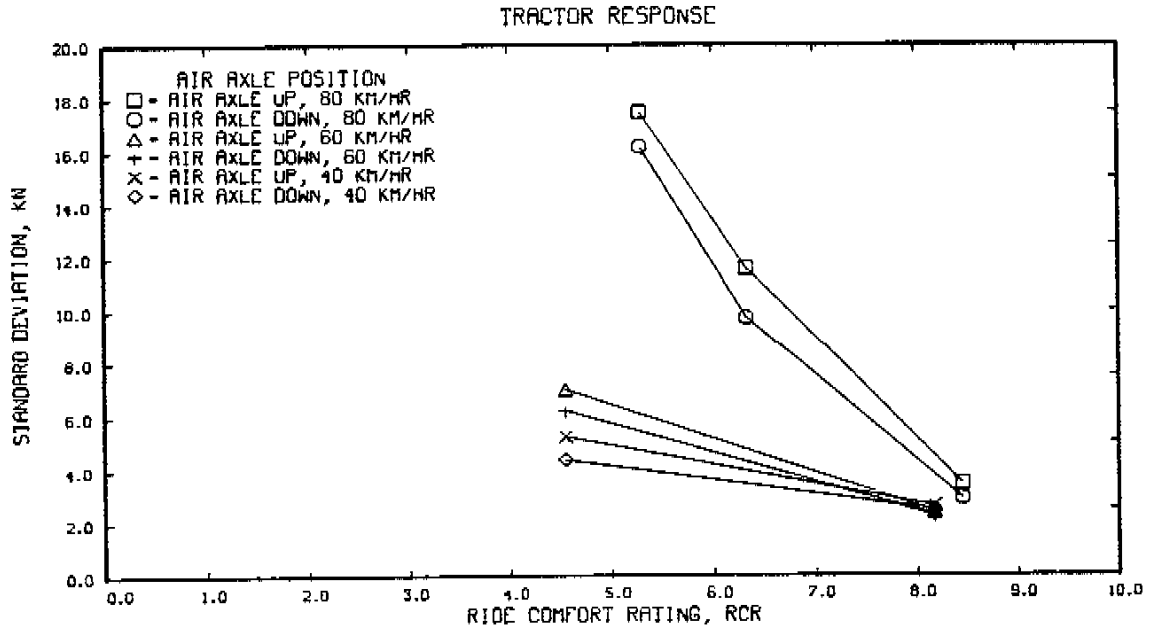


Figure 22 (upper), 23 (lower)

In some cases, however, the percentage reduction in dynamic wheel load can be very near the percentage decrease in static wheel load. Take for example the rubber spring walking beam suspension. With a vehicle speed of 80 km/hr and a RCR of 5.2, the triaxle group reduced the dynamic component of the wheel load by 17%. This is not surprising in light of the observation that much of the dynamic signal was generated by the low frequency whole body reaction. By adding a third suspending element the dynamic component of the sprung mass was distributed over three support members rather than two. It can be concluded therefore that the addition of a third axle will not likely result in an increase in dynamic wheel load within the bogie. The experimental results show that if the sprung mass is held constant the addition of a third axle will result in a decrease in dynamic wheel load.

6.3.4 Axle to Axle Dynamics for Load Sharing Suspensions

The series of plots on pages E20 to E29 of Appendix E show the axle dynamics for each axle of a given suspension. From these graphs it is clear that the lead drive axle has a slightly higher dynamic load (5%) than that of the trailing axle. This difference in dynamic axle load is attributed to the added mass of the interaxle differential on the lead axle.

The trailer axle dynamics do not show consistent load biasing between the lead and trailing axles. Load variations are within 5% and show similar trends. When comparing suspensions the standard deviation of the lead and trailing axles of a suspension were averaged.

6.3.5 Load Transfer Due to Braking

The four spring suspension was the only suspension tested that exhibited load transfer due to braking. For a moderate brake application of 5 KN-m (4400 lb-in) the trailing axle of the four spring suspension increased in load by 15-20%, while the lead axle decreased by a similar amount.

6.3.6 The Air Suspended Lift Axle

The air suspended lift axle was of special interest to the study. The unit tested had the same dynamic characteristics as the tandem axle air suspension. The lift axle maintains its axle loading by means of a constant pressure air regulator. The ability of this suspension to accept its share of the vehicle load over various conditions of road roughness and discontinuities was found to be excellent. Because it operates under constant air pressure settings, its load carrying ability is sensitive to vertical displacement variations. It is important, therefore, that the suspension mounting height specifications be adhered to and that axle spread be minimized so that optimum performance can be achieved. Failure to do so will result in variation of the mean axle load.

Provided that the air pressure regulator is properly set, this suspension can be classified as a load sharing suspension when used in conjunction with other suspension types in the appropriate manner. Regulators will want to consider the questions of where the control system should be mounted (i.e. cab or trailer) and when it is appropriate to lift the axle. A method of verifying that the air

regulator is properly set would be useful. Perhaps a single axle weight scale should be used at inspection stations.

6.4 PAVEMENT DEFLECTION DUE TO DYNAMIC WHEEL LOADS

A limited experimental study was undertaken to determine if there was a first order connection between pavement deflection and strain transducers as described in Reference 12. The intent of the experiment was to relate pavement deflection with vehicle speed and wheel loads monitored by the test vehicle.

The dynamic impulse to the axle was generated with a simple wooden plank fixed to the roadway directly over the deflection transducers and laying parallel to the axis of the vehicle's axles. The cross section of the plank measured 4 cm x 24 cm and was sufficiently long that all wheels of a given axle impacted the plank.

The axle loads for the test program are listed in Table 4. The axle number refers to the particular axle on the truck. The tractor steering axle is "1" and the last trailer axle is "6".

TABLE 4. Static Axle Loads in Metric Tonnes

Axle Number					
1	2	3	4	5	6
Not Measured	7.5	7.5	7.0	6.7	6.7

NOTE: - Axle loads were slightly lower than those used during the main study.

Three vehicle speeds were used for the above loading sequence, i.e. 18, 37, and 60 km/hr. Tests were run with and without a plank in place.

RESULTS

Dynamic axle loads as measured by the truck were compared with pavement deflection data recorded on site.

Upon review of the data, it became clear that selective analysis was required to eliminate confusion and convey the primary findings needed by the study. The source of confusion centered on the behaviour of the trailing axle of any of the load sharing suspensions. The fact that the lead and trailing axles of a given suspension are coupled in terms of load sharing, and the fact that the axles are in close proximity to each other, gave deflection results which were in some ways mysterious.

When, on the other hand, only the lead axles of the suspensions were studied, the results were found to be sufficiently clear and simple so that basic conclusions could be drawn.

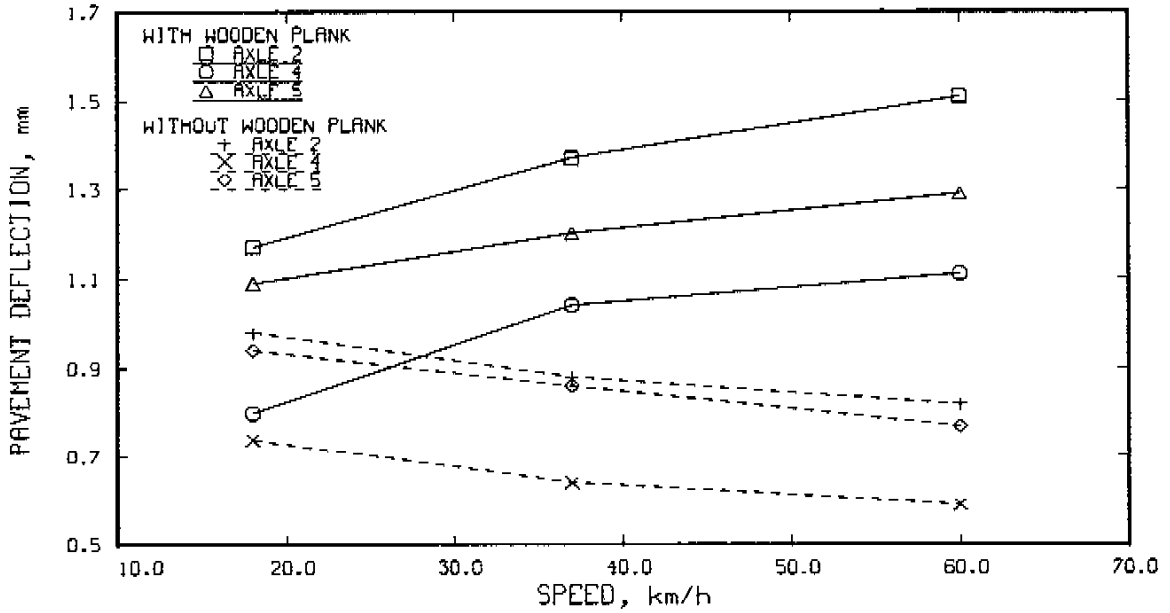
All results are presented in graphical form.

Figure 24 shows pavement deflection as a function of vehicle speed with and without a bump. It is interesting to note that without a bump pavement deflection diminishes with increased vehicle speed. However, with a bump, the deflection increases with speed and in one case the deflection changed by a factor of 1.8 when compared with the same run without a bump.

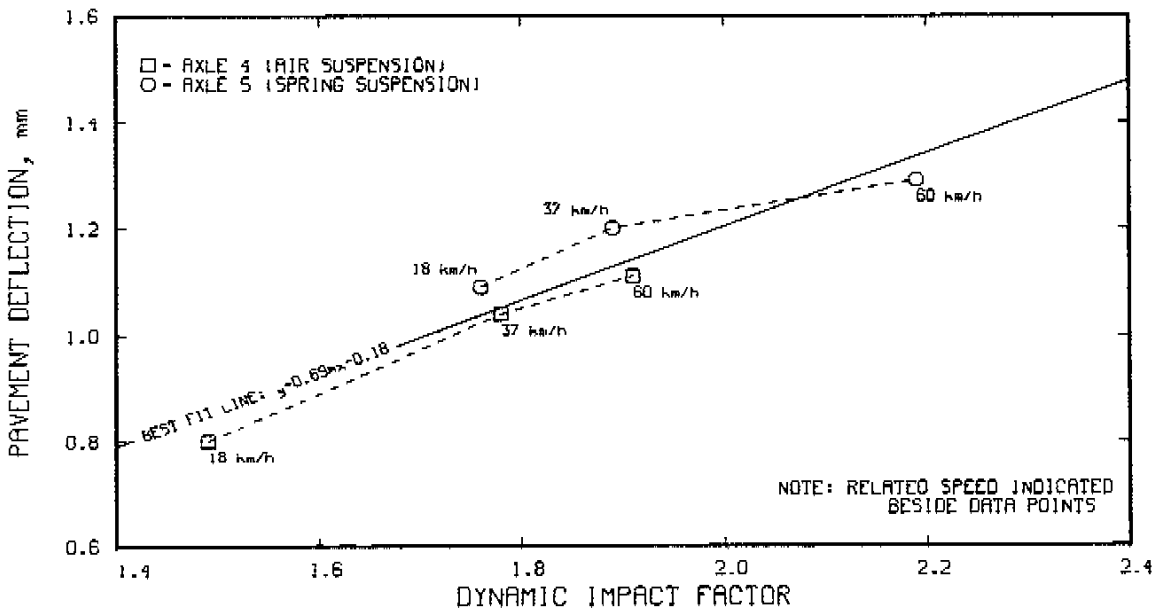
Figure 25 shows pavement deflection versus dynamic impact factor for two separate axles at 3 test speeds.

$$\text{dynamic impact factor} = \frac{\text{peak dynamic force}}{\text{static axle load}}$$

PAVEMENT DEFLECTION vs. SPEED



PAVEMENT DEFLECTION vs. DYNAMIC IMPACT FACTOR
 WOODEN PLANK FIXED TO ROADWAY



Figures 24 (upper), 25 (lower)

As can be expected, the experimental results show that pavement deflection increases with the dynamic impact factor. The best line fit drawn through the entire data set shows first order correlation between pavement deflection and dynamic wheel load. The scatter about the line can be attributed to secondary effects associated with the time history leading to peak dynamic forces. In turn, the time histories are related to the mechanical behaviour of individual suspensions. Also included in Figure 25 are dashed lines joining data points for each axle tested.

7.0 CONCLUDING REMARKS

7.1 INTERPRETATION OF EXPERIMENTAL RESULTS

The experimental results presented in this paper are pertinent to specific products which have been clearly indentified by the manufacturer's product number. It should be emphasized that the experimental results should in no circumstances reflect the whole product line of an individual manufacturer nor should the results be used to generalize on the performance of a generic suspension type. Subtle design variations in suspension components could in some cases lead to substantial changes in the performance of a suspension group. The objective of the study was not to endorse a product but rather to investigate the range of performance possible with these diverse systems.

7.2 RELATING STUDY FINDINGS TO VEHICLE WEIGHTS AND DIMENSION REGULATION

Findings from this study can be applied to the decision making process of heavy vehicle weights and dimensions regulations. Some of the results are straightforward and clear while others are rather complex and must be considered in conjunction with other findings.

Dealing with the straightforward findings first, we can draw two simple conclusions:

1. Axle Spread Sensitivities

a) Dynamic wheel load was found to be insensitive to axle spread per se. For mechanically dependent suspensions where variations

of axle spread imply a different mechanical configuration of the suspension, then substantial variations in dynamic wheel load can be expected. For these suspensions an optimum axle spacing will be difficult to establish since the order of preferred axle spread varies with road roughness.

b) Closer axle spreads for a given suspension group reduced tire scuffing and improved the pitch induced axle load equalization. This implies that, in a multi axle suspension group, with or without lift axles, the spacing between the first and the last axle should be minimized.

2. The Number of Axles in a Suspension Group

The addition of a third axle to a tandem axle suspension group reduced the dynamic wheel loads. However, as seen in section 6.3.2, for a given percentage increase in static wheel load we can generally expect a smaller percentage increase in the dynamic wheel load. The difference between the two percentages varies according to the type of suspension tested. These differences range from no perceptible increase to an increase proportional to the change in static wheel load. Hence, a conservative approach in estimating the total pavement load due to an increase in static wheel load is to expect a proportionate increase in dynamic wheel load.

Comparative Considerations of Various Suspension Systems

To compare various suspension systems requires the consideration of a number of factors. What follows is a brief discussion focusing on some of these factors with some thoughts on how they might be treated in the evaluation process.

Heavy truck load sharing suspensions serve to distribute the load of a vehicle evenly between axles and to mitigate the vertical dynamics of the whole vehicle body. It must do this over a wide range of road roughness conditions, vehicle speeds and hardware variations.

This study demonstrated that all suspensions show convergences to low dynamic activity on smooth roads even at highway speeds. On moderate to rough roads however, the dynamic characteristics of the suspensions vary widely depending on the suspension type examined. There is a clear order of suspension preference in terms of dynamic wheel loading. The following list of trailer suspensions tested is arranged in order from the lowest to the highest dynamic wheel loading.

1. Air suspension
2. Four spring suspension
3. Walking beam

On the basis of these findings one may be tempted to favour or restrict the use of particular suspensions through some regulatory means such as added or restricted load allowances. It would be inappropriate to make such a decision on the basis of the dynamic wheel loading alone. Other factors such as the sensitivity of the suspension to static load equalization, load transfer due to braking and pitch should also be considered. In addition, the contribution of the suspension to vehicle stability and control must be evaluated.

Clearly, the criteria listed above do not necessarily carry the same weight in the evaluation process. Consider the following points.

Load Equalization

a) A suspension group is said to have unfavorable load equalization characteristics if the axles of a given suspension do not share load equally. Pronounced load unbalance between axles of a tandem suspension becomes critical in all cases where road and bridge structures are designed on the assumption of perfect load equalization.

b) Brake induced load transfer is of little concern on major highways except on down hill grades. Highway junctions and city intersections would suffer most from this effect.

c) Load transfer due to pitch attitude would occur when tractor and trailer coupling heights are poorly matched. This would represent a small percentage of the vehicle population and therefore may be considered to be of less significance.

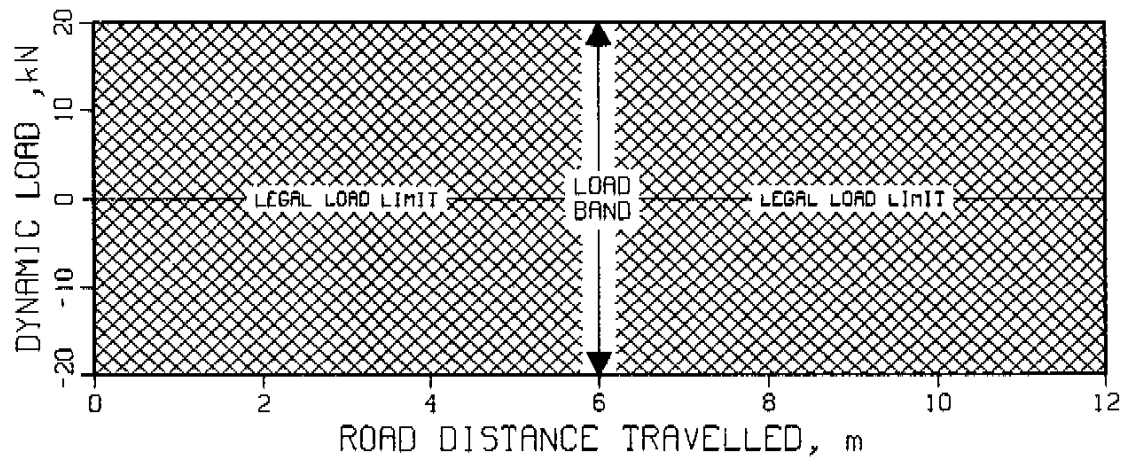
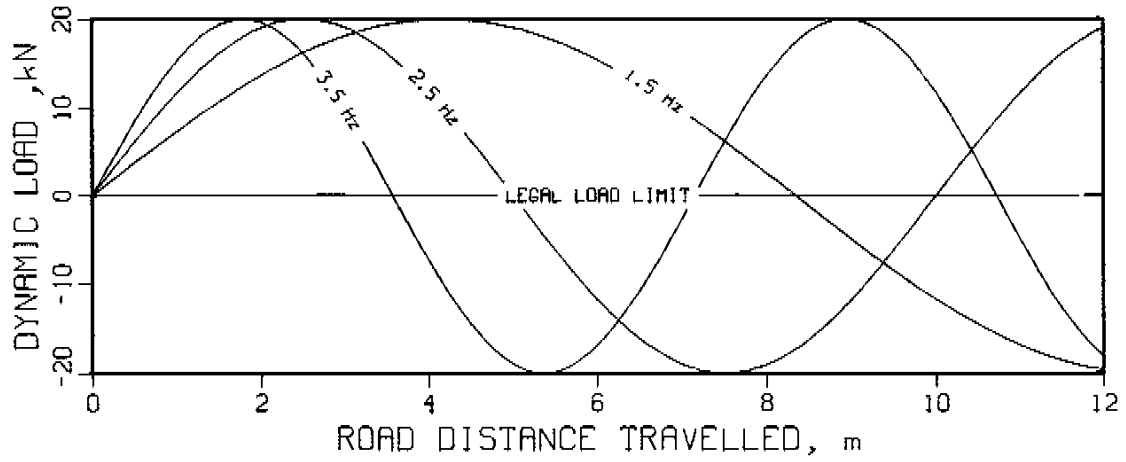
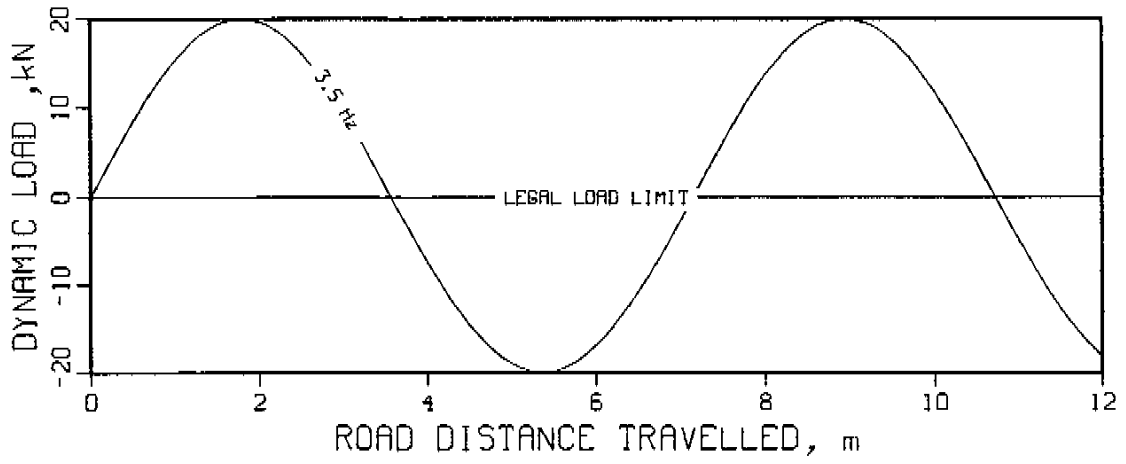
Dynamic Wheel Loads

Dynamic wheel loads are a function of suspension type, vehicle speed and road roughness. The largest variation in dynamic wheel load characteristics of the various suspensions occurred at highway speeds. For suspensions showing high dynamic activity, the majority of the wheel force is from the vertical response of the whole vehicle body which is in the frequency range of 1.5 to 3.5 Hz. Both axles of the suspension experience this portion of dynamic load in phase with each other. All wheel loads of a given suspension are greater than the nominal static loads for half of the period of the vehicle body oscillation. Conversely, for the other half of the period the wheel loads are less than the nominal static loads.

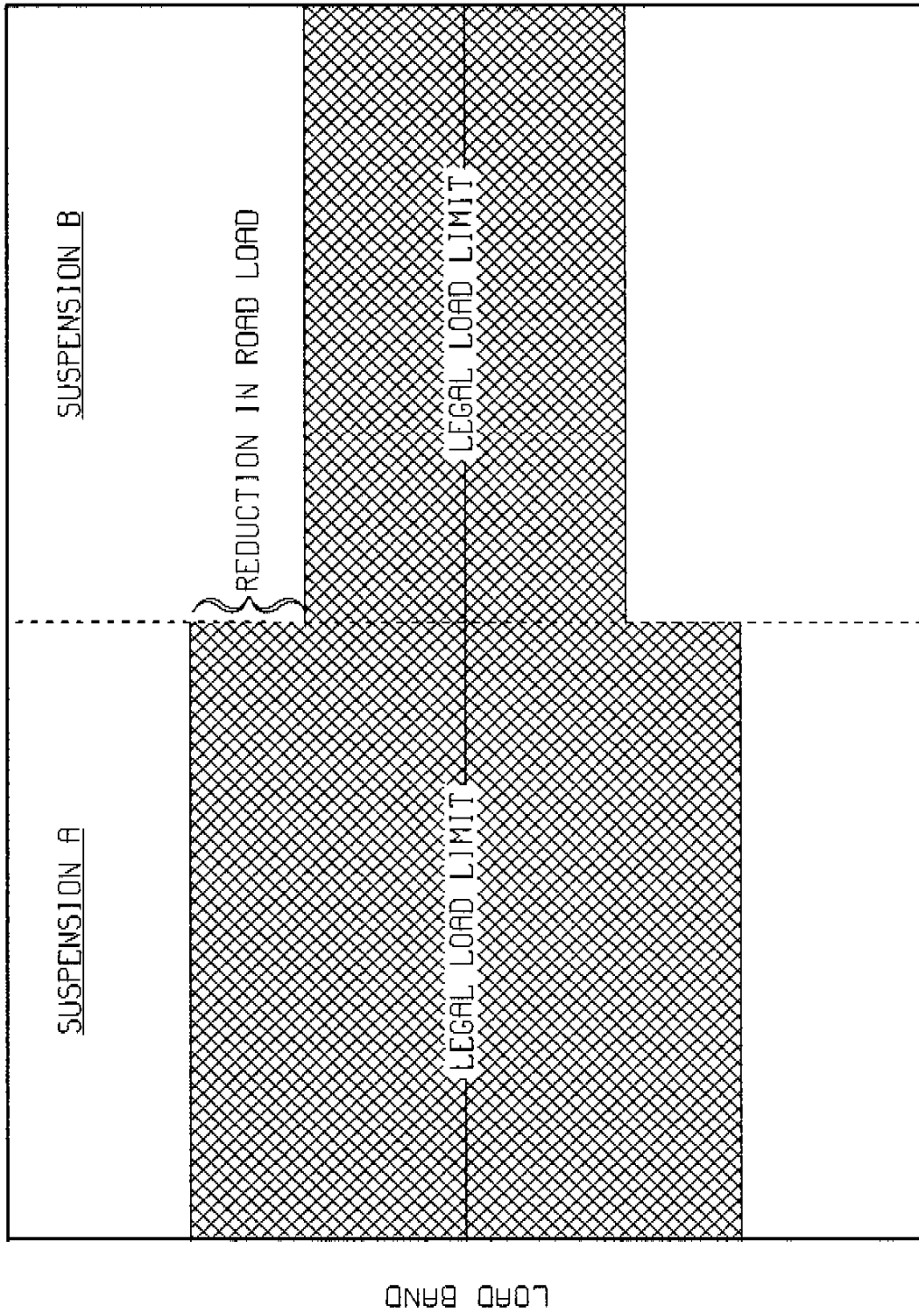
Consider for example a simplified vehicle with a linear suspension loaded to the legal limit traveling at 90 km/hr. We will assume that the natural frequency of the whole body is 3.5 Hz. For these conditions the vehicle will travel 7.1 meters for every complete cycle of the vehicle mass. As seen in Figure 26 this means that 3.6 meters of the highway will experience loads in excess of the desired legal limit and the following 3.6 meters of highway will experience loads below the legal limit. Consider a second and third vehicle with a natural frequency of 1.5 and 2.5 Hz, superimposed on the same stretch of roadway as shown in Figure 27. It becomes clear that, because every vehicle has different dynamic characteristics, a general band of loading can be expected. We will call this the Load Band as shown in Figure 28.

Consider the Load Band generated by the two suspensions, A and B, shown in Figure 29. Suspension A has a higher Load Band than does suspension B. Thus suspension A imposes higher maximum road loading forces than suspension B. Considering the effects of the fourth power law of pavement damage, a small reduction in Load Band should reflect a sizable gain in the expected fatigue life of the road structure.

In view of all the road loading factors discussed here, it is clear that dynamic wheel loading emerges as the single most significant suspension performance factor. When examining the dynamic wheel load performance of the various suspensions tested it is the opinion of the authors that the spread between the best and the worst performers is



Figures 26 (upper), 27 (middle), 28 (lower)



ROAD DISTANCE TRAVELLED

Figure 29

too high. This suggests the need for the establishment of an evaluation procedure which would establish acceptable suspension performance criteria. The key considerations should include vehicle stability and control performance, dynamic wheel load characteristics, and interaxle load sharing capabilities.

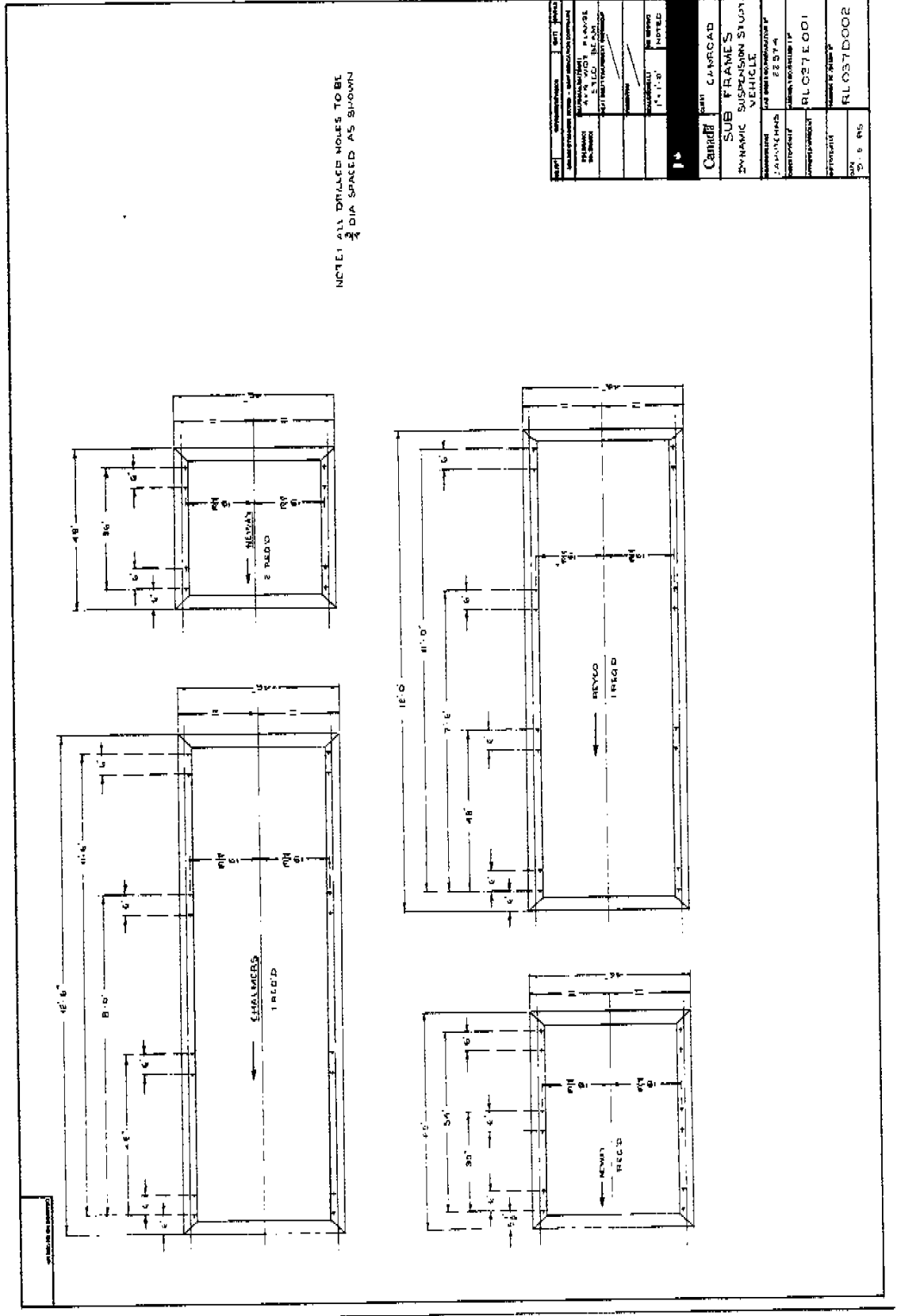
Further research should also consider the use of single axle enforcement weigh in motion scales. Because axle dynamics diminish with speed and roughness, precise axle load measurements should be possible with the vehicle rolling at slow speeds (≈ 10 km/hr). With the use of existing technology, this would provide information on single axle loads and total group loads. One would then be in a position to monitor axle load equalization which would likely promote longer pavement life.

REFERENCES

1. Sweatman, P.F. (1983) 'A Study of Dynamic Wheel Forces in Axle Group Suspensions of Heavy Vehicles', Australian Road Research Board, Special Report No. 27, Vermont South, Australia.
2. Sweatman, P.F. (1980) 'Effect of Heavy Vehicle Suspension on Dynamic Road Loading', Australian Road Research Board, AAR No. 116, Vermont South, Australia.
3. Heath, A.N. and Good, M.G. (1985) 'Heavy Vehicle Design Parameters and Dynamic Pavement Loading', Australian Road Research, 15(4), pp. 249-263.
4. Gillespie, T.D. (1985) 'Heavy Truck Ride', Society of Automotive Engineers, The Thirty-First L. Ray Buckendale Lecture, SP-607.
5. Cebon, D. (1985) 'An Investigation of the Dynamic Interaction Between Wheeled Vehicles and Road Surfaces', Ph.D. thesis submitted to the Department of Engineering, University of Cambridge.
6. Görge, W. (1984) 'Evaluation of research reports concerning - The influence of commercial vehicle development and design on the road fatigue', Forschungsvereinigung automobiltechnik e.v., Frankfurt, West Germany.
7. Hooker, R.J. (1980) 'A Model for the radial dynamic behaviour of pneumatic tyres', Int. J. of Vehicle Design, vol. 1, no. 4, pp. 361-372.
8. Dickerson, R.S. and Mace, D.G.W. (1981) 'Dynamic pavement force measurements with a two-axle heavy good vehicle', Department of the Environment, TRRL Supplementary Report 688, Crawthorne, Berkshire (Transport and Road Research Laboratory).
9. Bergan, A.T., Churko, B.M., Papagianakis, A.T. and Burns, W.A. 'Axle and Suspension Systems of Heavy Trucks for Minimizing Pavement Distress'.
10. Magnusson, G., Carlsson, H.E. and Ohlsson, E. (1984) 'The influence of heavy vehicles' springing characteristics and tyre equipment on the deterioration of the road', Swedish Road and Traffic Research Institute (VTI), VTI Report No. 270, Linköping, Sweden.
11. Page, J. (1974) 'A Review of Dynamic Loading Caused by Vehicle Suspensions', Department of the Environment, TRRL Supplementary Report 82UC, Crawthorne, Berkshire (Transportation and Road Research Laboratory).
12. Christison, T. (1986) 'Canadian Vehicle Weights and Dimensions Study. Pavement impact investigation. Data summary report', Civil Engineering Department, Natural Resources Division, Alberta Research Council.

APPENDIX A

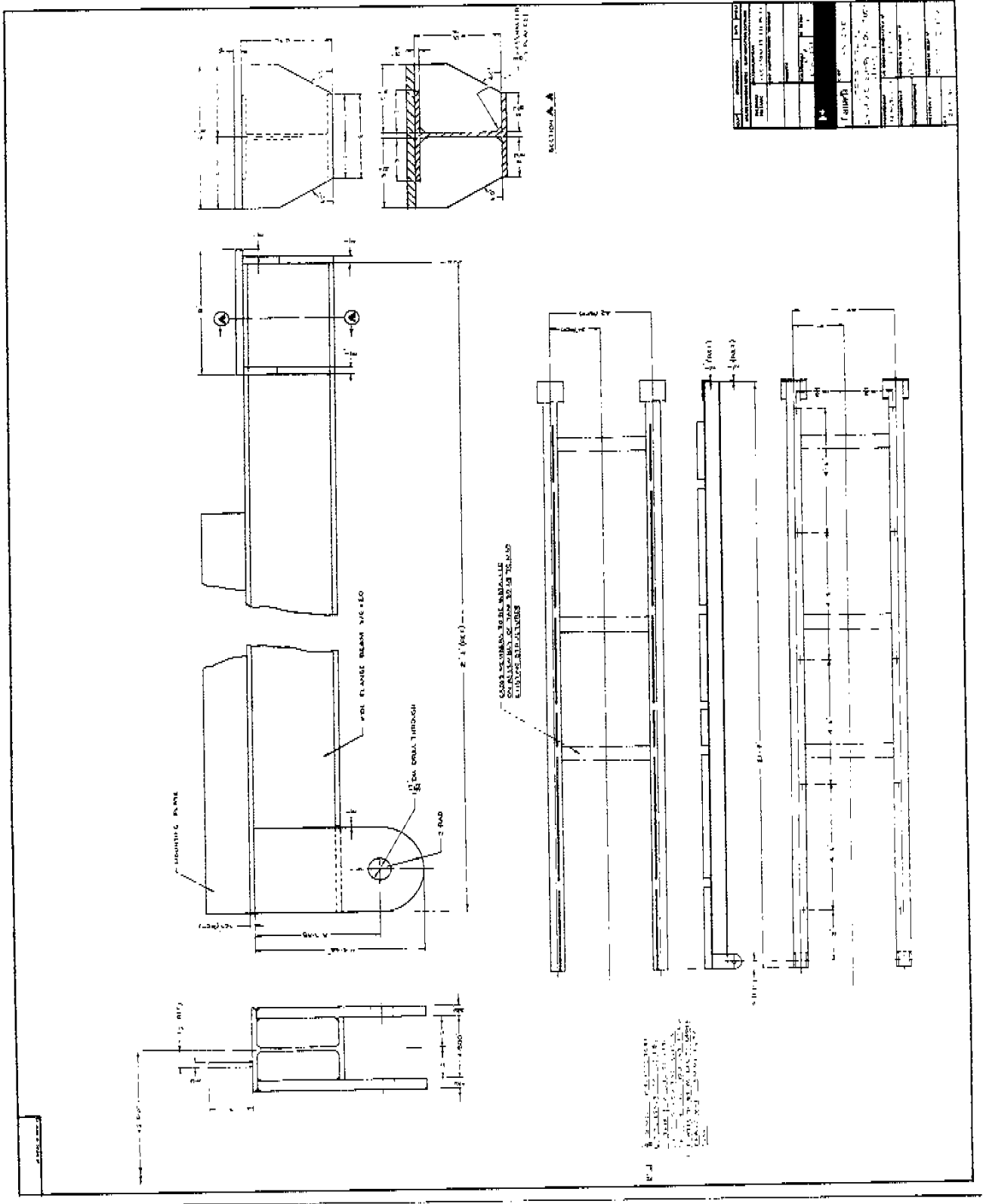
MECHANICAL DESIGN DRAWINGS OF HARDWARE FABRICATED FOR THIS STUDY



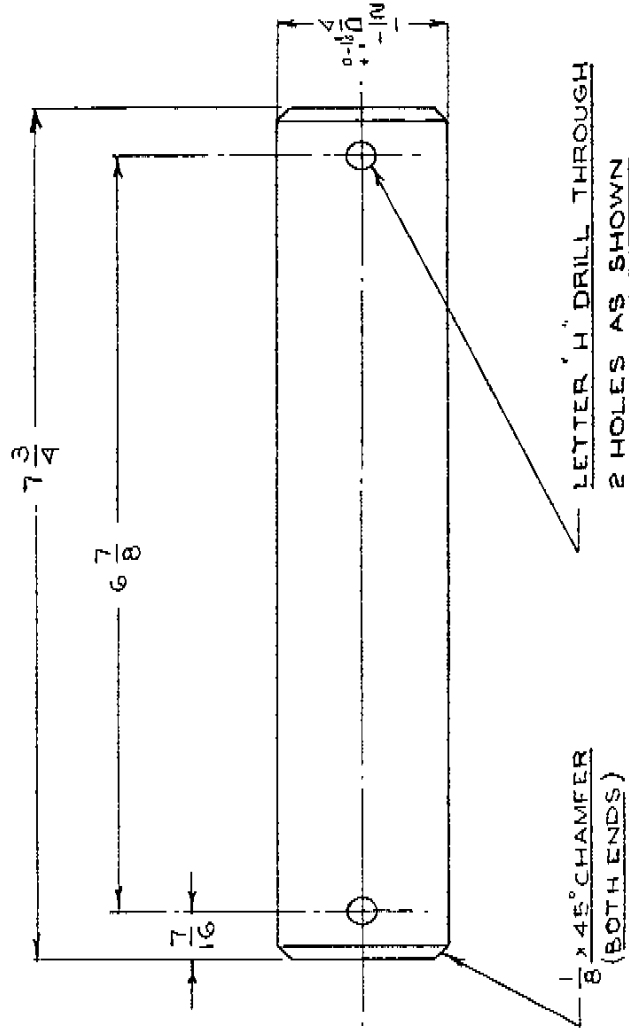
NOTE: ALL DRILLED HOLES TO BE 3/4" DIA SPACED AS SHOWN


REV	DESCRIPTION	DATE
1	ISSUED FOR CONSTRUCTION	11/10/68
2	REVISIONS	
3	REVISIONS	
4	REVISIONS	
5	REVISIONS	
6	REVISIONS	
7	REVISIONS	
8	REVISIONS	
9	REVISIONS	
10	REVISIONS	
11	REVISIONS	
12	REVISIONS	
13	REVISIONS	
14	REVISIONS	
15	REVISIONS	
16	REVISIONS	
17	REVISIONS	
18	REVISIONS	
19	REVISIONS	
20	REVISIONS	
21	REVISIONS	
22	REVISIONS	
23	REVISIONS	
24	REVISIONS	
25	REVISIONS	
26	REVISIONS	
27	REVISIONS	
28	REVISIONS	
29	REVISIONS	
30	REVISIONS	
31	REVISIONS	
32	REVISIONS	
33	REVISIONS	
34	REVISIONS	
35	REVISIONS	
36	REVISIONS	
37	REVISIONS	
38	REVISIONS	
39	REVISIONS	
40	REVISIONS	
41	REVISIONS	
42	REVISIONS	
43	REVISIONS	
44	REVISIONS	
45	REVISIONS	
46	REVISIONS	
47	REVISIONS	
48	REVISIONS	
49	REVISIONS	
50	REVISIONS	
51	REVISIONS	
52	REVISIONS	
53	REVISIONS	
54	REVISIONS	
55	REVISIONS	
56	REVISIONS	
57	REVISIONS	
58	REVISIONS	
59	REVISIONS	
60	REVISIONS	
61	REVISIONS	
62	REVISIONS	
63	REVISIONS	
64	REVISIONS	
65	REVISIONS	
66	REVISIONS	
67	REVISIONS	
68	REVISIONS	
69	REVISIONS	
70	REVISIONS	
71	REVISIONS	
72	REVISIONS	
73	REVISIONS	
74	REVISIONS	
75	REVISIONS	
76	REVISIONS	
77	REVISIONS	
78	REVISIONS	
79	REVISIONS	
80	REVISIONS	
81	REVISIONS	
82	REVISIONS	
83	REVISIONS	
84	REVISIONS	
85	REVISIONS	
86	REVISIONS	
87	REVISIONS	
88	REVISIONS	
89	REVISIONS	
90	REVISIONS	
91	REVISIONS	
92	REVISIONS	
93	REVISIONS	
94	REVISIONS	
95	REVISIONS	
96	REVISIONS	
97	REVISIONS	
98	REVISIONS	
99	REVISIONS	
100	REVISIONS	

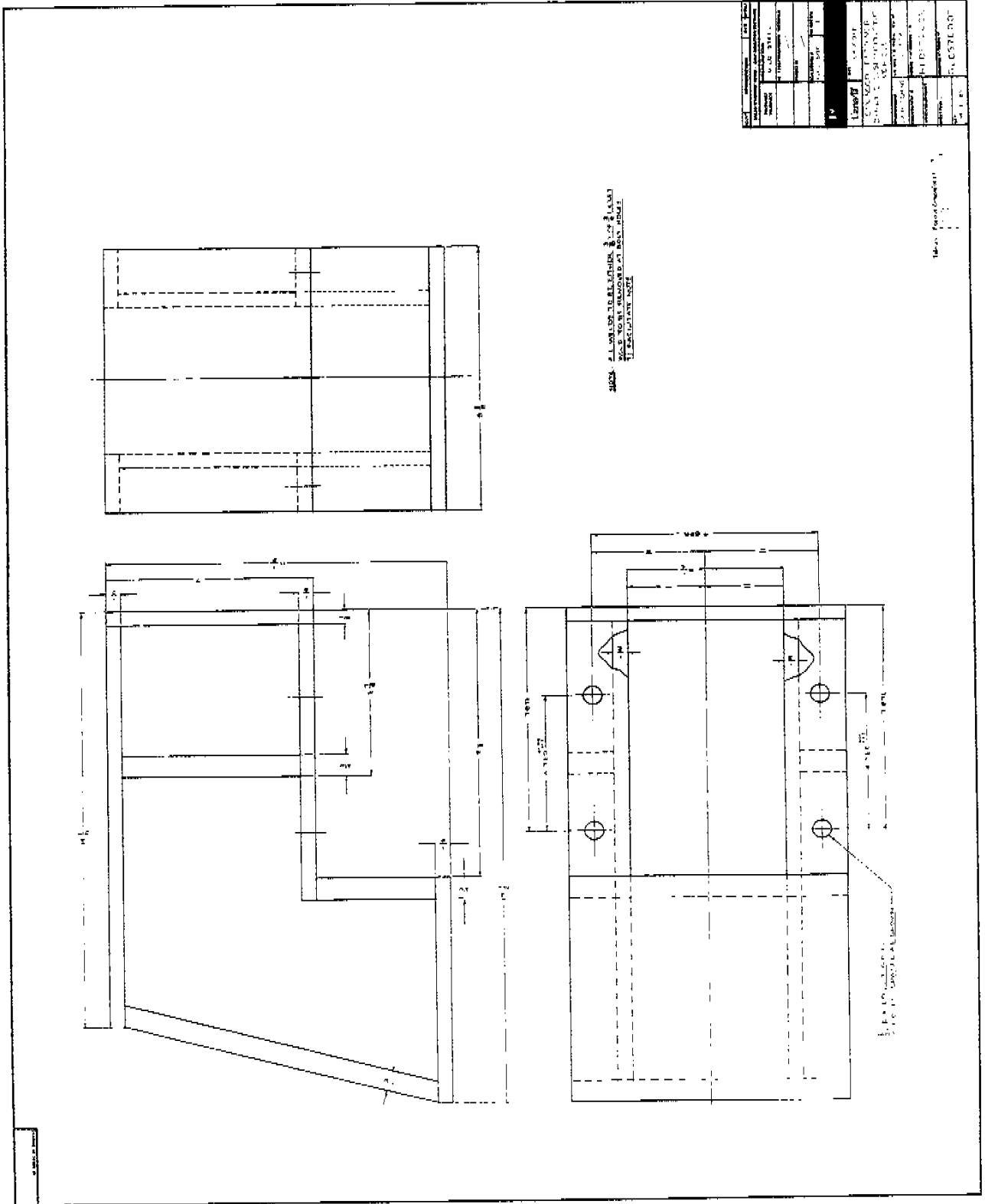
Cambridge PART **CONCORD**
SUB FRAMES
DYNAMIC SUSPENSION STUDY
VEHICLE
 DRAWING NO. **225 T-4**
 PROJECT NO. **RL037 E 001**
 DATE **11/10/68**
 DRAWN BY **W. B. BNS**
 CHECKED BY **W. B. BNS**
 APPROVED BY **W. B. BNS**



DRAWING NO / DESIGN NO

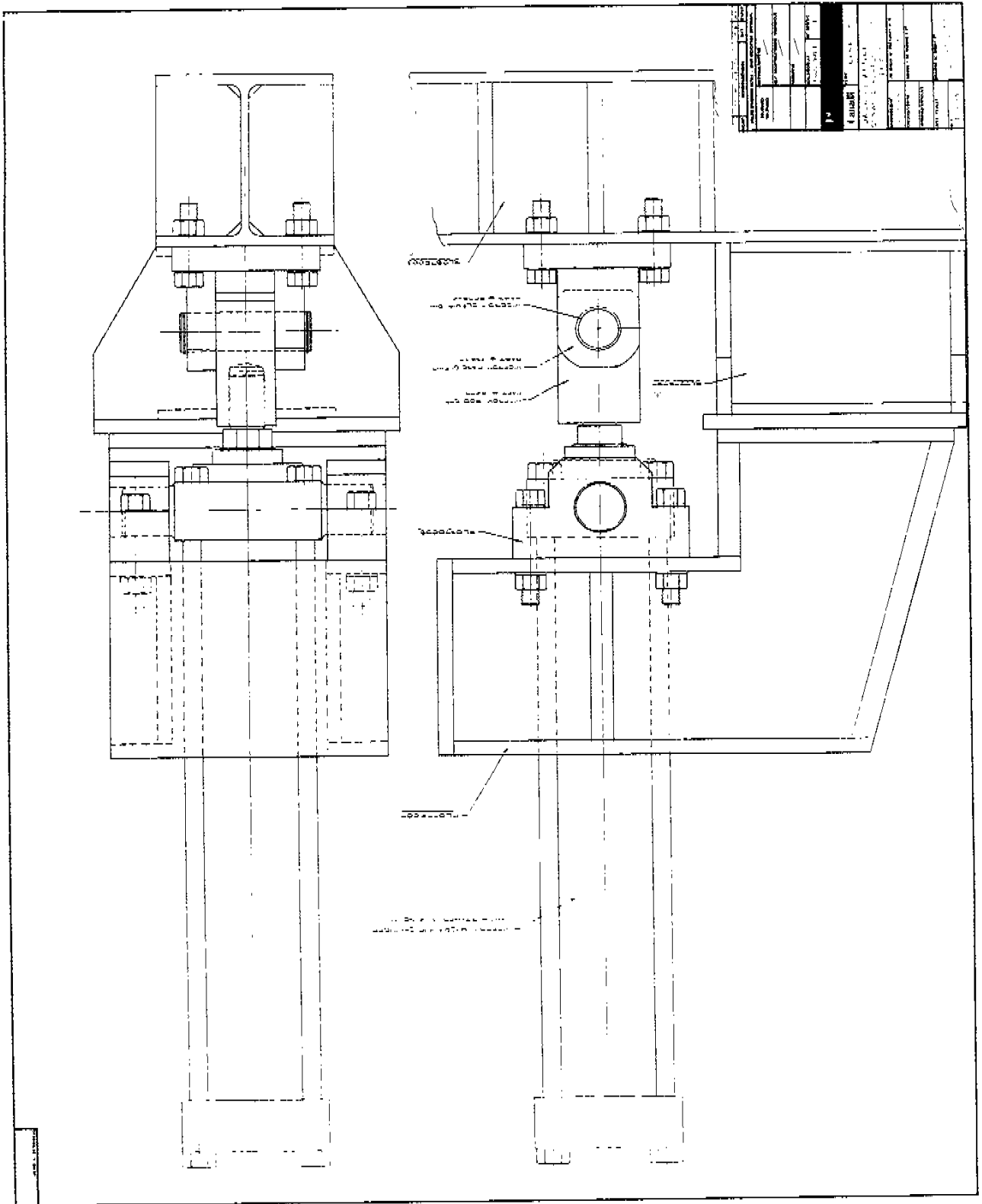


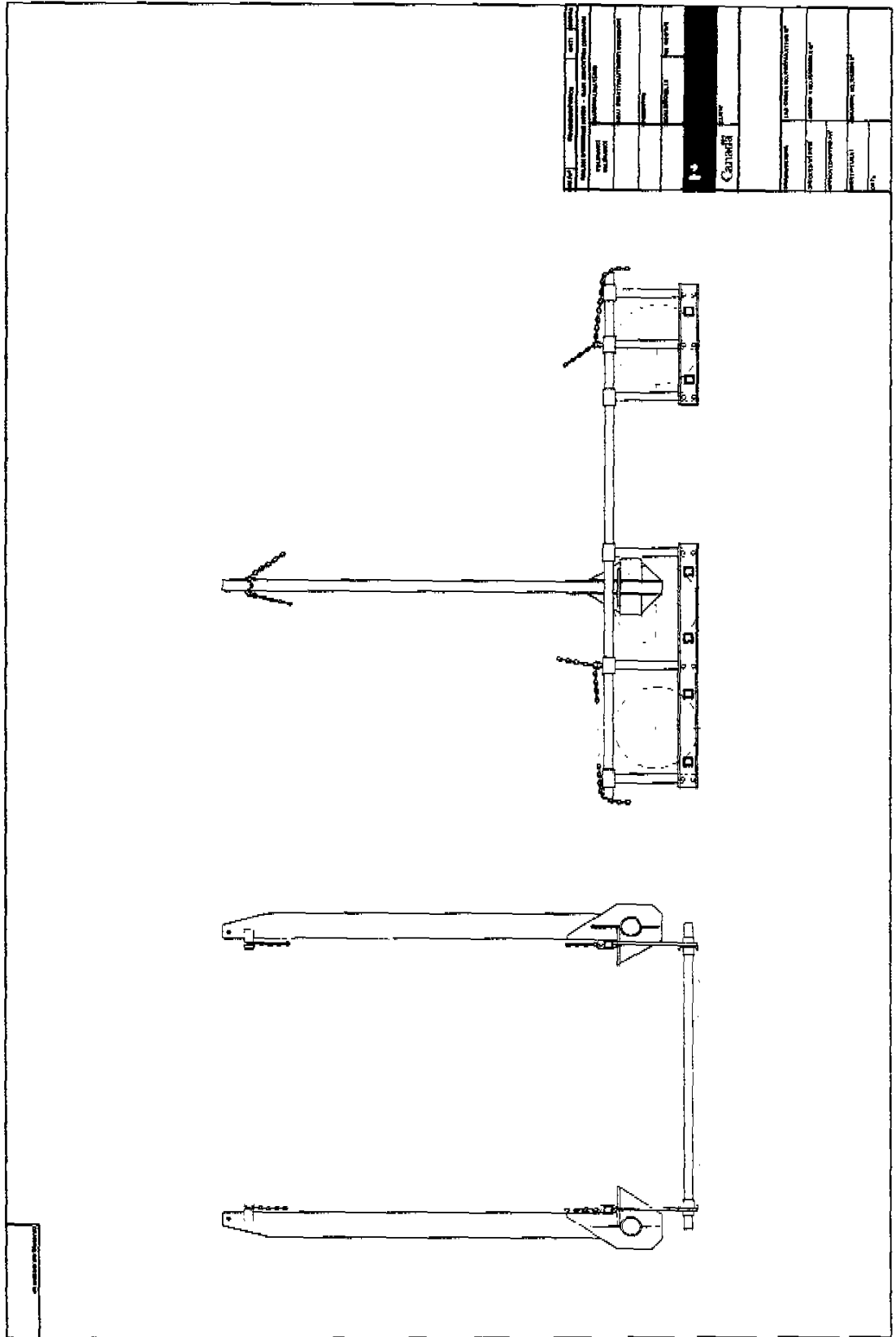
NO / N°	REVISION/REVISION	DATE	BY/PAR
UNLESS OTHERWISE NOTED - SAU/INDICATION CONTRAIRE			
TOLERANCE TOLÉRANCE	MATERIAL/MATÉRIEL ST ST 416		
	HEAT TREAT/TRAITEMENT THERMIQUE		
	FINISH/FINI	63	
	SCALE/ÉCHELLE	NO REDUC	
	FULL SIZE	E	
 National Research Council of Canada / Conseil national de recherches Canada			
Canada		CLIENT	CANROAD
PIVOT PIN DYNAMIC SUSPENSION STUDY VEHICLE			
DRAWN/DESINÉ	J.A. HUTCHINS	LAB. ORDER NO./PRÉPARATEUR N°	22574
CHECKED/VÉRIFIÉ		ASSEMBLY NO./ENSEMBLE N°	RLO37E001
APPROVED/APPROUVÉ			
SHEET/FEUILLE		DRAWING NO / DESIGN N°	RLO37B008
DATE	27-6-85		

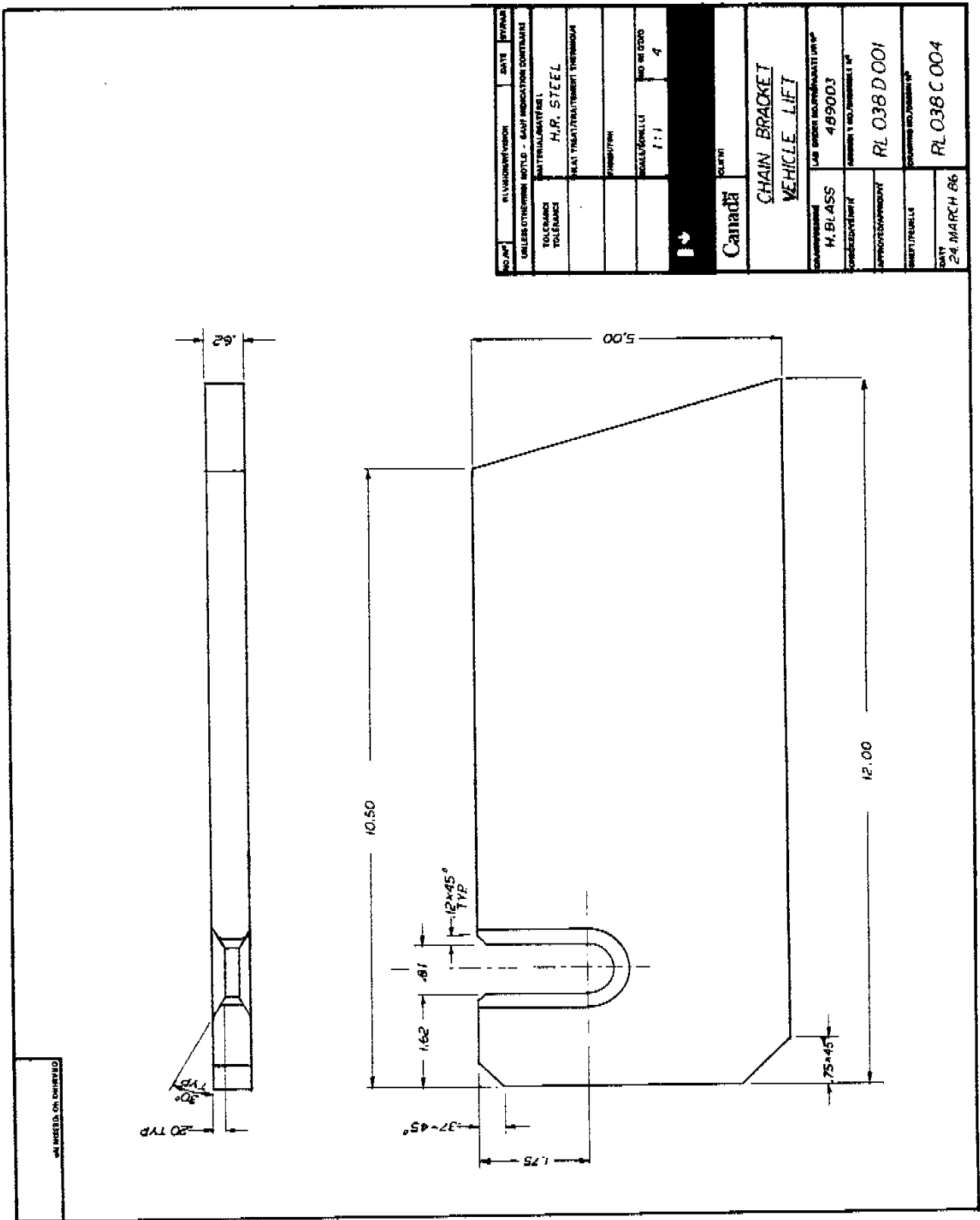


NOTES - ALL DIMENSIONS UNLESS OTHERWISE SPECIFIED ARE IN MILLIMETERS AND DECIMAL FRACTIONS THEREOF.

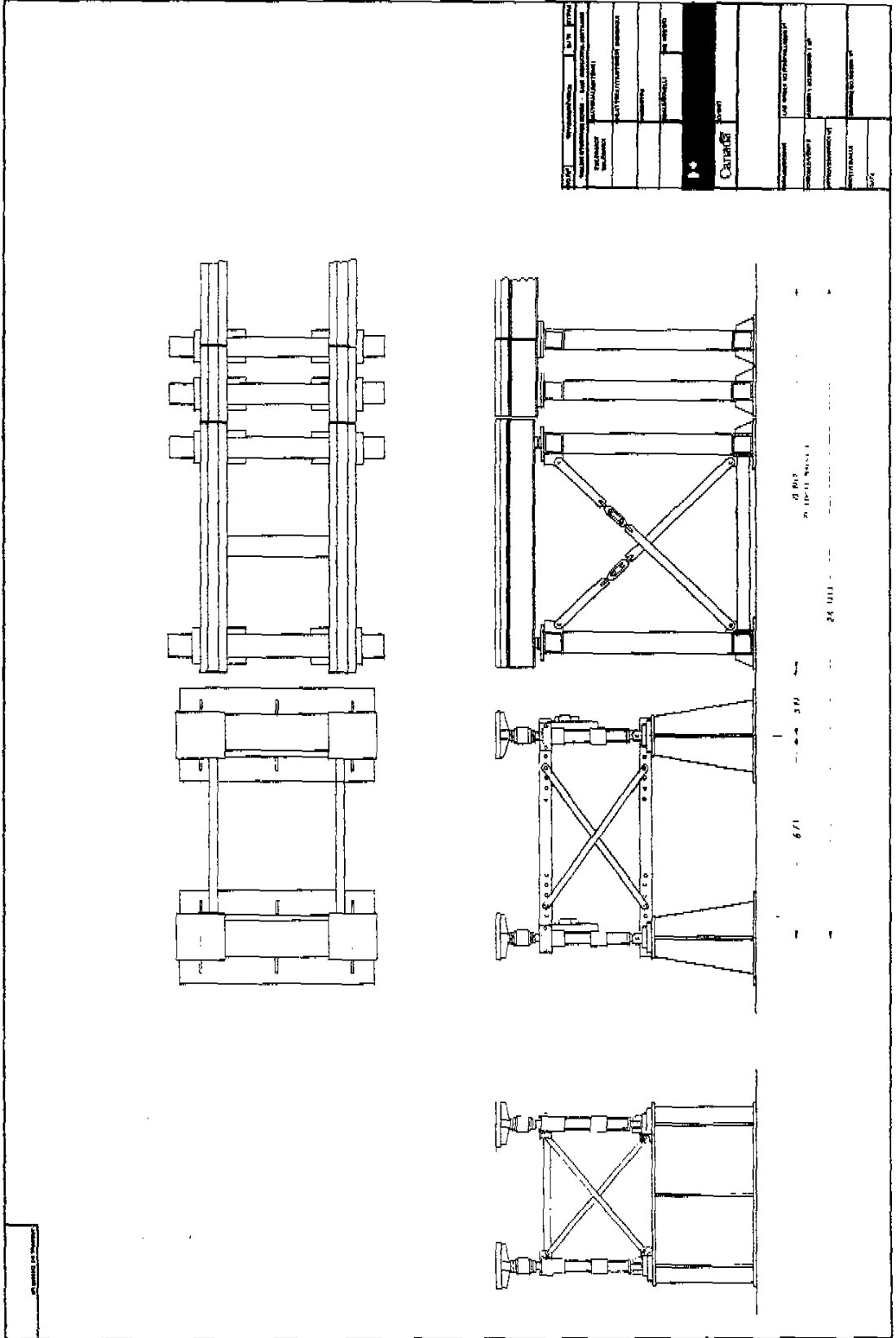
Part Name	[Blank]
Part No.	[Blank]
Rev.	[Blank]
Date	[Blank]
Drawn by	[Blank]
Checked by	[Blank]
Approved by	[Blank]
Title	[Blank]
Scale	[Blank]
Sheet No.	[Blank]
Total Sheets	[Blank]
Project No.	[Blank]
Customer	[Blank]

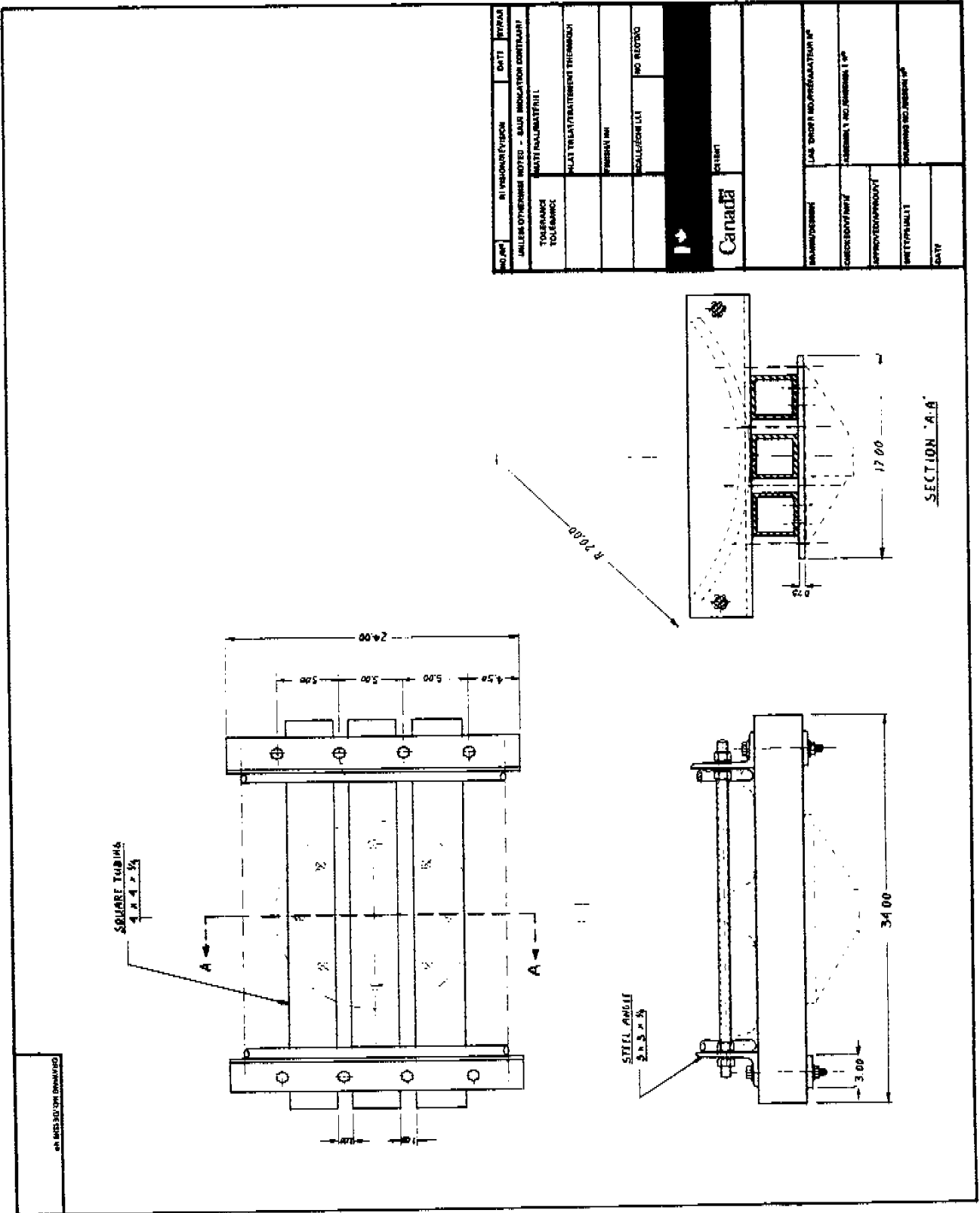






ALL DIMENSIONS UNLESS OTHERWISE SPECIFIED





CONSTRUCTION DRAWING

NO. 10	SI YHONKREYISOM	DATE	REVISED
MILLER OTHERSSE NOTED - SAIRI INDICATOR CONTINUIT			
TOLERANCE TOLÉRANCE			
NOTE IN ALUMINUM			
PLATE TREATMENT THERMO			
PARENT IN			
SCALE 1:1			
NO. 10 1000			
Canada			
PART			
L.A.S. SHOP & FABRICATION S.P.			
ADDRESS 1, rue de la Sablonnière S.P.			
APPROVED/APProuvé			
DATE			

APPENDIX B

VEHICLE CALIBRATION

Because of the importance of this subject to the success of this study, a formal report was written so that details would be available to those interested.

The calibration report was written by Mr. Karl R. LePiane, a third year Mechanical Engineering Co-Op student from Waterloo University who spent his work term at NRC Vehicle Dynamics Laboratory. The report constituted his required work term report for which he received the Babcock and Wilcox Award for best work term report in the Mechanical Engineering Department.

Readers will note that an alternative calibration method was suggested in the report. This procedure was carried out and the results formed our final axle load calibration standard. These final results are attached to the end of this appendix.

TABLE OF CONTENTS

	<u>PAGE</u>
SUMMARY	i
CONCLUSION	ii
RECOMMENDATIONS	iii
1. INTRODUCTION	
1.1 Background	1
1.2 Task	1
2. THE INSTRUMENTS USED AND THE MANUFACTURERS' SPECIFICATIONS	
2.1 Axles	1
2.2 Strain Gauge Transducers	3
2.3 Strain Gauge Conditioning Amplifier	3
2.4 Instruments Used for Torque Calibration	4
2.5 Instruments Used for Vertical Load Calibration	4
3. THEORETICAL BACKGROUND	
3.1 Torsional Shear Stress	5
3.2 Vertical Loading Stresses	7
3.3 Stress Strain Relationships	9
3.4 The Strain Gauge Transducer	10
3.5 Strain Gauge Orientation for Torsion	10
3.5.1 Transformation of Strain	12
3.5.2 Gauge Positioning on the Axle and the Wheatstone Bridge	13
3.5.3 Vertical Loading Effect on the Torsion Strain Gauges	17
3.5.4 Brake Force Effect on the Torsion Strain Gauges	19
3.6 Strain Gauge Orientation for Vertical Loading	20
3.6.1 Gauge Positioning on the Axle and the Wheatstone Bridge	22
3.7 The Strain Gauge Conditioning Amplifier	23

	<u>PAGE</u>
3.8 Calibration	25
3.8.1 Least Squares Method of Best Fit	26
3.8.2 Gauge Sensitivity	29
3.8.3 Electrical Calibration	31
3.9 Error Analysis	32
3.9.1 Error in Least Squares Calculation	32
3.9.2 Method of Application	33
4. TORQUE CALIBRATION	
4.1 Calibration Procedure	36
4.2 Data Analysis	38
4.2.1 Initial Tests	38
4.2.2 Brake Application Torque	40
4.2.3 Beam Torque and Bending Effect	41
4.2.4 Sign Convention	42
4.3 Final Calibration Tests	42
4.4 Discussion of Results	47
4.5 Sample Calculation	48
5. VERTICAL LOAD CALIBRATION	
5.1 Weigh Scale Preparation	49
5.1.1 Tractor Trailer Preparation	49
5.2 Calibration of Drive Axles	50
5.2.1 Procedure	50
5.2.2 Discussion of Results	51
5.3 Trailer Axle Calibration	52
5.3.1 Procedure Followed for the Reyco Tandem Set	52
5.3.2 Procedures Followed for the Neway Axle	53
5.4 Sensitivity of the Measurement System to Bias Tire Loading	53
5.4.1 Test Procedure	53
5.4.2 Results	54
5.4.3 Discussion of Results	54
5.5 An Alternate Solution	54
REFERENCES	57

Table of Contents (Cont'd)

APPENDIX A	Vishay Error
APPENDIX B	Confidence Intervals and the Student's t Distribution
APPENDIX C	Initial Torque Calibration Data Tables
APPENDIX D	Torque Calibration Results for Gauge ADS1 and BPS1
APPENDIX E	Torque Calibration Error Analysis Calculations and Results
APPENDIX F	Drive Axle Vertical Load Results
APPENDIX G	Trailer Axle Vertical Load Results
APPENDIX H	Reyco Axle Component Weights

LIST OF FIGURES

<u>Fig. #</u>	<u>Title</u>	<u>Page</u>
2.1	Axle Types	2
2.2	Strain Gauges Used	3
3.1	Torsional Shear Stress Effect	6
3.2	Vertical Load Shear Stress	8
3.3	Direct Stress Due to Bending	9
3.4	Direct Stress Due to Torsion	12
3.5	Gauge Orientation and Circuitry	14
3.6	Gauge Response to a C.W. Torque	15
3.7	Vertical Load Effect on Torque Gauges	18
3.8	Friction Force on Torque Gauges	21
3.9	Vertical Load Gauge Orientation and Circuitry	23
3.10	The Vishay and Its Functions	24
3.11	Least Squares Error	26
3.12	Least Squares Example	29
3.13	Electrical Calibration	31
3.14	Normal Distribution of Y Data Values	32
3.15	Error Analysis	35
4.1	Torque Gauge Locations	36
4.2	Calibration Configuration	37
4.3	Initial Torque Calibration	39
4.4	Brake Application Torque	40
4.5	Beam Torque	41
4.6	Sign Convention	43
4.7	Torque Calibration of ADS1	44
4.8	Torque Calibration of BPS1	45

LIST OF FIGURES (Cont'd)

<u>Fig. #</u>	<u>Title</u>	<u>Page</u>
4.9	Actual Orientation of Calibration Plots	46
5.1	Drive Axle Gauge Locations	50
5.2	Datum Level	51
5.3	Trailer Gauge Locations	52
5.4	Proposed Vertical Load Circuit	55

LIST OF TABLES

<u>Table #</u>	<u>Title</u>	<u>Page</u>
1	Material Properties and Dimensions of the Axle	1
2	Strain Gauge Specifications	2
3	Vishay Unit Serial Numbers	3
4	Torque Calibration Instruments	4
5	Gauge Sensitivities	38
6	Bending Effect for Gauges ADS1 and BPS1	42
7	Range For Electrical Calibration and Gauge Sensitivity of ADS1 and BPS1	47

SUMMARY

This report describes a calibration procedure performed on the strain gauged axles of a tractor-trailer. The calibration was performed to determine the loads imparted to the road during normal vehicle operation. A theoretical discussion of stresses and strains is provided as background to the calibration exercise.

The procedures followed in calibrating the vehicle are outlined. Errors inherent within the system were analysed and considered.

All calibrations produced linear results and good repeatability except those calibrations performed on the drive axles of the tractor-trailer unit. The tractor axle results were less linear but still within acceptable requirements.

The instrumentation used to monitor vertical road loading was found to be sensitive to bias tire loading. This requires that test sites be chosen with level pavement free of ruts.

Further studies are recommended for the drive axle calibration. Also consideration should be given to strain gauging sensitive to shear for vertical load instead of strain gauging sensitive to bending.

CONCLUSIONS

All calibration results showed very little hysteresis.

The trailer axle calibrations for torque and vertical load displayed excellent linearity and good sensitivity when plotted against voltage output. The drive axle gauges exhibited acceptable linearity but lower sensitivity.

It is imperative to maintain constant tire pressure in all tires to avoid bias tire loading which will lead to erroneous results while testing. Rutted roads will result in unequal tire loading also.

Three of the six torque gauges on the trailer were calibrated initially. Each displayed very similar gauge sensitivity. Therefore calibrating two torque gauges and documenting their behaviour was deemed sufficient to predict the torque experienced by all six torque gauges on the trailer.

Electrical calibration is required for all torque gauges because the lead wire lengths are not constant and therefore the wire resistance will cause different output voltages.

Brake application hardware induced a torque on the axle of large magnitude. This torque was considered in the data analysis.

RECOMMENDATIONS

The test sites chosen should be free of severe longitudinal road ruts as this may induce bias tire loading.

Each vertical load gauge should be calibrated independently that is, the actual load imparted to the road by one tire set should be plotted against its respective output voltage. The vertical load calibration followed in this report ordered the above output voltage with the total road load imparted via the axle. Independent calibration will serve to better predict axle load sharing.

Experiments should be performed to determine the appropriateness of using shear gauges in assessing vertical load. The purpose would be to investigate if there is a marked decrease in the bias tire loading errors experienced by the bending instrumentation. The voltage output cross talk of bending due to vertical loading and shear stress due to braking torque should be investigated.

The calibration loading procedure followed starts at a chosen datum level and is loaded incrementally. From the maximum, load is decremented by the same amount back to the minimum for the completion of one loading cycle. At least 30 data points should be recorded for calibration. Each increasing and decreasing cycle should contain approximately five increments. This will result in a scatter of points with no identical load values except at the extremes. A best fit line will then be calculated using all the data points.

1. INTRODUCTION

1.1 BACKGROUND

A nationwide weights and dimensions study is underway to determine the loading characteristics of different heavy vehicle suspension types under dynamic conditions. Under the supervision of Mr. J. Woodrooffe, at the National Research Council, an investigation of load sharing between axles, axle to road surface impact forces and axle load transfer resulting from normal vehicle braking are being considered. Once complete, the results will be presented to the Road Transportation Association of Canada (RTAC) in an attempt to equalize the heavy vehicle weights and dimensions regulations across Canada.

1.2 TASK

A heavy truck was instrumental to determine the dynamic axle loading characteristics of the vehicle. The task was to calibrate the instrumentation to accurately predict the dynamic vehicle loading.

This report covers the calibration procedures followed, a theoretical discussion describing the best locations of strain gauges to measure load and torque, and an error analysis such that the results are stated with confidence. These discussions are presented for the benefit of those not familiar with the subject.

2. THE INSTRUMENTS USED AND THE MANUFACTURER'S SPECIFICATIONS

2.1 AXLES

There are two round axle types commercially available. One type is designed with a forged hub and pilot shaft. The pilot shaft is inserted into the hollow axle and welded. The second axle type is manufactured using a hub without a pilot shaft. The hub is friction welded to the hollow axle shaft. This eliminates the pilot shaft from the axle tubing thereby providing a uniform cross section which can be strain gauged without the influence of localized stress anomalies associated with an abrupt cross sectional change.

Table 1 lists the material properties of the axle

High Strength Low Alloy Steel M5091 Algoma Steel Corp Ltd
Modulus of Elasticity (E) = 30×10^6 psi
Modulus of Rigidity (G) = 11.5×10^6 psi
O.D. = 5"
I.D. = 3.75"

TABLE 1
MATERIAL PROPERTIES AND DIMENSIONS OF THE AXLE

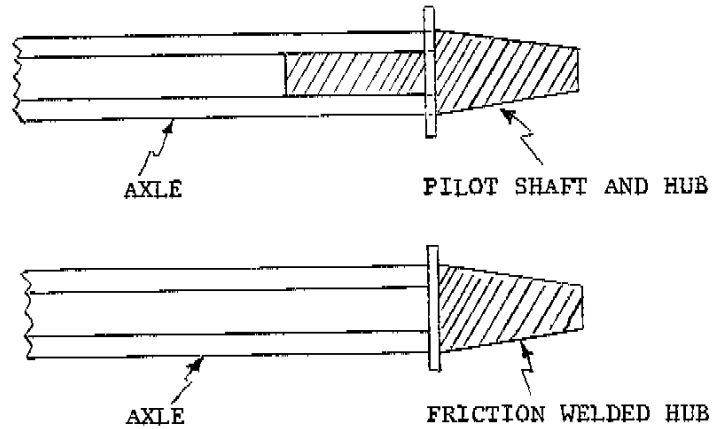


FIGURE 2.1
AXLE TYPES

2.2 STRAIN GAUGE TRANSDUCERS

Two strain gauge patterns are used. One type is used to monitor brake torque, and the other type is used to monitor vertical loading. The gauges are manufactured by Micro-Measurements. The manufacture's specifications are given in Table 2. Figure 2.2 shows the detail of both strain gauge types.

Use: Vertical Load Gauge
Type: CEA-06-250UW-120
Gage Resistance (R_G): $120 \pm 0.3\%$ ohms
Gage Factor (K_G): $2.045 \pm 0.5\%$

Use: Torsion Gauge
Type: EA-06-125TH-120
Gage Resistance (R_G): $120 \pm 0.2\%$ ohms
Gage Factor (K_G): $2.01 \pm 0.5\%$

TABLE 2
STRAIN GAUGE SPECIFICATIONS



VERTICAL LOAD
GAUGE

TORSION GAUGE

FIGURE 2.2
STRAIN GAUGES USED

2.3 STRAIN GAUGE CONDITIONING AMPLIFIER

The conditioning amplifier (Vishay units) are used to condition the input voltage needed to activate the strain gauges. It also amplifies and filters the output signal. These units are supplied by Intertechnology Limited. Table 3 contains the serial numbers of the units used during the calibration procedure. All units are Model #2310.

024155	024054
024079	024954
045349	043029
024076	045290
024072	

TABLE 3
VISHAY UNIT SERIAL NUMBERS

Before the calibration a bench test was performed on the Vishay units to check their outputs and stability. The procedure followed and results are documented in Appendix A. From the test it was concluded that each signal conditioned by the Vishay is within $\pm 1\%$.

2.4 INSTRUMENTS USED FOR TORQUE CALIBRATION

Table 4 lists the use and specifications of all the instruments used for calibrating for torque.

Manufacturer	Instrument Type	Model No.	Serial No.	Accuracy
Intertechnology	Load Cell	EP2-100K-10P3	30393	
Omega	Transducer indicator	DP420	420126	± 5 lbs
Owatonna Tool	55 ton hydraulic jack	RA556		
Owatonna Tool	hydraulic hand pump	3J	135510	

TABLE 4
TORQUE CALIBRATION INSTRUMENTS

2.5 INSTRUMENTS USED FOR VERTICAL LOAD CALIBRATION

The only instrument used to calibrate the vertical load, excluding the Vishay units, was a Fairbanks Morse Balance Scale, serial #E17049. Its rated capacity is 250000 lbs and has an accuracy of ± 25 lbs.

3. THEORETICAL BACKGROUND

During vehicle operation the axle is subjected to forces. These forces cause the axle to deform resulting in strain. Knowing the strain, which is easily measured using strategically placed strain gauges, the forces can be calculated.

An analysis of the stress strain behaviour due to torque and vertical loading are discussed in this section.

3.1 TORSIONAL STRESS

Torque caused by braking induces a shear stress on the axle. Torsional shear stress of a uniform cross section can be calculated knowing the following relationship:

$$\bar{\tau} = \frac{\bar{T}c}{J} = \frac{\text{FORCE}}{\text{AREA}} \quad [3.1i]$$

where: \bar{T} = magnitude and direction of the applied torque (units - ft*lbs)⁺
c = distance from the center of the member (ft)
J = polar moment of inertia (ft⁴)

The polar moment of inertia for the axle, a hollow tube, is

$$J = \frac{1}{2} \pi (c_2^4 - c_1^4)$$

where: c_2 = outer axle radius
 c_1 = inner axle radius

In reference to Fig. 3.1 and recalling one of the fundamental laws of nature, everything must maintain equilibrium, the behaviour of torsional shear stress on a small element will be discussed. The small element represents any point on the shaft, it is enlarged for clarity.

Logic dictates that twisting the member causes a stress in the positive y direction on the A face of the element. Multiplying this stress by the area of face A yields a force F_1 ($\frac{\text{FORCE}}{\text{AREA}} * \text{AREA} = \text{FORCE}$) in the direction of the shear stress (see Fig. 3.1a). By equilibrium; the sum of the forces in the y direction must equal zero. Therefore an equal but opposite force must be acting on the B face of the element. Since the member has a uniform cross section, the area of the A and B faces are equal, the result is $\tau_1 = \tau_2$ (see Fig. 3.1b).

The element is not yet in equilibrium. With just the forces, or stresses τ_1 and τ_2 the element would rotate in a counterclockwise direction. To maintain equilibrium the element must be experiencing equal but opposite forces to stop the rotational tendency (see Fig. 3.1c) Figure 3.1d shows the stresses experienced by any element in equilibrium on the shaft subjected to a clockwise torque.

Figure 3.1e shows how this torsional shear stress flows through any cross sectional portion of the axle. Figure 3.1f describes the relationship between the magnitude of shear stress and c the distance from the shaft's center.

⁺ft*lbs were chosen as the units for torque because it was felt that people have a better physical feel for 1 ft*lb versus 1 Newton meter the SI equivalent.

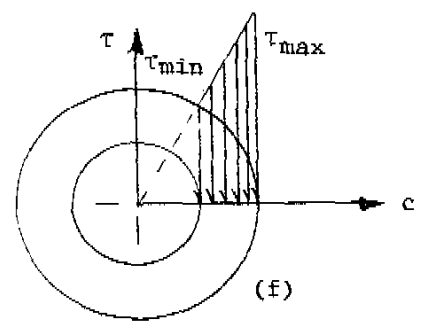
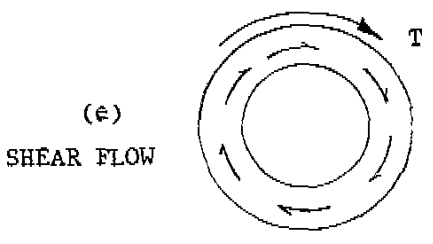
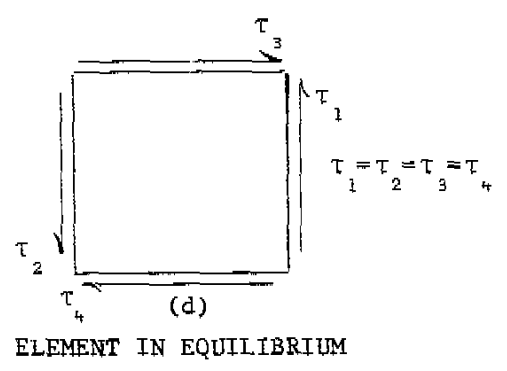
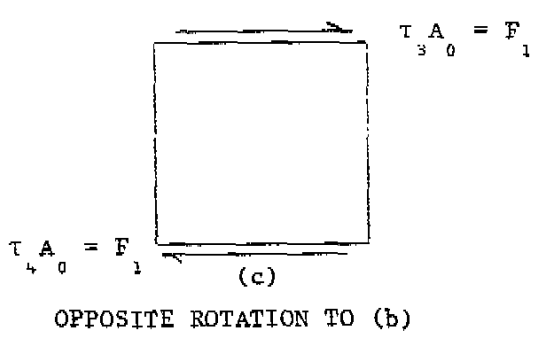
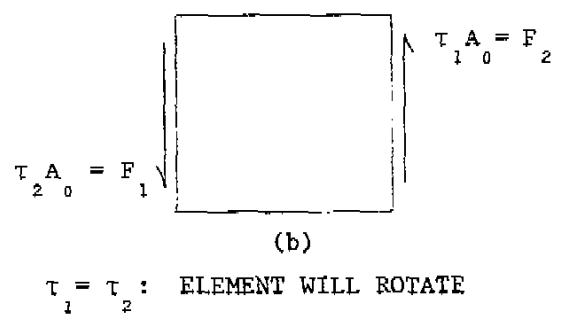
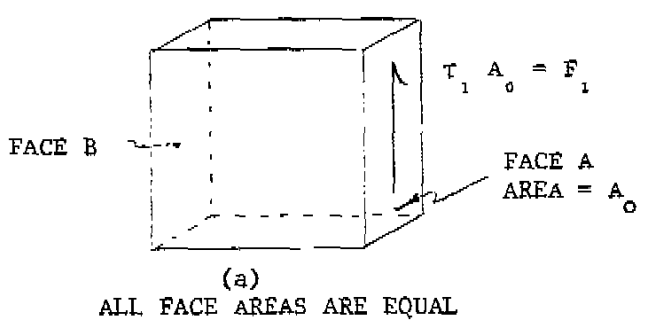
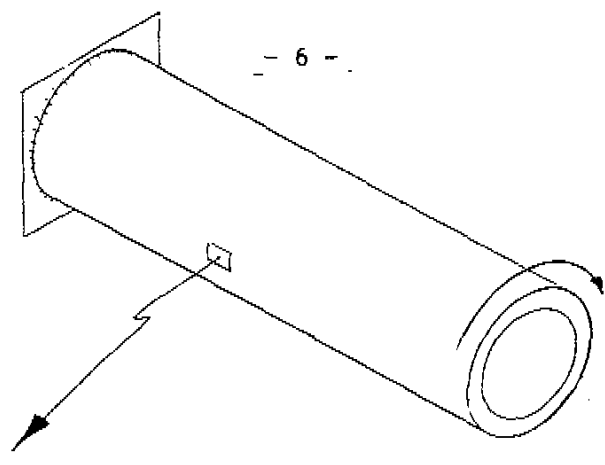


FIGURE 3.1
TORSIONAL SHEAR STRESS EFFECT

3.2 VERTICAL LOADING STRESSES

The axle experiences vertical loading from tire contact with the road surface and the trailer weight at the points of suspension spring attachment. Vertical forces are termed shear forces.

- Two types of stresses are associated with shear forces;
- i) direct stress due to bending and,
 - ii) shear stress

Shear stress is calculated in the following manner:

$$\bar{\tau} = \frac{\bar{F}Q}{I\tau} = \frac{\text{FORCE}}{\text{AREA}} \quad [3.21]$$

where \bar{F} = magnitude and direction of the shear force (lbs)
 Q = first moment of area (ft³)
 I = moment of inertia (ft⁴)
 τ = material thickness (ft)

Figure 3.2a shows a small element on a member experiencing a shear stress*. Figure 3.2b describes how this stress flows through any cross section of the axle. Notice along the vertical axis, through the center of the member, the shear stress is zero.

Direct stress due to bending is calculated by:

$$\sigma_{\text{BEND}} = \frac{\bar{F}(x)y}{I} = \frac{\text{FORCE}}{\text{AREA}} \quad [3.2ii]$$

where \bar{F} = direction and magnitude of the shear force (lbs)
 x = distance from the force to the element in question along the axle's horizontal axis (ft)
 y = distance along the vertical axis from the center of the axle or its neutral axis (ft)
 I = moment of inertia (ft⁴)

The moment of inertia is given by

$$I = \frac{1}{4} \pi (c_2^4 - c_1^4)$$

where c_1 and c_2 = inner and outer axle radius

Figure 3.3a graphically describes the stress distribution induced by bending. The important characteristics of this distribution are:

*The same equilibrium argument can be used to reach the shear stress directions on the element as in the previous section.

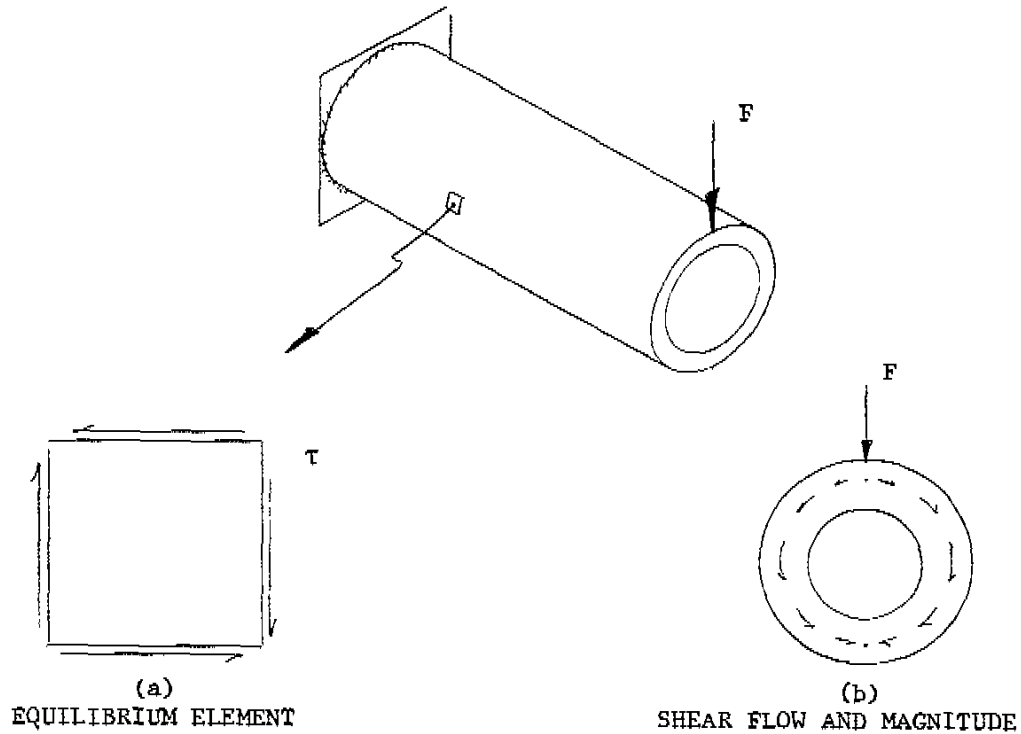


FIGURE 3.2
VERTICAL LOAD SHEAR STRESS

- i) the shaft experiences zero stress anywhere along its neutral axis
- ii) any portion of the material above the neutral axis experiences tension
- iii) any portion of the material below the neutral axis experiences compression
- iv) if the applied moment ($\bar{F}X$) is in the opposite direction the top half would be in compression, the bottom half would be in tension, and zero stress is along the neutral axis.

Figure 3.3b depicts the equilibrium configuration of a small element under direct stress.

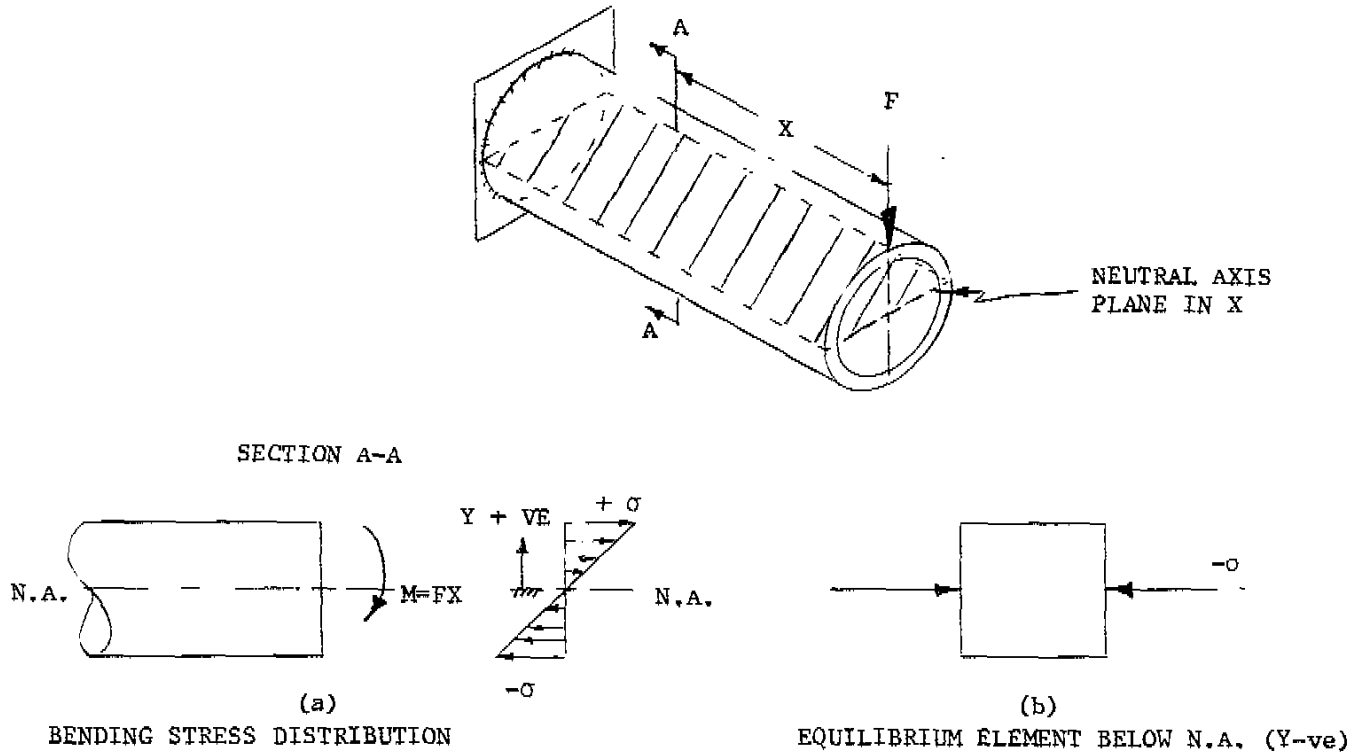


FIGURE 3.3
DIRECT STRESS DUE TO BENDING

3.3 STRESS STRAIN RELATIONSHIPS

When a material is subjected to a direct stress it behaves either elastically or plastically depending upon the magnitude of the stress and the material properties. In the plastic range the material suffers permanent deformation, in contrast, the material returns to its original length when the stress inducing force is removed in the elastic range. The change in length divided by the true length of the material in the elastic region is termed strain:

$$\epsilon = \frac{\Delta l}{l} \quad [3.3i]$$

where ϵ = denotes strain

Stress is proportional to strain when no plastic deformation occurs. The proportionality constant is called the modulus of elasticity and is a material property. It is denoted by a capital E.

$$\sigma = E \epsilon \quad [3.3ii]$$

A material subjected to a stress along the x axis, for example, experiences strains in all three dimensions but for our purpose these relationships are unnecessary. We need only to consider the strain in the x direction, therefore:

$$\sigma_x = E \epsilon_x \quad [3.3iii]$$

Shear stress also induces a strain, called a shear strain. These two physical properties are also proportional in the elastic range of the material. They are related by the modulus of rigidity (G) also a material property.

$$\tau = G \gamma \quad [3.3iv]$$

3.4 THE STRAIN GAUGE TRANSDUCER (From Ref. #4 p. 729)

A bonded resistance strain gauge is an electrically excited device used to measure strain. It is made of a grid of fine resistance wire bonded to a thin paper backing. When the gauge is cemented to a member under test, any deformation of the member results in a change in dimension and therefore a change in resistance of the gauge if the gauge's effective axis is oriented along an axis of either compression or tension. The relation between strain and resistance change is:

$$\frac{\Delta R}{R_G} = K_G \epsilon = K_G \frac{\Delta l}{l} \quad [3.4i]$$

where ΔR = gauge resistance change
 R_G = unstrained gauge resistance
 K_G = the gauge factor
 ϵ = the strain seen by the gauge

3.5 STRAIN GAUGE ORIENTATION FOR TORSION

When a small element in equilibrium, drawn parallel to the shaft's neutral axis, is subjected to pure torsion it does not experience direct stresses. Therefore, to instrument the axle with strain gauges it is necessary to find the orientation of an element which will sustain direct stress.

Figure 3.4a depicts an element under the influence of shear stresses due to a clockwise torque. Recalling from section 3.1, all these shear stresses are of equal magnitude and act over face areas also of equal magnitude. Cutting this element at any angle, θ , to the AD face, starting at A, results in the triangular element ADE. This

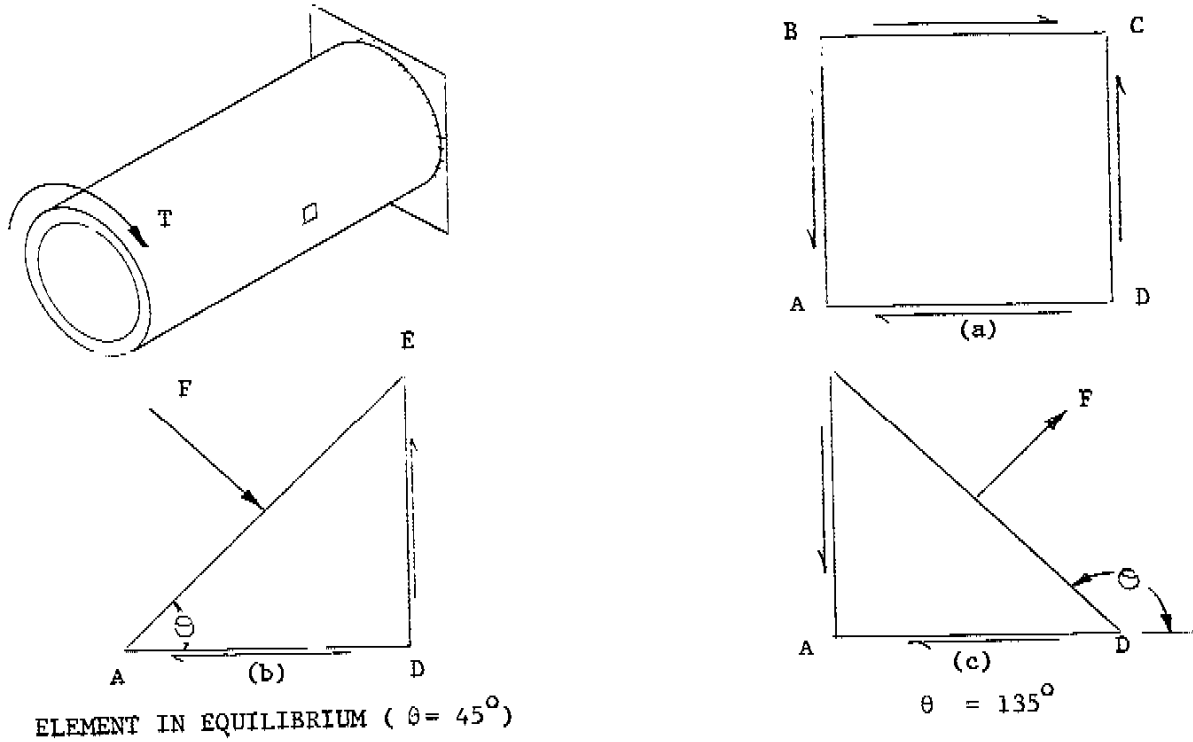


FIGURE 3.4
DIRECT STRESS DUE TO TORSION

3.5.1 Transformation of Strain

Thus far, we have only discussed methods of calculating strain due to direct stress and shear stress of elements oriented parallel to the neutral axis of the member (along the x axis). It is possible to compute strains at any angle to the x axis by the following formula,

$$\epsilon_{\theta} = \epsilon_x \cos^2\theta + \gamma \sin\theta \cos\theta \quad [3.511i]$$

where;

$$\epsilon_x = \frac{\sigma_x}{E} \quad [\text{from eq'n 3.311i}]$$

$$\gamma = \frac{1}{G} \quad [\text{from eq'n 3.31v}]$$

Since we are concerned with strains at 45° and 135° to the x axis, equation [3.5iii] becomes:
for 45°;

$$\begin{aligned}\epsilon_{45^\circ} &= \frac{\sigma_x}{E} \cos^2 45^\circ + \frac{\tau}{G} \sin 45^\circ \cos 45^\circ \\ &= \frac{\sigma_x}{E} * \frac{1}{2} + \frac{\tau}{G} * \frac{1}{2}\end{aligned}$$

therefore;

$$\epsilon_{45^\circ} = \frac{1}{2} * \left(\frac{\sigma_x}{E} + \frac{\tau}{G} \right) \quad [3.5iva]$$

for 135°

$$\epsilon_{135^\circ} = \frac{1}{2} * \left(\frac{\sigma_x}{E} - \frac{\tau}{G} \right) \quad [3.5ivb]$$

3.5.2 Gauge Positioning on the Axle and the Wheatstone Bridge

Four strain gauges are used to monitor torsion, two on each side of the axle. They are placed at identical points on each side of the axle over the neutral axis plane. Figure 3.5a shows their angle of orientation and location on the axle.

The four gauges are wired into a wheatstone bridge circuit. This circuit requires an excitation voltage (V^+) to activate the strain gauges. When the member is subjected to a torque the strain gauges deform resulting in a voltage output (V_o) due to the resistance change in the gauges. This voltage output across the nodes a and b can be calculated using the voltage divider concept (see Fig. 3.5b).

$$V_o = V^+ \left[\frac{R_1}{R_4 + R_1} - \frac{R_2}{R_2 + R_3} \right] * AF \quad [3.5v]$$

where V_o = output voltage

V^+ = excitation voltage

$R_{1,2,3,4}$ = strained resistance of the gauges

AF = amplification factor

Equation [3.5v] can be reduced further if we consider the following implicit example.

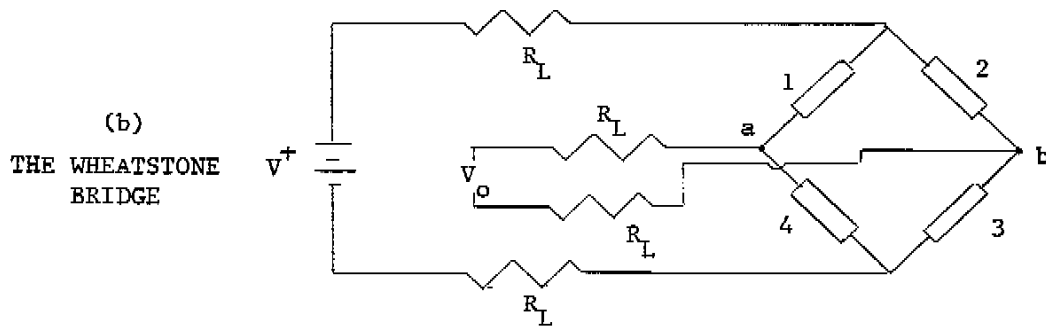
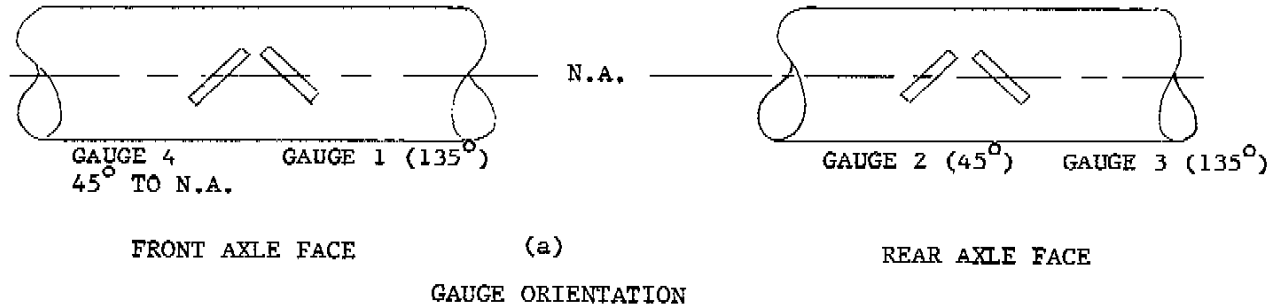


FIGURE 3.5
GAUGE ORIENTATION AND CIRCUITRY

A shaft experiences a torque of $x \text{ ft} \cdot \text{lbs}$ applied in a clockwise direction. Describe the strain gauge behaviour.

Figure 3.6 shows the two equilibrium elements containing the strain gauges and the strain gauge orientation within these elements. Before we proceed it is important to note the following properties;

- i) All shear stresses are of equal magnitude. The distance of these elements from the center of the shaft, are equal (refer to Figure 3.1f, p. 6).
- ii) The two elements are identical when comparing the directions of the effective shears.
- iii) The elements experience no direct stress.

NOTE: SMALL
ARROWS INDICATE
DEFORMATION OF
ELEMENT DUE TO
SHEAR

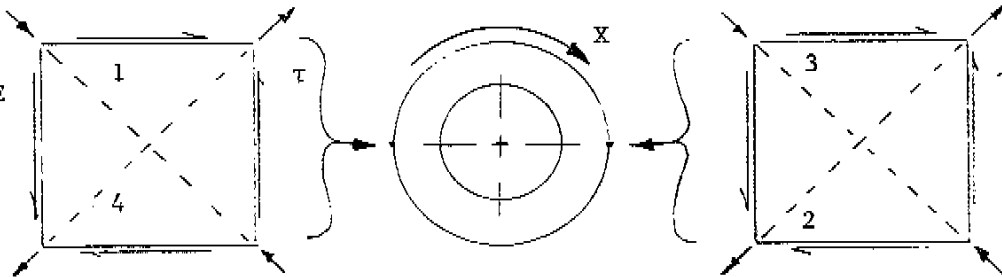


FIGURE 3.6
GAUGE RESPONSE TO A C.W. TORQUE

Calculating the strain in gauge 1 using [3.5ivb]:

$$\sigma_x = 0$$

$$\epsilon_1 = -\frac{1}{2} \frac{\tau}{G}$$

since the shear stress is constant on all elements and G (the modulus of rigidity) is also constant for all elements, let;

$$\epsilon_1 = -y \frac{\Delta l}{l} = -y \mu \text{ strains}^*$$

The strain in gauge 4 is; using [3.5iva];

$$\sigma_x = 0$$

$$\epsilon_4 = +\frac{1}{2} \frac{\tau}{G} = +y \mu \text{ strains}$$

Using the appropriate formula, depending on the angle of orientation, the strains in gauges 2 and 3 can be calculated.

Summarizing,

$$\epsilon_1 = -y \mu \text{ strains}$$

$$\epsilon_2 = +y \mu \text{ strains}$$

$$\epsilon_3 = -y \mu \text{ strains}$$

$$\epsilon_4 = +y \mu \text{ strains}$$

* μ strains represents $10^{-6} \frac{\Delta l}{l}$, the common units of strain.

from,

$$\frac{\Delta R}{R_G} = K_G \epsilon \quad [3.4i]$$

the change in gauge resistance can be calculated.

Noting that,

- i) all strain gauges are identical, therefore, the gauge resistance (R_G) and gauge factors (K_G) are constant
- ii) the magnitudes of the strains in each of the gauges are equal

therefore for all gauges;

$$\Delta R = +r \text{ (for positive strain)}$$

$$\Delta R = -r \text{ (for negative strain)}$$

for a clockwise torque, the voltage output is, from equation [3.5v]:

$$V_o = V^+ \left[\frac{R_G - r}{(R_G + r) + R_G - r} - \frac{R_G + r}{(R_G + r) + R_G - r} \right] * AF$$

As shown in Figure 3.5b on page 14 the lead wires connecting the instruments which provide the excitation voltage and monitor the voltage output from the wheatstone bridge are quite long and their resistance must be considered for accurate calculation of the output voltage.

The lead wire used is hard drawn, solid copper wire, AWG size 22. It's resistance per foot is 0.016 ohms/ft. The strain gauges are connected in series with these wires (see Fig. 3.5b, p. 14). The corrected gauge resistance is:

$$R_G^* = R_G + 2R_L \quad [3.5vi]$$

where R_G = gauge resistance
 R_L = lead wire resistance (0.016 * x ft of wire)

Therefore the correct voltage output formula for a clockwise torque is;

$$V_o = V^+ \left[\frac{R_G^* - r}{R_G^* - r + R_G^* + r} - \frac{R_G^* + r}{R_G^* - r + R_G^* + r} \right] * AF$$

Because the magnitude of the strain is in the order of 10^{-6} , ΔR will be small. This is why an amplification factor (AF) is necessary.

To further simplify the output voltage formula the amplification factor and excitation voltage are always constant in our applications:

$$AF = 1000$$

$$V^* = 5V$$

If the torque was applied in the opposite direction of the same magnitude the shear stress would be of the same magnitude but in the opposite sense thus reversing the sense of the strain seen by each gauge. Therefore equation [3.5v] reduces to:

$$V_o = 5000 \left[\frac{R_G^* \pm r}{R_G^* \pm r + R_G^* \mp r} - \frac{R_G^* \mp r}{R_G^* \pm r + R_G^* \mp r} \right]$$

$$V_o = 5000 \left[\frac{R_G^* \pm r}{2R_G^*} - \frac{R_G^* \mp r}{2R_G^*} \right]$$

$$V_o = \frac{2500}{R_G^*} [R_G^* \pm r - R_G^* \mp r]$$

$$V_o = \frac{2500}{R_G^*} (\pm 2r)$$

therefore, for pure torsion the voltage output is,

$$V_o = \frac{5000}{R_G^*} (\pm r) \quad [3.5vii]$$

where V_o = output voltage

R_G^* = gauge resistance [from eq'n 3.5vi]

$\pm r$ = calculated resistance change due to strain

[from eq'n 3.4i]

The gauge resistance in equation [3.4i] is not corrected due to lead wire resistance because the change in resistance depends on the strain experienced by the gauge as a ratio to the gauge's unstrained resistance.

3.5.3 Vertical Loading Effect on the Torsion Strain Gauges

During vehicle operation the axle will experience both torsional and vertical forces. Therefore, it is necessary to determine the effect of shear stress and direct stress due to bending on the torsion strain gauges.

As discussed in the preceding section the torsion strain gauges are placed at identical points on each side of the axle straddling the plane containing the neutral axis (see Fig. 3.5a, p. 14). Referring to Figure 3.3a on page 9, the direct stress due to bending is zero at the neutral axis. The gauges are larger than a point, but, if they are placed over the center of the neutral axis at identical points on the axle the net effect of the bending stress will be zero. Thus the voltage output of the wheatstone bridge circuit is not affected by the direct stress due to bending if the gauges are accurately placed (see Fig. 3.7a).

Figure 3.7b describes the effect on the elements A and B, containing strain gauges 1,4 and 2,3 respectively, due to a shear stress caused by vertical loading. All stresses are of equal magnitude, but, element A is influenced by a stress opposite to that of element B. Element A will be considered as the positive sense.

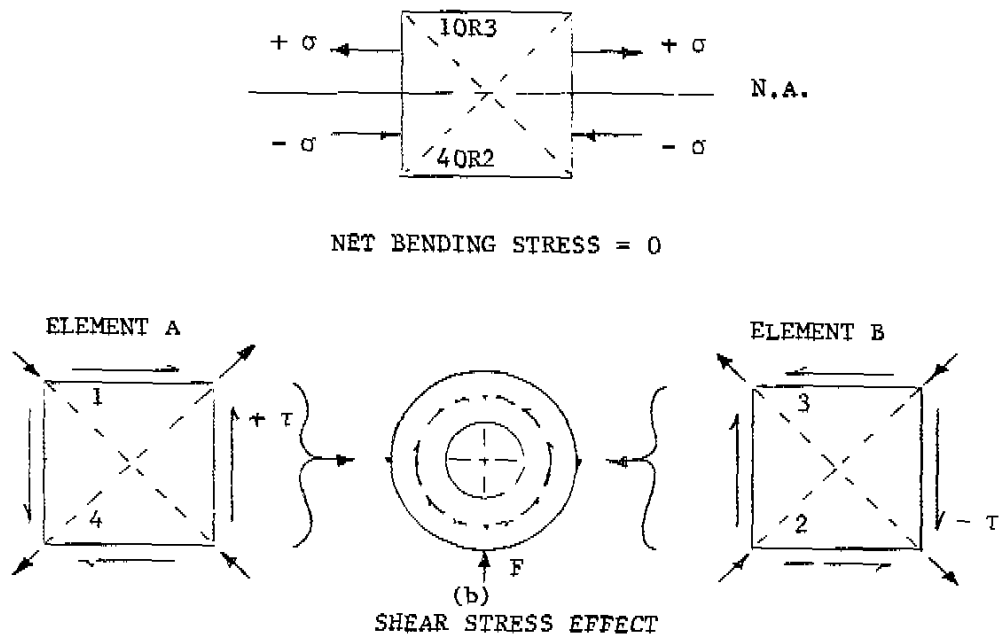


FIGURE 3.7
VERTICAL LOAD EFFECT ON TORQUE GAUGES

The net effect of the bending stress is zero therefore, gauges 1 and 4 experiencing a positive shear stress of τ see strains of;

$$\epsilon_1 = -y \mu \text{ strains} \quad [\text{from eq'n 3.51vb}]$$

$$\epsilon_4 = +y \mu \text{ strains} \quad [\text{from eq'n 3.51va}]$$

gauges 2 and 3 experience negative shear stress of $-\tau$ and see strains of;

$$\epsilon_2 = -y \mu \text{ strains} \quad [\text{from eq'n 3.51va}]$$

$$\epsilon_3 = +y \mu \text{ strains} \quad [\text{from eq'n 3.51vb}]$$

As discussed earlier the resistance change in each gauge will be of the same magnitude and the sign will be determined by the direction of the strain, therefore;

$$R_1 = R_2 = R_G^* - \tau$$

$$R_3 = R_4 = R_G^* + \tau$$

from equation [3.5v]

$$V_o = V^+ \left[\frac{R_G^* - \tau}{R_G^* - \tau + R_G^* + \tau} - \frac{R_G^* - \tau}{R_G^* - \tau + R_G^* + \tau} \right] * AF$$

$$V_o = V^+ \left[\frac{R_G^* - \tau - R_G^* + \tau}{2R_G^*} \right] * AF$$

therefore;

$$V_o = 0$$

Therefore equation [3.5vii] remains unchanged. It is not sensitive to stresses induced by vertical loading.

3.5.4 Brake Force Effect on the Torsion Strain Gauges

The force of braking at the tire to ground contact point generates a torque in the axle known as brake torque.

This force induces a shear stress on the axle as shown in Figure 3.8a. The gauges are located at the point of zero shear stress, thus, they will not be strained if they are placed accurately.

Also of concern is the bending effect caused by the braking force (see Fig. 3.8b). Gauges 1 and 4 are subjected to tension under the force while gauges 2 and 3 are compressed. Using equations [3.51va and b] and [3.4i];

$$R_1 = R_4 = R_G^* + r$$

$$R_2 = R_3 = R_G^* - r$$

substituting the above values into equation [3.5v] yields;

$$V_o = V^+ \left[\frac{R_G^* + r}{2(R_G^* + r)} - \frac{R_G^* - r}{2(R_G^* - r)} \right] * A.F.$$

$$V_o = V^+ \left[\frac{1}{2} - \frac{1}{2} \right] * A.F.$$

$$V_o = 0$$

No correction is necessary for the braking force.

3.6 STRAIN GAUGE ORIENTATION FOR VERTICAL LOADING

Strain gauges respond to directional strain. The stress distribution due to bending is directed perpendicular to the plane of the neutral axis. Recalling that the bending stress distribution is a maximum at the outer surface of the material (see Figure 3.3a, page 9) the logical choice is to place the strain gauges at the top and bottom of the axles oriented as shown in Figure 3.9.

Using the transformation of strain formula [3.5iii] it will be proven that any type of shear stress does not affect a gauge oriented as in Figure 3.9a on page 23.

gauge orientation: 0° to the x axis
from [3.3iv]
 $\gamma = \tau/G$

from [3.5iii]

$$\epsilon_o = \epsilon_x \cos^2 0^\circ + \gamma \sin 0^\circ \cos 0^\circ$$

$$\epsilon_{0^\circ} = \epsilon_x$$

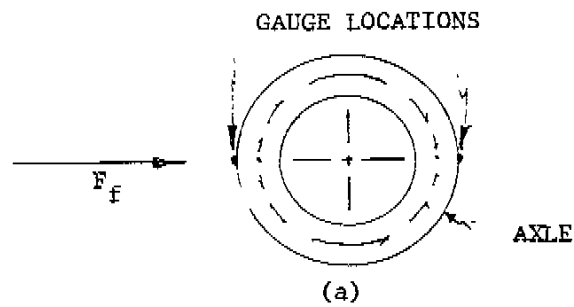
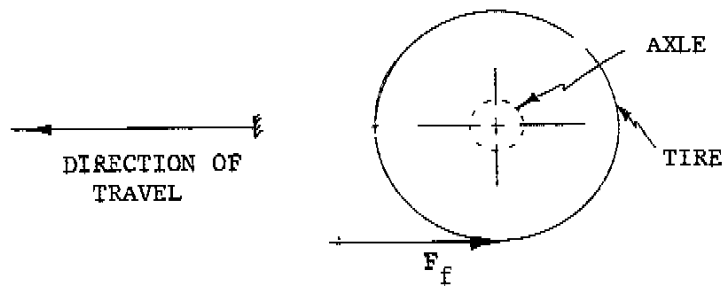
Bending caused by the brake force will not affect the gauges if they are oriented correctly. This stress distribution is zero at the top and bottom of the axle.

Therefore the gauges experience the effect of bending only.

Recalling equations [3.2ii] and [3.3ii]

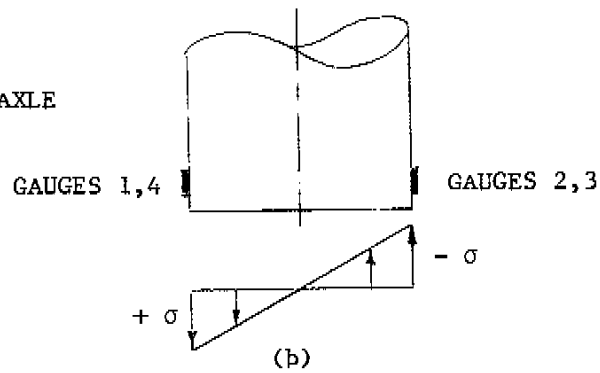
$$\sigma_x = \frac{F * x * y}{I} \quad [3.2ii]$$

$$\epsilon_x = \frac{\sigma_x}{E} \quad [3.3ii]$$



SHEAR STRESS EFFECT

TOP VIEW OF AXLE



BENDING EFFECT

FIGURE 3.8
FRICTION FORCE ON TORQUE GAUGES

3.6.1 Gauge Positioning on the Axle and the Wheatstone Bridge

Figure 3.9a depicts the gauge positioning used to monitor vertical loading. Figure 3.9b shows the wheatstone bridge circuit and the lead wire resistance.

Assuming the strain gauges are aligned without error along the axis of direct stress and are situated over each other they will see the same magnitude of strain but opposite senses. That is, one will be in compression and the other in tension depending on the direction of the applied moment, therefore from equation [3.4i]

$$\Delta R = \pm r$$

the output voltage expression for this bridge is;

$$V_o = V^+ \left[\frac{120}{R_G^* \pm r + 120} - \frac{120}{R_G^* \mp r + 120} \right] * A.F.$$

since the excitation voltage and amplification factor are constants;

$$V_o = 5000 \left[\frac{120}{R_G^* \pm r + 120} - \frac{120}{R_G^* \mp r + 120} \right]$$

$$V_o = 6.0 \times 10^5 \left[\frac{1}{R_G^* \pm r + 120} - \frac{1}{R_G^* \mp r + 120} \right] \quad [3.6i]$$

where R_G^* = given by eq'n [3.5vi].

3.7 THE STRAIN GAUGE CONDITIONING AMPLIFIER

Both vertical load and torsion bridge circuits require amplification and an excitation voltage. These two functions along with three others are provided by the strain gauge conditioning amplifiers, also known as a Vishay unit. This section will summarize the functions provided by the Vishay.

- i) It supplies the excitation voltage necessary for the gauges within the wheatstone bridge circuit.
- ii) It measures the differential voltage across the bridge.
- iii) Once a datum level for testing is chosen the Vishay can adjust the output voltage to zero volts. This is known as "balancing the bridge".
- iv) Amplification factor, or gain, is supplied by the Vishay unit. This function amplifies the bridge output voltage such that its signal is of sufficient magnitude to be recorded.

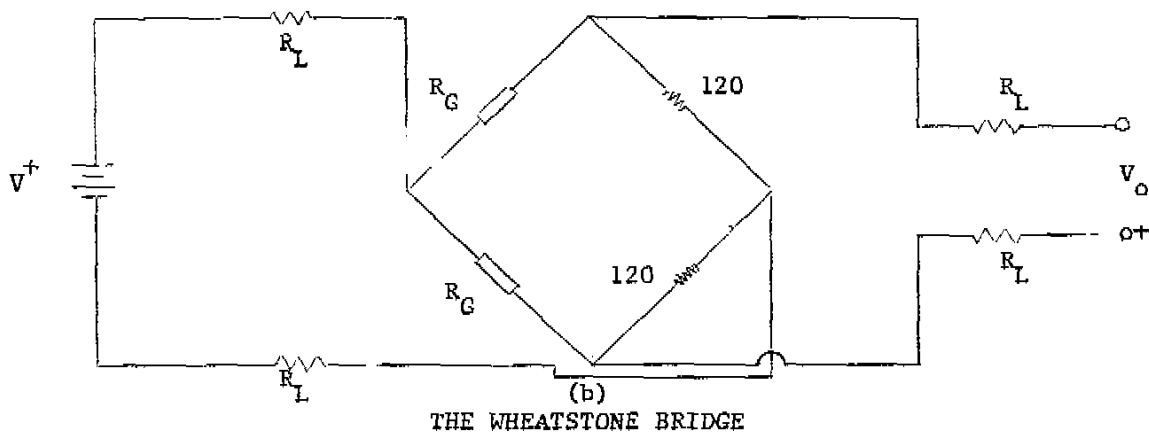
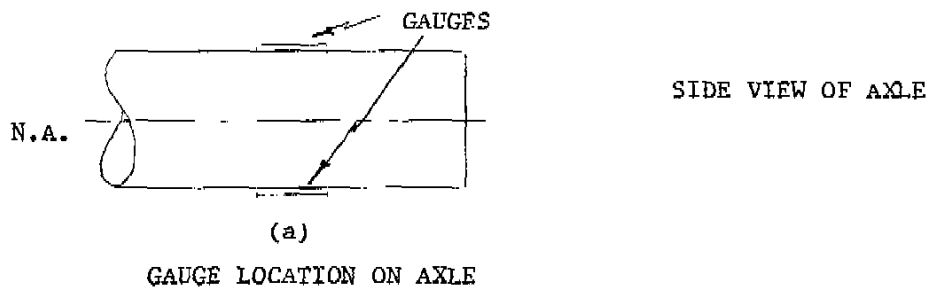
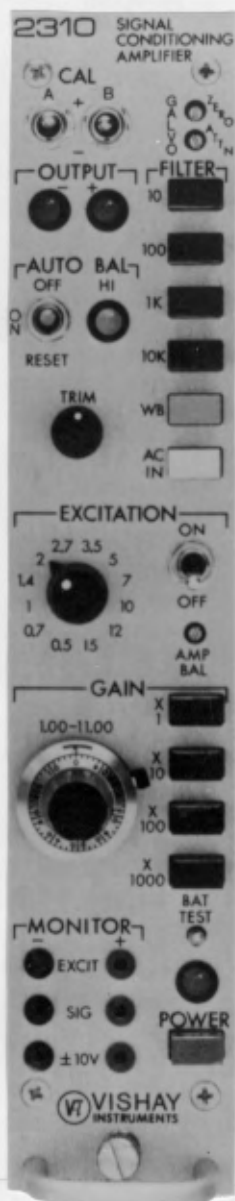


FIGURE 3.9
VERTICAL LOAD GAUGE ORIENTATION AND CIRCUITRY



WHEATSTONE BRIDGE

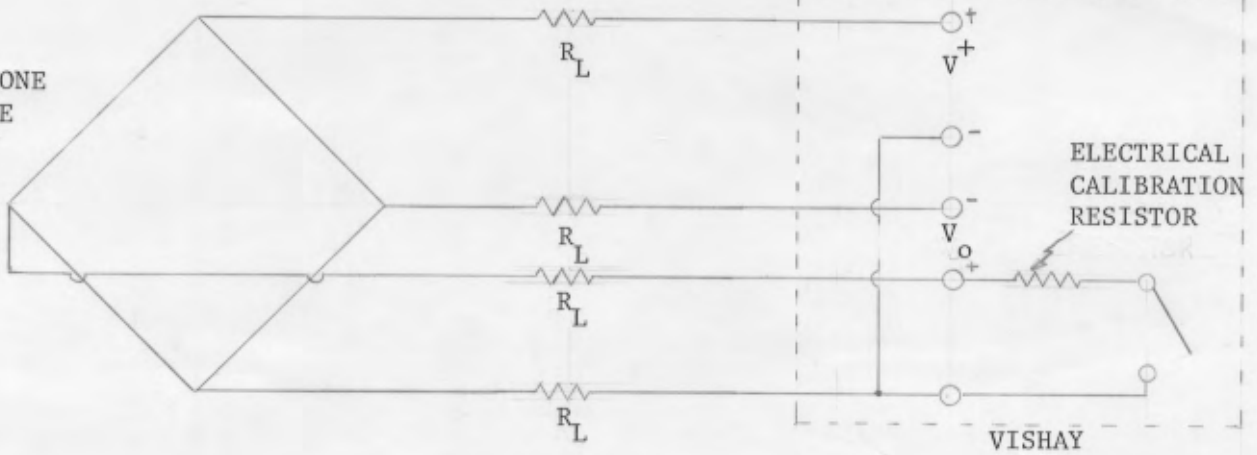


FIGURE 3.10
THE VISHAY AND ITS FUNCTIONS

- v) The Vishay also provides for electrical calibration. A switch is engaged allowing a resistor to be shunted across one arm of the bridge circuit. This function will be discussed in the next section.

Figure 3.10 shows the front panel of a Vishay unit and how it is integrated into the wheatstone bridge circuit.

3.8 CALIBRATION

To calibrate the gauges a known torque or vertical load is applied to the axle. Due to the axle's elastic behaviour it is strained and an output voltage is emitted from the bridge circuit. The load* and output voltage is recorded.

A linear relationship is predicted for load and output voltage by the following reasoning; consider the torque instrumentation on one axle from [3.2i];

$$\tau = \frac{Tc}{J}$$

the only variable in this equation is T, the applied torque all others are constant, therefore;

$$\tau \propto T$$

As torque increases so does the shear stress. This is a linear relationship. From [3.3.iv]:

$$\tau \propto \gamma$$

this is also a linear relation because the induced torque, and therefore, the induced shear stress does not exceed the elastic limit of the material. From [3.5iii] recall that $\alpha_x = 0$, therefore $\epsilon_x = 0$

$$\epsilon_{45^\circ}, \epsilon_{135^\circ} \propto \gamma$$

and from [3.4i]

$$\Delta R \propto \epsilon$$

the change in gauge resistance behaves linearly with strain. From [3.5vii]:

$$V_o \propto r(\Delta R)$$

Therefore, the torque induced on the axle is linearly proportional to the bridge output voltage.

*the word load implies both torque and vertical load.

$$\text{LOAD} \propto V_o$$

A similar argument can be made of the relationship between vertical load and output voltage leading to the same conclusion.

The recorded data is plotted with the bridge output on the ordinate (y) axis and the abscissa (x axis) represents the load configuration. This convention was adopted because the output voltage depends on the induced load. A straight line is fitted to the data of the form;

$$y = Mx + C$$

where $M = \text{slope of the line} = \frac{\text{RISE}}{\text{RUN}}$
 $C = y \text{ intercept.}$

3.8.1 Least Squares Method of Best Fit

Because of errors within the system, all data points do not fall exactly on a straight line as predicted. It is necessary to calculate the best fit line using the least squares method.

Consider the following data points

$$\frac{x}{y} \mid \frac{x_1}{y_1} \mid \frac{x_2}{y_2} \mid \dots \mid \frac{x_i}{y_i} \mid \dots \mid \frac{x_n}{y_n}$$

The data is anticipated to fall on a straight line

$$y' = MX + C$$

It is desired to find values of M and C which will best predict the true values of the recorded y data points. The ith value of y is given by:

$$y'_i = MX_i + C$$

It is desired to minimize the total error incurred without having positive error cancelling with negative error.

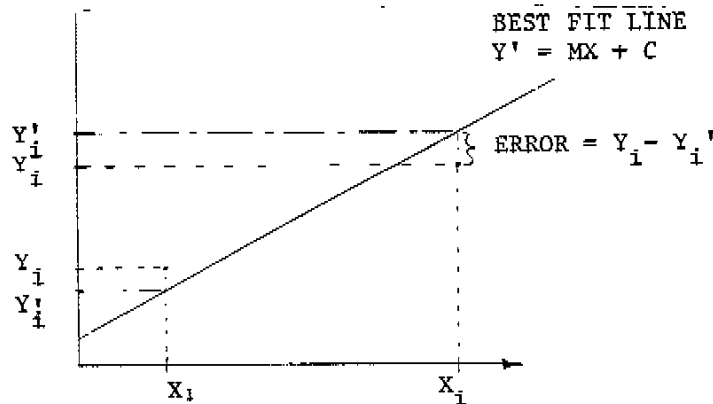


FIGURE 3.11
 LEAST SQUARES ERROR

To avoid the above cancellation it is required to minimize the sum of the squares of the error. Therefore,

$$\sum_{i=1}^n [y_i - (MX_i + C)]^2 = S$$

M and C must be determined such that S is a minimum.

Taking the partial derivative of S with respect to C and M respectively and letting the result equal zero will minimize S.

$$\frac{\partial S}{\partial C} = 0$$

therefore;

$$2 \sum_{i=1}^n [y_i - MX_i - C] [-1] = 0 \quad [3.8ia]$$

$$\frac{\partial S}{\partial M} = 0$$

therefore;

$$2 \sum_{i=1}^n [y_i - MX_i - C] [-x_i] = 0 \quad [3.8ib]$$

Dividing equation [3.8ia] by 2, therefore[†];

$$\begin{aligned} - \sum y_i + C \sum (1) + M \sum x_i &= 0 \\ \sum y_i &= Cn + M \sum x_i \end{aligned}$$

dividing equation [3.8ib] by 2,

$$\sum x_i y_i = C \sum x_i + M \sum x_i^2$$

Summarizing;

$$\sum y_i = Cn + M \sum x_i \quad [3.8iia]$$

$$\sum x_i y_i = C \sum x_i + M \sum x_i^2 \quad [3.8iib]$$

where n = number of data points

$\sum x_i$ = sum of all x data points

$\sum x_i^2$ = sum of all squared x data points

$\sum x_i y_i$ = sum of the product of corresponding pairs of data points

$\sum y_i$ = sum of all y data points

[†]all summation signs have bounds from 1 to n data points.

The unknowns are M and C. They can be calculated from equations [3.8iia] and [3.8iib]. A demonstration of the least squares method is given here.

The following data points were recorded during a calibration:

$$\frac{X}{Y} \mid \frac{1}{1.1} \mid \frac{2}{1.9} \mid \frac{3}{2.8} \mid \frac{4}{4.3}$$

From this data it is acceptable to assume the best fit line has the form,

$$y = MX + C$$

using equations [3.8iia] and [3.8iib]:

$$n = 4$$

$$\sum x_i = 1 + 2 + 3 + 4 = 10$$

$$\sum x_i^2 = 1^2 + 2^2 + 3^2 + 4^2 = 30$$

$$\sum x_i y_i = 1(1.1) + 2(1.9) + 3(2.8) + 4(4.3) = 30.5$$

$$\sum y_i = 1.1 + 1.9 + 2.8 + 4.3 = 10.1$$

substituting the above values in the appropriate equations of [3.8iia] and [3.8iib];

$$10.1 = 4C + 10M \quad [1]$$

$$30.5 = 10C + 30M \quad [2]$$

From [1]

$$C = \frac{10.1 - 10M}{4}$$

substituting into [2]

$$30.5 = 10 \left[\frac{10.1 - 10M}{4} \right] + 30M$$

$$M = 1.05$$

therefore from [1]

$$C = -0.1$$
$$\therefore y = 1.05x - 0.1$$

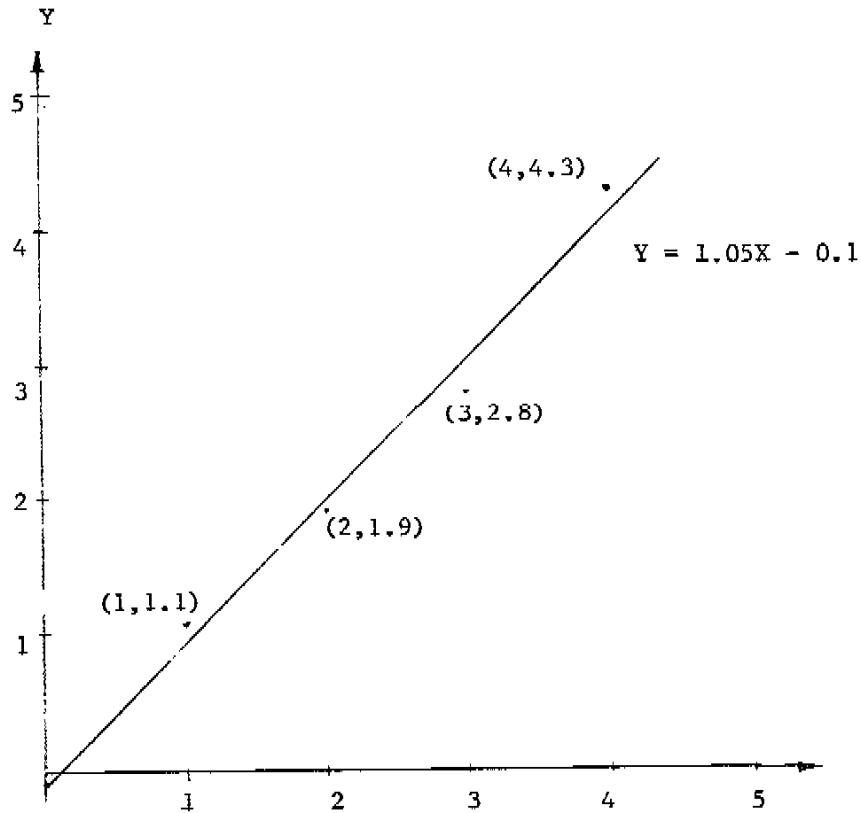


FIG. 3.12
LEAST SQUARES EXAMPLES

3.8.2 Gauge Sensitivity

The gauge sensitivity describes the slope of the best fit line, $y = MX + C$ in physical units.

The general expression for the gauge sensitivity is;

$$\frac{Y}{Z \text{ VOLT EXCITATION}} \equiv x \text{ LOAD UNITS} \quad [3.81va]$$

where y = bridge voltage output in mV
 x = corresponding load value
 z = excitation voltage value

Gauge sensitivity is calculated in the following manner given the best fit line;

$$Y = MX + C$$

where $y = \text{volts}$

$$M = \frac{\text{VOLTS}}{\text{LOAD}}$$

$X = \text{load}$

$C = \text{volts}$

let the output voltage be 1 volt; disregard the value of C;

$$1 = Mx$$

$$\therefore x(\text{Load}) = \frac{1 (\text{VOLT})}{M \left(\frac{\text{VOLTS}}{\text{LOAD}} \right)} \quad [3.81vb]$$

therefore using [3.81va] and [3.81vb]

$$1 \text{ VOLT} \equiv \frac{1}{M} \text{ LOAD UNITS}$$

The gain (G) and excitation voltage ($Z V^+$) affect the bridge output voltage; dividing the voltage output by these factors yields the gauge sensitivity.

$$\frac{1 \text{ VOLT}}{G * ZV^+} \equiv \frac{1}{M} \text{ LOAD UNITS} \quad [3.8v]$$

Given the equation of a best fit line calculated for a torque calibration with a gain of 1000 and an excitation voltage of 5 volts, we will determine the gauge sensitivity

$$y = 0.238x + 0.18$$

let $y = 1 \text{ VOLT}$ and disregard the value of C;

$$1 = 0.238x$$

$$x = \frac{1}{0.238} = 4.202 \text{ ft} * \text{lbs} \quad [\text{from } 3.81vb]$$

therefore;

$$1 \text{ VOLT} \equiv 4.202 \text{ ft} * \text{lbs}$$

dividing by the gain and excitation voltage yields the gauge sensitivity

$$\frac{1 \text{ VOLT}}{1000 * 5 \text{ V}^+} = 4.202 \text{ ft} * \text{lbs}$$

in its standard form the gauge sensitivity is;

$$\frac{0.2 \text{ mV}}{V^+} = 4.202 \text{ ft}^2\text{lbs}$$

3.8.3 Electrical Calibration

Electrical calibration is performed when the wheatstone bridge is balanced ($V_o=0$). At this point engaging a switch on the Vishay unit shunts a resistor across one arm of the bridge network (see Fig. 3.10, p. 24). This results in a voltage output. The voltage output will always be of the same value to within $\pm 1\%$. The error incurred is due to the Vishay.

Once a gauge is calibrated and its best fit line is calculated, the gauge behaviour is therefore, established. The electrical calibration voltage is substituted into the line equation to give a resulting load value. Consider the following implicit example;

i) gauge behaviour

$$y = MX + C$$

ii) electrical calibration result;

$$y = V_o \text{ (output volts)}$$

iii) resulting load

$$X_{\text{ECAL}} = \frac{V_o - C}{M}$$

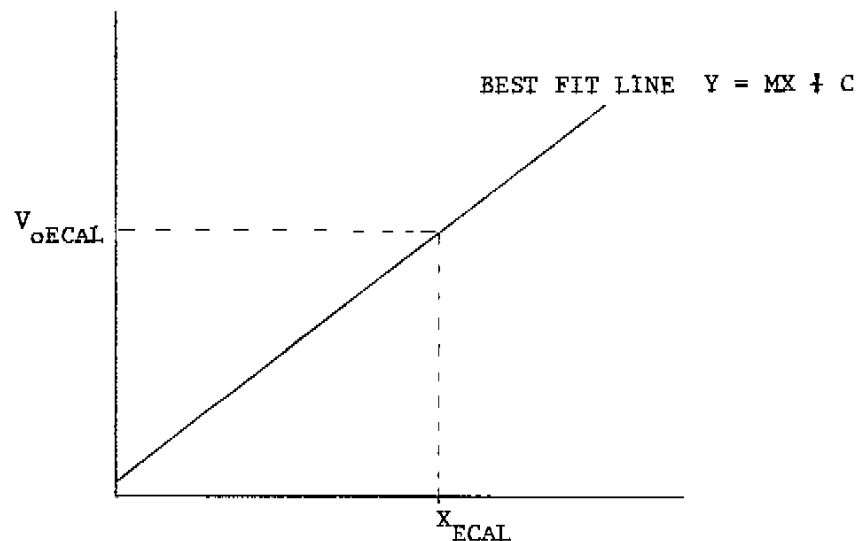


FIGURE 3.13
ELECTRICAL CALIBRATION

During an actual test a chart recorder is used to monitor a specific load gauge. The wheatstone bridge is balanced and electrical calibration is performed resulting in a deflection of, for example, ten divisions on the chart paper. The gauge behaviour is known to be linear (from the line $y = MX + C$) and the voltage output caused by the electrical calibration is known, therefore, the corresponding load can be calculated. On the chart recorder 10 divisions is therefore equivalent to the calculated load due to electrical calibration. The result is the magnitude of all loads can be determined from the recorded data. Electrical calibration is the most important function of calibration.

3.9 ERROR ANALYSIS

3.9.1 Error in Least Squares Calculation (From Ref. #2 p. 296)

The least squares method of curve fitting is only an estimator to the true line. This true line can be found if an infinite number of data points were collected resulting in the following equation.

$$y_i = \alpha + \beta x_i$$

The values of y_i recorded are independently normally distributed about the true line $\alpha + \beta x_i$ representing the mean value of this distribution. Each i th value of y has this distribution characteristic and all of these distributions have the same shape, or, common variance (see Fig. 3.14).

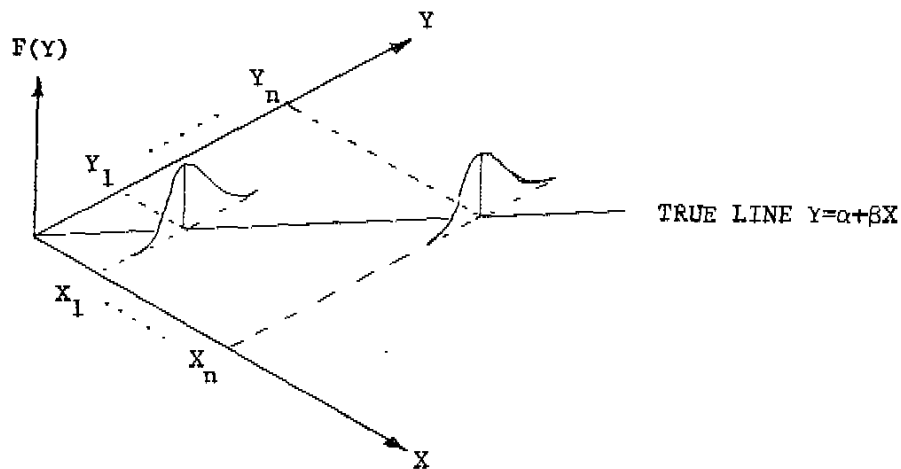


FIGURE 3.14
NORMAL DISTRIBUTION OF Y DATA VALUES

The method of least squares is used only to estimate the true line, that is, C and M are just estimates of the true values α and β respectively.

To evaluate the range of the true line coefficients the following expression will be used. Their development is beyond the scope of this report.

$$S_{xx} = n \sum_{i=1}^n x_i^2 - \left(\sum_{i=1}^n x_i \right)^2 \quad [3.9ia]$$

$$S_{yy} = n \sum_{i=1}^n y_i^2 - \left(\sum_{i=1}^n y_i \right)^2 \quad [3.9ib]$$

$$S_{xy} = n \sum_{i=1}^n x_i y_i - \left(\sum_{i=1}^n x_i \right) \left(\sum_{i=1}^n y_i \right) \quad [3.9ic]$$

$$S_e = \left[\frac{S_{xx} S_{yy} - (S_{xy})^2}{n(n-2) S_{xx}} \right]^{\frac{1}{2}} \quad [3.9id]$$

Using the Student's t distribution we can construct a confidence interval for α and β^* .

For α ;

$$C - t_{n/2} \cdot Se \left[\frac{S_{xx} + (\sum x_i)^2}{n S_{xx}} \right]^{\frac{1}{2}} < \alpha < C + t_{n/2} \cdot Se \left(\frac{S_{xx} + (\sum x_i)^2}{n S_{xx}} \right)^{\frac{1}{2}} \quad [3.9iia]$$

For β ;

$$M - t_{n/2} \cdot Se \left[\frac{n}{S_{xx}} \right]^{\frac{1}{2}} < \beta < M + t_{n/2} \cdot Se \left[\frac{n}{S_{xx}} \right]^{\frac{1}{2}} \quad [3.9iib]$$

The confidence level used throughout this report will be 95%. Therefore;

$$n = 1 - 0.95$$

$$n/2 = 0.025$$

3.9.2 Method of Application

From the Vishay units listed in Appendix A it was determined that each output voltage recorded is in error to $\pm 1\%$, thus, the assumption that y is normally distributed with common variance about the true line is reasonable and the M and C estimator error method is applicable. But x , the load configuration, is also in error due to instrument accuracy.

*See Appendix B for discussion of confidence intervals and the Student's t distribution.

The method of incorporating these two sources of error is outlined in a step by step procedure below. The data is recorded in the following manner:

x_i = represents the measured load
 y_i = represents the corresponding voltage output

1) from the measured load, add the load configuration error.
For example:

$$x_i + 10 \text{ lbs}$$

2) calculate the best fit line through this new data set[†];

$$x_i + 10 \text{ lbs}, y_i$$

3) apply the least squares error calculation therefore;

$$C_1 < \alpha < C_2 \quad [3.9iia]$$

$$M_1 < \beta < M_2 \quad [3.9iib]$$

4) determine the lowest extreme line from the above. In this case;

$$y_{\text{LOW}} = M_1 X + C_1$$

5) repeat steps 1 through 3 subtracting the load configuration error ($x_i - 10 \text{ lbs}$). This yields;

$$C_3 < \alpha < C_4 \quad [3.9iia]$$

$$M_3 < \beta < M_4 \quad [3.9iib]$$

6) determine the highest extreme line

$$y_{\text{HIGH}} = M_4 x + C_4$$

7) from the electrical calibration voltage add and subtract the Vishay error ($\pm 1\%$).

$$V_{\text{OECAL}} + 0.01(V_{\text{OECAL}}) = V_{\text{OHIGH}}$$

$$V_{\text{OECAL}} - 0.01(V_{\text{OECAL}}) = V_{\text{OLOW}}$$

8) from V_{OHIGH} calculate the corresponding load using the low extreme equation

[†]This best fit line will be shifted to the right of the original line, having lower slope and y intercept.

$$x_R = \frac{V_{oHIGH} - C_1}{M_1} \quad [3.9iia]$$

9) from V_{oLOW} calculate the corresponding load using the high extreme equation:

$$x_L = \frac{V_{oLOW} - C_4}{M_4} \quad [3.9iib]$$

Figure 3.15 graphically describes the above procedure, the end result is a range for electrical calibration.

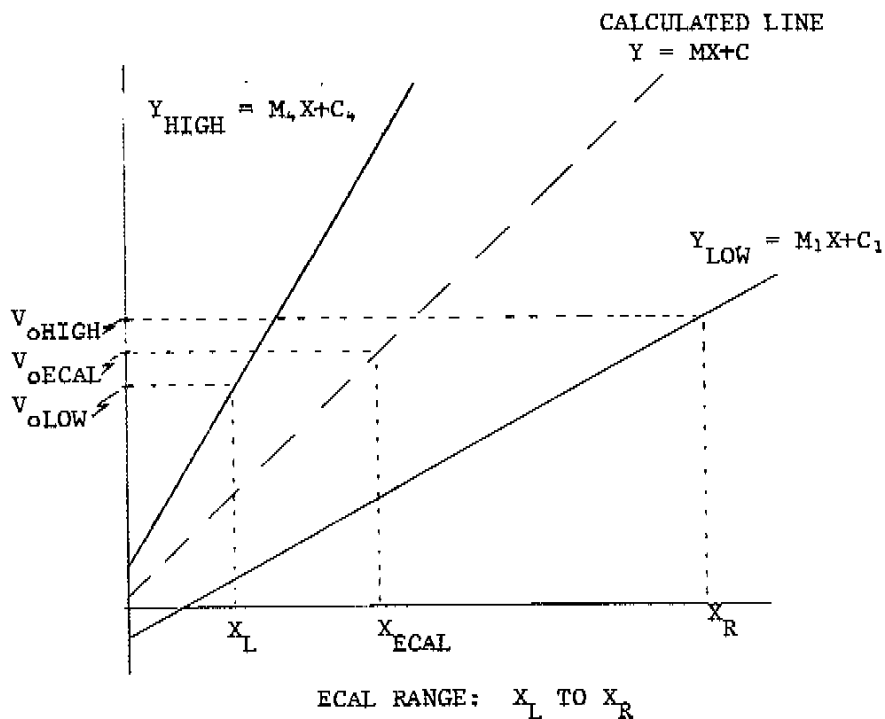


FIGURE 3.15
ERROR ANALYSIS

4. TORQUE CALIBRATION

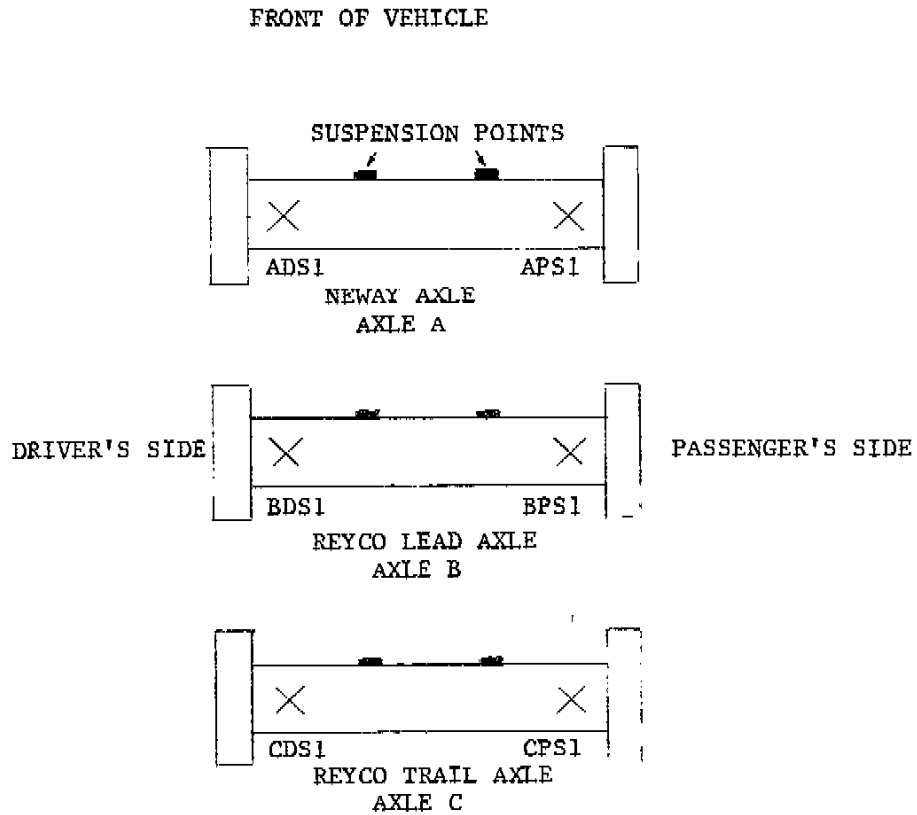


FIGURE 4.1
TORQUE GAUGE LOCATIONS

4.1 CALIBRATION PROCEDURE

To induce a torque on the axle a disk was cut from a one inch steel plate. Holes were drilled to match the trailer wheel bolt pattern. A six foot long I beam, measured from the axle center, was welded to the disk.

The axle was raised off the ground, the outside tire removed and the beam arrangement bolted to the axle. The beam was leveled and the brakes applied. A hydraulic jack was placed under the free end of the beam with a load cell situated on top of the jack (see Fig. 4.2).

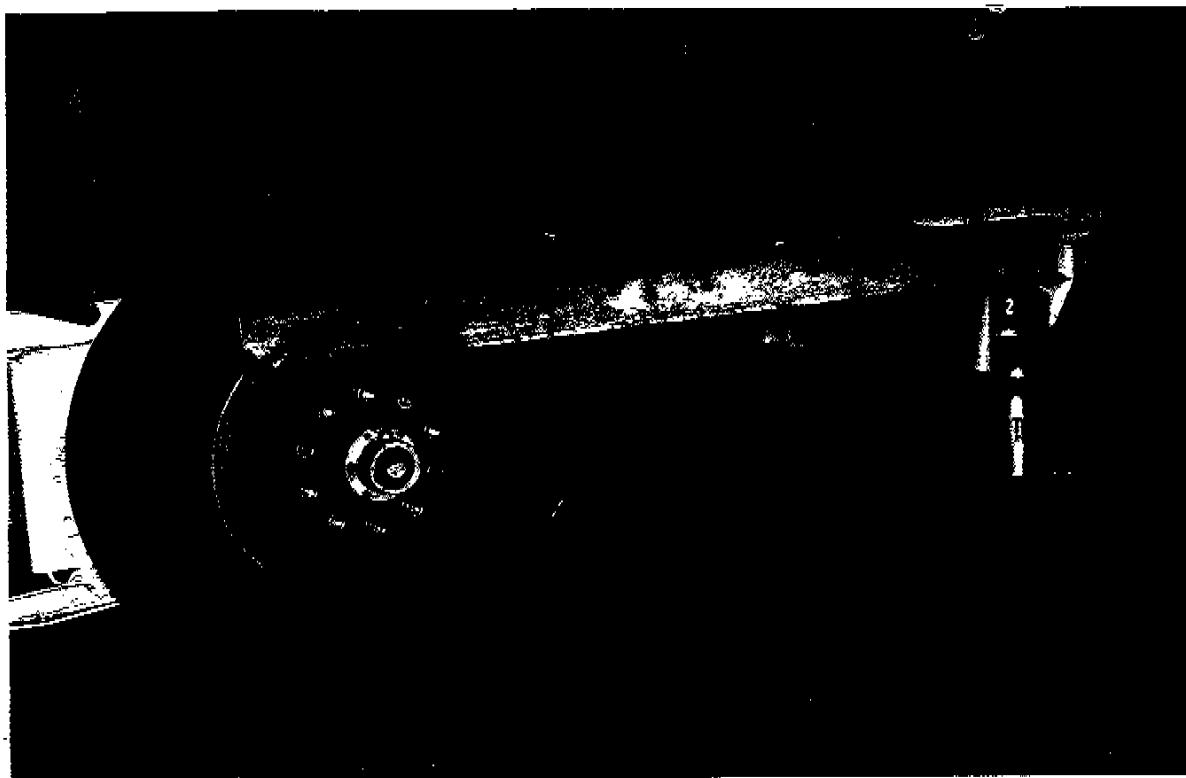


FIGURE 4.2
CALIBRATION CONFIGURATION

The jack and load cell were raised with a hand pump to induce a force six feet away from the axle center. The load cell indicator displayed the force, in pounds, applied by the jack.

The force was incremented to a maximum and decremented by a release valve on the hand pump, to the datum level. At predetermined levels the torque (force readout * 6 ft) and corresponding output voltage were recorded. Electrical calibration was performed at the datum level. A best fit line was plotted and the corresponding electrically calibrated torque was calculated.

4.2 DATA ANALYSIS

4.2.1 Initial Tests

The datum level is determined by the following axle configuration;

- i) the brakes off
- ii) the axle on the ground and
- iii) the beam assembly removed

The vertical shear stress contribution is zero, as previously discussed. The effect of bending was assumed to be zero. The calibration was carried out as per the procedure outlined in the previous section.

Three gauges were calibrated: ADS1, BPS1 and CPS1. Positive torque was considered to be in the direction of the applied force induced by the jack. For these three gauges positive torque was therefore;

ADS1: counterclockwise direction
BPS1: counterclockwise direction
CPS1: clockwise direction

The bridge voltage output sign was neglected and just the magnitude of the voltage was recorded. The gauge sensitivities are listed below in Table 5 and the calibration curves generated for this test are in Figure 4.3. Refer to Appendix C for the data values plotted in Figure 4.3.

Gauge	Sensitivity
ADS1	$\frac{0.2 \text{ mV}}{V^+} \cong 3040 \text{ ft*lbs}$
BPS1	$\frac{0.2 \text{ mV}}{V^+} \cong 3279 \text{ ft*lbs}$
CPS1	$\frac{0.2 \text{ mV}}{V^+} \cong 3115 \text{ ft*lbs}$

TABLE 5
GAUGE SENSITIVITIES

INITIAL TORQUE CALIBRATION

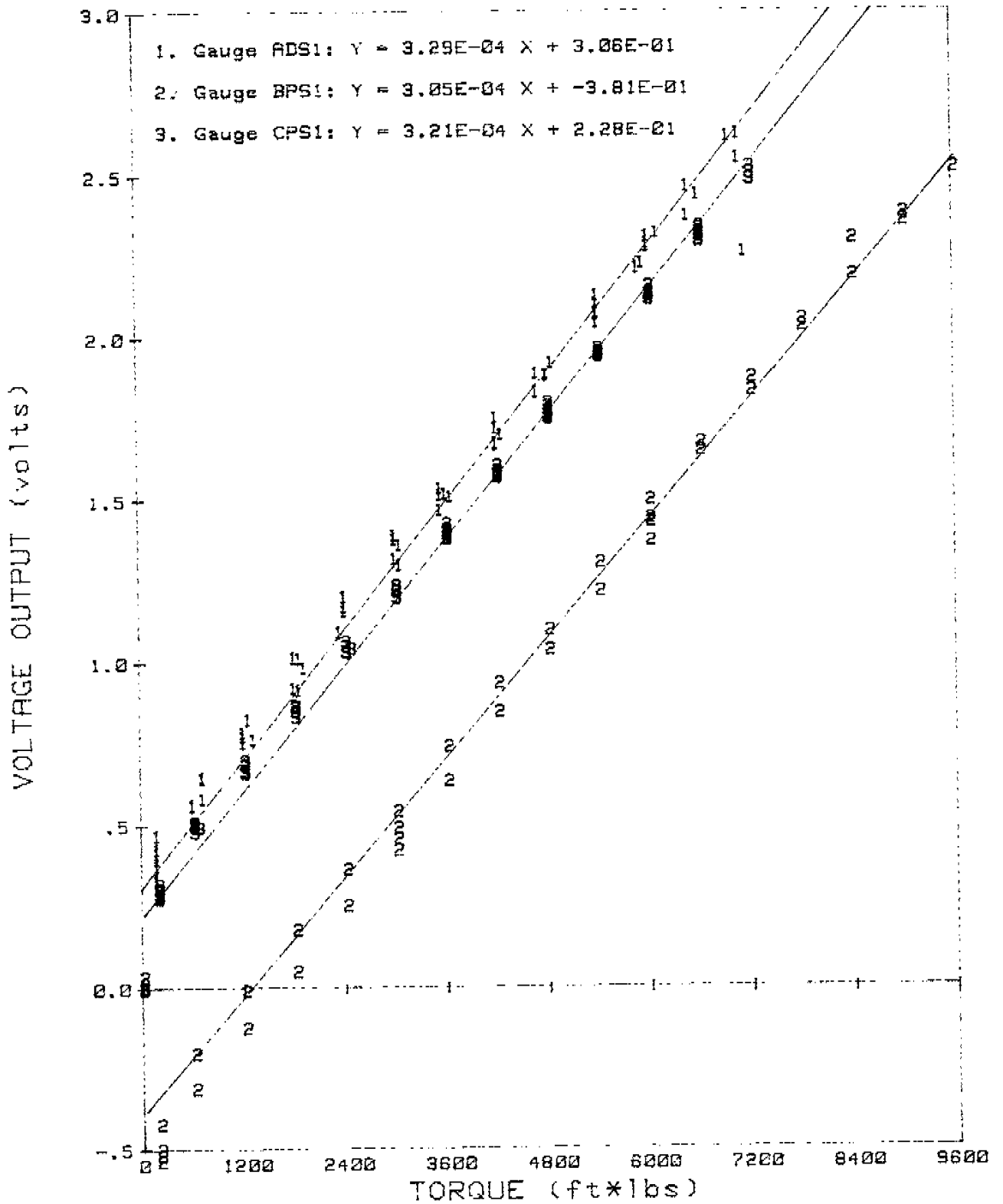


FIGURE 4.3

Conclusions drawn from the test were all torsion gauges behave virtually the same as seen in Table 5, and not all torque contributing factors were considered as can be seen by the marked offset from the origin of the graph in Figure 4.3

4.2.2 Brake Application Torque

The mechanism which activates the brakes induces a torque on the axle.

The brake pod, which is fixed to the axle by a bracket, is supplied with air. A diaphragm expands within the pod pushing a rod which is attached to the slack adjuster. The slack adjuster pivots and turns the S arm which activates the brakes (see Fig. 4.4).

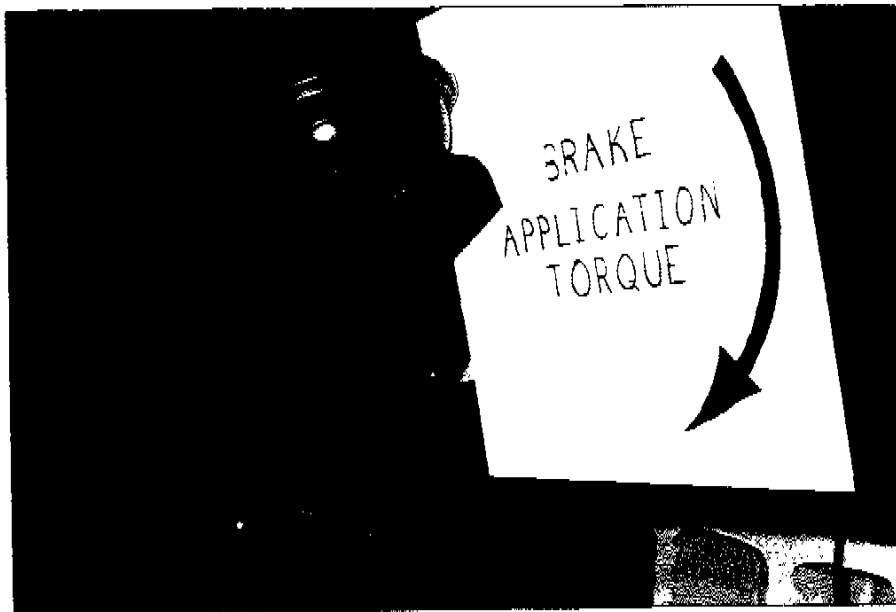


FIGURE 4.4
BRAKE APPLICATION TORQUE

When charged with air the diaphragm is forced against the brake pod. This force pushes the rod and activates the slack adjuster. The moment arm of the force is the rod center to the axle center, six inches (6"). The diaphragm area is 30 square inches. Knowing the air pressure supplied to the diaphragm gives the force pushing the rod and multiplying by the moment arm results in the brake application torque.

$$T_{BR} = 30 \text{ in}^2 * \text{SUPPLIED AIR PRESSURE} \left(\frac{\text{lbs}}{\text{in}^2}\right) * \frac{1}{2} \text{ ft}$$

$$T_{BR} = 15(\text{in}^2 * \text{ft}) * \text{PSI} = \text{ft} * \text{lbs} \quad [4.2i]$$

Because of the brake mechanism orientation on the axle it applies a clockwise torque to all driver's side gauges and a counter-clockwise torque to all passenger side gauges when activated. The supplied air pressure does not remain constant during calibration, therefore it had to be recorded with each output voltage and applied torque.

4.2.3 Beam Torque and Bending Effect

The beam arrangement was not made from weightless material. Therefore its contribution to the results had to be considered. The beam torque always opposed the torque induced by the jack.

To ascertain the magnitude of the torque the free end of the beam arrangement was allowed to rest on a sensitive scale. The moment arm was measured and the torque obtained. The contribution of the beam arrangement used on the drivers side was 250 ft*lbs and 240 ft*lbs for the passenger side arrangement.

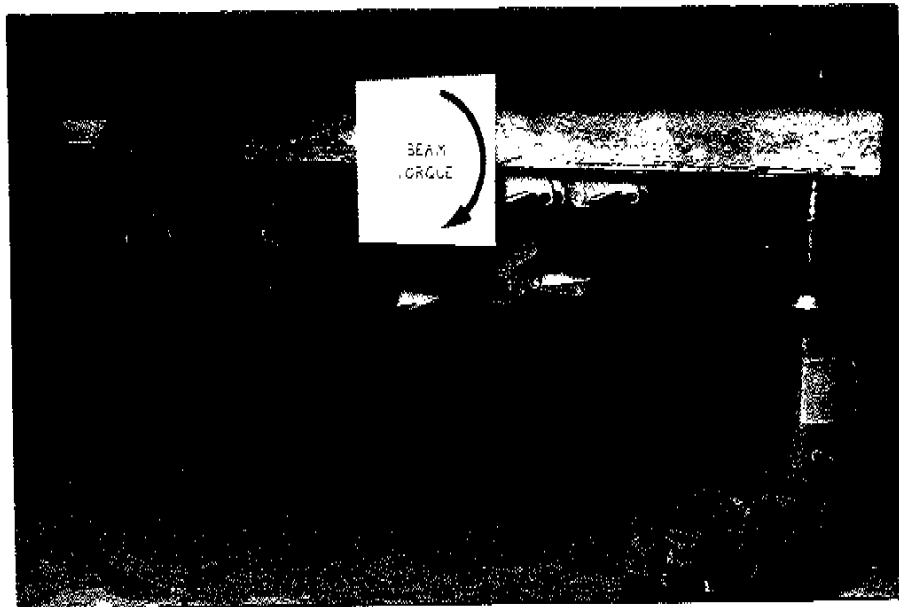


FIGURE 4.5
BEAM TORQUE

The effect of bending was determined during the vertical load calibration. The datum level was maintained consistent. The result being no matter what the vertical load the bending effect contaminates the voltage output on the torque gauges by a constant amount.

4.2.4 Sign Convention

A sign convention was developed for the sake of consistency.

Positive torques will be those torques which act in the direction of wheel rotation while travelling forward. Therefore torques induced in the counterclockwise (CCW) direction on the driver's side are positive and those torques which are applied in the clockwise (CW) direction on the passengers side are positive.

These positive senses are determined by looking directly at the axle side being calibrated.

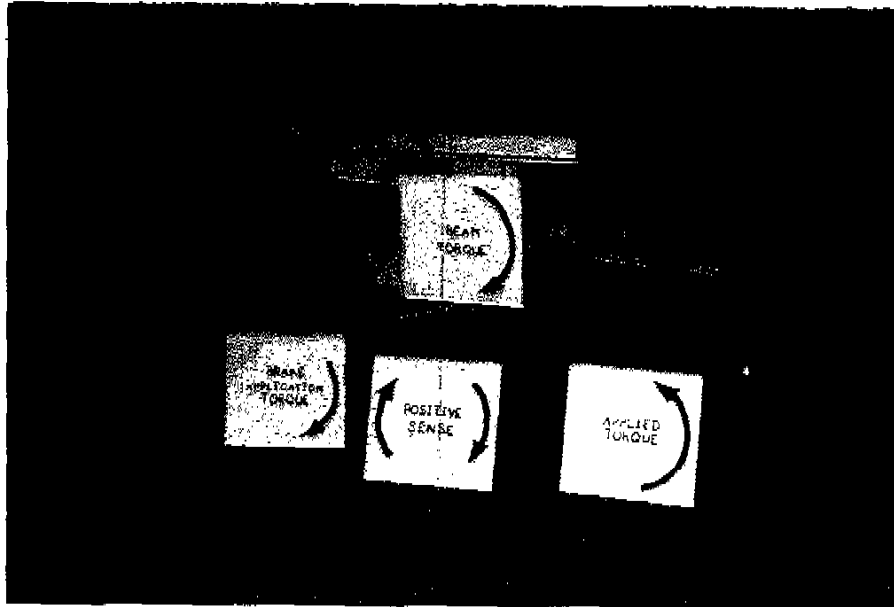
4.3 FINAL CALIBRATION TEST

For this test two gauges were monitored with consideration given to all variables. Gauge ADS1 was calibrated applying the torque via the jack, in the positive sense. Gauge BPS1 was calibrated with the applied torque in the negative direction.

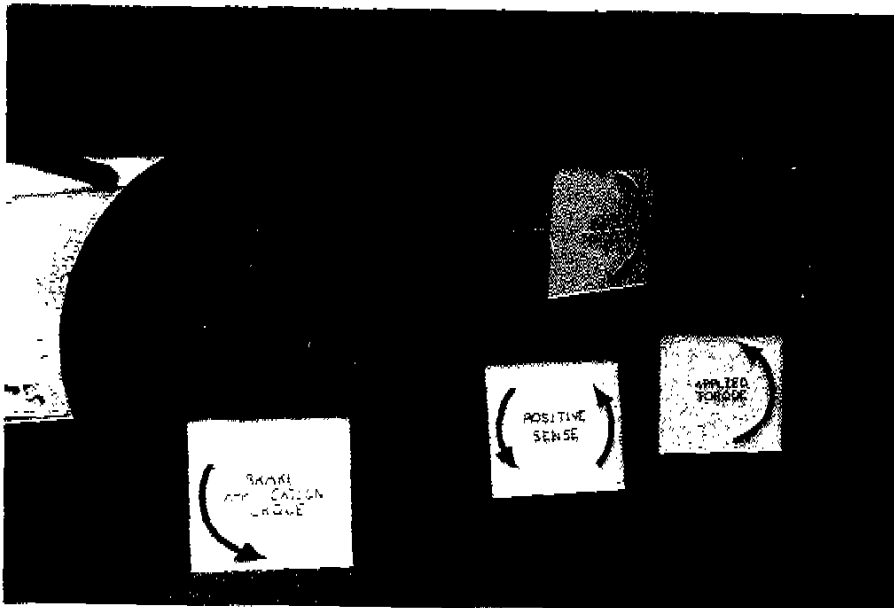
Figure 4.6 shows the sense of all contributing torques with respect to the positive sign convention adopted for each gauge.

Gauge; ADS1 Vertical Load Range; V_o Due to Bending	Gauge; BPS1 Vertical Load Range; V_o Due to Bending
-0.002	-0.011
-0.008	-0.022
-0.007	-0.036
-0.007	-0.040
-0.003	-0.021
-0.005	-0.020
-0.005	-0.032
-0.004	-0.036
-0.004	-0.020
-0.006	-0.014
-0.006	-0.023
$\bar{X} = -0.005$	-0.030
	-0.037
	-0.041
	-0.032
	-0.025
	-0.011
	$\bar{X} = -0.027$

TABLE 6
BENDING EFFECT FOR GAUGES ADS1 AND BPS1



PASSENGER'S SIDE



DRIVER'S SIDE

FIGURE 4.6
SIGN CONVENTION

DEC., 16, 1985

TORQUE CALIBRATION OF ADS1

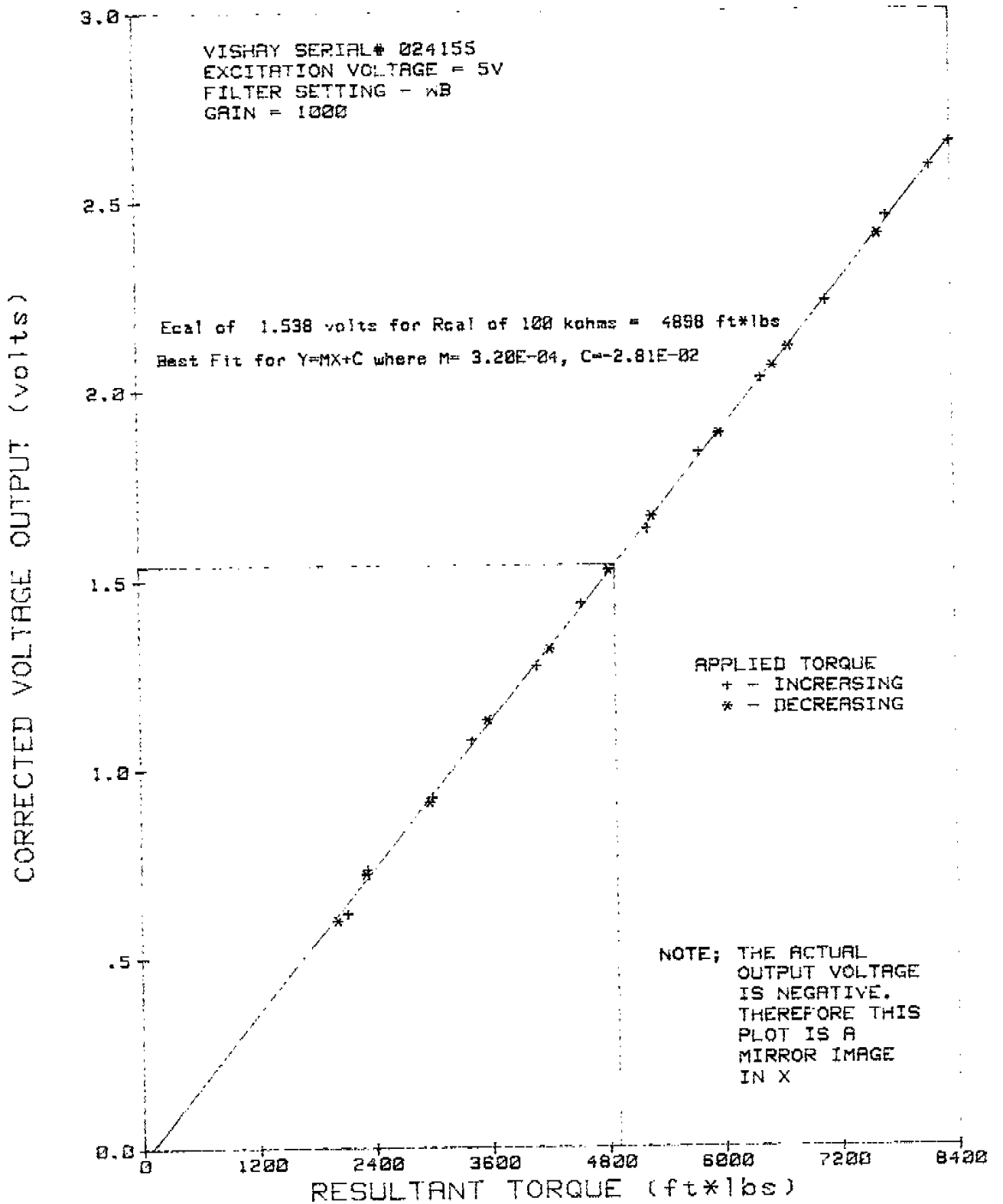


FIGURE 4.7

TORQUE CALIBRATION OF BPS1

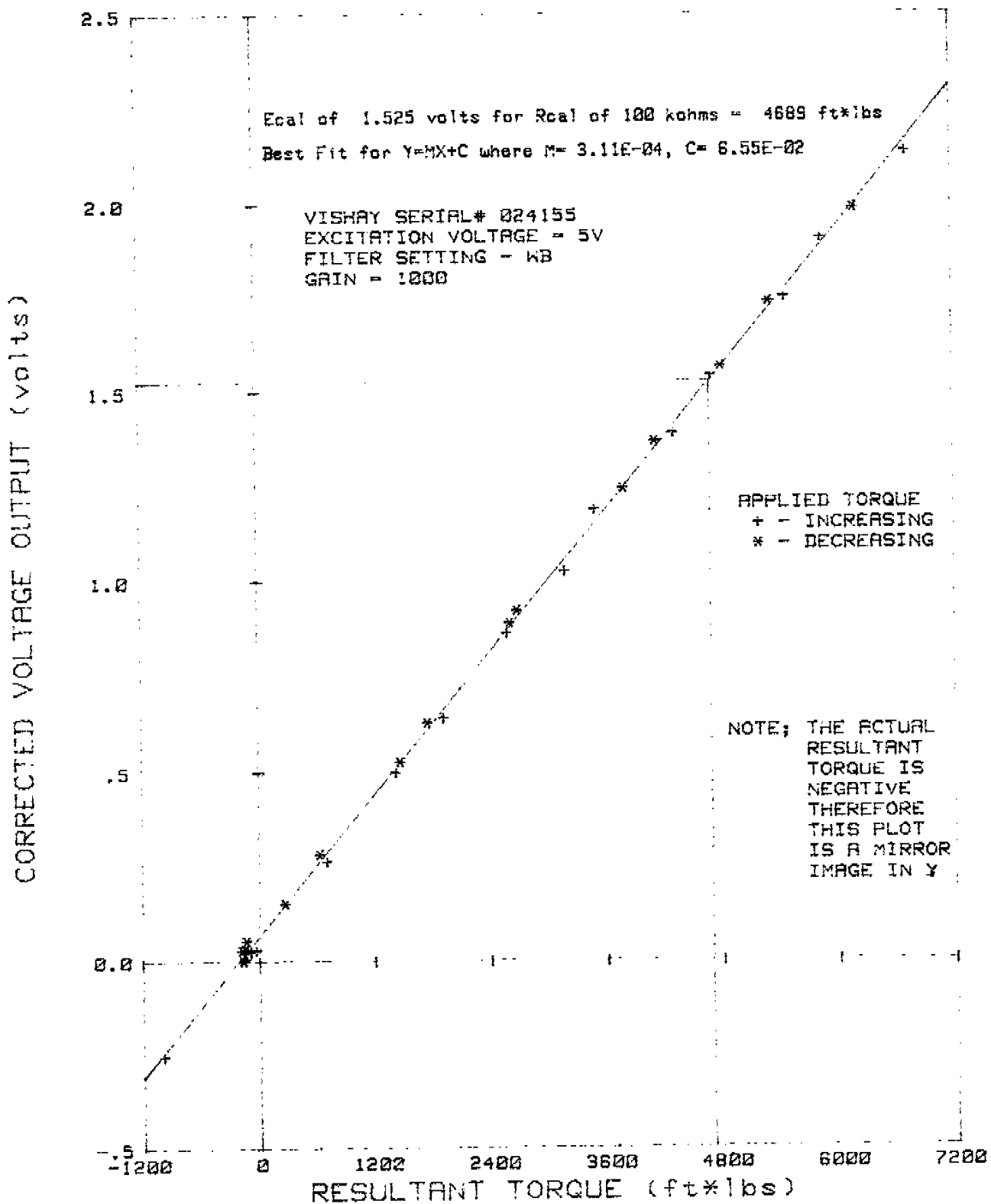


FIGURE 4.8

ACTUAL ORIENTATION OF CALIBRATION PLOTS

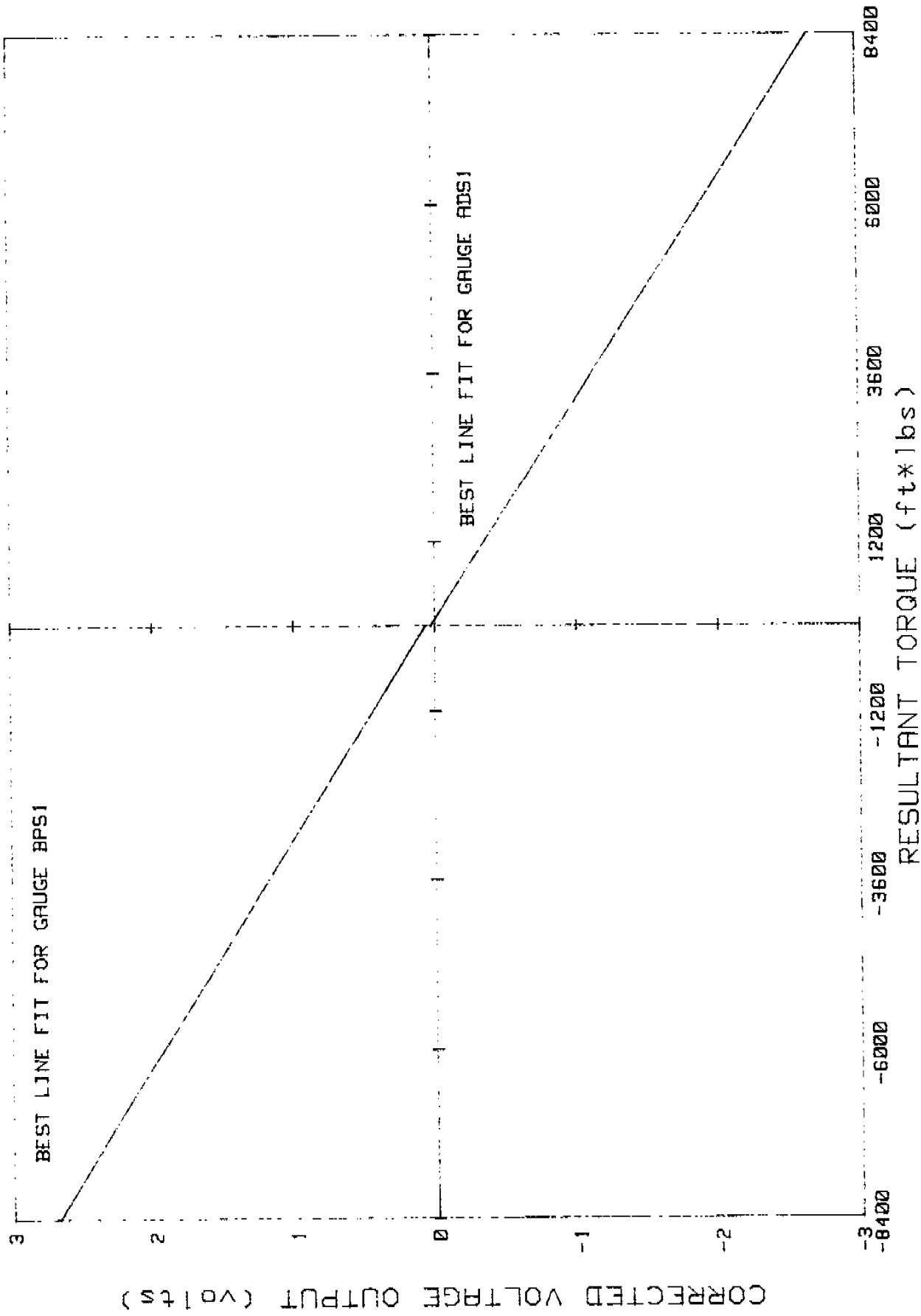


FIGURE 4.9

Table 6 on page 42 lists the bending effect of each gauge being calibrated. The average bending cross table for gauge ADS1 is -0.005 volts therefore 0.005 volts is added to the recorded voltage readings to compensate for bending. A factor of 0.027 volts is added to gauge BPS1 by the same reasoning.

The graphical results for the calibration of gauge ADS1 are presented in Figure 4.7. Figure 4.8 exhibits the results of calibration on gauge BPS1. Appendix D gives the table of results plotted for both gauges.

4.4 DISCUSSION OF RESULTS

The two gauges ADS1 and BPS1 displayed good sensitivity, linearity, and repeatability.

For the purpose of error analysis the calibration plots (Figures 4.7 and 4.8) were transformed into the first quadrant of the Cartesian plane. The ADS1 calibration plot in Figure 4.7 is a mirror image in X and Figure 4.8 is a mirror image in Y. These transformations do not affect the magnitude of the plotted values. If our sign convention were different for torque and the voltage output recorder was connected reversing the polarity these mirror images would be the actual plots. The error analysis is documented in Appendix E the results are reported in Table 7 below;

Gauge ADS1

ECAL Range; $1.538 \pm 1\%$ volts $\equiv 4898 \pm 5.2\%$ ft*lbs

Sensitivity Range; $\frac{0.2 \pm 1\% \text{ mV}}{V^+} \equiv 3125 \pm 0.7\%$ ft*lbs

Gauge BPS1

ECAL Range; $1.525 \pm 1\%$ volts $\equiv 4689 \pm 5.4\%$ ft*lbs

Sensitivity Range; $\frac{0.2 \pm 1\% \text{ mV}}{V^+} \equiv 3215 \pm 1.3\%$ ft*lbs

TABLE 7
ERROR BOUNDS FOR GAUGES ADS1 AND BPS1

From Table 7 the gauge sensitivity ranges indicate that the estimated measurement errors listed in Appendix E are reasonable and the error analysis procedure is valid.

The best fit line for gauge BPS1 is:

$$y = 3.11 \times 10^{-4} X + 6.55 \times 10^{-2}$$

calculating the torque for the electrical calibration voltage of gauge ADS1 using the BPS1 best fit line yields 4735 ft*lbs. This value falls within the electrical calibration range calculated for ADS1.

The best fit line for gauge ADS1 is;

$$y = 3.20 \times 10^{-4} X - 2.81 \times 10^{-2}$$

calculating the torque at 1.525 volts, BPS1 electrical calibration value, yields 4853 ft*lbs. This is within the range of electrical calibration for gauge BPS1.

Therefore all torque gauges will behave similarly when all torque contributing factors are considered.

The strain gauge missalignment errors resulting in voltage outputs due to bending may also produce a voltage output due to the shear stress caused by braking friction. All torque gauges should be tested to determine the bending and shear effects.

4.5 SAMPLE CALCULATION

A voltage output of -1.5 volts is recorded from gauge ADS1. What is magnitude of the applied torque assuming the lead wire lengths of 50 ft, and given a gain of 1000 and an excitation voltage of 5V.

From [3.5vii]

$$V_o = \frac{5000}{R_G^*} (\pm r)$$

$$\therefore -1.5 R_G^* = 5000 (-r)$$

from [3.5vi]

$$R_G^* = R_G + 2 R_L$$

$$R_G^* = 120 + 2(50)(0.015) = 121.6 \Omega$$

$$\therefore r = 3.648 \times 10^{-2}$$

from [3.4i]

$$\Delta R = r$$

$$\frac{r}{R_G} = K_G \epsilon$$

$$\frac{3.648 \times 10^{-2}}{120} = 2.01 \epsilon$$

$$\epsilon = 151.2 \mu \text{ strains} = 151.2 \times 10^{-6} \frac{\Delta L}{L}$$

from [3.5iva]

$$\epsilon_{45^\circ} = \frac{1}{2} * \left(\frac{\sigma_x}{E} + \frac{\tau}{G} \right)$$

$$\sigma_x = 0$$

$$G = 11.5 \times 10^6 \text{ lbs/in}^2$$

$$\tau = 3.48 \times 10^4 \text{ lb/in}^2$$

from [3.1i]

$$\tau = \frac{Tc}{J}$$

$$c = 2.5 \text{ in}^4$$

$$J = \frac{1}{2} \pi (2.5^4 - 1.875^4) = 41.9 \text{ in}^4$$

$$\therefore T = 5.83 \times 10^4 \text{ ft*in} = 4857 \text{ ft*lbs}$$

Using the best fit line of gauge ADS1 and an output voltage of 1.5 volts (due to the transformation used) results in a torque of 4775 ft*lbs. This is within 2% of the above calculated value. Therefore the assumed lead wire length of 50 ft is reasonably accurate.

5. VERTICAL LOAD CALIBRATION

5.1 WEIGH SCALE PREPARATION

The weigh scale used was designed to weigh railway cars. To serve the purpose of monitoring axle weight a $\frac{1}{2}$ " plate was placed over the weight scales' rail section. This plate was of a sufficient width to accommodate both dual wheels of a single axle.

To monitor only one axle of a tandem set a 'C' channel was placed over the rails and raised clear of the scale by placing four one inch thick pieces of steel on both sides of each rail. The axle that is not of concern in the tandem set is driven onto this channel where it would not affect the scale reading.

5.1.1 Tractor Trailer Preparation

The front and rear compartments of the tanker trailer were filled with water. The purpose of this exercise was to induce an appropriate full scale load. The compartments were completely filled to prevent liquid slosh.

At zero, or the datum level, an electrical calibration was performed.

The data and a best fit line was plotted. The same process was followed to calibrate the Rear Drive Axle. The gauges monitored were D6, P6, D9, P9.



FIGURE 5.2
DATUM LEVEL

5.2.2 Discussion of Results

All gauges displayed a low sensitivity and non linear results. A further investigation is necessary before the results can be reported with confidence (see Appendix F for results).

5.3 TRAILER AXLE CALIBRATION

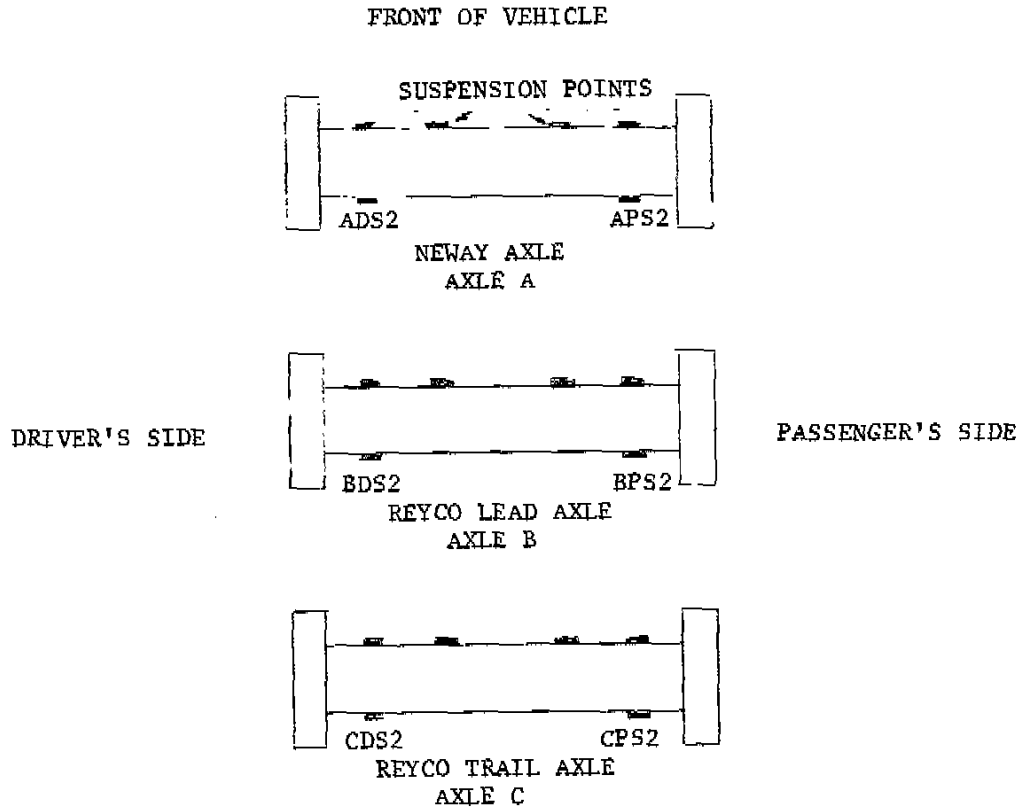


FIGURE 5.3
TRAILER GAUGE LOCATIONS

5.3.1 Procedure Followed for the Reyco Tandem Set

Axle B, the lead tandem axle, was calibrated first. Axle C was on the C channel clear of the scale. Gauges BDS2, BPS2 and BPS1 were monitored. The reaction of gauge BPS1, the torque gauge, was monitored to establish the effect of vertical loading.

With the brakes off and the axle lifted clear of the scale by a vertical hoisting crane all gauges in question were zeroed. This configuration was chosen as the datum level because it is the point where the road experiences zero load.

The scale was preset to 2 tonnes and the axle was slowly lowered onto the plate until a deflection on the scale was detected. The hoist was stopped and an accurate scale reading was obtained. The voltage readings for all gauges were recorded.

Load was increased in approximately 2 tonne intervals following the above procedure until full axle load was achieved. The process was then reversed lifting the axle off the scale in 2 tonne intervals.

At the datum level an electrical calibration was performed. The data for each vertical load gauge was plotted on a graph of output voltage versus the total road load. The procedure was repeated for axle C.

5.3.2 Procedure Followed for the Neway Axle

Calibration of the Neway axle, axle A, followed the same basic outline, the difference being that the hoist was not needed. The Neway axle is an air lift axle and increasing and decreasing the load on the plate was accomplished by restricting the air flow to the lift mechanism.

5.4 SENSITIVITY OF THE MEASUREMENT SYSTEM TO BIAS TIRE LOADING

A test was performed to simulate the load gauge response while driving on non level ground, that is when all wheels on an axle set are not in contact with the road.

5.4.1 Test Procedure

This test was performed using axle A and monitoring gauge ADS2. The gauge was zeroed in the raised position, zero pavement load. The axle was lowered with the outside tire resting on a 1" steel plate, a reading was taken. This procedure was repeated with the plate under the inside tire and then no plate at all.

5.4.2 Results

	Voltage
Axle Up	0.0
Axle Down	
Plate under Outside tire	+1.480
Plate under I/S tire	+0.510
No Plate	+0.915
Axle Up	0.0
O/S Tire	+1.524
I/S Tire	+0.516
No Plate	+1.061

5.4.3 Discussion of Results

The strain gauges for vertical loading are affected by the direct stress due to bending.

$$\sigma = \frac{F \cdot xy}{I} \quad [3.211]$$

The same vertical load produced varying results because the bending stress depends on the induced force and the distance that force is to the strain gauge location on the axle. Therefore two variables determine the amount of stress, thus strain, experienced by the axle. Care must be taken in selecting test sites. Rutted roads should be avoided for better loading predictions. Also the tire pressure must be maintained constant in all tires to avoid bias tire loading. All calibration plots showed very little deviation from the best fit line.

Each wheel should be calibrated with respect to the load which that wheel imparts on the road to determine the load sharing activity of the axles. This will also provide a check for the calibrations performed and listed in Appendix G.

5.5 AN ALTERNATE SOLUTION

A shear stress is also produced by vertical loading:

$$\tau = \frac{FQ}{It} \quad [3.21]$$

The only possible variable which can change the value of this shear stress is F , the vertical load or shear force. All other variables remain constant as long as the strain gauge remains fixed on the axle circumference.

Figure 3.2b on page 8 describes how the shear stress flows through the axle's cross section. The location of maximum stress is at the neutral axis.

Strain gauges will respond to shear stress if they are oriented at 45° and 135° to the neutral axis as discussed in section 3.5. A slight variation in the Wheatstone Bridge circuit used to detect strain due to torsion will result in a voltage output from strains caused by the shear stress due to vertical loading.

Figure 5.4 presents the proposed Wheatstone bridge circuit to be used for shear force. Comparing this circuit to the torsion circuit (Fig. 3.5 p. 14), the gauges will have the same orientation on the axle but gauges 2 and 3 have been interchanged.

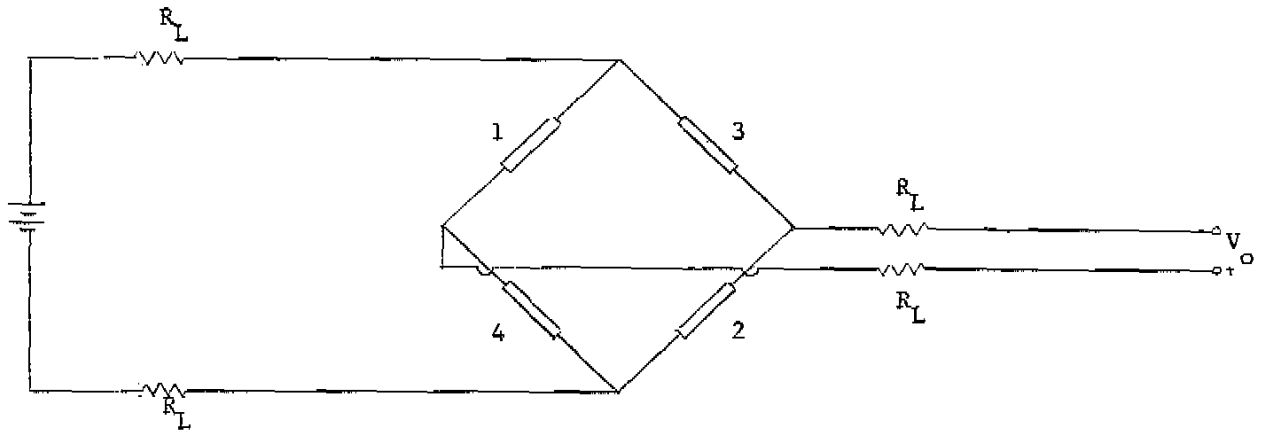


FIGURE 5.4
PROPOSED VERTICAL LOAD CIRCUIT

The voltage output for the shear force bridge is given by the following equation:

$$V_o = V^+ \left[\frac{R_1}{R_1 + R_4} - \frac{R_3}{R_2 + R_3} \right] * AF \quad [5.41]$$

Figure 3.7 on page 18 describes the gauge reactions to a shear stress caused by vertical loading. Element A, on the rear face of the axle, contains gauges 1 and 4. Element B, on the front face of the axle includes gauges 2 and 3. As noted in section 3.5.3 the elements are experiencing stresses in opposite directions when compared to each other.

The shear stress in element A will be considered positive. Knowing the gauge orientation with respect to the neutral axis and using formulae [3.5iva and b] (keeping in mind the above sign convention) strain experienced by the gauges due to the shear force F are:

$$\epsilon_1 = -y \mu \text{ strains}$$

$$\epsilon_2 = -y \mu \text{ strains}$$

$$\epsilon_3 = +y \mu \text{ strains}$$

$$\epsilon_4 = +y \mu \text{ strains}$$

From [3.4i] the change in gauge resistance is:

$$\Delta R = \pm r$$

where the sign of the resistance change will be the same as the sign of strain and all gauge resistances (R_G^* from [3.5vi]) are equal. Therefore from [5.41]:

$$V_o = V^+ \left[\frac{R_G^* - r}{2R_G^*} - \frac{R_G^* + r}{2R_G^*} \right] * AF$$

$$V_o = V^+ \left[\frac{-2r}{2R_G^*} \right] * AF$$

$$V_o = \frac{-V^+ * r * AF}{R_G^*}$$

for a shear force applied in the upward direction.

Considering both possible loading directions where shear in the upward direction is positive:

$$V_o = \frac{V^+ * \pm r * AF}{R_G^*} \quad [5.4ii]$$

Applying a torque in either direction will have no effect on the Wheatstone bridge circuit as will be proven.

Consider a clockwise torque as positive and an oppositely applied torque as negative. Both shear stress elements on the axle containing the gauges will be oriented in the same direction. Below are listed the strains experienced by the gauges. Positively applied torque is the top sign. From [3.5iva and b] and from [3.4i]:

$$\epsilon_1 = \pm y \mu \text{ strains and } \Delta R = \pm r$$

$$\epsilon_2 = \mp y \mu \text{ strains and } \Delta R = \mp r$$

$$\epsilon_3 = \pm y \mu \text{ strains and } \Delta R = \pm r$$

$$\epsilon_4 = \mp y \mu \text{ strains and } \Delta R = \mp r$$

From [5.4i]

$$V_o = V^+ \left[\frac{R_G^* \pm r}{R_G^* \pm r + R_G^* \mp r} - \frac{R_G^* \pm r}{R_G^* \pm r + R_G^* \mp r} \right] * AF$$

therefore $V_o = 0$ and torque has no effect.

Bending due to vertical and frictional forces will also have no effect if the gauges are placed carefully at the same spots over the neutral axis on both faces of the axle. Refer to section 3.5.3 and 3.5.4 where these effects are considered with respect to the torque instrumentation. The same arguments apply here.

This gauge arrangement should be investigated to determine if it shows good sensitivity and reduces the sensitivity to error as shown in the bending gauge arrangement due to bias tire loading.

REFERENCES

1. Beer, Ferdinand P., E. Russell Johnston Jr., 1981. Mechanics of Materials, McGraw-Hill Book Company, New York.
2. Miller, Irwin, John E. Freund, 1977. Probability and Statistics for Engineers, 2nd Edition, Prentice-Hall Inc., New Jersey.
3. Perry, C.C., H.R. Lissner, 1955. The Strain Gauge Primer, 2nd Edition, McGraw-Hill Book Company, New York.
4. Smith, Ralph J., 1976. Circuits Devices and Systems, 3rd Edition, John Wiley and Sons Inc., New York.

APPENDIX A

VISHAY ERROR

A bench test was performed to determine the error in each reading conditioned by a Vishay.

All Vishay units used during the calibration procedure were interfaced with an Intertechnology 1550 Strain Indicator Calibrator (S.I.C.) which simulates the different resistance changes due to varying strains.

The excitation voltage and gain were set as in the calibration procedure, 5 volts and 1000 respectively.

Test Procedure:

1. Each vishay was balanced at zero μ strains.
2. 600 μ strains then 1600 μ strains were induced via the S.I.C. and the voltage output recorded.
3. Electrical calibration voltage output was also recorded.
4. Steps 2 and 3 were repeated 3 times for each vishay.
5. The average output voltage of the three reading for 600 μ strains were calculated for each vishay. The readings of 1600 μ strains and electrical calibration were also averaged for each Vishay to yield the mean Vishay reading.
6. The overall average was then calculated for each strain level.
7. The overall average was subtracted from the individual mean Vishay readings for each strain level.
8. An average of these values was calculated giving the mean change in readings.
9. The error was determined by dividing the overall reading average into the mean change in readings and multiplying by 100%. The results are documented in Table A1.

Vishay Serial #	Reading at 600 μ strains (in volts)	$\bar{X} - \bar{X}_1$	Reading at 1600 μ strains (in volts)	$\bar{X} - \bar{X}_1$	Reading at Electrical calibration (in volts)	$\bar{X} - \bar{X}_1$
024155	1.454 1.455 <u>1.456</u> $\bar{X}_1 = 1.455$	0.043	3.896 3.899 <u>3.899</u> $\bar{X}_2 = 3.898$	0.102	1.466 1.466 <u>1.467</u> $\bar{X}_1 = 1.466$	0.049
024074	1.527 1.527 <u>1.531</u> $\bar{X}_2 = 1.528$	-0.030	4.077 4.077 <u>4.081</u> $\bar{X}_2 = 4.077$	-0.077	1.544 1.545 <u>1.548</u> $\bar{X}_2 = 1.546$	-0.031
045349	1.497 1.496 <u>1.495</u> $\bar{X}_3 = 1.496$	+0.002	3.994 3.992 <u>3.992</u> $\bar{X}_3 = 3.993$	0.007	1.508 1.597 <u>1.506</u> $\bar{X}_3 = 1.507$	0.008
024076	1.505 1.505 <u>1.501</u> $\bar{X}_4 = 1.504$	-0.006	4.015 4.015 <u>4.015</u> $\bar{X}_4 = 4.015$	-0.015	1.515 1.515 <u>1.515</u> $\bar{X}_4 = 1.515$	0.0
024072	1.484 1.484 <u>1.483</u> $\bar{X}_5 = 1.484$	0.014	3.955 3.955 <u>3.956</u> $\bar{X}_5 = 3.955$	0.045	1.513 1.513 <u>1.513</u> $\bar{X}_5 = 1.513$	0.002
024054	1.497 1.496 <u>1.483</u> $\bar{X}_6 = 1.496$	0.002	3.990 3.989 <u>3.985</u> $\bar{X}_6 = 3.988$	0.012	1.509 1.507 <u>1.507</u> $\bar{X}_6 = 1.508$	0.007
024954	1.525 1.524 <u>1.522</u> $\bar{X}_7 = 1.524$	-0.026	4.069 4.070 <u>4.068</u> $\bar{X}_7 = 4.069$	-0.059	1.537 1.537 <u>1.537</u> $\bar{X}_7 = 1.537$	-0.022
043029	1.498 1.495 <u>1.497</u> $\bar{X}_8 = 1.497$	0.001	4.006 4.005 <u>4.007</u> $\bar{X}_8 = 4.006$	-0.006	1.527 1.525 <u>1.523</u> $\bar{X}_8 = 1.525$	-0.01
AVERAGES	1.498	0.016	4.000	0.042	1.515	0.016

$$E_{600\mu\epsilon} = \frac{0.016}{1.498} \times 100\% = 1\%$$

$$E_{1600\mu\epsilon} = \frac{0.42}{4.000} \times 100\% = 1\%$$

$$E_{ECAL} = \frac{0.016}{1.515} \times 100\% = 1\%$$

TABLE A1
VISHAY ERROR TESTS AND RESULTS

APPENDIX B

CONFIDENCE INTERVALS AND THE STUDENT'S t DISTRIBUTION

Since point estimates cannot be expected to coincide with the quantities they are intended to estimate, it is sometimes preferable to replace them with interval estimates, that is, intervals for which one can assert with a reasonable degree of certainty that they contain the parameter under consideration.

The Student's t distribution is used to estimate the confidence interval because the y data points are assumed to be a normally distributed population about the mean α and βx but we do not have an infinite number of data points to use the normal distribution with certainty.

The Student's t distribution has a similar shape to that of a normal distribution, but its variance (shape) depends upon a parameter called the number of degrees of freedom (see Fig. B.1).

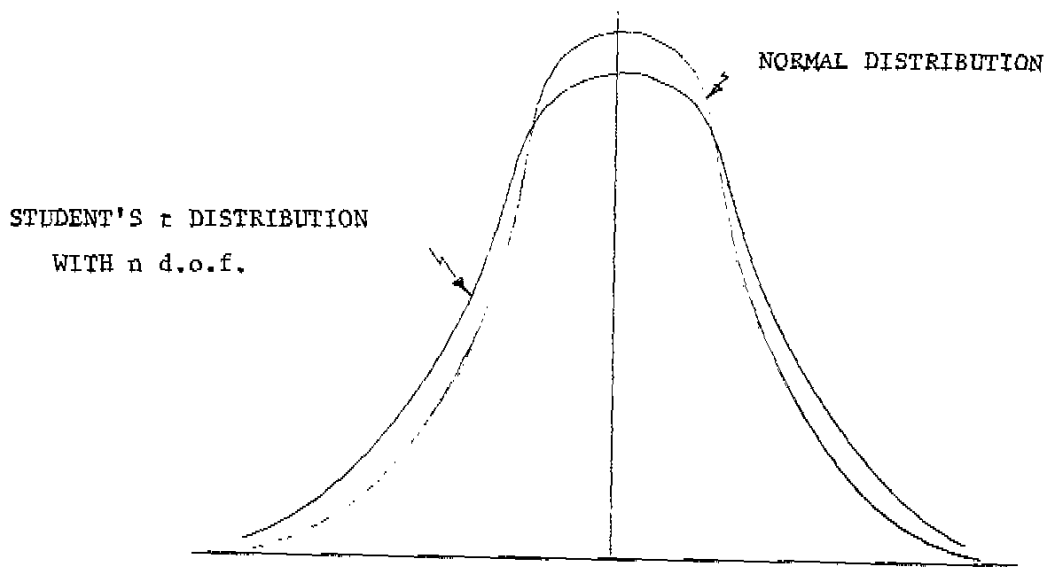


FIGURE B.1

For our purpose we have $n-2$ degrees of freedom, where n represents the number of data points. Two degrees of freedom are lost because α and β are replaced by their least squares estimations.

A confidence interval of 95% establishes a range of acceptable numbers for α and β doing away with the other 5%. The deleted 5% is split such the last 2.5% of the numbers lying within the distribution range are omitted from the right tail and the other 2.5% omitted from the left tail (see Fig. B.2).

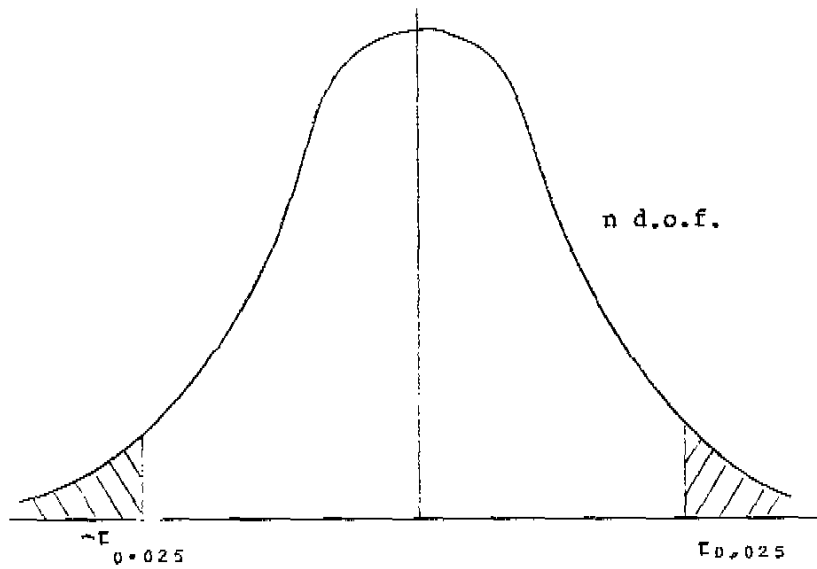


FIGURE B.2

Degrees of Freedom	$t_{0.025}$	Degrees of Freedom	$t_{0.025}$
1	12.706	16	2.120
2	4.303	17	2.110
3	3.182	18	2.101
4	2.776	19	2.093
5	2.571	20	2.086
6	2.447	21	2.080
7	2.365	22	2.074
8	2.306	23	2.069
9	2.262	24	2.064
10	2.228	25	2.060
11	2.201	26	2.056
12	2.179	27	2.052
13	2.160	28	2.048
14	2.145	29	2.045
15	2.131	30	1.960

TABLE B.1
CONFIDENCE VALUES

APPENDIX C

INITIAL TORQUE CALIBRATION DATA TABLES

 * DATA MANIPULATION *

 INITIAL CALIBRATION OF GUAGE ADS1

Data file name: DATA
 Number of observations: 70
 Number of variables: 2

Variables names:
 1. APPL TORQ
 2. VOITS OUT

Subfiles: NONE

INITIAL CALIBRATION OF GUAGE ADS1

OBS#	Variable # 1	Variable # 2
1	180.00000	.37600
2	600.00000	.56100
3	1200.00000	.75700
4	1800.00000	.92200
5	2400.00000	1.20000
6	3000.00000	1.31600
7	3600.00000	1.51800
8	4200.00000	1.67500
9	4800.00000	1.88400
10	5400.00000	2.06900
11	5880.00000	2.21200
12	6600.00000	2.43900
13	7140.00000	2.26200
14	6000.00000	2.27900
15	5400.00000	2.07500
16	4800.00000	1.88000
17	4260.00000	1.70000
18	3660.00000	1.50900
19	3000.00000	1.39000
20	2400.00000	1.20000
21	1800.00000	1.01500
22	1260.00000	.82800
23	720.00000	.64600
24	180.00000	.42700
25	0.00000	.00200
26	1200.00000	.77700
27	2400.00000	1.17000
28	3540.00000	1.51500
29	4860.00000	1.92100
30	6120.00000	2.32200
31	7080.00000	2.62400
32	6000.00000	2.29000

33	5400.00000	2.10400
34	4200.00000	1.72000
35	3060.00000	1.35900
36	1920.00000	.98400
37	600.00000	.56500
38	180.00000	.39800
39	0.00000	.00400
40	180.00000	.46900
41	1200.00000	.78900
42	2400.00000	1.15600
43	3540.00000	1.53500
44	4680.00000	1.88500
45	6000.00000	2.30900
46	6960.00000	2.61600
47	6480.00000	2.46400
48	5400.00000	2.12700
49	4200.00000	1.75100
50	3000.00000	1.37700
51	1860.00000	1.01300
52	720.00000	.65100
53	180.00000	.41600
54	0.00000	0.00000
55	180.00000	.33100
56	1320.00000	.76800
57	2340.00000	1.09100
58	3540.00000	1.46800
59	4680.00000	1.82900
60	5940.00000	2.22700
61	7080.00000	2.55000
62	6480.00000	2.37400
63	5400.00000	2.04400
64	4200.00000	1.67000
65	3060.00000	1.29700
66	1860.00000	.91600
67	720.00000	.58300
68	180.00000	.33800
69	0.00000	0.00000
70	0.00000	0.00000

 * DATA MANIPULATION *

 INITIAL CALIBRATION OF GAUGE BPS1

Data file name: DATA
 Number of observations: 42
 Number of variables: 2

Variables names:
 1. APPL TORQ
 2. VOLTS OUT

Subfiles: NONF

INITIAL CALIBRATION OF GAUGE BPS1

OBS#	Variable # 1	Variable # 2
1	0.00000	0.00000
2	180.00000	-.51600
3	600.00000	-.31300
4	1200.00000	-.12400
5	1800.00000	.05000
6	2400.00000	.25200
7	3000.00000	.45700
8	3600.00000	.63600
9	4200.00000	.84900
10	4800.00000	1.03700
11	5400.00000	1.21600
12	6000.00000	1.44000
13	6600.00000	1.64900
14	7200.00000	1.83000
15	7800.00000	2.03000
16	8400.00000	2.18600
17	9000.00000	2.37900
18	8400.00000	2.30000
19	7800.00000	2.05200
20	7200.00000	1.86900
21	6600.00000	1.67400
22	6000.00000	1.49800
23	5400.00000	1.30300
24	4800.00000	1.09700
25	4200.00000	.93500
26	3600.00000	.74300
27	3000.00000	.54200
28	2400.00000	.36300
29	1800.00000	.17900
30	1200.00000	-.00900
31	600.00000	-.20300
32	180.00000	-.42200
33	0.00000	.03500

34	180.00000	-.53600
35	3000.00000	.42200
36	6000.00000	1.37000
37	9000.00000	2.35500
38	9600.00000	2.51700
39	6000.00000	1.43000
40	3000.00000	.49100
41	180.00000	-.50000
42	0.00000	.01300

```

*****
*                               DATA MANIPULATION
*****
INITIAL CALIBRATION OF GAUGE CPS1

```

```

Data file name: DATA
Number of observations: 84
Number of variables: 2

```

```

Variables names:
  1. APPL TORQ
  2. VOLTS OUT

```

```

Subfiles: NONE

```

INITIAL CALIBRATION OF GAUGE CPS1

OBS#	Variable # 1	Variable # 2
1	0.00000	0.00000
2	180.00000	.28800
3	600.00000	.50200
4	1200.00000	.66500
5	1800.00000	.83500
6	2400.00000	1.03200
7	3000.00000	1.19800
8	3600.00000	1.37800
9	4200.00000	1.57000
10	4800.00000	1.75900
11	5400.00000	1.94200
12	6000.00000	2.11500
13	6600.00000	2.29500
14	7200.00000	2.48500
15	6600.00000	2.30800
16	6000.00000	2.12900
17	5400.00000	1.94500
18	4800.00000	1.75000
19	4200.00000	1.57500
20	3600.00000	1.38800
21	3000.00000	1.21600
22	2400.00000	1.03000
23	1800.00000	.85200
24	1200.00000	.66900
25	600.00000	.48000
26	180.00000	.27900
27	0.00000	0.00000
28	180.00000	.28000
29	660.00000	.49300
30	1800.00000	.86500
31	3000.00000	1.23000
32	4200.00000	1.60300
33	5400.00000	1.96300

34	6600.00000	2.33200
35	7200.00000	2.52400
36	6000.00000	2.15600
37	4800.00000	1.79600
38	3600.00000	1.42400
39	2400.00000	1.06200
40	1200.00000	.70000
41	180.00000	.31900
42	8.00000	.00300
43	180.00000	.30600
44	1200.00000	.66400
45	2460.00000	1.04100
46	3600.00000	1.39600
47	4800.00000	1.76000
48	6000.00000	2.12400
49	7200.00000	2.48600
50	6600.00000	2.31600
51	5400.00000	1.94800
52	4200.00000	1.59000
53	3000.00000	1.21900
54	1800.00000	.86400
55	600.00000	.49600
56	180.00000	.30000
57	0.00000	0.00000
58	0.00000	0.00000
59	180.00000	.30500
60	600.00000	.51000
61	1200.00000	.68900
62	1800.00000	.87000
63	2400.00000	1.04900
64	3000.00000	1.22000
65	3600.00000	1.40200
66	4200.00000	1.58200
67	4800.00000	1.77200
68	5400.00000	1.95300
69	6000.00000	2.13300
70	6600.00000	2.32200
71	7200.00000	2.50300
72	6600.00000	2.33900
73	6000.00000	2.15400
74	5400.00000	1.96200
75	4800.00000	1.78600
76	4200.00000	1.60400
77	3600.00000	1.40800
78	3000.00000	1.23400
79	2400.00000	1.06200
80	1800.00000	.86300
81	1200.00000	.68900
82	600.00000	.50600
83	180.00000	.28700
84	0.00000	.00200

APPENDIX D

TORQUE CALIBRATION RESULTS FOR GAUGES ADS1 AND BPS1

 * DATA MANIPULATION *

 TORQUE CALIBRATION RESULTS OF GAUGE ADS1

Data file name: BRAKAD:F8
 Number of observations: 24
 Number of variables: 7

- Variables names:
 1. APPL TORK
 2. BRAKE PSI
 3. BRAKE TORK
 4. BEAM TORK
 5. TOTAL TORK
 6. BENDING Vo
 7. CORRECT Vo

Subfiles: NONE

TORQUE CALIBRATION RESULTS OF GAUGE ADS1

URS#	Variable # 1 Variable # 6	Variable # 2 Variable # 7	Variable # 3	Variable # 4	Variable # 5
1	1200.00000 .00500	92.00000 -.73900	1380.00000	-250.00000	2330.000
2	2280.00000 .00500	92.00000 -1.07600	1380.00000	-250.00000	3410.000
3	3420.00000 .00500	92.00000 -1.43800	1380.00000	-250.00000	4550.000
4	4680.00000 .00500	90.00000 -1.83300	1350.00000	-250.00000	5780.000
5	6000.00000 .00500	90.00000 -2.23500	1350.00000	-250.00000	7100.000
6	7080.00000 .00500	90.00000 -2.58700	1350.00000	-250.00000	8180.000
7	6540.00000 .00500	90.00000 -2.40800	1350.00000	-250.00000	7640.000
8	5460.00000 .00500	89.00000 -2.06300	1335.00000	-250.00000	6545.000
9	4200.00000 .00500	89.00000 -1.66500	1335.00000	-250.00000	5285.000
10	3120.00000 .00500	90.00000 -1.31700	1350.00000	-250.00000	4220.000
11	1800.00000 .00500	95.00000 -.91400	1425.00000	-250.00000	2975.000
12	660.00000 .00500	107.00000 -.60300	1605.00000	-250.00000	2015.000
13	900.00000 .00500	98.00000 -.62100	1470.00000	-250.00000	2120.000
14	1800.00000 .00500	97.00000 -.92600	1455.00000	-250.00000	3005.000
15	2880.00000 .00500	97.00000 -1.27100	1455.00000	-250.00000	4085.000
16	4080.00000	94.00000	1410.00000	-250.00000	5240.000

Oct-04-00 04:55pm From-TAC/CCMTA

+6137361395

T-251 P.16/45 F-805

	.00500	-2.02900			
18	6600.00000	92.00000	1380.00000	-250.00000	7730.0000
	.00500	-2.45500			
19	7260.00000	92.00000	1380.00000	-250.00000	8390.0000
	.00500	-2.65000			
20	5580.00000	92.00000	1380.00000	-250.00000	6710.0000
	.00500	-2.11500			
21	4860.00000	92.00000	1380.00000	-250.00000	5990.0000
	.00500	-1.88200			
22	3720.00000	91.00000	1365.00000	-250.00000	4835.0000
	.00500	-1.52600			
23	2460.00000	91.00000	1365.00000	-250.00000	3575.0000
	.00500	-1.12900			
24	1200.00000	91.00000	1365.00000	-250.00000	2315.0000
	.00500	-.72600			

 * DATA MANIPULATION *

 TORQUE CALIBRATION RESULTS OF GAUGE BPS1

Data file name: BRAKBP:F8
 Number of observations: 30
 Number of variables: 7

- Variables names:
 1. APPL TORQ
 2. BRAKE PSI
 3. BRAKE TORQ
 4. BEAM TORQ
 5. TOTAL TORQ
 6. BENDING Vo
 7. CORRECT Vo

Subfiles: NONE

TORQUE CALIBRATION RESULTS OF GAUGE BPS1

OBS#	Variable # 1 Variable # 6	Variable # 2 Variable # 7	Variable # 3	Variable # 4	Variable # 5
1	-600.00000 .02700	90.00000 -.25300	1350.00000	240.00000	990.000
2	-1440.00000 .02700	90.00000 .00700	1350.00000	240.00000	150.000
3	-1500.00000 .02700	90.00000 .02600	1350.00000	240.00000	90.000
4	-3000.00000 .02700	89.00000 .49800	1335.00000	240.00000	-1425.000
5	-4200.00000 .02700	92.00000 .86200	1380.00000	240.00000	-2580.000
6	-5340.00000 .02700	107.00000 1.19000	1605.00000	240.00000	-3495.000
7	-6600.00000 .02700	110.00000 1.54000	1650.00000	240.00000	-4710.000
8	-7740.00000 .02700	110.00000 1.90700	1650.00000	240.00000	-5850.000
9	-7200.00000 .02700	110.00000 1.73800	1650.00000	240.00000	-5310.000
10	-6000.00000 .02700	109.00000 1.38900	1635.00000	240.00000	-4125.000
11	-4560.00000 .02700	109.00000 .92100	1635.00000	240.00000	-2685.000
12	-3600.00000 .02700	107.00000 .62900	1605.00000	240.00000	-1755.000
13	-2460.00000 .02700	106.00000 .28000	1590.00000	240.00000	-630.000
14	-1680.00000 .02700	105.00000 .05400	1575.00000	240.00000	135.000
15	-1620.00000 .02700	104.00000 .02900	1560.00000	240.00000	180.000
16	-1500.00000 .02700	95.00000 .00100	1425.00000	240.00000	165.000

180

	.02700	.03000			
18	-2340.00000	93.00000	1395.00000	240.00000	-705.0000
	.02700	.26100			
19	-3540.00000	92.00000	1380.00000	240.00000	-1920.0000
	.02700	.64200			
20	-4800.00000	92.00000	1380.00000	240.00000	-3180.0000
	.02700	1.02500			
21	-5940.00000	92.00000	1380.00000	240.00000	-4320.0000
	.02700	1.39100			
22	-7080.00000	91.00000	1365.00000	240.00000	-5475.0000
	.02700	1.75000			
23	-8340.00000	91.00000	1365.00000	240.00000	-6735.0000
	.02700	2.13300			
24	-7800.00000	91.00000	1365.00000	240.00000	-6195.0000
	.02700	1.98500			
25	-6420.00000	91.00000	1365.00000	240.00000	-4815.0000
	.02700	1.56600			
26	-5400.00000	91.00000	1365.00000	240.00000	-3795.0000
	.02700	1.24600			
27	-4200.00000	90.00000	1350.00000	240.00000	-2610.0000
	.02700	.88900			
28	-3060.00000	90.00000	1350.00000	240.00000	-1470.0000
	.02700	.52600			
29	-1860.00000	90.00000	1350.00000	240.00000	-270.0000
	.02700	.15100			
30	-1440.00000	90.00000	1350.00000	240.00000	150.0000
	.02700	.03200			

APPENDIX E

TORQUE CALIBRATION ERROR ANALYSIS CALCULATIONS AND RESULTS

The physical errors present in the system while calibrating are;

for Brake Application Torque;

$$T_{BR} = (\text{moment arm})(\text{brake air pressure})(\text{diaphragm area})$$

errors;

$$\begin{aligned} \text{moment arm} &= 0.5 \text{ ft} \pm 0.1/12 \text{ ft} \\ \text{brake air pressure} &= \text{recorded reading} \pm 3 \text{ psi} \\ \text{diaphragm area} &= 30 \text{ in}^2 \pm 1 \text{ in}^2 \end{aligned}$$

for Applied Torque;

$$T_{APPL} = (\text{load cell reading}) (6 \text{ ft})$$

errors;

$$\text{load cell reading} = \text{recorded reading} \pm 5 \text{ lbs}$$

$$\therefore T_{APPL} = \text{recorded } T_{APPL} \pm 30 \text{ ft*lbs}$$

The beam torque contribution is error free.

It is desired to combine these errors in order to find the extreme limits of the resultant torque.

For gauge ADS1 positive is in the CCW direction. Therefore the resultant torque is given by;

$$T_{RES} = T_{APPL} + T_{BR} - T_{BEAM}$$

$$T_{RES} = T_{APPL} + T_{BR} - 250$$

for the lowest extreme torque (to be used in calculating the highest extreme line).

$$\begin{aligned} T_{RES_{LOW}} &= (T_{APPL}-30) + [(\text{recorded psi} - 3\text{psi})(0.5\text{ft} - \frac{0.1}{12} \text{ ft}) \\ &\quad (30 \text{ in}^2 - 1 \text{ in}^2)] - 250 \end{aligned}$$

for the highest extreme torque (to be used in calculating the lowest extreme line).

$$\begin{aligned} T_{RES_{HIGH}} &= (T_{APPL}+30) + [(\text{recorded psi} + 3 \text{ psi})(0.5\text{ft} + \frac{0.1}{12} \text{ ft}) \\ &\quad (30 \text{ in}^2 + 1 \text{ in}^2)] - 250 \end{aligned}$$

The error analysis is only valid if we transform the actual calibration plot into the first quadrant of the cartesian plane. This is accomplished by ignoring the negative bridge output voltage, that is, a mirror image in X.

For gauge BPS1 positive torque is in the CW direction, therefore;

$$T_{RES} = T_{BR} + T_{BEAM} - T_{APPL}$$

A transformation of the BPS1 calibration plot requires all torque to change sign, a mirror image in Y.

$$-T_{RES} = -(-T_{APPL}) - T_{BR} - T_{BEAM}$$

To calculate the best fit line giving the lowest extreme line we require the greatest possible resultant torque where the brake torque contribution has to be the lowest possible value because of our sign convention.

$$T_{RES_{HIGH}} = -(-T_{APPL}-30) - [(recorded\ psi - 3\ psi)(0.5 - \frac{0.01}{12}) \\ (30\ in^2 - 1\ in^2)] - 240$$

Using the same logic, the highest extreme line is given by the lowest resultant torque.

$$T_{RES_{LOW}} = -(-T_{APPL}+30) - [(recorded\ psi + 3)(0.5 + \frac{0.01}{12})(30\ in^2 + 1\ in^2)] \\ - 240$$

The procedure explained in section 3.9.2 is followed giving the error in electrical calibration and gauge sensitivity. The resultant torques and voltage outputs used for these calculations are listed in the tables which follow under columns 4 and 5 respectively.

Sample Calculation Using the Results of Gauge ADS1

For the highest extreme line; a best fit line is calculated using the ordered pairs,

$$(T_{RES_{LOW}}, Vo_i)$$

to yield;

$$y = 3.20 \times 10^{-4} X + 1.22 \times 10^{-2}$$

Applying the least squares error calculation for the range of α :

from [3.911a]

$$C - t_{\eta/2} \cdot Se \left[\frac{S_{xx} + (\sum x_i)^2}{n S_{xx}} \right]^{\frac{1}{2}} < \alpha < C + t_{\eta/2} \cdot Se \left[\frac{S_{xx} + (\sum x_i)^2}{n S_{xx}} \right]^{\frac{1}{2}}$$

where using a 95% confidence interval $t_{0.025}$

for 22 degrees of freedom = 2.074

$$n = 24$$

$$Se = 0.012$$

$$S_{xx} = 229.1 \times 10^7$$

$$(\sum x_i)^2 = 1.381 \times 10^{10}$$

We want to calculate the highest extreme line therefore;

$$C_4 = 1.22 \times 10^{-2} + 2.074(0.012) \left[\frac{229.1 \times 10^7 + 1.381 \times 10^{10}}{24(229.1 \times 10^7)} \right]^{\frac{1}{2}}$$

$$C_4 = 2.485 \times 10^{-2}$$

Calculating the highest extreme slope from [3.9iib]

$$M_4 = M + t_{n/2} \cdot Se \left[\frac{n}{S_{xx}} \right]^{\frac{1}{2}}$$

$$= 3.2 \times 10^{-4} - 2.074(0.012) \left[\frac{24}{229.1 \times 10^7} \right]^{\frac{1}{2}}$$

$$M_1 = 3.221 \times 10^{-4}$$

Therefore the highest extreme line is;

$$y_{HIGH} = 3.221 \times 10^{-4} x + 2.485 \times 10^{-2}$$

Using the ordered pairs;

$$(T_{RES_{HIGH}_i}, Vo_i)$$

yields;

$$y = 3.20 \times 10^{-4} x - 6.95 \times 10^{-2}$$

Calculating the range of the true line to achieve the lowest system line from equations [3.9iia and b]

$$C_1 = C - t_{n/2} \cdot Se \left[\frac{S_{xx} + (\sum x_i)^2}{n(S_{xx})} \right]^{\frac{1}{2}}$$

and

$$M_1 = M + t_{n/2} \cdot Se \left[\frac{n}{S_{xx}} \right]^{\frac{1}{2}}$$

where;

$$t_{0.025} = 2.074$$

$$n = 24$$

$$Se = 0.012$$

$$S_{xx} = 229.1 \times 10^7$$

$$(\sum x_i)^2 = 1.381 \times 10^{10}$$

$$C = -6.95 \times 10 \times 10^{-2}$$

$$M = 3.2 \times 10^{-4}$$

therefore the lowest extreme line is

$$y_{\text{LOW}} = 3.173 \times 10^{-4} x - 8.355 \times 10^{-2}$$

summarizing;

$$y_{\text{LOW}} = 3.173 \times 10^{-4} x - 8.355 \times 10^{-2} = M_1 x + C_1$$

$$y_{\text{HIGH}} = 3.221 \times 10^{-4} x + 2.485 \times 10^{-2} = M_4 x + C_4$$

Considering the Vishay error in electrical calibration, ($\pm 1\%$ of the voltage reading).

$$V_{\text{OECAL}} = 1.538$$

$$V_{\text{OHIGH}} = (1.01)(1.538) = 1.553$$

$$V_{\text{OLOW}} = (0.99)(1.538) = 1.523$$

from equation [3.9iia] the upper electrical calibration bound, using the lowest extreme line, is;

$$X_{\text{RIGHT}} = \frac{V_{\text{OHIGH}} - C_1}{M_1} = 5158 \text{ ft*lbs}$$

from equation [3.9iib] the lower electrical calibration bound is;

$$X_{\text{LEFT}} = \frac{V_{\text{OLOW}} - C_4}{M_4} = 4651 \text{ ft*lbs}$$

The actual electrical calibration recorded is;

$$1.538 \text{ volts} \equiv 4898 \text{ ft*lbs}$$

$$\frac{X_{\text{RIGHT}} - 4898}{4898} \times 100\% = +5.3\%$$

$$\frac{X_{\text{LEFT}} - 4898}{4898} \times 100\% = -5.0\%$$

Therefore for gauge ADS1;

$$1.538 \pm 1\% \text{ volts} \equiv 4898 \pm 5\% \text{ ft*lbs}$$

Calculating the gauge sensitivity range;

$$\text{Gain} = 1000$$

$$\text{Excitation Voltage} = 5\text{V}$$

calibrated gauge sensitivity from [3.8v]

$$\frac{0.2 \text{ mV}}{\text{V}^+} \equiv 3.125 \text{ ft*lbs}$$

from the highest extreme line;

$$\frac{0.2 \text{ mV}}{V^+} \cong 3105 \text{ ft*lbs}$$

from the lowest extreme line;

$$\frac{0.2 \text{ mV}}{V^+} \cong 3152 \text{ ft*lbs}$$

calculating the percentage deviation

$$\frac{3105 - 3125}{3125} \times 100\% = -0.6\%$$

$$\frac{3153 - 3125}{3124} \times 100\% = +0.8\%$$

summarizing;

electrical calibration error for ADS1;

$$1.538 \pm 1\% \text{ volts} \cong 4898 \pm 5.2\% \text{ ft*lbs}$$

gauge sensitivity

$$\frac{0.2 \pm 1\% \text{ mV}}{V^+} \cong 3125 \pm 0.7\% \text{ ft*lbs}$$

electrical calibration error for BPS1;

$$n = 30$$

$$t_{n/2} \text{ for } 28 \text{ d.o.f.} = 2.048$$

$$y_{\text{low}} = 3.08 \times 10^{-4}X + 1.69 \times 10^{-2}$$

$$y_{\text{high}} = 3.146 \times 10^{-4}X + 1.156 \times 10^{-1}$$

$$1.525 \pm 1\% \text{ volts} \cong 4689 \pm 5.4\% \text{ ft*lbs}$$

gauge sensitivity

$$\frac{0.2 \pm 1\% \text{ mV}}{V^+} \cong 3215 \pm 1.3\%$$

 * DATA MANIPULATION *

 ADJUSTED TORQUE VALUES FOR THE HIGHEST EXTREME LINE OF ADS1

Data file name: UPERRA:F8
 Number of observations: 24
 Number of variables: 5

- Variables names:
 1. APPL TORQ
 2. BRAKE PSI
 3. BRAKE TORQ
 4. TOTAL TORQ
 5. CORRECT Vo

Subfiles: NONE

ADJUSTED TORQUE VALUES FOR THE HIGHEST EXTREME LINE OF ADS1

OBS#	Variable # 1	Variable # 2	Variable # 3	Variable # 4	Variable # 5
1	1170.00000	89.00000	1288.34917	2208.00000	.739
2	2250.00000	89.00000	1288.34917	3288.00000	1.076
3	3390.00000	89.00000	1288.34917	4428.00000	1.438
4	4650.00000	87.00000	1259.39750	5659.00000	1.833
5	5970.00000	87.00000	1259.39750	6979.00000	2.235
6	7050.00000	87.00000	1259.39750	8059.00000	2.587
7	6510.00000	87.00000	1259.39750	7519.00000	2.408
8	5430.00000	86.00000	1244.92167	6425.00000	2.063
9	4170.00000	86.00000	1244.92167	5165.00000	1.665
10	3090.00000	87.00000	1259.39750	4099.00000	1.317
11	1770.00000	92.00000	1331.77667	2852.00000	.914
12	630.00000	104.00000	1505.48667	1885.00000	.603
13	870.00000	95.00000	1375.20417	1995.00000	.621
14	1770.00000	94.00000	1360.72833	2881.00000	.926
15	2850.00000	94.00000	1360.72833	3961.00000	1.271
16	4050.00000	91.00000	1317.30083	5117.00000	1.632
17	5250.00000	90.00000	1302.82500	6303.00000	2.025
18	6570.00000	89.00000	1288.34917	7608.00000	2.455
19	7230.00000	89.00000	1288.34917	8268.00000	2.650
20	5550.00000	89.00000	1288.34917	6588.00000	2.115
21	4830.00000	89.00000	1288.34917	5868.00000	1.885
22	3690.00000	88.00000	1273.87333	4714.00000	1.528
23	2430.00000	88.00000	1273.87333	3454.00000	1.129
24	1170.00000	88.00000	1273.87333	2194.00000	.728

HIGHEST EXTREME PARAMETERS FOR GAUGE ADS1

SIGMA X_i = 1.175E+05
SIGMA Y_i = 3.784E+01
SIGMA X_i*Y_i = 2.158E+05
SIGMA X_i*X_i = 6.709E+08
SIGMA Y_i*Y_i = 6.941E+01

OF DATA PTS. = 2.400E+01
 $r_{0.025}$ = 2.074E+00
 S_{xx} = 2.291E+09
 S_{yy} = 2.341E+02
 S_{xy} = 7.321E+05
 S_e = 1.167E-02

THE UPPER EXTREME LINE IS;

$$Y = 3.221E-04 X + 2.485E-02$$

 * DATA MANIPULATION *

 ADJUSTED TORQUE VALUES FOR THE LOWEST EXTREME LINE OF ADS1

Data file name: LTERRA:F8
 Number of observations: 24
 Number of variables: 5

- Variables names:
 1. APPL TORQ
 2. BRAKE PSI
 3. BRAKE TORQ
 4. TOTAL TORQ
 5. CORRECT V₀

Subfiles: NONE

ADJUSTED TORQUE VALUES FOR THE LOWEST EXTREME LINE OF ADS1

DRS#	Variable # 1	Variable # 2	Variable # 3	Variable # 4	Variable # 5
1	1230.00000	95.00000	1474.95417	2455.00000	.739
2	2310.00000	95.00000	1474.95417	3535.00000	1.076
3	3450.00000	95.00000	1474.95417	4675.00000	1.438
4	4710.00000	93.00000	1443.90250	5904.00000	1.833
5	6030.00000	93.00000	1443.90250	7224.00000	2.235
6	7110.00000	93.00000	1443.90250	8304.00000	2.587
7	8570.00000	93.00000	1443.90250	7764.00000	2.408
8	5490.00000	92.00000	1428.37667	6668.00000	2.063
9	4230.00000	92.00000	1428.37667	5408.00000	1.665
10	3150.00000	93.00000	1443.90250	4344.00000	1.317
11	1830.00000	98.00000	1521.53167	3102.00000	.914
12	690.00000	110.00000	1707.84167	2148.00000	.603
13	930.00000	101.00000	1568.10917	2248.00000	.621
14	1830.00000	100.00000	1552.58333	3133.00000	.926
15	2910.00000	100.00000	1552.58333	4213.00000	1.271
16	4110.00000	97.00000	1506.00583	5366.00000	1.632
17	5310.00000	96.00000	1490.48000	6550.00000	2.029
18	6630.00000	95.00000	1474.95417	7855.00000	2.459
19	7290.00000	95.00000	1474.95417	8515.00000	2.650
20	5610.00000	95.00000	1474.95417	6835.00000	2.119
21	4890.00000	95.00000	1474.95417	6115.00000	1.882
22	3750.00000	94.00000	1459.42833	4959.00000	1.521
23	2490.00000	94.00000	1459.42833	3699.00000	1.129
24	1230.00000	94.00000	1459.42833	2439.00000	.721

LOWEST EXTREME PARAMETERS FOR GAUGE ADS1

SIGMA X_i = 1.235E+05
SIGMA Y_i = 3.784E+01
SIGMA X_i*Y_i = 2.251E+05
SIGMA X_i*X_i = 7.303E+08
SIGMA Y_i*Y_i = 6.941E+01

OF DATA PTS. = 2.400E+01
t@0.025 = 2.074E+00
Sxx = 2.286E+09
Syy = 2.341E+02
Sxy = 7.313E+05
Se = 1.237E-02

THE LOWER EXTREME LINE IS ;

$$Y = 3.173E-04 X + -8.355E-02$$

 * DATA MANIPULATION *

 ADJUSTED TORQUE VALUES FOR THE HIGHEST EXTREME LINE OF BPS1

Data file name: UPERRB:F8
 Number of observations: 30
 Number of variables: 5

- Variables names:
 1. APPL TORQ
 2. BRAKE PSI
 3. BRAKE TORQ
 4. TOTAL TORQ
 5. CORRECT Vo

Subfiles: NONE

ADJUSTED TORQUE VALUES FOR THE HIGHEST EXTREME LINE OF BPS1

UBS#	Variable # 1	Variable # 2	Variable # 3	Variable # 4	Variable # 5
1	570.00000	93.00000	-1443.90250	-1114.00000	-.253
2	1410.00000	93.00000	-1443.90250	-274.00000	.007
3	1470.00000	93.00000	-1443.90250	-214.00000	.026
4	2970.00000	92.00000	-1428.37667	1302.00000	.498
5	4170.00000	95.00000	-1474.95417	2455.00000	.852
6	5310.00000	110.00000	-1707.84167	3362.00000	1.190
7	6570.00000	113.00000	-1754.41917	4576.00000	1.540
8	7710.00000	113.00000	-1754.41917	5716.00000	1.907
9	7170.00000	113.00000	-1754.41917	5176.00000	1.738
10	5970.00000	112.00000	-1738.89333	3991.00000	1.369
11	4530.00000	112.00000	-1738.89333	2551.00000	.921
12	3570.00000	110.00000	-1707.84167	1622.00000	.629
13	2430.00000	109.00000	-1692.31583	498.00000	.280
14	1650.00000	108.00000	-1676.79000	-267.00000	.054
15	1590.00000	107.00000	-1661.26417	-311.00000	.029
16	1470.00000	98.00000	-1521.53167	-292.00000	.001
17	1590.00000	97.00000	-1506.00583	-156.00000	.031
18	2310.00000	96.00000	-1490.48000	580.00000	.261
19	3510.00000	95.00000	-1474.95417	1795.00000	.841
20	4770.00000	95.00000	-1474.95417	3055.00000	1.021
21	5910.00000	95.00000	-1474.95417	4195.00000	1.391
22	7050.00000	94.00000	-1459.42833	5351.00000	1.751
23	8310.00000	94.00000	-1459.42833	6611.00000	2.131
24	7770.00000	94.00000	-1459.42833	6071.00000	1.981
25	6390.00000	94.00000	-1459.42833	4691.00000	1.561
26	5370.00000	94.00000	-1459.42833	3671.00000	1.241
27	4170.00000	93.00000	-1443.90250	2486.00000	.881
28	3030.00000	93.00000	-1443.90250	1346.00000	.521
29	1830.00000	93.00000	-1443.90250	146.00000	.151
30	1410.00000	93.00000	-1443.90250	-274.00000	.031

HIGHEST EXTREME PARAMETERS FOR GAUGF BPS1

SIGMA Xi= 6.835E+04
SIGMA Yi= 2.443E+01
SIGMA Xi*Yi= 1.036E+05
SIGMA Xi*X_i= 3.096E+08
SIGMA Yi*Yi= 3.482E+01

OF DATA PTS.= 3.000E+01
τ_{0.025}= 2.048E+00
S_{xx}= 4.618E+09
S_{yy}= 4.479E+02
S_{xy}= 1.438E+06
S_e= 2.016E-02

THE UPPER EXTREME LINE IS;

$$Y = 3.146E-04 X + 1.156E-01$$

 * DATA MANIPULATION *

 ADJUSTED TORQUE VALUES FOR THE LOWEST EXTREME LINE OF BPS1

Data file name: LTERRB:F8
 Number of observations: 30
 Number of variables: 5

- Variables names:
 1. APPL TORQ
 2. BRAKE PSI
 3. BRAKE TORQ
 4. TOTAL TORQ
 5. CORRECT Vo

Subfiles: NONE

ADJUSTED TORQUE VALUES FOR THE LOWEST EXTREME LINE OF BPS1

OBS#	Variable # 1	Variable # 2	Variable # 3	Variable # 4	Variable # 5
1	630.00000	87.00000	-1259.39750	-869.00000	-.253
2	1470.00000	87.00000	-1259.39750	-29.00000	.007
3	1530.00000	87.00000	-1259.39750	31.00000	.026
4	3030.00000	86.00000	-1244.92167	1548.00000	.498
5	4230.00000	89.00000	-1288.34917	2702.00000	.862
6	5370.00000	104.00000	-1505.48667	3625.00000	1.190
7	6630.00000	107.00000	-1548.91417	4841.00000	1.540
8	7770.00000	107.00000	-1548.91417	5981.00000	1.907
9	7230.00000	107.00000	-1548.91417	5441.00000	1.738
10	6030.00000	106.00000	-1534.43833	4256.00000	1.369
11	4590.00000	106.00000	-1534.43833	2816.00000	.921
12	3630.00000	104.00000	-1505.48667	1885.00000	.629
13	2490.00000	103.00000	-1491.01083	759.00000	.280
14	1710.00000	102.00000	-1476.53500	-7.00000	.054
15	1650.00000	101.00000	-1462.05917	-52.00000	.029
16	1530.00000	92.00000	-1331.77667	-42.00000	.001
17	1650.00000	91.00000	-1317.30083	93.00000	.031
18	2370.00000	90.00000	-1302.82500	827.00000	.261
19	3570.00000	89.00000	-1288.34917	2042.00000	.641
20	4830.00000	89.00000	-1288.34917	3302.00000	1.021
21	5970.00000	89.00000	-1288.34917	4442.00000	1.39
22	7110.00000	88.00000	-1273.87333	5596.00000	1.75
23	8370.00000	88.00000	-1273.87333	6856.00000	2.13
24	7830.00000	88.00000	-1273.87333	6316.00000	1.98
25	6450.00000	88.00000	-1273.87333	4936.00000	1.56
26	5430.00000	88.00000	-1273.87333	3916.00000	1.24
27	4230.00000	87.00000	-1259.39750	2731.00000	.88
28	3090.00000	87.00000	-1259.39750	1591.00000	.52
29	1890.00000	87.00000	-1259.39750	391.00000	.15
30	1470.00000	87.00000	-1259.39750	-29.00000	.03

LOWEST EXTREME PARAMETERS FOR GAUGE BPS1

SIGMA Xi= 7.589F+04
SIGMA Yi= 2.443E+01
SIGMA Xi*Yi= 1.097E+05
SIGMA Xi*Xi= 3.461E+08
SIGMA Yi*Yi= 3.482E+01

OF DATA PTS.= 3.000E+01
t@0.025= 2.048F+00
Sxx= 4.624E+09
Syy= 4.479E+02
Sxy= 1.439E+06
Se= 1.818E-02

THE LOWER EXTREME LINE IS ;

$$Y = 3.081E-04 X + 1.690E-02$$

APPENDIX F

DRIVE AXLE VERTICAL LOAD RESULTS

 * DATA MANIPULATION *

 NEW ZERO FOR REAR DRIVE AXLE (CALIBRATION DATA)

Data file name: CAL2RD:F8
 Number of observations: 13
 Number of variables: 5

Variables names:
 1. TONNES
 2. GAGE D9
 3. GAGE D6
 4. GAGE P9
 5. GAGE P6

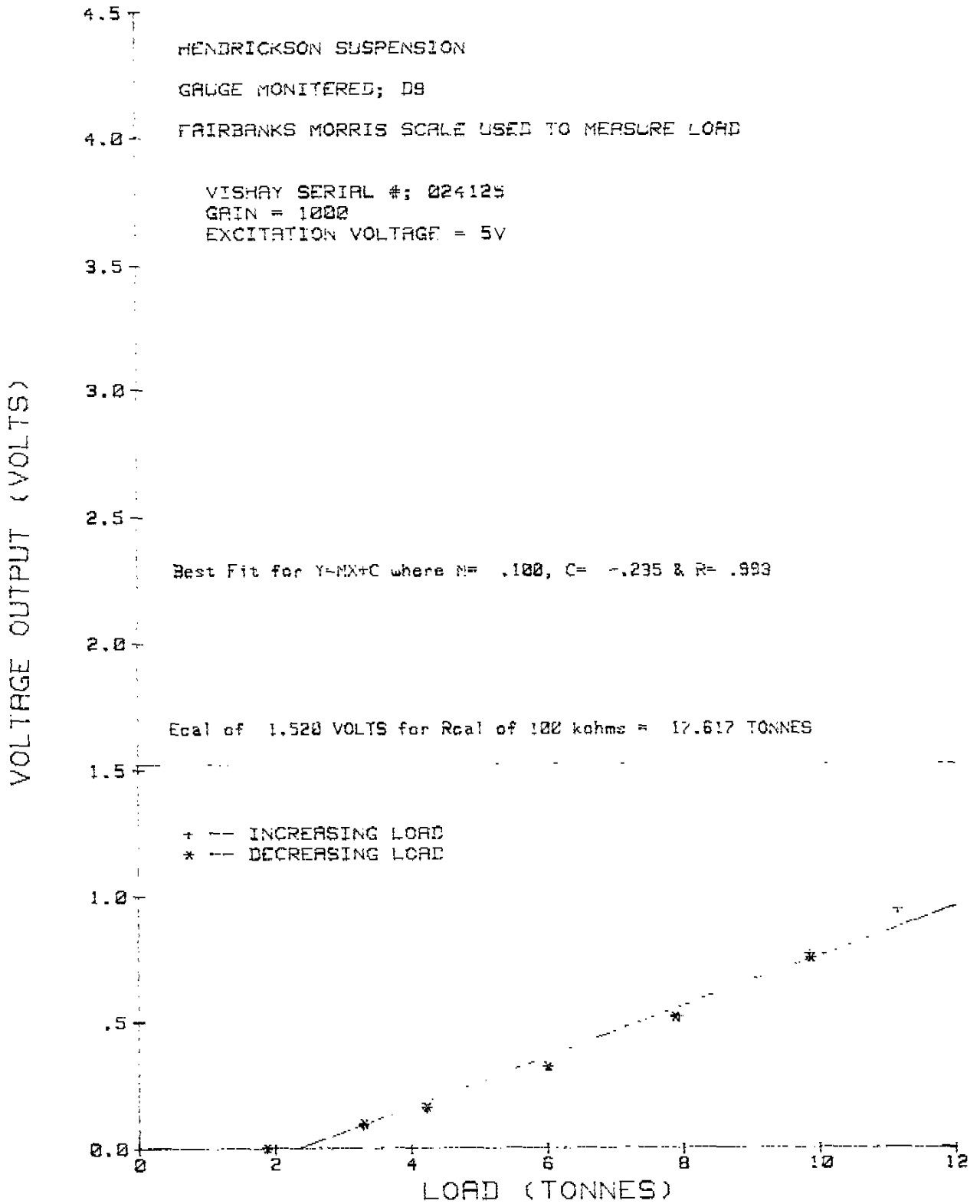
Subfile name	beginning observation	number of observations
1. INC LOAD	1	7
2. DEC LOAD	8	6

NEW ZERO FOR REAR DRIVE AXLE (CALIBRATION DATA)

OBS#	Variable # 1	Variable # 2	Variable # 3	Variable # 4	Variable # 5
1	1.88000	.00200	-.00200	-.00200	.002
2	3.29000	.09200	.13100	.24200	.433
3	4.23000	.16000	.22300	.39000	.743
4	6.01000	.32400	.47600	.67000	1.319
5	7.93000	.52100	.80900	.94600	1.889
6	9.86000	.76800	1.29800	1.17700	2.324
7	11.15000	.94800	1.67500	1.29200	2.535
8	9.88000	.75100	1.23800	1.20000	2.403
9	7.88000	.51700	.78800	.95500	1.930
10	6.01000	.32400	.45200	.69900	1.401
11	4.23000	.15400	.21400	.42400	.817
12	3.30000	.09900	.13200	.25700	.475
13	1.88000	.00100	0.00000	.00900	-.005

NOV., 28, 1985

VERTICAL LOAD CALIBRATION



NOV., 28, 1985

VERTICAL LOAD CALIBRATION

4.5 -

HENDRICKSON SUSPENSION

GAUGE MONITERED; D6

4.0 -

FAIRBANKS MORRIS SCALE USED TO MEASURE LOAD

VISHAY SERIAL #; 024079

GAIN = 1000

EXCITATION VOLTAGE = 5V

3.5 -

VOLTAGE OUTPUT (VOLTS)

3.0 -

2.5 -

Best Fit for $Y=MX+C$ where $M= .171$, $C= -.448$ & $R= .981$

2.0 -

Eqal of 1.523 VOLTS for Resl of 100 kohms = 11.815 TONNES

1.5 -

+ -- INCREASING LOAD
* -- DECREASING LOAD

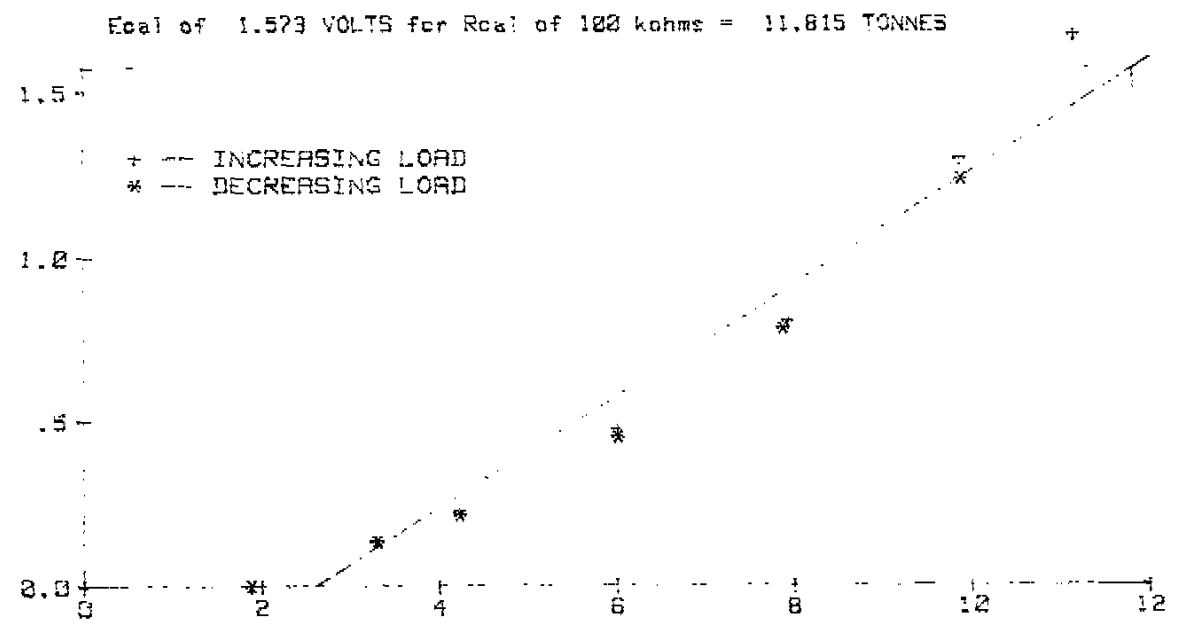
1.0 -

.5 -

0.0 -

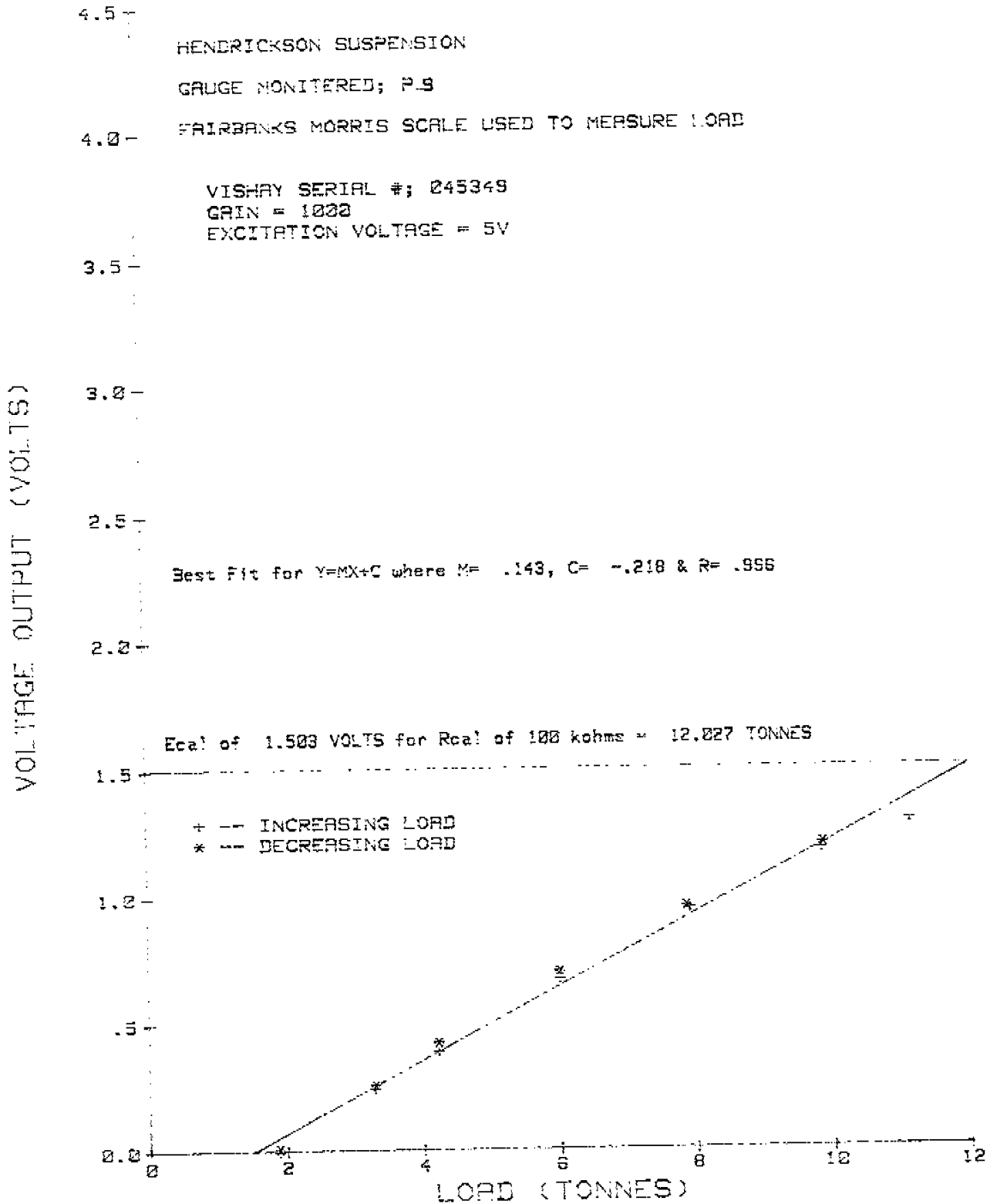
LOAD (TONNES)

0 2 4 6 8 10 12



NOV., 28, 1985

VERTICAL LOAD CALIBRATION



 * DATA MANIPULATION *

 CALIBRATION - FRONT DRIVE AXLE

Data file name: DATA
 Number of observations: 13
 Number of variables: 5

- Variables names:
 1. TONNES
 2. GAGE D2
 3. GAGE D5
 4. GAGE P2
 5. GAGE P5

Subfile name	beginning observation	number of observations
1. INC LOAD	1	6
2. DEC LOAD	7	5
3. EXTREMES	12	2

CALIBRATION - FRONT DRIVE AXLE

URS#	Variable # 1	Variable # 2	Variable # 3	Variable # 4	Variable # 5
1	2.13000	.00800	.00300	-.00100	.002
2	4.08000	.10600	.18400	.31500	.727
3	6.06000	.24200	.44600	.60400	1.385
4	8.03000	.41100	.80600	.85200	1.940
5	10.04000	.64600	1.35800	1.04700	2.332
6	11.26000	.81800	1.78500	1.12800	2.472
7	9.91000	.61900	1.25400	1.05200	2.371
8	7.91000	.38600	.70700	.85000	1.958
9	6.00000	.23300	.39500	.60300	1.370
10	4.13000	.11200	.17700	.32000	.692
11	2.12000	.00700	.02000	.01000	-.001
12	2.21000	.02200	-.00700	.03000	.012
13	11.30000	.82700	1.78500	1.14000	2.46.

NOV., 28, 1985

VERTICAL LOAD CALIBRATION

HENDRICKSON SUSPENSION

GAUGE MONITERED; D2

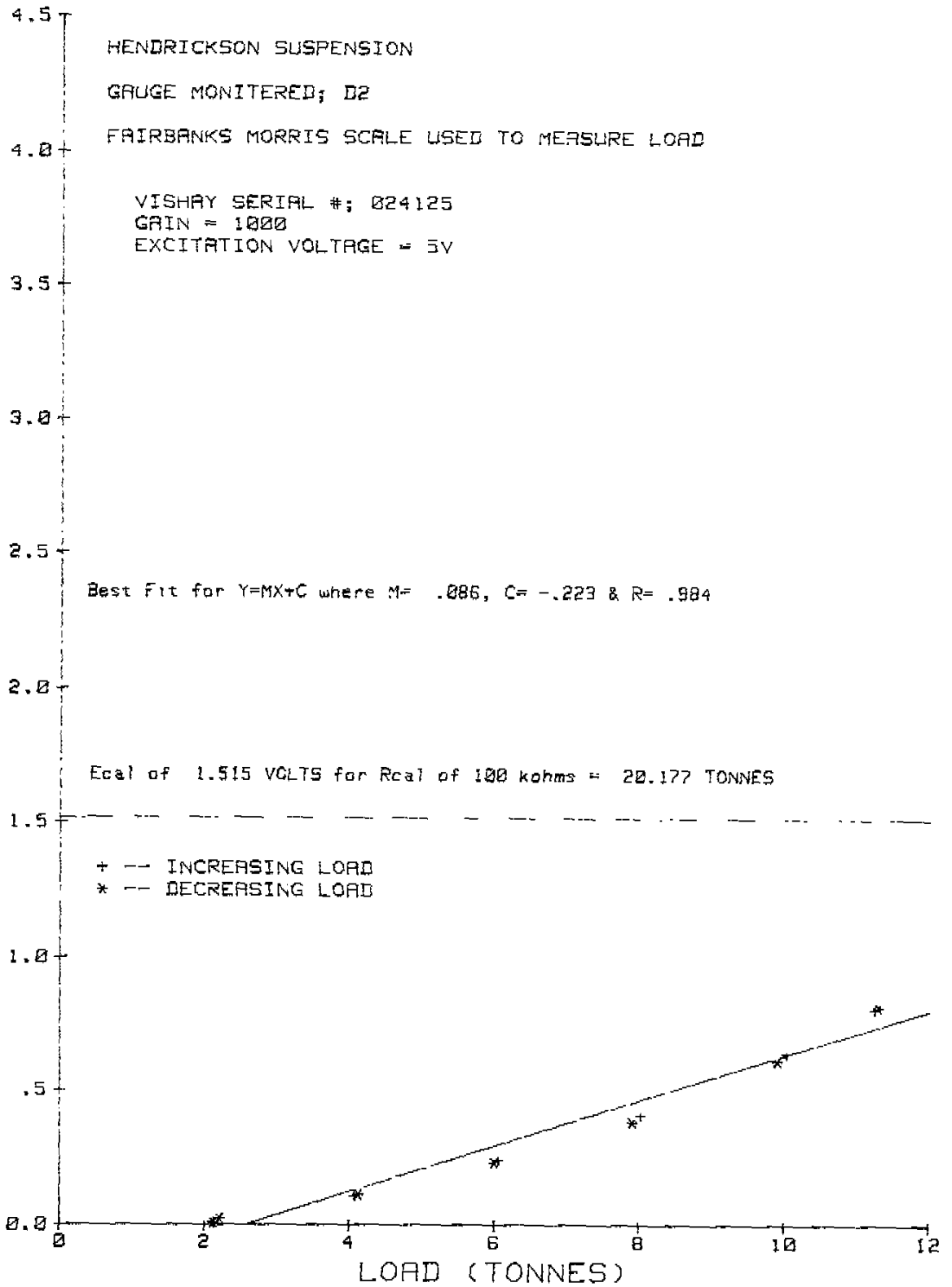
FAIRBANKS MORRIS SCALE USED TO MEASURE LOAD

VISHAY SERIAL #: 024125

GAIN = 1000

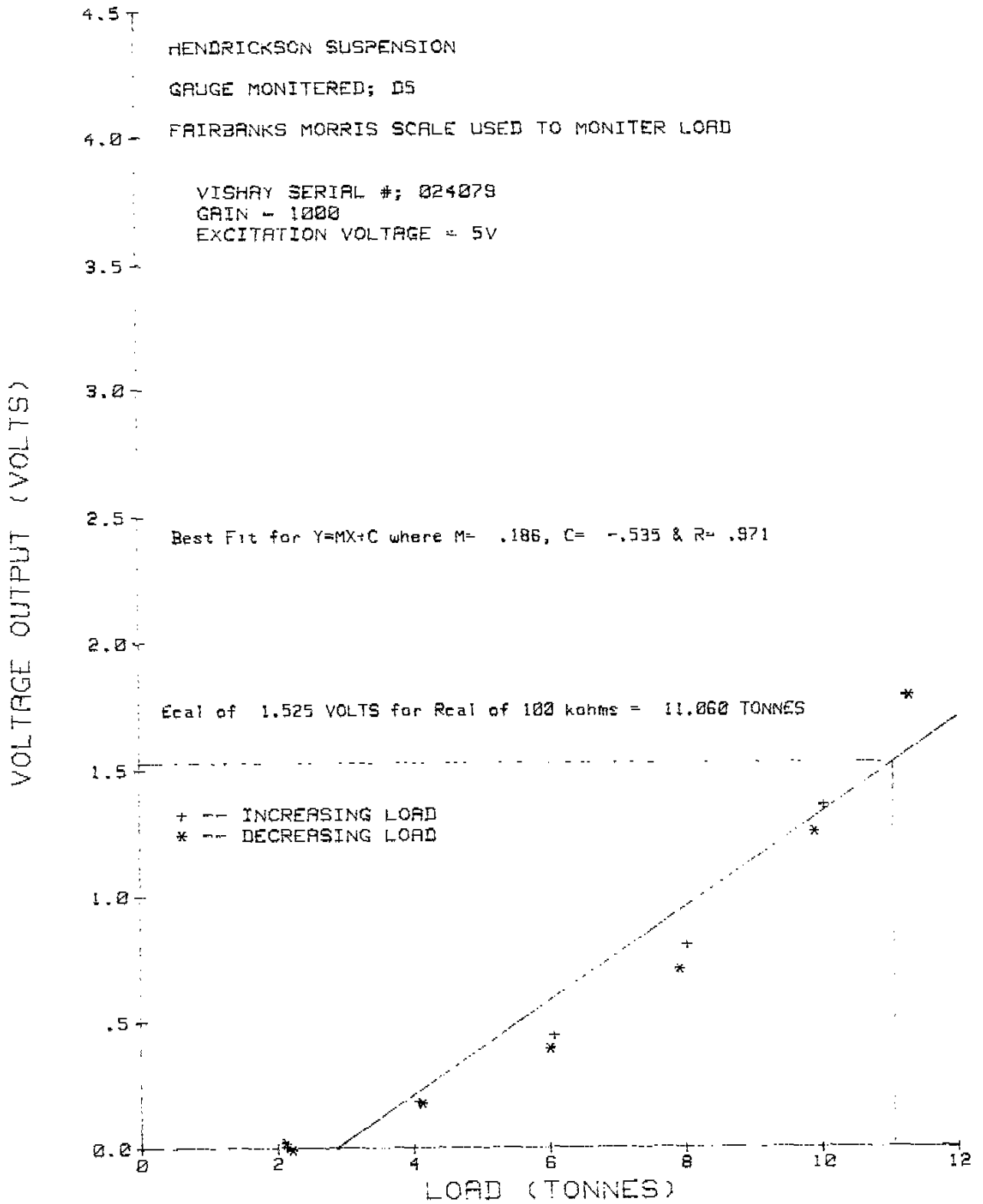
EXCITATION VOLTAGE = 5V

VOLTAGE OUTPUT (VOLTS)



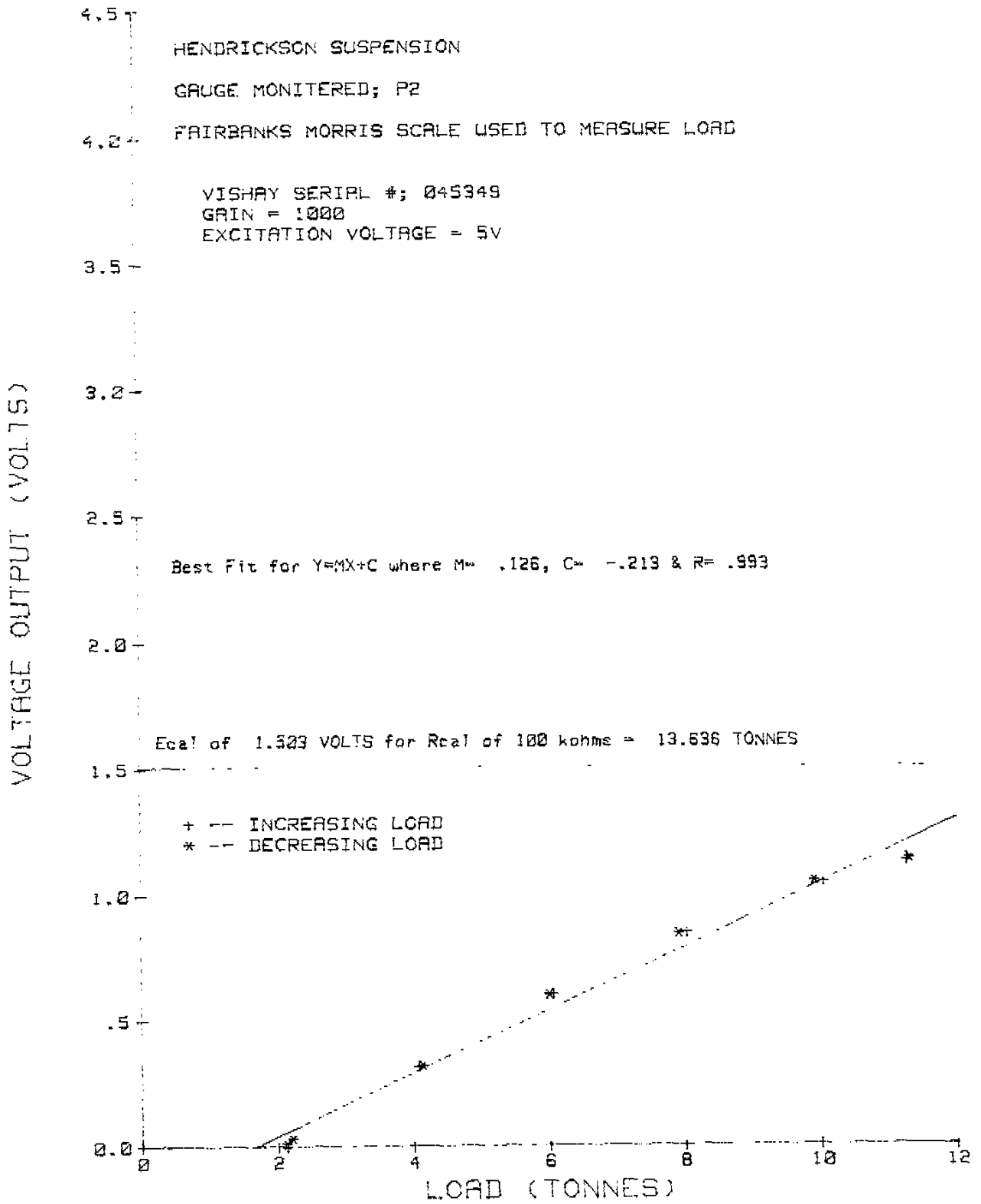
NOV., 28, 1985

VERTICAL LOAD CALIBRATION



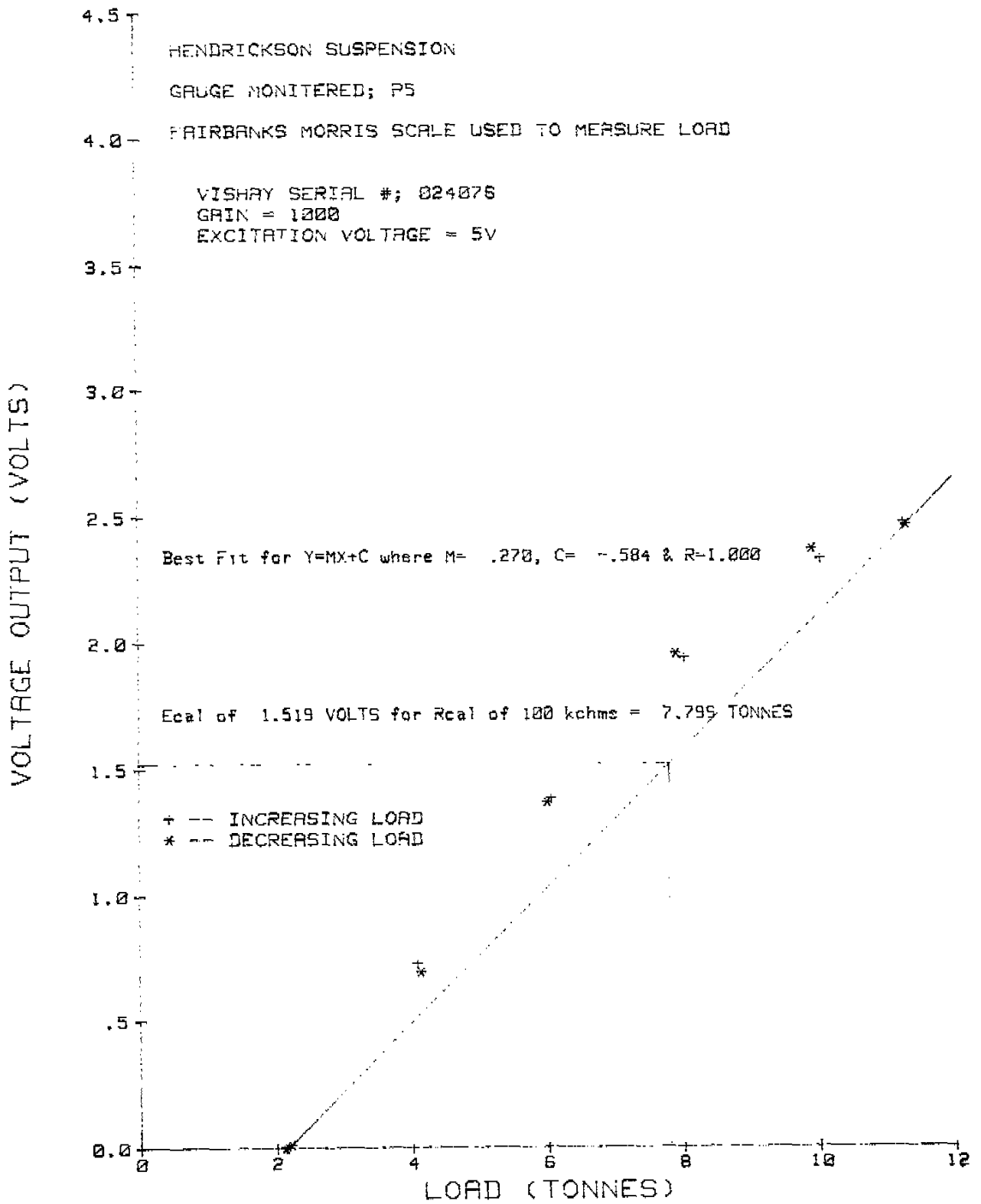
NOV., 28, 1985

VERTICAL LOAD CALIBRATION



NOV., 28, 1985

VERTICAL LOAD CALIBRATION



APPENDIX G

TRAILER AXLE VERTICAL LOAD RESULTS

 * DATA MANIPULATION *

 CALIBRATION OF TRAILER AXLE #1

Data file name: DATA
 Number of observations: 10
 Number of variables: 3

Variables names:
 1. TONNES
 2. ADS2
 3. APS2

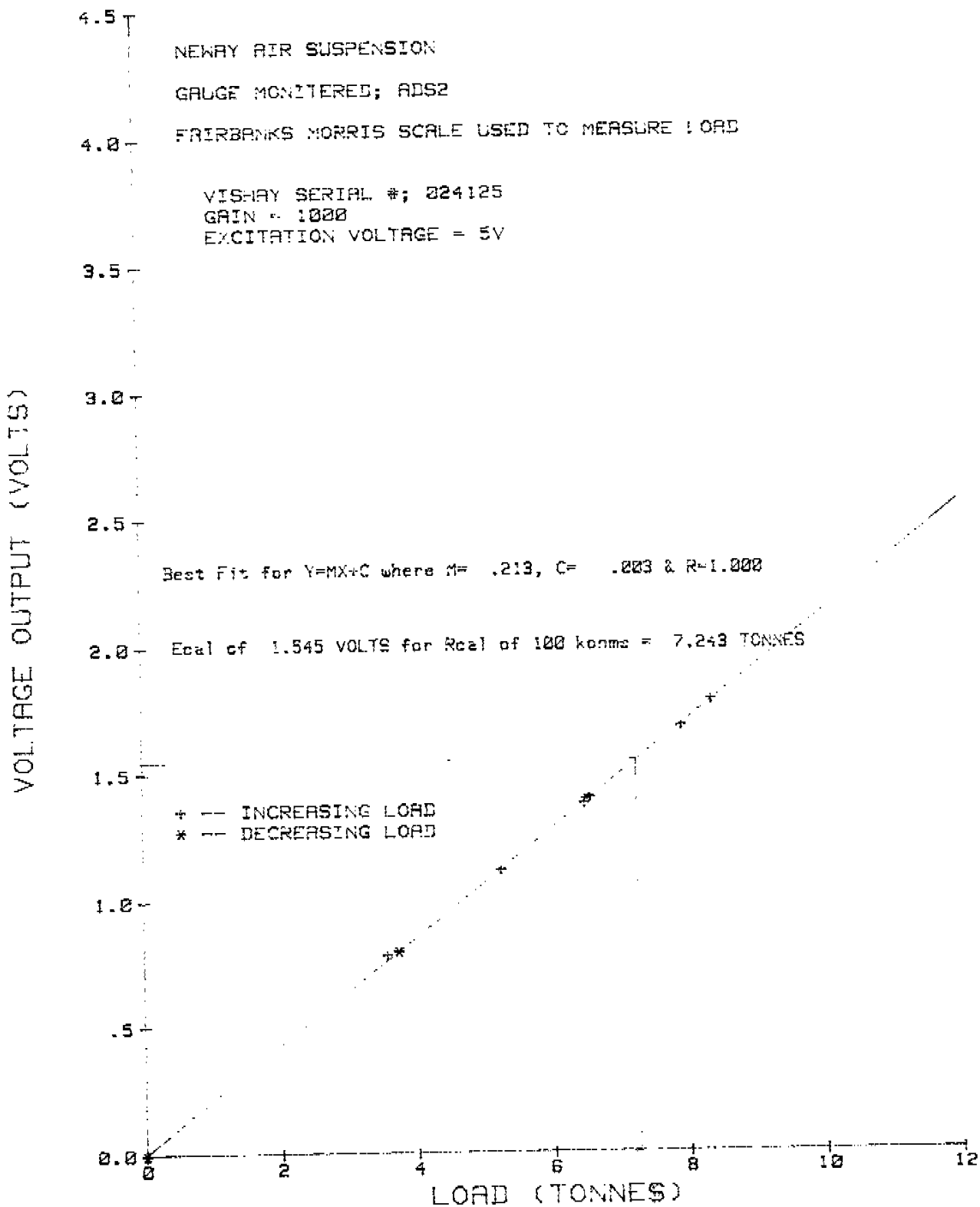
Subfiles: NONE

CALIBRATION OF TRAILER AXLE #1

OBS#	Variable # 1	Variable # 2	Variable # 3
1	0.00000	-.00060	-.00010
2	3.57000	.78390	.84550
3	5.25000	1.11790	1.22310
4	6.48000	1.37630	1.49110
5	6.57000	1.40000	1.50740
6	7.92000	1.68220	1.79380
7	8.36000	1.78500	1.90050
8	6.51000	1.39470	1.51100
9	3.74000	.79900	.91780
10	0.00000	-.00400	.01430

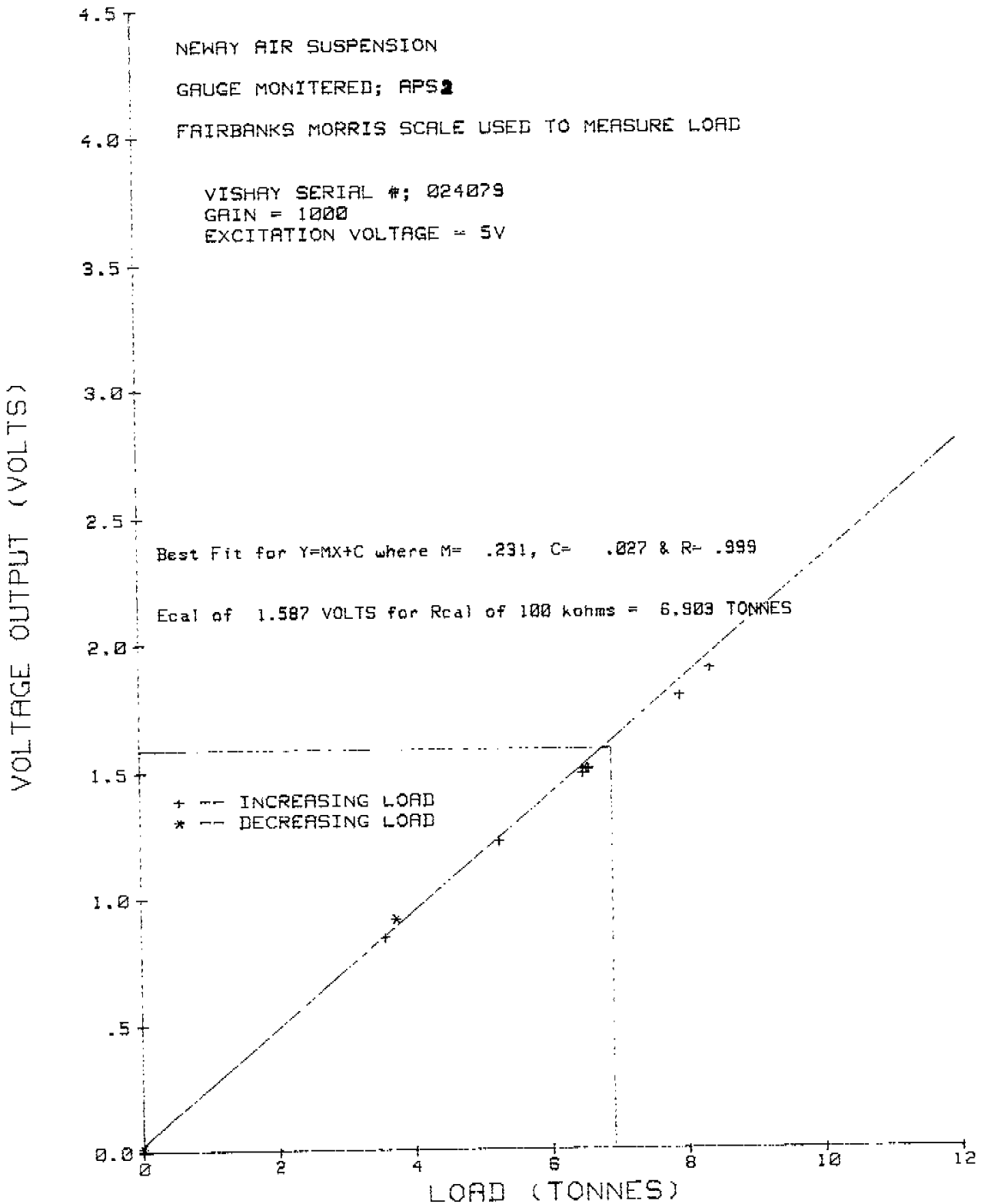
NOV., 28, 1985

VERTICAL LOAD CALIBRATION



NOV., 28, 1985

VERTICAL LOAD CALIBRATION



 * DATA MANIPULATION *

 CALIBRATION OF TRAILER AXLE #2

Data file name: DATA
 Number of observations: 26
 Number of variables: 3

Variables names:
 1. TONNES
 2. BDS2
 3. BPS2

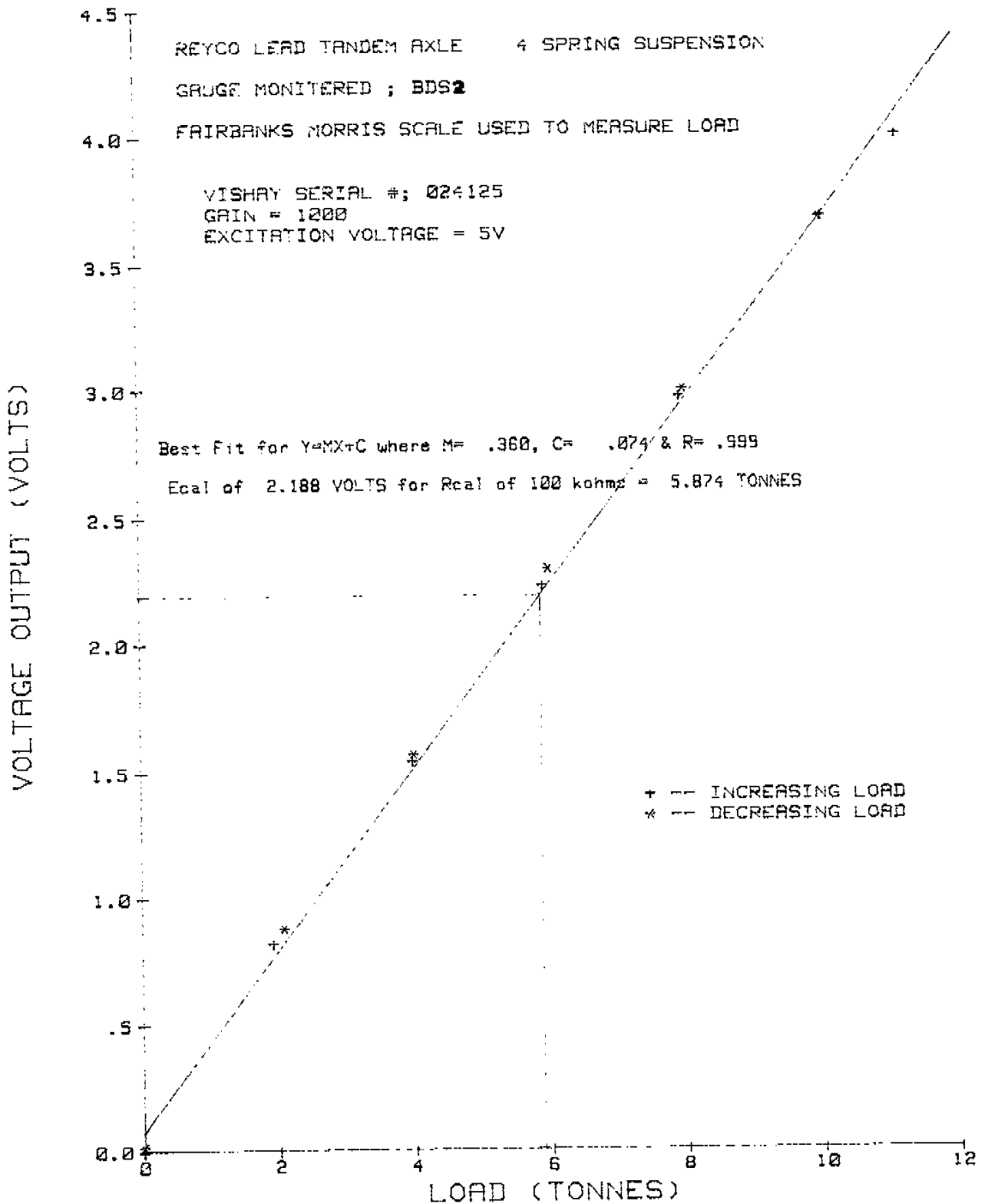
Subfiles: NONE

CALIBRATION OF TRAILER AXLE #2

ORS#	Variable # 1	Variable # 2	Variable # 3
1	0.00000	-.00460	.00290
2	1.92000	.82000	.42800
3	3.99000	1.54050	.93980
4	5.91000	2.22800	1.47700
5	7.95000	2.97000	1.99000
6	10.04000	3.68400	2.52800
7	11.15000	4.00100	2.91200
8	10.02000	3.68200	2.55800
9	8.00000	2.99800	2.00000
10	6.00000	2.29500	1.51400
11	4.01000	1.56820	.98320
12	2.08000	.88000	.47050
13	0.00000	.01600	-.01300
14	0.00000	.01300	-.01600
15	3.93000	1.54200	.92900
16	7.91000	2.96000	1.97000
17	11.21000	4.02000	2.90900
18	7.96000	2.96600	1.97500
19	3.95000	1.52700	.95860
20	0.00000	0.00000	0.00000
21	3.94000	1.53570	.96080
22	7.97000	2.95800	2.00600
23	11.21000	4.00300	2.92200
24	7.95000	2.95400	2.00800
25	3.94000	1.51820	.98470
26	0.00000	.00600	.00300

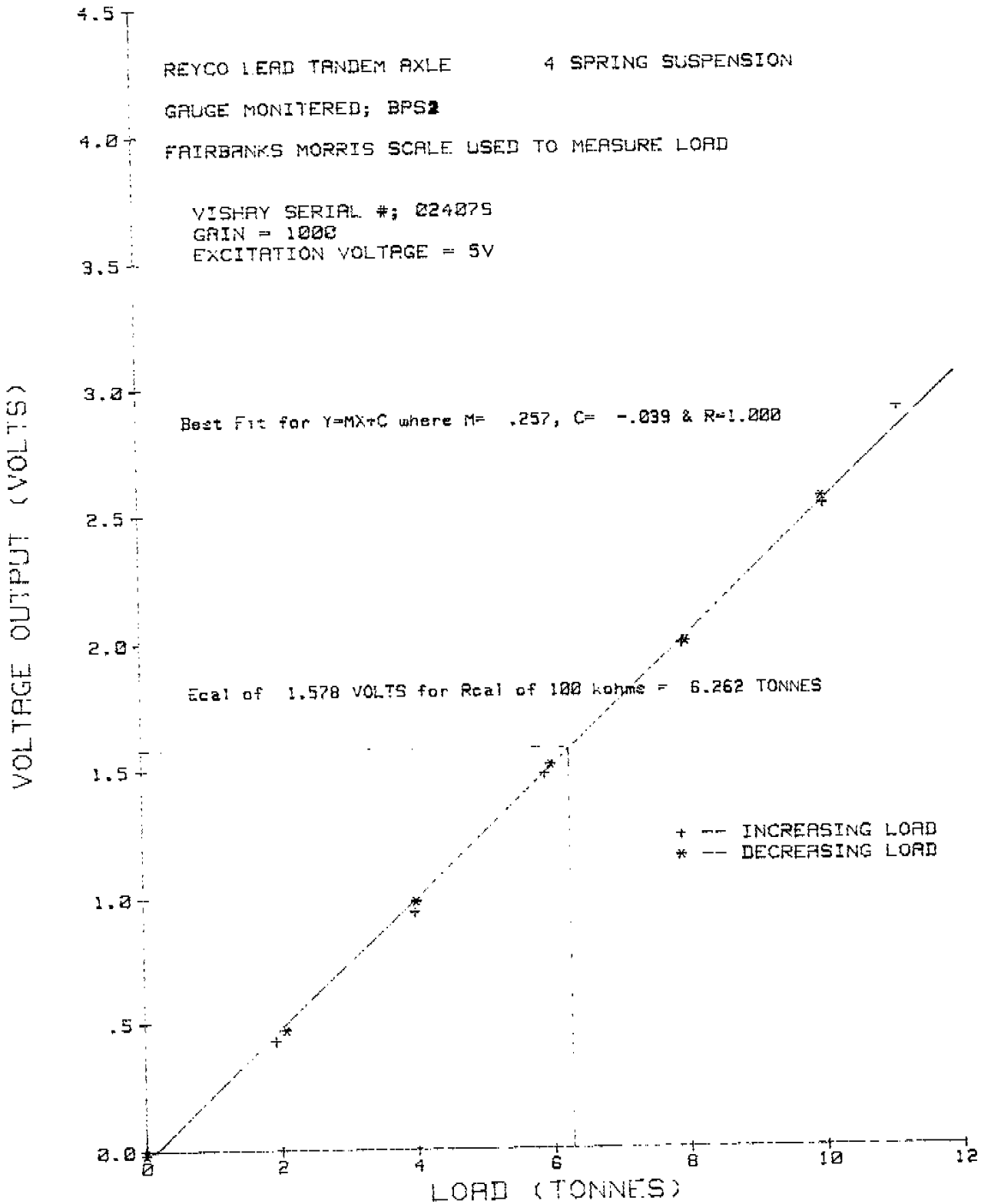
NOV., 28, 1985

VERTICAL LOAD CALIBRATION



NOV., 28, 1985

VERTICAL LOAD CALIBRATION



 * DATA MANIPULATION *

 CALIBRATION OF TRAILER AXLE #3

Data file name: DATA
 Number of observations: 29
 Number of variables: 3

Variables names:
 1. TONNES
 2. CPS2
 3. CPS2

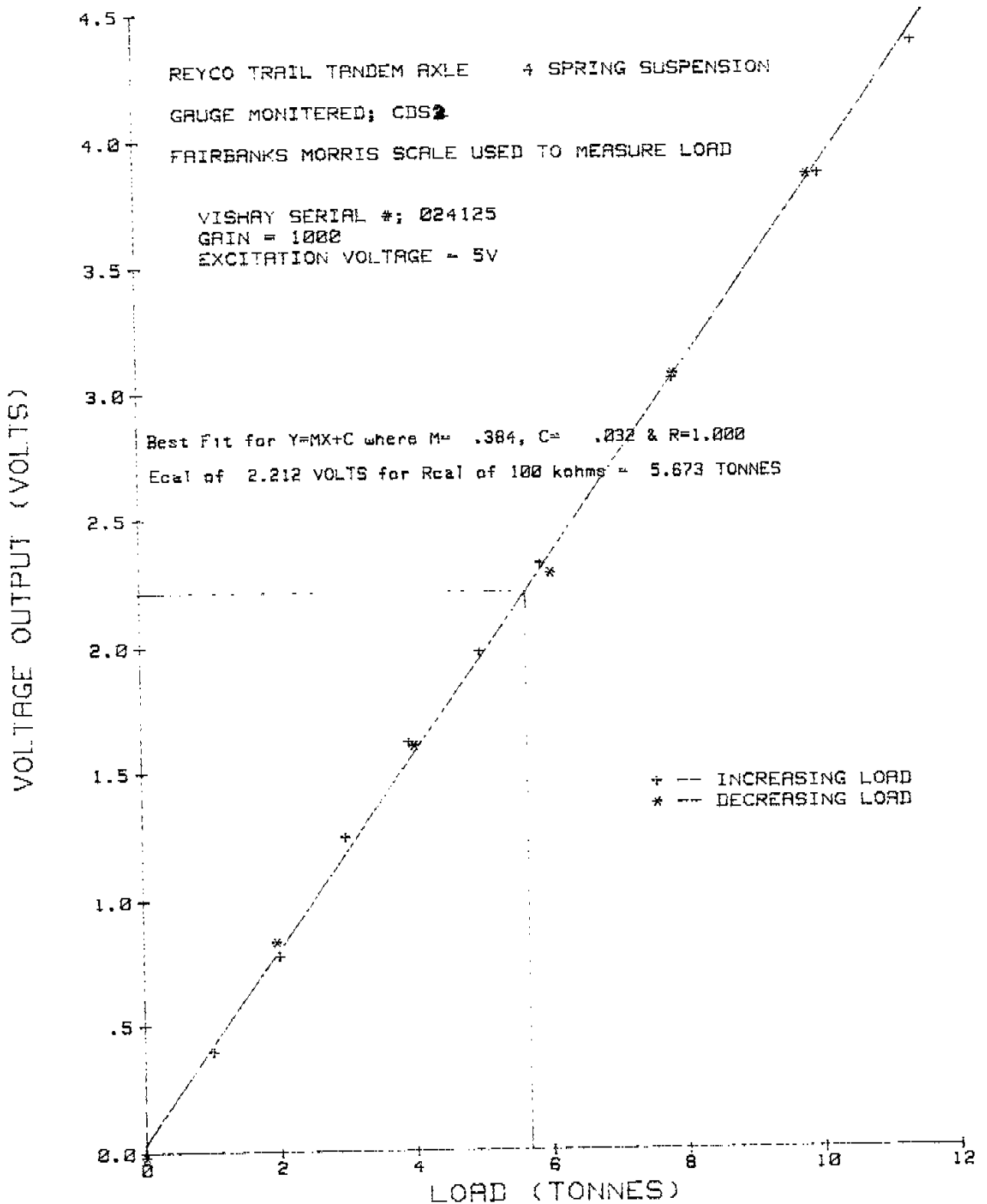
Subfiles: NONE

CALIBRATION OF TRAILER AXLE #3

OBS#	Variable # 1	Variable # 2	Variable # 3
1	0.00000	0.00000	0.00000
2	1.01000	.39540	.22850
3	2.00000	.77680	.46190
4	2.99000	1.24680	.63940
5	3.94000	1.61770	.88870
6	4.99000	1.97840	1.12930
7	5.90000	2.32200	1.37700
8	7.88000	3.05100	1.85500
9	10.06000	3.85700	2.36000
10	11.46000	4.37900	2.73600
11	9.89000	3.85400	2.32600
12	7.89000	3.06800	1.86100
13	6.05000	2.28500	1.38200
14	4.02000	1.60350	.95040
15	1.96000	.83440	.44030
16	0.00000	-.01630	.00010
17	0.00000	-.00810	.00940
18	4.23000	1.71670	.96300
19	7.68000	2.98200	1.82000
20	11.46000	4.39200	2.74400
21	7.71000	3.01300	1.83400
22	4.31000	1.70800	1.03200
23	0.00000	-.01600	.00640
24	4.19000	1.71090	.94750
25	7.72000	3.00100	1.81230
26	11.48000	4.43000	2.73400
27	7.87000	3.09200	1.85800
28	4.32000	1.70650	1.02040
29	0.00000	-.02020	.00260

NOV., 28, 1985

VERTICAL LOAD CALIBRATION



NOV., 28, 1985

VERTICAL LOAD CALIBRATION

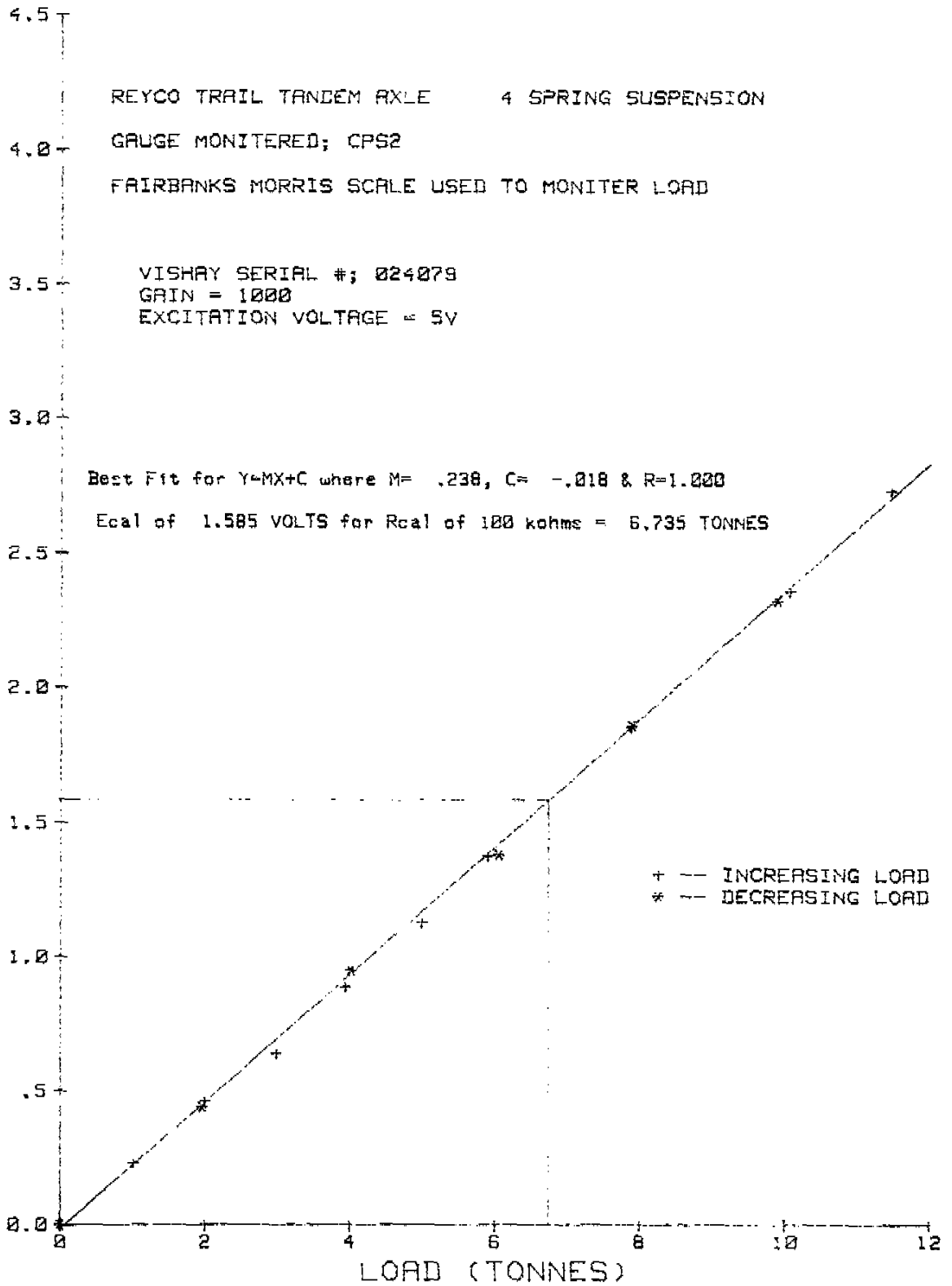
REYCO TRAIL TANDEM AXLE 4 SPRING SUSPENSION
GAUGE MONITERED; CPS2
FAIRBANKS MORRIS SCALE USED TO MONITER LOAD

VISHAY SERIAL #; 024079
GAIN = 1000
EXCITATION VOLTAGE = 5V

Best Fit for $Y=MX+C$ where $M= .230$, $C= -.018$ & $R=1.000$

Ecal of 1.585 VOLTS for Rcal of 100 kohms = 6.735 TONNES

VOLTAGE OUTPUT (VOLTS)



APPENDIX H

HAYES DANA AXLE COMPONENT WEIGHTS

Description	Weight	Quantity Per Axle	Total Weight
Nuts	2 lbs* (set of 10)	2	4 lbs
Studs	3 lbs 9.5 oz (set of 10)	2	7
Tire and Rim	228 1/3	4	913
Cam Shaft	14	2	28
Brake Shoes & Lining	18	4	72
Hub & Drum	137	2	274
Bare Axle	235	1	235
Spring Suspension Assembly (Reyco Leaf)	139	2	278
Air Chamber	10	2	20
Brake Arm	7	2	14
Springs, Cam Holder	24 1/2	2	49

Total Weight = 1894 Lbs

Hayes Dana Axle Component Weights

FINAL CALIBRATION STANDARDS

1.0 INTRODUCTION

Nine tractor-trailer axles strain gauged to measure vertical load were calibrated using an aircraft weighing scale and a Vishay strain gauge conditioning amplifier. The gauges were located on the passenger side at midpoint between the wheel hub and the suspension point.

Of the nine axles, two are tractor drive axles while the remaining are trailer axles. The tractor front and rear drive axles are supported by a Hendrickson RTE 440 tandem suspension. The trailer axles are numbered from the front end of the trailer. Axle #1 is fixed to a Neway air suspension while axles #2 and #3 form an axle group at the rear of the trailer. The axles for three different trailer suspension types were calibrated; namely these were a Reyco 4 spring suspension, a Neway air suspension and a Chalmers walking beam rubber suspended suspension.

Equipment

- ten single element (uniaxial) strain gauges
- aircraft weighing scale
- Vishay signal conditioning amplifier,
Ser. No. 045312
- voltmeter, Ser. No. 10343
- two 3/4" steel plates, 14" x 18"
- White Freightliner tractor
- NRC modified Fruehauf tanker-trailer
- air and hydraulic jacks
- level

Test Setup

The calibration was performed in a temperature controlled environment of 20°C.

The tractor axles were calibrated by jacking the rear end of the tractor and positioning load cells under the dual wheel of the axle being calibrated. The three load cells were sandwiched between two 3/4" steel plates. They were placed in a manner to record approximately equal loads. Lift blocks were placed under the remaining tractor drive wheels to maintain the walking beam level with the horizontal. Photographs 1 to 6 show the load cell and jacking arrangement used for calibrating the vehicle.

The same type of load cell configuration was used to record the vertical load on the trailer axles. The trailer was kept level to the horizontal (less than 1°) during all three trailer axle calibrations by jacking the unmonitored dual wheels on lift blocks.

2.0 CALIBRATION

In all cases the load cells and the Vishay unit were zeroed with the dual wheel in the jacked position (no contact between dual wheel and top steel plate).

The vertical load was generated to the tractor axles by lowering the tractor with the use of two air jacks. A level was installed on the tractor chassis to ensure zero roll angle during calibration.

3.0 RESULTS AND OBSERVATIONS

A plot of nine calibration curves is shown in Graphs 1 to 9. The nine calibrations are found to be accurate within 0.15 tonne for any given voltage output.

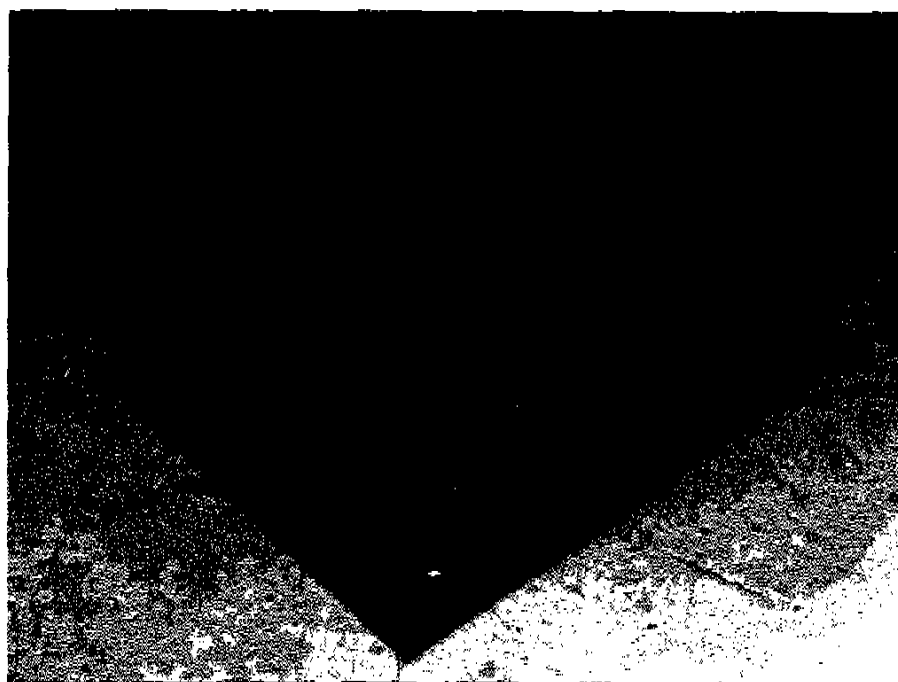
The voltage output for the front drive axle oscillated consistently during calibration with an amplitude of approximately 5 mV for any given vertical load. The voltage output used for the least-square fitting was the average of the maximum and minimum values recorded.

The loading system on the Neway air suspension required about five minutes for the applied load to settle to a reasonably constant load. For every observation point the voltage output was recorded followed by the three load cell readings and a final voltage output reading. Hence, the average load and average voltage output over the time of the reading was recorded. The loading increased or decreased from the average load by less than 0.02 tonne during the time of the recording.

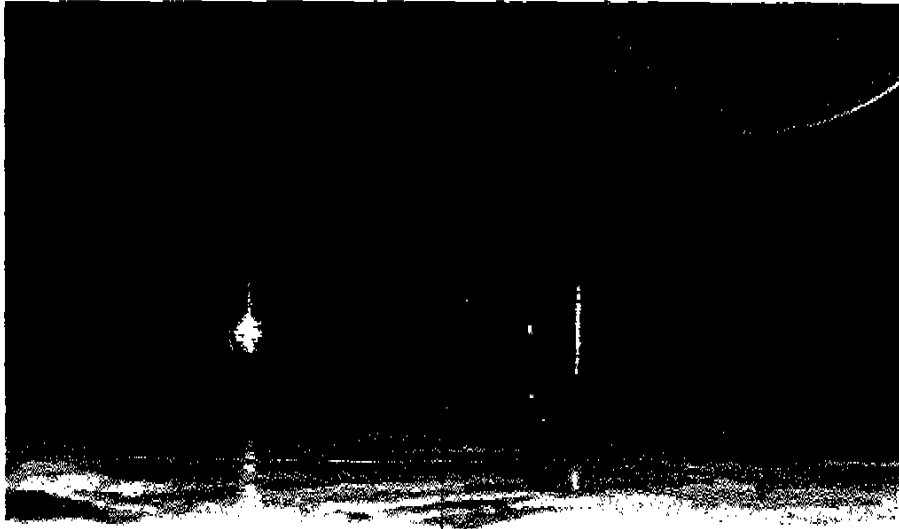
The voltage output and the load cell force for the rear drive axle and axles #2 and #3 were recorded without any appreciable drift.

4.0 CONCLUSION

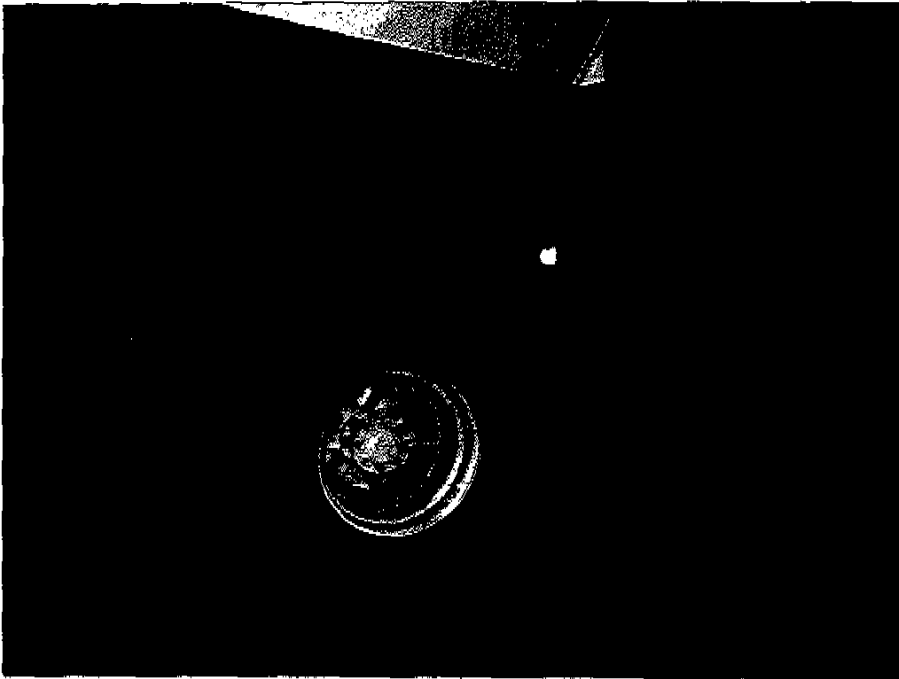
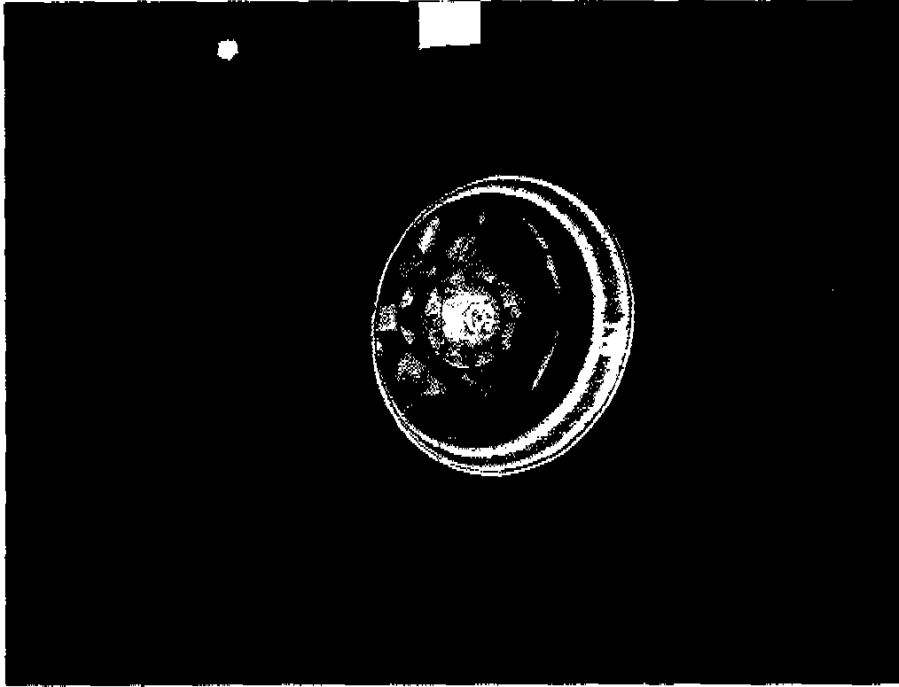
The calibration curves plotted on Graphs 1 to 9 meet the accuracy requirements for the study and were therefore used as the calibration data in the dynamic suspension response testing.



FIGURES 1, 2 THREE LOAD CELLS AND TWO STEEL PLATES
WHICH COMPRISED THE CALIBRATION SCALE



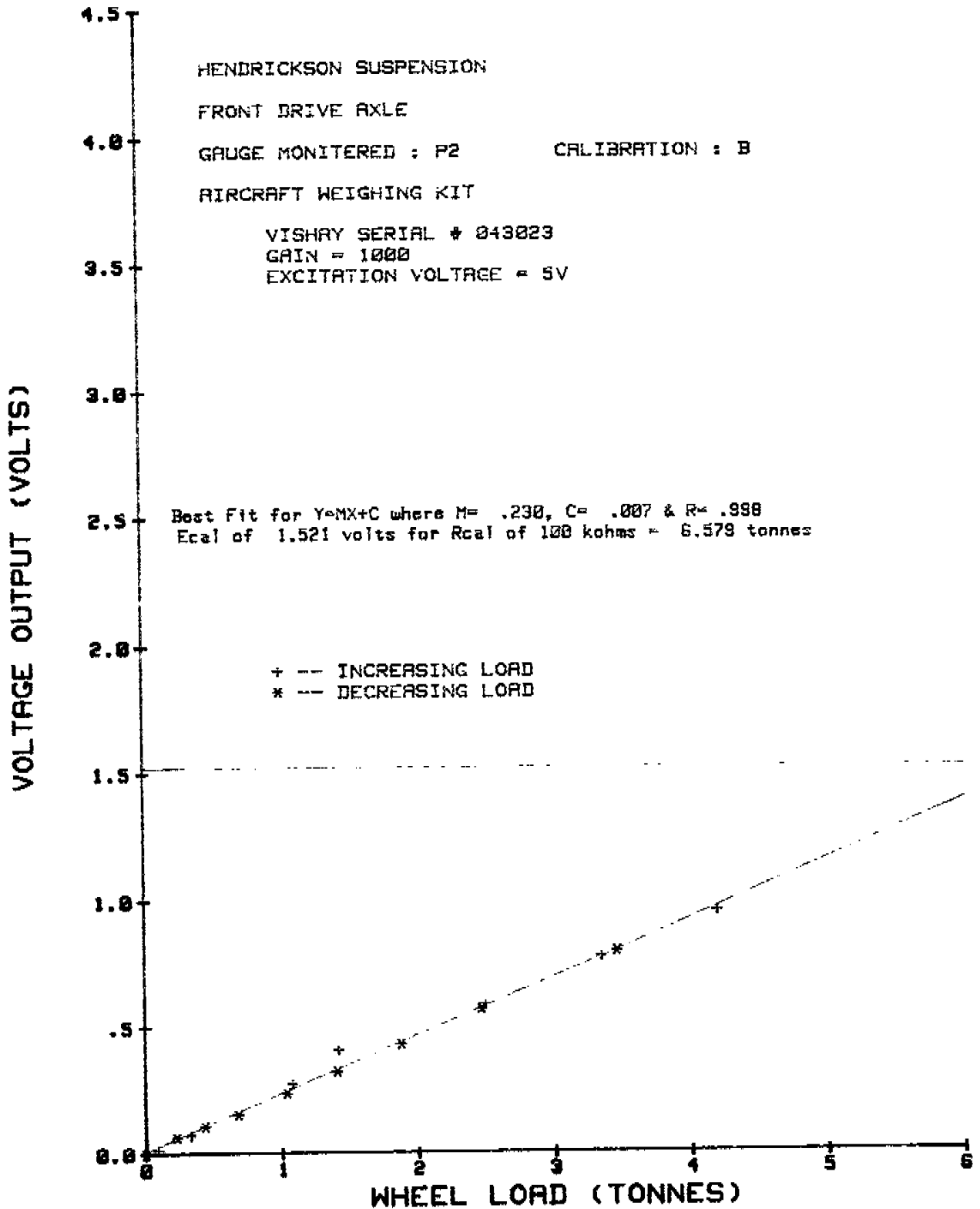
FIGURES 3, 4 LOCATION OF THE SCALE DURING CALIBRATION OF THE AXLE



FIGURES 5, 6 VIEW OF AXLES AND WEIGH SCALE DURING CALIBRATION

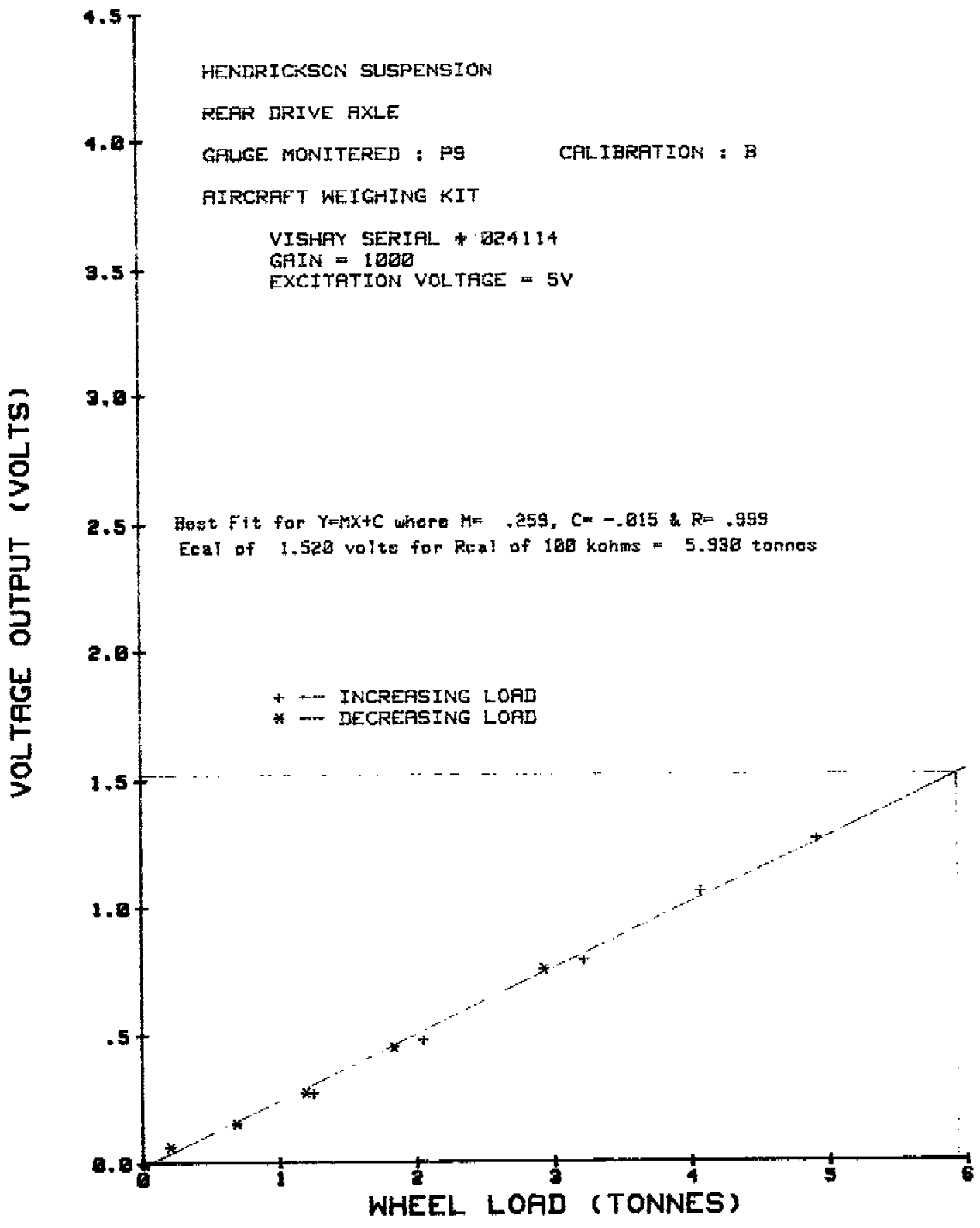
24 APR 1986

VERTICAL LOAD CALIBRATION



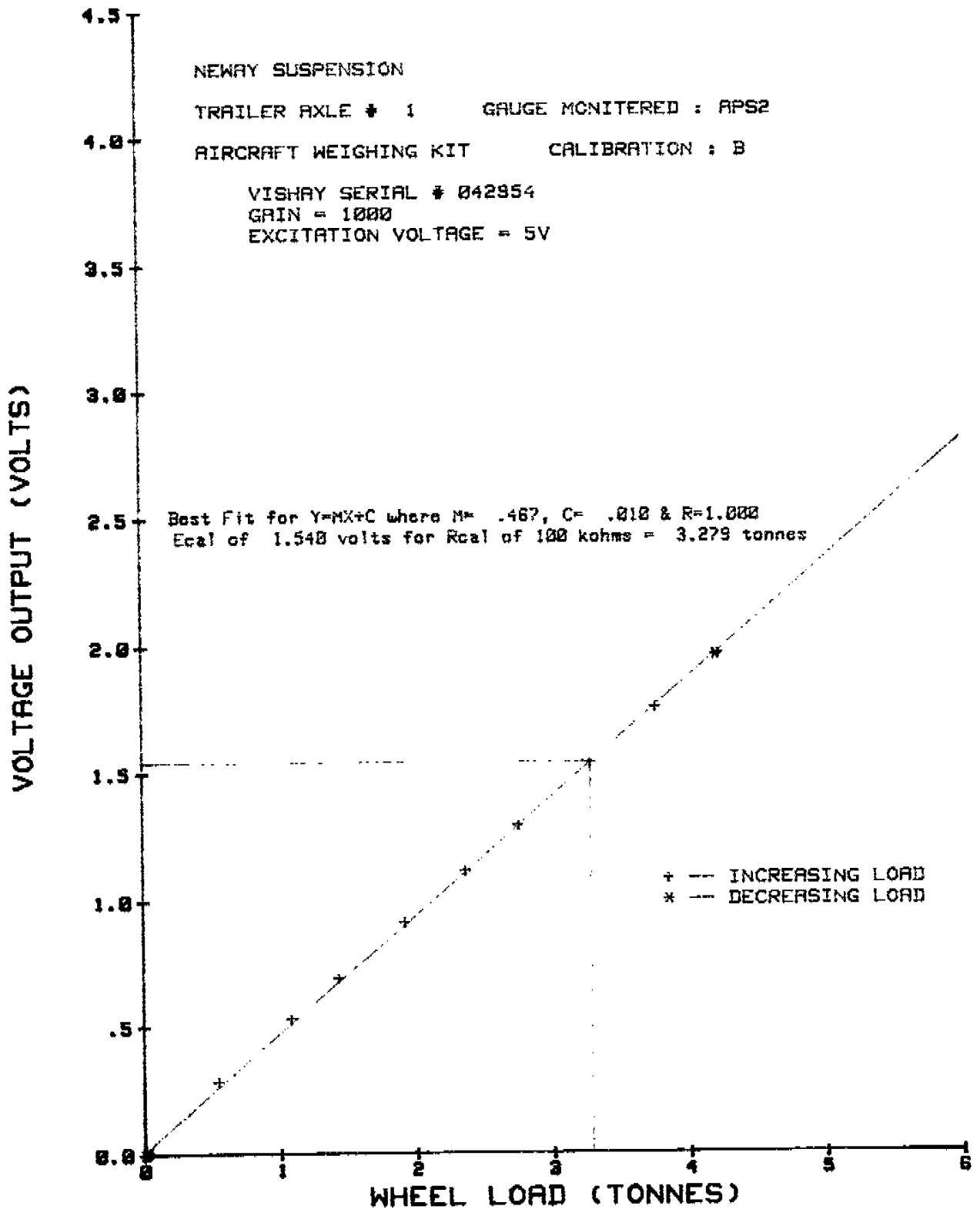
24 APR 1986

VERTICAL LOAD CALIBRATION



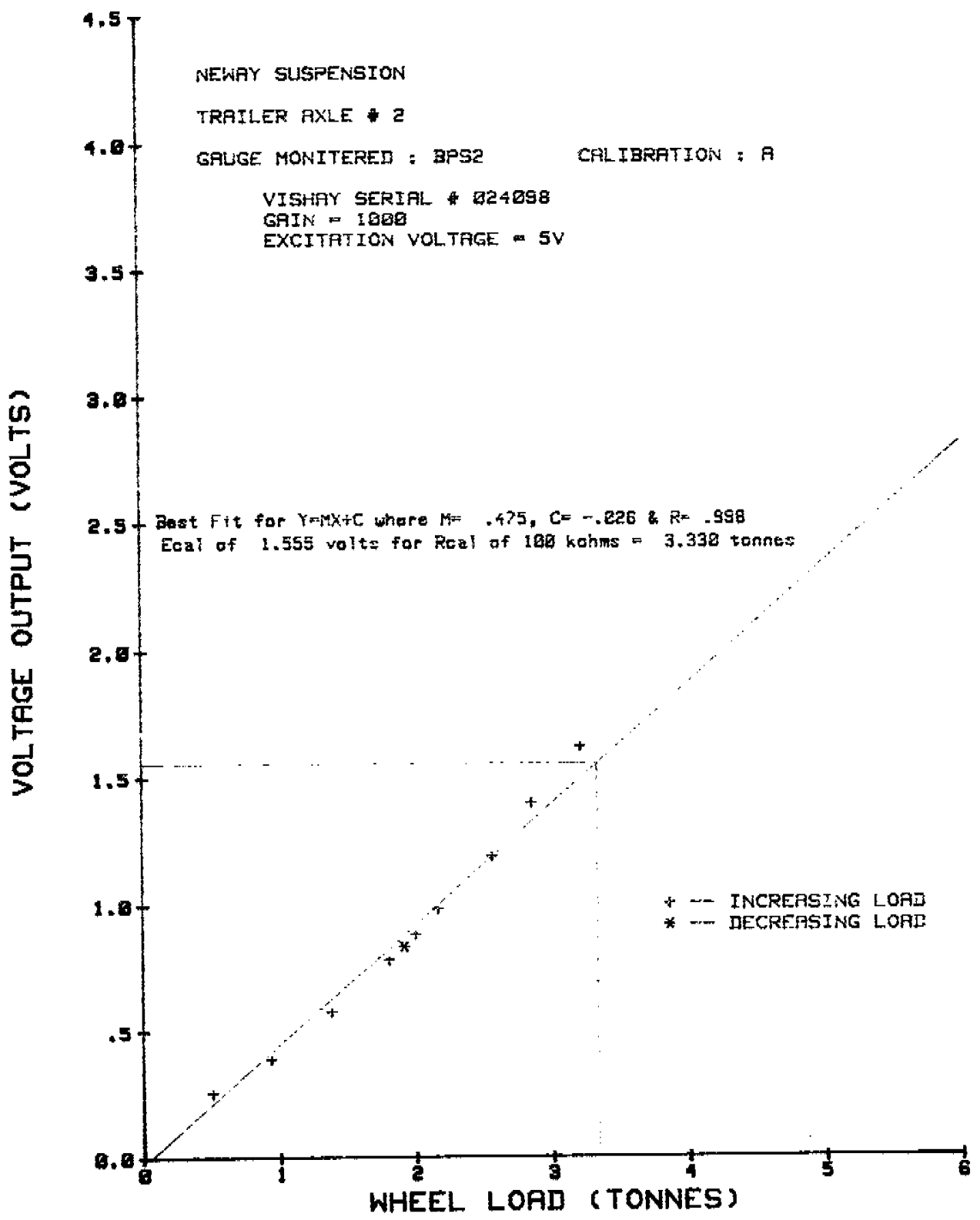
24 APR 1986

VERTICAL LOAD CALIBRATION



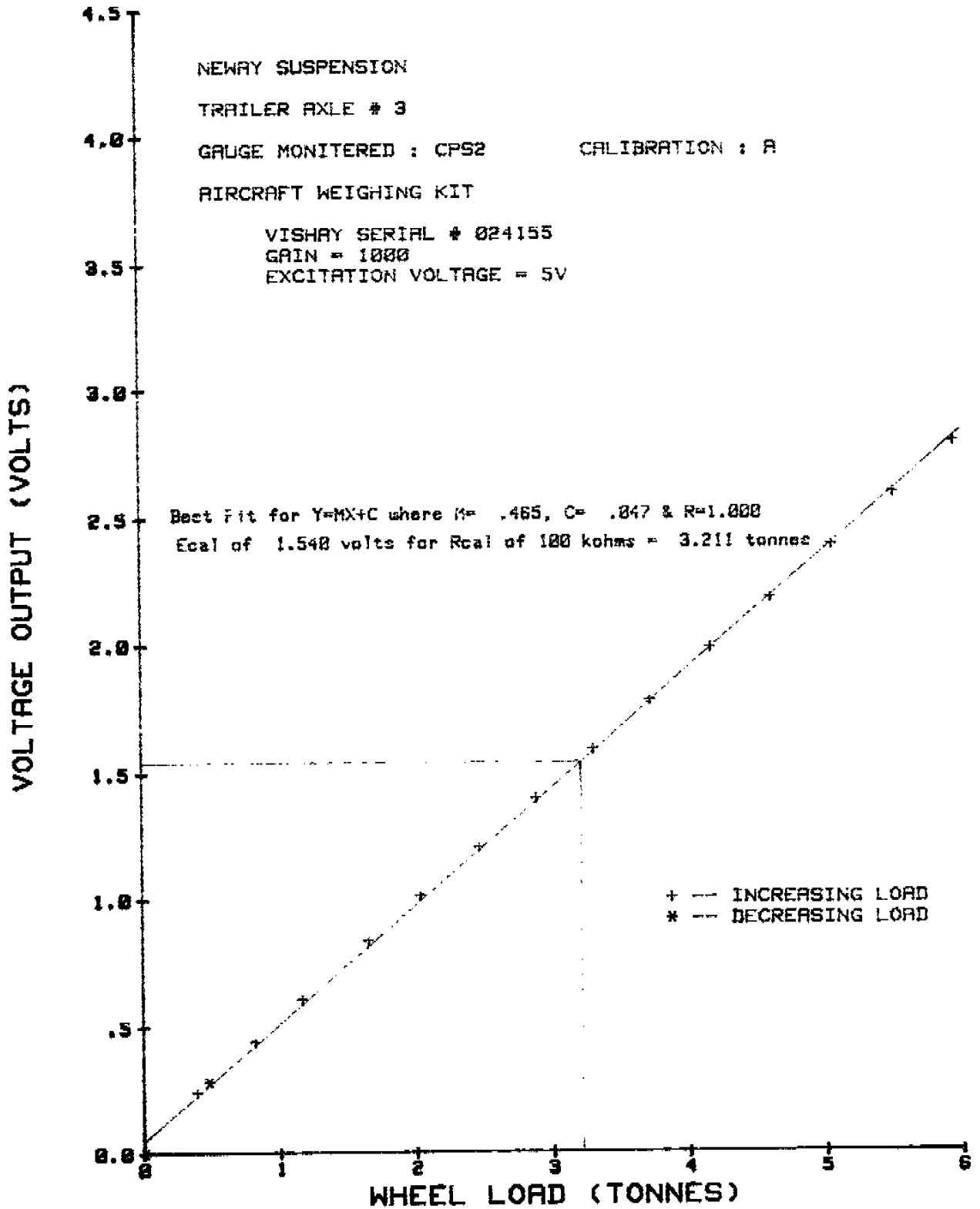
24 APR 1986

VERTICAL LOAD CALIBRATION



24 APR 1986

VERTICAL LOAD CALIBRATION



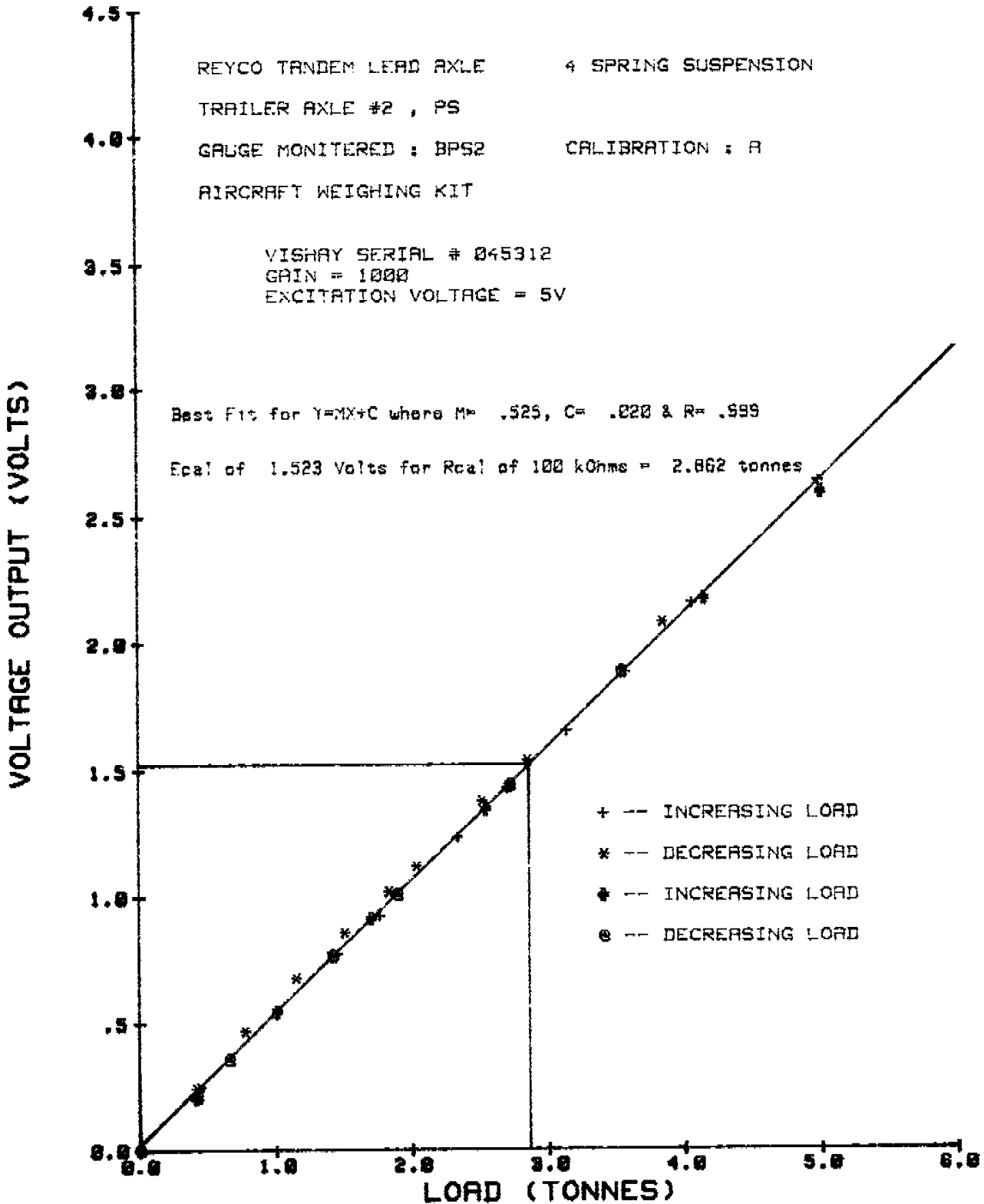
VERTICAL LOAD CALIBRATION

REYCO TANDEM LEAD AXLE 4 SPRING SUSPENSION
 TRAILER AXLE #2 , PS
 GAUGE MONITERED : BPS2 CALIBRATION : A
 AIRCRAFT WEIGHING KIT

VISHAY SERIAL # 045312
 GAIN = 1000
 EXCITATION VOLTAGE = 5V

Best Fit for $Y=MX+C$ where $M= .525$, $C= .020$ & $R= .999$

Eqal of 1.523 Volts for Reqal of 100 kOhms = 2.862 tonnes



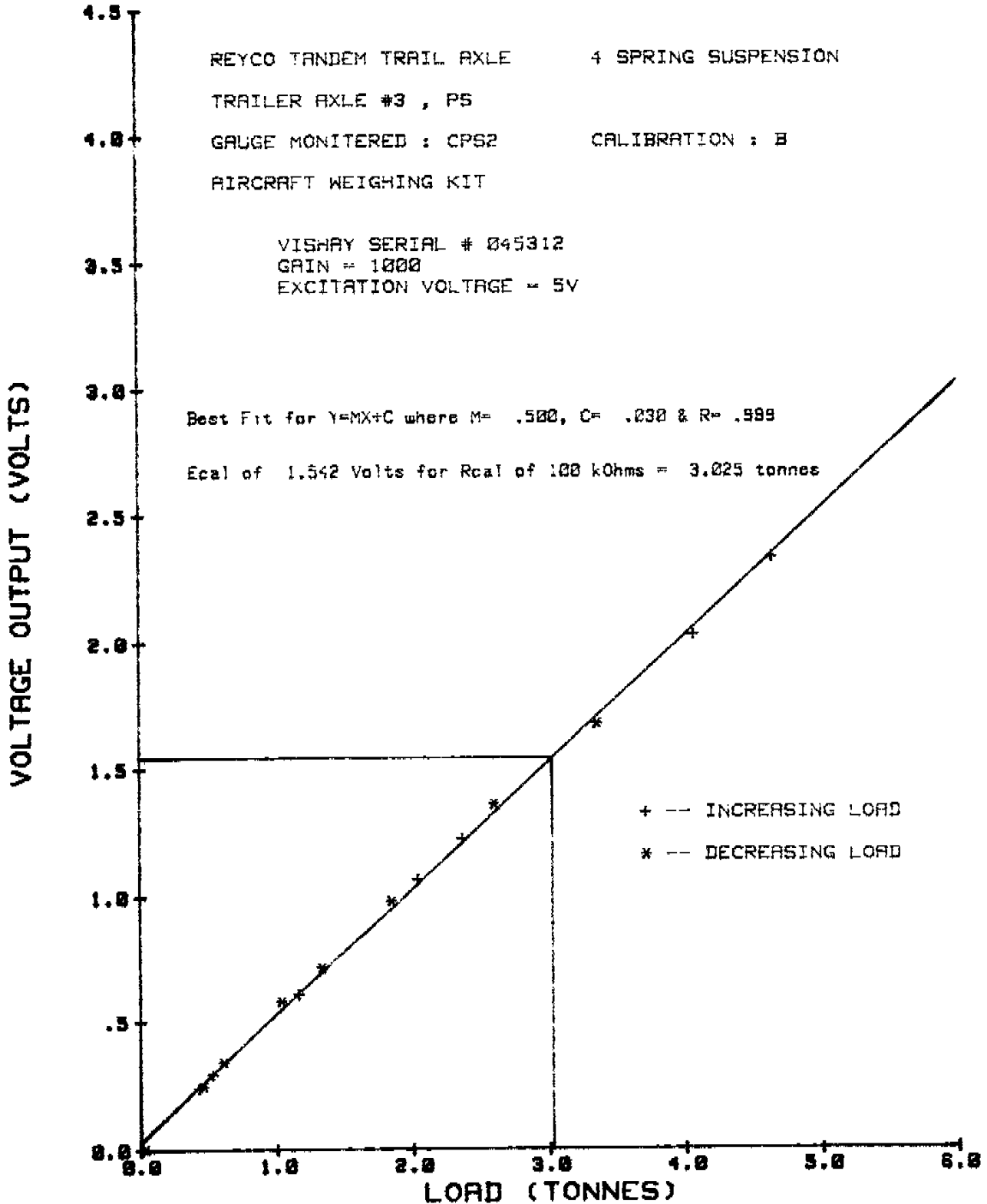
VERTICAL LOAD CALIBRATION

REYCO TANDEM TRAIL AXLE 4 SPRING SUSPENSION
TRAILER AXLE #3 , P5
GAUGE MONITERED : CPS2 CALIBRATION : B
AIRCRAFT WEIGHING KIT

VISHAY SERIAL # 045312
GAIN = 1000
EXCITATION VOLTAGE = 5V

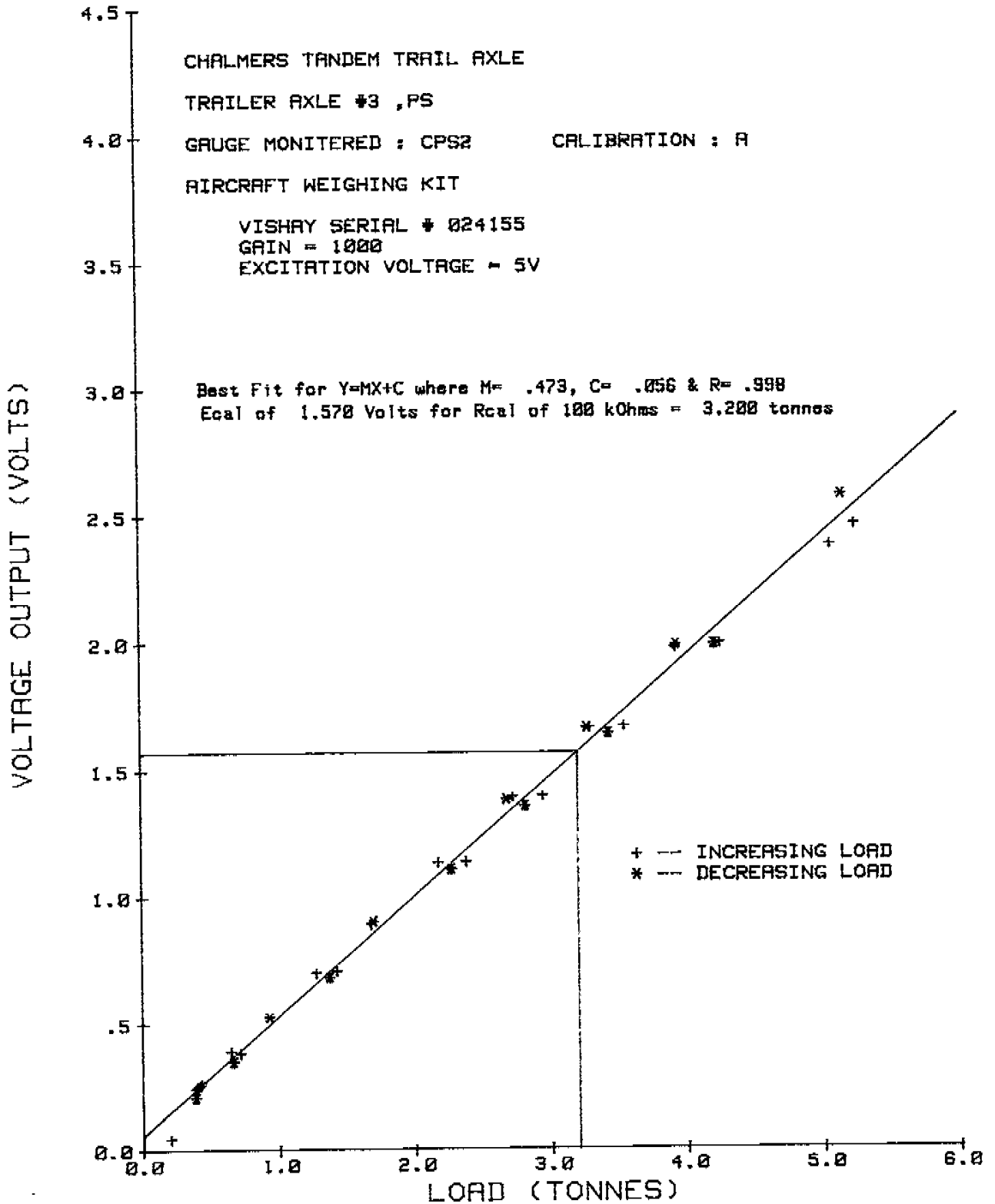
Best Fit for $Y=MX+C$ where $M= .500$, $C= .030$ & $R= .999$

Ecal of 1.542 Volts for Rcal of 100 kOhms = 3.025 tonnes



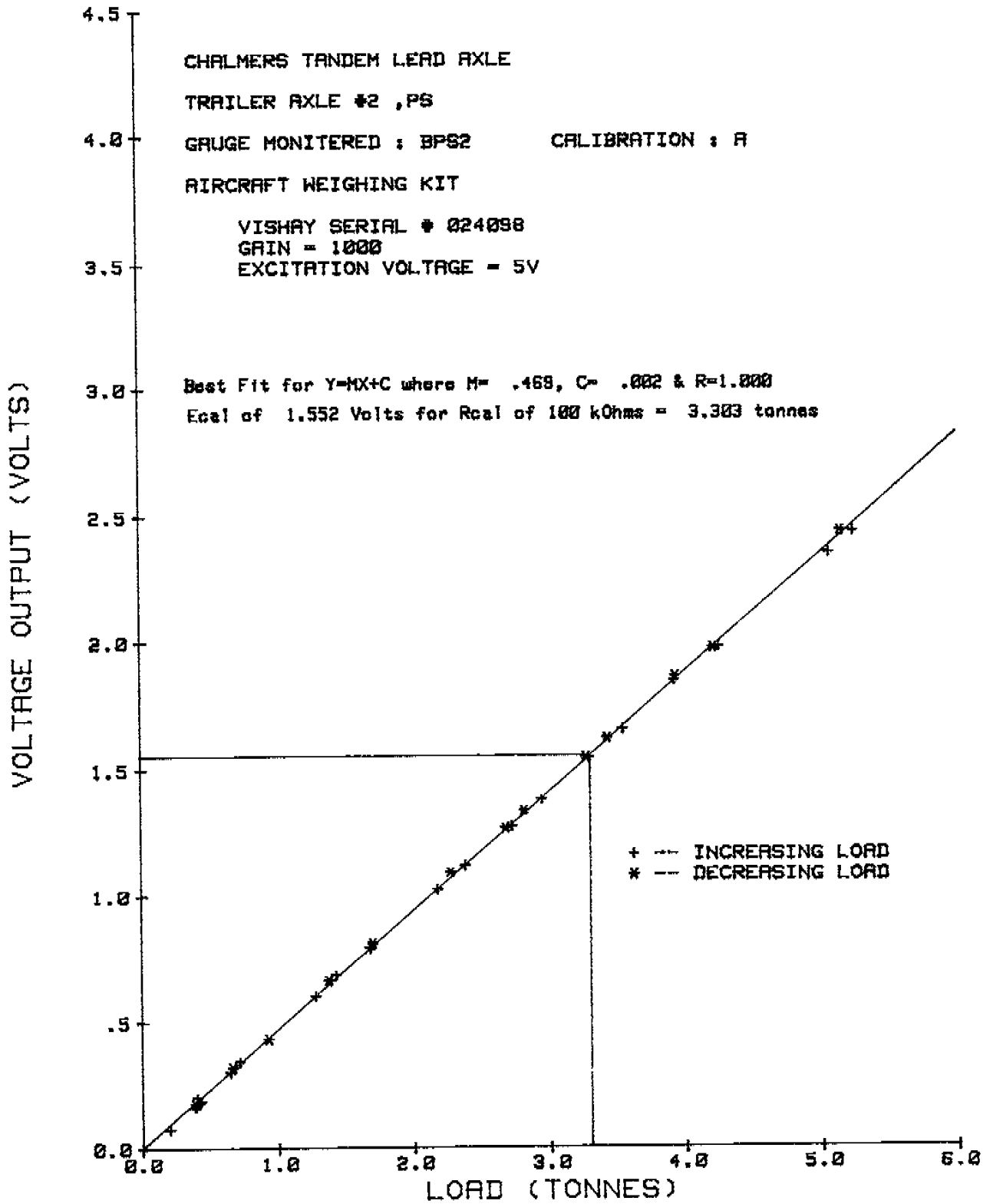
2 JUNE 1986

VERTICAL LOAD CALIBRATION



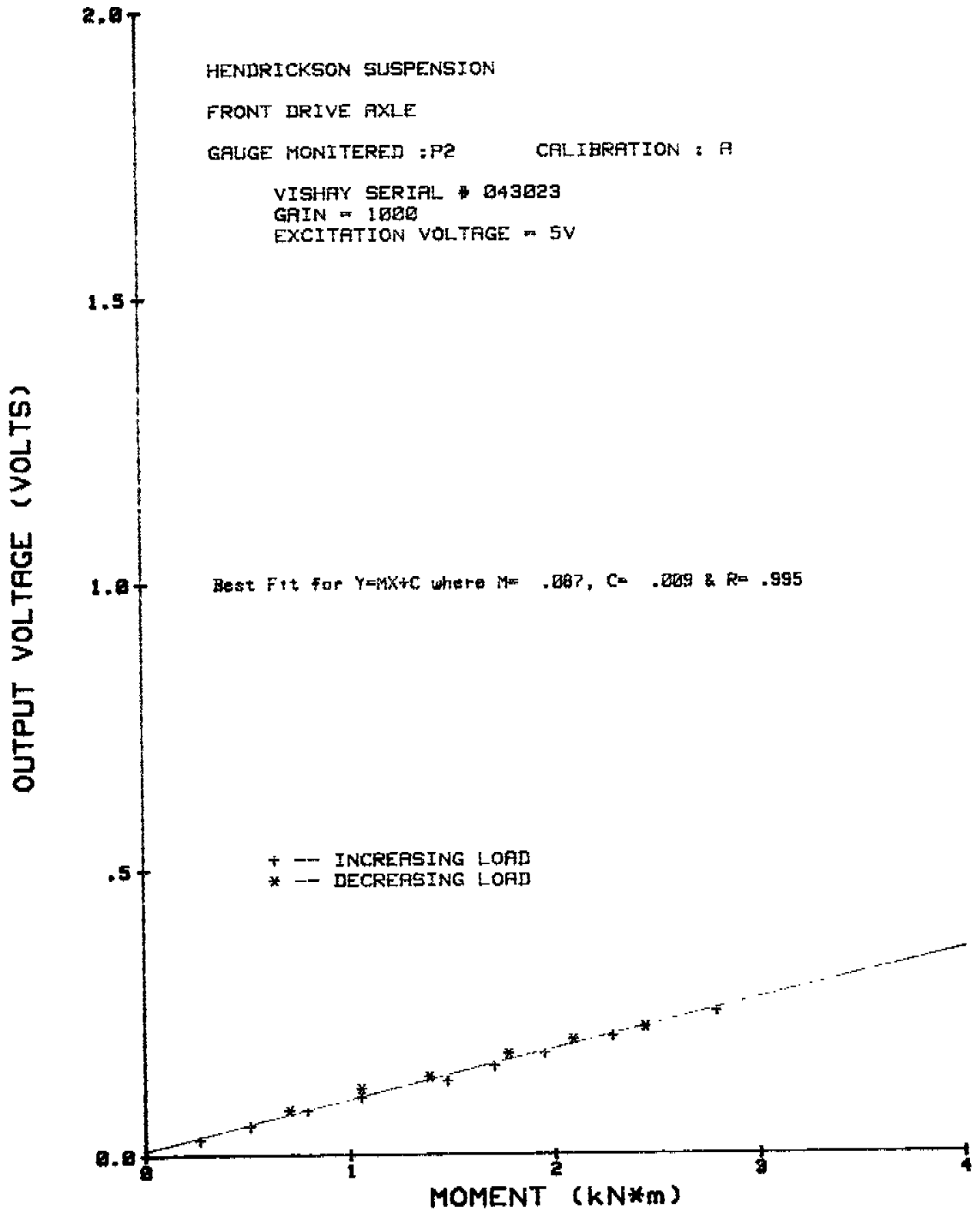
2 JUNE 1986

VERTICAL LOAD CALIBRATION



23 APR 1986

BENDING MOMENT CALIBRATION



23 APR 1986

BENDING MOMENT CALIBRATION

HENDRICKSON SUSPENSION

REAR DRIVE AXLE

GAUGE MONITERED : P9

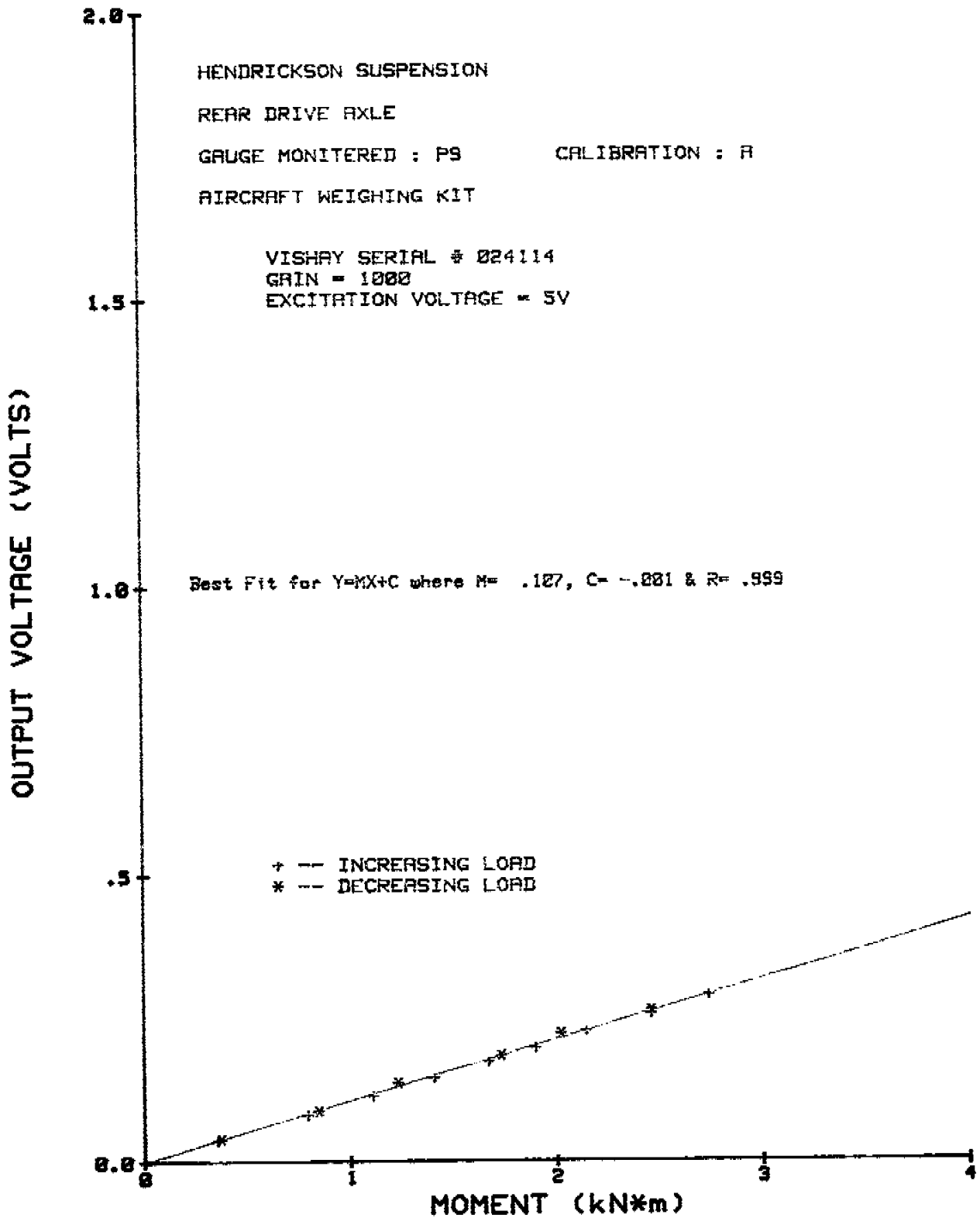
CALIBRATION : A

AIRCRAFT WEIGHING KIT

VISHAY SERIAL # 024114

GAIN = 1000

EXCITATION VOLTAGE = 5V



23 APR 1986

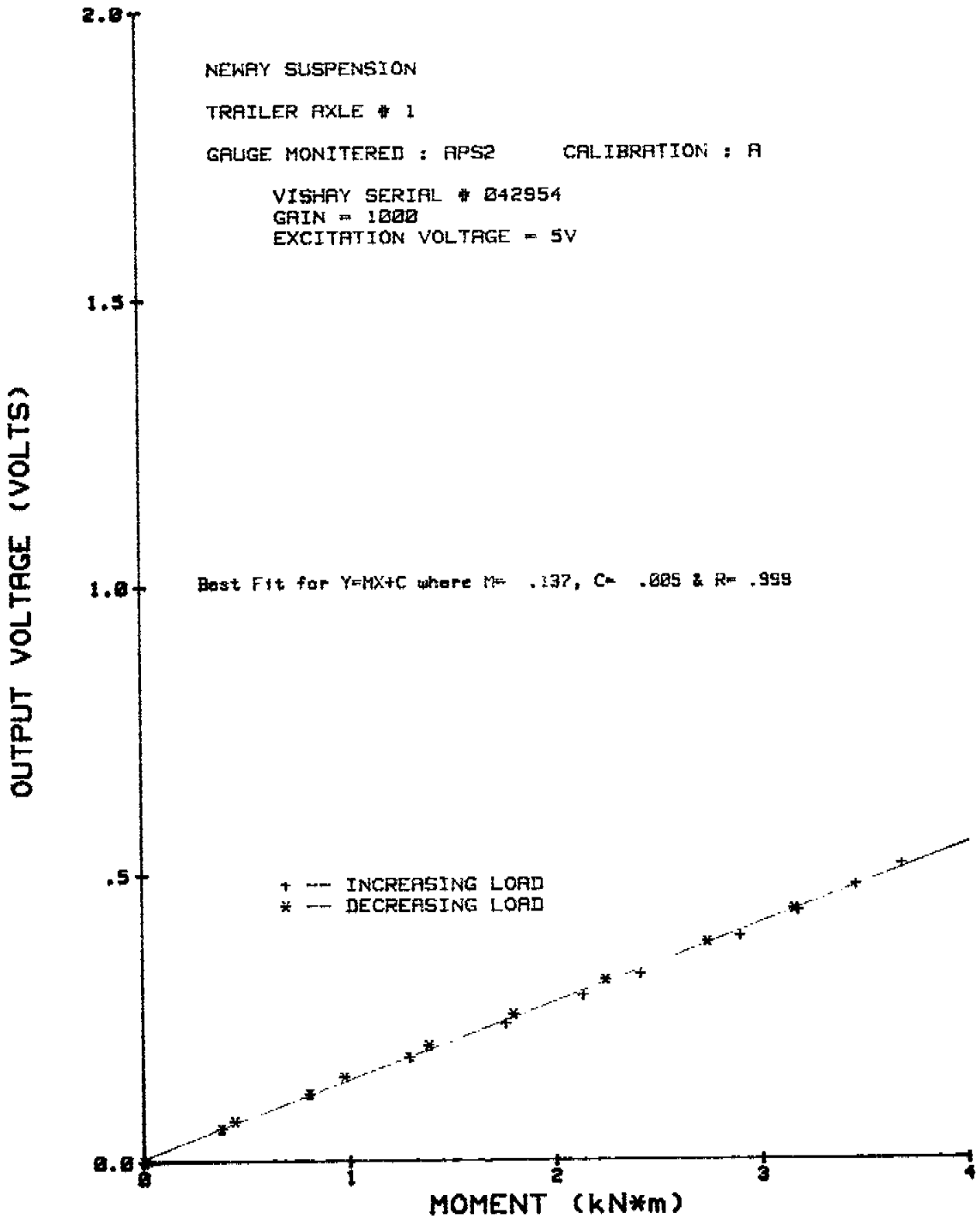
BENDING MOMENT CALIBRATION

NEWAY SUSPENSION

TRAILER AXLE # 1

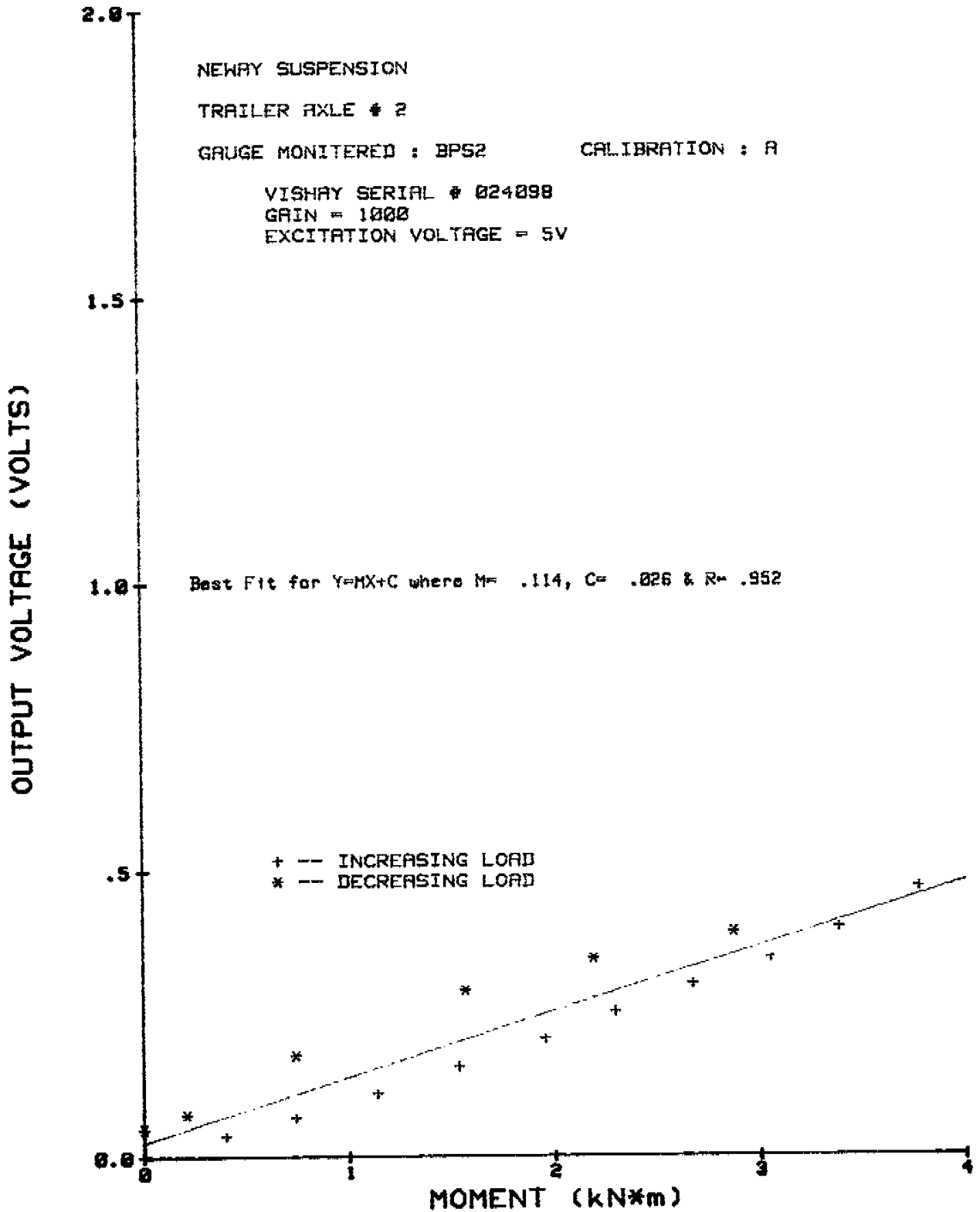
GAUGE MONITERED : APS2 CALIBRATION : A

VISHAY SERIAL # 042954
GAIN = 1000
EXCITATION VOLTAGE = 5V



23 APR 1986

BENDING MOMENT CALIBRATION



23 APR 1986

BENDING MOMENT CALIBRATION

NEWAY SUSPENSION

TRAILER AXLE #3

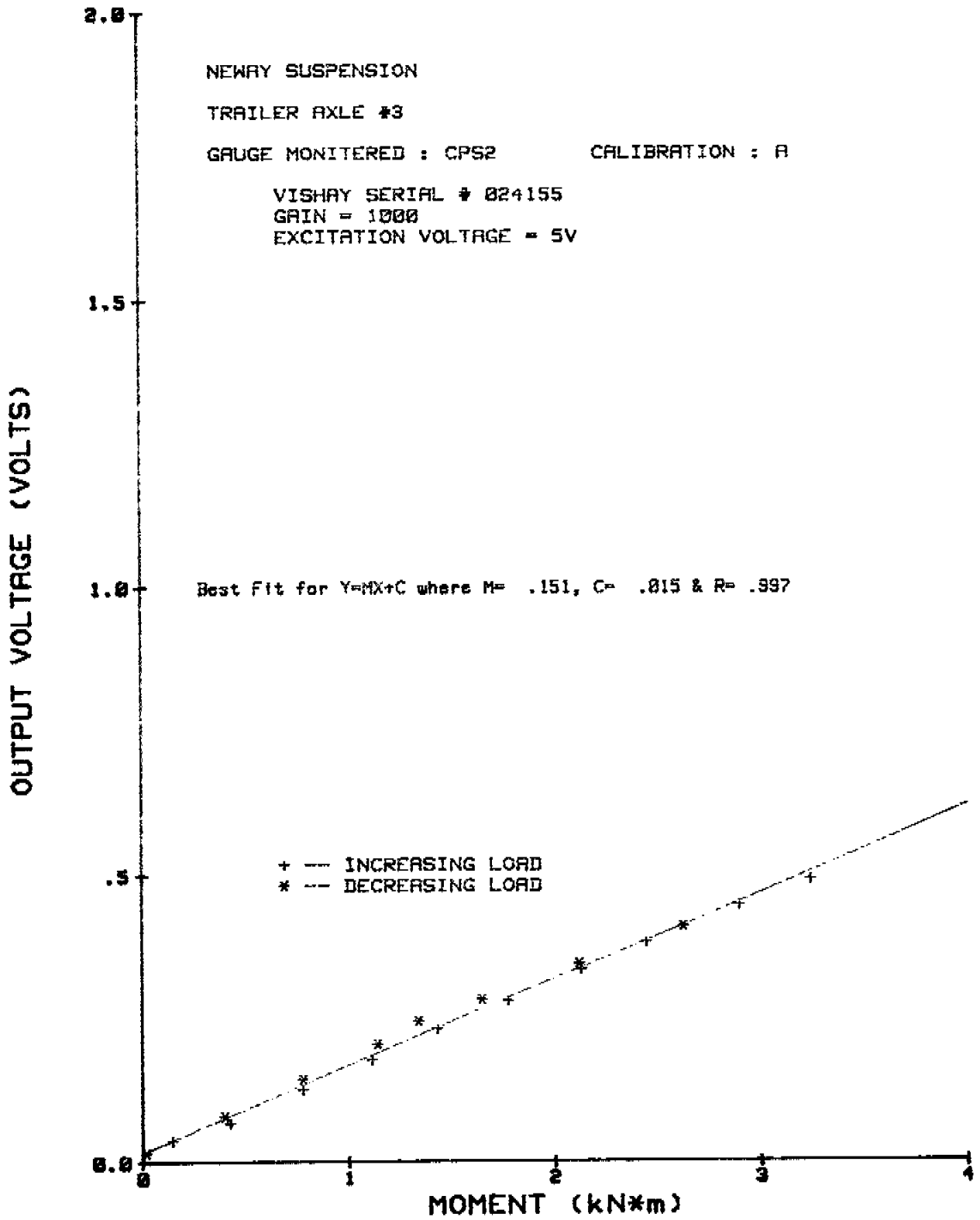
GAUGE MONITERED : CPS2

CALIBRATION : A

VISHAY SERIAL # 024155

GAIN = 1000

EXCITATION VOLTAGE = 5V



APPENDIX C
ROAD ROUGHNESS REPORT

A P P E N D I X

ROUGHNESS MEASUREMENTS

By

A.T.Papagianakis * R.C.G.Haas ** T.Khan *** F.Marciello ****

* Ph.D. student, Dep. of Civil Eng., U. of Waterloo, N2L 3G1

** Professor, Dep. of Civil Eng., U. of Waterloo, N2L 3G1

*** Pavement Research Technician, MTCO, Downsview, Ont., M3M 3E6

**** Highway Design Technician, MTCO, Downsview, Ont., M3M 3E6

Acknowledgment :Thanks are expressed to Mr. J.H.F. Woodrooffe of the National Research Council for his cooperation. Technical support for the roughness measurements was provided by the Ministry of Transportation and Communications of Ontario. Special thanks are addressed to Mr. W.A. Phang for his assistance with the project

TABLE OF CONTENTS

	<u>Page</u>
1. Content Description	1
2. Mays-Meter Roughness Measurements	3
2.1 Woodroffe Avenue	3
2.2 Uplands Road	5
2.3 Highway 417	7
3. Rod-and-Level Measurements	10

1. Content Description

This appendix presents pavement roughness data for three street sections in the city of Ottawa. The National Research Council uses the three sections for its dynamic load measurements obtained by a specially instrumented vehicle. The instrumentation was developed as part of the Heavy Vehicles Weights and Dimensions Study carried-out under the auspices of the RTAC. The three sections tested are:

- (i) Woodrofe Avenue from the CNR trucks 1.7 Km to the Slack Road approach sign
- (ii) Uplands Road from the International Airport sign 1.19 Km Northly to a drainage ditch
- (iii) Highway 417 from the Maitland Road overpass 5.0 Km easterly to the Preston Boulevard intersection

Two methods were used for measuring pavement roughness. First, a Mays-meter device was used to obtain a response-type statistic expressed in the form of inches/mile. This reflects the sum of the vertical displacement of the axle of a standardized trailer with respect to its frame. Measurements were obtained for the full length of all three sections.

Second, true pavement profile was obtained for the first 320 meters of the first two sections by a rod-and-level survey. A sampling interval of 0.5 meters was used. A self-leveling automatic level was used, generating a reference plane by a single laser beam rotating at 300 rpm. The rod contains a sensor that automatically locks into the laser beam.

The roughness measurements described in the following sections are expected to allow a direct comparison between dynamic load on the pavement and roughness profile. This is a pilot study of a project attempting to relate pavement roughness with dynamic vehicle loads. The goal of the project is to develop damage functions to be used in Pavement Management. This project is related to work carried-out by the first of the authors as part of his Ph.D. thesis.

The following sections include the roughness data organized in two parts. First, the output of the Mays-meter is presented and second, the true profile elevations are shown.

2. Mays-meter Roughness Measurements

The following sections present the roughness statistics obtained by the Mays-meter.

2.1 Woodroffe Avenue

```

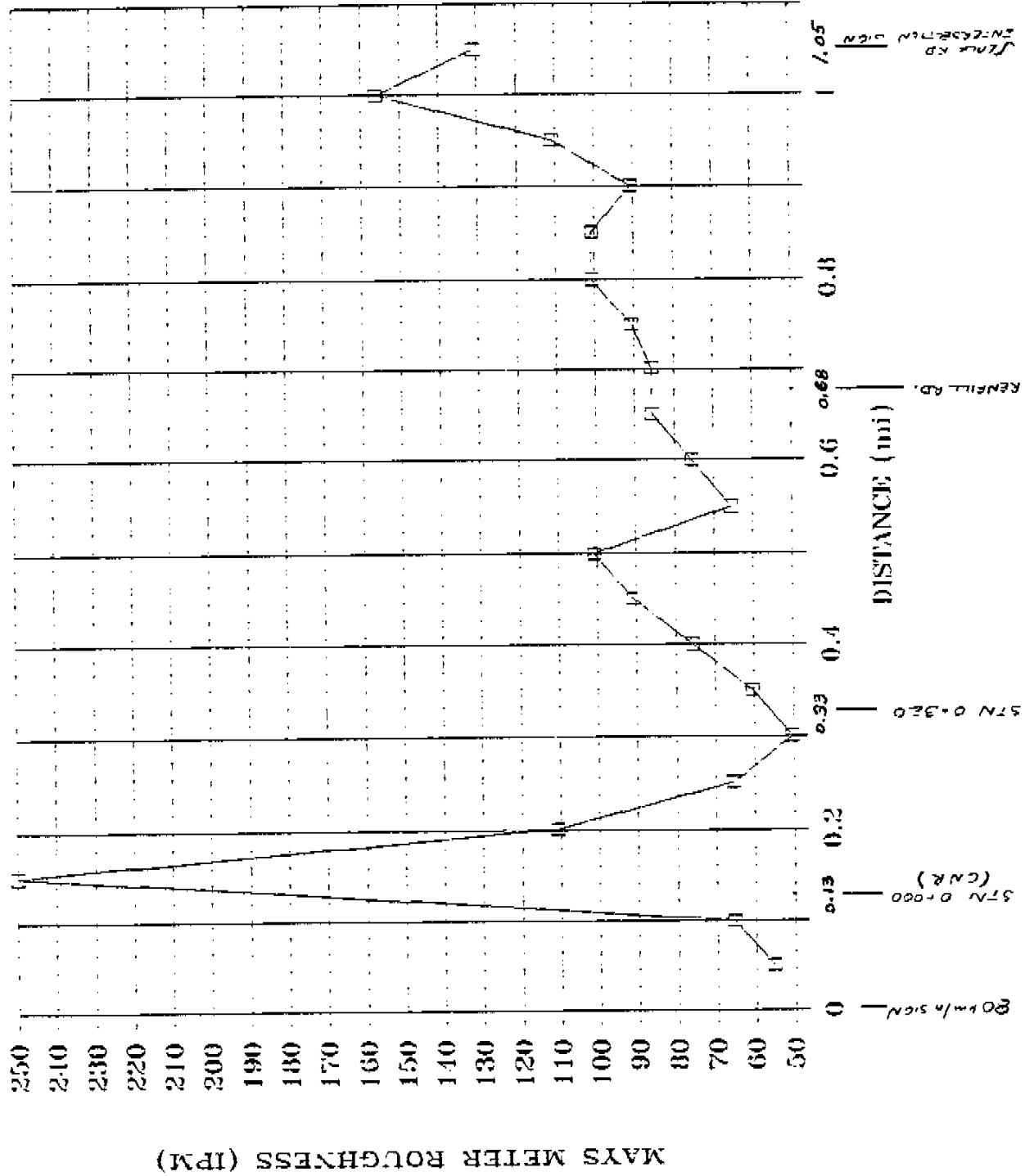
=====
DISTRICT: 9      HWY: WOODROOFE LANE: 1      DIR: NB      CONT/WP:-
LOCATION: FROM SOUTH OF CNR TRACKS N'LY TO SLACK RD. APPROACH SIGN
From LHRS/O.S.  To LHRS/O.S.  LENGTH  AVG. IPM = 96  RANGE: 50- 252
  -/ 0.0        -/ 0.0        1.7km  STD. DEV.= 43.9  DATE : 86 04 02
=====
    
```

Distance (mi)	Landmarks	Roughness (I.P.M.)	Profile			
			0	100	200	300
0.00	POSTED 80km/h SIGN					
0.05		55	*****			
0.10	0.13 STN 0+000 (CNR)	66	*****			
0.15		252	*****			
0.20		111	*****			
0.25		66	*****			
0.30	0.33 STN 0+320	50	*****			
0.35		60	*****			
0.40		76	*****			
0.45		91	*****			
0.50		101	*****			
0.55		66	*****			
0.60		76	*****			
0.65	0.68 RENFILL RD.	86	*****			
0.70		86	*****			
0.75		91	*****			
0.80		101	*****			
0.85		101	*****			
0.90		91	*****			
0.95		111	*****			
1.00	1.05 SLACK RD. APPROACH SIGN	156	*****			
1.05		131	*****			

REMARKS :

WOODROFF AVE. NB ONLY

FROM JUST SOUTH OF CNR NLY



2.2 Uplands Road

```

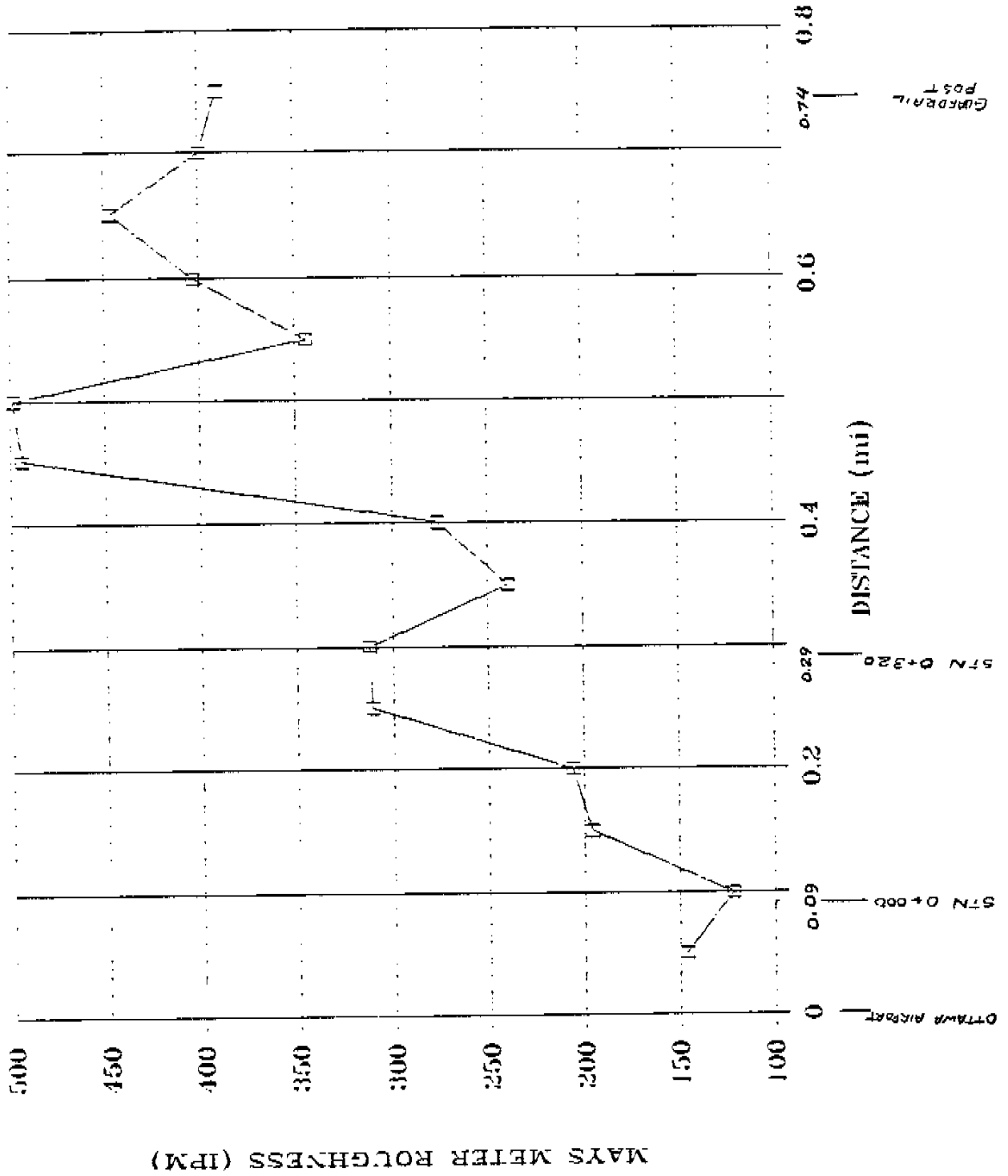
=====
DISTRICT: 9      HWY: UPLANDS  LANE: 1      DIR: NB      CONT/WP:-
LOCATION: OTTAWA INT'L AIRPORT SIGN N'LY 1.19km
From LHR5/O.S.  To LHR5/O.S.  LENGTH  AVG. IPM = 317  RANGE: 121~ 499
- /  0.0        - /  0.0        1.2km   STD. DEV.=121.1  DATE : 86 04 03
=====
    
```

Distance (mi)	Landmarks	Roughness (I.P.M.)	Profile			
			0	100	200	300
0.00	OTTAWA INT'L AIRPORT SIGN		----- ----- ----- -----			
0.05	0.09 STN. 0+000	146	*****			
0.10		121	*****			
0.15		191	*****			
0.20		202	*****			
0.25	0.29 STN. 0+320	307	*****			
0.30		312	*****			
0.35		237	*****			
0.40		272	*****			
0.45		494	*****			
0.50		499	*****			
0.55		343	*****			
0.60		403	*****			
0.65		443	*****			
0.70	0.74 GUARDRAIL POST	398	*****			
0.75		388	*****			

REMARKS : PROFILES FOR AREAS EXCEEDING 350IPM NOT PLOTTED

UPLANDS RD. NB ONLY

FROM AIRPORT SIGN ONLY



2.3 Highway 417

```

=====
DISTRICT: 9      HWY: 417      LANE: 2      DIR: EB      CONT/WP: 83-22/84-69
LOCATION: MAITLAND RD. E'LY TO PRESTON BR.
From LHR5/O.S.  To LHR5/O.S.  LENGTH  AVG. IPM = 106  RANGE: 32- 297
  49490/ 0.0     49450/ 0.1     5.0km  STD. DEV. = 60.1  DATE : 86 04 03
=====
    
```

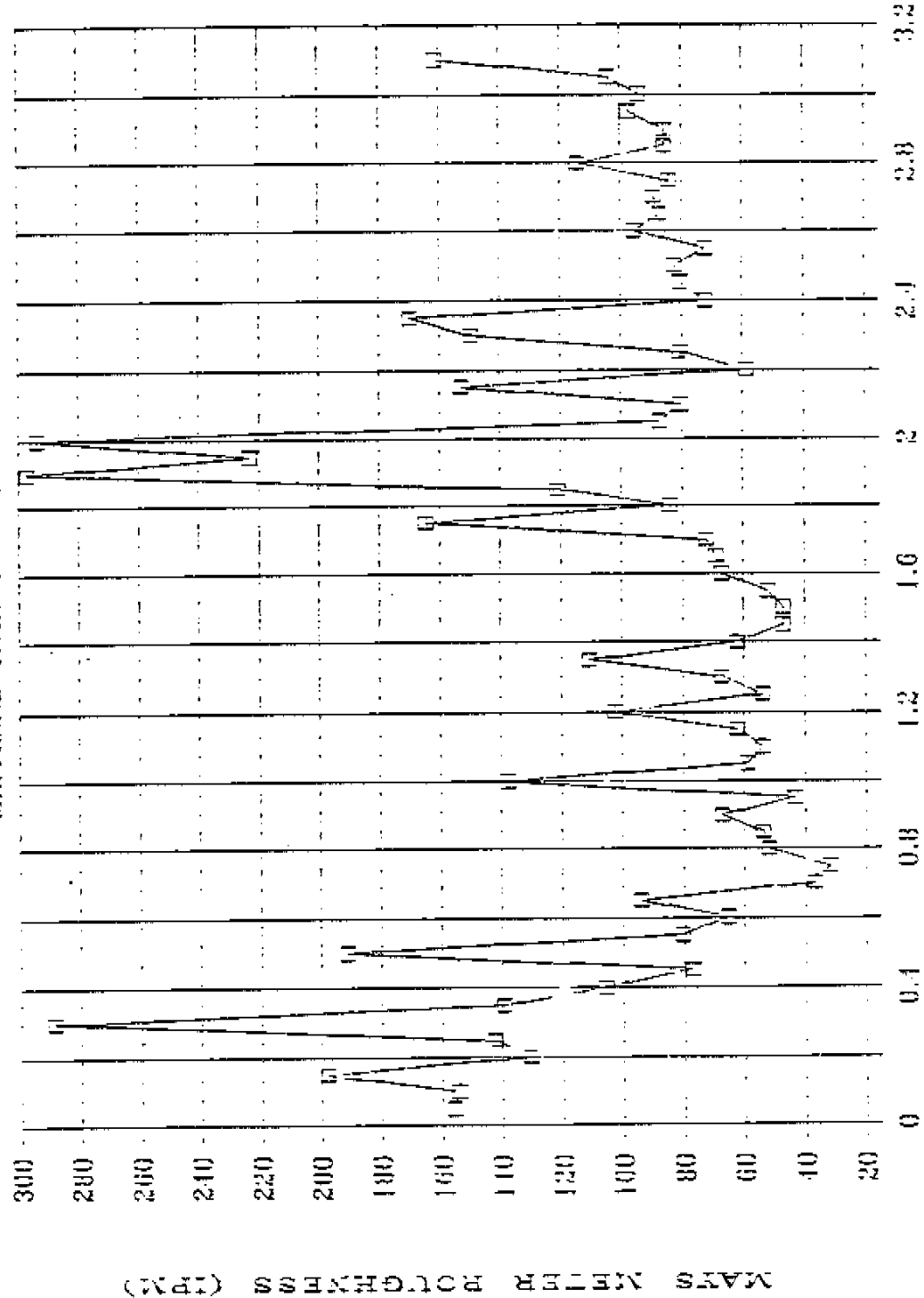
Distance (mi)	Landmarks	Roughness (I.P.M.)	Profile			
			0	100	200	300
0.00	MAITLAND AVE.		----- ----- ----- -----			
0.05		156	*****			
0.10		155	*****			
0.15		198	*****			
0.20		131	*****			
0.25		143	*****			
0.30		289	*****			
0.35		139	*****			
0.40		106	*****			
0.45		77	*****			
0.50	0.50 COLE AVE.	191	*****			
0.55		81	*****			
0.60		66	*****			
0.65		94	*****			
0.70		37	****			
0.75		32	***			
0.80		52	****			
0.85		54	****			
0.90		67	*****			
0.95	0.97 CARLING AVE.	44	****			
1.00		138	*****			
1.05		59	*****			
1.10		54	*****			
1.15	1.17 KIRKWOOD	62	*****			
1.20		102	*****			
1.25		54	*****			
1.30	1.32 CARLING AVE WB BR.	67	*****			
1.35		111	*****			
1.40		62	*****			
1.45		47	****			
1.50		47	****			
1.55		52	****			
1.60		67	*****			
1.65		69	****			
1.70	1.71 ISLAND PARK DR.	72	*****			
1.75		165	*****			
1.80		84	*****			
1.85	1.86 pavement change	121	*****			
1.90		297	*****			
1.95	1.99 PARKDALE CATWALK	223	*****			
2.00		294	*****			
2.05		87	*****			
2.10		81	*****			

Distance (mi)	Landmarks	Roughness (I.P.M.)	Profile			
			0	100	200	300
2.15		153	*****			
2.20		59	*****			
2.25		81	*****			
2.30	2.30 PARKDALE BR.	149	*****			
2.35		170	*****			
2.40		72	*****			
2.45		81	*****			
2.50	2.54 LANE 2 TO LANE 3	82	*****			
2.55		72	*****			
2.60		96	*****			
2.65		87	*****			
2.70		89	*****			
2.75		84	*****			
2.80		114	*****			
2.85		86	*****			
2.90		86	*****			
2.95		97	*****			
3.00		94	*****			
3.05	3.08 PRESTON BR.	104	*****			
3.10		161	*****			

REMARKS :

HWY. 417 EASTBOUND ONLY

MAYLAND AVE. TO PRESTON BR.



APRIL 1986

3. Rod-and-Level Measurements

CHAINAGE (M)	UPLANDS ROAD		WOODROFE AVENUE	
	TRUE ELEVATION RIGHT WHEEL PATH	TRUE ELEVATION LEFT WHEEL PATH	TRUE ELEVATION RIGHT WHEEL PATH	TRUE ELEVATION LEFT WHEEL PATH
0	1.02	1.02	0.436	0.414
0.5	1.023	1.023	0.444	0.42
1	1.023	1.023	0.455	0.425
1.5	1.023	1.023	0.464	0.431
2	1.027	1.027	0.466	0.438
2.5	1.024	1.024	0.473	0.444
3	1.023	1.023	0.494	0.448
3.5	1.023	1.023	0.485	0.456
4	1.023	1.023	0.491	0.461
4.5	1.024	1.024	0.498	0.464
5	1.018	1.018	0.505	0.472
5.5	1.014	1.014	0.515	0.478
6	1.016	1.016	0.524	0.485
6.5	1.01	1.01	0.535	0.496
7	1.003	1.003	0.543	0.501
7.5	1.003	1.003	0.552	0.509
8	1.004	1.004	0.562	0.519
8.5	1.018	1.018	0.57	0.526
9	1.011	1.011	0.577	0.535
9.5	1.019	1.019	0.588	0.55
10	0.993	0.975	0.615	0.568
10.5	0.995	0.991	0.614	0.564
11	0.989	0.991	0.611	0.562
11.5	0.981	0.996	0.625	0.571
12	0.998	1.005	0.637	0.581
12.5	1.008	1.008	0.645	0.59
13	1.014	1.014	0.651	0.601
13.5	1.023	1.023	0.665	0.605
14	1.027	1.035	0.675	0.616
14.5	1.038	1.041	0.681	0.624
15	1.048	1.051	0.687	0.635
15.5	1.058	1.053	0.7	0.649
16	1.073	1.059	0.705	0.656
16.5	1.083	1.059	0.709	0.664
17	1.088	1.063	0.716	0.675
17.5	1.090	1.072	0.722	0.678
18	1.095	1.077	0.735	0.688
18.5	1.096	1.084	0.741	0.701
19	1.098	1.091	0.745	0.706
19.5	1.104	1.094	0.754	0.717
20	1.105	1.101	0.761	0.724
20.5	1.113	1.102	0.77	0.731
21	1.118	1.107	0.776	0.742
21.5	1.121	1.110	0.786	0.745
22	1.126	1.113	0.79	0.756
22.5	1.131	1.115	0.801	0.766
23	1.136	1.119	0.811	0.781
23.5	1.142	1.122	0.82	0.788
24	1.145	1.124	0.832	0.796

24.5	1.151	1.125	0.835	0.805
25	1.155	1.130	0.842	0.814
25.5	1.160	1.135	0.851	0.823
26	1.166	1.141	0.855	0.831
26.5	1.175	1.145	0.864	0.837
27	1.180	1.153	0.87	0.852
27.5	1.193	1.158	0.882	0.861
28	1.191	1.159	0.891	0.868
28.5	1.196	1.163	0.9	0.872
29	1.202	1.168	0.905	0.882
29.5	1.205	1.174	0.908	0.884
30	1.206	1.176	0.919	0.89
30.5	1.214	1.175	0.923	0.895
31	1.215	1.175	0.93	0.9
31.5	1.219	1.172	0.934	0.907
32	1.224	1.178	0.939	0.914
32.5	1.222	1.176	0.946	0.923
33	1.225	1.176	0.955	0.93
33.5	1.229	1.179	0.96	0.936
34	1.232	1.180	0.966	0.943
34.5	1.227	1.180	0.975	0.95
35	1.231	1.181	0.98	0.957
35.5	1.235	1.185	0.989	0.961
36	1.234	1.190	0.996	0.969
36.5	1.234	1.194	1	0.973
37	1.236	1.195	1.009	0.978
37.5	1.236	1.199	1.011	0.985
38	1.238	1.199	1.017	0.992
38.5	1.237	1.202	1.025	0.997
39	1.236	1.204	1.032	1.003
39.5	1.235	1.206	1.042	1.01
40	1.238	1.211	1.045	1.011
40.5	1.237	1.207	1.049	1.015
41	1.239	1.206	1.055	1.02
41.5	1.242	1.207	1.064	1.028
42	1.245	1.205	1.066	1.037
42.5	1.245	1.209	1.074	1.045
43	1.248	1.210	1.083	1.053
43.5	1.251	1.211	1.091	1.057
44	1.253	1.212	1.095	1.063
44.5	1.258	1.215	1.101	1.069
45	1.259	1.219	1.109	1.071
45.5	1.259	1.218	1.115	1.083
46	1.264	1.222	1.119	1.09
46.5	1.263	1.224	1.129	1.095
47	1.269	1.226	1.134	1.104
47.5	1.268	1.229	1.139	1.111
48	1.275	1.229	1.145	1.117
48.5	1.275	1.231	1.155	1.125
49	1.277	1.236	1.159	1.127
49.5	1.279	1.241	1.165	1.134
50	1.285	1.243	1.173	1.139
50.5	1.285	1.245	1.178	1.145
51	1.288	1.245	1.186	1.151
51.5	1.291	1.248	1.193	1.157
52	1.294	1.248	1.203	1.164

52.5	1.299	1.248	1.209	1.168
53	1.301	1.249	1.214	1.173
53.5	1.302	1.255	1.224	1.18
54	1.301	1.254	1.226	1.189
54.5	1.306	1.256	1.231	1.191
55	1.305	1.258	1.239	1.198
55.5	1.308	1.261	1.256	1.204
56	1.308	1.264	1.258	1.21
56.5	1.310	1.265	1.265	1.216
57	1.311	1.265	1.271	1.223
57.5	1.312	1.268	1.278	1.231
58	1.316	1.268	1.285	1.236
58.5	1.317	1.271	1.29	1.242
59	1.318	1.274	1.293	1.251
59.5	1.320	1.275	1.296	1.253
60	1.316	1.274	1.296	1.256
60.5	1.319	1.276	1.301	1.264
61	1.324	1.277	1.305	1.264
61.5	1.322	1.277	1.312	1.272
62	1.325	1.281	1.316	1.272
62.5	1.329	1.281	1.32	1.28
63	1.330	1.284	1.325	1.283
63.5	1.330	1.285	1.333	1.288
64	1.334	1.289	1.335	1.294
64.5	1.336	1.289	1.341	1.298
65	1.340	1.293	1.34	1.301
65.5	1.344	1.297	1.342	1.309
66	1.350	1.301	1.346	1.311
66.5	1.349	1.304	1.348	1.314
67	1.353	1.305	1.352	1.318
67.5	1.355	1.307	1.357	1.321
68	1.357	1.308	1.359	1.324
68.5	1.359	1.310	1.359	1.33
69	1.361	1.308	1.364	1.332
69.5	1.362	1.310	1.362	1.332
70	1.363	1.311	1.368	1.336
70.5	1.364	1.314	1.37	1.342
71	1.364	1.316	1.374	1.352
71.5	1.365	1.316	1.372	1.353
72	1.365	1.320	1.369	1.351
72.5	1.365	1.320	1.37	1.351
73	1.366	1.319	1.376	1.355
73.5	1.368	1.324	1.384	1.36
74	1.369	1.324	1.386	1.369
74.5	1.370	1.325	1.389	1.369
75	1.368	1.326	1.391	1.375
75.5	1.370	1.325	1.395	1.376
76	1.370	1.329	1.397	1.38
76.5	1.371	1.332	1.396	1.381
77	1.371	1.332	1.399	1.382
77.5	1.374	1.336	1.399	1.385
78	1.374	1.336	1.4	1.386
78.5	1.373	1.337	1.4	1.385
79	1.374	1.336	1.402	1.386
79.5	1.375	1.335	1.403	1.386
80	1.375	1.336	1.405	1.386

80.5	1.375	1.339	1.408	1.385
81	1.374	1.336	1.407	1.386
81.5	1.374	1.337	1.408	1.387
82	1.373	1.335	1.41	1.387
82.5	1.372	1.336	1.41	1.39
83	1.371	1.335	1.407	1.392
83.5	1.372	1.336	1.405	1.391
84	1.369	1.335	1.406	1.391
84.5	1.370	1.336	1.414	1.397
85	1.369	1.336	1.415	1.399
85.5	1.368	1.335	1.417	1.401
86	1.380	1.338	1.421	1.404
86.5	1.371	1.342	1.425	1.405
87	1.372	1.337	1.428	1.406
87.5	1.373	1.340	1.432	1.408
88	1.374	1.342	1.435	1.408
88.5	1.376	1.344	1.439	1.413
89	1.376	1.345	1.442	1.416
89.5	1.376	1.347	1.446	1.419
90	1.378	1.349	1.446	1.42
90.5	1.376	1.350	1.449	1.425
91	1.380	1.352	1.45	1.424
91.5	1.380	1.355	1.454	1.426
92	1.381	1.356	1.455	1.428
92.5	1.384	1.360	1.453	1.43
93	1.385	1.363	1.455	1.433
93.5	1.389	1.365	1.455	1.439
94	1.392	1.365	1.457	1.442
94.5	1.392	1.365	1.458	1.447
95	1.393	1.370	1.461	1.449
95.5	1.395	1.369	1.461	1.445
96	1.395	1.370	1.46	1.445
96.5	1.395	1.375	1.46	1.451
97	1.395	1.375	1.46	1.45
97.5	1.396	1.375	1.46	1.449
98	1.395	1.374	1.463	1.447
98.5	1.395	1.375	1.465	1.449
99	1.396	1.375	1.464	1.449
99.5	1.395	1.374	1.465	1.448
100	1.395	1.373	1.466	1.446
100.5	1.395	1.374	1.465	1.446
101	1.395	1.374	1.465	1.442
101.5	1.396	1.372	1.464	1.451
102	1.396	1.374	1.462	1.442
102.5	1.396	1.372	1.46	1.444
103	1.397	1.370	1.459	1.444
103.5	1.398	1.375	1.456	1.448
104	1.398	1.375	1.458	1.445
104.5	1.398	1.373	1.46	1.449
105	1.397	1.375	1.462	1.452
105.5	1.398	1.375	1.466	1.452
106	1.399	1.375	1.465	1.453
106.5	1.396	1.374	1.468	1.454
107	1.396	1.375	1.468	1.451
107.5	1.396	1.375	1.471	1.449
108	1.398	1.376	1.47	1.443

108.5	1.398	1.375	1.468	1.44
109	1.398	1.377	1.468	1.436
109.5	1.400	1.376	1.467	1.436
110	1.400	1.376	1.465	1.435
110.5	1.399	1.375	1.463	1.435
111	1.401	1.378	1.462	1.434
111.5	1.400	1.380	1.458	1.437
112	1.400	1.379	1.457	1.435
112.5	1.400	1.381	1.456	1.432
113	1.405	1.382	1.457	1.432
113.5	1.405	1.383	1.458	1.431
114	1.406	1.386	1.46	1.43
114.5	1.407	1.385	1.46	1.43
115	1.410	1.386	1.46	1.427
115.5	1.414	1.385	1.459	1.424
116	1.411	1.385	1.453	1.423
116.5	1.412	1.386	1.45	1.419
117	1.411	1.389	1.45	1.416
117.5	1.414	1.390	1.451	1.415
118	1.415	1.392	1.446	1.412
118.5	1.415	1.395	1.435	1.41
119	1.417	1.395	1.435	1.41
119.5	1.418	1.395	1.433	1.408
120	1.419	1.396	1.431	1.401
120.5	1.422	1.395	1.429	1.397
121	1.425	1.397	1.428	1.396
121.5	1.427	1.396	1.425	1.394
122	1.428	1.397	1.422	1.392
122.5	1.429	1.396	1.419	1.391
123	1.430	1.399	1.415	1.39
123.5	1.432	1.396	1.413	1.388
124	1.433	1.400	1.41	1.387
124.5	1.435	1.400	1.408	1.386
125	1.435	1.402	1.405	1.384
125.5	1.437	1.400	1.401	1.385
126	1.436	1.404	1.401	1.384
126.5	1.436	1.404	1.399	1.38
127	1.438	1.406	1.397	1.375
127.5	1.440	1.407	1.395	1.371
128	1.440	1.410	1.394	1.368
128.5	1.441	1.415	1.391	1.364
129	1.445	1.414	1.387	1.361
129.5	1.446	1.417	1.384	1.356
130	1.444	1.420	1.381	1.355
130.5	1.444	1.422	1.376	1.35
131	1.444	1.423	1.376	1.347
131.5	1.445	1.422	1.375	1.345
132	1.448	1.422	1.375	1.344
132.5	1.450	1.422	1.376	1.344
133	1.451	1.425	1.371	1.344
133.5	1.452	1.427	1.372	1.342
134	1.454	1.427	1.368	1.338
134.5	1.455	1.43	1.366	1.336
135	1.458	1.432	1.356	1.33
135.5	1.459	1.435	1.35	1.326
136	1.460	1.436	1.346	1.325

136.5	1.460	1.429	1.344	1.321
137	1.462	1.442	1.344	1.317
137.5	1.463	1.442	1.346	1.318
138	1.463	1.443	1.345	1.315
138.5	1.464	1.444	1.34	1.314
139	1.465	1.447	1.336	1.309
139.5	1.468	1.45	1.333	1.308
140	1.468	1.448	1.329	1.307
140.5	1.469	1.449	1.331	1.31
141	1.470	1.449	1.332	1.31
141.5	1.471	1.452	1.334	1.312
142	1.470	1.452	1.332	1.311
142.5	1.470	1.452	1.332	1.311
143	1.474	1.454	1.332	1.31
143.5	1.475	1.457	1.333	1.31
144	1.475	1.457	1.334	1.312
144.5	1.475	1.457	1.334	1.313
145	1.476	1.46	1.335	1.313
145.5	1.477	1.462	1.336	1.311
146	1.476	1.461	1.336	1.31
146.5	1.476	1.464	1.335	1.315
147	1.478	1.464	1.336	1.315
147.5	1.479	1.464	1.337	1.317
148	1.479	1.466	1.337	1.316
148.5	1.479	1.466	1.335	1.314
149	1.480	1.467	1.336	1.312
149.5	1.483	1.468	1.335	1.312
150	1.481	1.466	1.335	1.312
150.5	1.483	1.472	1.333	1.315
151	1.483	1.472	1.334	1.309
151.5	1.486	1.471	1.335	1.308
152	1.488	1.475	1.336	1.31
152.5	1.489	1.477	1.335	1.31
153	1.492	1.475	1.335	1.31
153.5	1.492	1.476	1.339	1.31
154	1.492	1.478	1.34	1.309
154.5	1.495	1.478	1.338	1.308
155	1.496	1.479	1.341	1.31
155.5	1.496	1.482	1.339	1.309
156	1.496	1.482	1.337	1.304
156.5	1.498	1.481	1.34	1.303
157	1.498	1.484	1.339	1.299
157.5	1.499	1.485	1.338	1.296
158	1.499	1.487	1.332	1.298
158.5	1.500	1.487	1.331	1.297
159	1.499	1.49	1.329	1.293
159.5	1.499	1.494	1.326	1.29
160	1.500	1.5	1.322	1.285
160.5	1.504	1.5	1.319	1.281
161	1.504	1.502	1.316	1.276
161.5	1.505	1.503	1.316	1.277
162	1.506	1.503	1.312	1.269
162.5	1.507	1.507	1.312	1.267
163	1.508	1.51	1.311	1.267
163.5	1.509	1.51	1.311	1.266
164	1.509	1.509	1.311	1.265

164.5	1.509	1.511	1.313	1.262
165	1.507	1.509	1.312	1.265
165.5	1.508	1.511	1.315	1.265
166	1.508	1.51	1.319	1.265
166.5	1.507	1.512	1.321	1.265
167	1.509	1.511	1.315	1.265
167.5	1.507	1.512	1.309	1.262
168	1.507	1.511	1.306	1.266
168.5	1.509	1.514	1.304	1.268
169	1.511	1.512	1.298	1.265
169.5	1.510	1.511	1.295	1.257
170	1.512	1.513	1.29	1.254
170.5	1.513	1.514	1.289	1.252
171	1.516	1.513	1.287	1.253
171.5	1.517	1.515	1.286	1.252
172	1.519	1.517	1.292	1.251
172.5	1.518	1.517	1.301	1.251
173	1.516	1.517	1.309	1.255
173.5	1.519	1.518	1.303	1.264
174	1.520	1.522	1.309	1.268
174.5	1.520	1.521	1.31	1.274
175	1.521	1.522	1.308	1.277
175.5	1.524	1.526	1.305	1.271
176	1.527	1.527	1.304	1.268
176.5	1.530	1.531	1.303	1.269
177	1.532	1.532	1.305	1.268
177.5	1.537	1.536	1.306	1.266
178	1.539	1.539	1.301	1.26
178.5	1.545	1.541	1.297	1.259
179	1.548	1.546	1.294	1.259
179.5	1.552	1.545	1.299	1.255
180	1.555	1.549	1.298	1.256
180.5	1.560	1.549	1.297	1.258
181	1.564	1.554	1.297	1.256
181.5	1.570	1.552	1.3	1.253
182	1.574	1.558	1.298	1.253
182.5	1.578	1.562	1.292	1.255
183	1.580	1.563	1.295	1.25
183.5	1.584	1.566	1.293	1.247
184	1.588	1.566	1.296	1.248
184.5	1.590	1.567	1.293	1.248
185	1.595	1.571	1.291	1.25
185.5	1.597	1.573	1.29	1.25
186	1.598	1.576	1.292	1.252
186.5	1.602	1.578	1.295	1.25
187	1.607	1.583	1.295	1.251
187.5	1.609	1.586	1.293	1.25
188	1.612	1.592	1.289	1.25
188.5	1.617	1.593	1.29	1.249
189	1.619	1.595	1.294	1.254
189.5	1.620	1.597	1.294	1.252
190	1.628	1.598	1.295	1.251
190.5	1.632	1.602	1.294	1.251
191	1.635	1.605	1.3	1.252
191.5	1.639	1.611	1.296	1.25
192	1.641	1.616	1.296	1.251

192.5	1.646	1.618	1.294	1.253
193	1.652	1.621	1.295	1.248
193.5	1.654	1.628	1.289	1.246
194	1.658	1.63	1.291	1.246
194.5	1.662	1.635	1.291	1.24
195	1.665	1.636	1.293	1.247
195.5	1.668	1.639	1.29	1.243
196	1.674	1.645	1.289	1.24
196.5	1.675	1.649	1.288	1.24
197	1.676	1.652	1.285	1.24
197.5	1.678	1.657	1.286	1.238
198	1.682	1.662	1.281	1.239
198.5	1.685	1.666	1.276	1.238
199	1.690	1.668	1.275	1.238
199.5	1.693	1.671	1.281	1.239
200	1.695	1.672	1.28	1.244
200.5	1.698	1.678	1.278	1.244
201	1.700	1.682	1.278	1.242
201.5	1.704	1.684	1.274	1.234
202	1.706	1.687	1.268	1.236
202.5	1.710	1.688	1.268	1.233
203	1.715	1.69	1.271	1.23
203.5	1.716	1.695	1.265	1.23
204	1.720	1.697	1.262	1.227
204.5	1.724	1.7	1.254	1.222
205	1.726	1.704	1.253	1.221
205.5	1.727	1.706	1.254	1.218
206	1.729	1.708	1.259	1.215
206.5	1.731	1.707	1.256	1.215
207	1.734	1.711	1.257	1.213
207.5	1.735	1.716	1.252	1.213
208	1.736	1.717	1.254	1.208
208.5	1.737	1.72	1.255	1.21
209	1.740	1.719	1.255	1.208
209.5	1.740	1.723	1.262	1.212
210	1.744	1.727	1.259	1.214
210.5	1.746	1.728	1.264	1.214
211	1.746	1.727	1.259	1.213
211.5	1.747	1.728	1.261	1.208
212	1.751	1.729	1.259	1.21
212.5	1.752	1.729	1.265	1.21
213	1.751	1.732	1.264	1.213
213.5	1.754	1.735	1.265	1.217
214	1.756	1.737	1.264	1.212
214.5	1.758	1.737	1.263	1.21
215	1.758	1.739	1.26	1.213
215.5	1.761	1.742	1.263	1.211
216	1.763	1.741	1.271	1.213
216.5	1.765	1.744	1.273	1.218
217	1.765	1.745	1.272	1.217
217.5	1.766	1.746	1.272	1.217
218	1.770	1.745	1.265	1.219
218.5	1.770	1.747	1.258	1.219
219	1.771	1.748	1.256	1.217
219.5	1.772	1.749	1.254	1.216
220	1.775	1.752	1.259	1.214

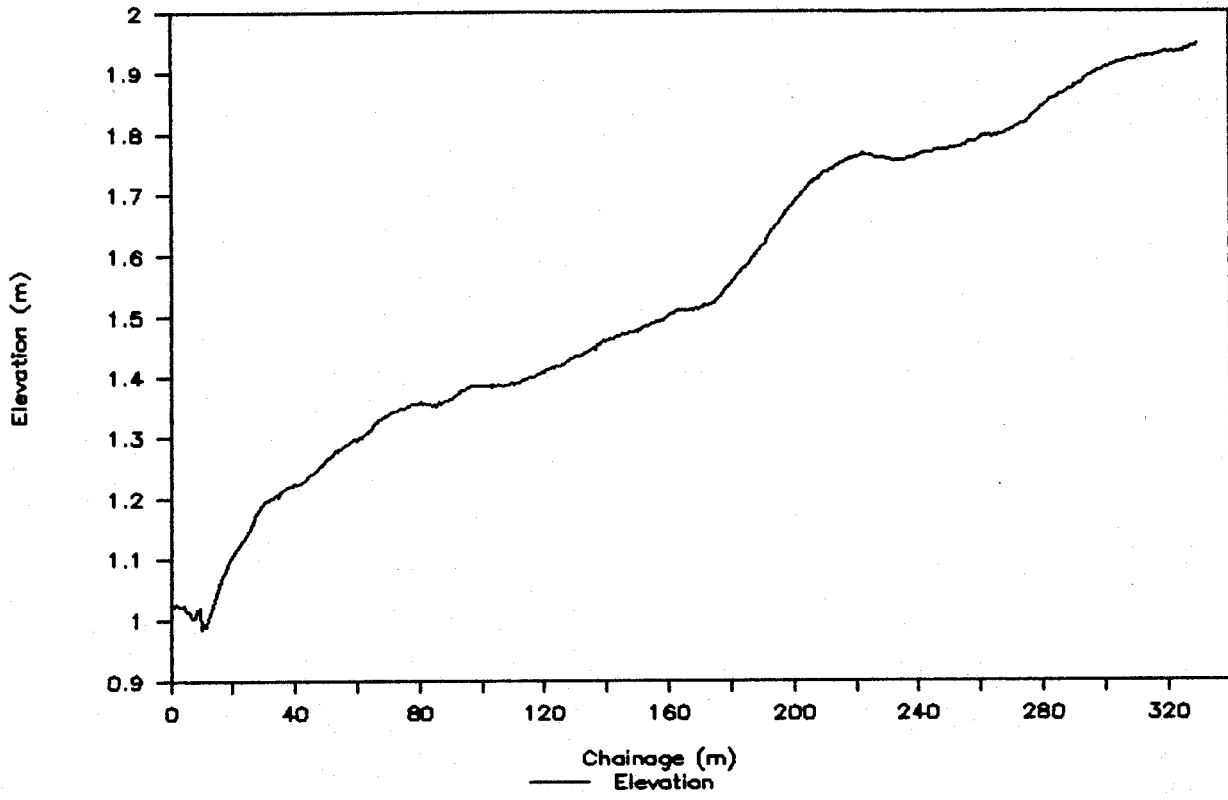
220.5	1.771	1.751	1.259	1.212
221	1.773	1.752	1.257	1.212
221.5	1.777	1.752	1.254	1.21
222	1.776	1.753	1.255	1.213
222.5	1.777	1.756	1.252	1.213
223	1.778	1.756	1.254	1.211
223.5	1.777	1.751	1.253	1.21
224	1.777	1.752	1.253	1.209
224.5	1.777	1.752	1.253	1.206
225	1.777	1.751	1.253	1.208
225.5	1.777	1.752	1.25	1.206
226	1.774	1.75	1.249	1.205
226.5	1.772	1.749	1.243	1.209
227	1.773	1.75	1.246	1.208
227.5	1.772	1.75	1.241	1.203
228	1.771	1.749	1.242	1.199
228.5	1.770	1.751	1.239	1.203
229	1.771	1.75	1.239	1.197
229.5	1.770	1.749	1.239	1.196
230	1.771	1.747	1.235	1.193
230.5	1.769	1.746	1.237	1.191
231	1.773	1.744	1.238	1.191
231.5	1.772	1.741	1.232	1.192
232	1.772	1.739	1.232	1.183
232.5	1.772	1.737	1.228	1.184
233	1.773	1.738	1.231	1.183
233.5	1.772	1.741	1.227	1.181
234	1.772	1.741	1.223	1.18
234.5	1.772	1.741	1.222	1.177
235	1.772	1.74	1.222	1.181
235.5	1.772	1.741	1.22	1.178
236	1.771	1.741	1.223	1.177
236.5	1.772	1.743	1.224	1.177
237	1.775	1.745	1.225	1.174
237.5	1.776	1.744	1.227	1.172
238	1.773	1.746	1.215	1.169
238.5	1.776	1.744	1.213	1.165
239	1.776	1.747	1.212	1.163
239.5	1.778	1.749	1.212	1.161
240	1.778	1.748	1.21	1.161
240.5	1.782	1.75	1.216	1.161
241	1.782	1.751	1.216	1.158
241.5	1.781	1.752	1.213	1.152
242	1.781	1.754	1.211	1.155
242.5	1.782	1.756	1.212	1.152
243	1.782	1.756	1.21	1.154
243.5	1.781	1.756	1.213	1.149
244	1.783	1.755	1.213	1.143
244.5	1.782	1.757	1.209	1.146
245	1.781	1.759	1.207	1.145
245.5	1.782	1.761	1.206	1.143
246	1.783	1.763	1.202	1.14
246.5	1.783	1.764	1.202	1.138
247	1.784	1.765	1.203	1.138
247.5	1.784	1.762	1.198	1.136
248	1.784	1.763	1.197	1.136

248.5	1.785	1.761	1.193	1.132
249	1.787	1.762	1.19	1.128
249.5	1.785	1.761	1.183	1.125
250	1.788	1.761	1.184	1.124
250.5	1.788	1.763	1.183	1.119
251	1.790	1.763	1.178	1.115
251.5	1.790	1.764	1.175	1.113
252	1.790	1.762	1.171	1.114
252.5	1.791	1.762	1.163	1.117
253	1.793	1.764	1.16	1.112
253.5	1.792	1.765	1.157	1.113
254	1.792	1.766	1.156	1.118
254.5	1.793	1.767	1.158	1.118
255	1.793	1.767	1.16	1.124
255.5	1.795	1.768	1.158	1.121
256	1.797	1.77	1.155	1.12
256.5	1.798	1.771	1.151	1.122
257	1.800	1.772	1.153	1.118
257.5	1.802	1.772	1.156	1.119
258	1.803	1.772	1.152	1.121
258.5	1.803	1.772	1.151	1.118
259	1.805	1.772	1.147	1.113
259.5	1.807	1.773	1.143	1.112
260	1.808	1.774	1.137	1.113
260.5	1.811	1.778	1.133	1.111
261	1.813	1.777	1.129	1.108
261.5	1.813	1.778	1.128	1.109
262	1.817	1.779	1.125	1.111
262.5	1.815	1.778	1.127	1.111
263	1.816	1.778	1.128	1.113
263.5	1.817	1.777	1.129	1.108
264	1.815	1.774	1.129	1.108
264.5	1.817	1.775	1.124	1.109
265	1.818	1.776	1.12	1.111
265.5	1.818	1.775	1.125	1.108
266	1.819	1.776	1.121	1.103
266.5	1.820	1.778	1.12	1.103
267	1.821	1.776	1.12	1.1
267.5	1.822	1.776	1.121	1.103
268	1.823	1.777	1.128	1.104
268.5	1.824	1.78	1.13	1.102
269	1.826	1.782	1.13	1.103
269.5	1.828	1.782	1.131	1.103
270	1.828	1.785	1.126	1.104
270.5	1.829	1.786	1.124	1.1
271	1.832	1.787	1.126	1.1
271.5	1.832	1.788	1.129	1.099
272	1.833	1.788	1.127	1.1
272.5	1.836	1.791	1.123	1.099
273	1.838	1.791	1.121	1.095
273.5	1.838	1.792	1.118	1.092
274	1.837	1.794	1.123	1.093
274.5	1.839	1.796	1.123	1.093
275	1.841	1.796	1.128	1.091
275.5	1.845	1.798	1.123	1.091
276	1.846	1.8	1.123	1.088

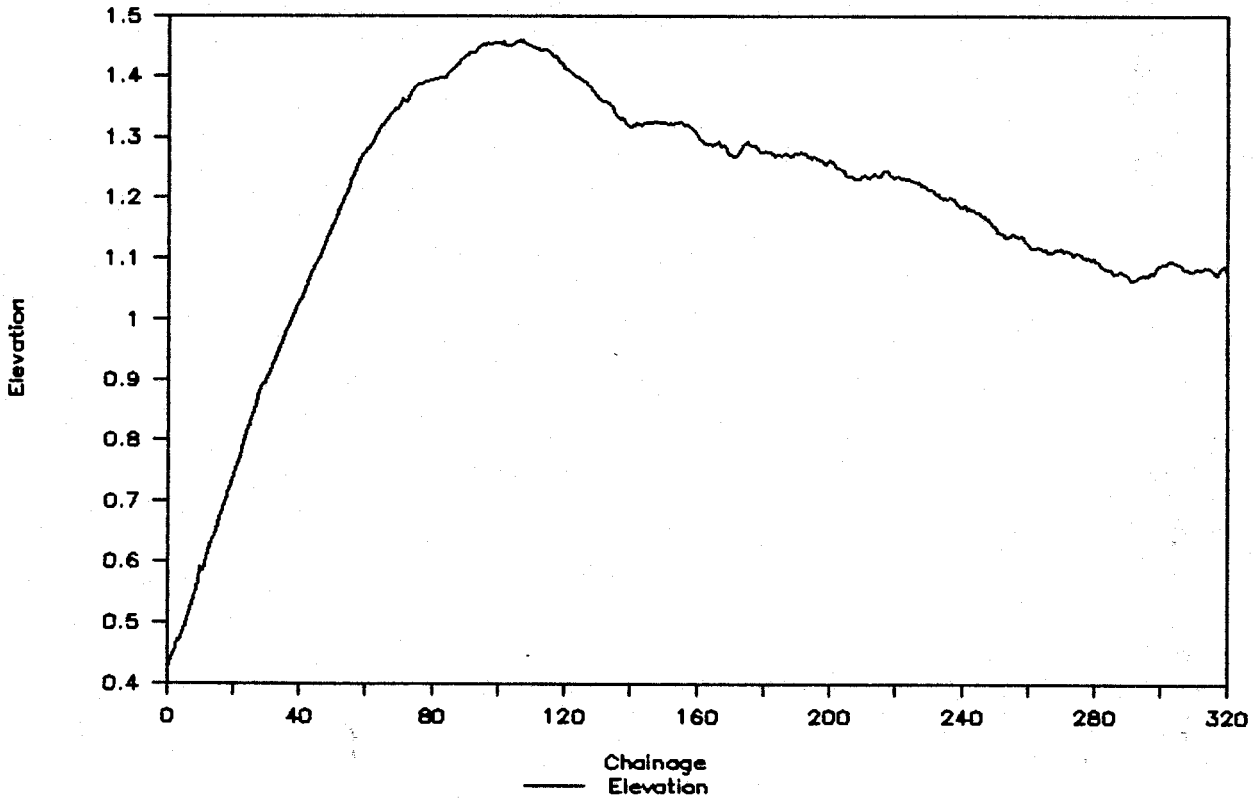
276.5	1.849	1.802	1.117	1.089
277	1.852	1.805	1.117	1.087
277.5	1.853	1.807	1.116	1.086
278	1.857	1.81	1.118	1.089
278.5	1.858	1.811	1.117	1.083
279	1.861	1.813	1.116	1.082
279.5	1.863	1.817	1.115	1.084
280	1.865	1.821	1.112	1.087
280.5	1.868	1.822	1.11	1.082
281	1.869	1.823	1.109	1.081
281.5	1.872	1.826	1.108	1.077
282	1.875	1.827	1.104	1.073
282.5	1.877	1.833	1.1	1.074
283	1.878	1.832	1.098	1.07
283.5	1.881	1.832	1.097	1.072
284	1.883	1.833	1.098	1.069
284.5	1.886	1.834	1.099	1.065
285	1.885	1.836	1.102	1.059
285.5	1.889	1.837	1.099	1.054
286	1.888	1.838	1.103	1.05
286.5	1.889	1.839	1.102	1.05
287	1.891	1.842	1.104	1.05
287.5	1.893	1.843	1.108	1.051
288	1.896	1.845	1.107	1.05
288.5	1.897	1.848	1.103	1.048
289	1.900	1.846	1.107	1.046
289.5	1.899	1.848	1.105	1.042
290	1.902	1.85	1.103	1.041
290.5	1.904	1.852	1.097	1.033
291	1.904	1.852	1.097	1.033
291.5	1.907	1.854	1.096	1.035
292	1.907	1.856	1.095	1.036
292.5	1.909	1.858	1.099	1.034
293	1.910	1.863	1.105	1.033
293.5	1.911	1.863	1.103	1.038
294	1.913	1.868	1.106	1.038
294.5	1.915	1.869	1.108	1.038
295	1.916	1.872	1.108	1.037
295.5	1.917	1.874	1.107	1.039
296	1.919	1.875	1.103	1.038
296.5	1.921	1.876	1.104	1.043
297	1.922	1.878	1.107	1.047
297.5	1.923	1.878	1.104	1.049
298	1.924	1.881	1.104	1.048
298.5	1.926	1.883	1.109	1.05
299	1.928	1.881	1.115	1.054
299.5	1.929	1.883	1.122	1.055
300	1.930	1.885	1.123	1.06
300.5	1.931	1.887	1.118	1.063
301	1.930	1.886	1.113	1.068
301.5	1.932	1.888	1.113	1.071
302	1.933	1.89	1.114	1.076
302.5	1.933	1.892	1.114	1.079
303	1.938	1.892	1.109	1.082
303.5	1.938	1.892	1.108	1.082
304	1.938	1.894	1.108	1.078

304.5	1.938	1.894	1.108	1.079
305	1.938	1.895	1.109	1.074
305.5	1.940	1.895	1.111	1.073
306	1.940	1.897	1.11	1.069
306.5	1.942	1.897	1.103	1.069
307	1.943	1.897	1.097	1.069
307.5	1.943	1.898	1.094	1.069
308	1.944	1.897	1.093	1.07
308.5	1.943	1.899	1.088	1.071
309	1.942	1.899	1.087	1.073
309.5	1.943	1.899	1.089	1.072
310	1.944	1.902	1.087	1.073
310.5	1.943	1.903	1.085	1.078
311	1.945	1.906	1.088	1.08
311.5	1.945	1.907	1.086	1.08
312	1.945	1.907	1.083	1.083
312.5	1.947	1.907	1.083	1.081
313	1.945	1.907	1.085	1.083
313.5	1.947	1.908	1.089	1.083
314	1.948	1.908	1.089	1.082
314.5	1.947	1.909	1.089	1.083
315	1.946	1.908	1.09	1.081
315.5	1.948	1.909	1.09	1.076
316	1.948	1.908	1.086	1.07
316.5	1.949	1.911	1.08	1.066
317	1.948	1.912	1.082	1.066
317.5	1.948	1.91	1.091	1.072
318	1.951	1.911	1.097	1.073
318.5	1.949	1.914	1.101	1.075
319	1.951	1.915	1.105	1.073
319.5	1.952	1.916	1.097	1.069
320	1.951	1.916	1.09	1.063
321.5	1.953	1.917		
322	1.949	1.917		
322.5	1.949	1.915		
323	1.952	1.916		
323.5	1.954	1.916		
324	1.953	1.914		
324.5	1.956	1.918		
325	1.953	1.917		
325.5	1.956	1.919		
326	1.957	1.919		
326.5	1.958	1.918		
327	1.958	1.921		
327.5	1.959	1.923		
328	1.959	1.925		
328.5	1.959	1.926		
329	1.960	1.928		
329.5	1.960	1.927		
330	1.962	1.931		

Woodroffee



Uplands



APPENDIX D
A LISTING OF SOFTWARE DEVELOPED FOR THE
ANALYSIS OF DYNAMIC DATA

The interactive program converts analog signals to digital values,
applies calibration factors, performs the statistical analysis, stores
data and plots the distribution.

Program VW

```

c
implicit integer*2 (a-z)
integer*4 size,intary(4000)
dimension nochan(3),time(3),rate(3)
c
common/gracom/size,intary
c
size=4000
c
50 print 1
1   format(/'          main  menu')
   print 2
2   format(/'  1- convert analog signal      4- decalibrate')
   print 3
3   format('  2- plot digitized signal      5- plot distribution')
   print 4
4   format('  3- statistical analysis        6- store data')
   print 7
7   format('          7- exit VW')
   print 5
5   format(/' Enter code number : ')
   read 6,code
6   format(i1)
   if(code.eq.1)call convert(nochan,time,rate)
   if(code.eq.2)call plotsign(nochan,time,rate,code)
   if(code.eq.3)call stats(nochan,time,rate)
   if(code.eq.4)call decal(nochan,time,rate)
   if(code.eq.5)call plotdist(nochan,time,rate,code)
   if(code.eq.6)call store(nochan,time,rate)
   if(code.eq.7)goto 51
   goto 50
c
51  stop
   end

```

```

subroutine convert(nochan,time,rate)
c
implicit integer*2 (a-z)
dimension tape(8),comp(8),vector1(30000),vector2(30000)
dimension vector3(1000),nochan(3),time(3),rate(3)
character*1 ans1,yes,ans2,ans3
integer*4 count1,rate41,count2,rate42,count3,rate43
c
common/comp/tape
common/conv/vector1,vector2
c
data yes/'y'/
do 56 i=1,3
nochan(i)=0
time(i)=0
56 rate(i)=0
call comptape
print 1
1 format('/' Enter first and last computer channels to be converted
* : ')
read 2,chanlo1,chanhi1
2 format(i1,1x,i1)
nochan(1)=chanhi1-chanlo1+1
print 3
3 format(' Enter A to D converting time in tenths of seconds : ')
read 4,time(1)
4 format(i3)
print 5
5 format(' Enter A to D converting rate in counts per second : ')
read 6,rate(1)
6 format(i4)
print 11
11 format(' Is there a second vector to be generated ? ')
read 15,ans1
15 format(a1)
if(ans1.eq.yes)then
print 1
read 2,chanlo2,chanhi2
nochan(2)=chanhi2-chanlo2+1
print 3
read 4,time(2)
print 5
read 6,rate(2)
print 16
16 format(' Is there a time lapse between the 2 vectors ? ')
read 17,ans2
17 format(a1)
if(ans2.eq.yes)then
print 18
18 format(' Enter time lapse in tenths of seconds : ')

```

```

19      read 19,time(3)
      format(13)
      adapt3=0
      device3=9
      chanlo3=0
      chanhi3=3
      nochan(3)=4
      rate(3)=10
      points3=time(3)
      ctrl3=0
      mode3=0
      stor3=0
      count3=time(3)
      rate43=rate(3)
      stat3=0
      endif
      if(ans2.ne.yes)then
20      print 20
      format(' Do you want to link vector1 with vector2 ? ')
      read 21,ans3
21      format(a1)
      if(ans3.eq.yes)time1=time(1)+time(2)
      endif
      endif
c
      adapt1=0
      adapt2=0
      device1=9
      device2=9
      ctrl1=0
      ctrl2=0
      model=0
      mode2=0
      stor1=0
      stor2=0
      points1=rate(1)/10*nochan(1)*time(1)
      points2=rate(2)/10*nochan(2)*time(2)
      count1=rate(1)/10*time(1)
      count2=rate(2)/10*time(2)
      rate41=rate(1)
      rate42=rate(2)
      stat1=0
      stat2=0
      call ainsc(adapt1,device1,chanlo1,chanhi1,ctrl1,model,
*stor1,count1,rate41,vector1,stat1)
      if(stat1.ne.0)goto 100
      if(ans1.eq.yes.and.ans2.eq.yes)call ainsc(adapt3,device3,chanlo3,
*chanhi3,ctrl3,mode3,stor3,count3,rate43,vector3,stat3)
      if(stat3.ne.0)goto 100
      if(ans1.eq.yes)call ainsc(adapt2,device2,chanlo2,chanhi2,ctrl2,

```

```
*mode2,stor2,count2,rate42,vector2,stat2)
  if(stat2.ne.0)goto 100
  goto 101
100  print 7,stat1,stat2,stat3
7    format(1x,' Execution errors ',3i8/)
  stop
c
101  if(ans3.eq.yes)time(1)=time1
c
  return
end
```

```

subroutine stats(nochan,time,rate)
c
implicit integer*2 (a-z)
real*4 sumv(4),sumv2(4),avg(4),sigma(4),one(4)
dimension vector1(30000),vector2(30000),tape(8)
dimension nochan(3),time(3),rate(3),prob(4,4096)
character*78 fileid(4)
c
common/conv/vector1,vector2
common/sta/prob,avg,sigma,code
c
print 1
1 format(/'                                stats menu')
print 2
2 format(/' 1- analysis of vector1          3- analysis of virtual data')
print 3
3 format(' 2- analysis of vector2          4- last menu')
print 4
4 format(/' Enter code number : ')
read 5,code
5 format(i1)
c
if(code.eq.4)return
c
if(code.eq.3)then
open(2,file='d:virtual.dat',status='old')
read(2,14)tape
14 format(8i3)
read(2,15)nochan(1),time(1),rate(1)
15 format(3i8)
points=rate(1)/10*nochan(1)*time(1)
if(points.gt.30000)then
read(2,16)(vector1(i),i=1,30000)
read(2,16)(vector2(i),i=30001,points-30000)
endif
if(points.le.30000)read(2,16)(vector1(i),i=1,points)
16 format(8i8)
read(2,17)fileid
17 format(a78)
close(2,status='keep')
print 17,fileid
endif
c
c Calculate average and standard deviation
c
c
if(code.eq.1.or.code.eq.3)then
noch=nochan(1)
rat=rate(1)
tim=time(1)
endif
if(code.eq.2)then
noch=nochan(2)

```

```

    rat=rate(2)
    tim=time(2)
    endif
    do 50 i=1,noch
    do 52 j=1,4096
52    prob(i,j)=0
    one(i)=0.
    sumv(1)=0.
50    sumv2(1)=0.
    points=rat/10*noch*tim
    if(code.eq.2)goto 100
    if(points.gt.30000)then
    do 59 k=1,30000-nochan(1)+1,nochan(1)
    do 60 l=1,nochan(1)
    ichan=k+l-1
    sumv(1)=1.0*vector1(ichan)+sumv(1)
    sumv2(1)=1.0*vector1(ichan)*vector1(ichan)+sumv2(1)
    bin=vector1(ichan)+1
60    prob(1,bin)=prob(1,bin)+1
59    continue
    p=points-30000-nochan(1)+1
    do 58 k=1,p,nochan(1)
    do 65 l=1,nochan(1)
    ichan=k+l-1
    sumv(1)=1.0*vector2(ichan)+sumv(1)
    sumv2(1)=1.0*vector2(ichan)*vector2(ichan)+sumv2(1)
    bin=vector1(ichan)+1
65    prob(1,bin)=prob(1,bin)+1
58    continue
    endif
    if(points.le.30000)then
    do 66 k=1,points-nochan(1)+1,nochan(1)
    do 67 l=1,nochan(1)
    ichan=k+l-1
    sumv(1)=1.0*vector1(ichan)+sumv(1)
    sumv2(1)=1.0*vector1(ichan)*vector1(ichan)+sumv2(1)
    bin=vector1(ichan)+1
67    prob(1,bin)=prob(1,bin)+1
66    continue
    endif
100    if(code.eq.2)then
    do 68 k=1,points-nochan(2)+1,nochan(2)
    do 69 l=1,nochan(2)
    ichan=k+l-1
    sumv(1)=1.0*vector2(ichan)+sumv(1)
    sumv2(1)=1.0*vector2(ichan)*vector2(ichan)+sumv2(1)
    bin=vector2(ichan)+1
69    prob(1,bin)=prob(1,bin)+1
68    continue
    endif
c
    do 53 i=1,noch
    avg(i)=sumv(1)*10./rat/tim

```



```
53  sigma(i)=(sumv2(i)*10./rat/tim-avg(i)**2)**0.5
c
c  Evaluate probability for given voltage bins
c
c      do 63 i=1,noch
c      do 64 j=1,4096
64  one(i)=one(i)+prob(i,j)*10./tim/rat
63  continue
c
c  Print statistical output
c
c      print 6,(avg(i),i=1,noch)
6  format(' average      = ',8f8.2)
c      print 7,(sigma(i),i=1,noch)
7  format(' stand. dev. = ',8f8.2)
c      print 8,(one(i),i=1,noch)
8  format(' integral    = ',8f8.4)
c
c      return
c      end
```

```

subroutine decal(nochan,time,rate)
c
implicit integer*2 (a-z)
real*4 slope,constant,group,prob(4,100),eng(4,100),avgeng(4)
real*4 avg(4),sigma(4),percent,one(4),probbitr(4096)
real*4 static(4),dlc(4),percent5(4),percent95(4)
character*7 cal(14),dec
character*8 filename
character*12 filenamext
character*78 fileid(4)
dimension tape(8),comp(8),nochan(3),time(3),rate(3)
dimension probbit(4,4096)
c
common/dec/eng,prob
common/comp/tape
common/sta/probbit,avg,sigma,vect
c
data cal/'c01.dec','c02.dec','c03.dec','c04.dec','c05.dec',
*        'c06.dec','c07.dec','c08.dec','c09.dec','c10.dec',
*        'c11.dec','c12.dec','c13.dec','c14.dec'/
c
print 1
1  format(/'                decal menu')
print 2
2  format(/'  1- decalibrate RAM data      3-last menu')
print 3
3  format('  2- decalibrate raw data')
print 4
4  format(/' Enter code number : ')
read 5,code
5  format(i1)
   if(code.eq.3)return
   if(code.eq.1)then
   if(vect.eq.1.or.vect.eq.3)then
noch=nochan(1)
tim=time(1)
rat=rate(1)
endif
   if(vect.eq.2)then
noch=nochan(2)
tim=time(2)
rat=rate(2)
endif
endif
c
c Read statistical data file (*.raw)
c
   if(code.eq.2)then
print 12
12  format(' Enter raw data filename : ')
read 13,filename
13  format(a8)
   filenamext=filename//'.raw'

```

```

print 27,filenamext
27 format(1x,a12)
open(1,file=filenamext,status='old')
read(1,25) fileid
25 format(a78)
print 25,fileid
read(1,23) tape
23 format(8i3)
read(1,24) noch,tim,rat
24 format(3i8)
read(1,19) (avg(i),i=1,noch)
19 format(16x,8f8.2)
read(1,20) (sigma(i),i=1,noch)
20 format(16x,8f8.2)
read(1,22) ((probit(i,k),k=1,4096),i=1,noch)
22 format(12i6)
close(1,status='keep')
nochan(1)=noch
time(1)=tim
rate(1)=rat
endif

c
call comptape
open(1,file='stat',status='unknown')
do 54 j=1,noch
do 50 i=1,4096
50 probbitr(i)=probit(j,i)*10./tim/rat
c
c Read calibration constants
c
dec=cal(tape(j))
open(2,file=dec,status='old')
read(2,8) slope,constant,group
8 format(3f8.3)
close(2,status='keep')

c
c Decalibrate
c
percent=0.
percent5(j)=0.
percent95(j)=0.
one(j)=0.
do 55 i=1,100
55 prob(j,i)=0.
r1=-50.*2048./slope/5.+avg(j)
probability=0
do 53 i=1,100
r2=(-50.+i)*2048./slope/5.+avg(j)
if(r2.lt.1)goto 101
if(r1.lt.1.and.r2.ge.1)r1=1
if(r1.gt.4096)goto 101
if(r1.le.4096.and.r2.gt.4096)r2=4096
do 51 k=r1,r2

```

```

one(j)=one(j)+probbit(j,k)
51 prob(j,i)=prob(j,i)+probbitr(k)
prob(j,i)=prob(j,i)*100.
101 r1=r2+1
eng(j,i)=-50.5+i
percent=percent+prob(j,i)
if(percent.gt.5.0.and.percent5(j).eq.0.0)then
percent5(j)=eng(j,i)-(percent-5.)/prob(j,i)
endif
if(percent.gt.95.0.and.percent95(j).eq.0.0)then
53 percent95(j)=eng(j,i)-(percent-95.)/prob(j,i)
endif
one(j)=one(j)*10/tim/rat*100.
avgeng(j)=0.0
dlc(j)=slope*sigma(j)*5./2048.
static(j)=constant
c
c File statistical analysis results
c
write(1,17) dlc(j)
write(1,18) percent5(j)
write(1,26) percent95(j)
54 continue
close(1,status='keep')
c
c Print statistical analysis results
c
print 31,avgeng
15 format('          mean = ',f6.2,' kN')
31 format('          mean = ',4(2x,f6.2),' kN')
print 33,dlc
17 format(' standard deviation = ',f6.2,' kN')
33 format(' standard deviation = ',4(2x,f6.2),' kN')
print 37,percent5
18 format('      5th percentile = ',f6.2,' kN')
37 format('      5th percentile = ',4(2x,f6.2),' kN')
print 38,percent95
26 format('      95th percentile = ',f6.2,' kN')
38 format('      95th percentile = ',4(2x,f6.2),' kN')
print 36,one
36 format('          one = ',4(3x,f5.1))
c
return
end

```



```

24      print 24
24      format('          4- air suspension - trailer'//)
      print 25
25      format('      MAYS roughness in I3          Inertial forces'//)
      print 26
26      format('          1- with')
      print 27
27      format('          2- without'//)
      print 28
28      format('      Enter spread in F4.2          Air suspension'//)
      print 29
29      format('          1- up')
      print 30
30      format('          2- down'//)
      print 31
31      format('      Enter graph identification in sequential form : '//)
      read 32,run,speed,post,susp,surf,inert,spread,air
32      format(a10,1x,i2,1x,8(i1,1x),i3,1x,i1,1x,f4.2,1x,i1)
      open (1,file='id',status='unknown')
      do 56 i=1,nochan(1)
      write(1,33)run
33      format(' Run # ',a10)
      write(1,34)speed
34      format(' Speed = ',i2,' km/hr')
      write(1,35)surf
35      format(' MAYS roughness = ',i3,' IPM')
      write(1,37)
37      format(' Suspension :')
      write(1,36)suspension(susp(i))
36      format(3x,a30)
      write(1,38)axle(post(i))
38      format(1x,a10)
      write(1,39)force(inert)
39      format(1x,a25)
      write(1,40)spread
40      format(' Spread = ',f4.2,' meters')
      write(1,41)lift(air)
41      format(' Air suspension lift axle ',a4)
56      continue
      close(1,status='keep')
      endif
c
      open(1,file='stat',status='old')
      open(2,file='id',status='old')
      do 57 i1=1,nochan(1)
c
c      Open plotting system
c
      status=popnps()
c
c      Assign plotting system output device
c
      if(device.eq.1)status=ppsot('display')

```

```

        if(device.eq.2)status=ppspot('printer')
c
c Read statistical analysis results file
c
        read(1,18) (results(j),j=1,3)
18      format(a37)
        if(device.eq.2)then
            read(2,18) (ident(j),j=1,9)
        endif
c
c Set display surface size
c
        status=psurf(13.7,9.1)
c
c Define x-axis title string
c
        status=ptax(1,'dynamic loading (kN)')
c
c Define y-axis title string
c
        status=ptax(2,'frequency of occurrence')
c
c Set existence of chart & view area frame
c
        status=pxcfm(1,1)
        status=pxvfrm(0,1)
c
c Set axis extents
c
        status=paxext(1,-50.,50.,10.)
        status=paxext(2,0.,20.,2.)
c
c Set axis tick label type and height
c
        status=paxlty(1,1,2,1)
        status=ptahgt(1,1)
        status=ptahgt(2,1)
c
c Define x/y data set
c
        do 59 k=1,100
            ld(k)=load(11,k)
59      pb(k)=prob(11,k)
            status=pdsxy(2,100,ld,pb)
c
c Define data set to be a bar
c
        status=pbar(2)
c
c Set output primitives : data set 1 to solid bar and color
c
        status=pdsstl(2,2)
        status=pdsclr(2,3)

```

```

c
c Set notation height
c
      status=psnhgt(1)
c
c Define notation strings
c
      do 54 k=1,3
      yalign=90.-2.0*(k-1.0)
54      status=pnote(1,68.,yalign,results(k))
      do 55 k=1,9
      yalign=90.-2.*(k-1.)
55      status=pnote(1,9.5,yalign,ident(k))
c
c Output currently defined chart
c
      status=ppltit()
c
c View graph
c
      if(device.eq.1)status=ppsln('display')
      if(device.eq.2)status=ppsln('printer')
      status=prqst(1,1,echpt,26,string)
c
c Close I/O device
c
      if(device.eq.1)status=ppsot('display')
      if(device.eq.2)status=ppsot('printer')
c
c Reset defaults and viewing area
c
      status=pdeflt()
      status=prsvw()
c
c Close plotting system
c
      status=pcisps()
c
57      continue
      close(1,status='keep')
      close(2,status='keep')
c
      return
      end

```



```

subroutine store(nochan,time,rate)
c
implicit integer*2 (a-z)
real*4 average(4),sigma(4),eng(4,100),rprob(4,100)
character*1 ans,yes
character*8 filename
character*12 filenamext
character*40 stat(20)
character*70 fileid(4)
dimension tape(8),comp(8),prob(4,4096)
dimension nochan(3),time(3),rate(3)
c
common/dec/eng,rprob
common/comp/tape
common/sta/prob,average,sigma,vect
c
data yes/'y'/
print 9
9 format(/'                                store menu')
print 10
10 format(/'  1- store raw data                3- store raw and statist
*ical data')
print 11
11 format('  2- store statistical data        4- last menu')
print 12
12 format(/' Enter code number : ')
read 13,code
13 format(i1)
c
if(code.eq.4)return
if(vect.eq.0.or.vect.eq.1.or.vect.eq.3)then
noch=nochan(1)
tim=time(1)
rat=rate(1)
endif
if(vect.eq.2)then
noch=nochan(2)
tim=time(2)
rat=rate(2)
endif
c
sumtape=0
do 50 i=1,8
50 sumtape=sumtape+tape(i)
if(sumtape.eq.0)then
open(1,file='comptape.dat',status='old')
read(1,14) (comp(i),tape(i),i=1,8)
14 format(16i3)
close(1,status='keep')
endif
c
if(code.eq.1.or.code.eq.3)then
print 15

```

```

15  format(' Enter filename (up to 8 characters) : ')
    read 16,filename
16  format(a8)
    print 17
17  format(' Enter file identification (4 lines of 70 characters) :')
    read 18,fileid
18  format(a70)
    filenamext=filename//'.raw'
    open(1,file=filenamext,status='new')
    write(1,7) fileid
7   format(' I.D. : ',a70,3(/8x,a70))
    write(1,8) tape
8   format(8i3)
    write(1,3) noch,tim,rat
3   format(3i8)
    write(1,19) (average(i),i=1,noch)
19  format(' average      = ',8f8.2)
    write(1,20) (sigma(i),i=1,noch)
20  format(' stand. dev. = ',8f8.2)
    write(1,22) ((prob(i,k),k=1,4096),i=1,noch)
22  format(12i6)
    close(1,status='keep')
    endif
c
    if(code.eq.2.or.code.eq.3)then
    if(code.eq.2)then
    print 15
    read 16,filename
    print 23,filename
23  format(' Does data file ',a8,'.raw exist ? ')
    read 24,ans
24  format(a1)
    if(ans.eq.yes)then
    open(1,file=filename//'.raw',status='old')
    read(1,25)fileid
25  format(8x,a70,3(/8x,a70))
    close(1,status='keep')
    endif
    if(ans.ne.yes)then
    print 17
    read 18,fileid
    endif
    endif
    open(1,file='stat',status='unknown')
    read(1,26) (stat(i),i=1,3*noch)
26  format(a40)
    close(1,status='keep')
    open(1,file=filename//'.sta',status='new')
    write(1,7)fileid
    write(1,8)tape
    write(1,3)noch,tim,rat
    write(1,26) (stat(i),i=1,3*noch)
    write(1,27) (eng(1,i),i=1,100)

```

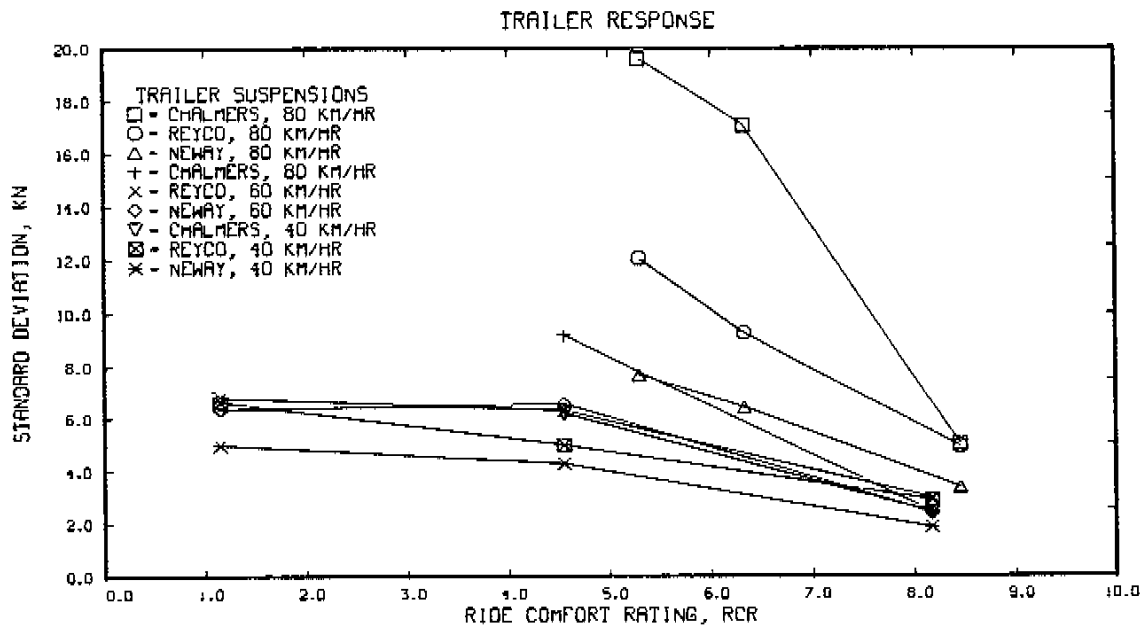
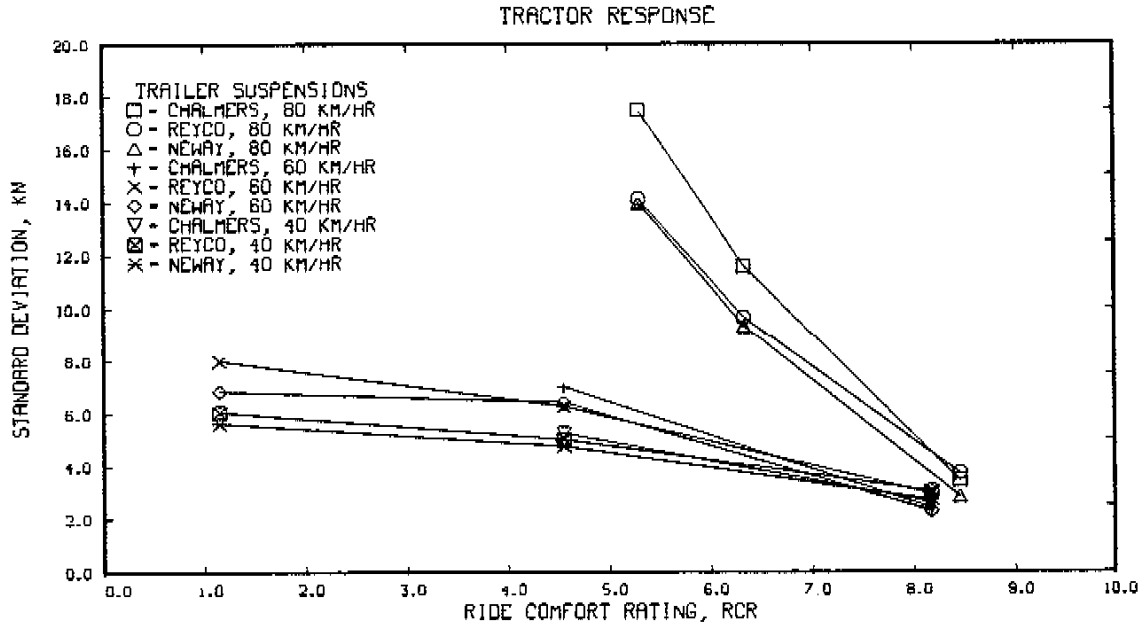
```
write(1,27)((rprob(1,j),j=1,100),i=1,noch)
27 format(2f8.3)
close(1,status='keep')
endif
c
return
end
```

```
subroutine comptape
c
c  implicit integer*2 (a-z)
c  dimension comp(8),tape(8)
c
c  common/comp/tape
c
c  print 7
7  format(/'          COMPUTER-TAPE RECORDER CHANNEL NUMBER CORRESPON
*DENCE ')
  open(1,file='comptape.dat',status='old')
  read(1,8) (comp(i),tape(i),i=1,8)
8  format(16i3)
  close(1,status='keep')
  print 9,comp
9  format(/'    Computer channel number      :',8i4)
  print 10,tape
10 format('    Tape recorder channel number :',8i4)
c
  return
end
```

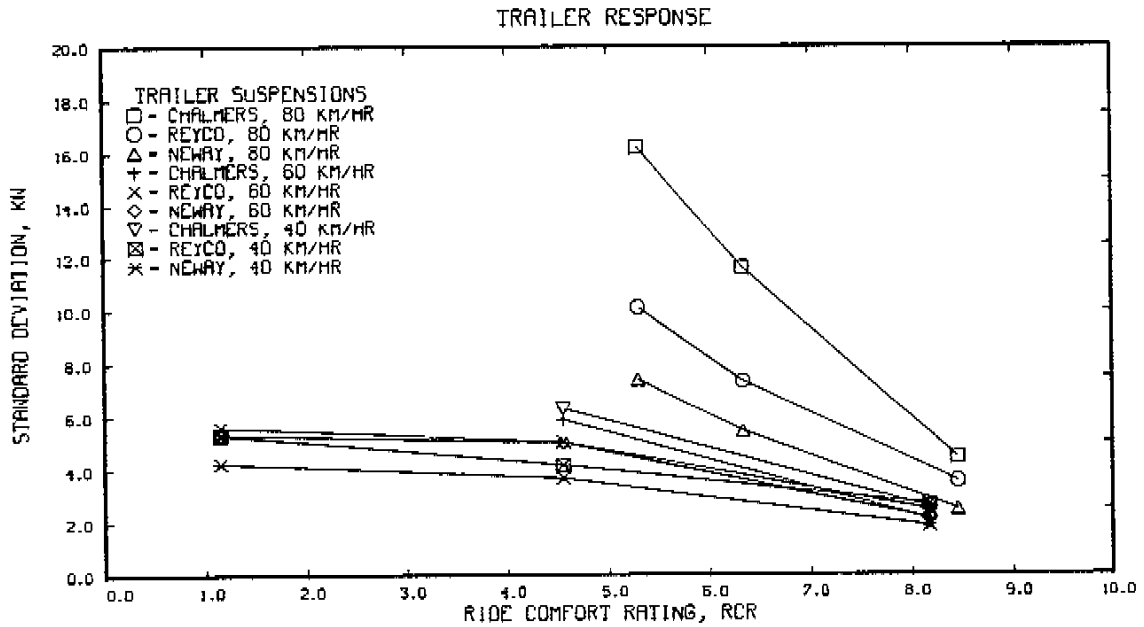
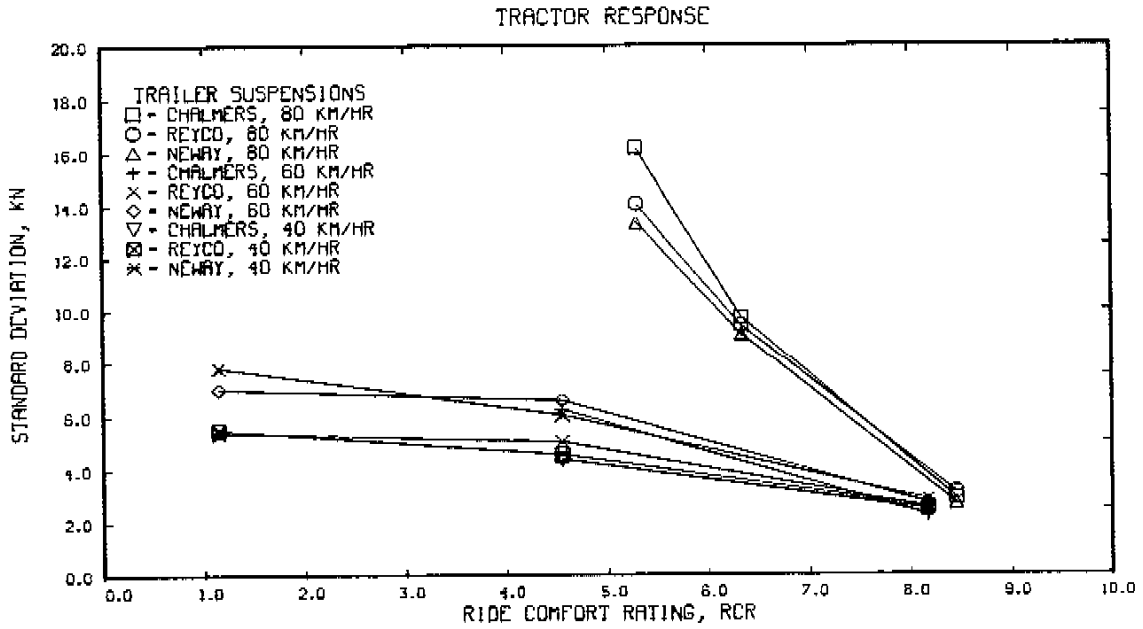
APPENDIX E

PLOTS OF WHEEL LOAD VS RIDE COMFORT RATING FOR VARIOUS
SUSPENSION COMBINATIONS

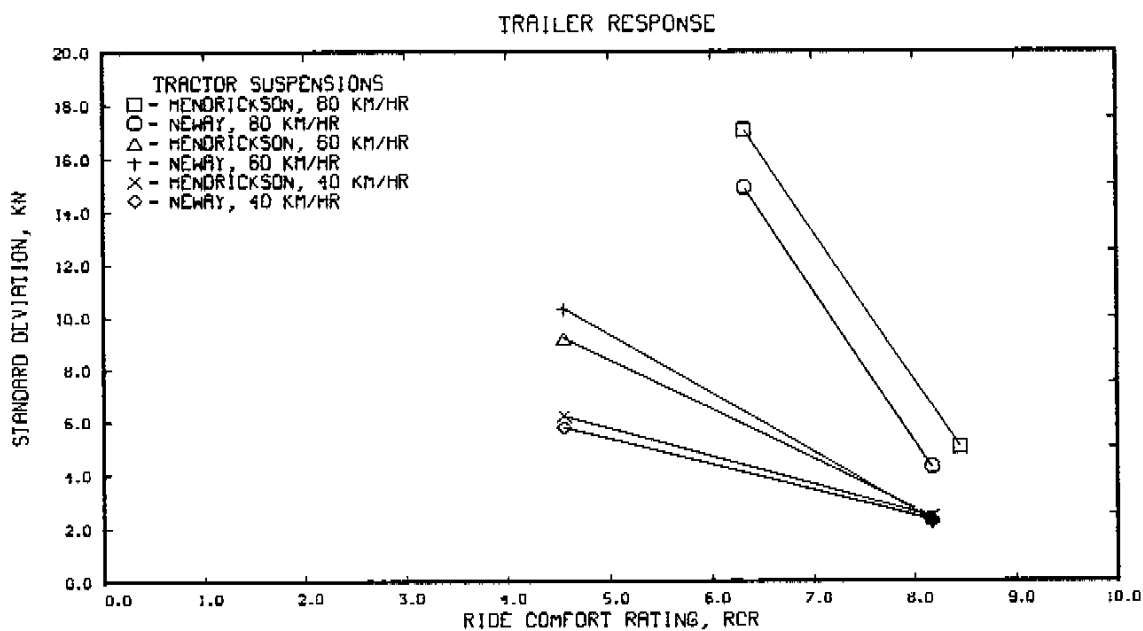
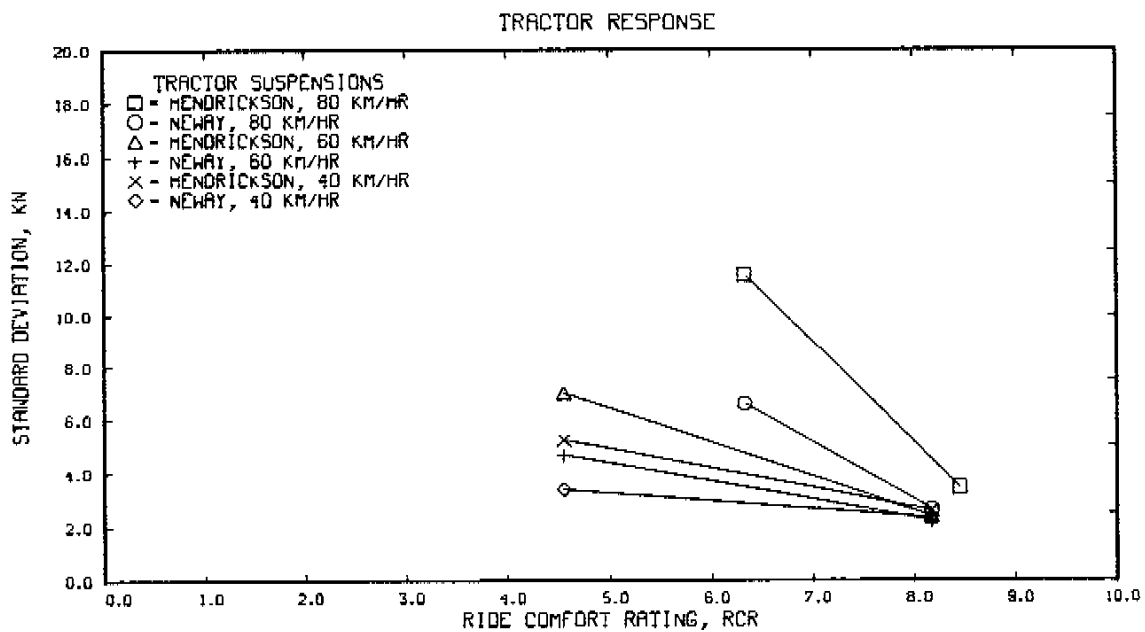
VARIATION OF TRAILER SUSPENSION TYPE
 TRACTOR SUSPENSION - HENDRICKSON
 AIR AXLE UP - NOMINAL WHEEL LOAD OF 50 KN
 NOMINAL TRAILER AXLE SPREAD OF 1.3 M



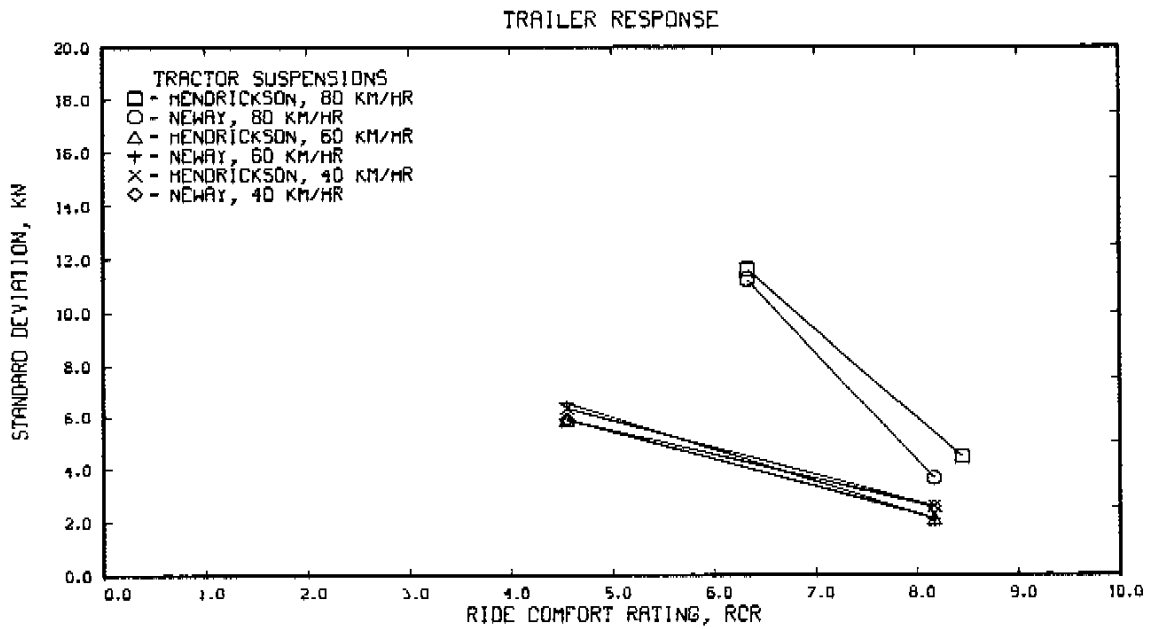
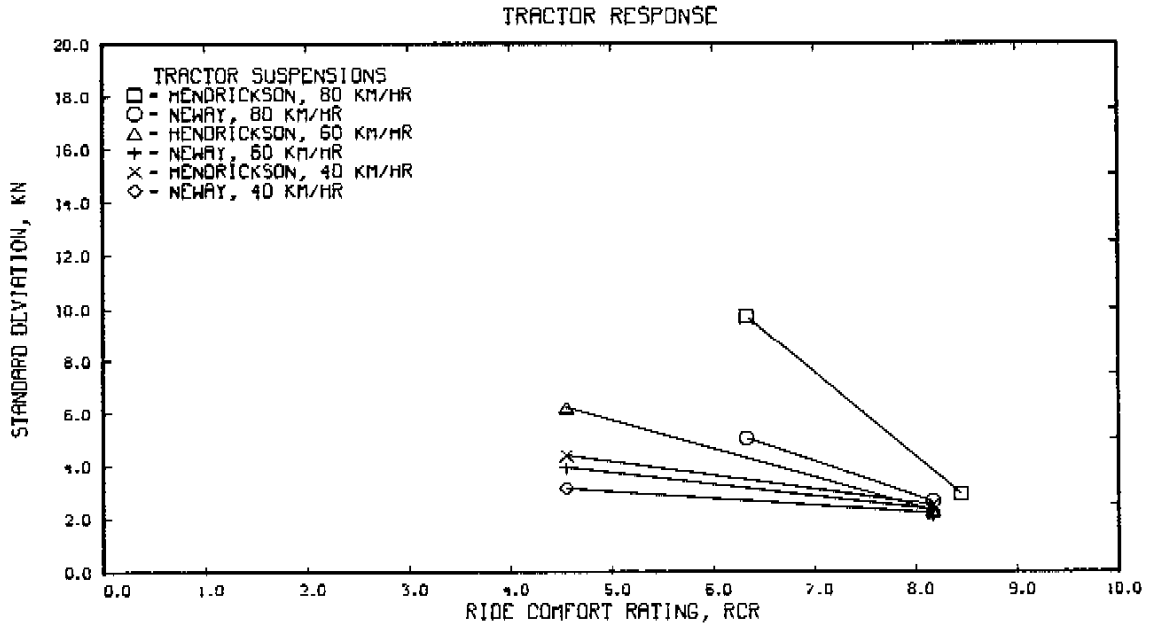
VARIATION OF TRAILER SUSPENSION TYPE
 TRACTOR SUSPENSION - HENDRICKSON
 AIR AXLE DOWN - NOMINAL WHEEL LOAD OF 40 KN
 NOMINAL TRAILER AXLE SPREAD OF 1.3 M



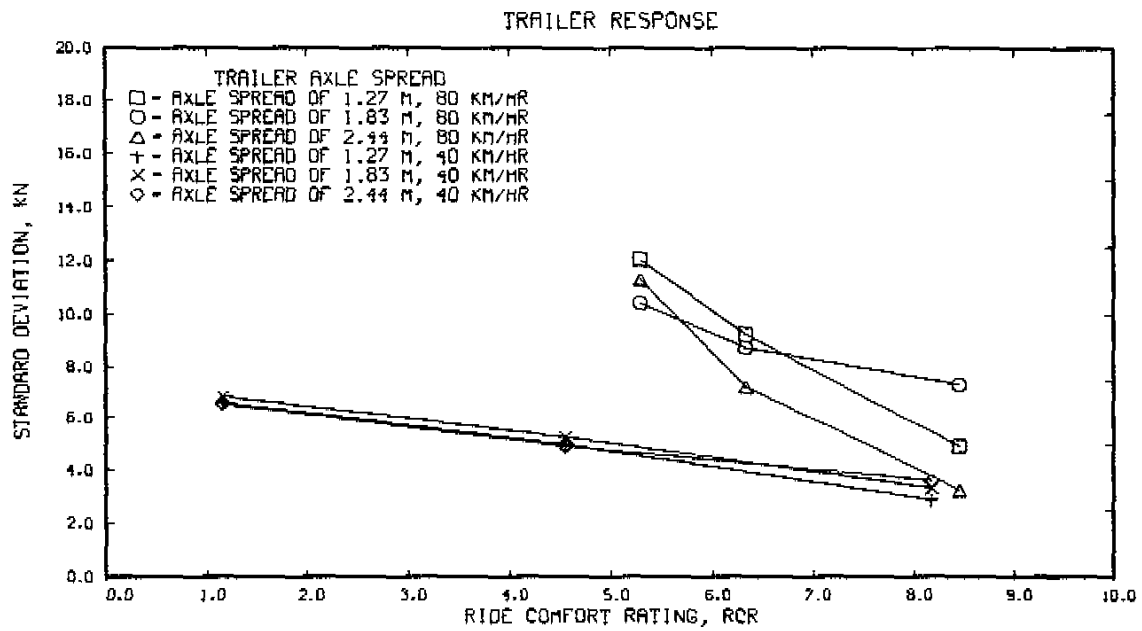
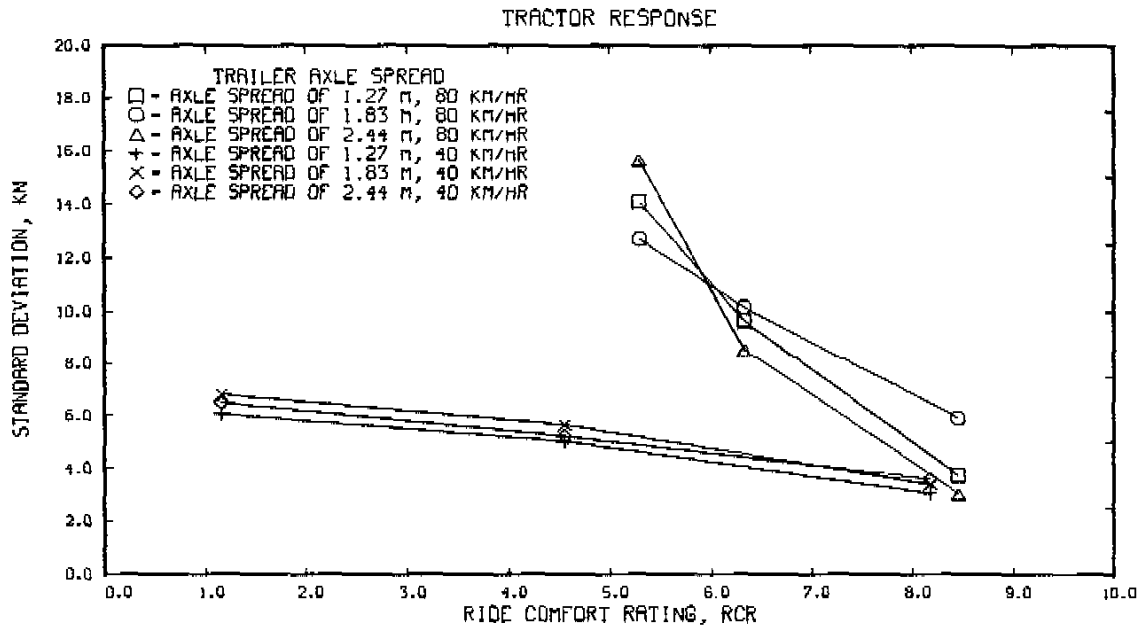
VARIATION OF TRACTOR SUSPENSION TYPE
 TRAILER SUSPENSION - CHALMERS
 AIR AXLE UP - NOMINAL WHEEL LOAD OF 50 KN
 NOMINAL TRAILER AXLE SPREAD OF 1.3 M



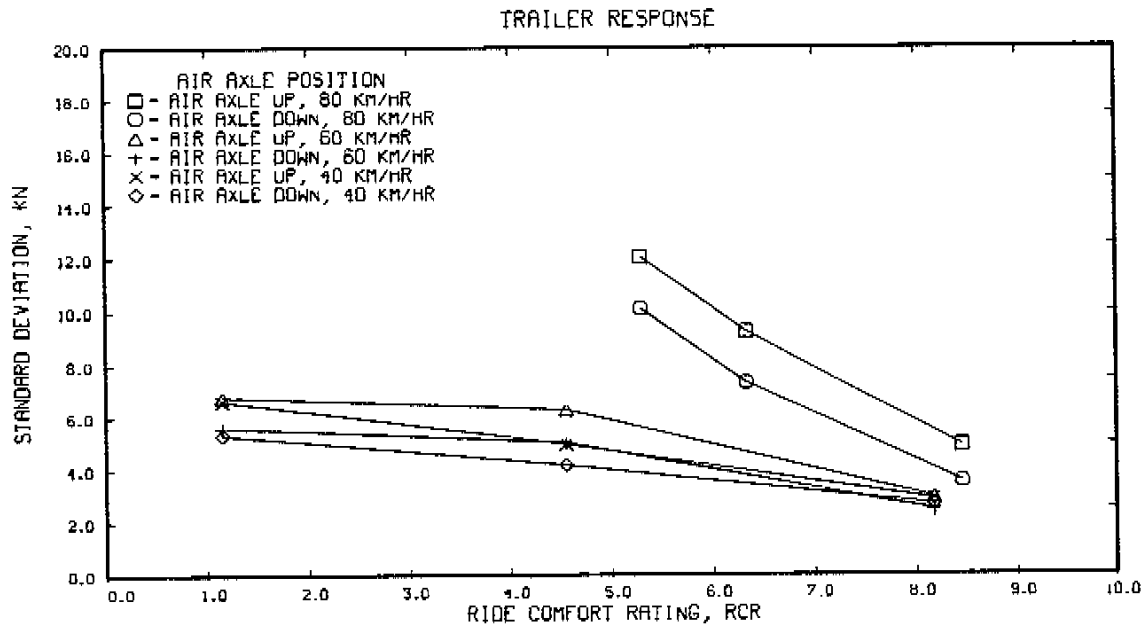
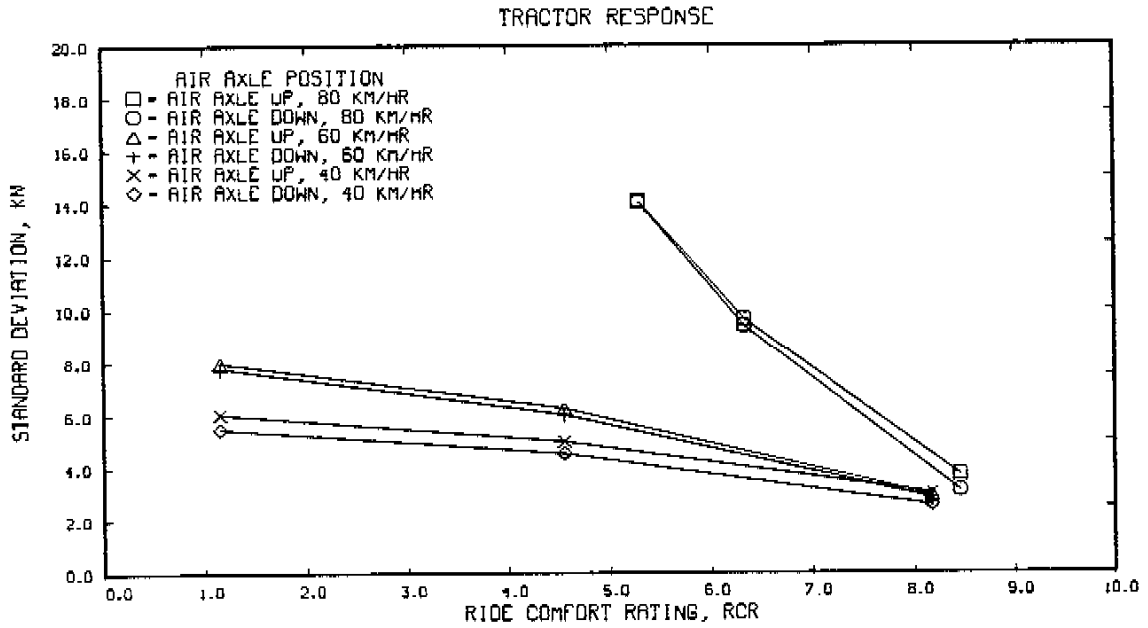
VARIATION OF TRACTOR SUSPENSION TYPE
 TRAILER SUSPENSION - CHALMERS
 AIR AXLE DOWN - NOMINAL WHEEL LOAD OF 40 KN
 NOMINAL TRAILER AXLE SPREAD OF 1.3 M



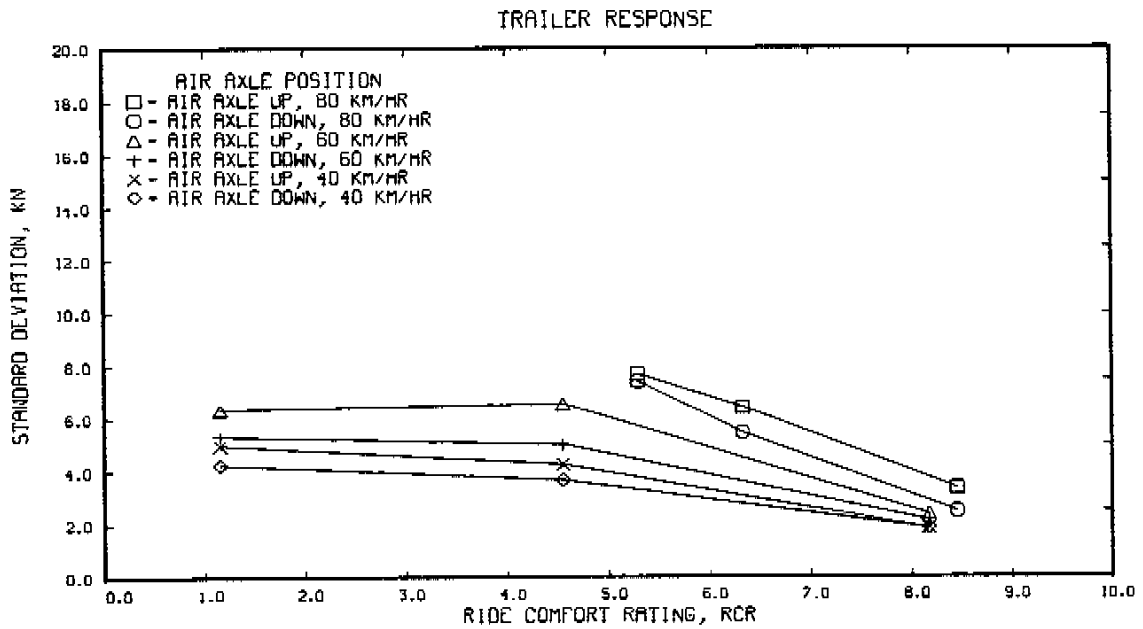
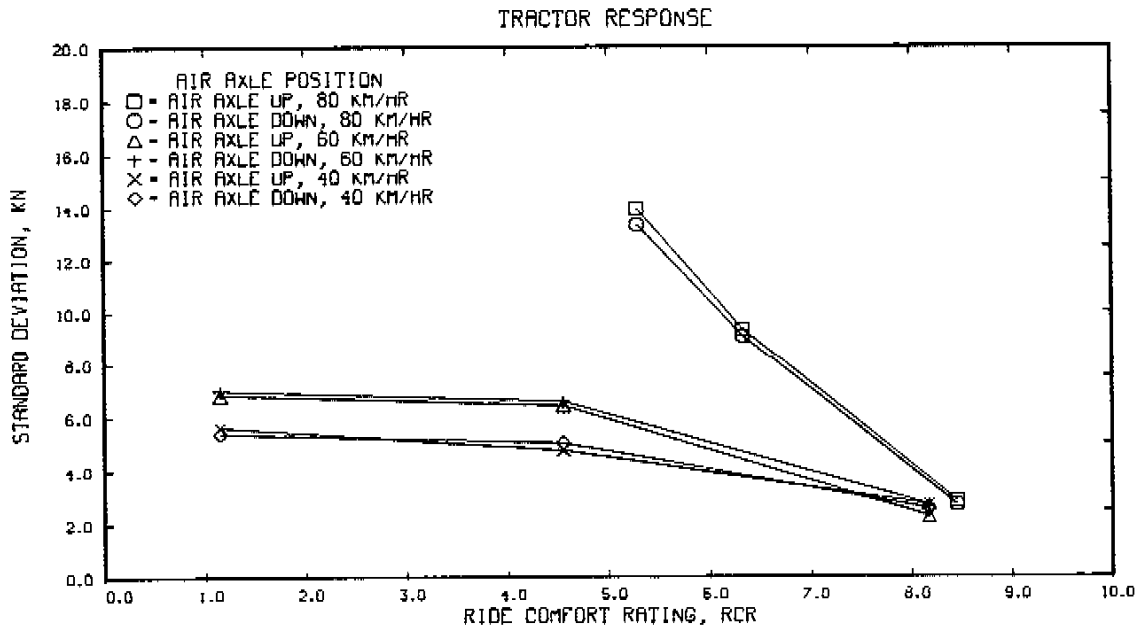
VARIATION OF TRAILER AXLE SPREAD
 TRACTOR SUSPENSION - HENDRICKSON
 TRAILER SUSPENSION - REYCO
 AIR AXLE UP - NOMINAL WHEEL LOAD OF 50 KN



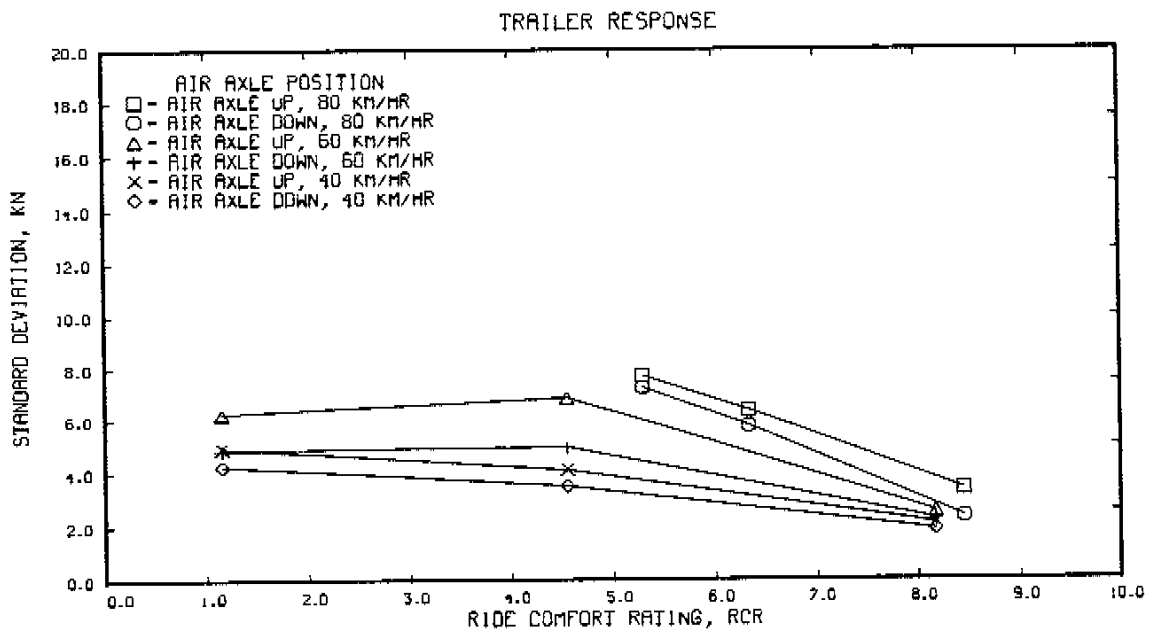
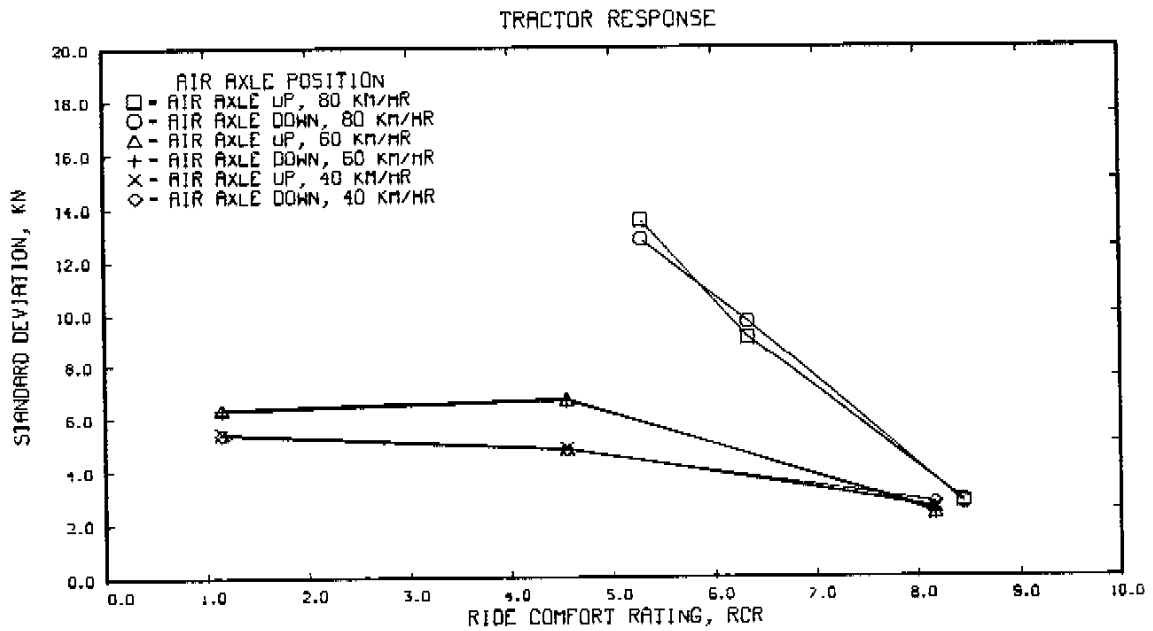
EFFECT OF AIR SUSPENSION LIFT AXLE
 TRACTOR SUSPENSION - HENDRICKSON
 TRAILER SUSPENSION - REYCO, AXLE SPREAD OF 1.27 M



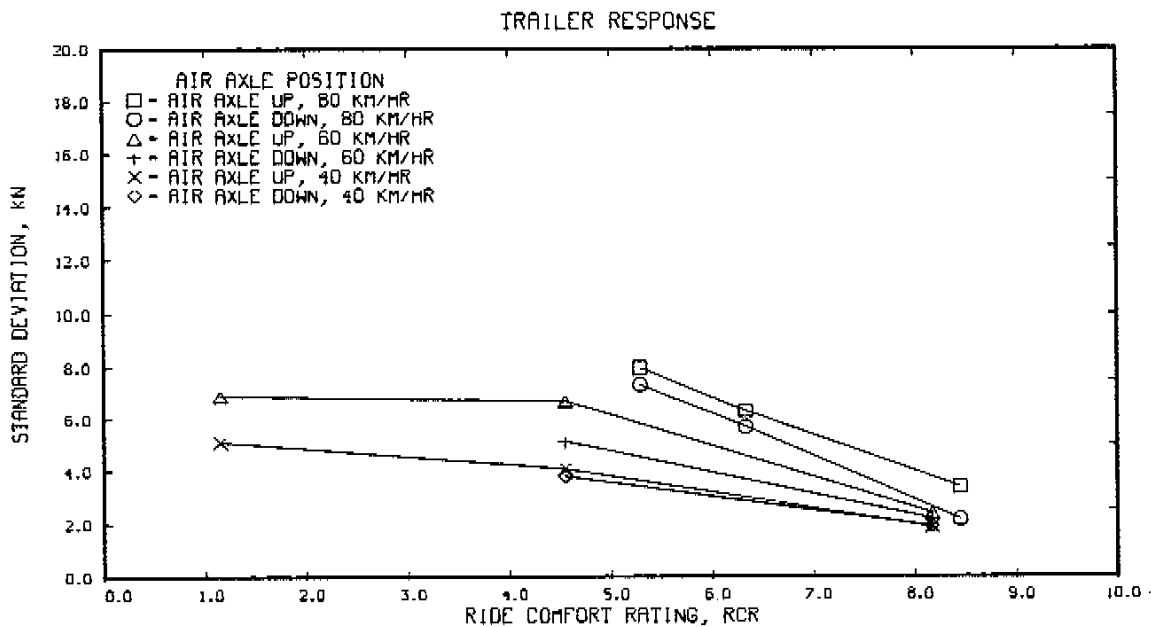
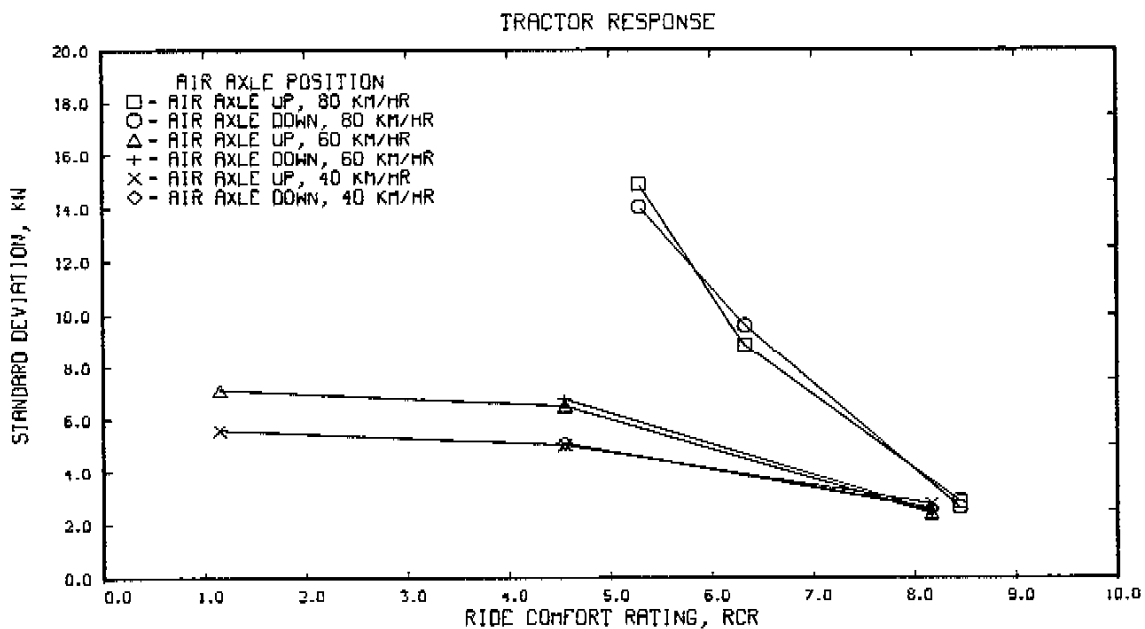
EFFECT OF AIR SUSPENSION LIFT AXLE
 TRACTOR SUSPENSION - HENDRICKSON
 TRAILER SUSPENSION - NEWAY, AXLE SPREAD OF 1.27 M



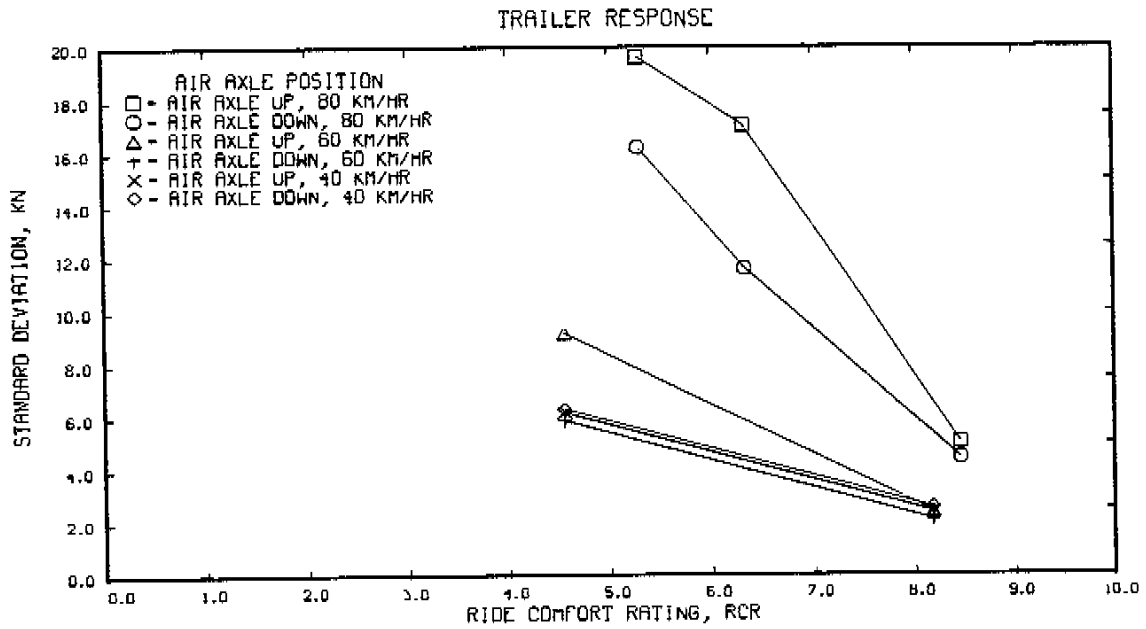
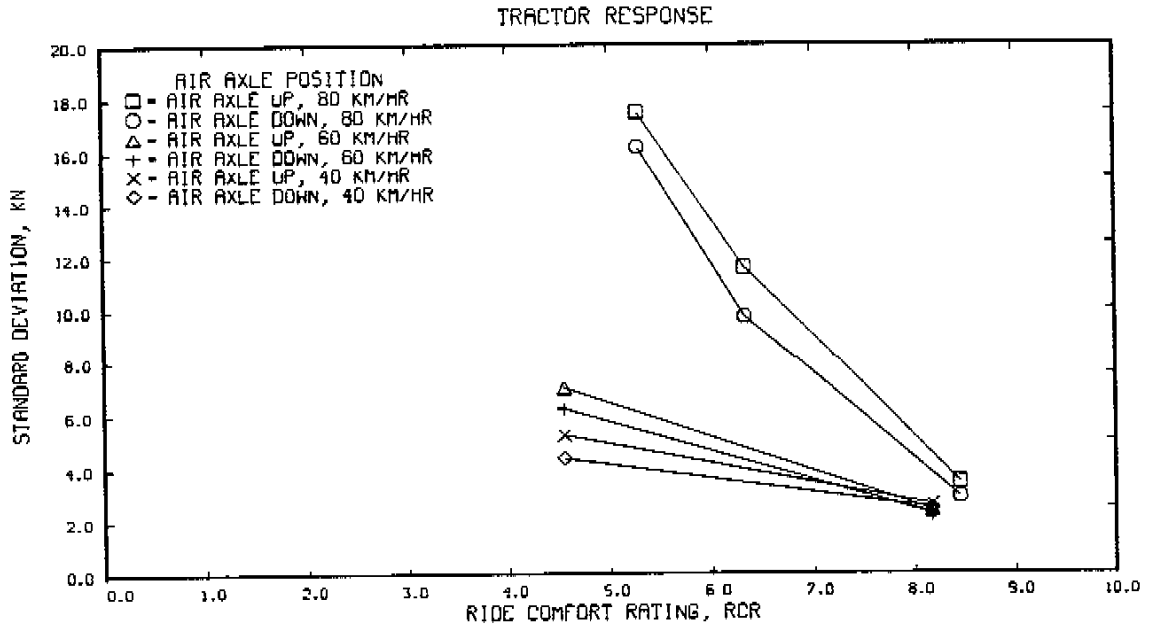
EFFECT OF AIR SUSPENSION LIFT AXLE
 TRACTOR SUSPENSION - HENDRICKSON
 TRAILER SUSPENSION - NEWAY, AXLE SPREAD OF 1.83 M



EFFECT OF AIR SUSPENSION LIFT AXLE
 TRACTOR SUSPENSION - HENDRICKSON
 TRAILER SUSPENSION - NEWAY, AXLE SPREAD OF 2.44 M

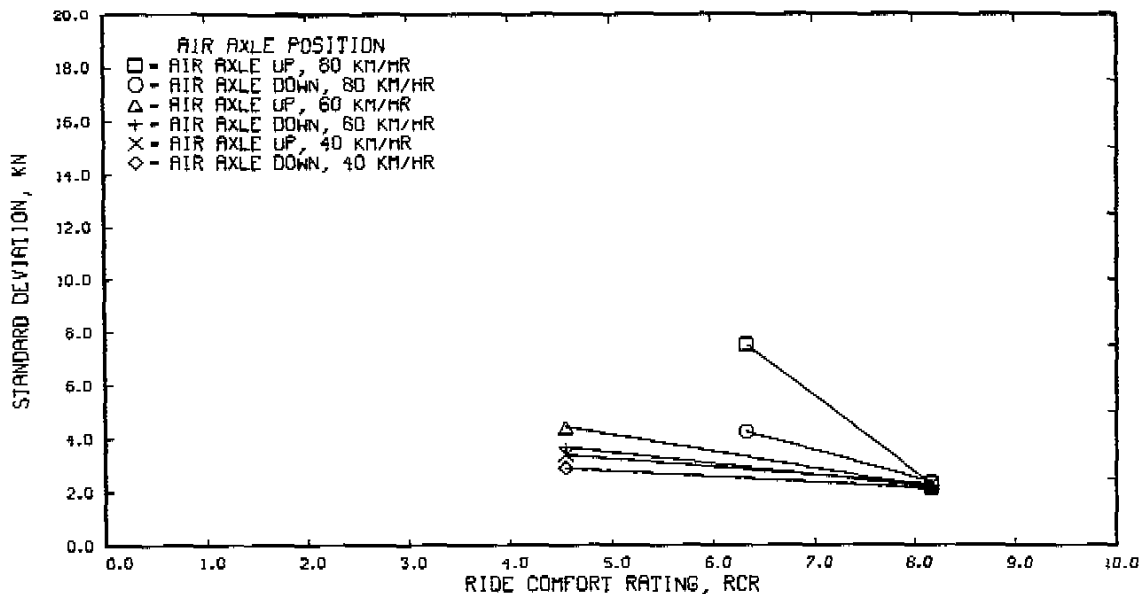


EFFECT OF AIR SUSPENSION LIFT AXLE
 TRACTOR SUSPENSION - HENDRICKSON
 TRAILER SUSPENSION - CHALMERS, AXLE SPREAD OF 1.37 M

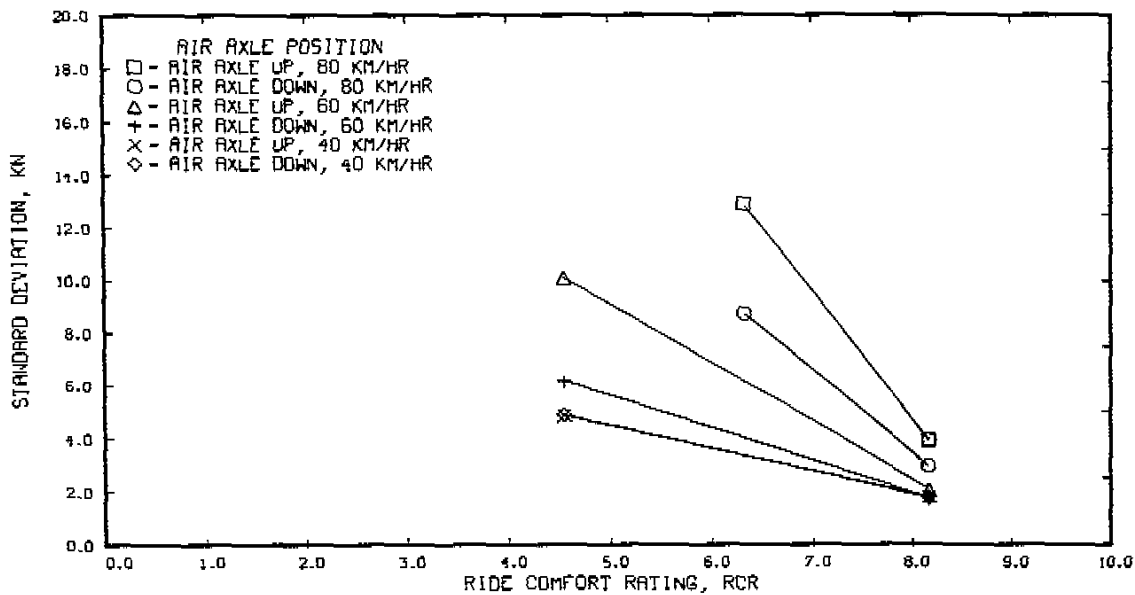


EFFECT OF AIR SUSPENSION LIFT AXLE
 TRACTOR SUSPENSION - NEWAY
 TRAILER SUSPENSION - CHALMERS, AXLE SPREAD OF 1.37 M

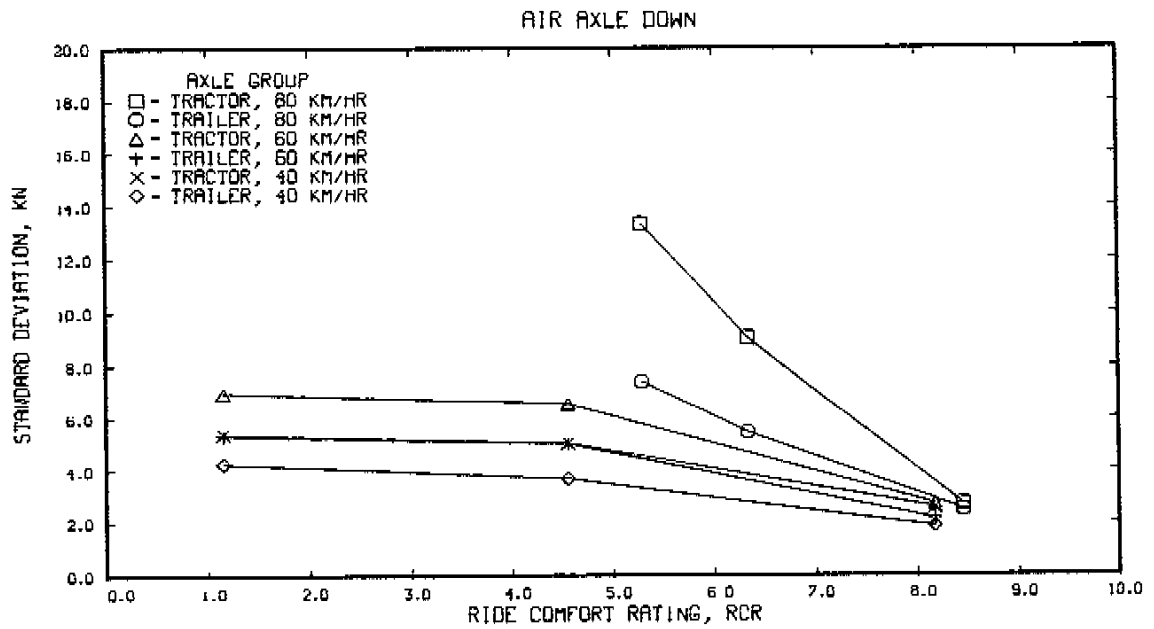
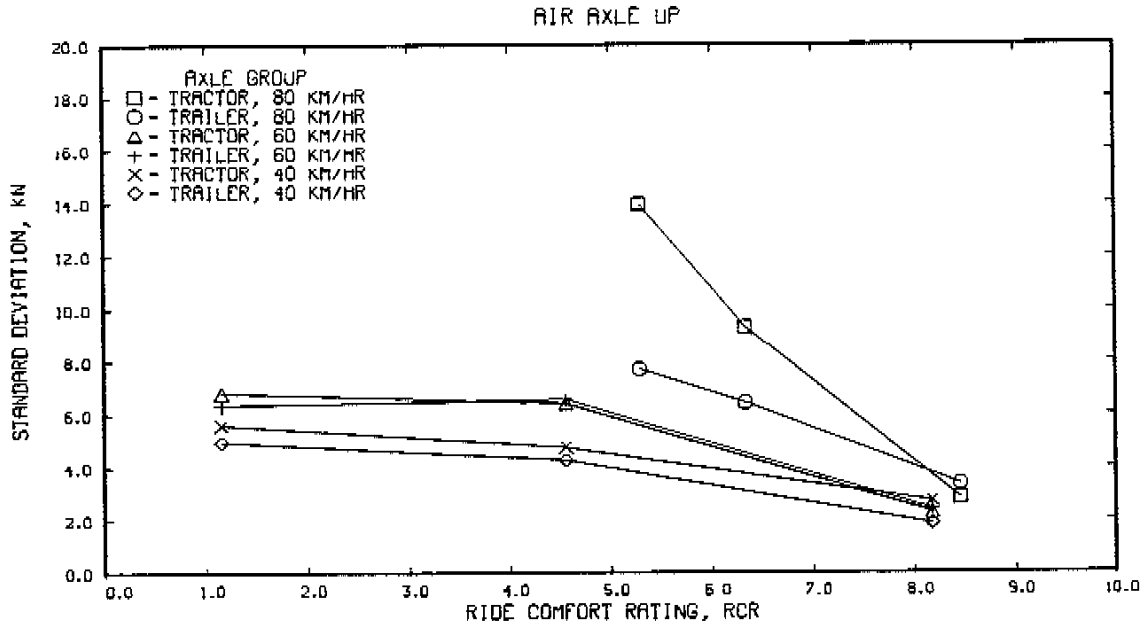
TRACTOR RESPONSE



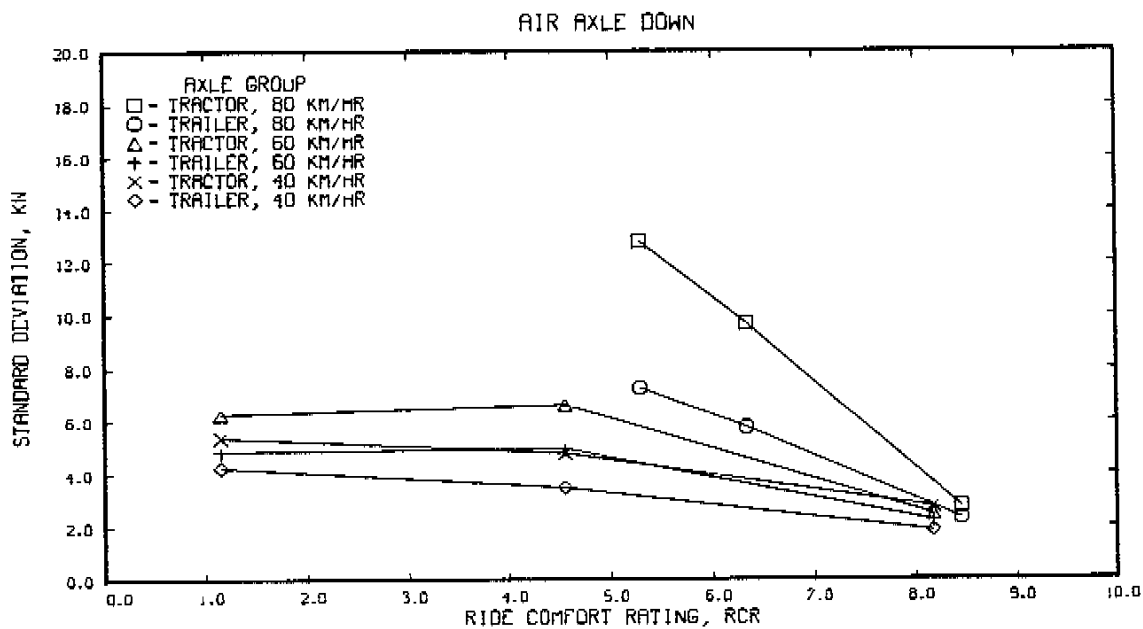
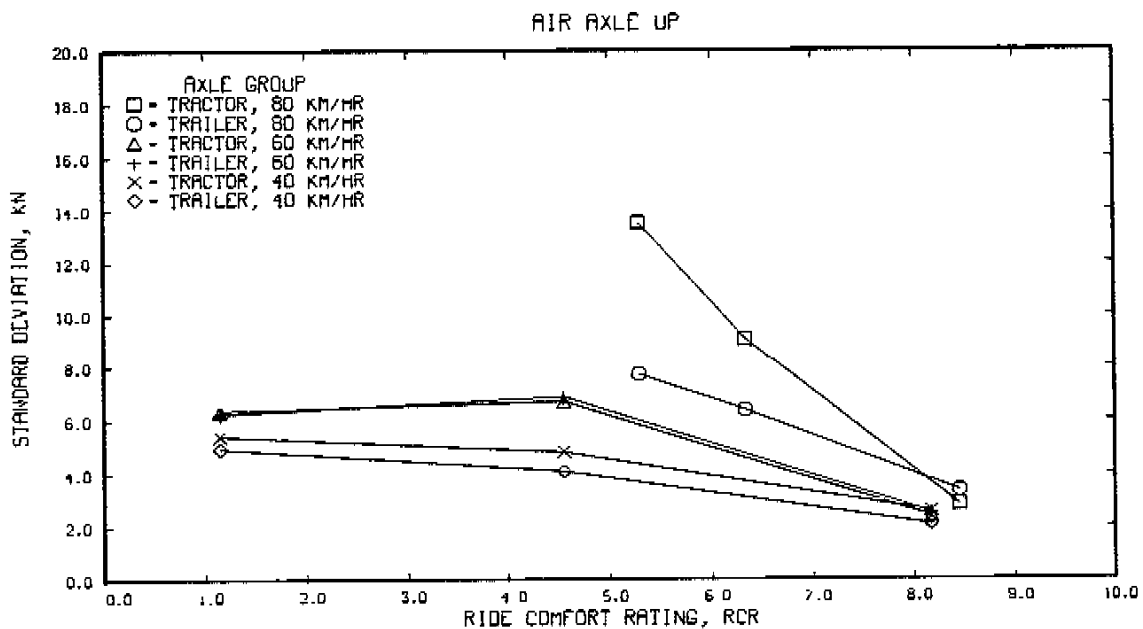
TRAILER RESPONSE



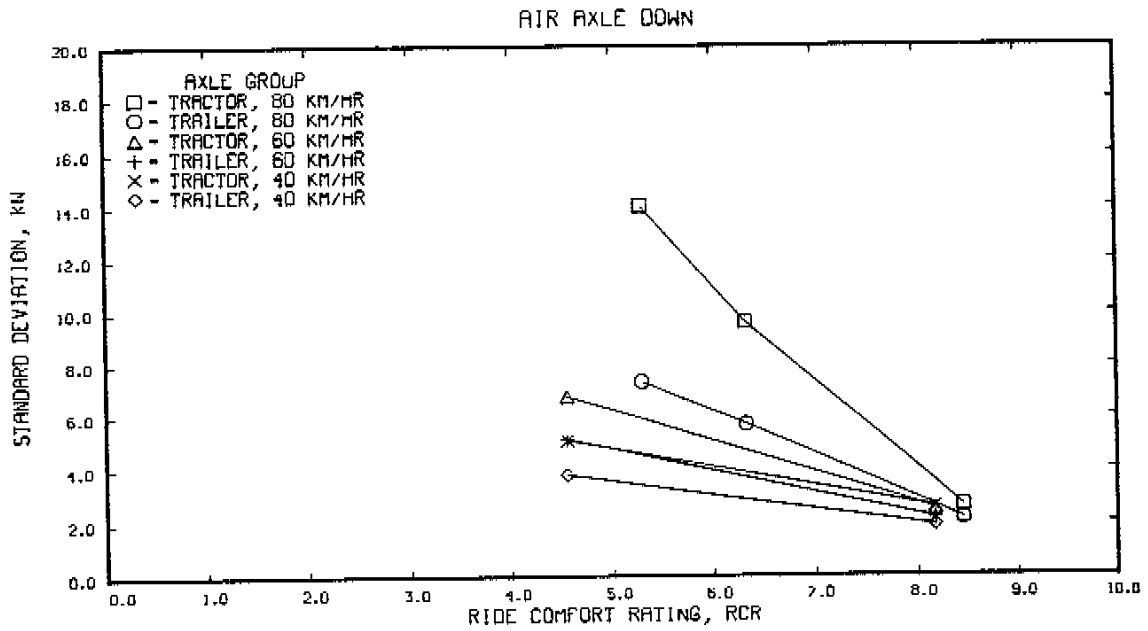
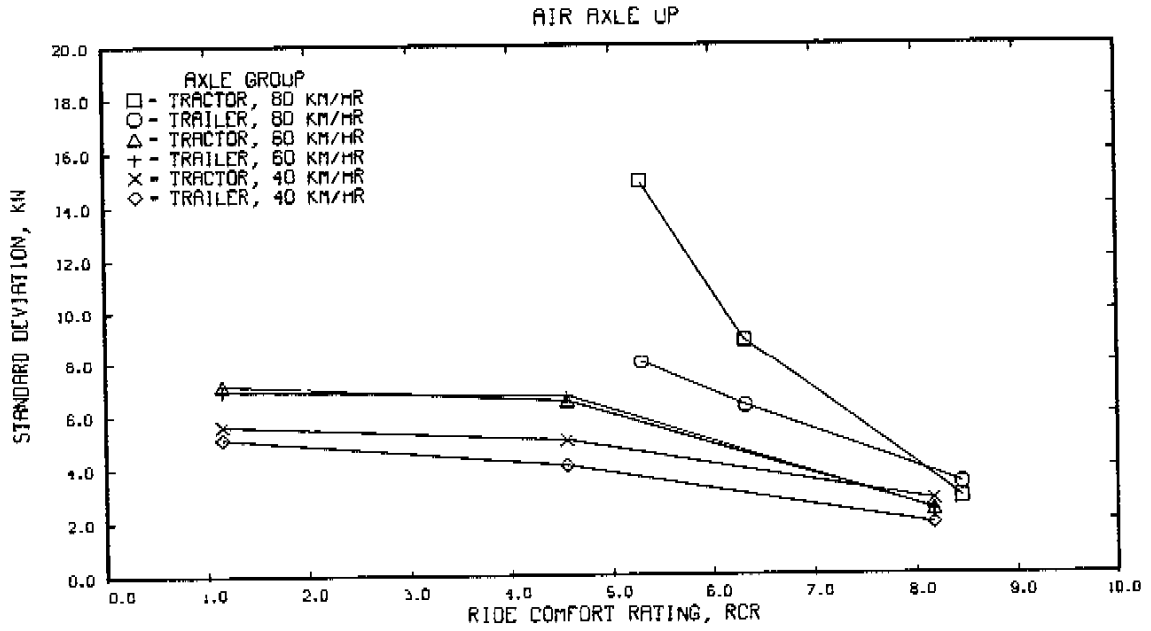
COMPARISON OF TRACTOR AND TRAILER RESPONSE
 TRACTOR SUSPENSION - HENDRICKSON
 TRAILER SUSPENSION - NEWAY, AXLE SPREAD OF 1.27 M



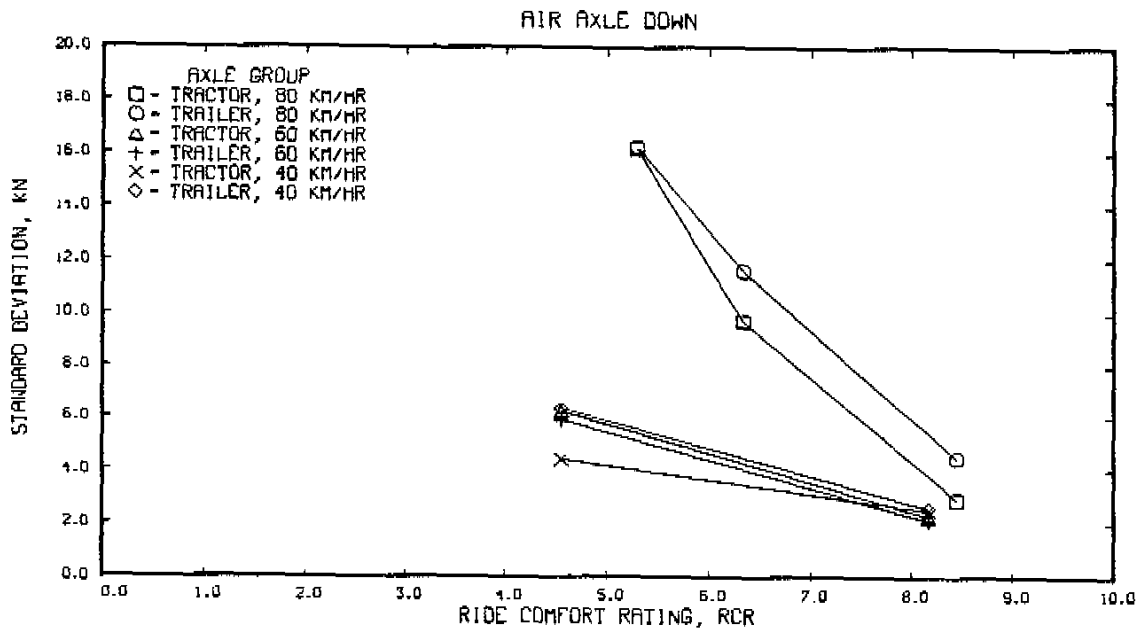
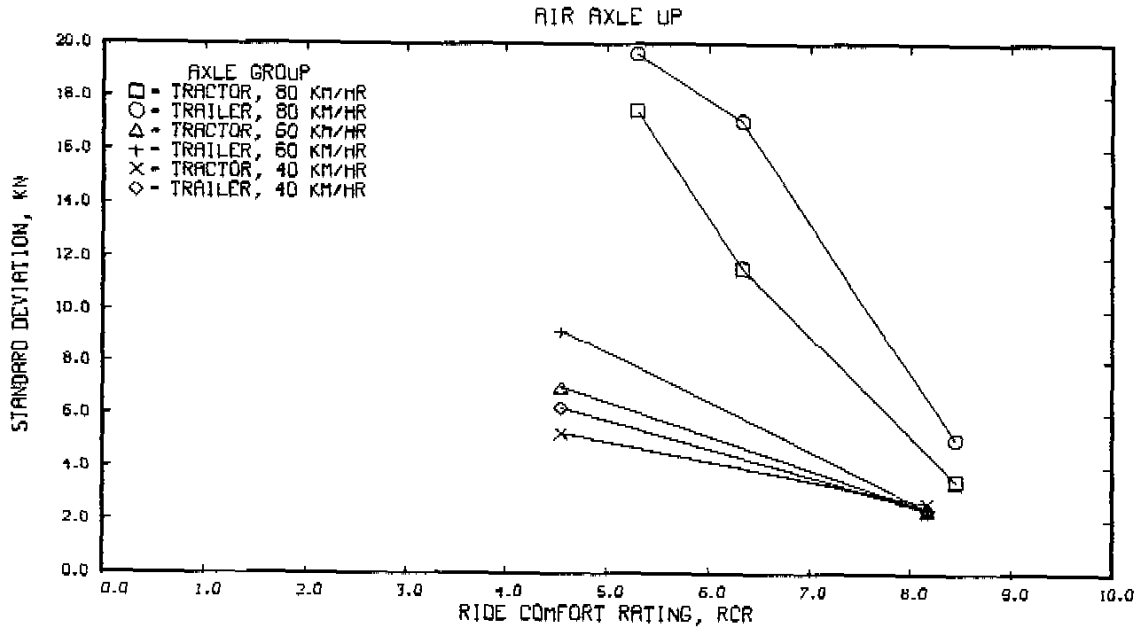
COMPARISON OF TRACTOR AND TRAILER RESPONSE
 TRACTOR SUSPENSION - HENDRICKSON
 TRAILER SUSPENSION - NEWAY, AXLE SPREAD OF 1.83 M



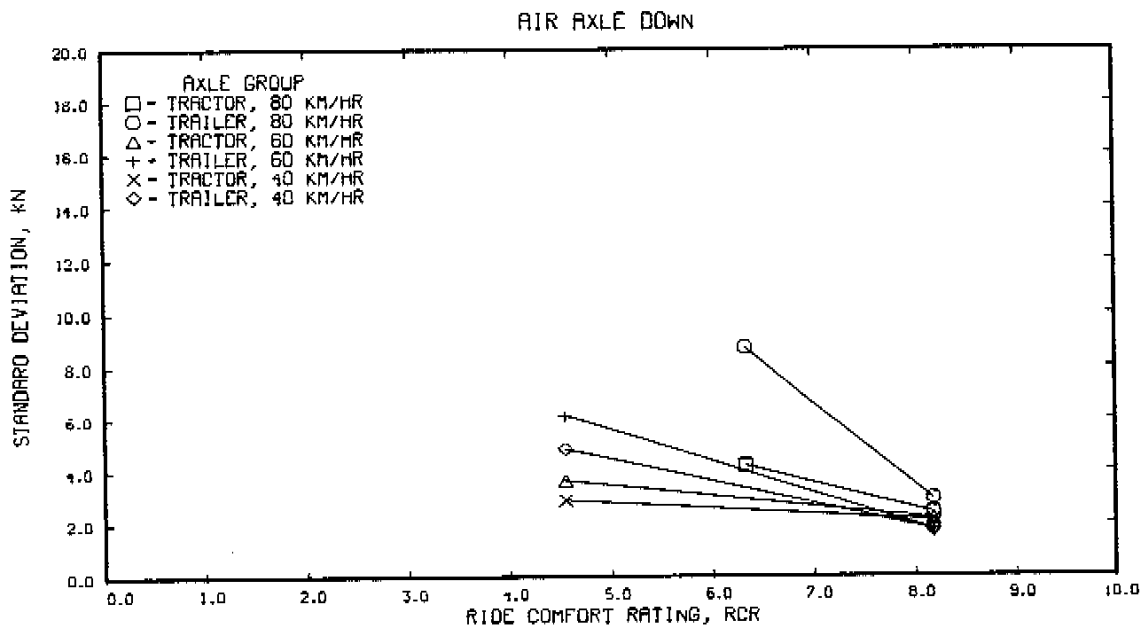
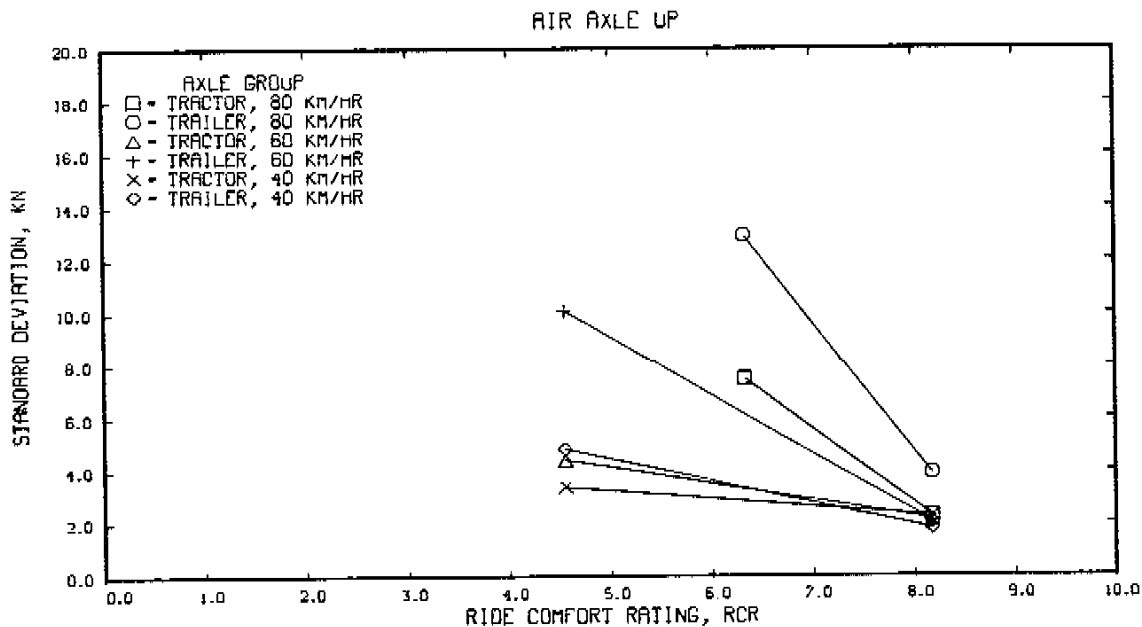
COMPARISON OF TRACTOR AND TRAILER RESPONSE
 TRACTOR SUSPENSION - HENDRICKSON
 TRAILER SUSPENSION - NEWAY, AXLE SPREAD OF 2.44 M



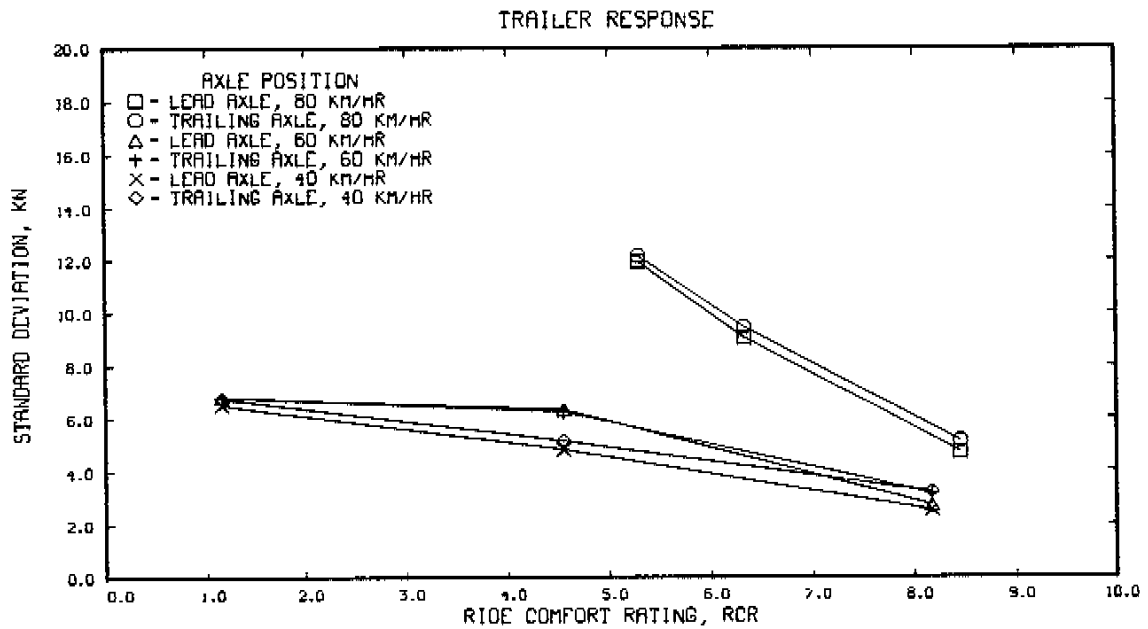
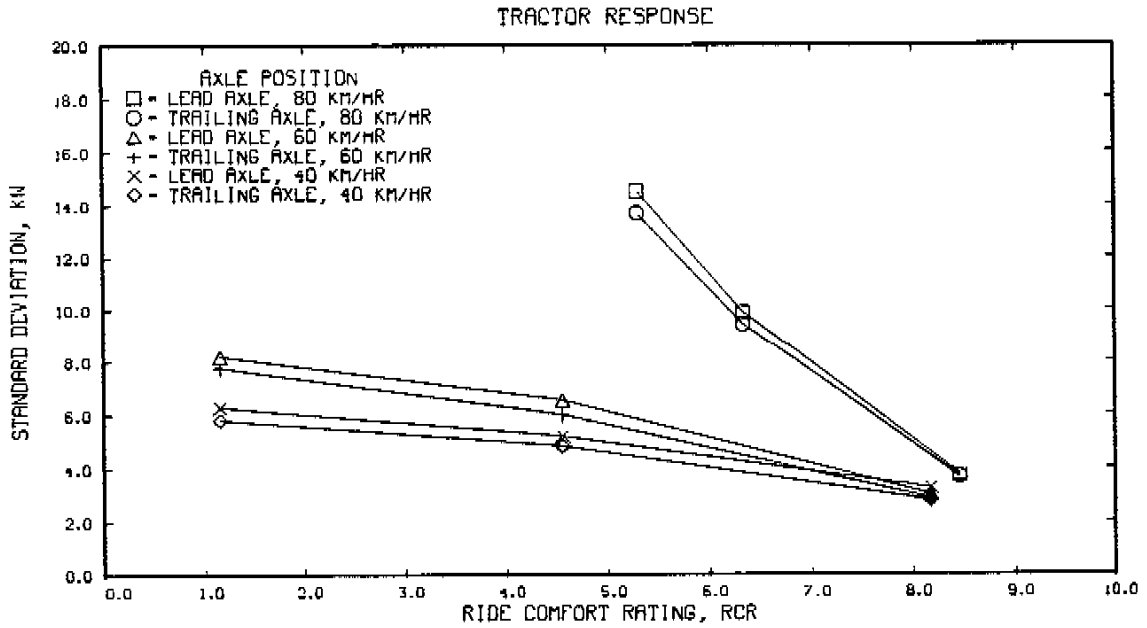
COMPARISON OF TRACTOR AND TRAILER RESPONSE
 TRACTOR SUSPENSION - HENDRICKSON
 TRAILER SUSPENSION - CHALMERS, AXLE SPREAD OF 1.37 M



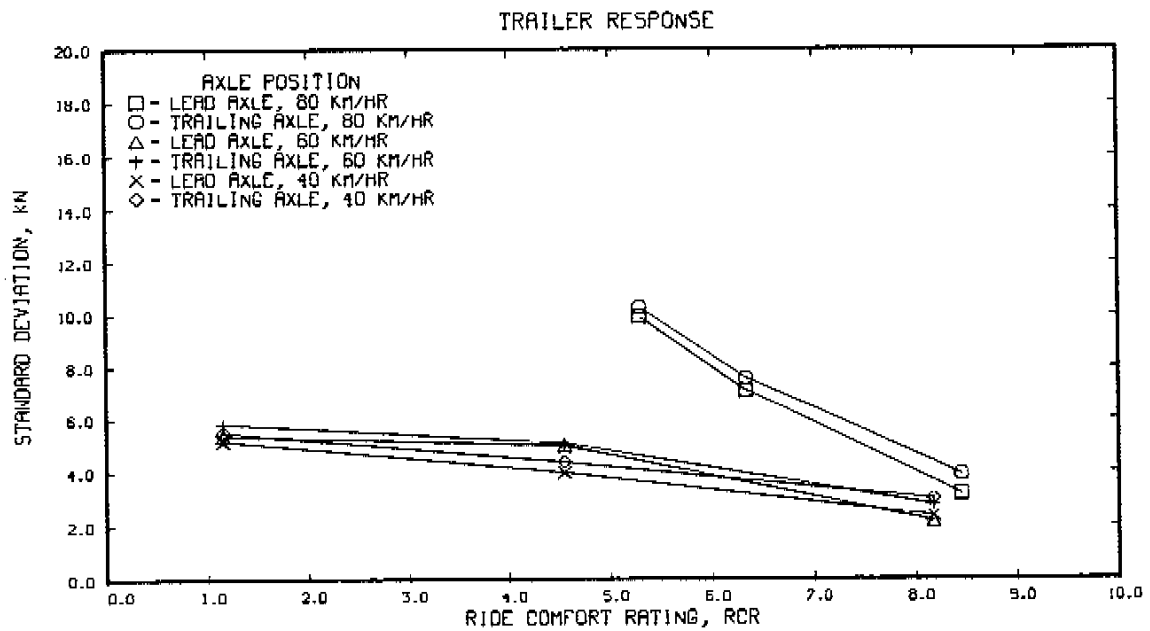
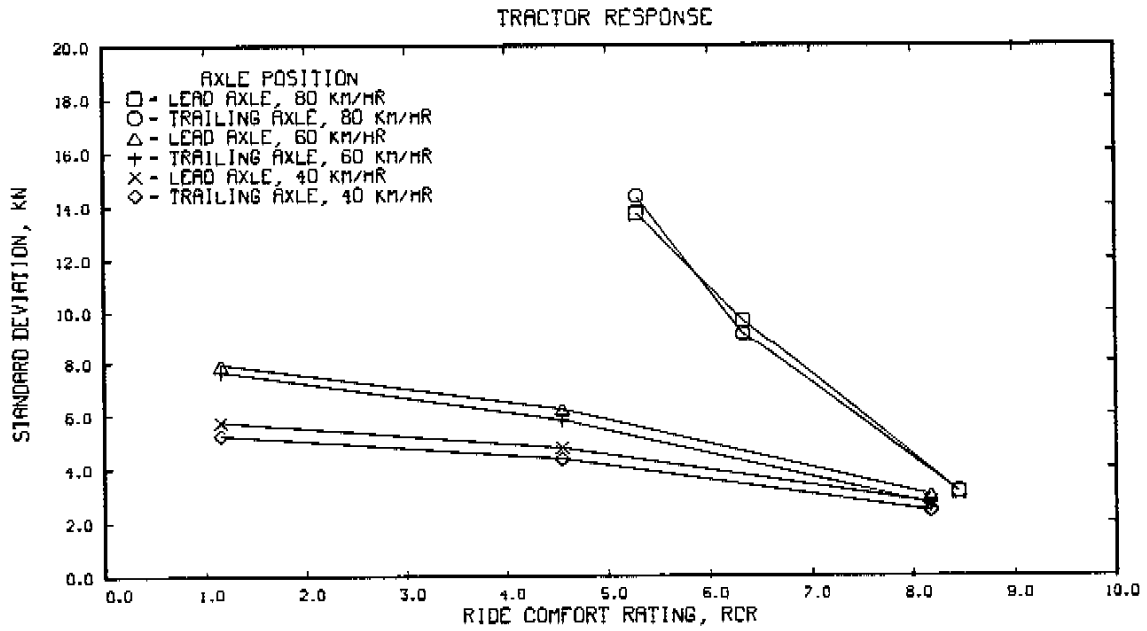
COMPARISON OF TRACTOR AND TRAILER RESPONSE
 TRACTOR SUSPENSION - NEWAY
 TRAILER SUSPENSION - CHALMERS, AXLE SPREAD OF 1.37 M



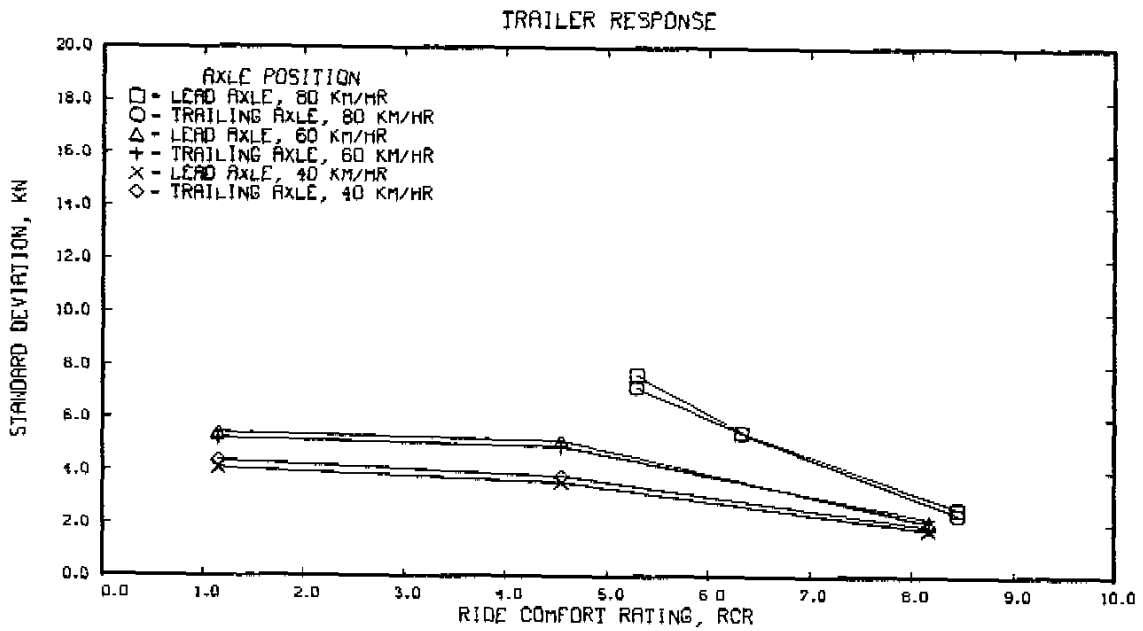
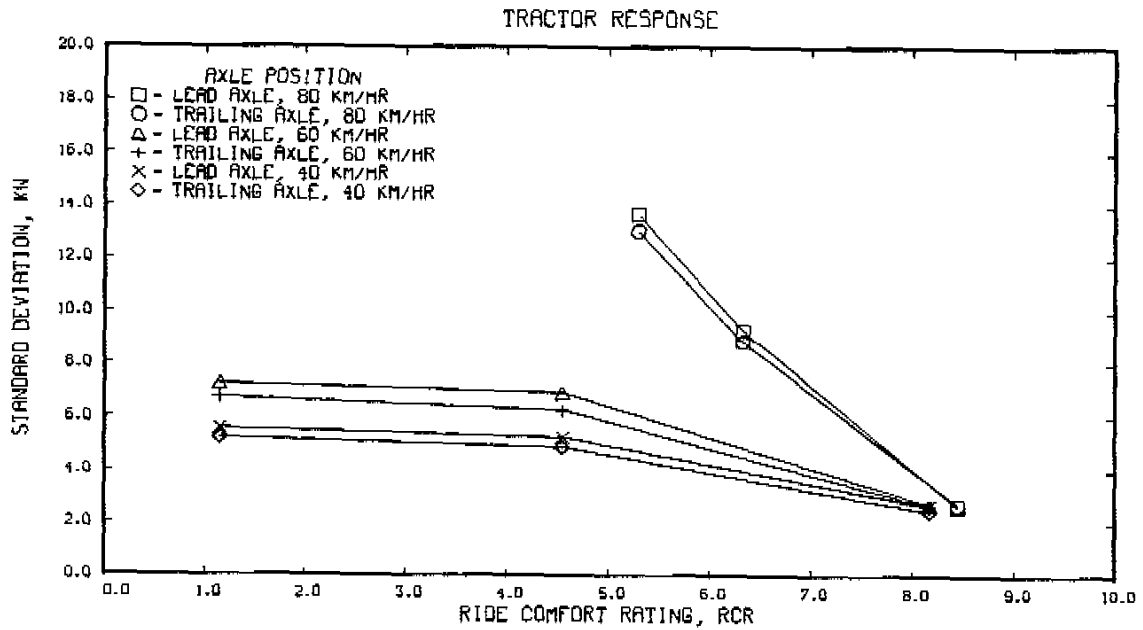
COMPARISON OF LEAD AND TRAILING AXLE RESPONSE
 TRACTOR SUSPENSION - HENDRICKSON
 TRAILER SUSPENSION - REYCO, AXLE SPREAD OF 1.27 M
 AIR AXLE UP - NOMINAL WHEEL LOAD OF 50 KN



COMPARISON OF LEAD AND TRAILING AXLE RESPONSE
 TRACTOR SUSPENSION - HENDRICKSON
 TRAILER SUSPENSION - REYCO, AXLE SPREAD OF 1.27 M
 AIR AXLE DOWN - NOMINAL WHEEL LOAD OF 40 KN

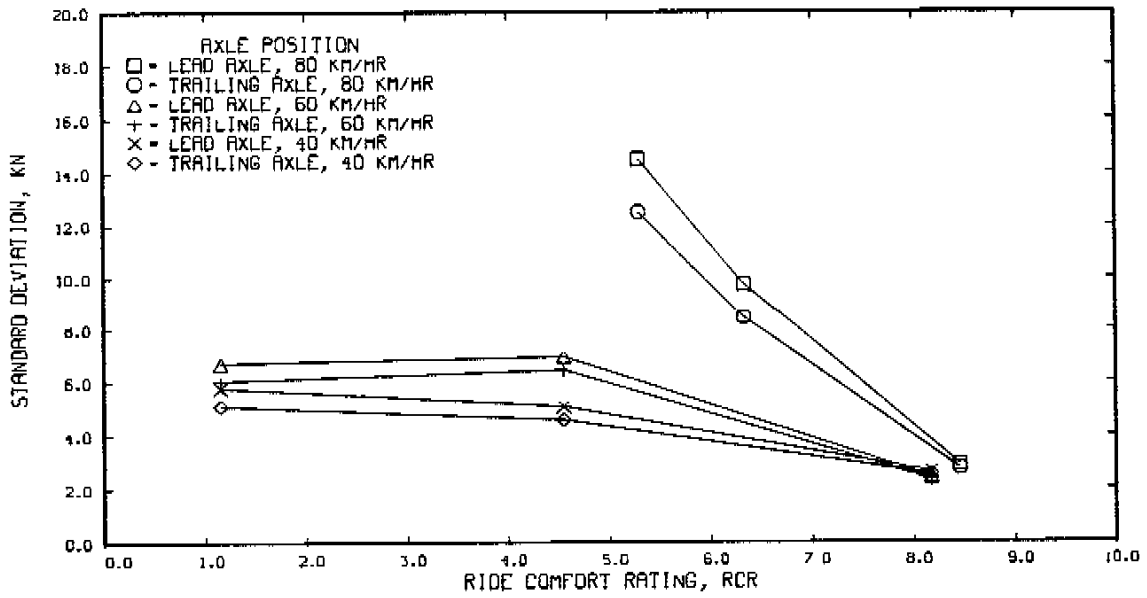


COMPARISON OF LEAD AND TRAILING AXLE RESPONSE
 TRACTOR SUSPENSION - HENDRICKSON
 TRAILER SUSPENSION - NEWAY, AXLE SPREAD OF 1.27 M
 AIR AXLE DOWN - NOMINAL WHEEL LOAD OF 40 KN

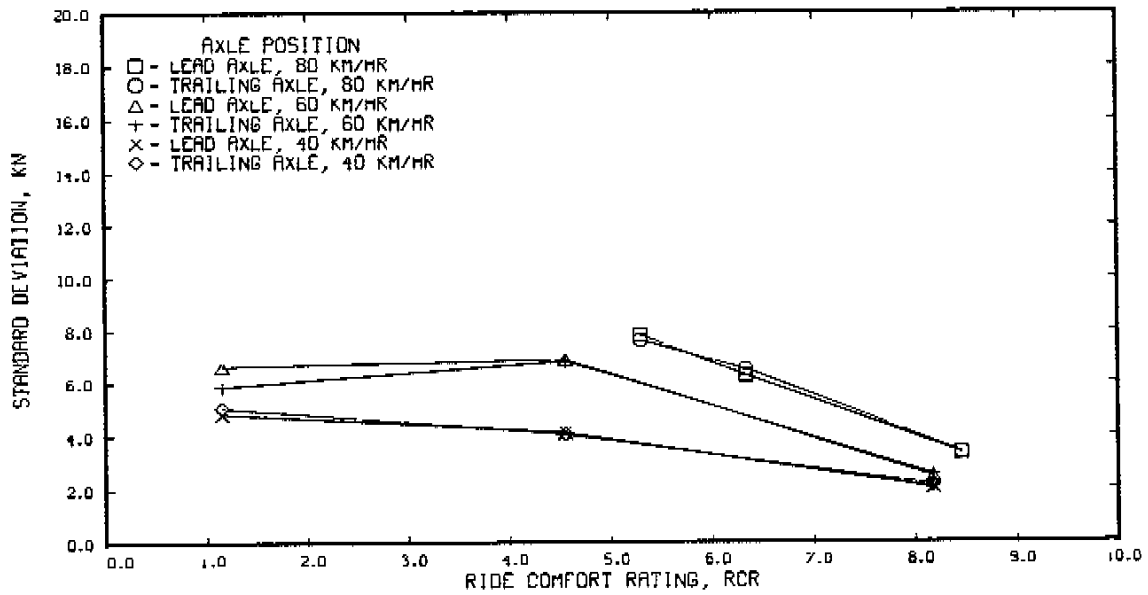


COMPARISON OF LEAD AND TRAILING AXLE RESPONSE
 TRACTOR SUSPENSION - HENDRICKSON
 TRAILER SUSPENSION - NEWAY, AXLE SPREAD OF 1.83 M
 AIR AXLE UP - NOMINAL WHEEL LOAD OF 50 KN

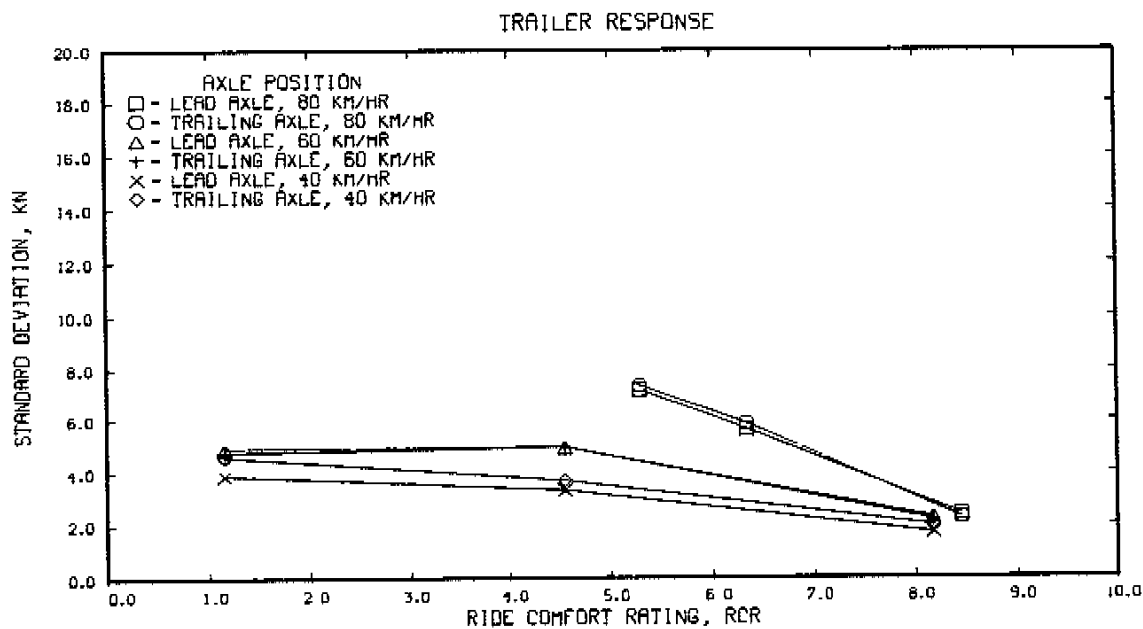
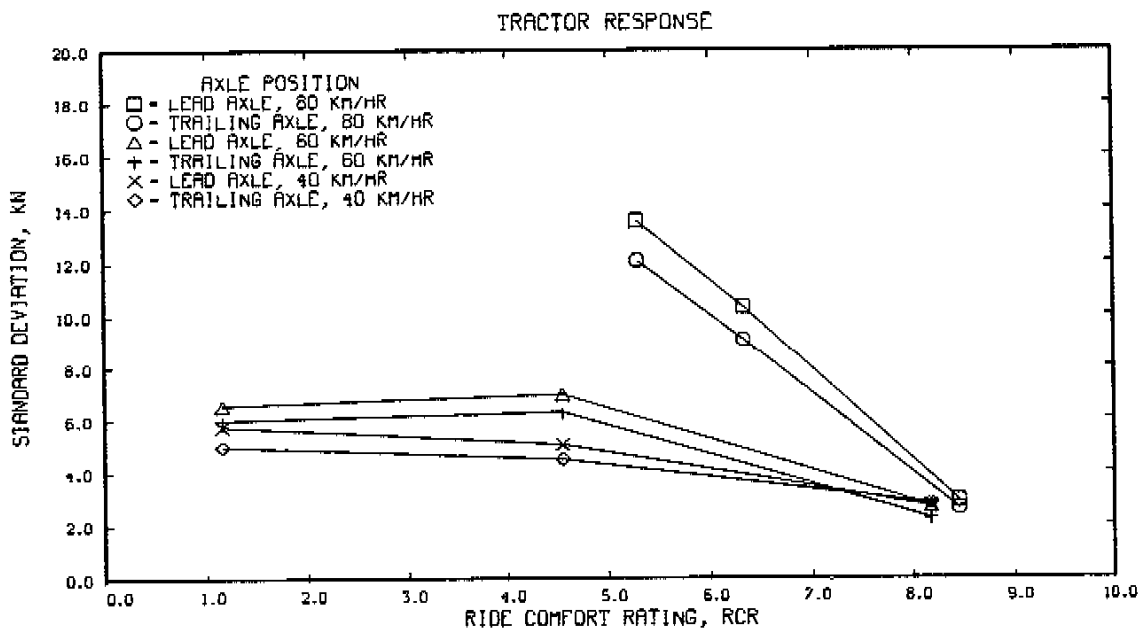
TRACTOR RESPONSE



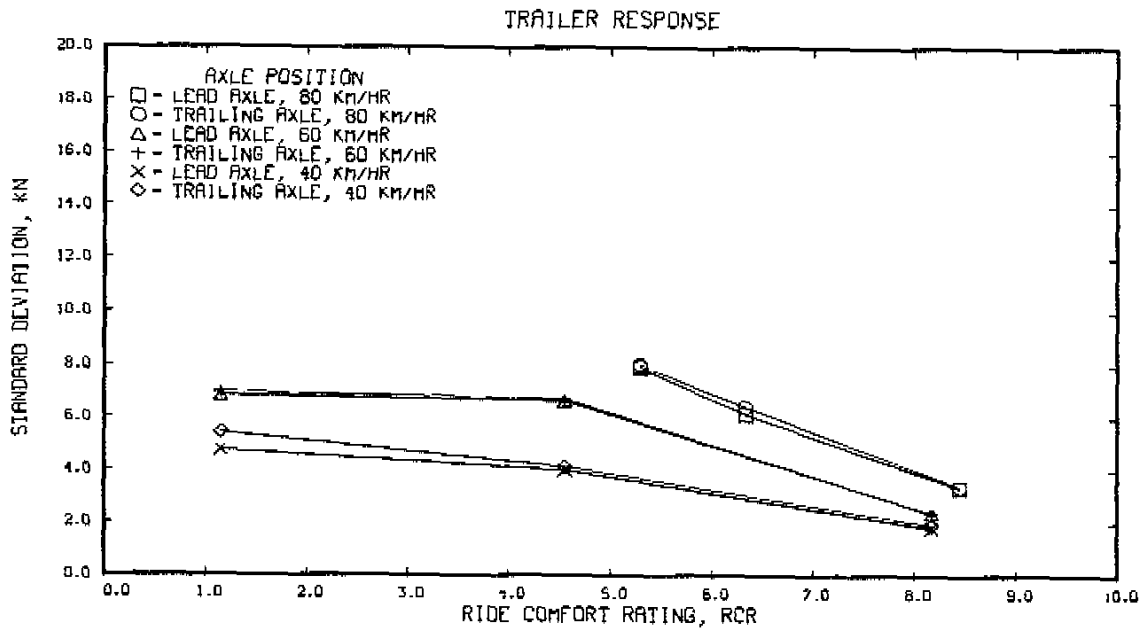
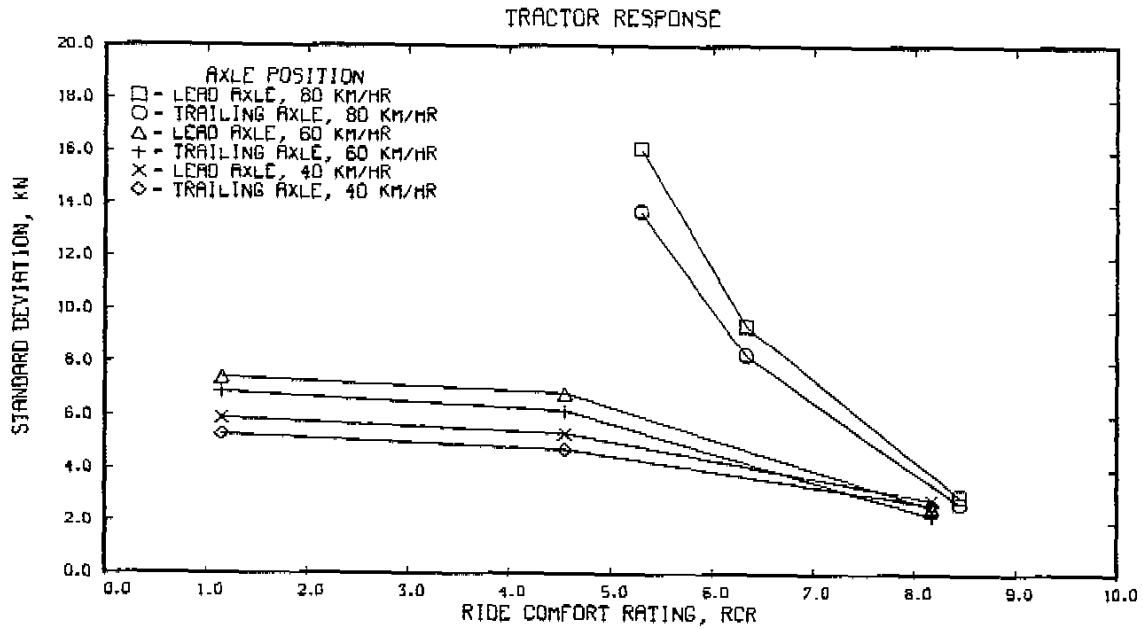
TRAILER RESPONSE



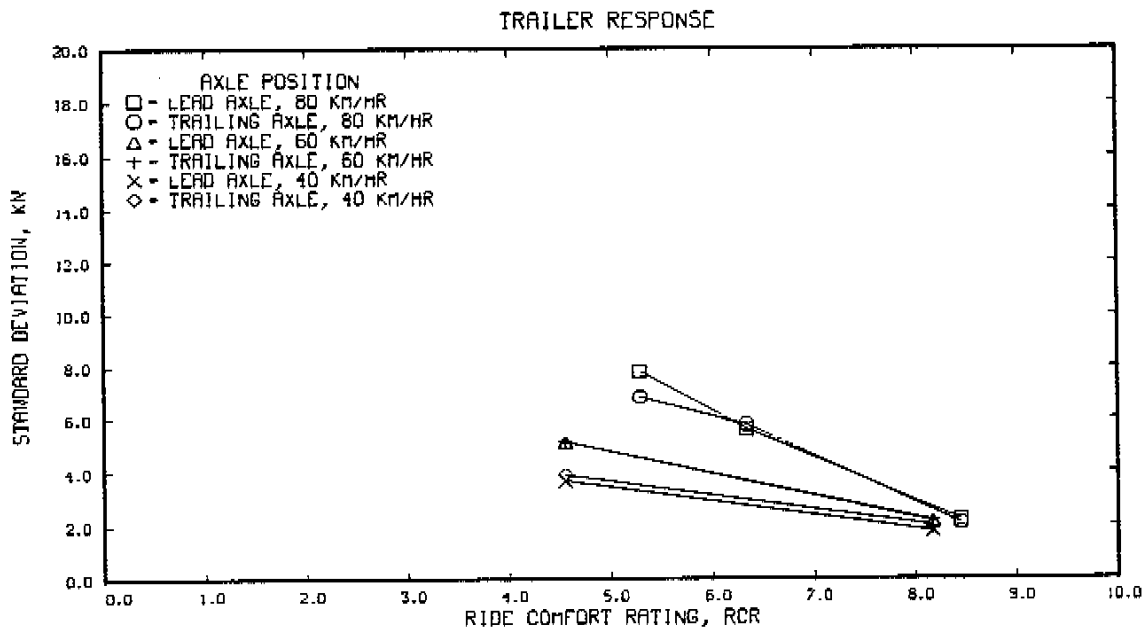
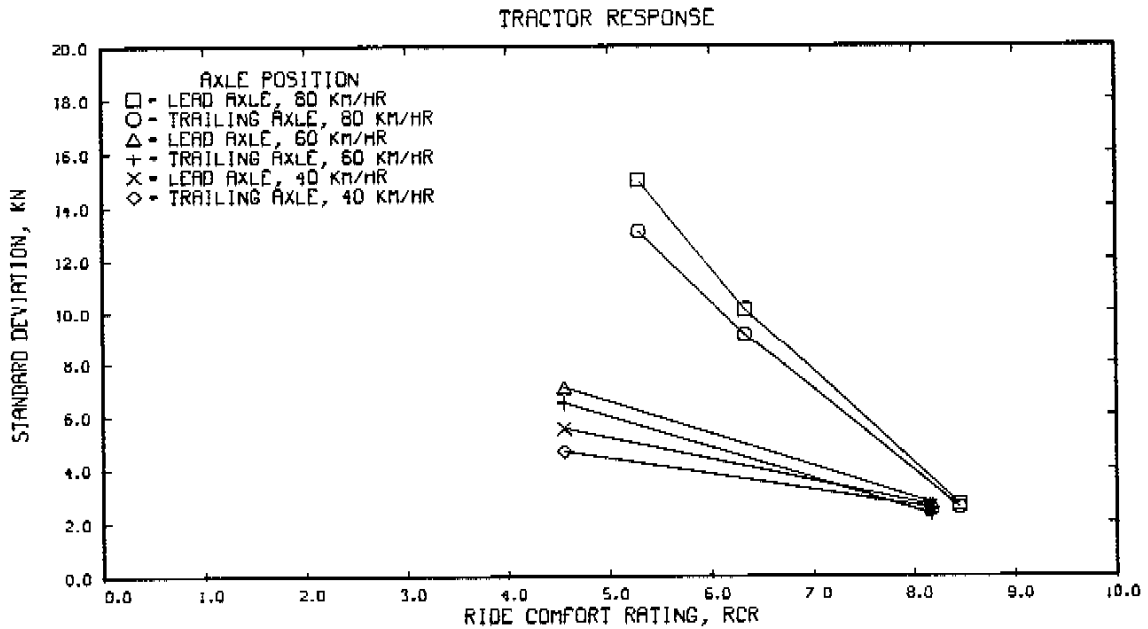
COMPARISON OF LEAD AND TRAILING AXLE RESPONSE
 TRACTOR SUSPENSION - HENDRICKSON
 TRAILER SUSPENSION - NEWAY, AXLE SPREAD OF 1.83 M
 AIR AXLE DOWN - NOMINAL WHEEL LOAD OF 40 KN



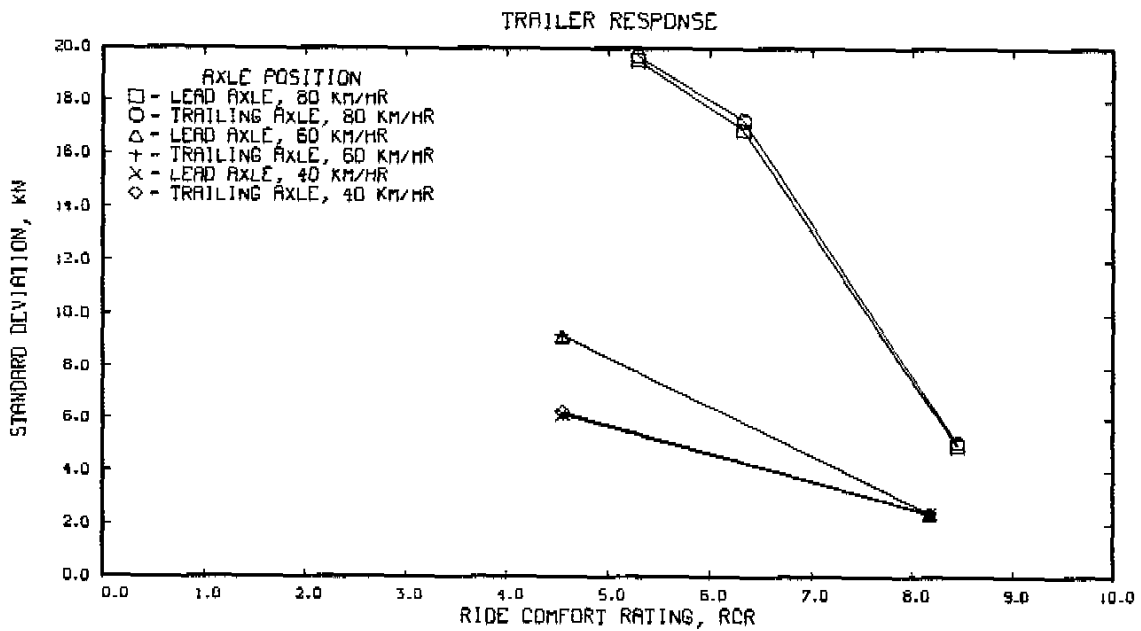
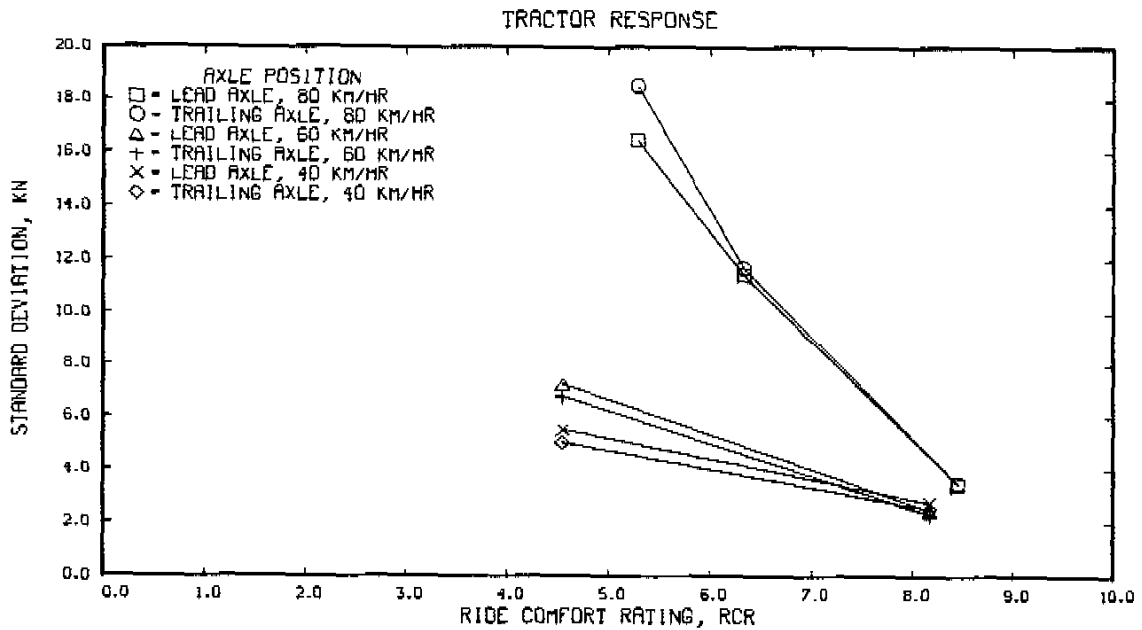
COMPARISON OF LEAD AND TRAILING AXLE RESPONSE
 TRACTOR SUSPENSION - HENDRICKSON
 TRAILER SUSPENSION - NEWAY, AXLE SPREAD OF 2.44 M
 AIR AXLE UP - NOMINAL WHEEL LOAD OF 50 KN



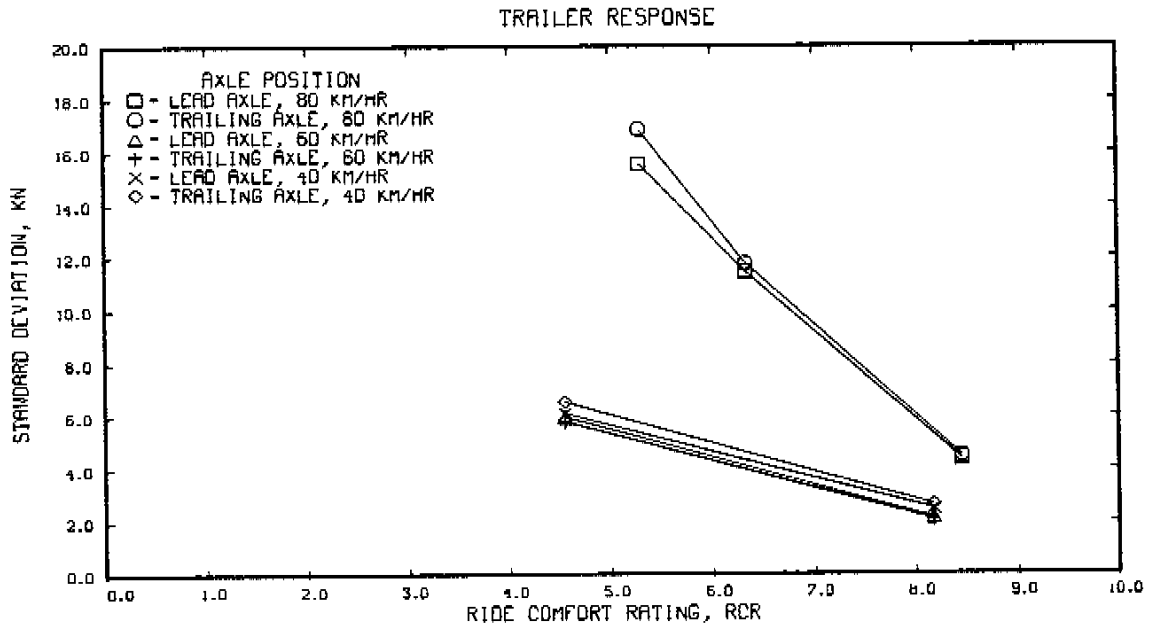
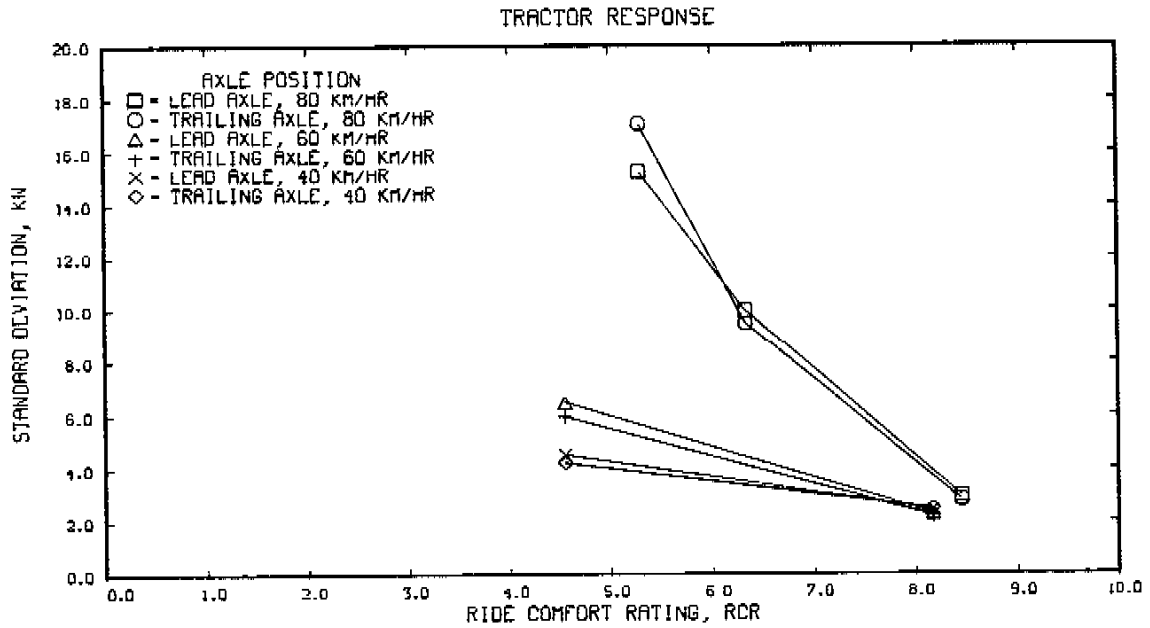
COMPARISON OF LEAD AND TRAILING AXLE RESPONSE
 TRACTOR SUSPENSION - HENDRICKSON
 TRAILER SUSPENSION - NEWAY, AXLE SPREAD OF 2.44 M
 AIR AXLE DOWN - NOMINAL WHEEL LOAD OF 40 KN



COMPARISON OF LEAD AND TRAILING AXLE RESPONSE
 TRACTOR SUSPENSION - HENDRICKSON
 TRAILER SUSPENSION - CHALMERS, AXLE SPREAD OF 1.37 M
 AIR AXLE UP - NOMINAL WHEEL LOAD OF 50 KN



COMPARISON OF LEAD AND TRAILING AXLE RESPONSE
 TRACTOR SUSPENSION - HENDRICKSON
 TRAILER SUSPENSION - CHALMERS, AXLE SPREAD OF 1.37 M
 AIR AXLE DOWN - NOMINAL WHEEL LOAD OF 40 KN



APPENDIX F

HISTOGRAMS OF DIGITIZED WHEEL LOAD DATA

Each run represented in the appendix illustrates the dynamic wheel load distributions of the lead and trailing axles for both the tractor and trailer. The tables on pages F1 and F2 serve to correlate the probability distributions with points on the line graphs of Appendix E.

Reyco - Hendrickson

speed km/hr	roughness IPM - RCR		1.27 meters		1.83 meters		2.44 meters	
			lift up	lift down	lift up	lift down	lift up	lift down
40	73	8.17	F3	F12	F21		F27	
	254	4.55	F4	F13	F22		F28	
	424	1.15	F5	F14	F23		F29	
60	73	8.17	F6	F15				
	254	4.55	F7	F16				
	424	1.15	F8	F17				
80	59	8.45	F9	F18	F24		F30	F33
	165	6.33	F10	F19	F25		F31	F34
	217	5.29	F11	F20	F26		F32	F35

Table F1 Pagation for Reyco distributions

Neway - Hendrickson

speed km/hr	roughness IPM - RCR		1.27 meters		1.83 meters		2.44 meters	
			lift up	lift down	lift up	lift down	lift up	lift down
40	73	8.17	F36	F45	F53	F62	F71	F80
	254	4.55	F37	F46	F54	F63	F72	F81
	424	1.15	F38	F47	F55	F64	F73	
60	73	8.17	F39	F48	F56	F65	F74	F82
	254	4.55	F40	F49	F57	F66	F75	F83
	424	1.15	F41		F58	F67	F76	
80	59	8.45	F42	F50	F59	F68	F77	F84
	165	6.33	F43	F51	F60	F69	F78	F85
	217	5.29	F44	F52	F61	F70	F79	F86

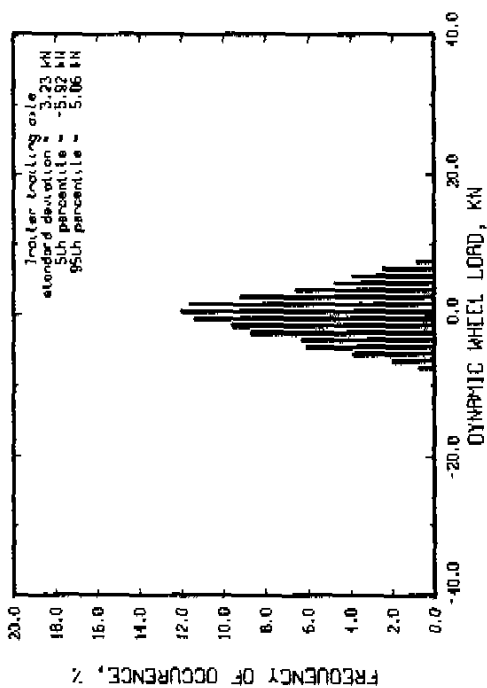
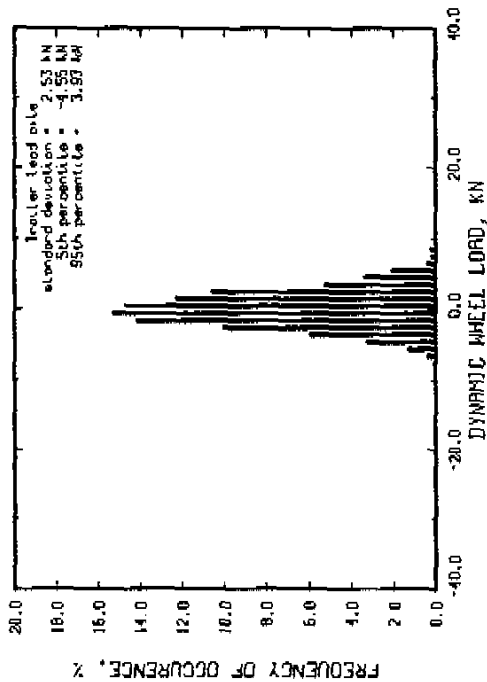
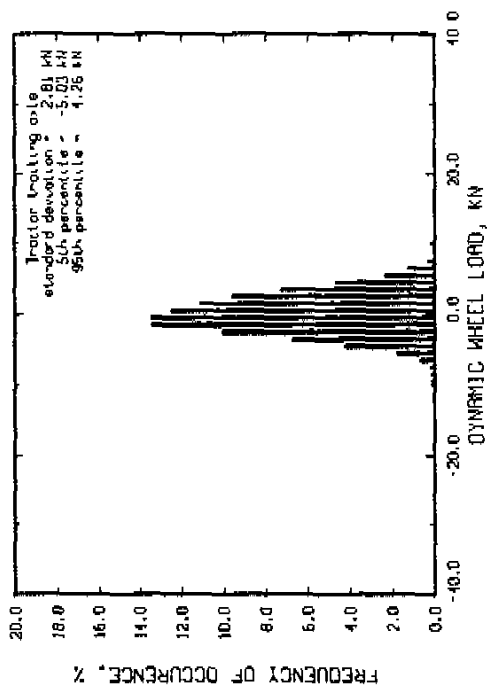
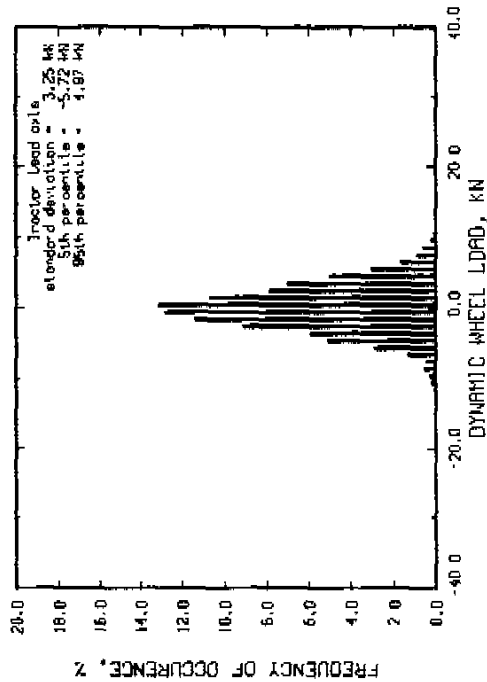
Table F2 Pagation for Neway distributions

Chalmers - Hendrickson

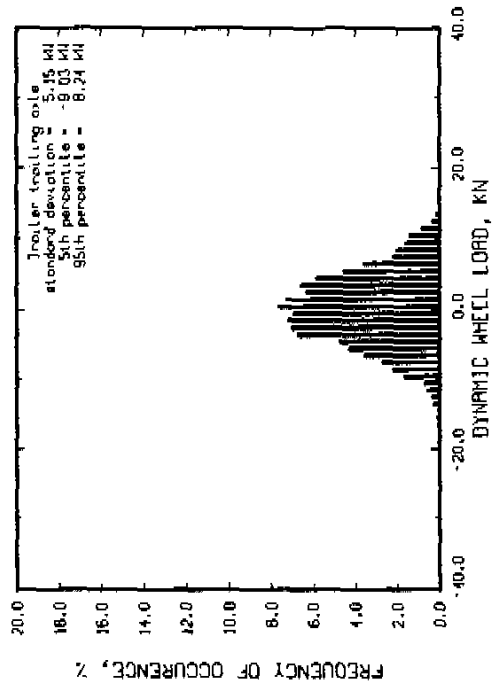
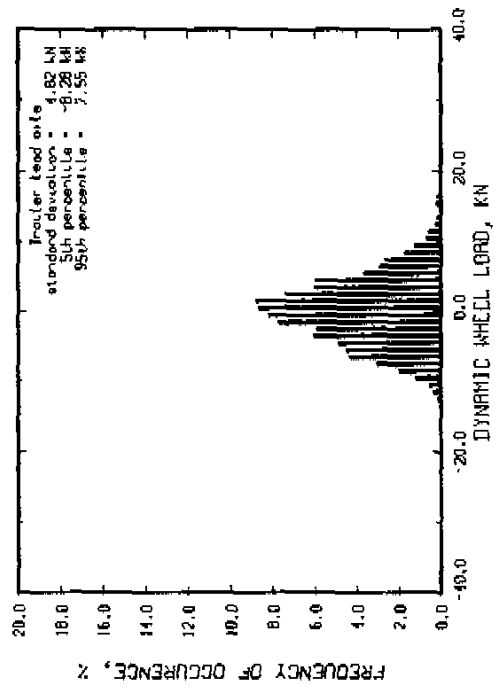
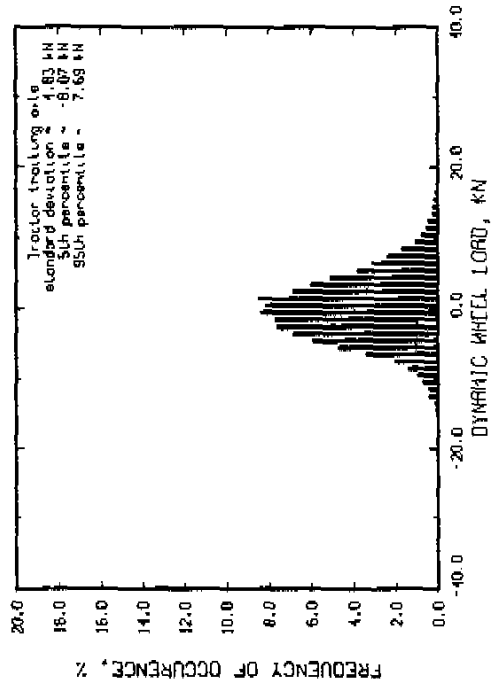
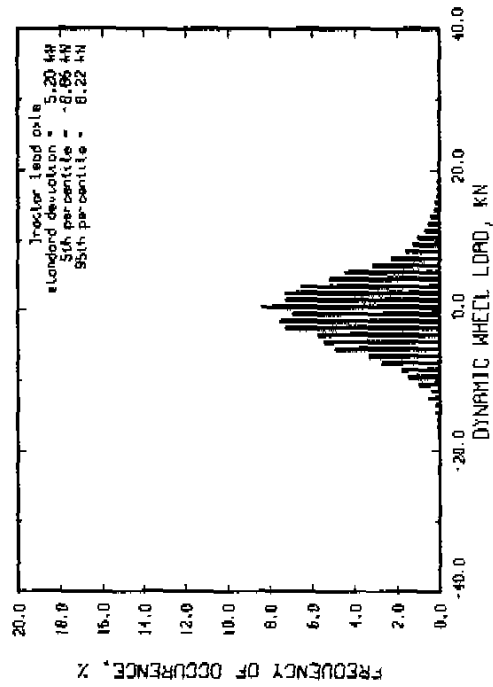
		1.37 meters		
speed km/hr	roughness IPM - RCR		lift up	lift down
40	73	8.17	F87	F94
	254	4.55	F88	F95
60	73	8.17	F89	F96
	254	4.55	F90	F97
80	59	8.45	F91	F98
	165	6.33	F92	F99
	217	5.29	F93	F100

Table F3 Pagination for Chalmers distributions

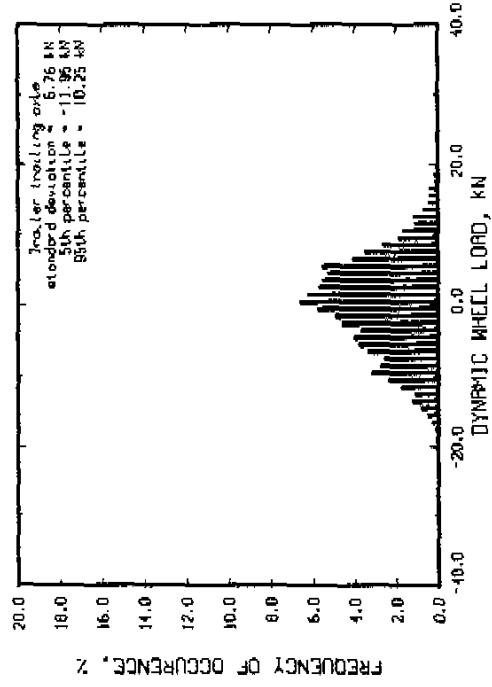
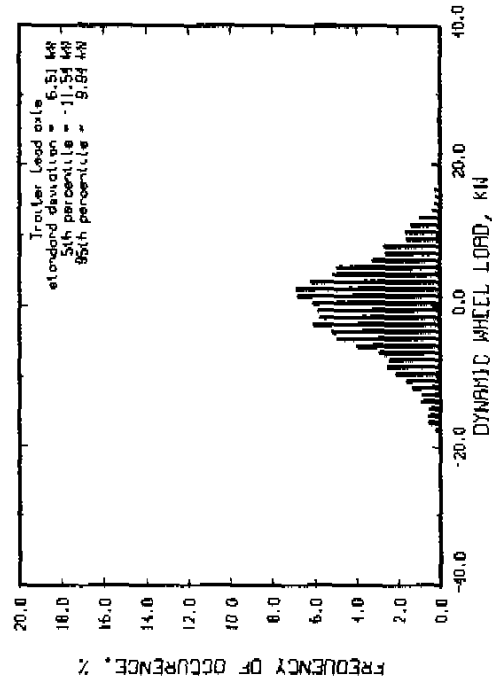
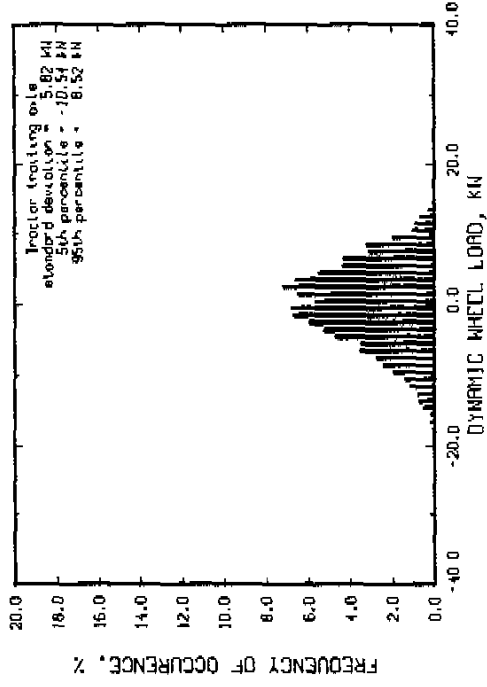
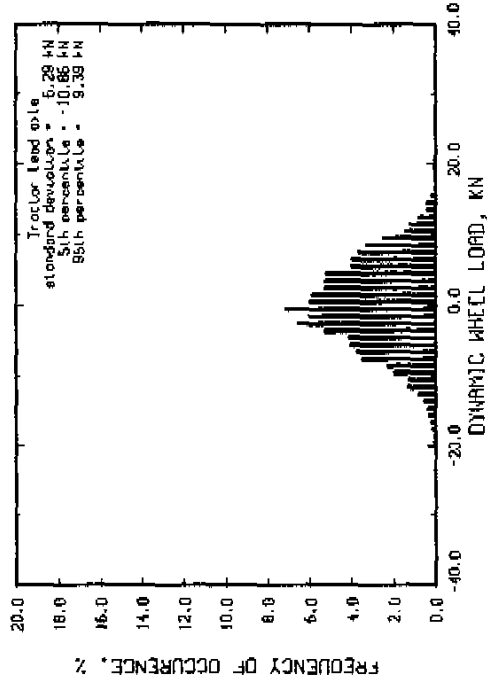
Run # 110 Speed = 40 km/hr
 Moys roughness = 73 IPM Trolley axle spread = 1.27 m
 Trolley suspension : spring suspended walking beam
 Trolley suspension : four spring
 Air suspension lift axle up



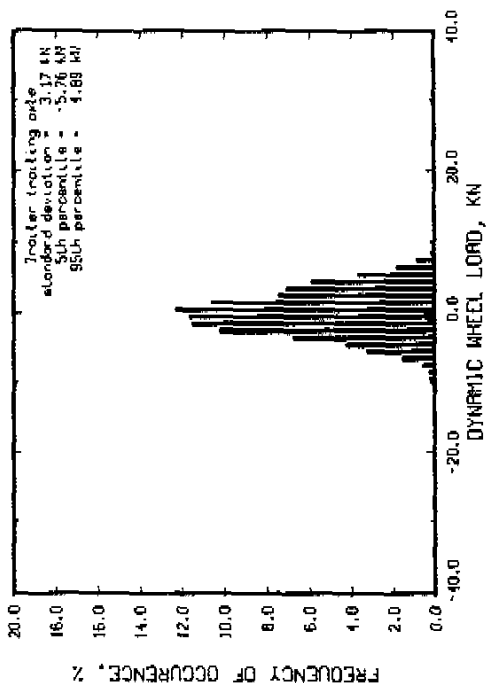
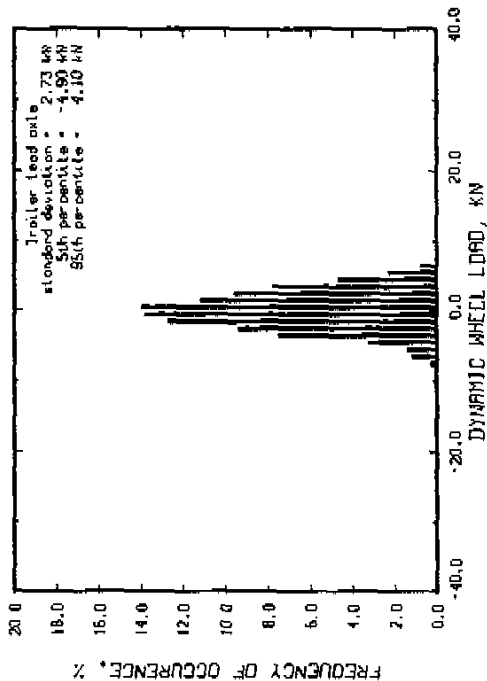
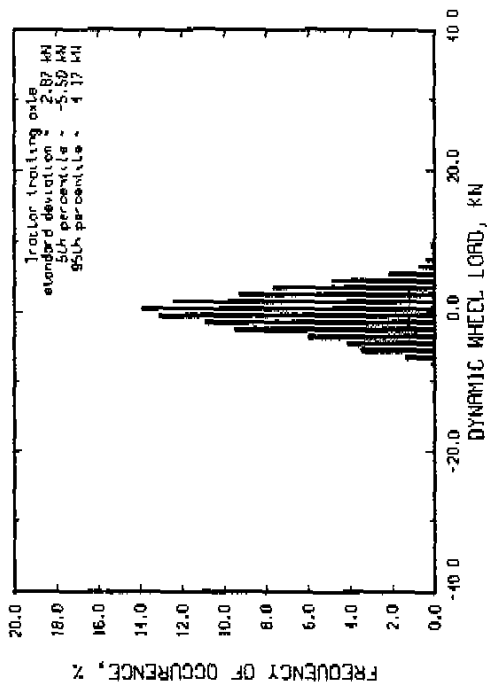
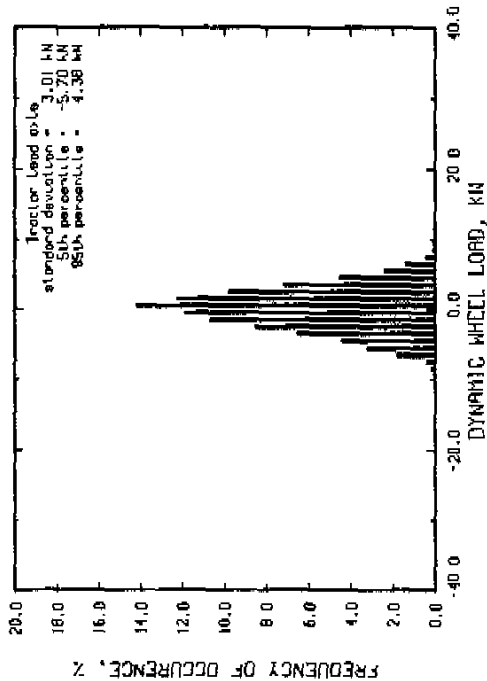
Run # 121 Part I Speed = 40 km/hr
 Moys roughness = 254 jPM Trailer axle spread = 1.27 m
 Tractor suspension : spring suspended walking beam
 Trailer suspension : four spring
 Rtr suspension lift axle up



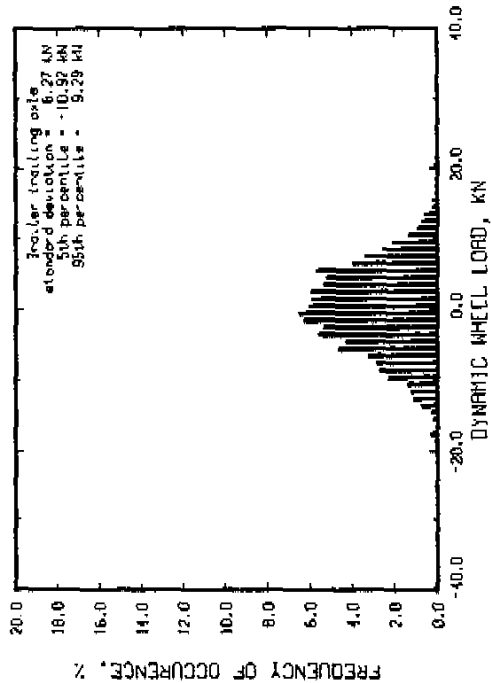
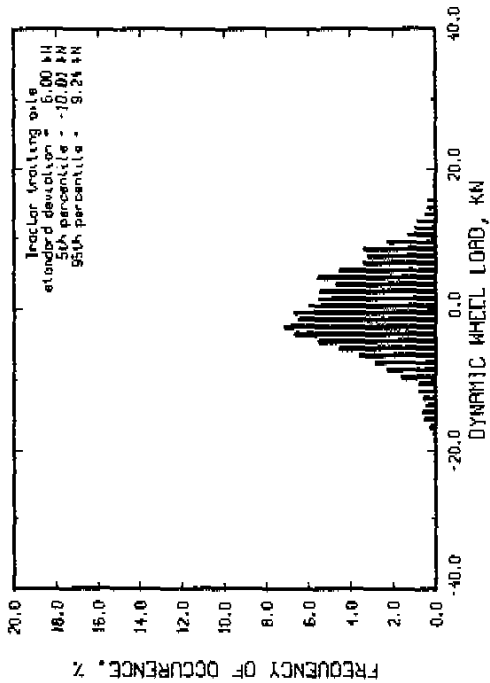
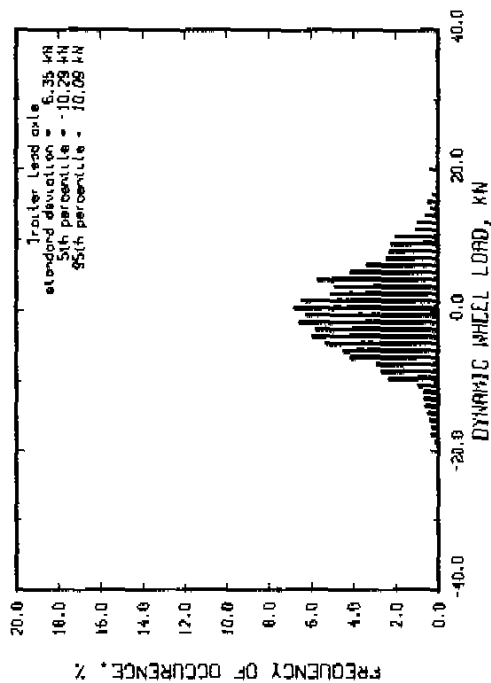
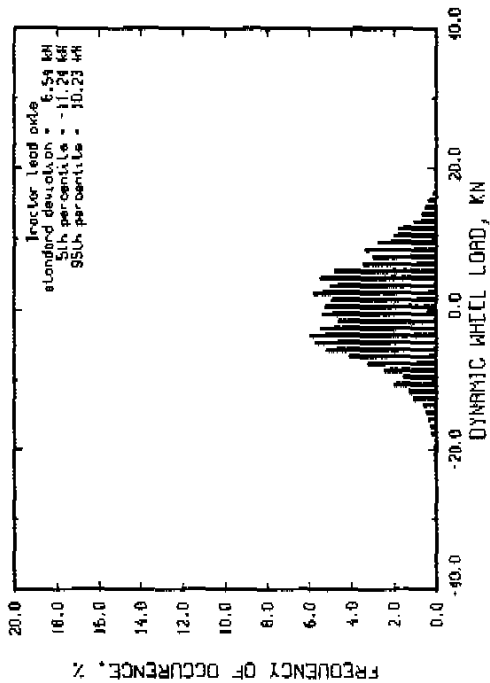
Run # 121 Part 2
 Moys roughness = 424 JPH
 Speed = 40 km/hr
 Tractor axle spread = 1.27 m
 Tractor suspension : sprung suspended walking beam
 Tractor suspension : four spring
 R/R suspension lift axle up



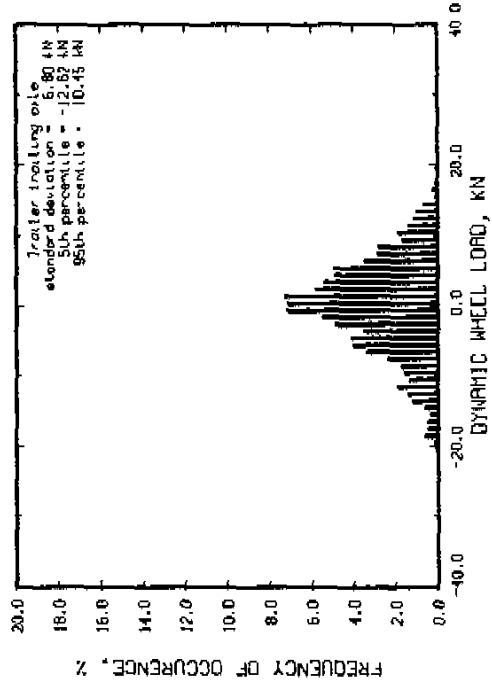
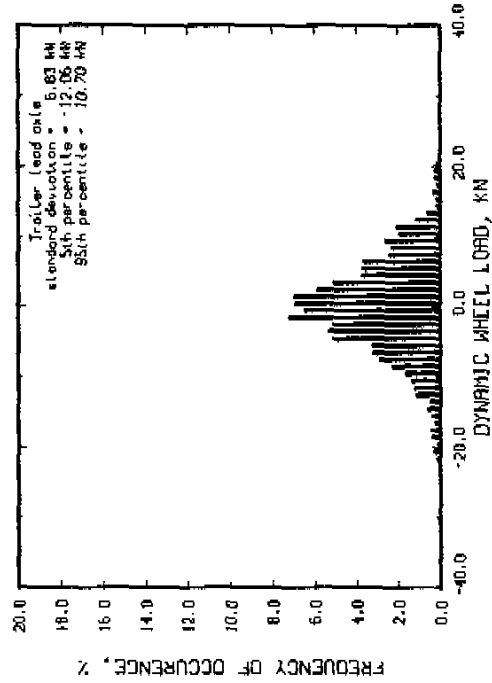
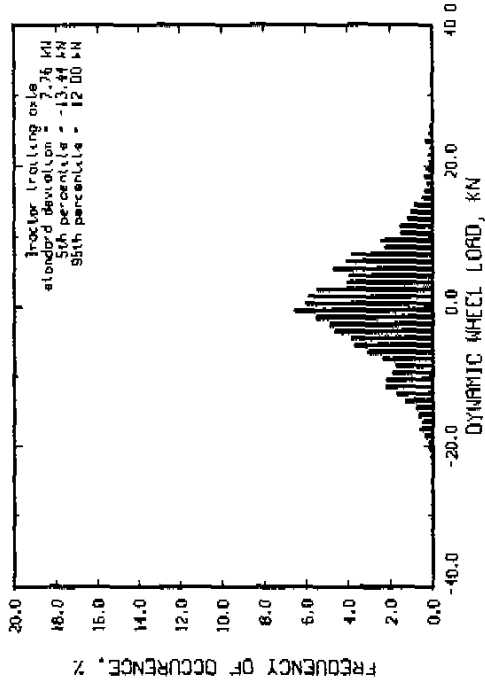
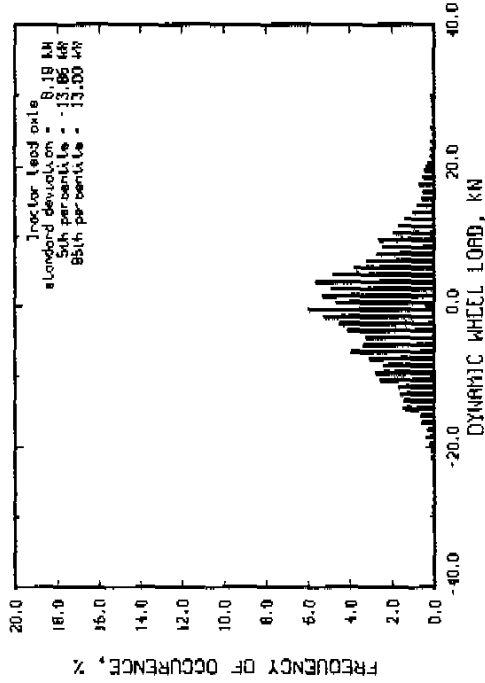
Run # 109 Speed = 60 km/hr
 Mays roughness = 73 IPM Iroller axle spread = 1.27 m
 Tractor suspension : spring suspended working beam
 Iroller suspension : four spring
 R/R suspension left axle up



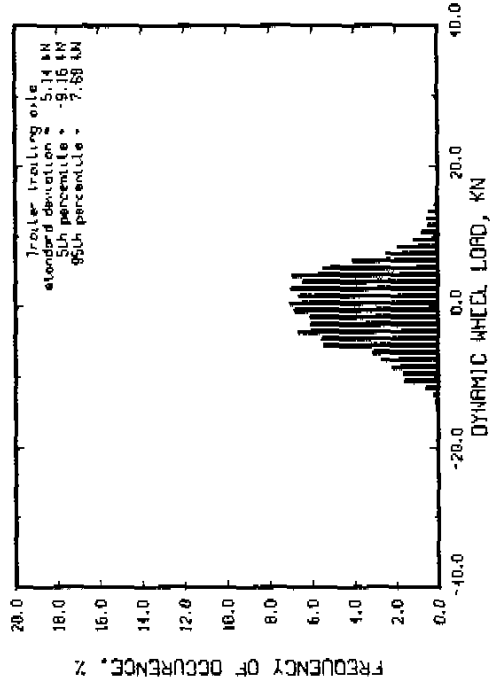
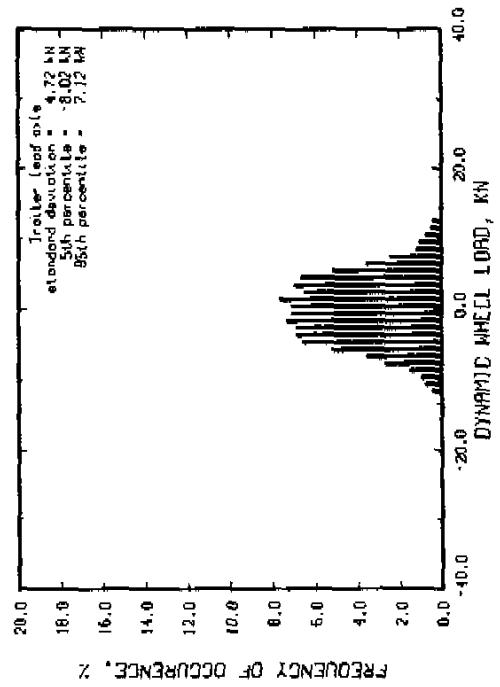
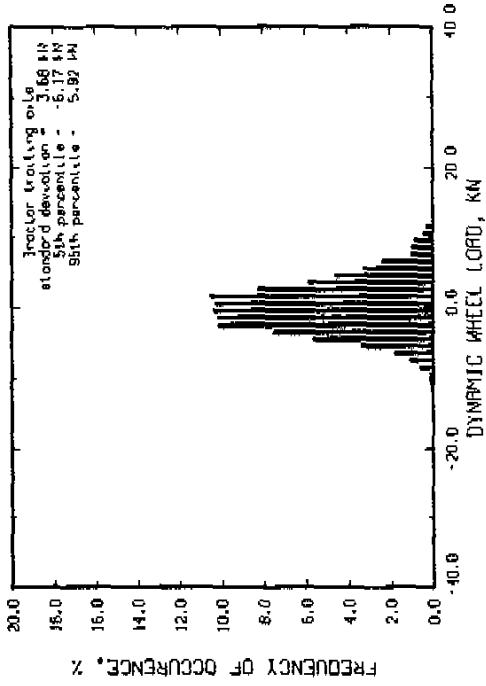
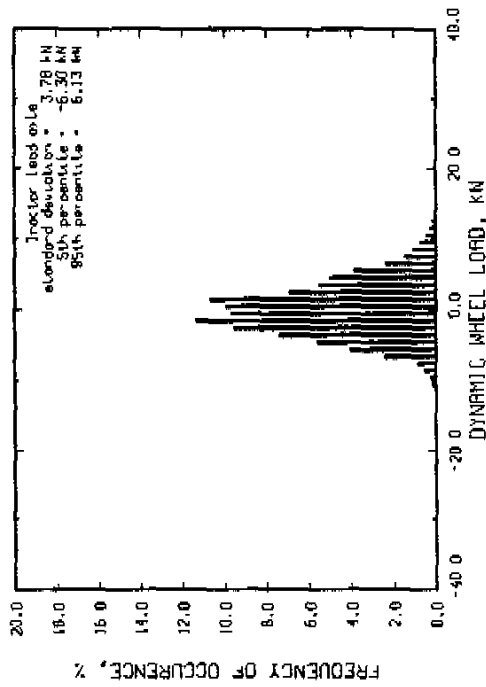
Run # 122 Part 1 Speed = 60 km/hr
 Hays roughness = 254 ipm Tractor axle spread = 1.27 m
 Tractor suspension : spring suspended walking bear
 Tractor suspension : four spring
 R/R suspension lift axle up



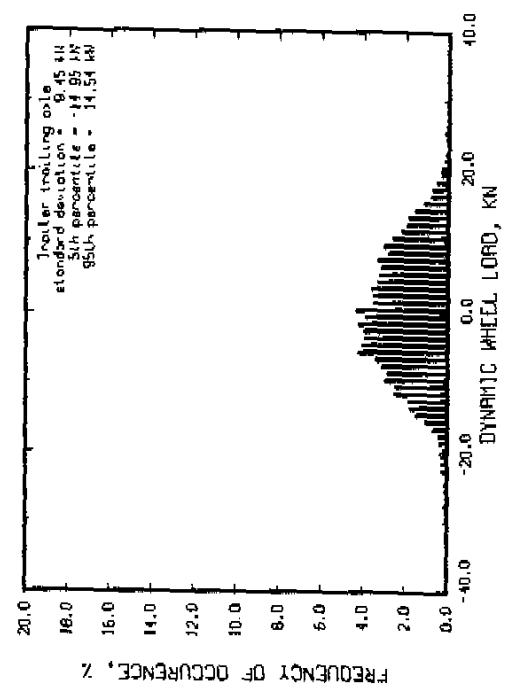
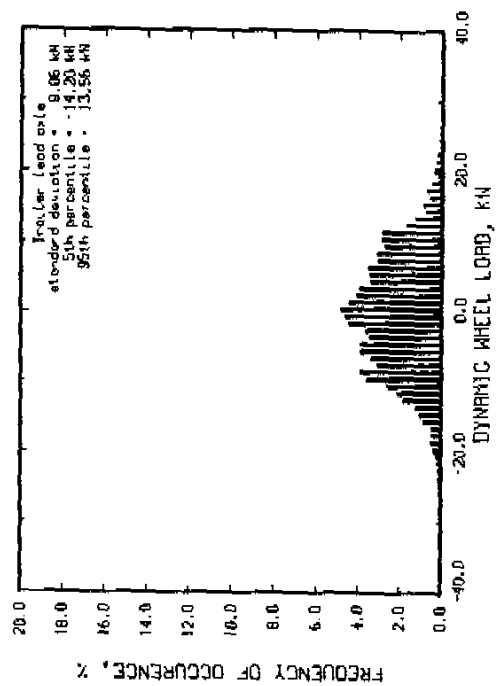
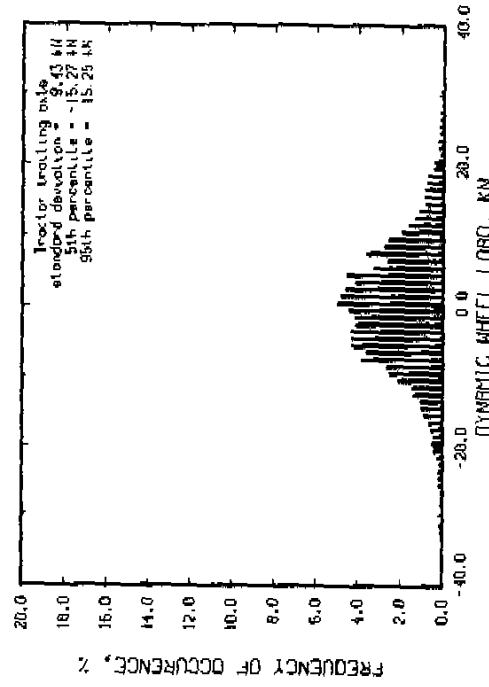
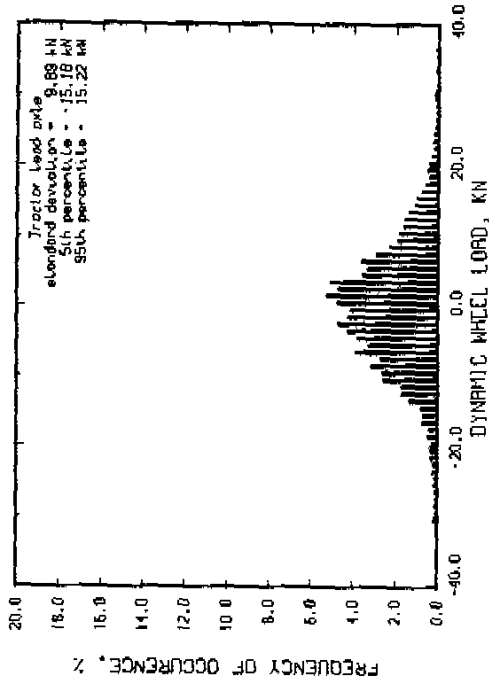
Run # 122 Part 2
 Speed = 60 km/hr
 Moys roughness = 424 IPH
 Trailer axle spread = 1.27 m
 Tractor suspension : sprung suspended walking beam
 Trailer suspension : four sprung
 R/R suspension lift axle up



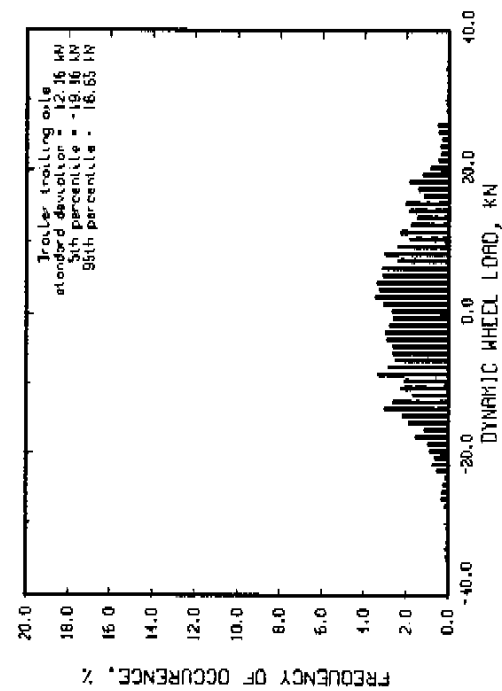
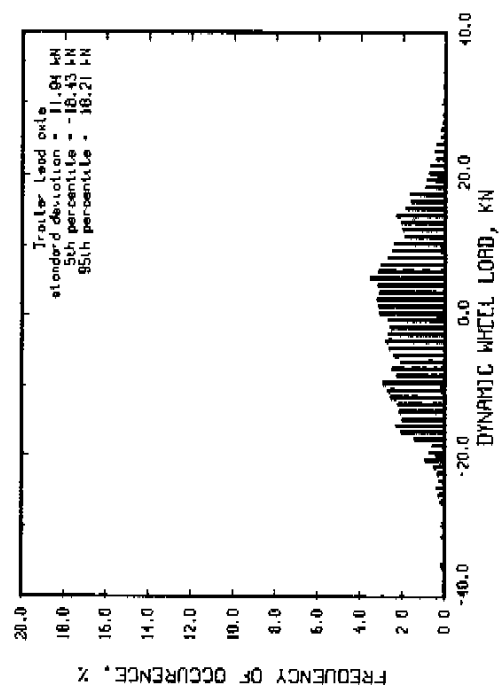
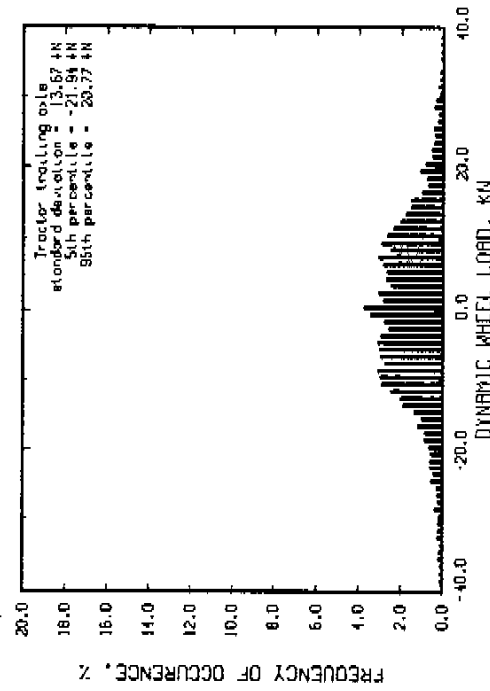
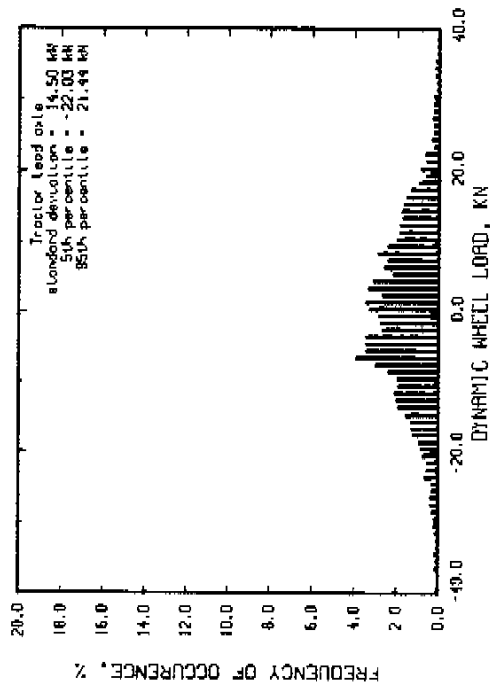
Run # 119 Part 2 Speed = 80 km/hr
 Moys roughness = 59 JPH Tractor axle spread = 1.27 m
 Tractor suspension : spring suspended walking beam
 Tractor suspension : four sprung
 Rtr suspension lift axle up



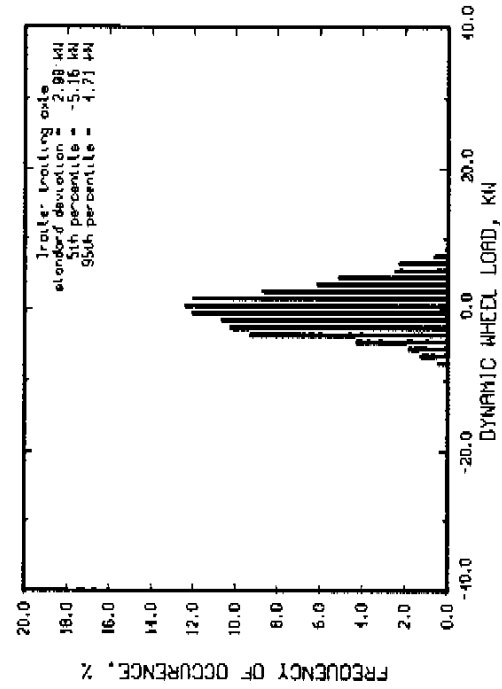
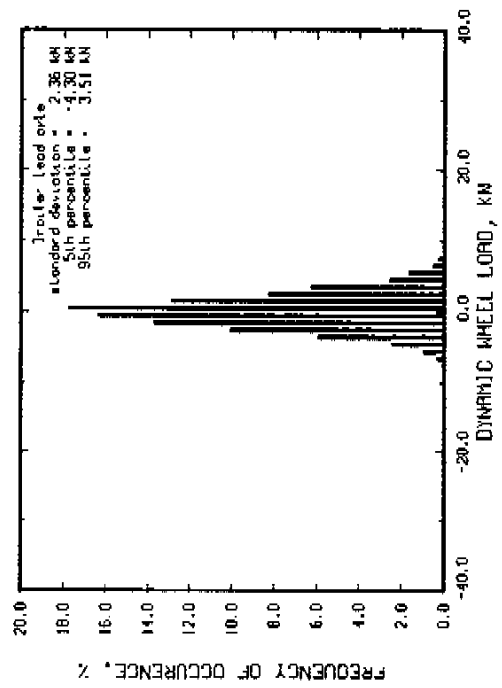
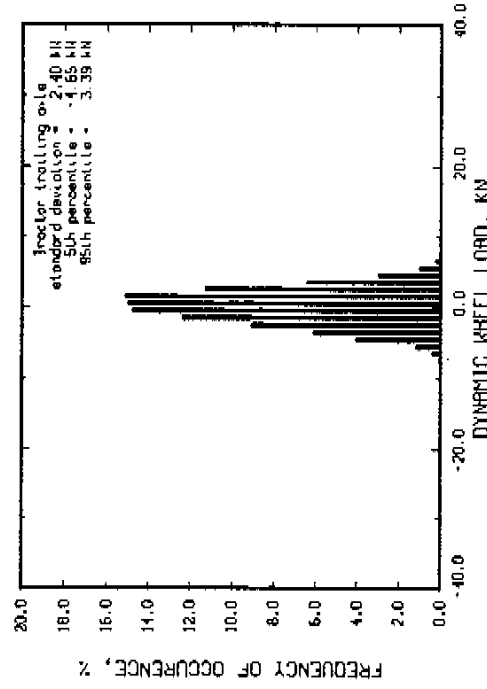
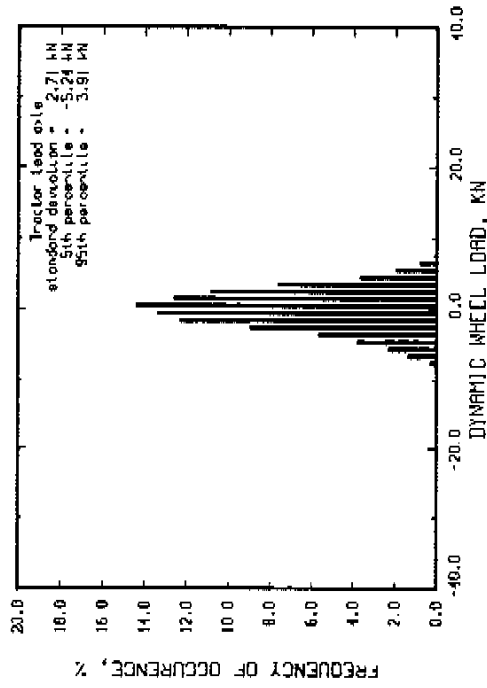
Run # 119 PART 1
 Moys roughness = 155 IPM
 Speed = 80 km/hr
 Troller axle spread = 1.27 m
 Troller suspension : spring suspended walking beam
 Tractor suspension : four spring
 Air suspension lift axle up



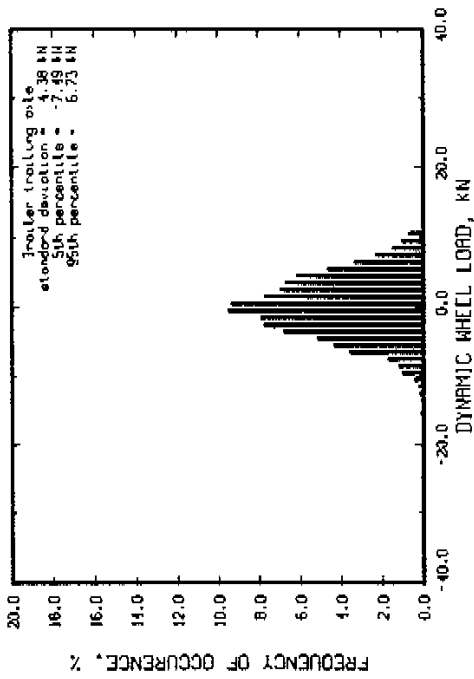
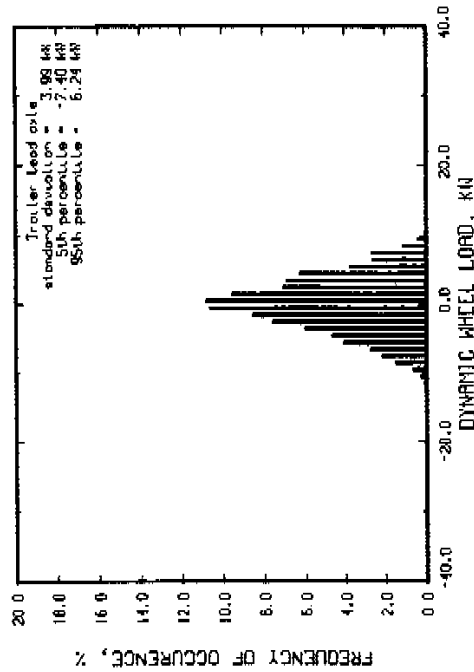
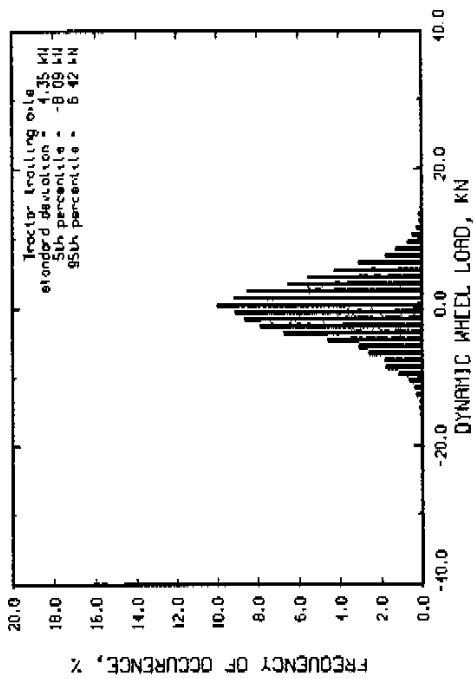
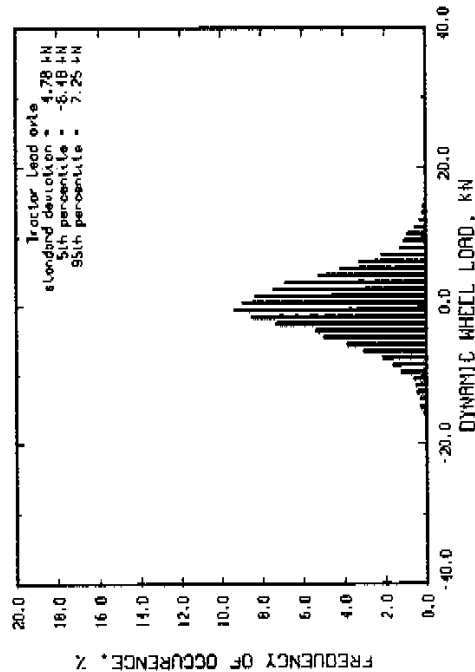
Run # 119 PART 3 Speed = 60 km/hr
 Ways roughness = 217 IPM Trolley axle spread = 1.27 m
 Tractor suspension : spring suspended walking beam
 Trolley suspension : four spring
 Rlr suspension Lfl axle up



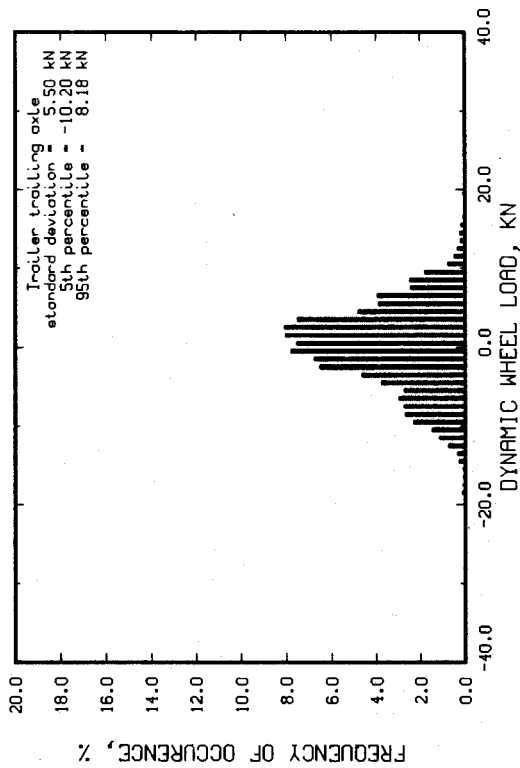
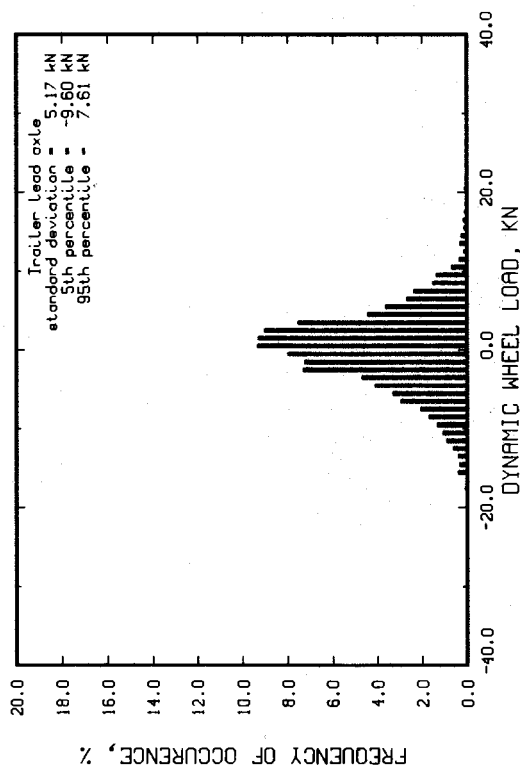
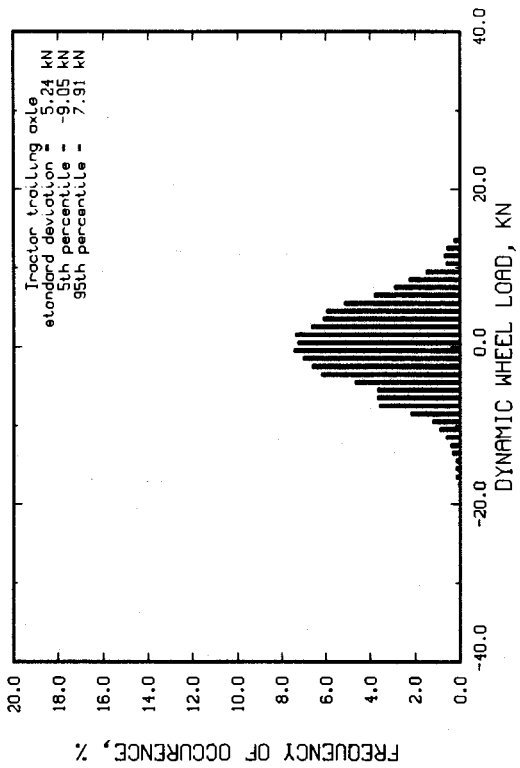
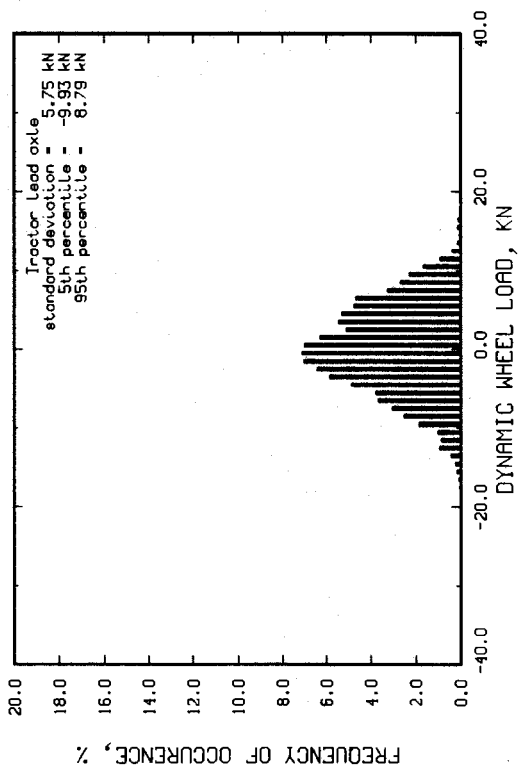
Run # 113 Speed = 40 km/hr
 Mays roughness = 73 JPH Tractor axle spread = 1.27 m
 Tractor suspension : sprung suspended walking beam
 Tractor suspension : four spring
 Axr suspension lift axle down



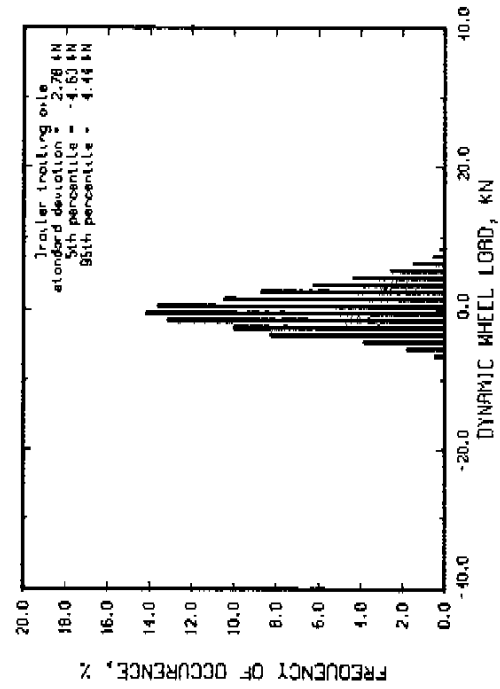
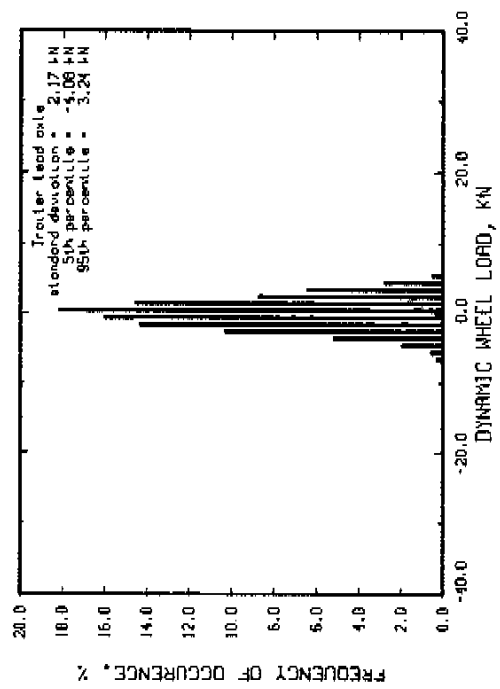
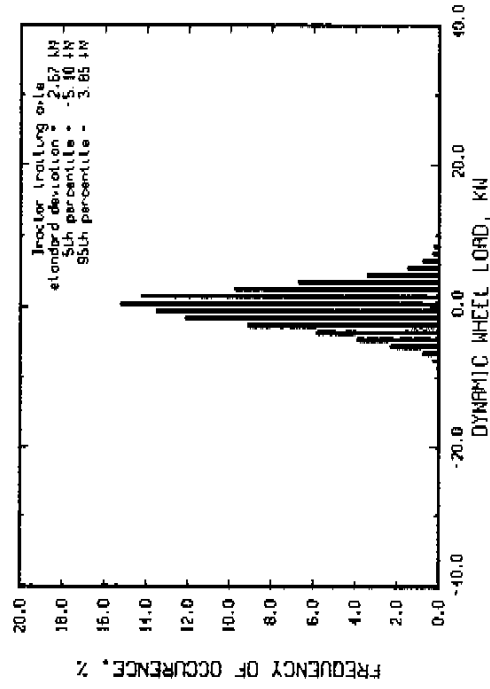
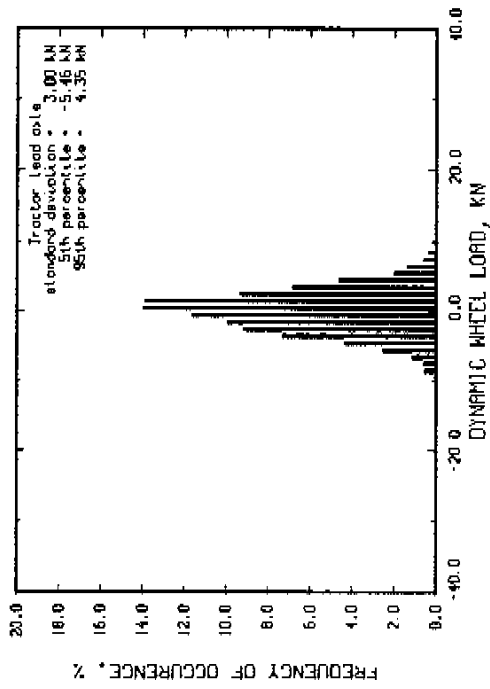
Run # 123 Part 1
 Speed = 40 km/hr
 Moys roughness = 254 IPI
 Tractor suspension : sprung suspended walking beam
 Trailer suspension : four spring
 R/R suspension lift axle down



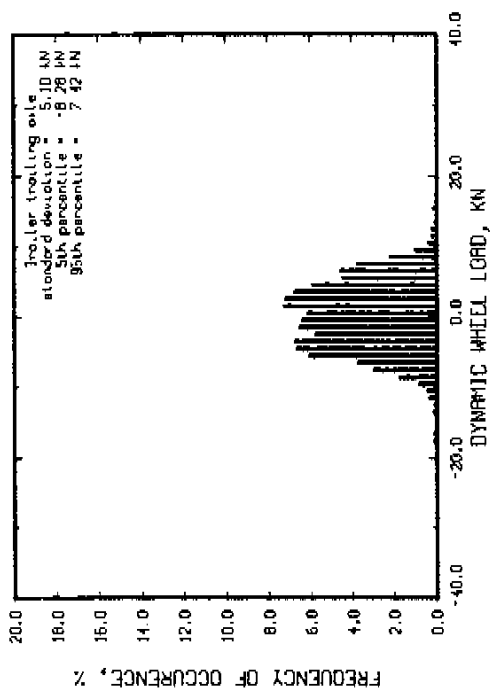
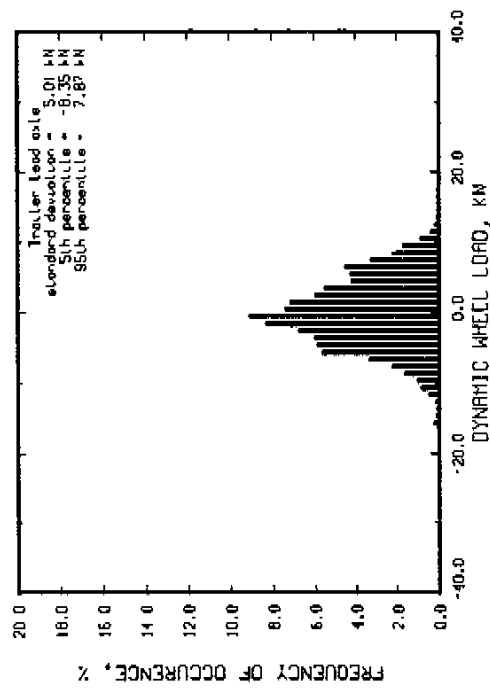
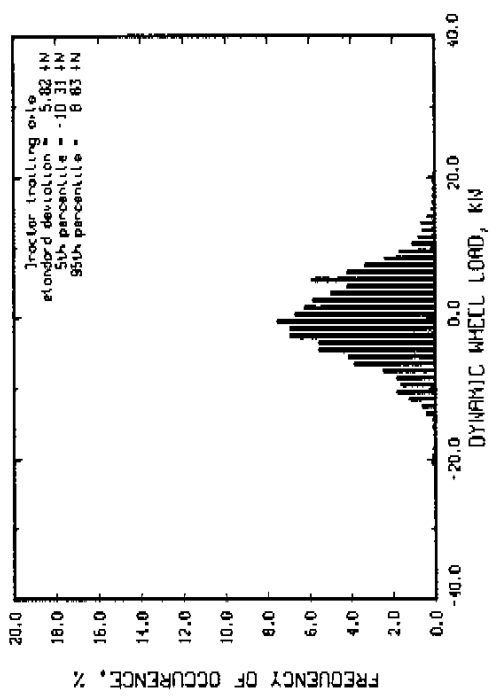
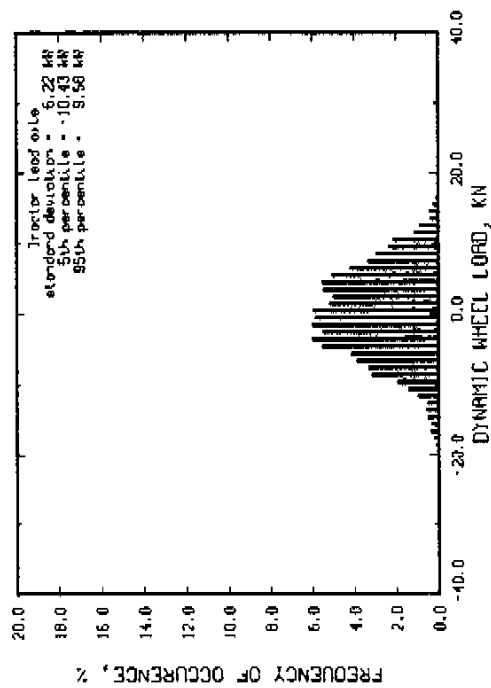
Run # 123 Part 2 Speed = 40 km/hr
 Mays roughness = 424 IPM Trailer axle spread = 1.27 m
 Tractor suspension : spring suspended walking beam
 Trailer suspension : four spring
 Air suspension lift axle down



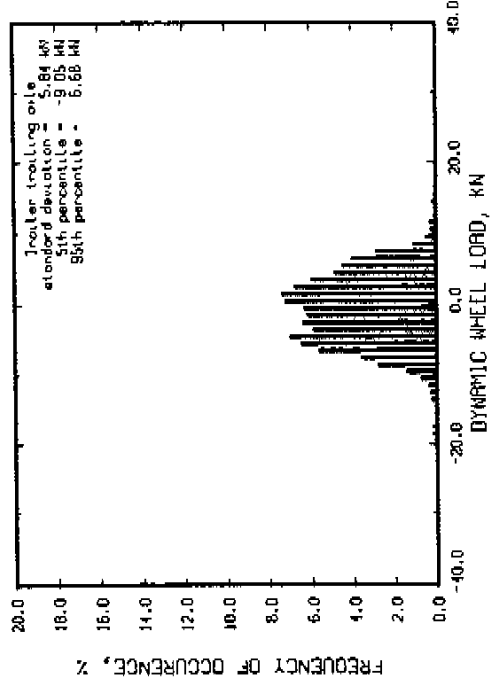
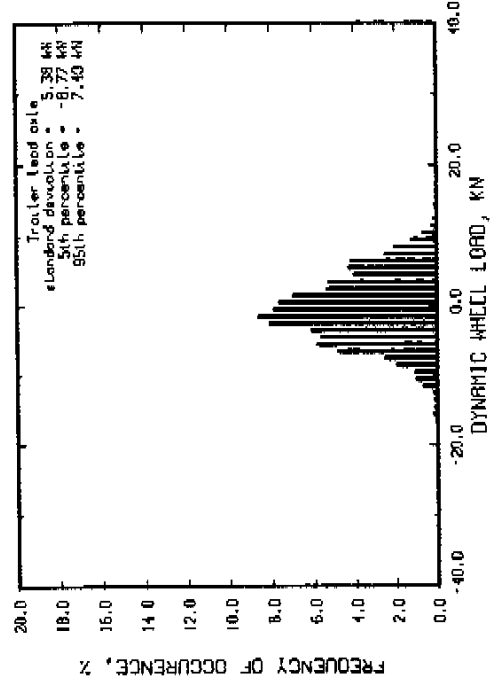
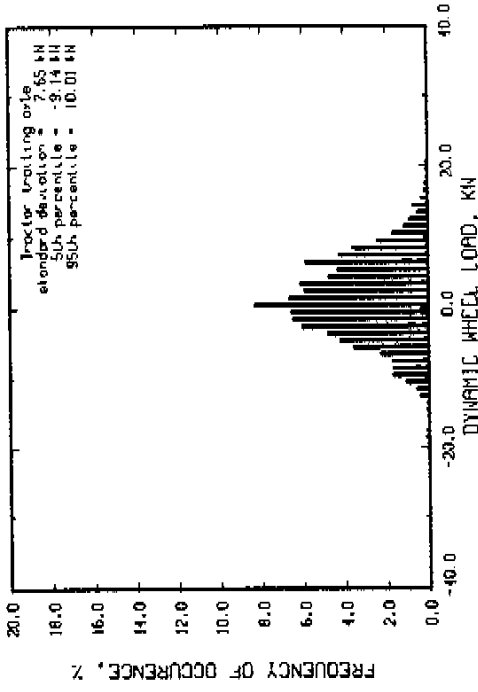
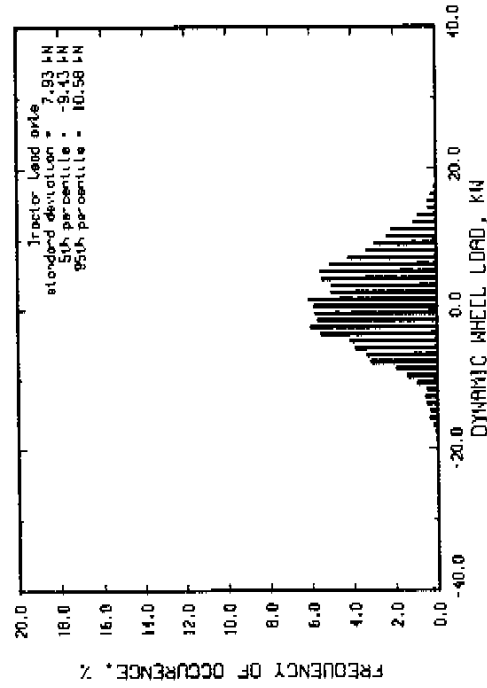
Run # 112 Speed = 60 km/hr
 Moys roughness = 73 JPH Tractor axle spread = 1.27 m
 Tractor suspension : spring suspended walking beam
 Tractor suspension : four spring
 Tractor suspension lift axle down



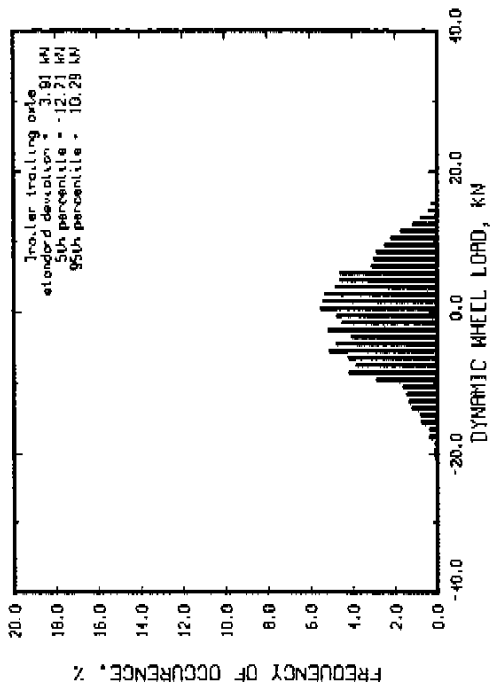
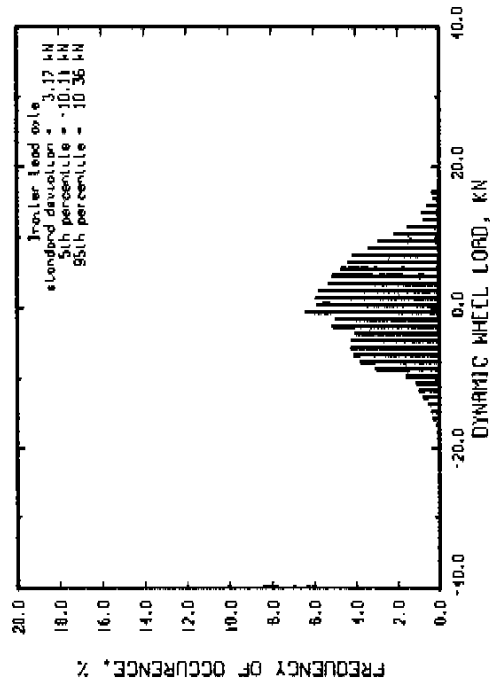
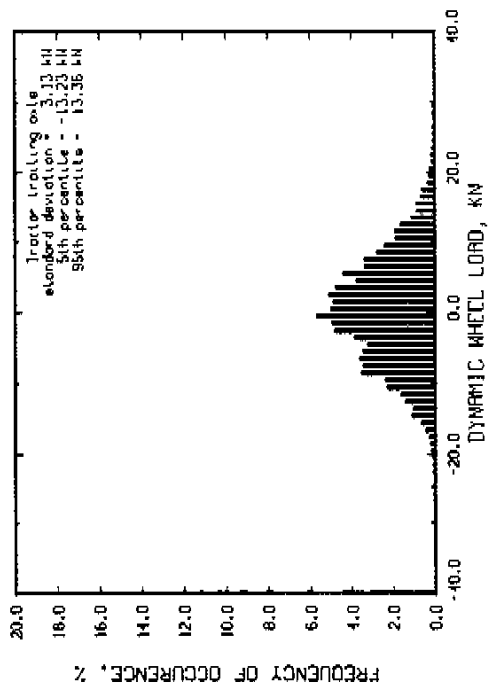
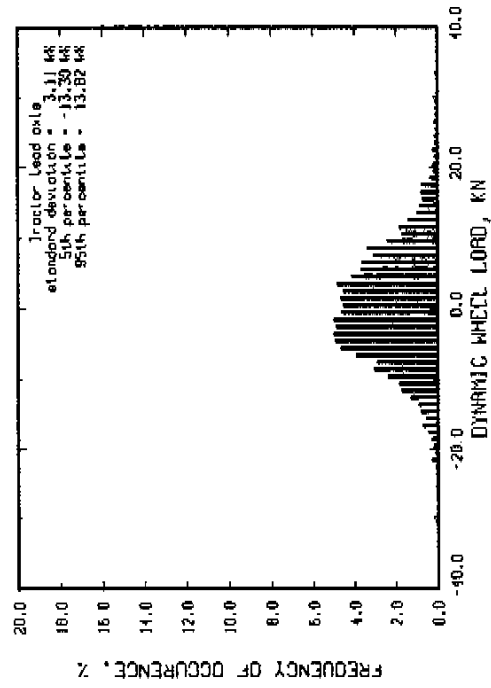
Run = 124 Part 1
 Major roughness = 254 IPH
 Tractor axle spread = 1.27 m
 Tractor suspension : sprung suspended walking beam
 Tractor suspension : four spring
 Tractor suspension lift axle down



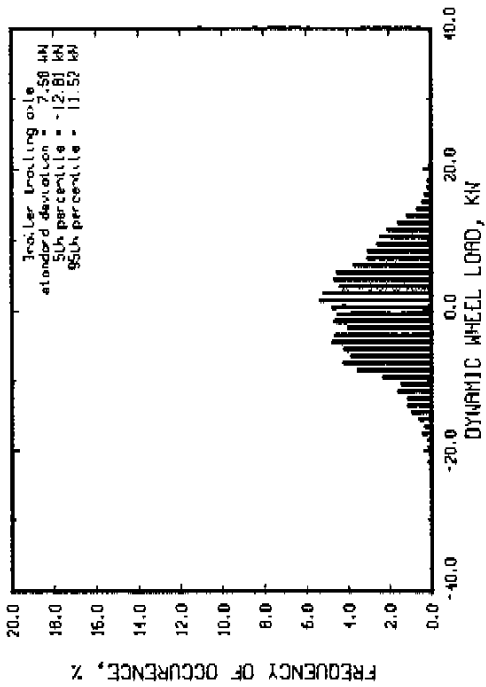
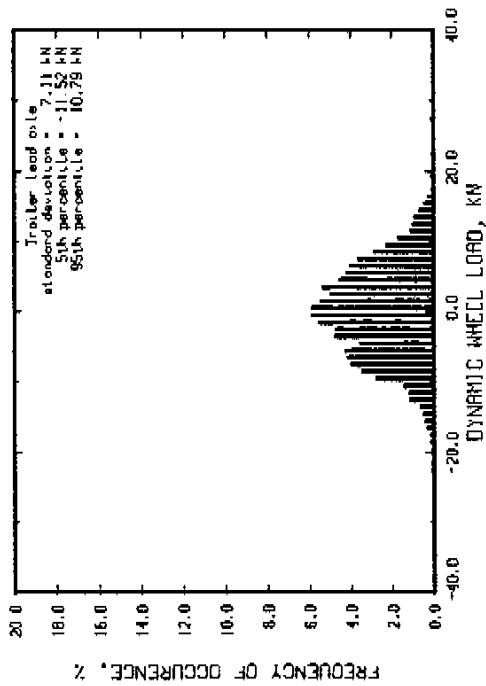
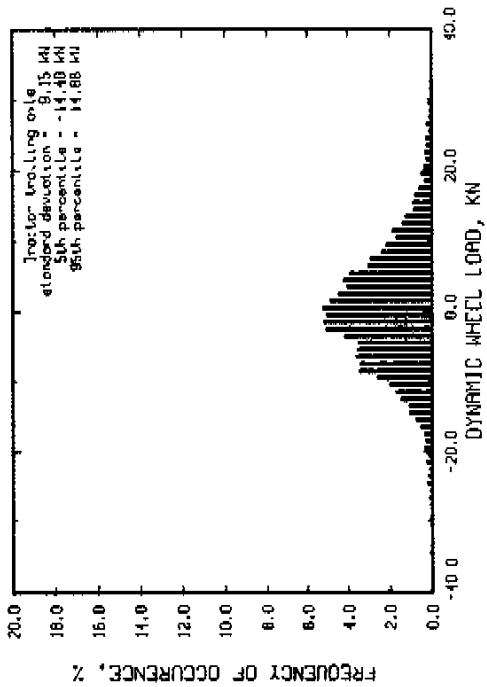
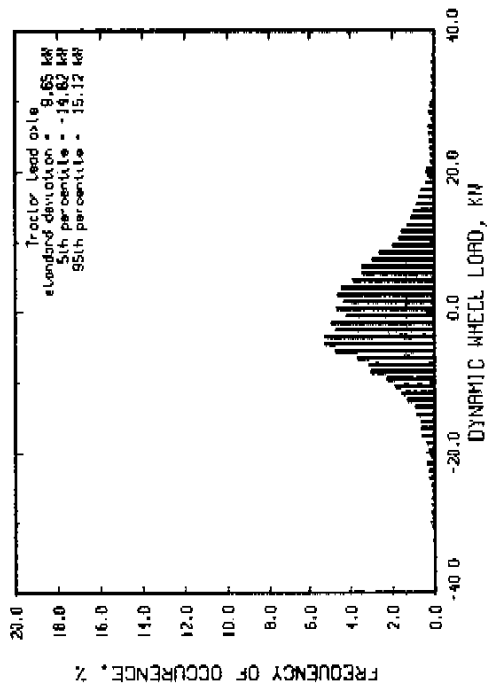
Run # 124 Part 2 Speed = 60 km/hr
 Moys roughness = 424 IPM Trailer axle spread = 1.27 m
 Tractor suspension : spring suspended walking beam
 Trailer suspension : four spring
 R/R suspension lift axle down



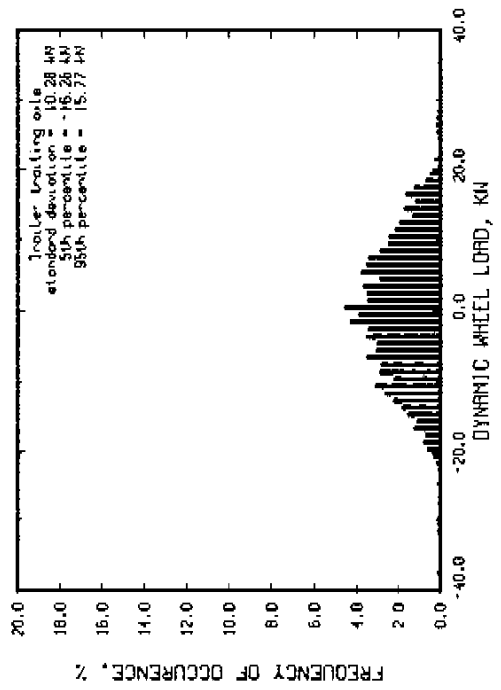
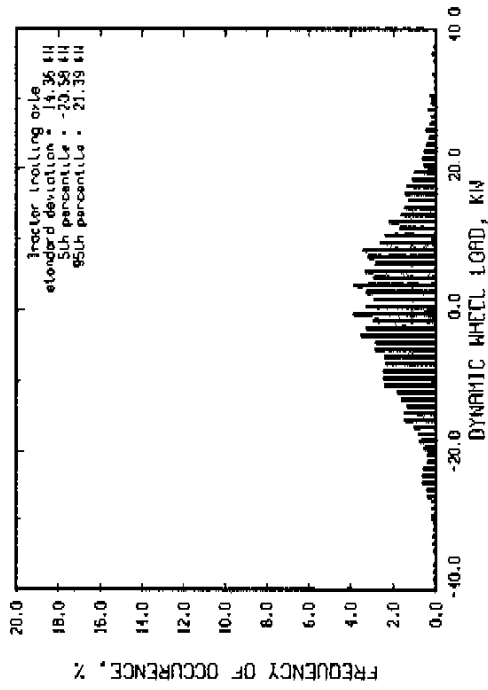
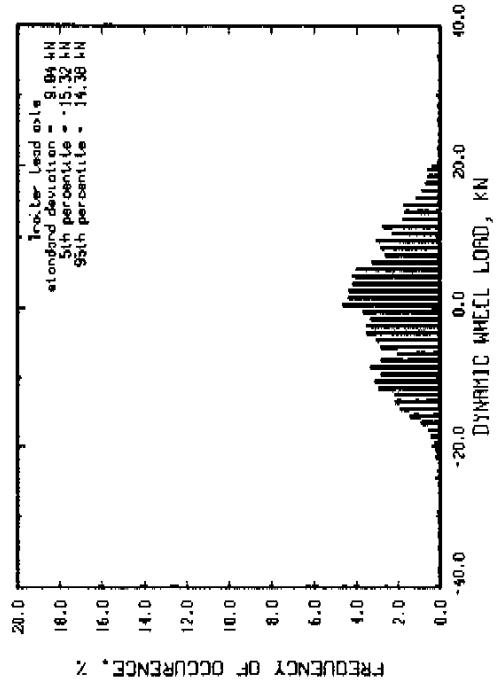
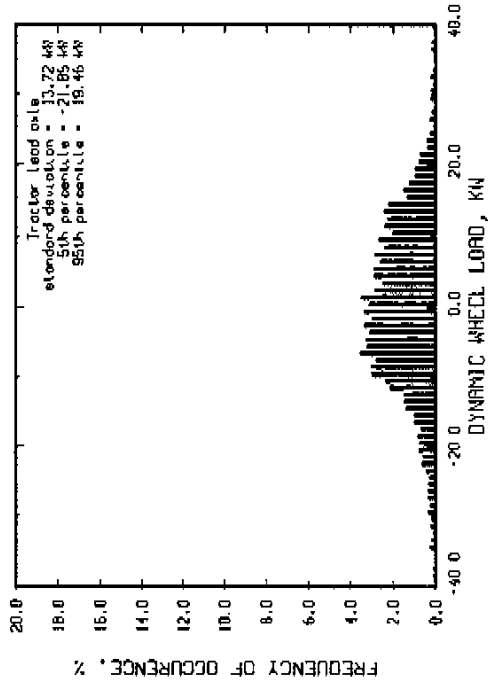
Run # 117 Part 2 Speed = 80 km/hr
 Mays roughness = 59 jPM Iroller axle spread = 1.27 m
 Itractor suspension i spring suspended walking beam
 Iroller suspension i four spring
 Itr suspension lift axle down



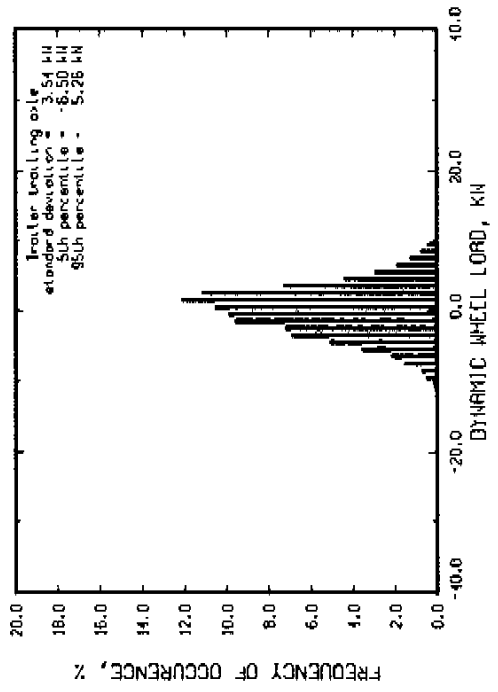
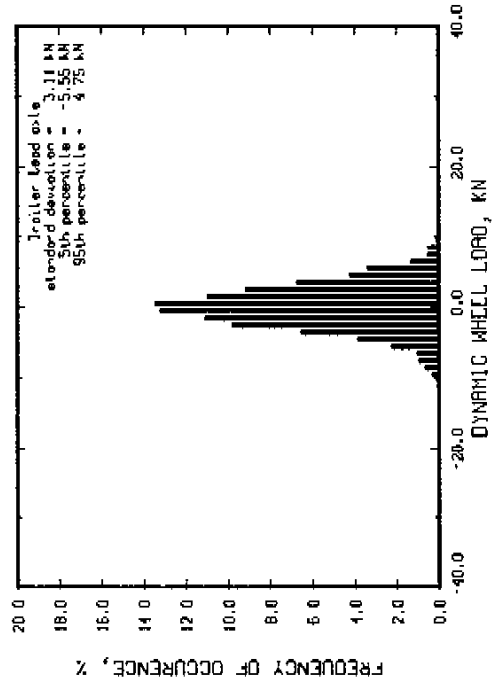
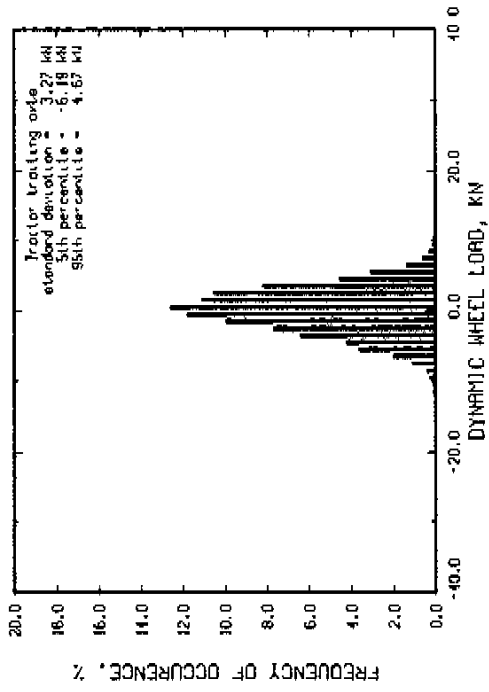
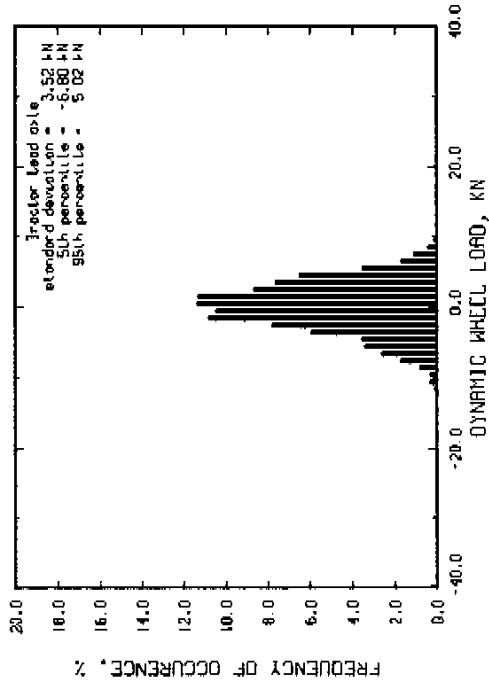
Run # 117 Part 1
 Speed = 80 km/hr
 Moje roughness = 165 IPM
 Tractor axle spread = 1.27 m
 Tractor suspension : sprung suspended walking beam
 Tractor suspension : four spring
 Air suspension lift axle down



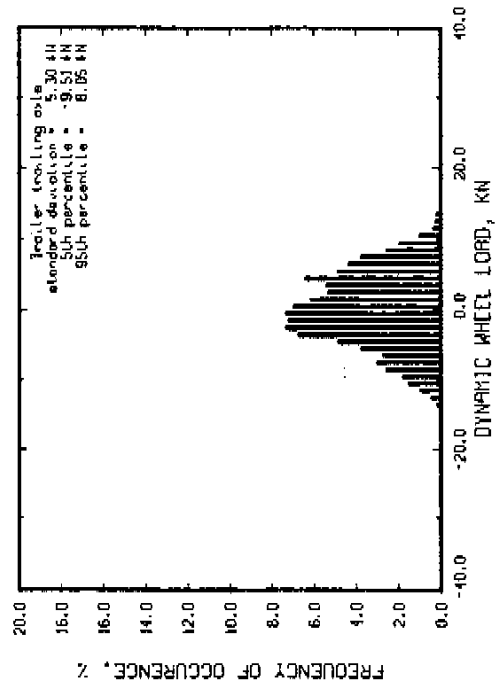
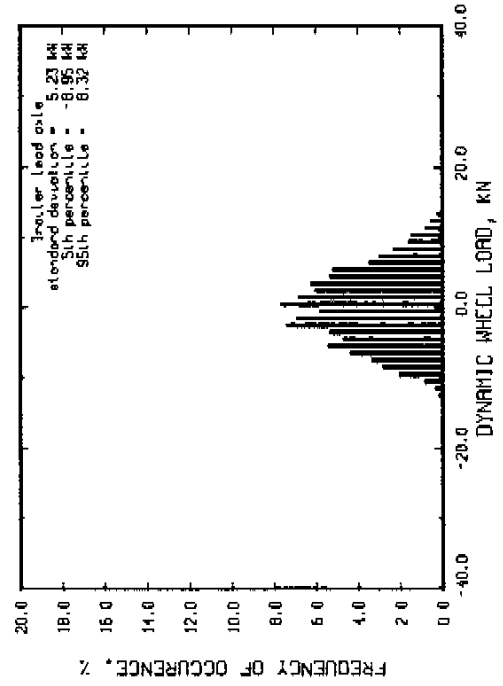
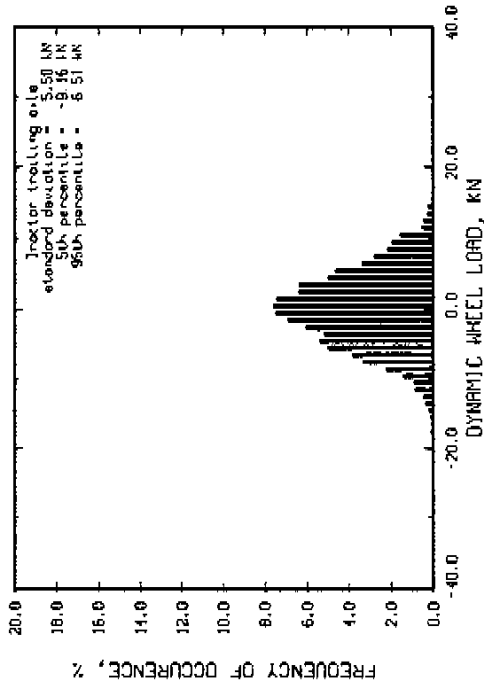
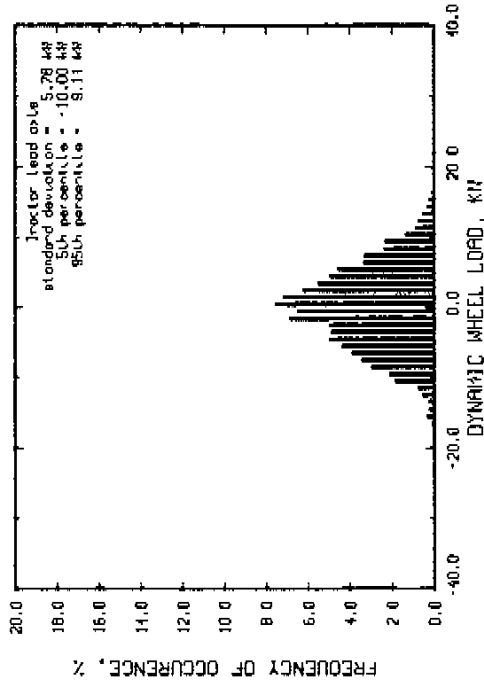
Run # 117 Part 3 Speed = 80 km/hr
 Hays roughness = 217 IPH Trailer axle spread = 1.27 m
 Tractor suspension : spring suspended walking beam
 Trailer suspension : four spring
 flr suspension lift axle down



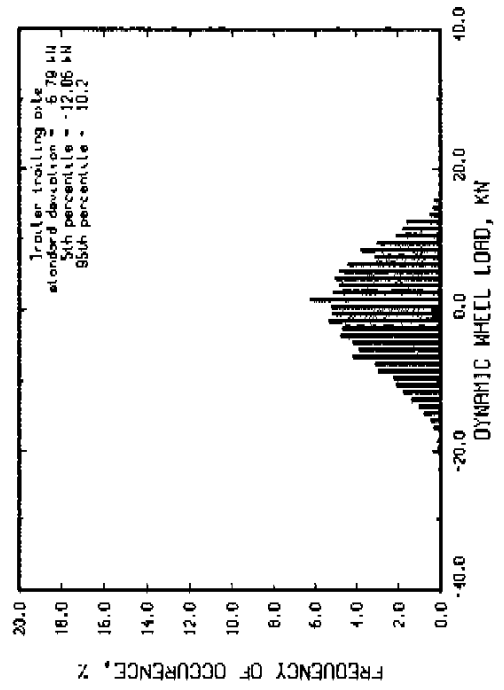
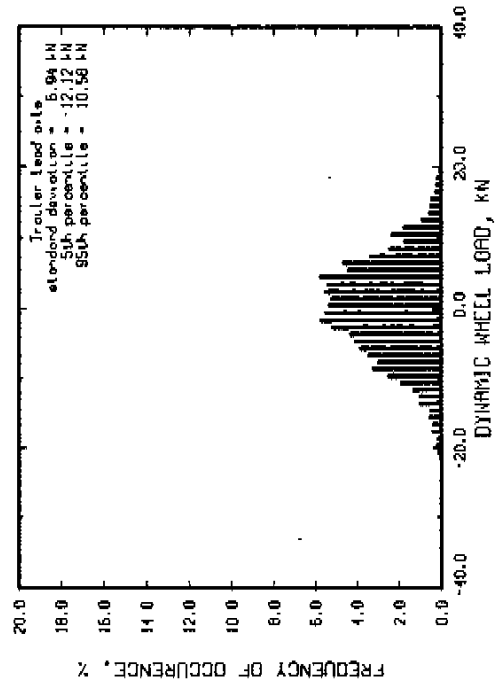
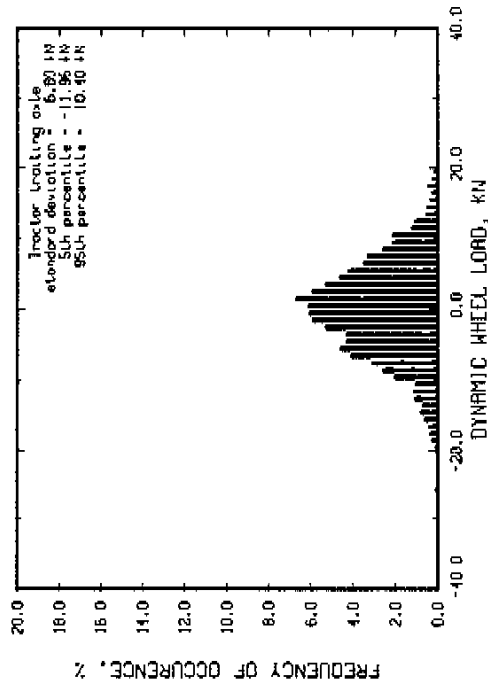
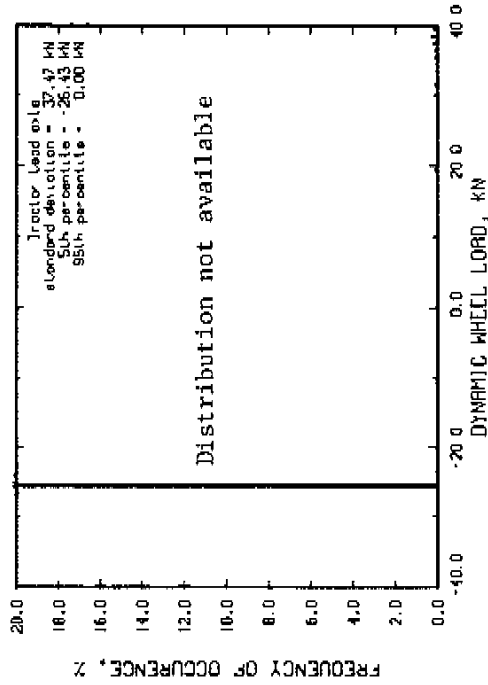
Run # 47 Speed = 40 km/hr
 Moys roughness = 73 IPM Trailer axle spread = 1.83 m
 Tractor suspension : spring suspended walking boom
 Trailer suspension : four spring
 Air suspension lift axle up



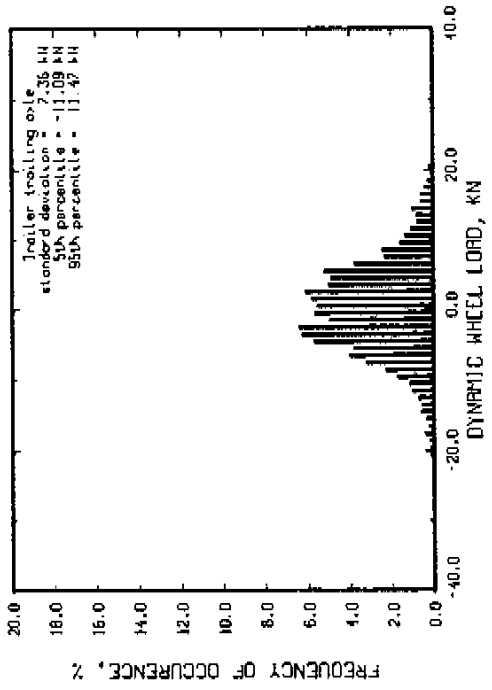
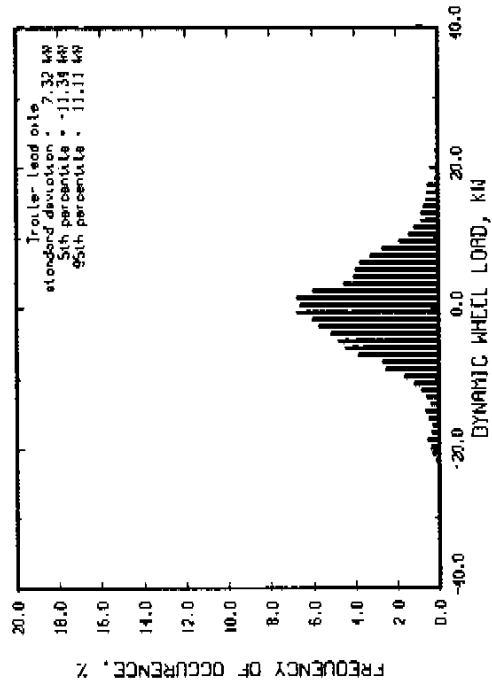
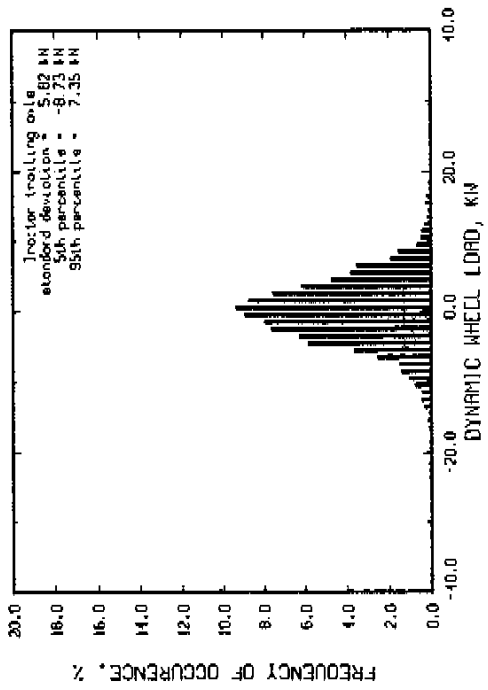
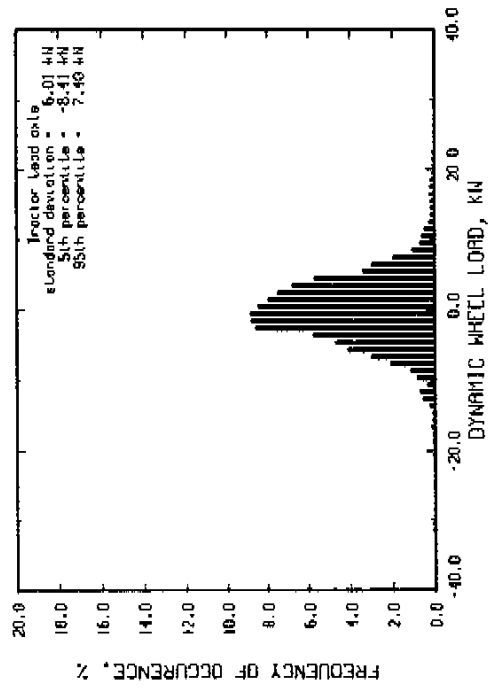
Run # 44 Part J Speed = 40 km/hr
 Moys roughness = 254 JPH Trailer axle spread = 1.83 m
 Trailer suspension : spring suspended walking beam
 Trailer suspension : four spring
 RLR suspension lift axle up



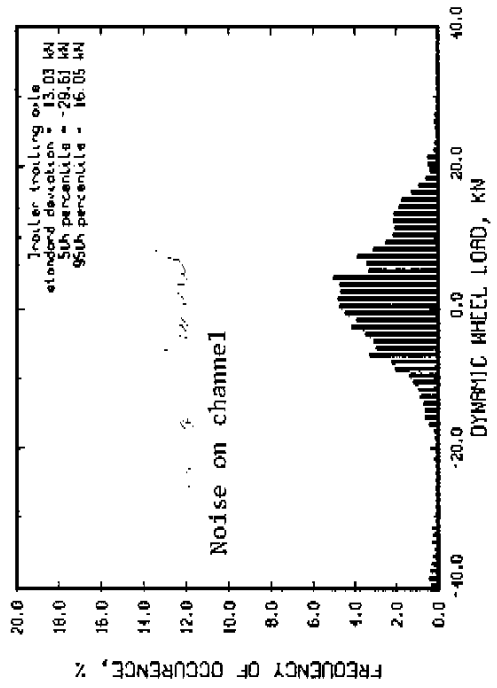
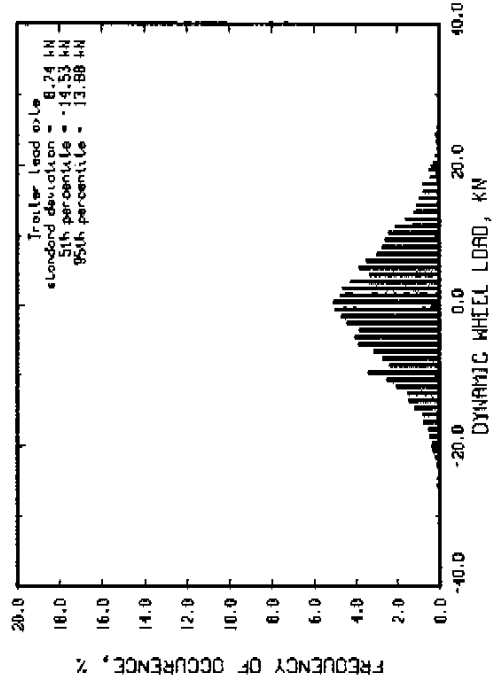
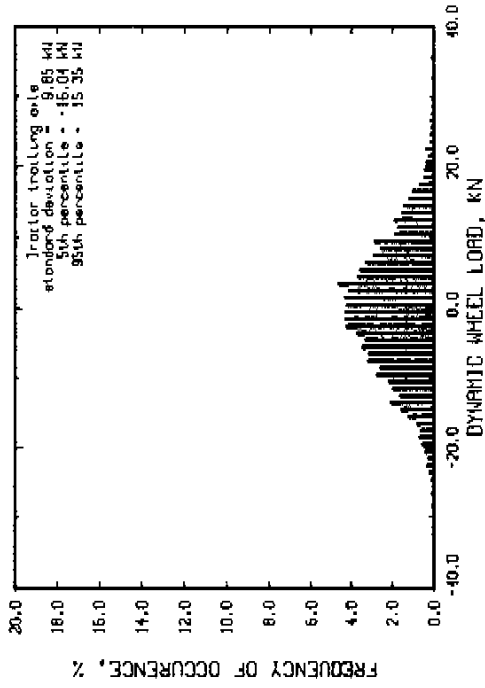
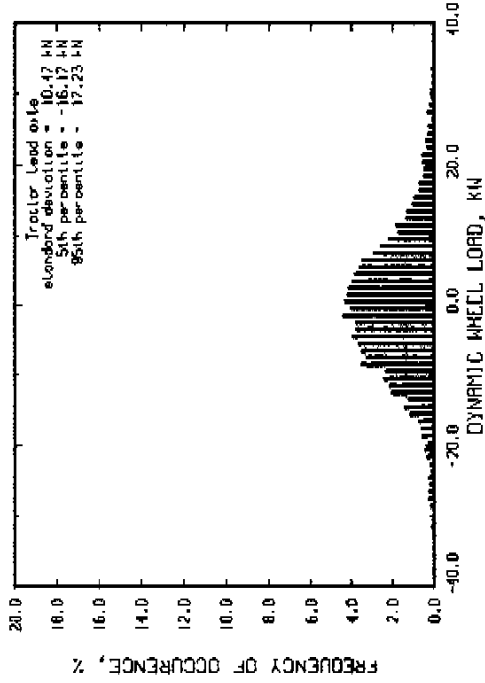
Run # 44 Part 2
 Speed = 40 km/hr
 Noys roughness = 424 IPM
 Tractor axle spread = 1.83 m
 Tractor suspension : spring suspended walking beam
 Tractor suspension lift axle up
 R/R suspension lift axle up



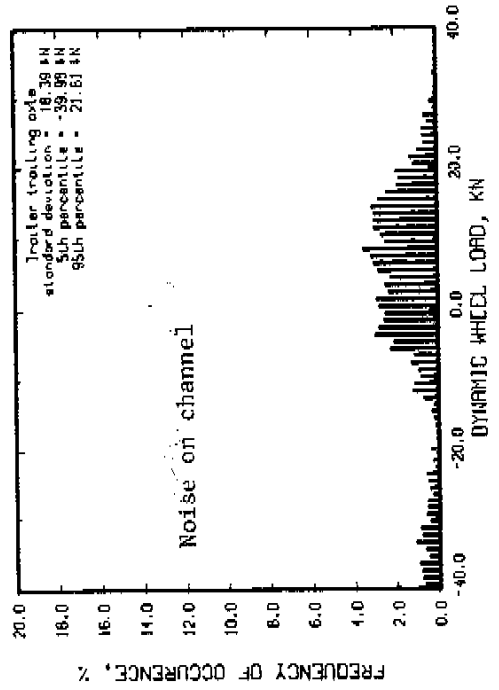
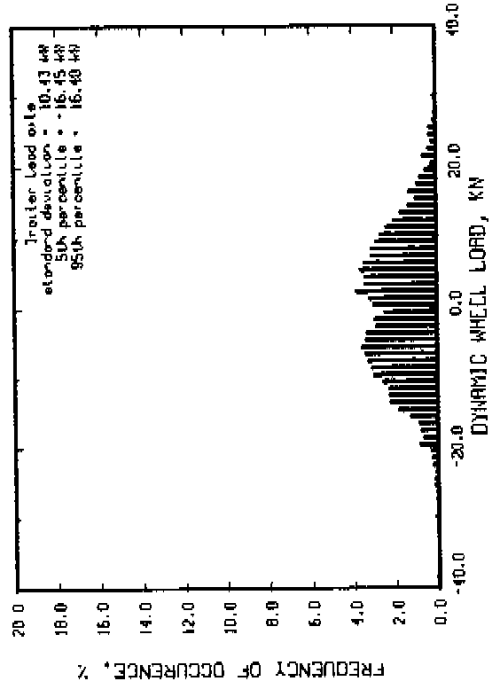
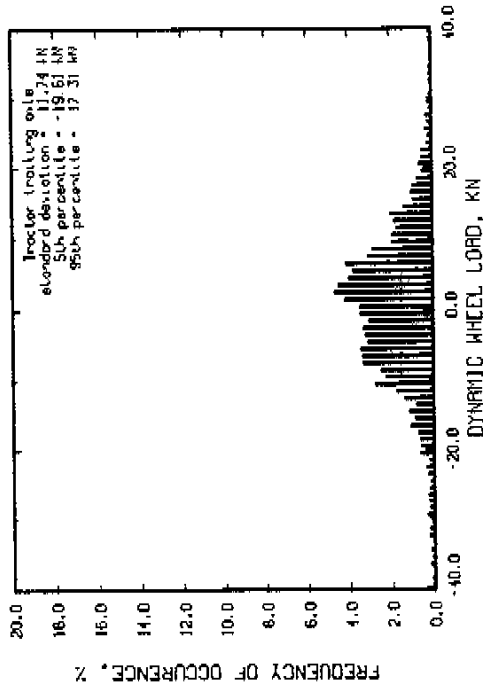
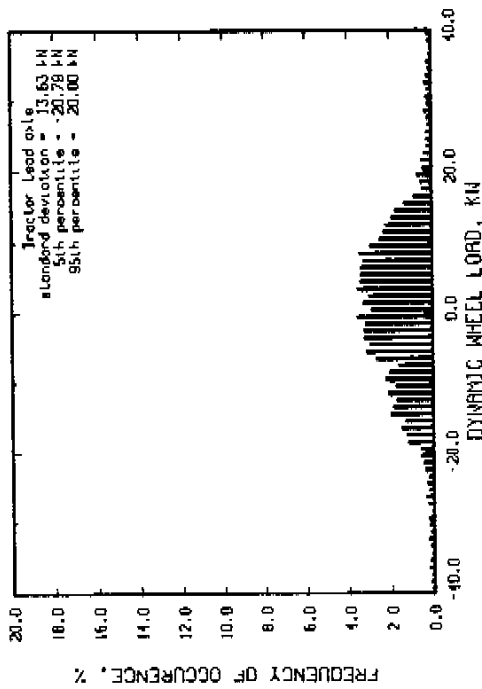
Run # 48 Part 2
 Speed = 80 km/hr
 Moys roughness = 59 JPH
 Tractor axle spread = 1.63 m
 Tractor suspension : spring suspended walking beam
 Trailer suspension : four spring
 Air suspension lift axle up



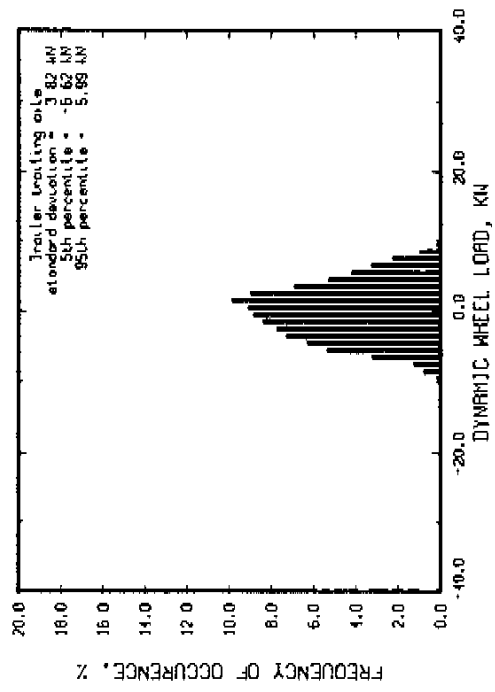
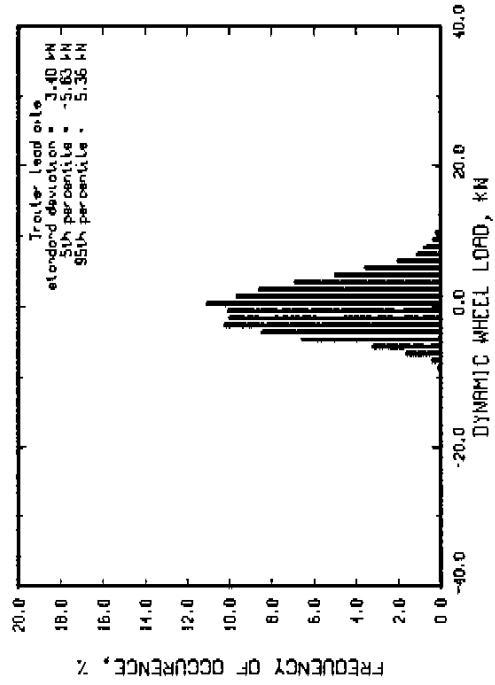
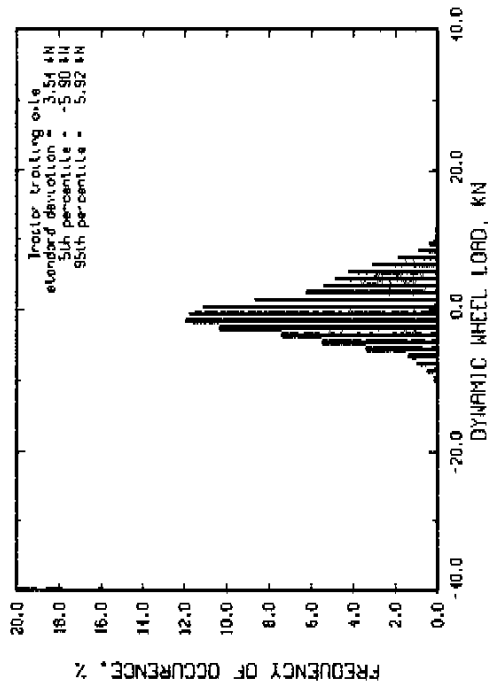
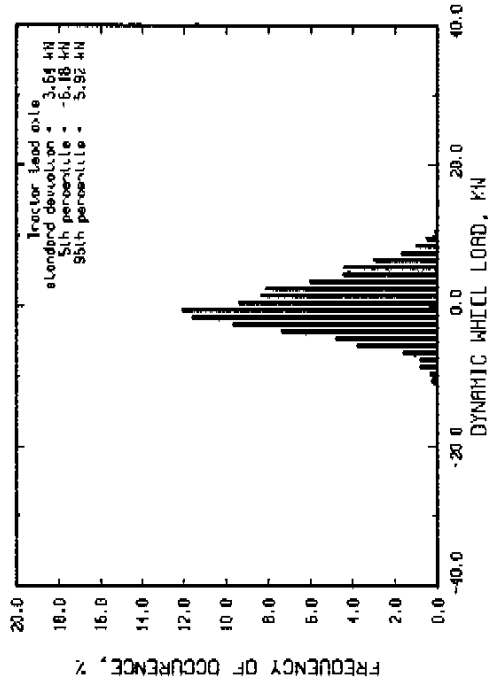
Run # 48 Part 1
 Speed = 80 km/hr
 Mays roughness = 155 IPM
 Tractor axle spread = 1.83 m
 Tractor suspension : spring suspended walking beam
 Tractor suspension : four spring
 Air suspension left axle up



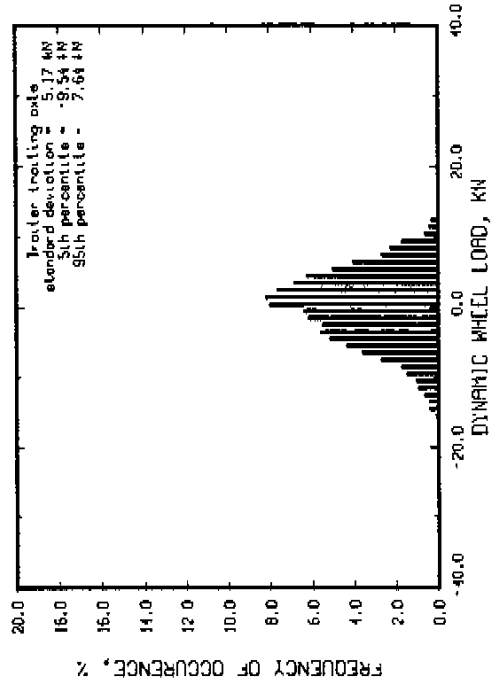
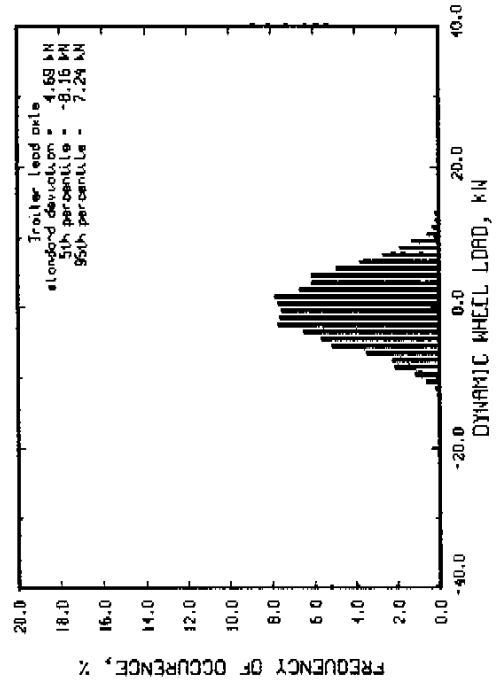
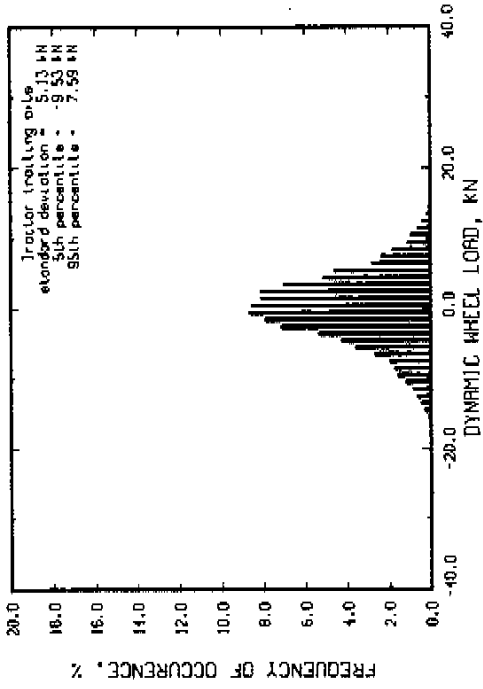
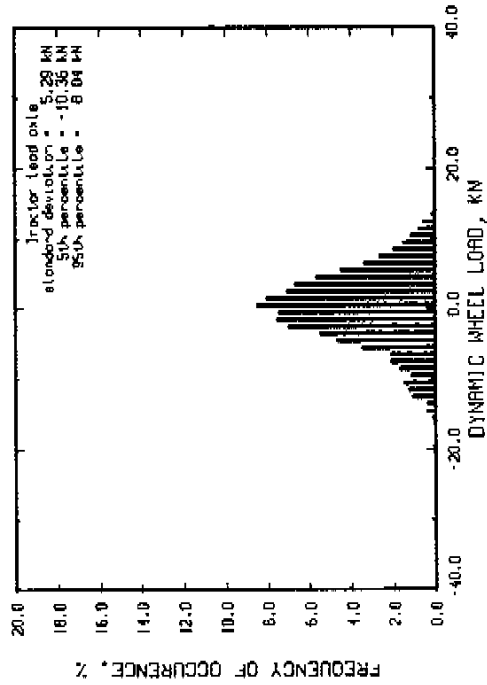
Run # 48 Fort 3 Speed = 60 km/hr
 Noise roughness = 217 JPH Trailer axle spread = 1.83 m
 Tractor suspension : spring suspended walking beam
 Trailer suspension : four spring
 Air suspension lift axle up



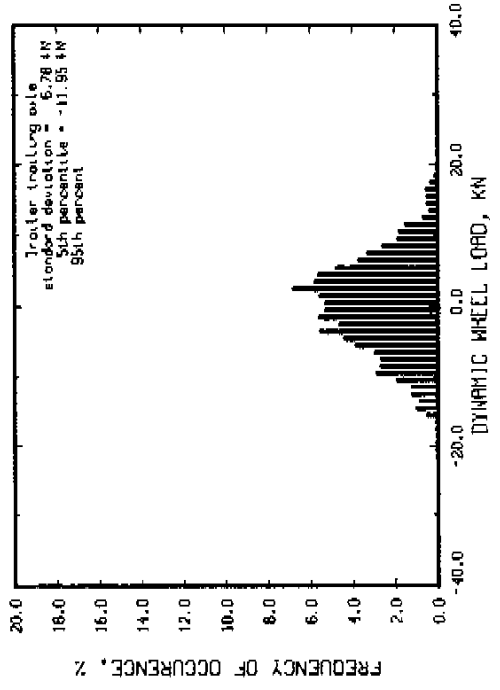
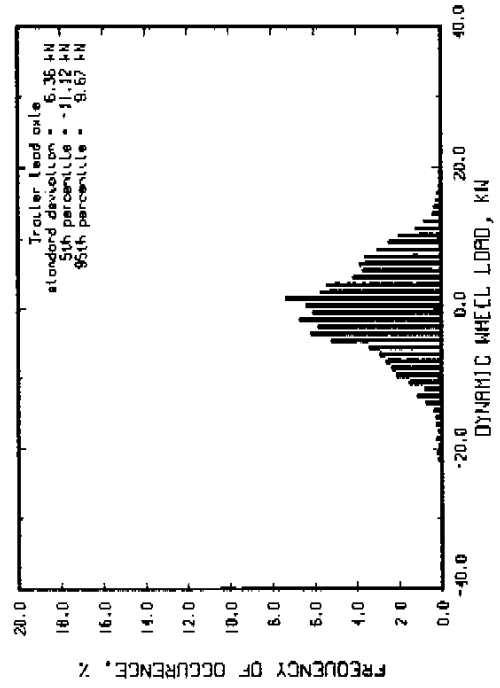
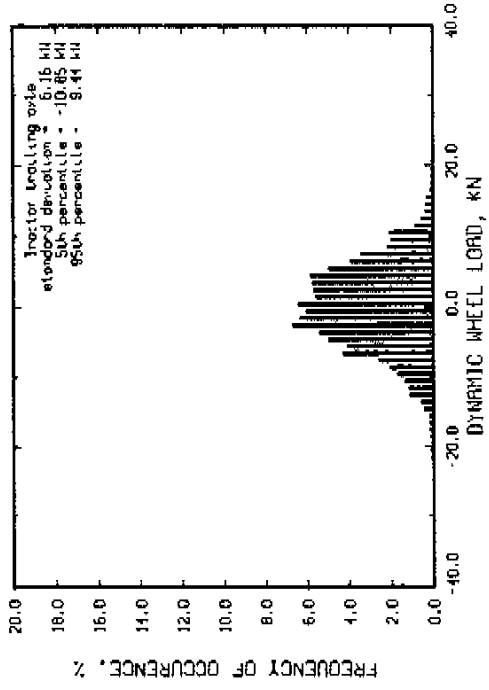
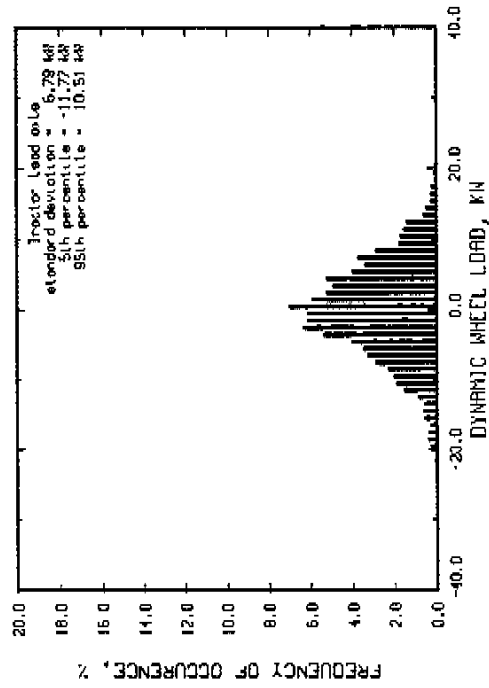
Run # 93 Speed = 40 km/hr
 Moys roughness = 73 IPI Tractor axle spread = 2.44 m
 Tractor suspension : spring suspended walking beam
 Tractor suspension : four spring
 Tractor suspension lift axle up



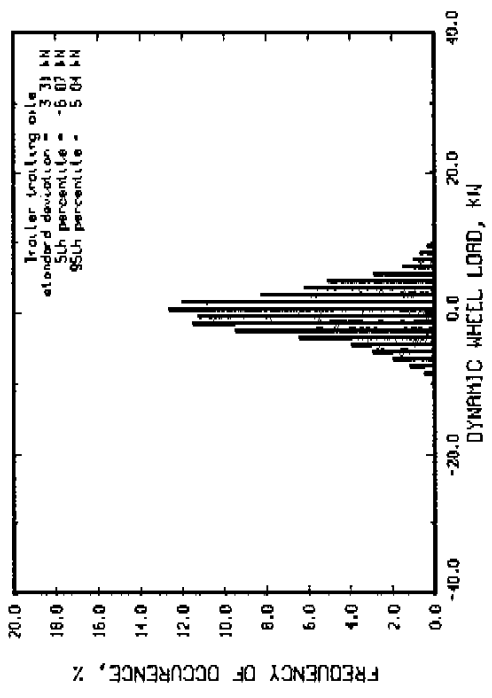
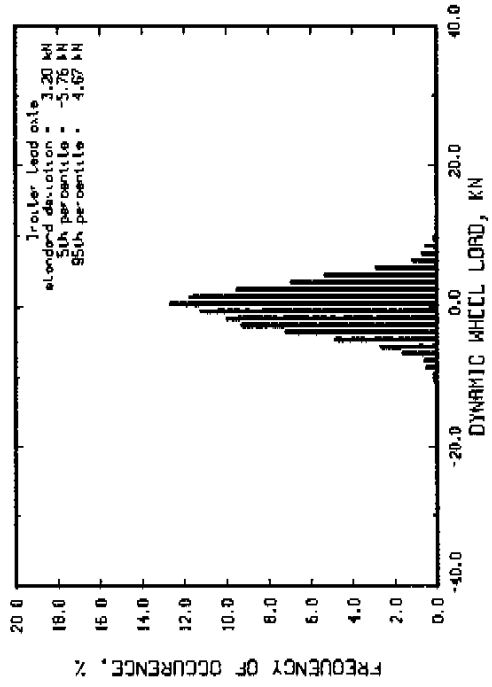
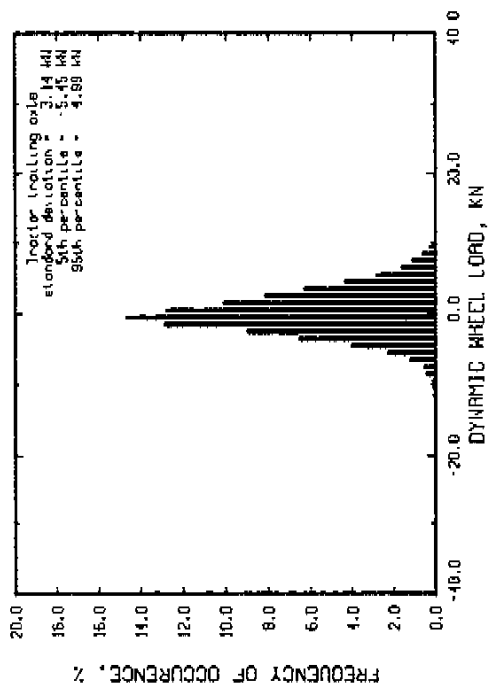
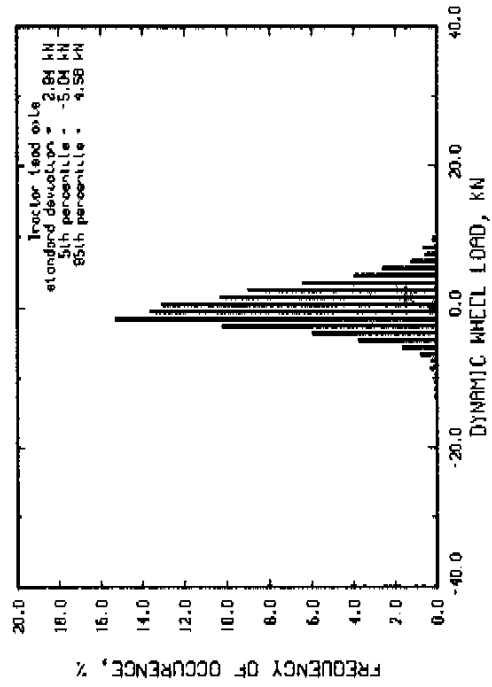
Run # 9] Part 1
 Hays roughness = 254 IPH
 Speed = 40 km/hr
 Tractor axle spread = 2.44 m
 Tractor suspension : spring suspended walking beam
 Tractor suspension : four spring
 Rtr suspension lift axle up



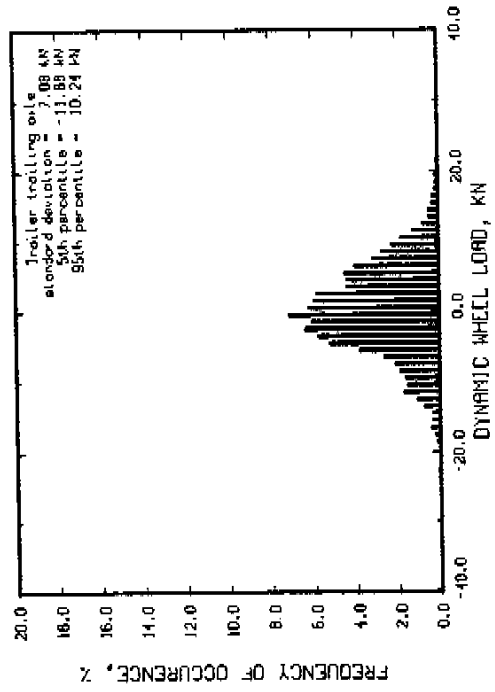
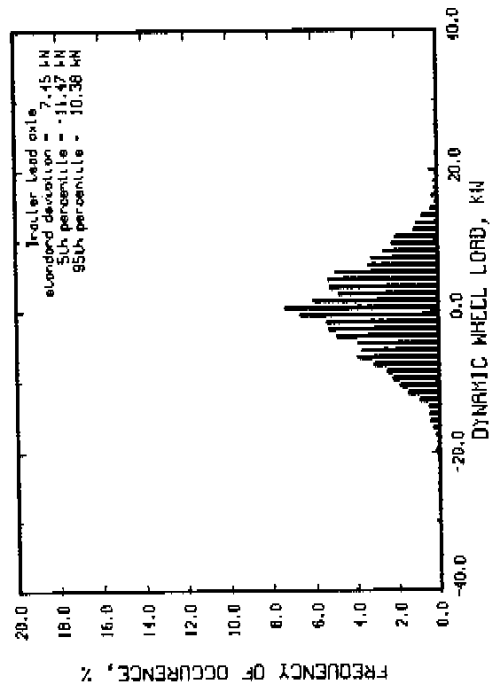
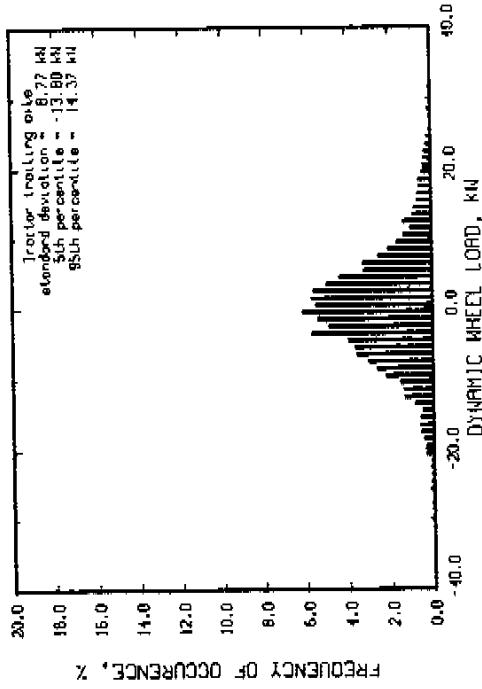
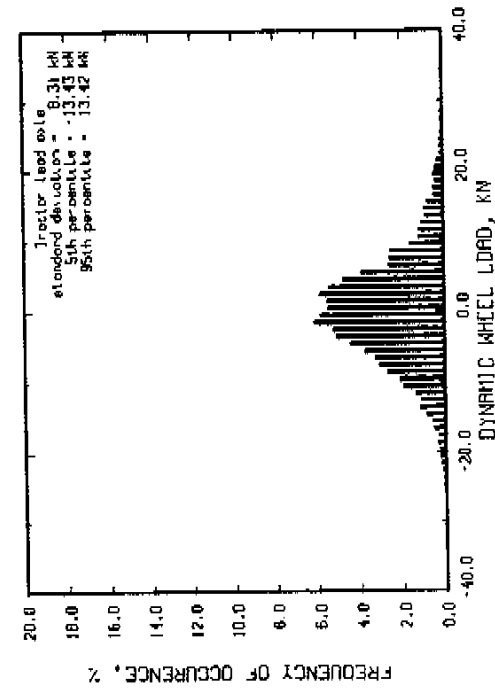
Run # 91 Part 2 Speed = 40 km/hr
 Moys roughness = 424 JPH Tractor axle spread = 2.44 m
 Tractor suspension : spring suspended walking beam
 Tractor suspension : four spring
 Tractor suspension lift axle up



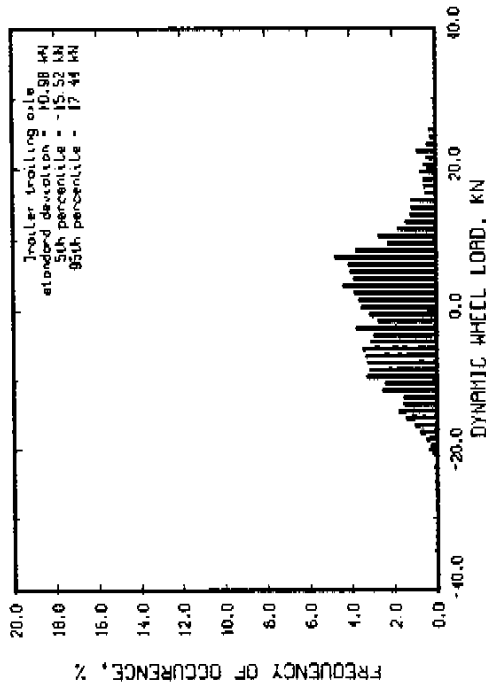
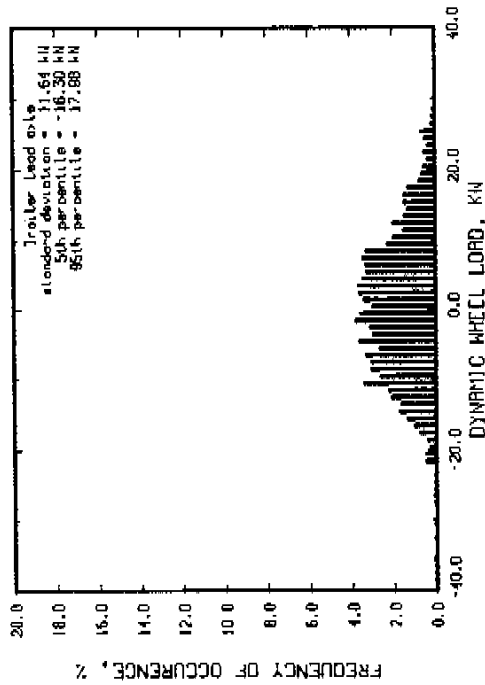
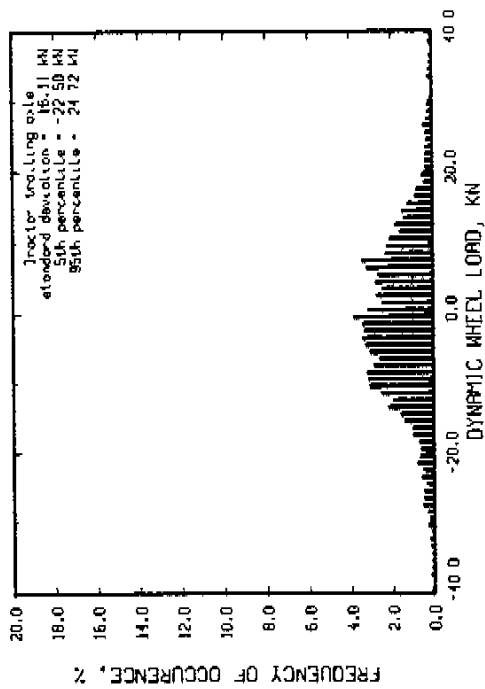
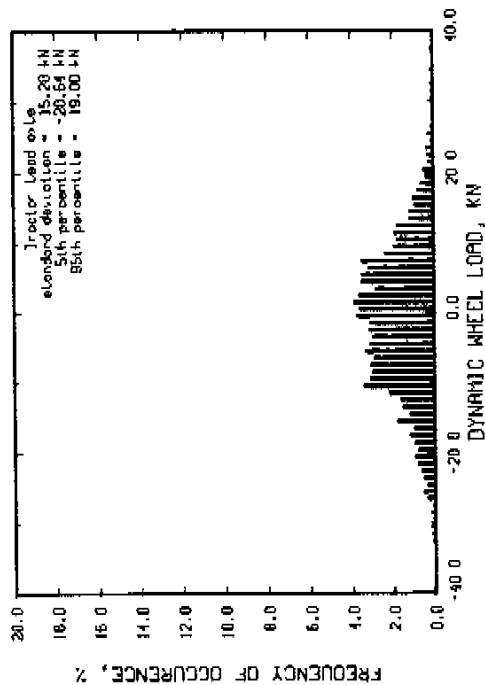
Run # 99 Part 2
 Speed = 80 km/hr
 Hoys roughness = 59 JPH
 Tractor axle spread = 2.44 m
 Tractor suspension : spring suspended walking beam
 Trailer suspension : four spring
 Air suspension lift axle up



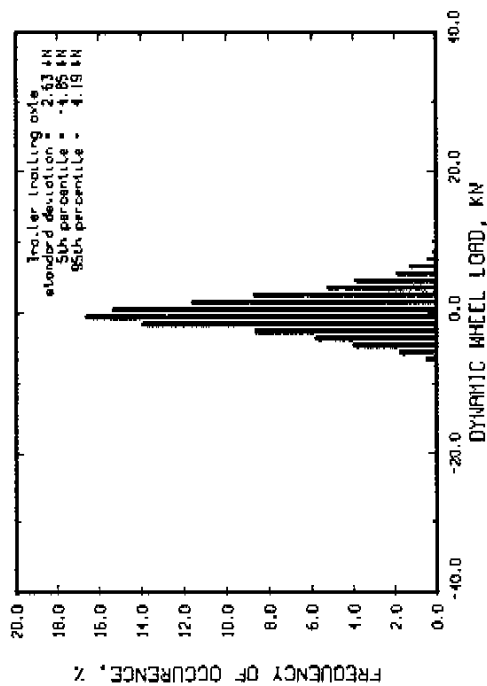
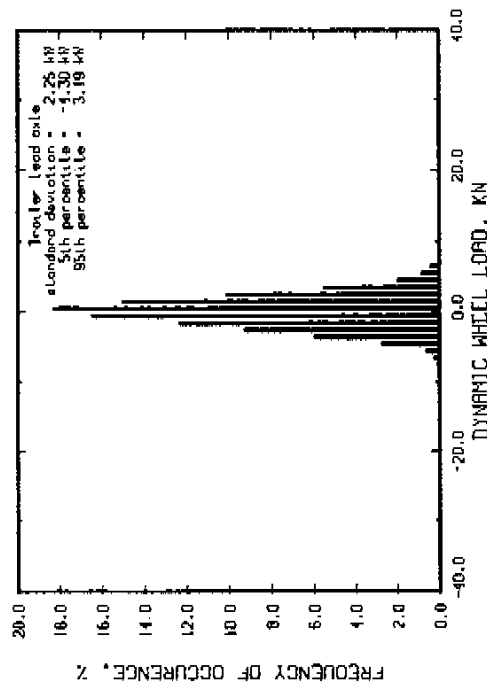
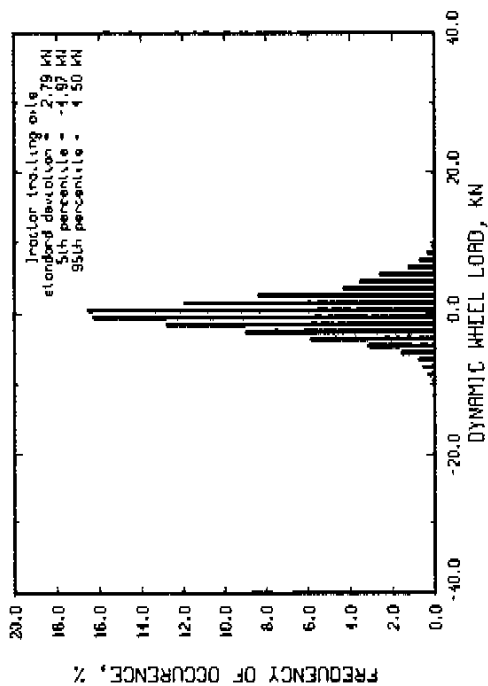
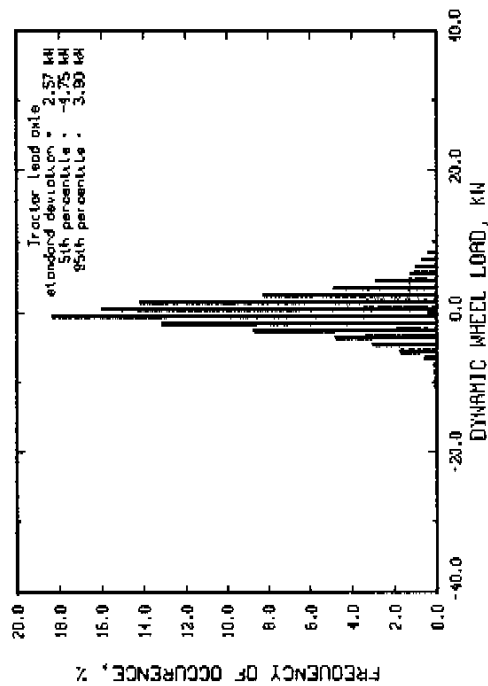
Run # 99 Part 1
 Speed = 80 km/hr
 Moys roughness = 165 IPH
 Trailer axle spread = 2.44 m
 Tractor suspension : sprung suspended walking beam
 Trailer suspension : four spring
 Air suspension left axle up



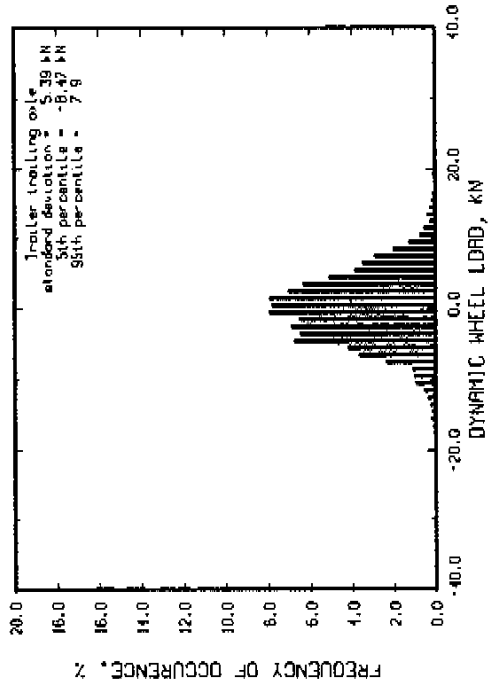
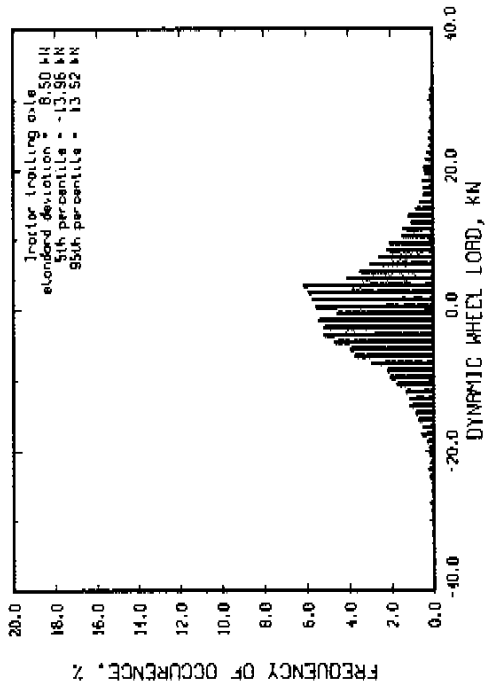
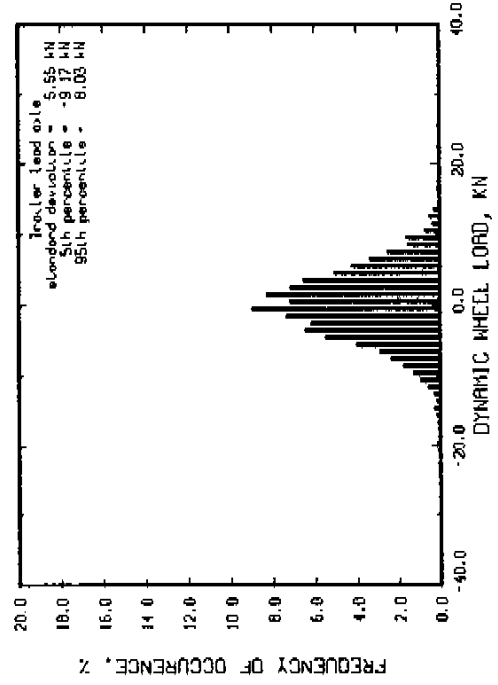
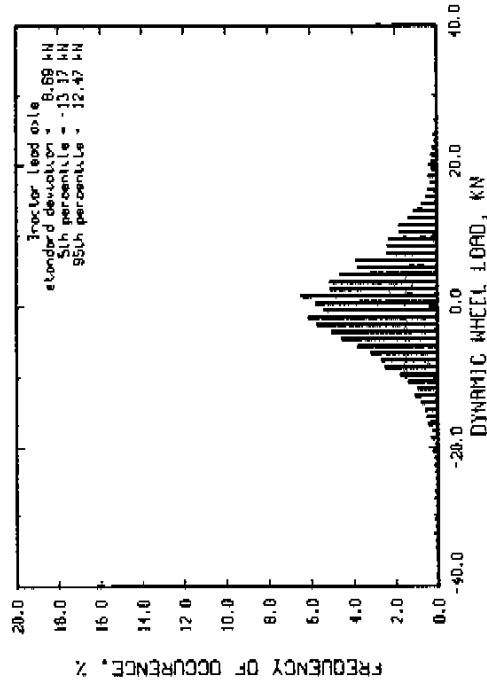
Run # 99 Port 3 Speed = 80 km/hr
 Moys roughness = 217 IPH Tractor axle spread = 2.44 m
 Tractor suspension : spring suspended walking beam
 Tractor suspension : four spring
 Rtr suspension Lxfl axle up



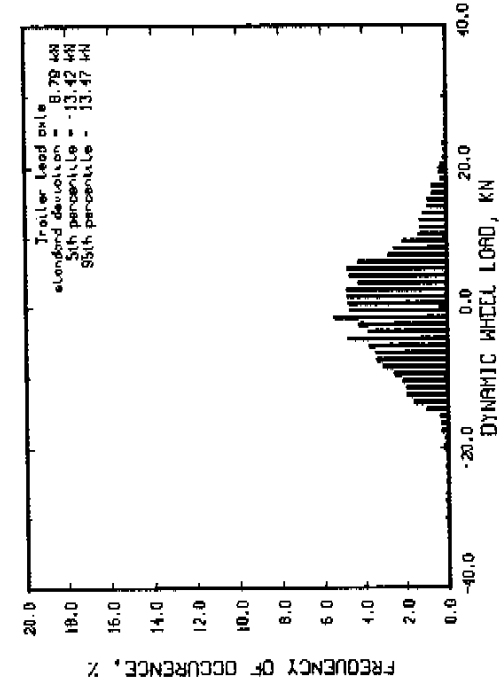
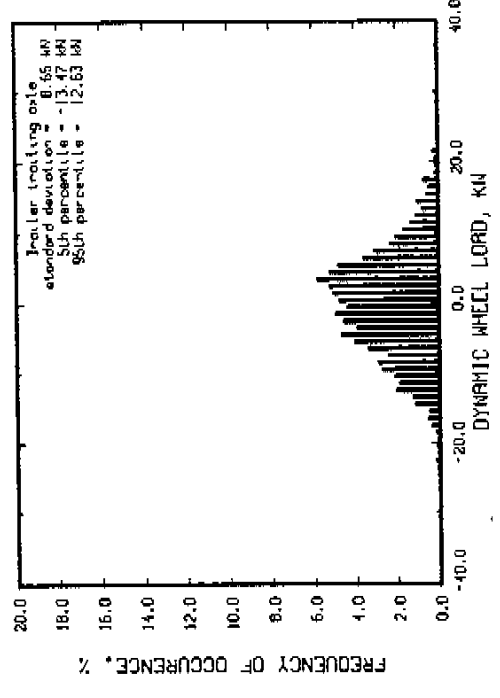
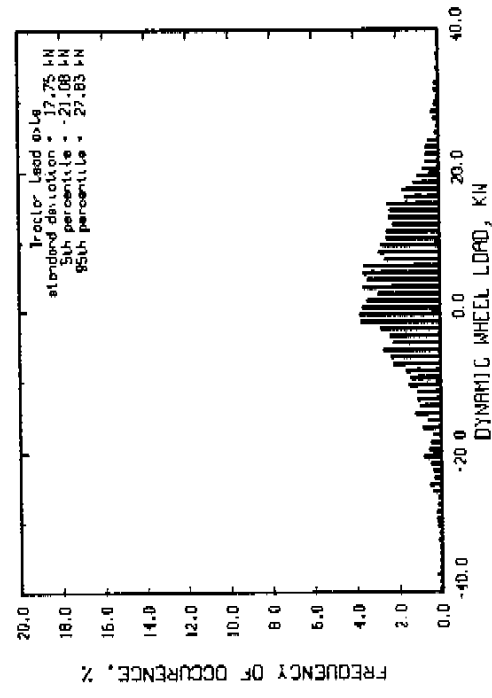
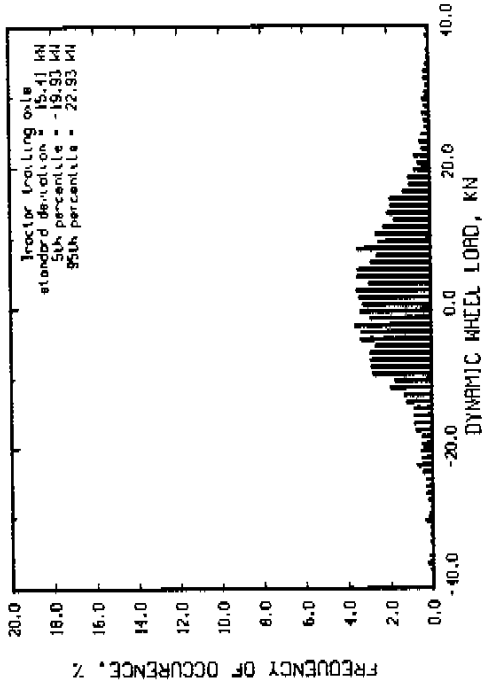
Run # 100 Part 2 Speed = 80 km/hr
 Moys roughness = 59 IPM Tractor axle spread = 2.44 m
 Tractor suspension : spring suspended walking beam
 Tractor suspension : four spring
 Rtr suspension lift axle down



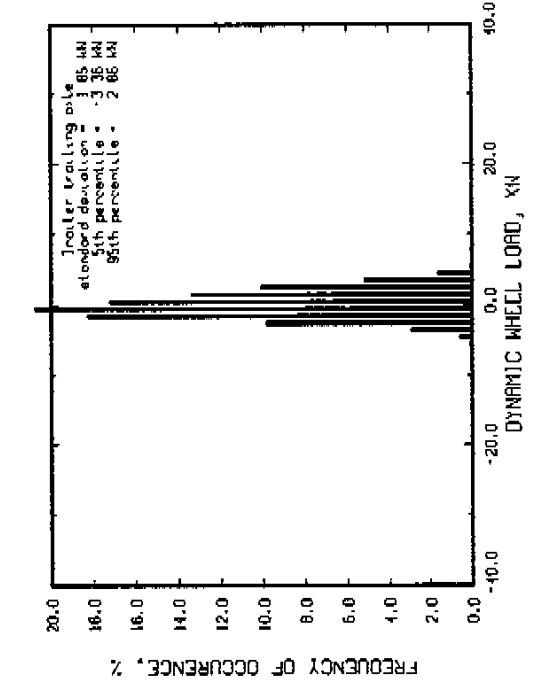
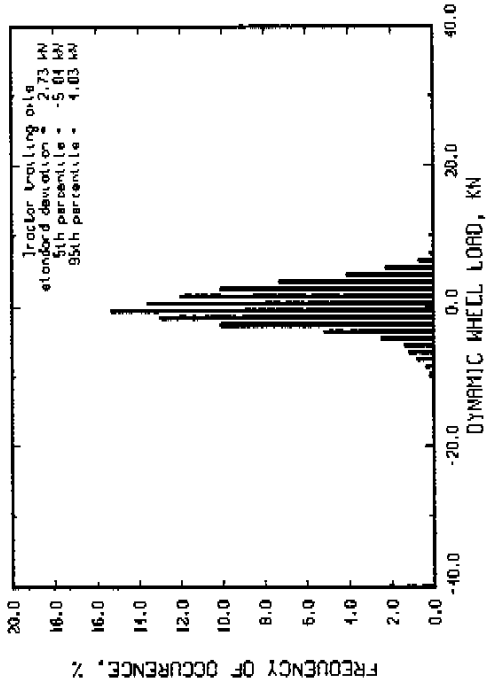
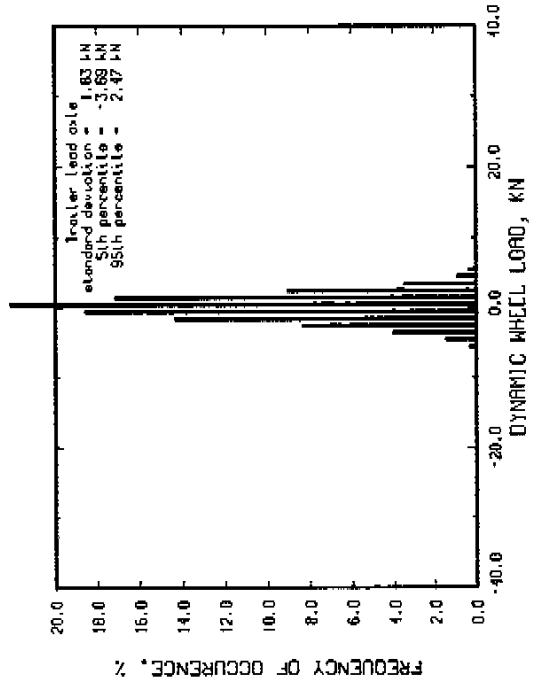
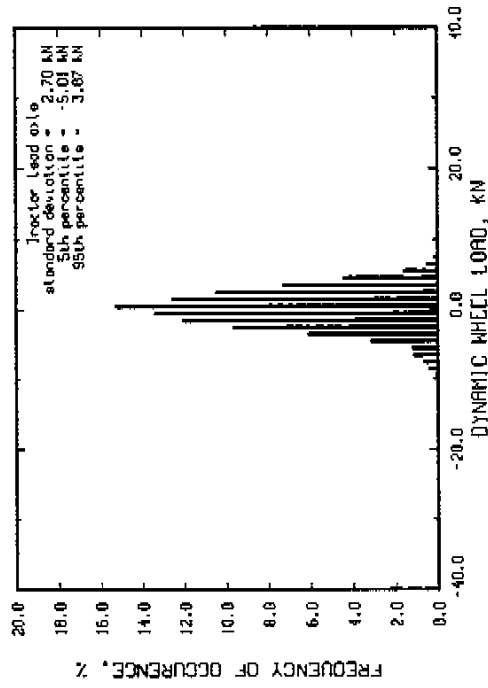
Run # 100 part 1
 Speed = 80 km/hr
 Moys roughness = 165 JPH
 Trailer axle spread = 2.44 m
 Tractor suspension : spring suspended walking beam
 Trailer suspension : four spring
 Air suspension lift axle down



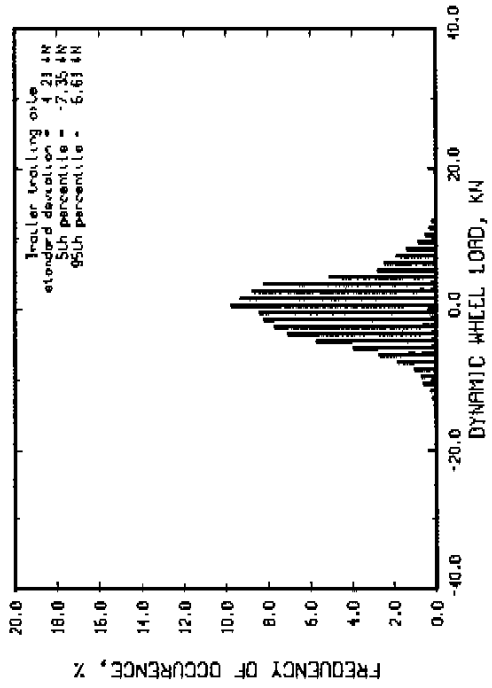
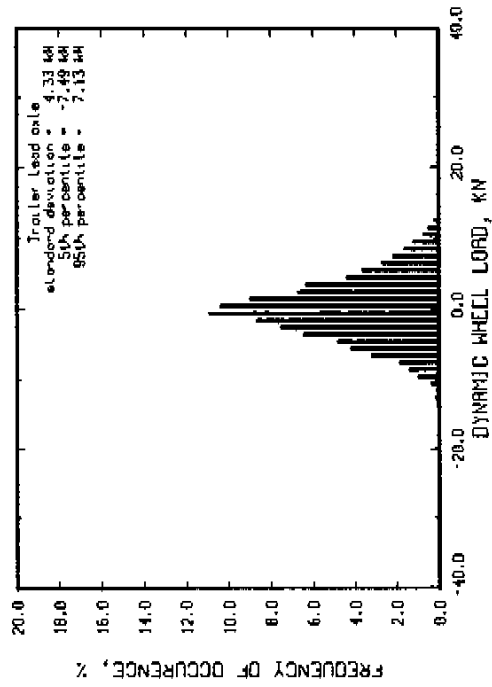
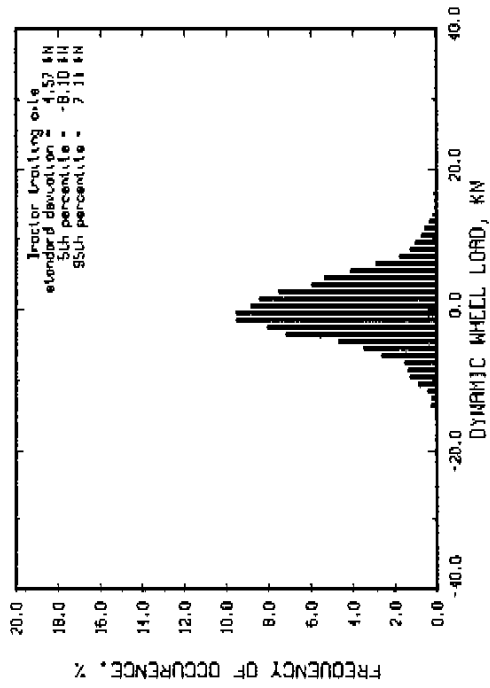
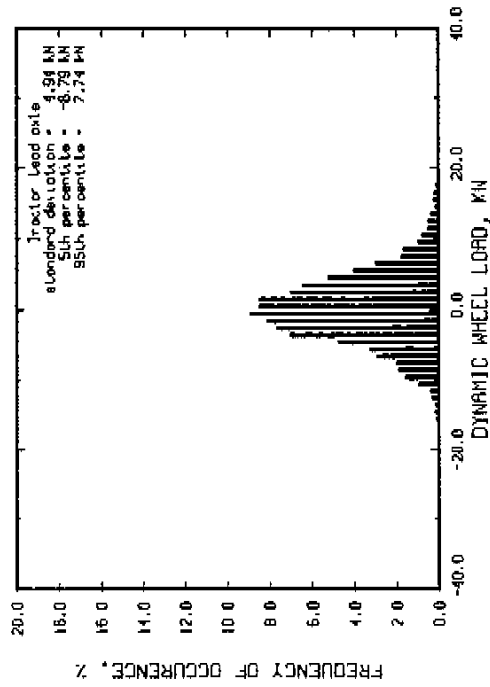
Run # 100 Part 3
 Speed = 80 km/hr
 Moys roughness = 217 IPH
 Trailer axle spread = 2.44 m
 Tractor suspension : spring suspended walking beam
 Trailer suspension : four spring
 air suspension lift axle down



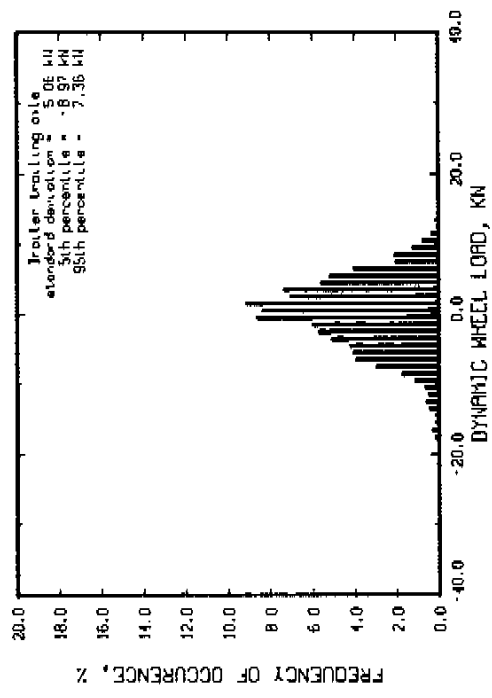
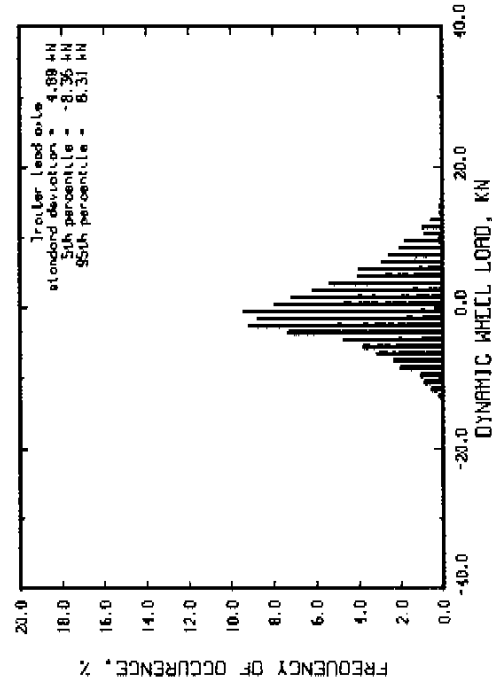
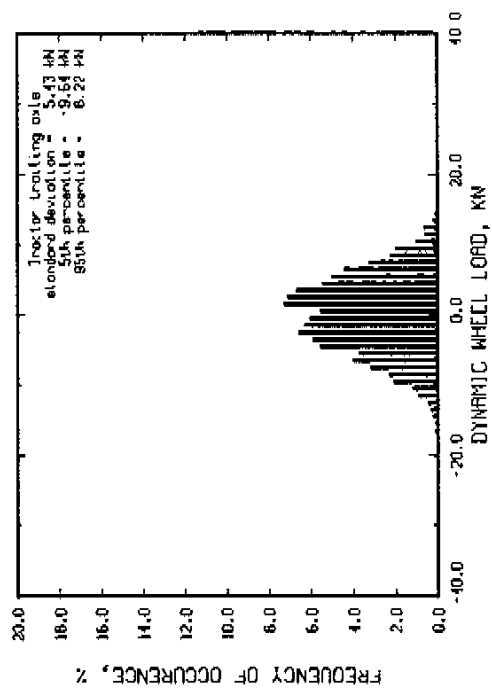
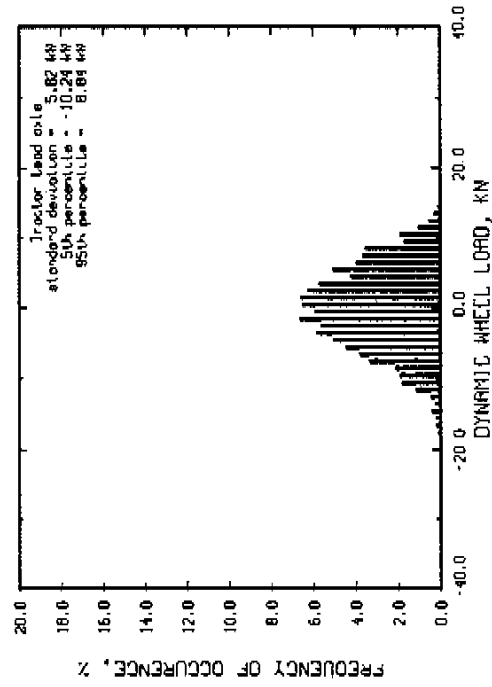
Run # 170 Speed = 40 km/hr
 Hoys roughness = 73 IPM Trailer axle spread = 1.27 m
 Tractor suspension : spring suspended walking beam
 Trailer suspension : air bags
 Air suspension lift axle up



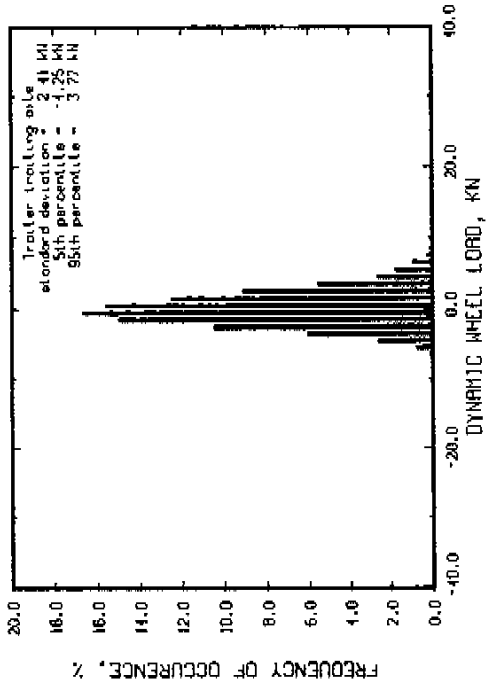
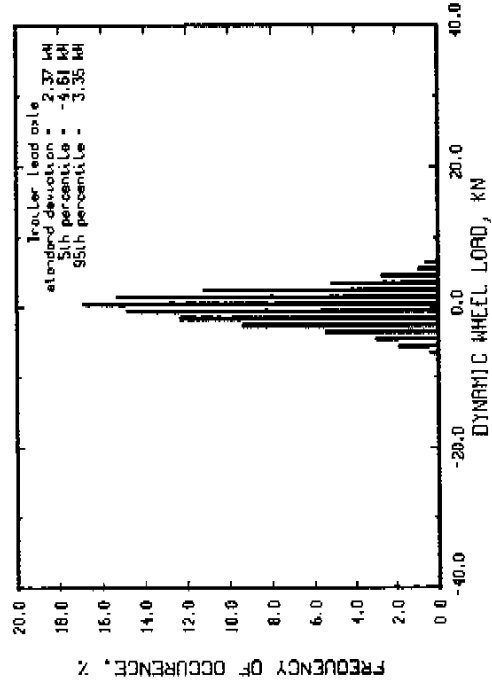
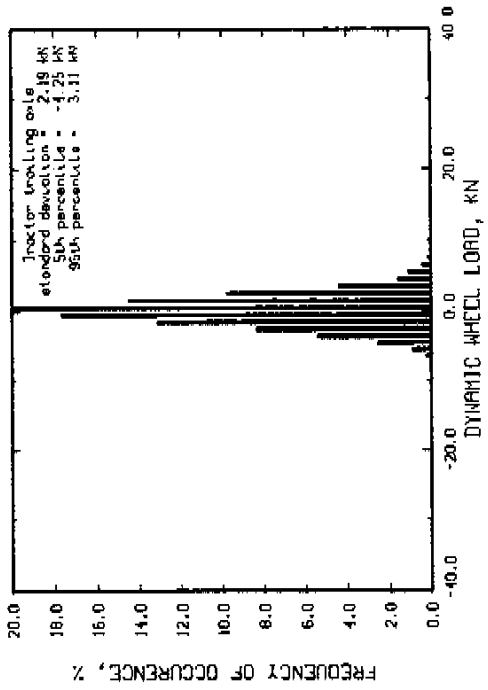
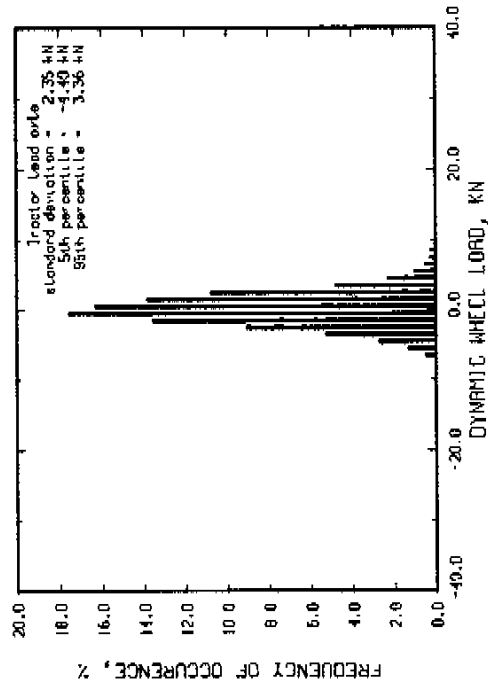
Run # 154 Part 1 Speed = 40 km/hr
 Moys roughness = 254 IPM Tractor axle spread = 1.27 m
 Tractor suspension : spring suspended walking beam
 Tractor suspension : air bags
 Rtr suspension lift axle up



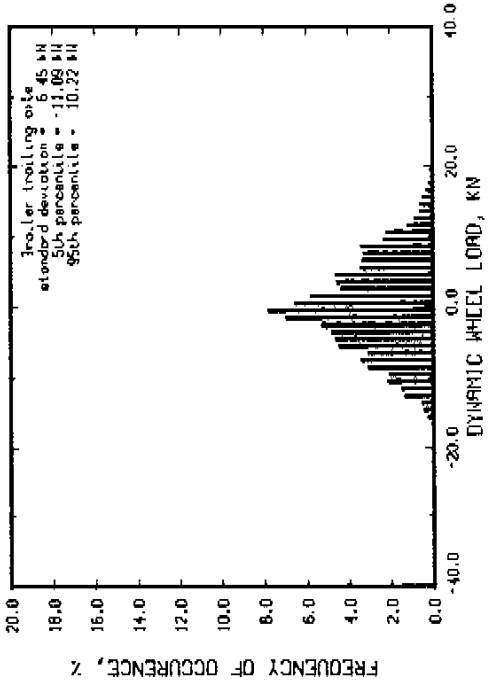
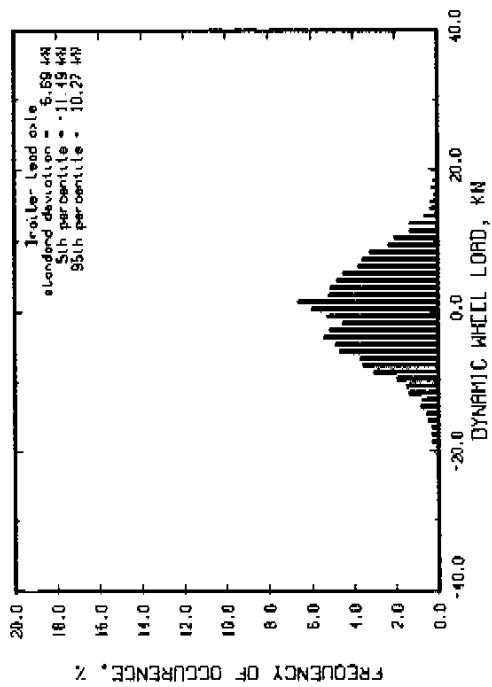
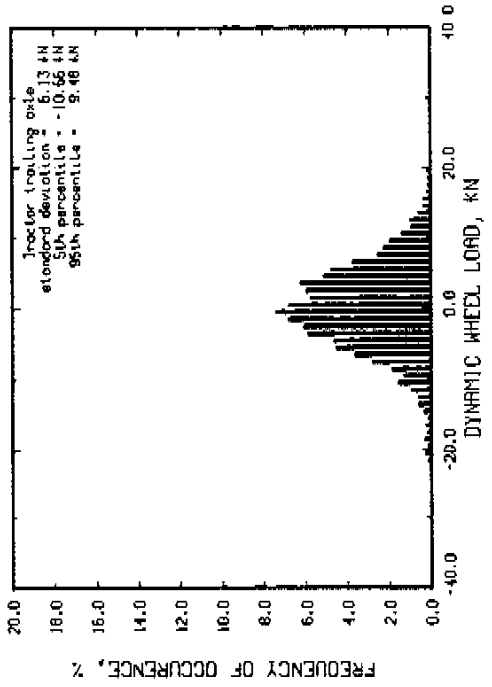
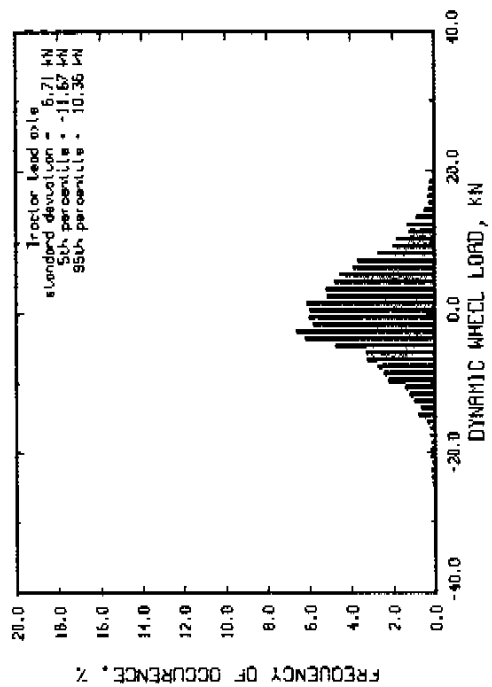
Run # 154 Part 2
 Speed = 40 km/hr
 Moys roughness = 424 JPH
 Trailer axle spread = 1.27 m
 Trailer suspension : spring suspended walking beam
 Trailer suspension : air bags
 flr suspension lift axle up



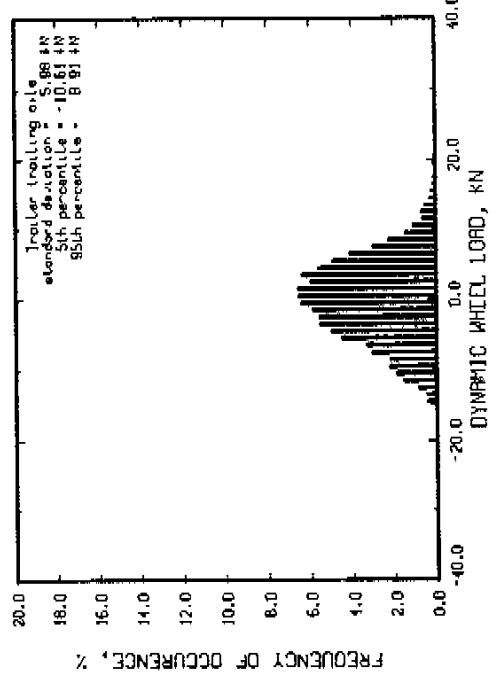
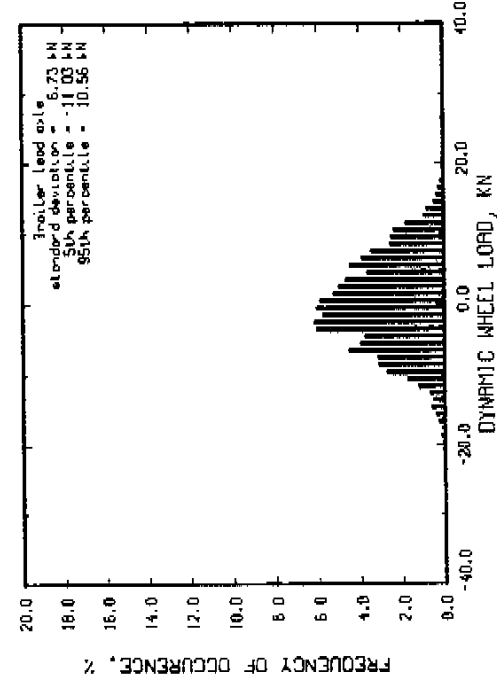
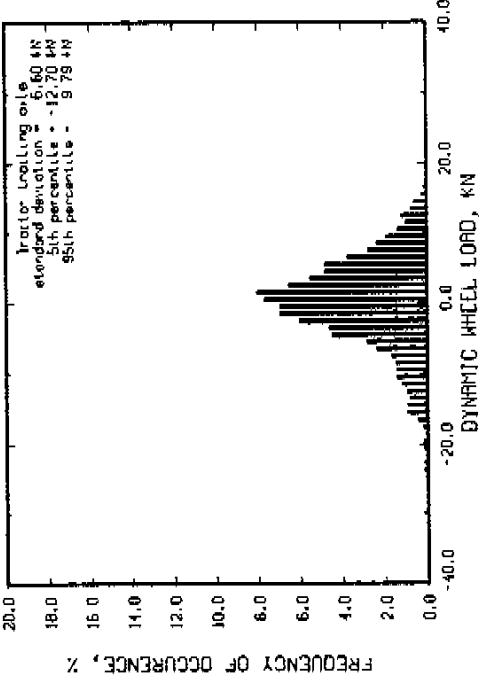
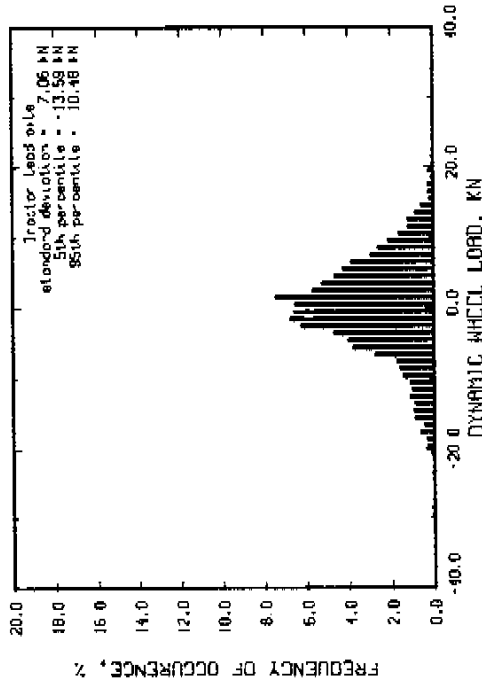
Run # 167 Speed = 60 km/hr
 Moys roughness = 73 IPI Tractor axle spread = 1.27 m
 Tractor suspension : spring suspended walking beam
 Tractor suspension : air bags
 Air suspension lift axle up



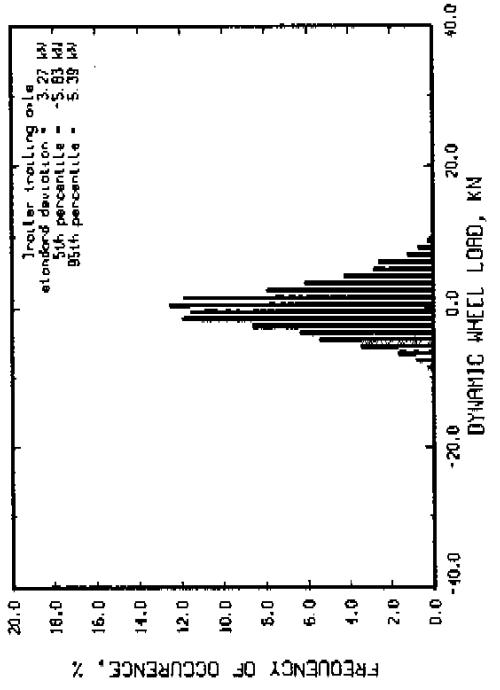
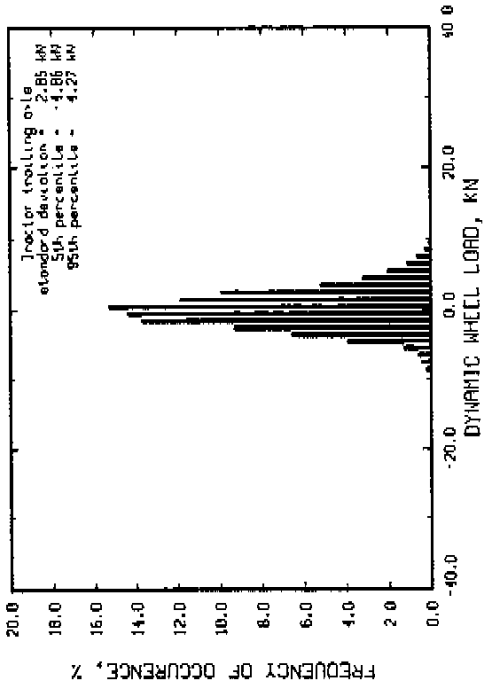
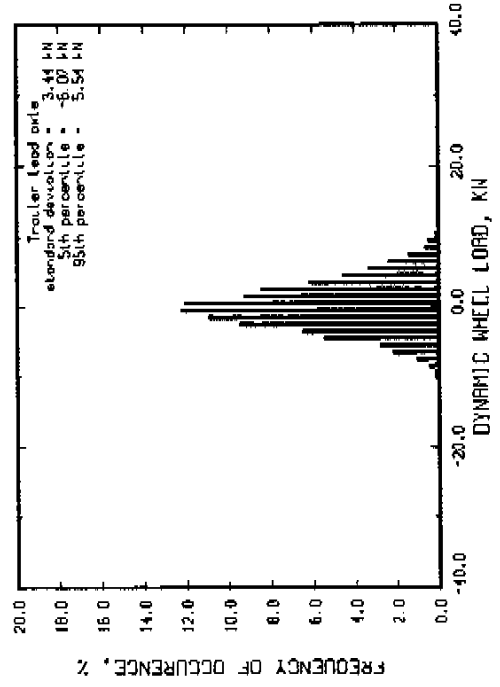
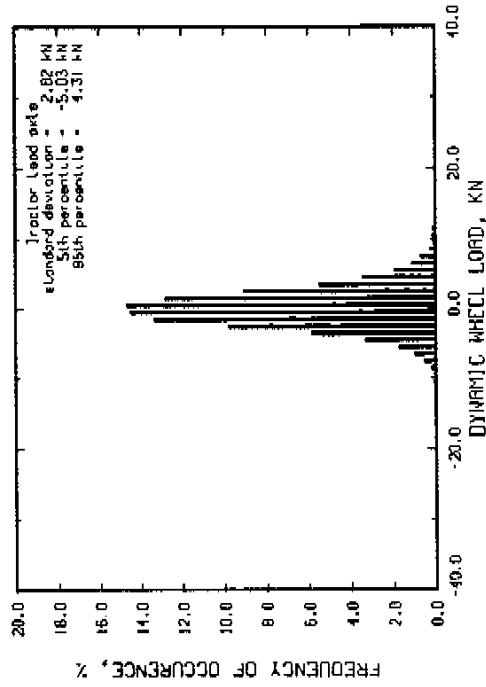
Run # 157 Part 1
 Max roughness = 254 IPM
 Speed = 60 km/hr
 Tractor axle spread = 1.27 m
 Tractor suspension : sprung suspended walking beam
 Tractor suspension : air bags
 Tractor suspension left axle up



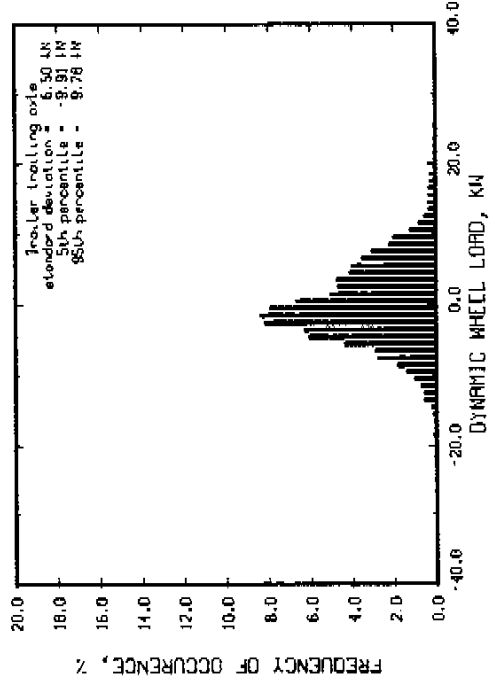
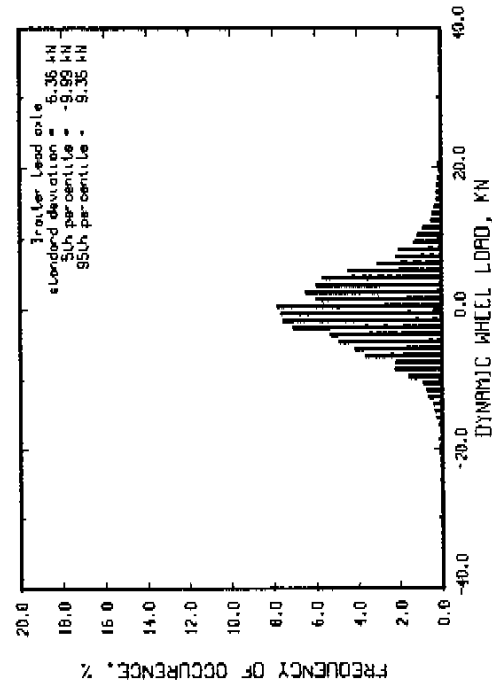
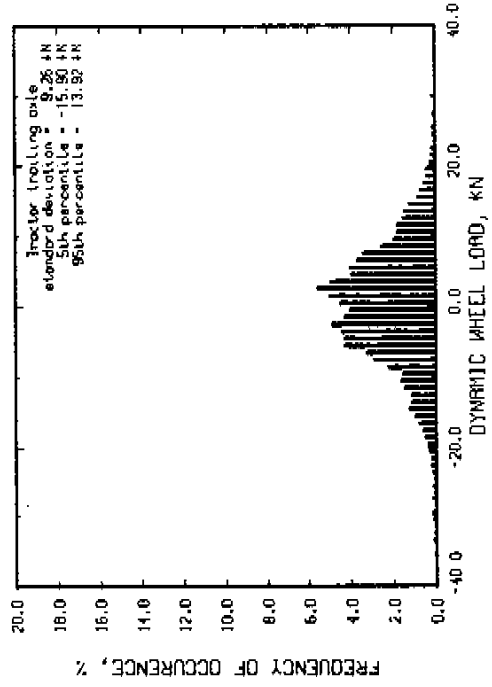
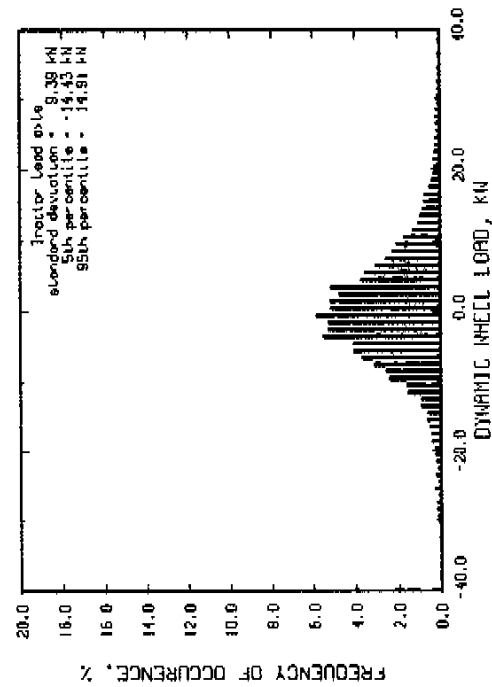
Run # 157 Part 2 Speed = 50 km/hr
 Hoys roughness = 424 JPH Tractor axle spread = 1.27 m
 Tractor suspension : spring suspended walking beam
 Trailer suspension : air bags
 Air suspension lift axle up



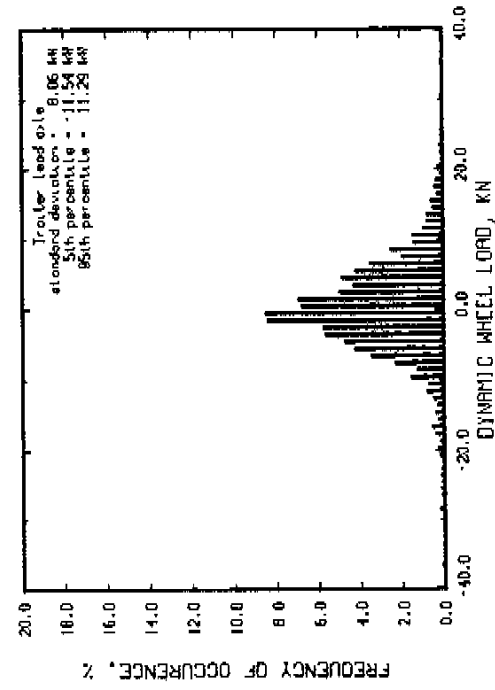
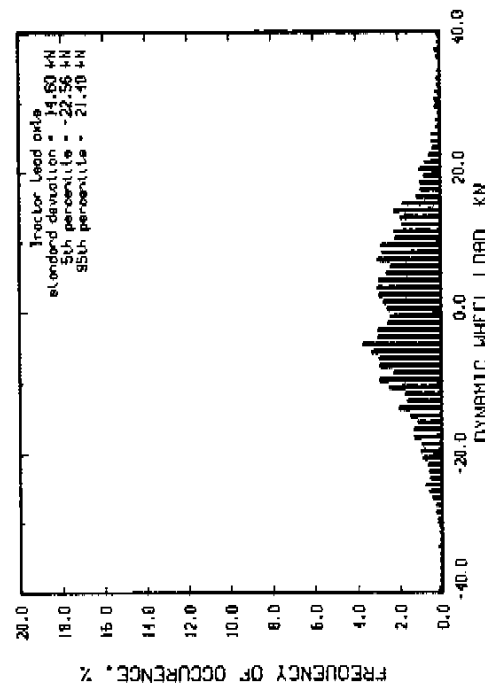
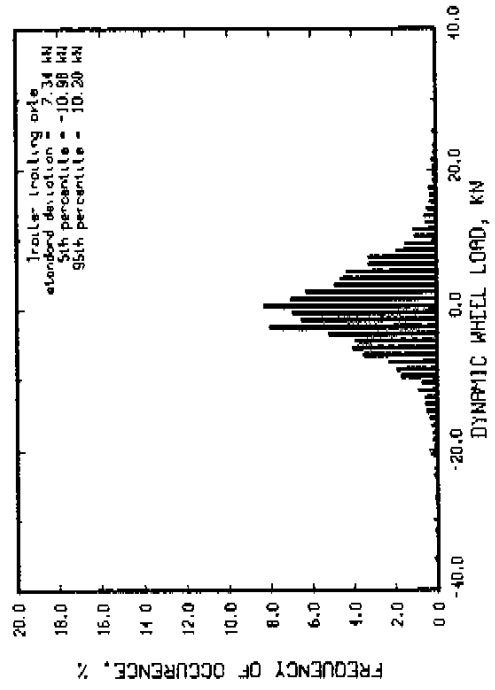
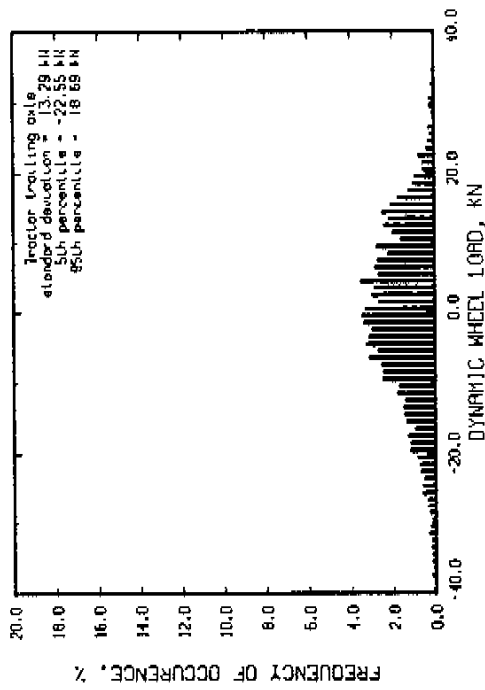
Run # 194 Part 2 Speed = 80 km/hr
 Moys roughness = 59 JPH Trailer axle spread = 1.27 m
 Tractor suspension : spring suspended walking beam
 Trailer suspension : air bags
 Air suspension left axle up



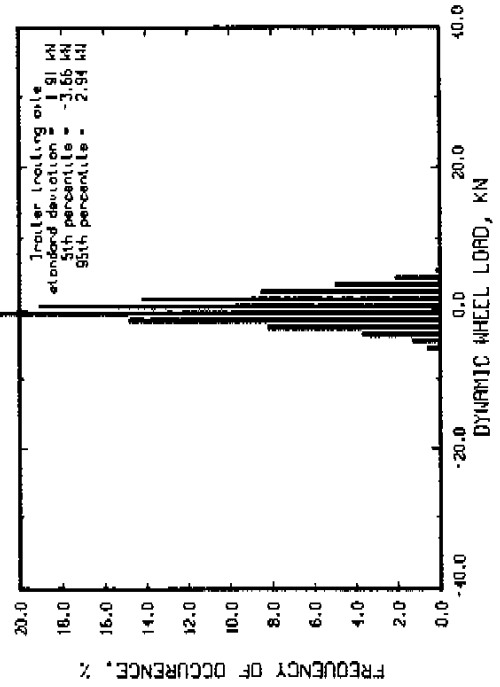
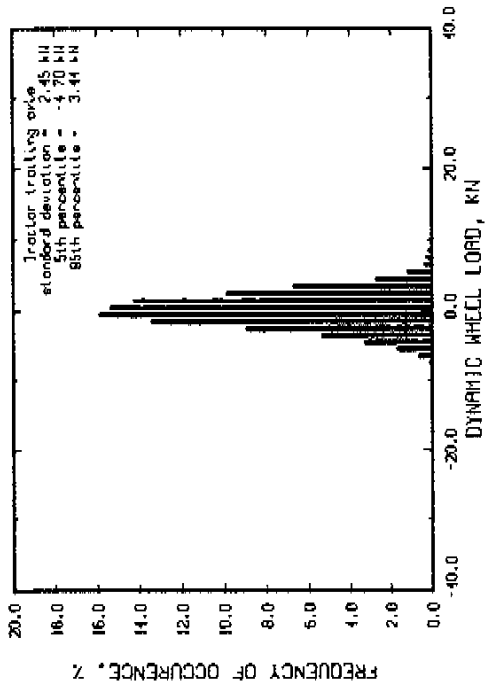
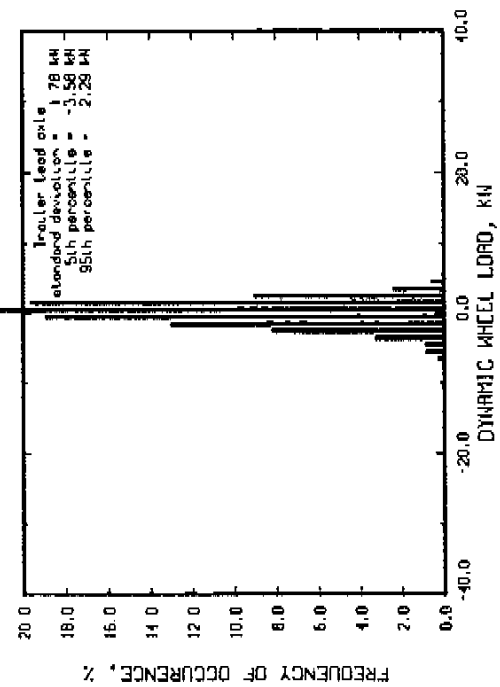
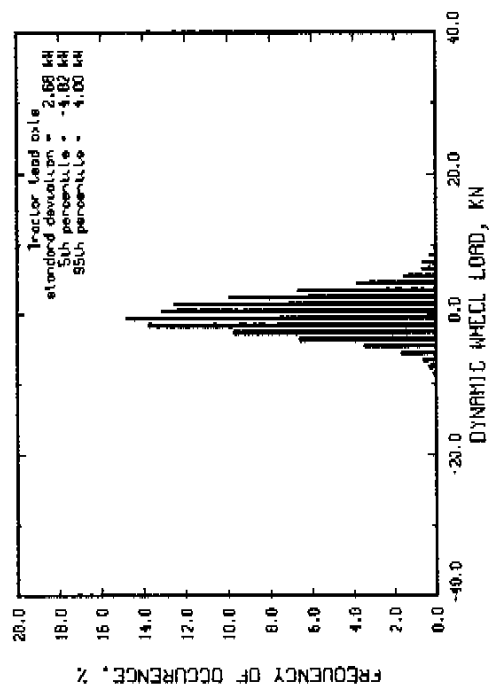
Run # 194 Part 1 Speed = 80 km/hr
 Tractor axle spread = 1.27 m
 Tractor suspension : sprung suspended walking beam
 Tractor suspension : air bugs
 Tractor suspension left axle up



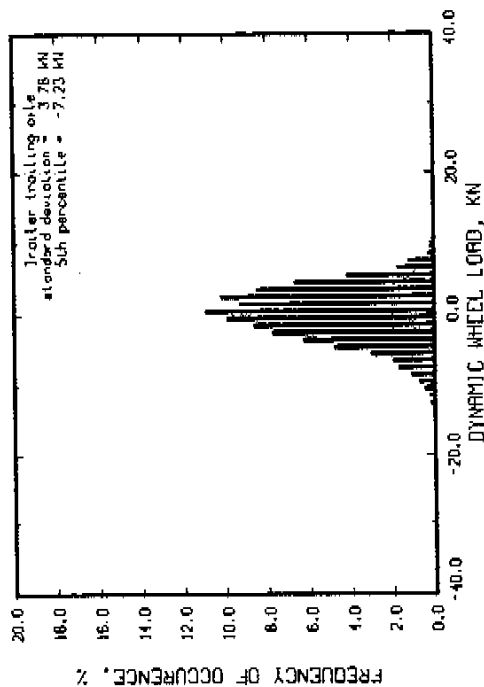
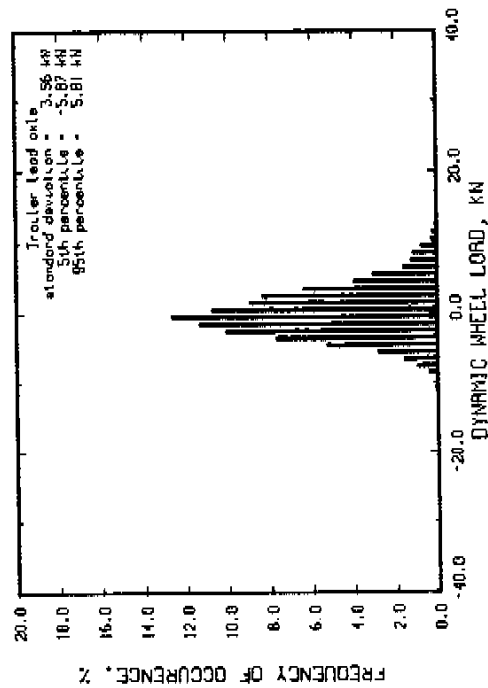
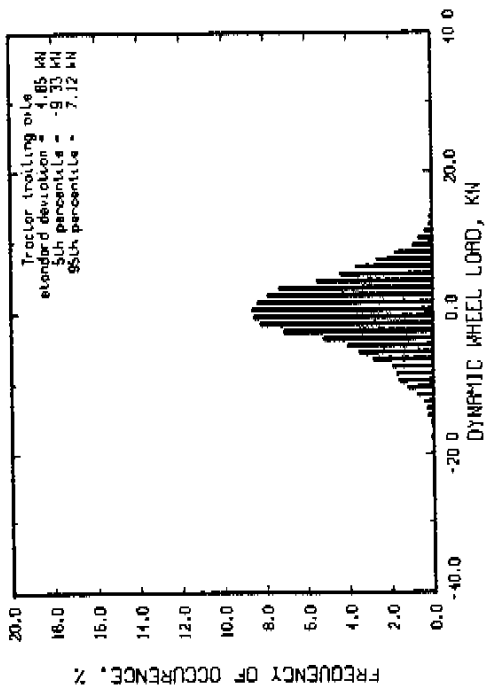
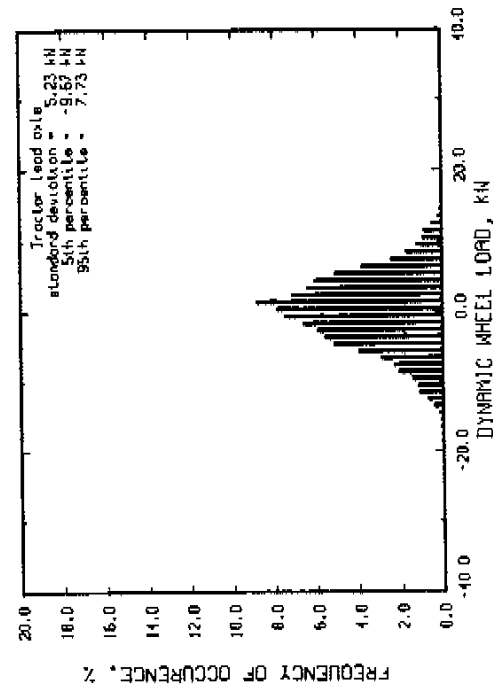
Run # 194 Part 3 Speed = 80 km/hr
 Moys roughness = 217 JPH
 Tractor axle spread = 1.27 m
 Tractor suspension : spring suspended walking beam
 Trailer suspension : air bags
 R/R suspension lift axle up



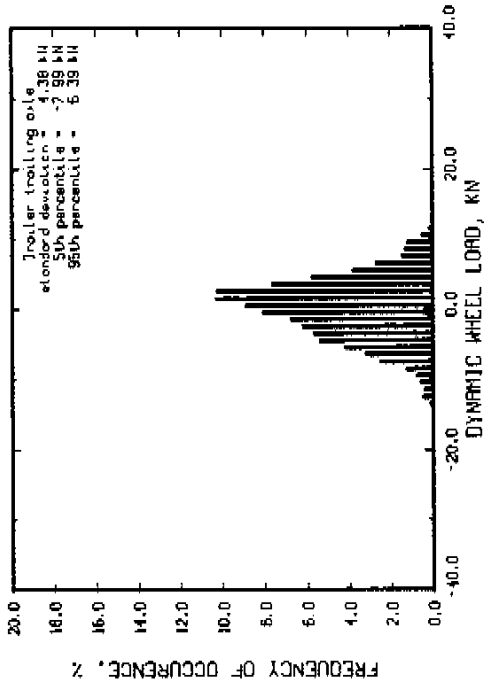
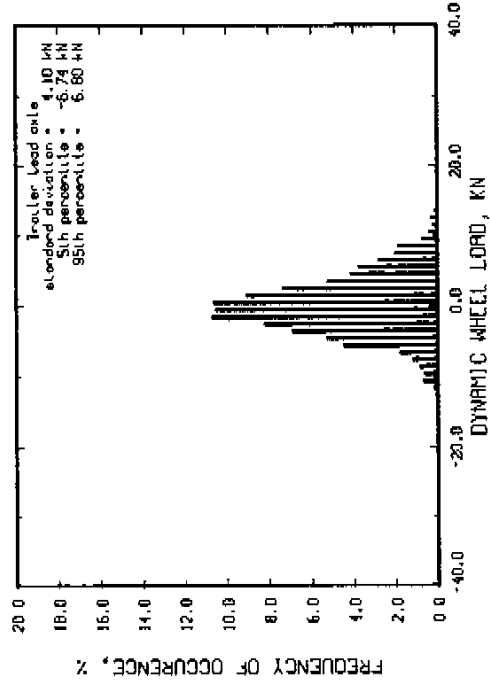
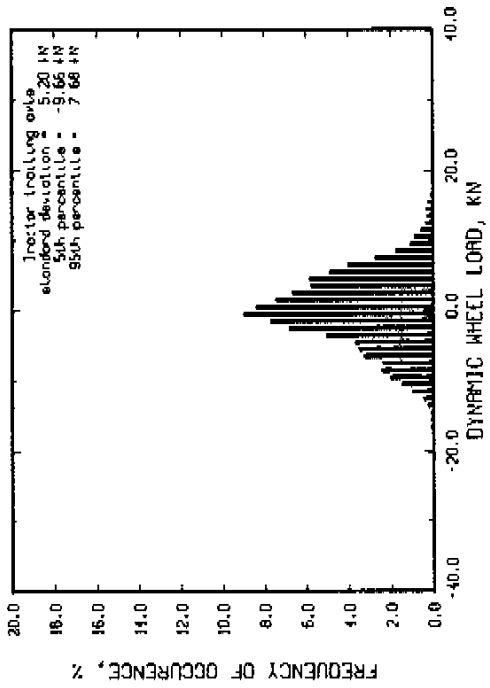
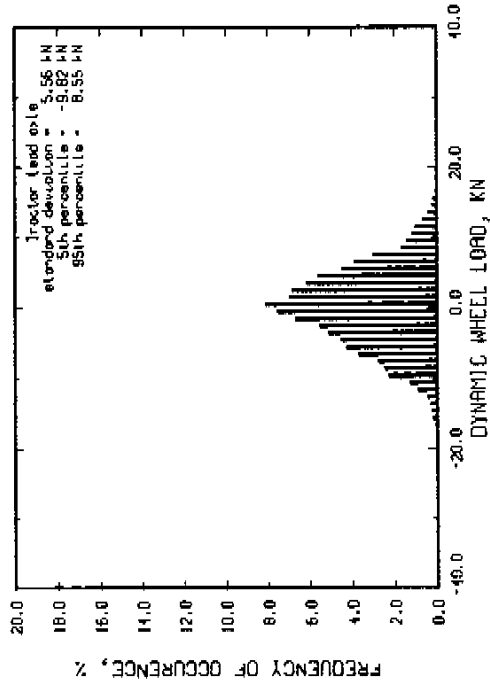
Run # 175 Speed = 40 km/hr
 Mays roughness = 73 IPH Trolley axle spread = 1.27 m
 Trolley suspension : spring suspended walking beam
 Trolley suspension : air bags
 flr suspension lift axle down



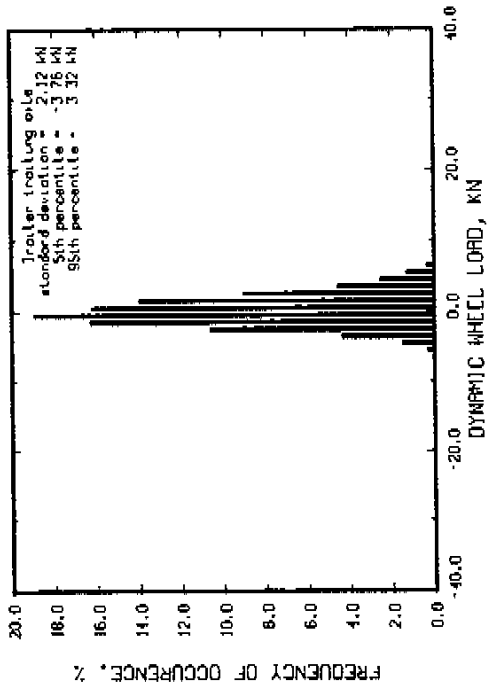
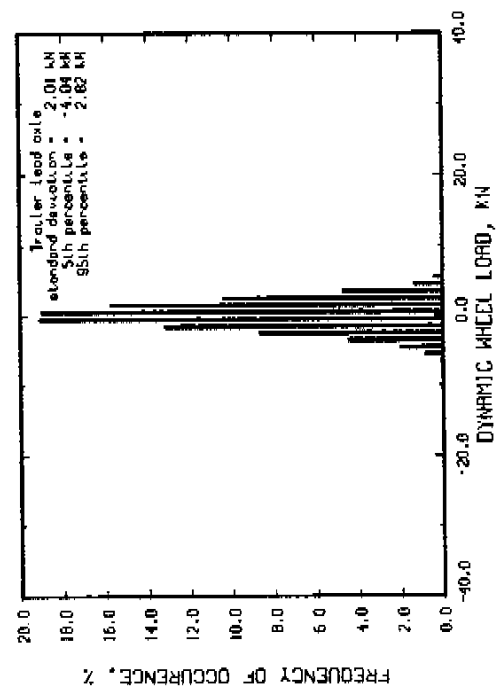
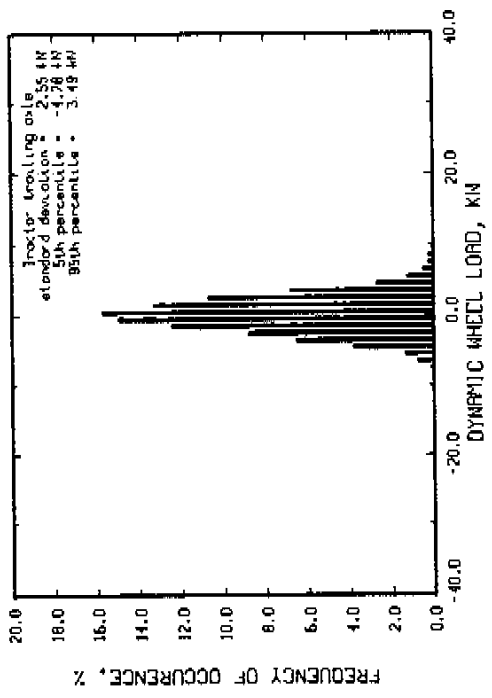
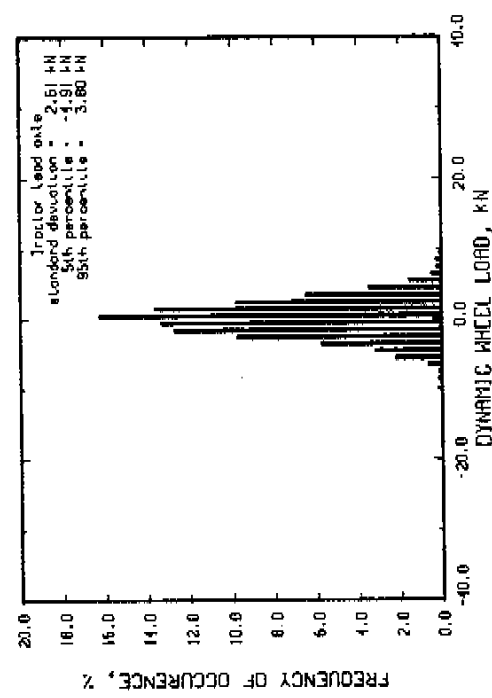
Run # 160 Part 1
 Speed = 40 km/hr
 Hoys roughness = 254 IPH
 Tractor axle spread = 1.27 m
 Tractor suspension : spring suspended walking beam
 Tractor suspension : air bags
 R/R suspension lift axle down



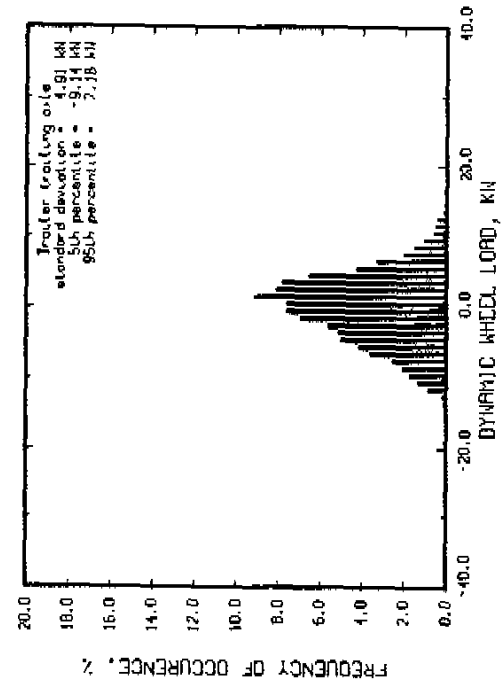
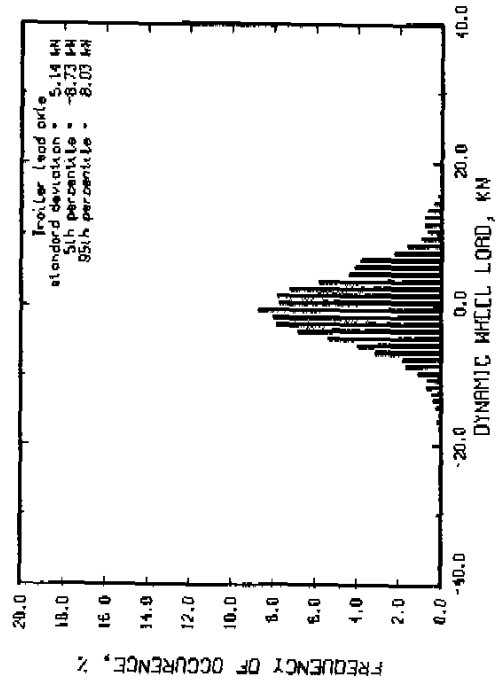
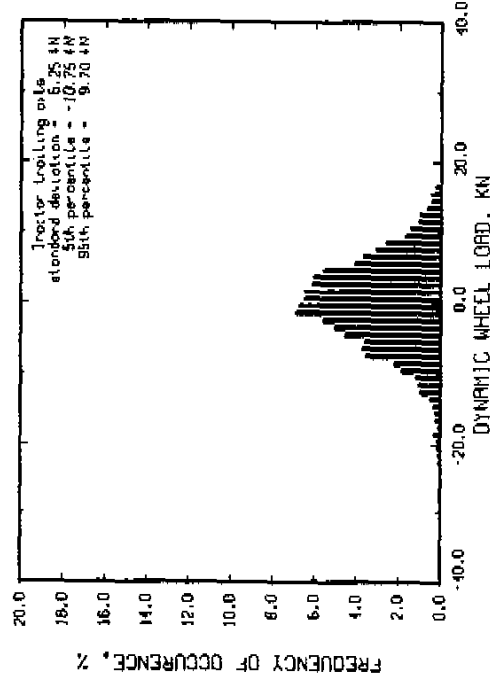
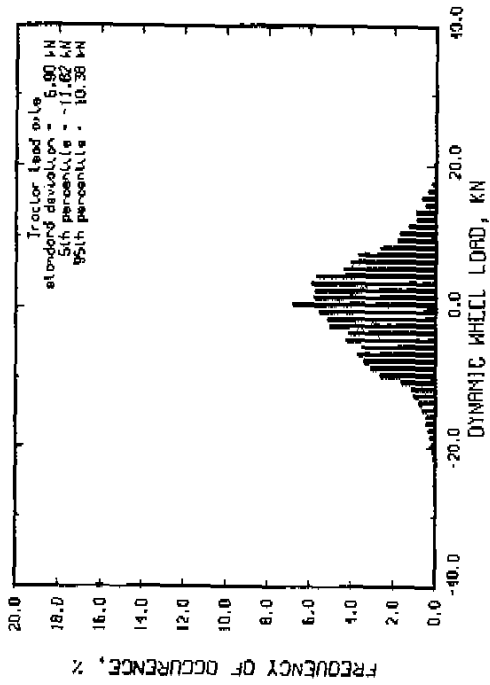
Run # 160 Part 2 Speed = 40 km/hr
 Hays roughness = 424 IPH Tractor axle spread = 1.27 m
 Tractor suspension : spring suspended walking beam
 Tractor suspension : air bogs
 Tractor suspension lift axle down



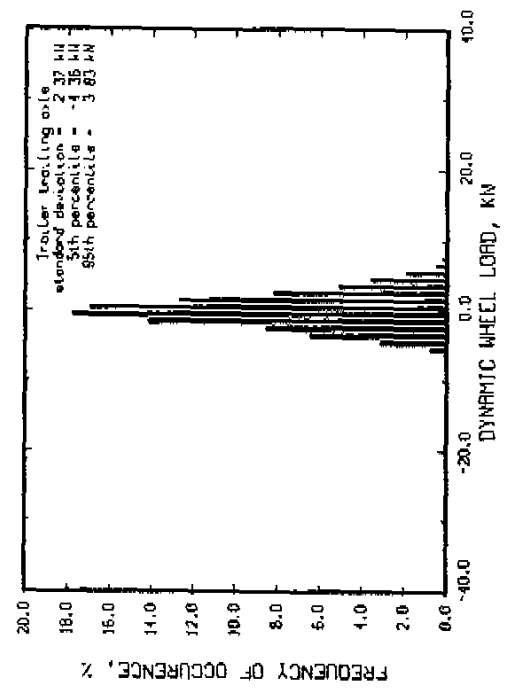
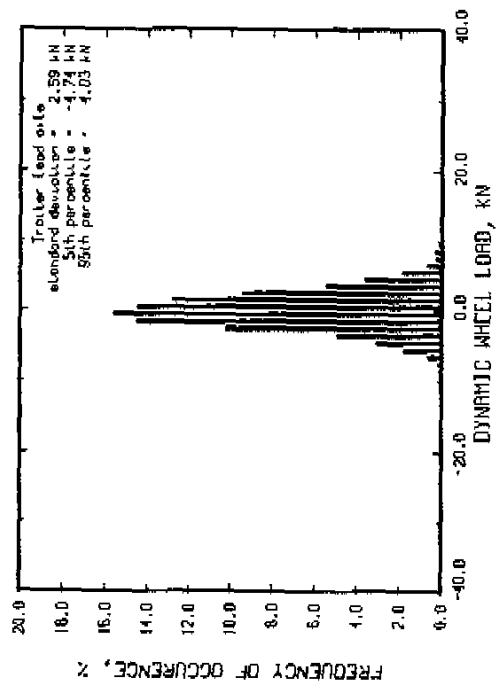
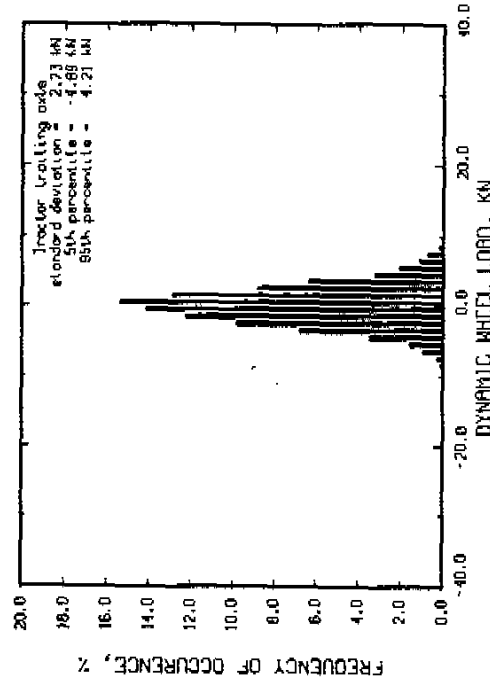
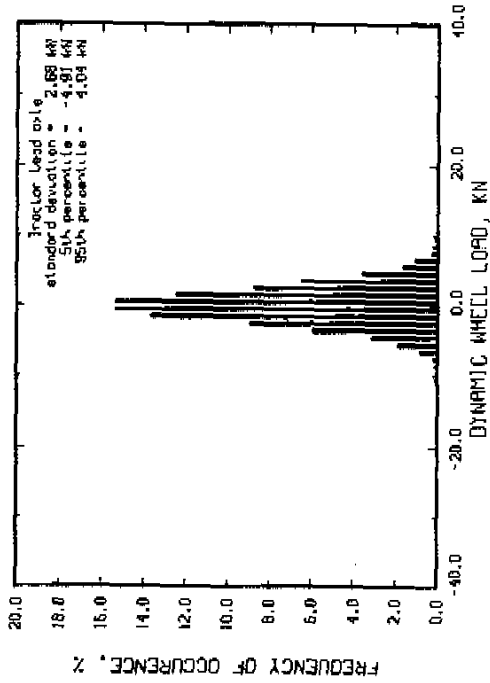
Run # 173 Speed = 60 km/hr
 Moys roughness = 73 JPM Trailer axle spread = 1.27 m
 Tractor suspension : spring suspended walking beam
 Trailer suspension : air bags
 Air suspension left axle down



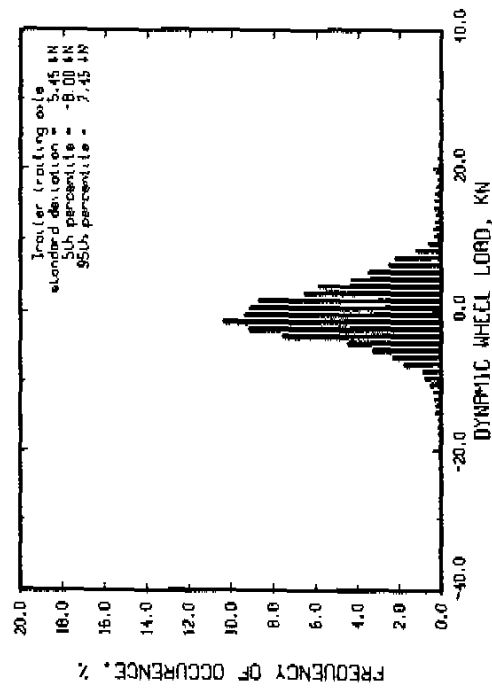
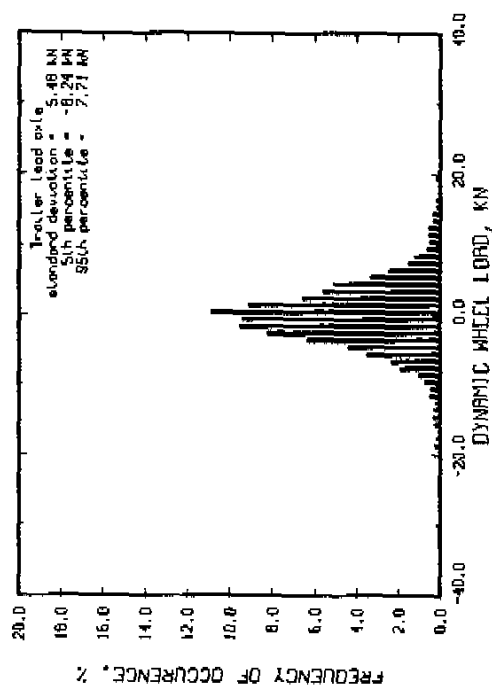
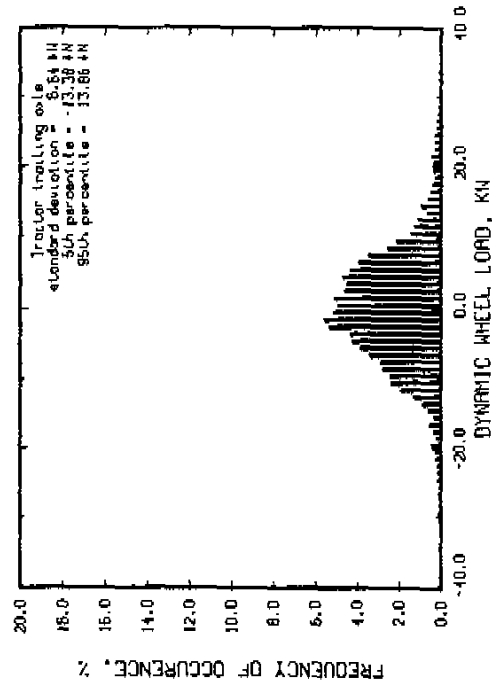
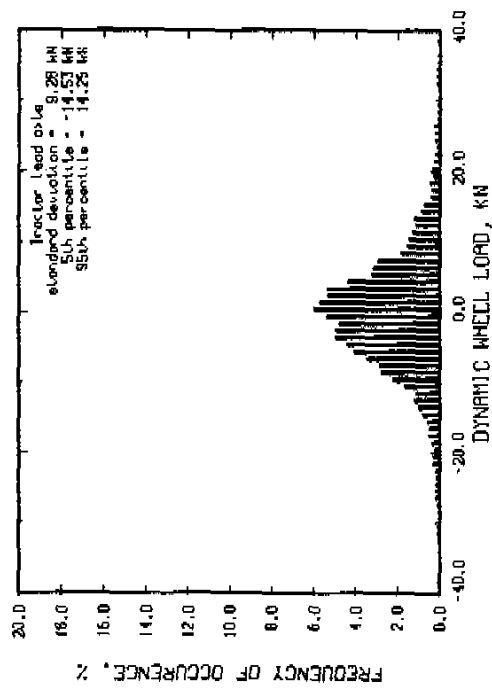
Run # 153 PART 1 Speed = 60 km/hr
 Hays roughness = 254 IPH Trailer axle spread = 1.27 m
 Tractor suspension : spring suspended walking beam
 Trailer suspension : air bags
 R/R suspension lift axle down



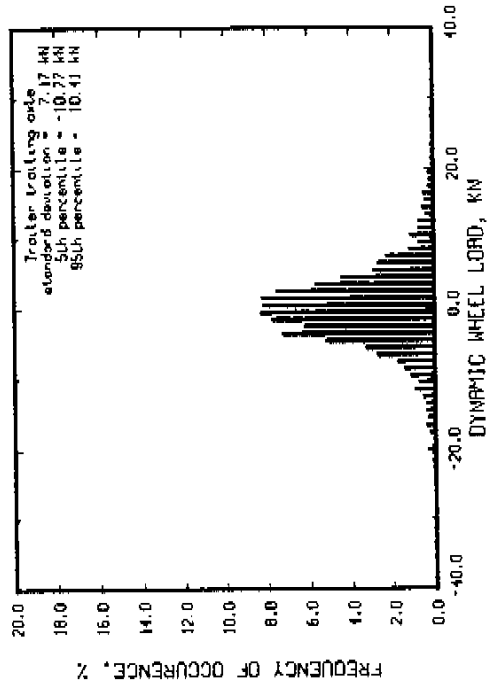
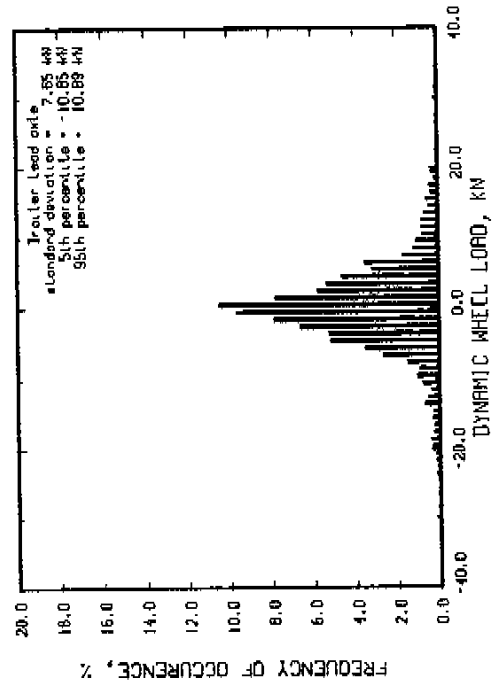
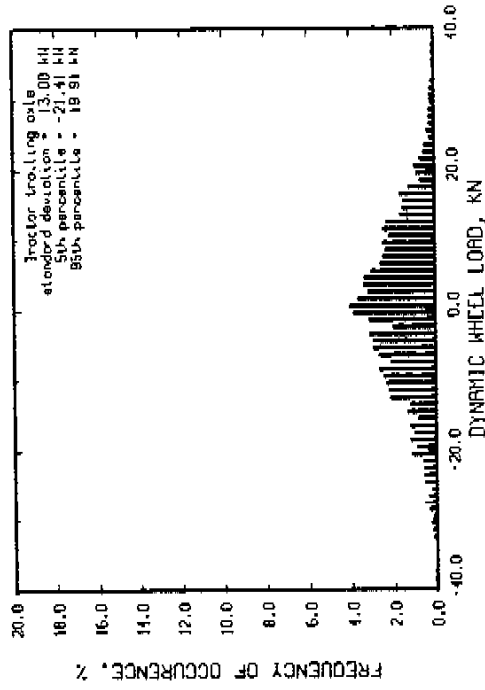
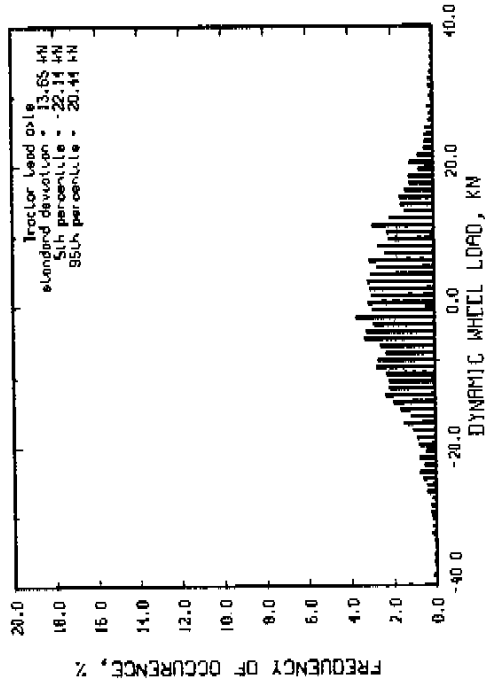
Run # 175 Part 2
 Max roughness = 59 IPH
 Speed = 80 km/hr
 Tractor axle spread = 1.27 m
 Tractor suspension : spring suspended walking beam
 Tractor suspension : air bags
 R/R suspension lift axle down



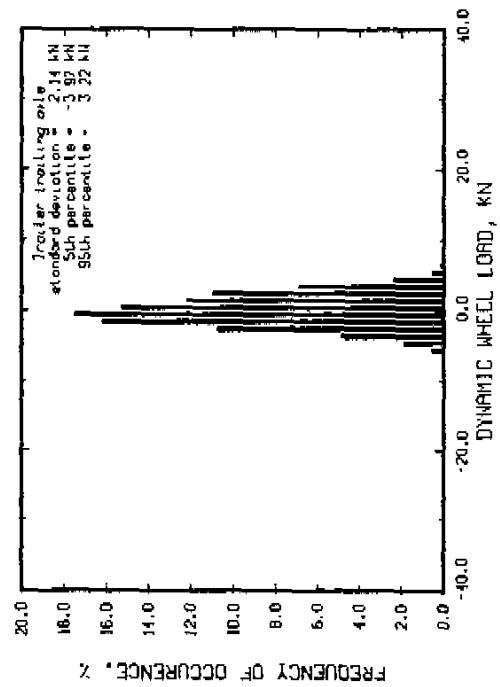
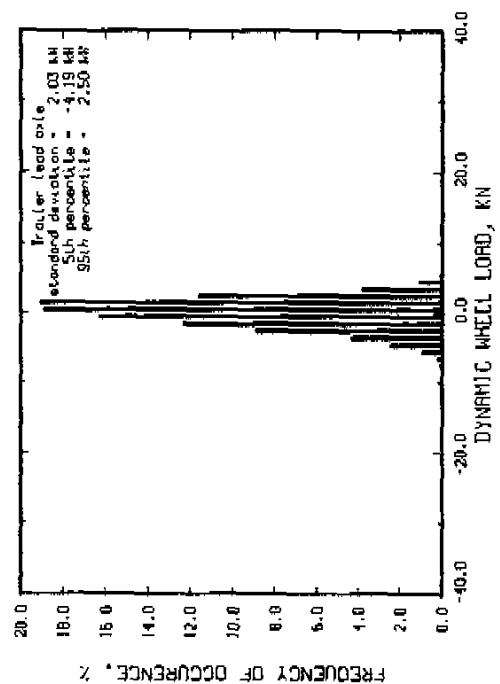
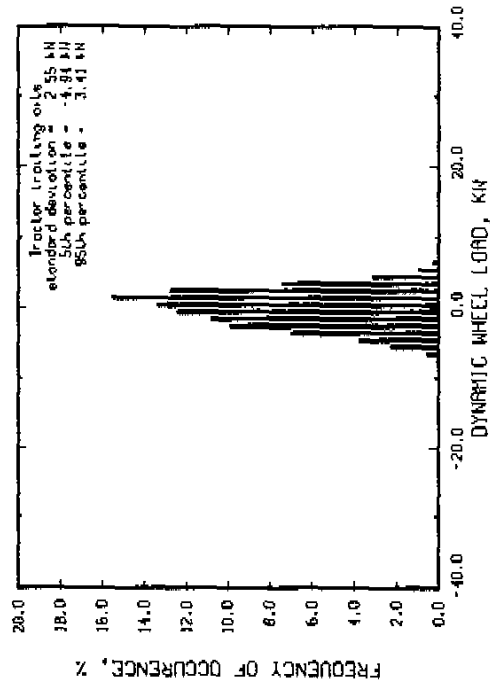
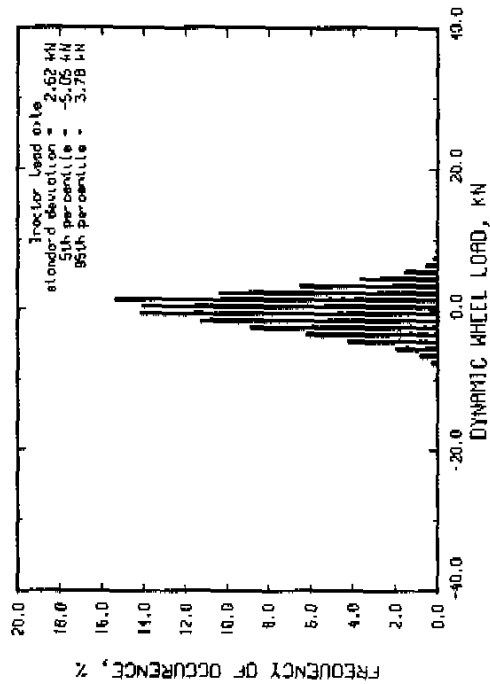
Run # 176 PART 1 Speed = 80 km/hr
 Moys roughness = 165 ipm Tractor axle spread = 1.27 m
 Tractor suspension : spring suspended walking beam
 Tractor suspension : air bags
 Air suspension lift axle down



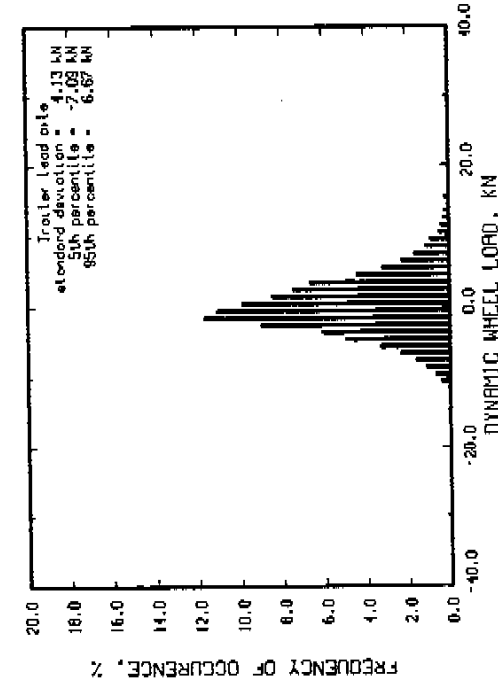
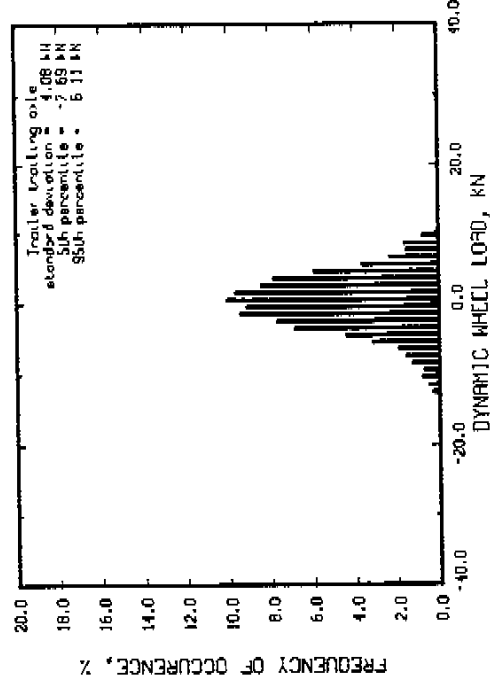
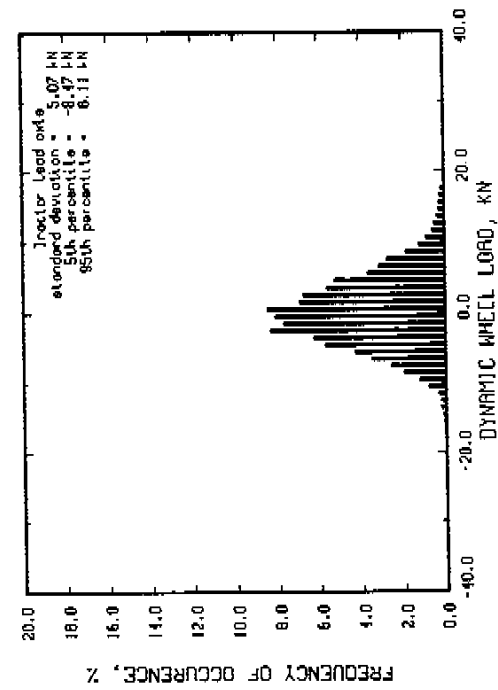
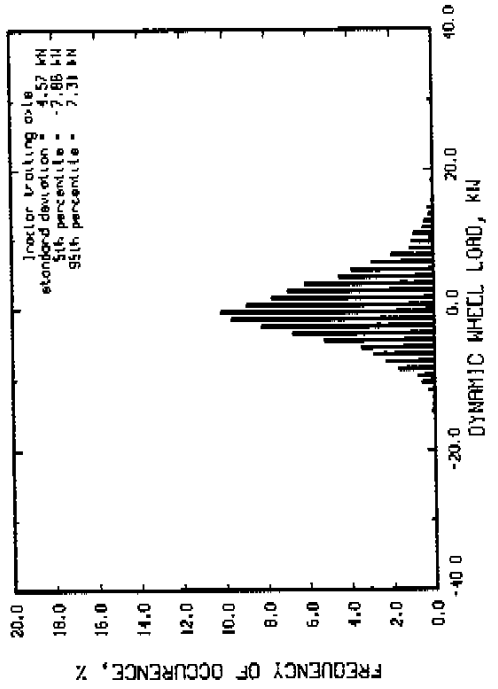
Run # 176 Part 3 Speed = 80 km/hr
 Moys roughness = 217 IPM Tractor axle spread = 1.27 m
 Tractor suspension : spring suspended walking beam
 Tractor suspension : air bags
 RLr suspension lift axle down



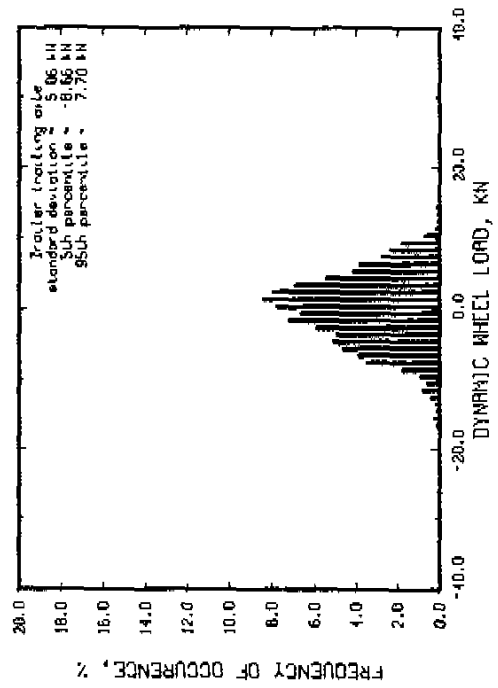
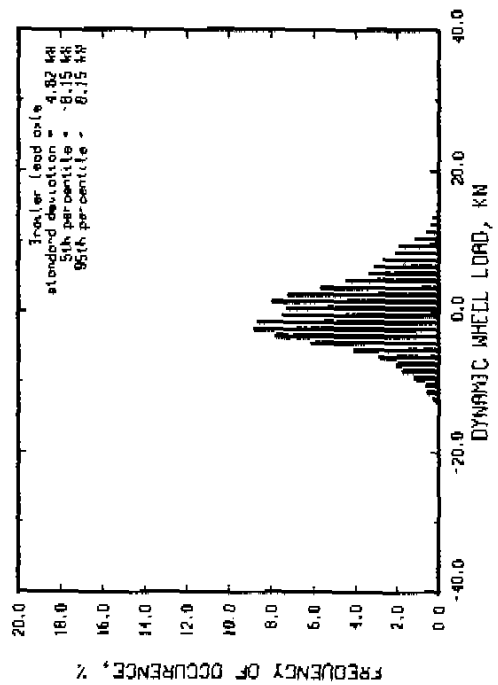
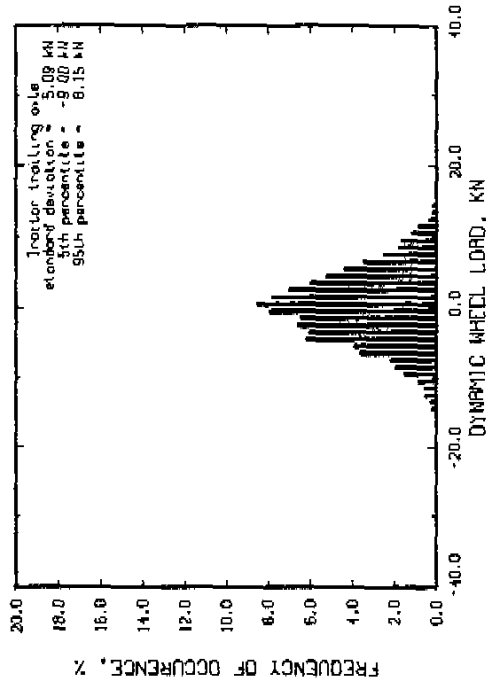
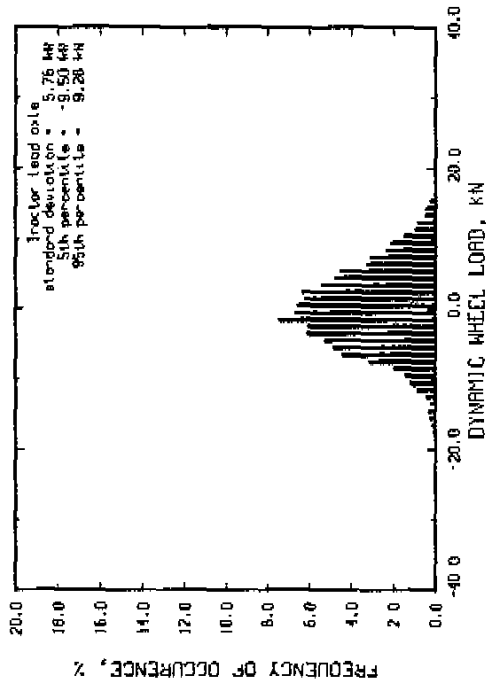
Run # 209
 Moys roughness = 73 IPI
 Speed = 40 km/hr
 Tractor suspension : spring suspended walking beam
 Trailer axle spread = 1.83 m
 Tractor suspension : air bags
 Air suspension lift axle up



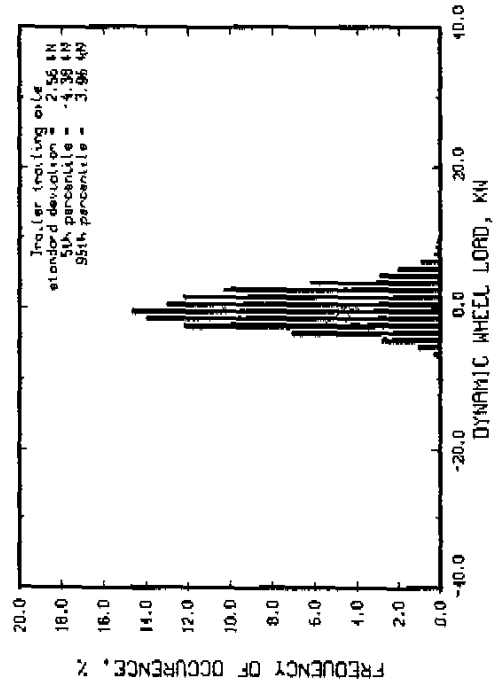
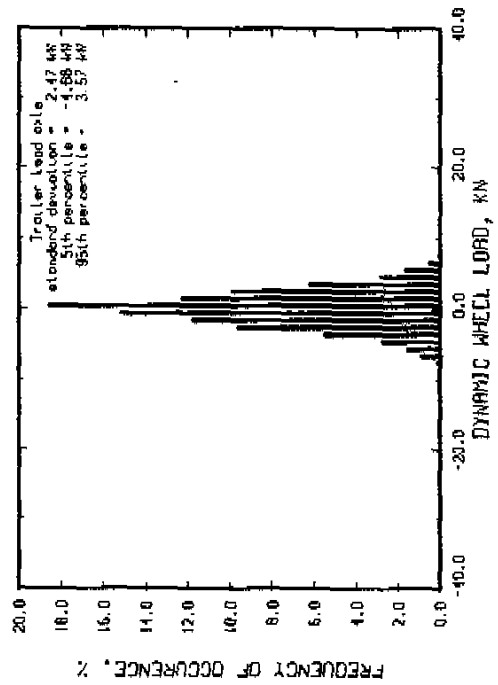
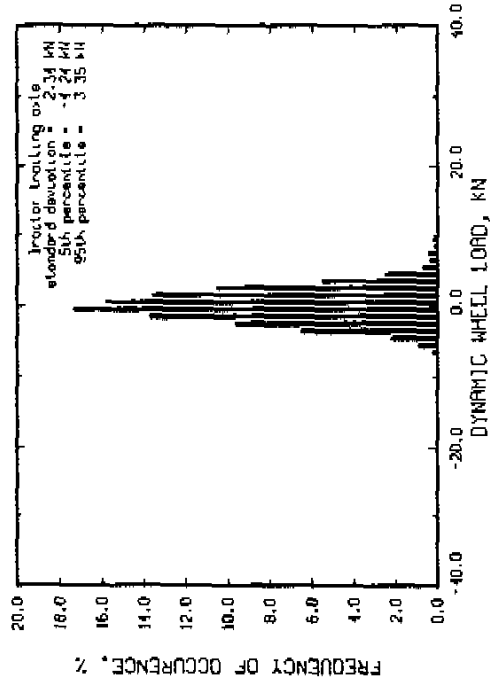
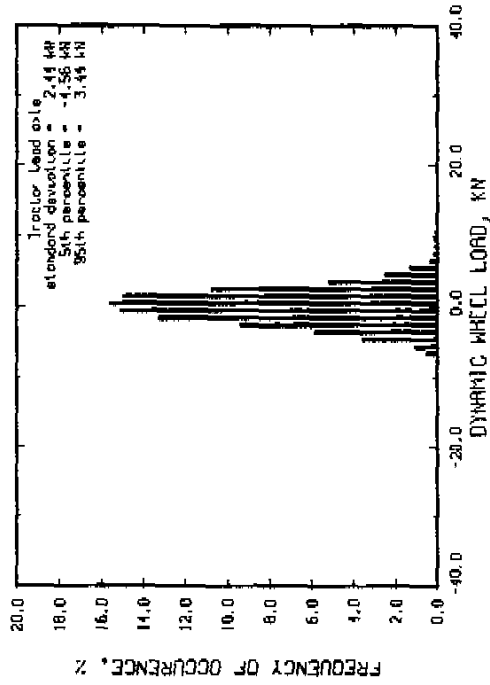
Run # 195 Part 1
 Speed = 40 km/hr
 Maye roughness = 254 IPM
 Trailer axle spread = 1.83 m
 Tractor suspension : spring suspended walking beam
 Trailer suspension : air bags
 Air suspension lift axle up



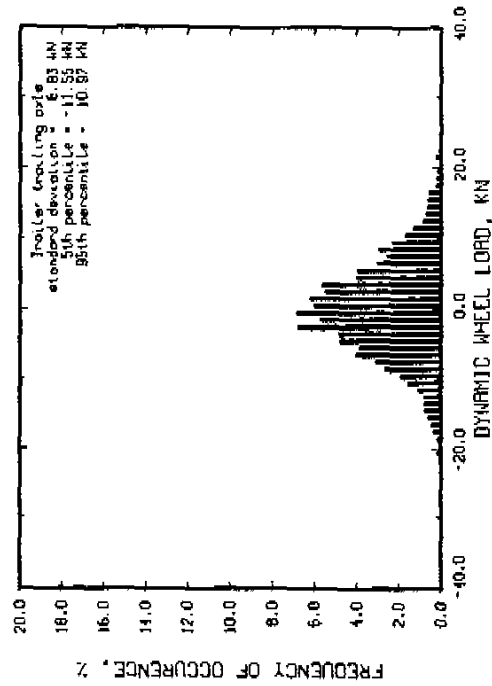
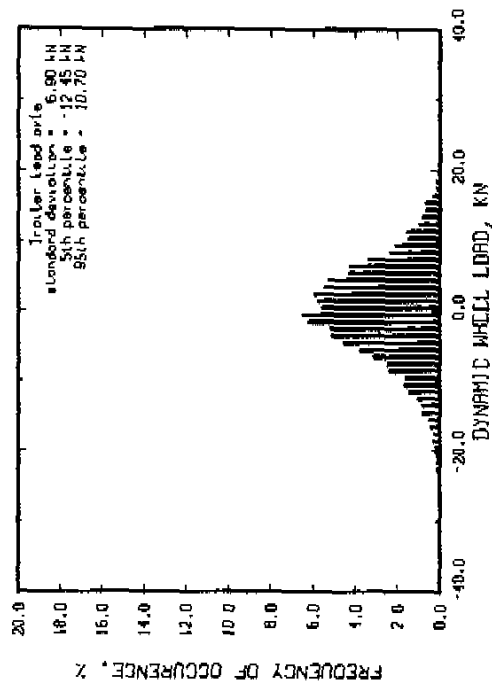
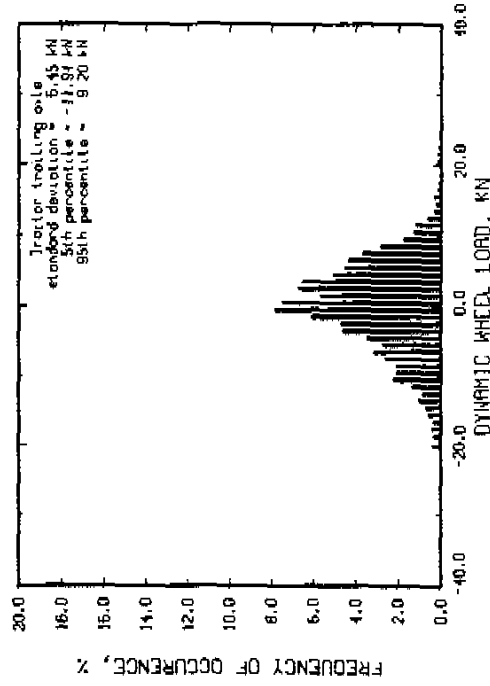
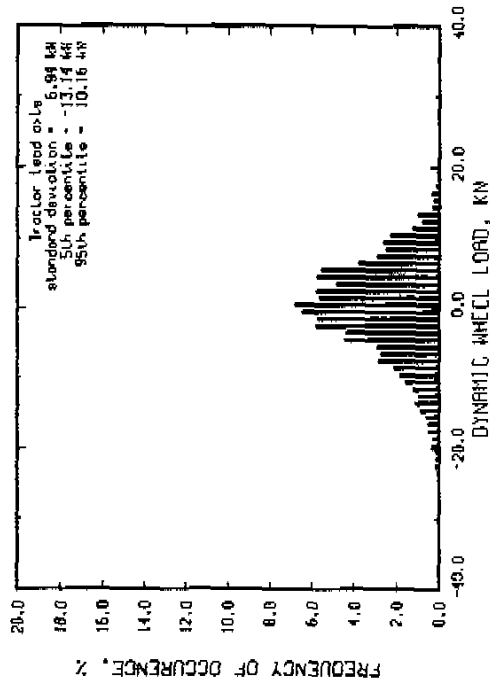
Run # 195 Part 2
 Moys roughness = 424 JPH
 Speed = 40 km/hr
 Trailer axle spread = 1.63 m
 tractor suspension : spring suspended walking beam
 tractor suspension : air bags
 air suspension lift axle up



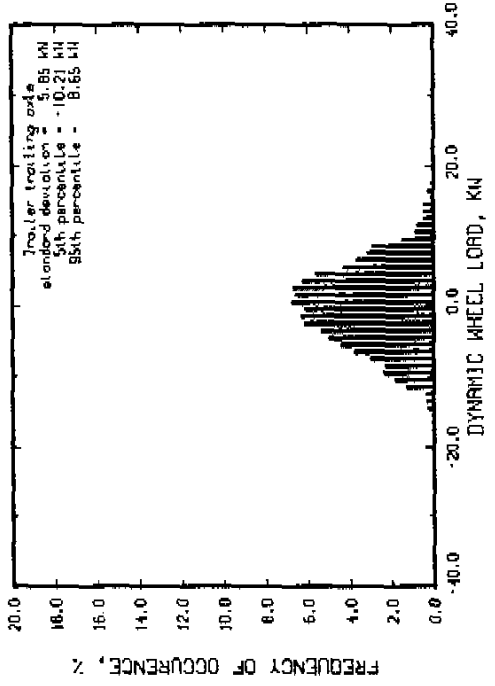
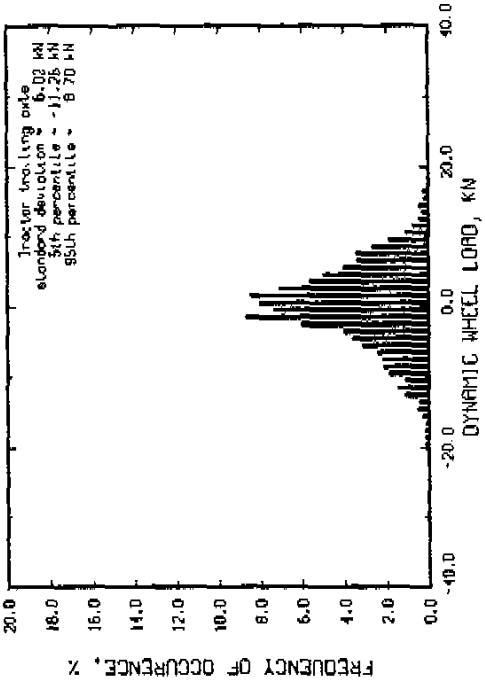
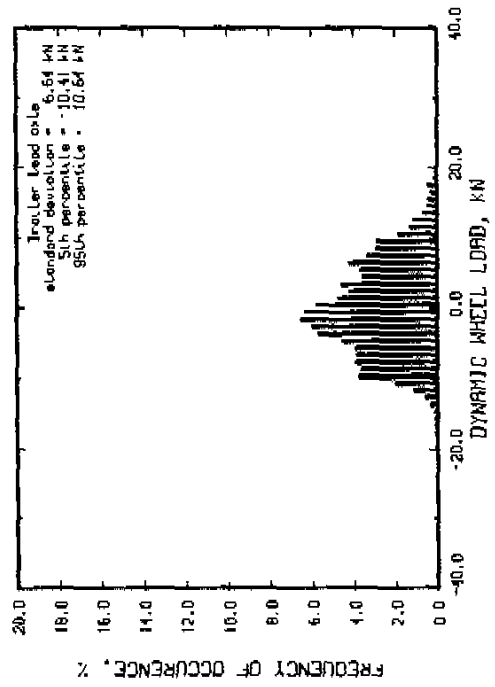
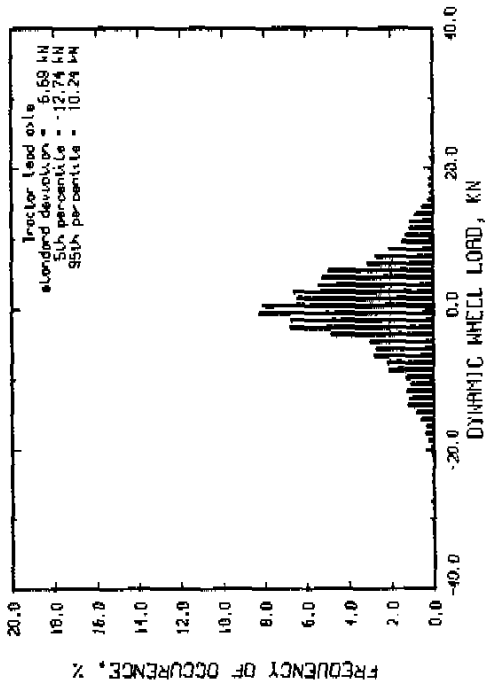
Run # 207 Speed = 50 km/hr
 Moys roughness = 73 JPH Tractor axle spread = 1.83 m
 Tractor suspension : sprung suspended working beam
 Tractor suspension : air bags
 Rtr suspension lift axle up



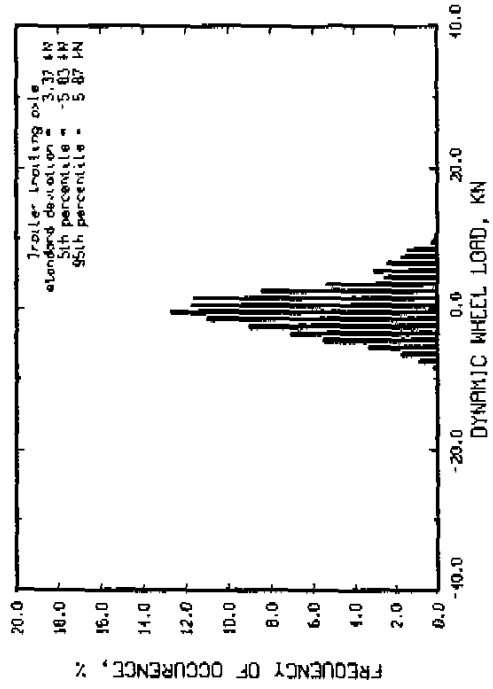
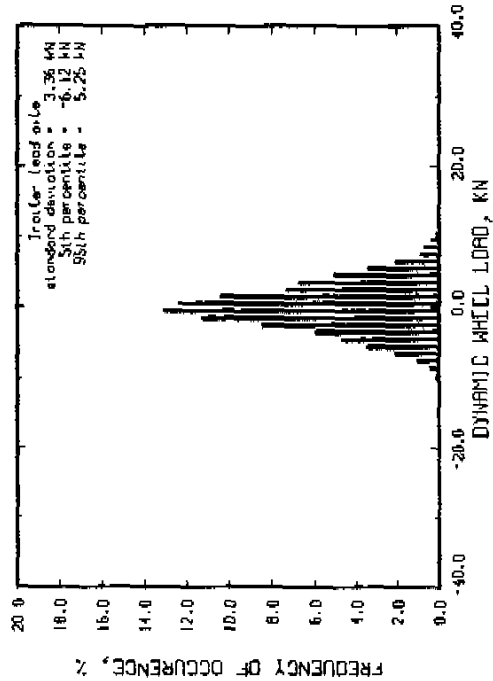
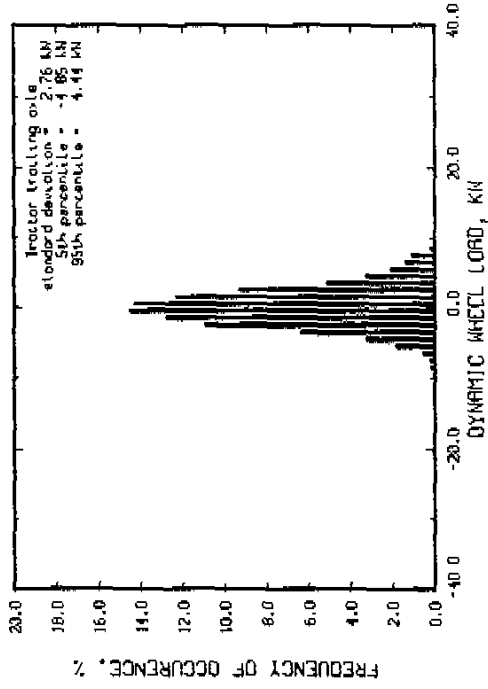
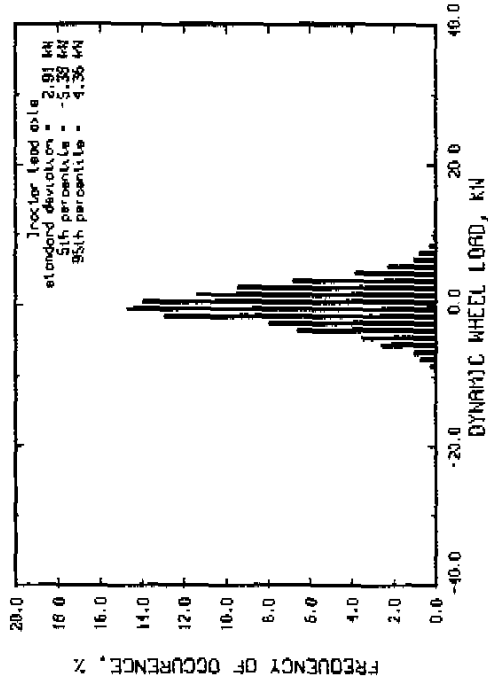
Run # 198 Part 1 Speed = 60 km/hr
 Hays roughness = 254 IPI Tractor axle spread = 1.83 m
 tractor suspension : spring suspended walking beam
 trailer suspension : air bags
 air suspension lift axle up



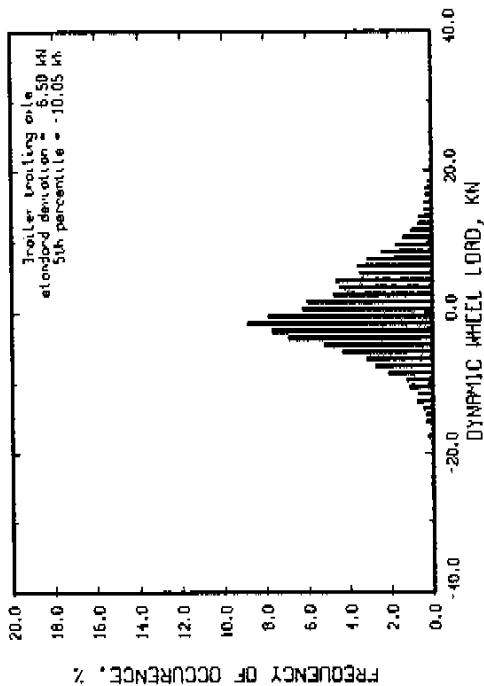
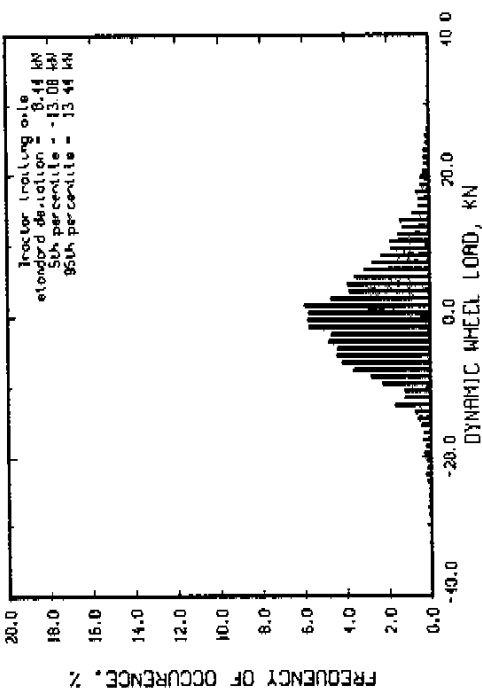
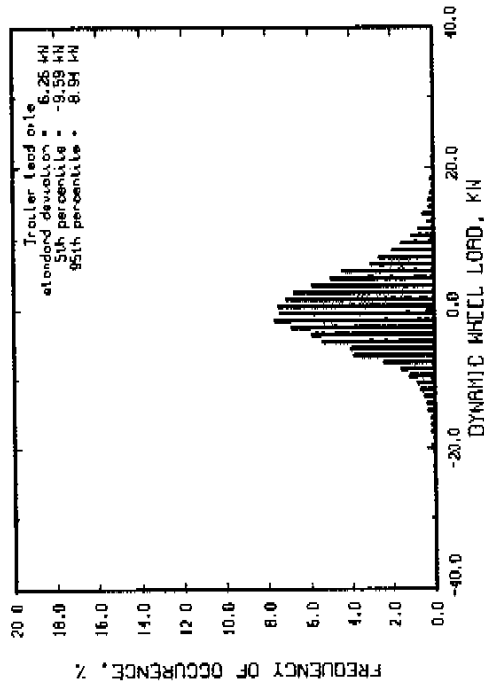
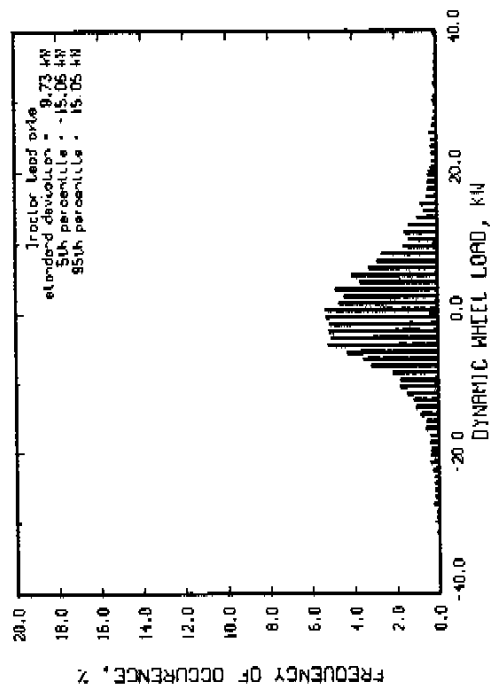
Run # 198 Part 2
 Speed = 60 km/hr
 Moys roughness = 424 JPH
 Tractor axle spread = 1.63 m
 Tractor suspension : sprung suspended walking beam
 Tractor suspension : air bogs
 R/R suspension lift axle up



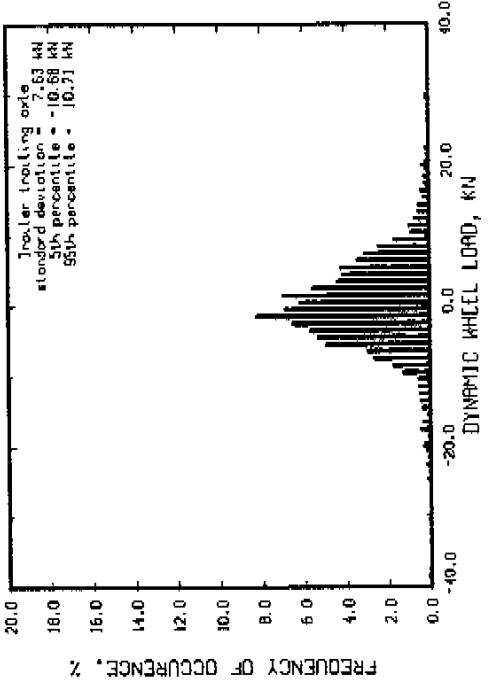
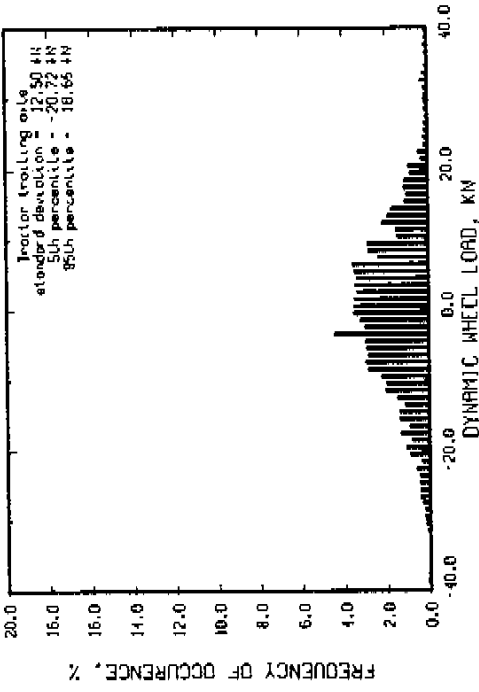
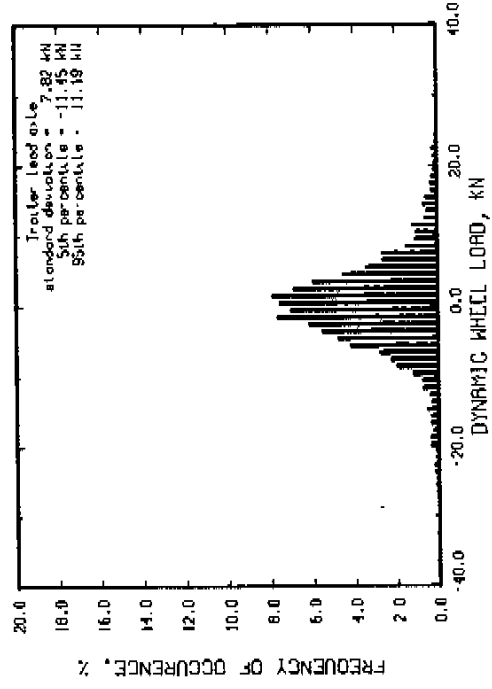
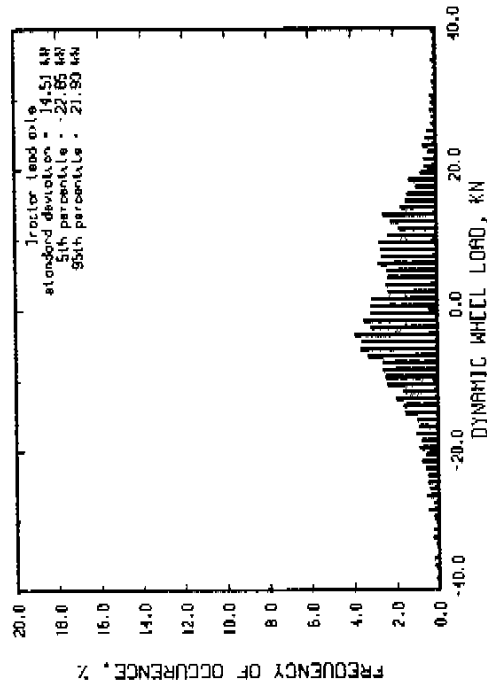
Run # 216 Part 2 Speed = 80 km/hr
 Moys roughness = 59 jpm Trailer axle spread = 1.83 m
 Trailer suspension : spring suspended walking beam
 Trailer suspension : air bags
 Air suspension left axle up



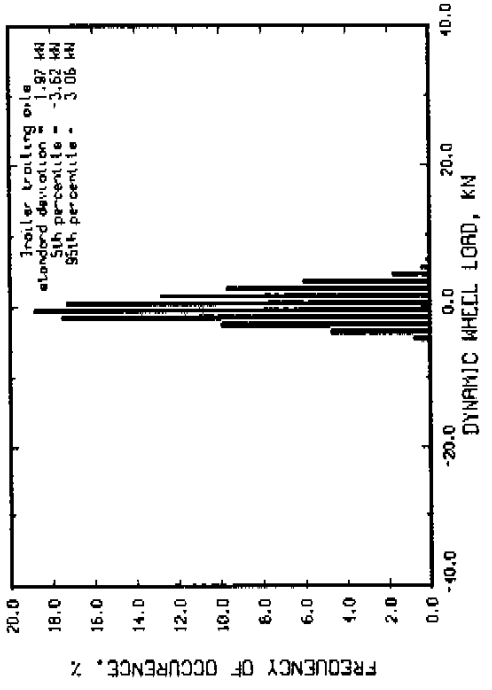
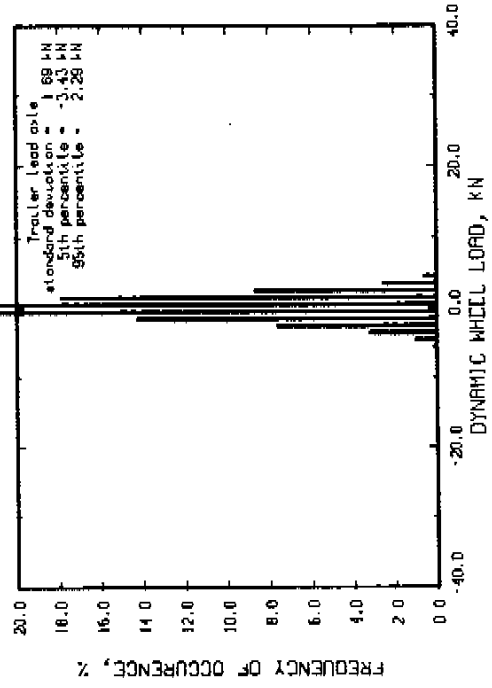
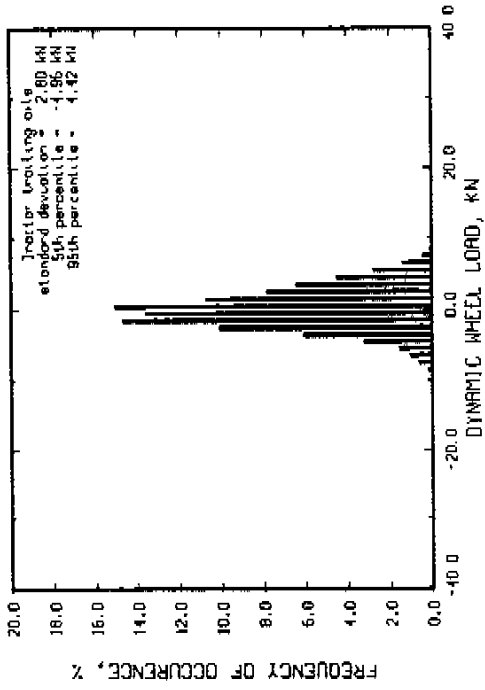
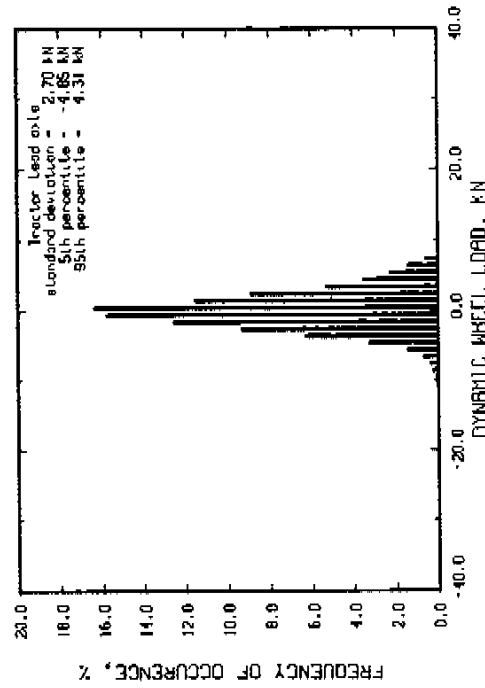
Run # 216 Part 1 Speed = 60 km/hr
 Mays roughness = 155 IPH Tractor axle spread = 1.83 m
 Tractor suspension : spring suspended walking beam
 Tractor suspension : air bags
 R/R suspension lift axle up



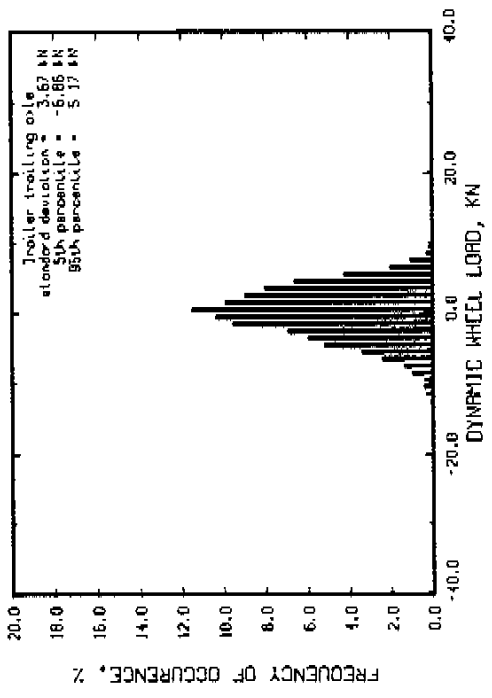
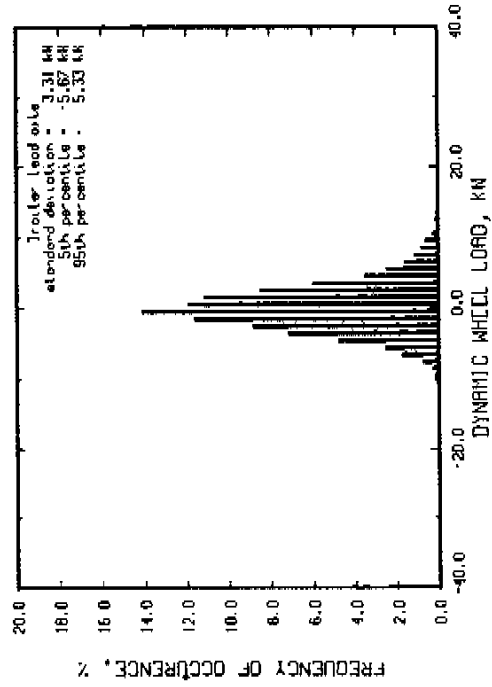
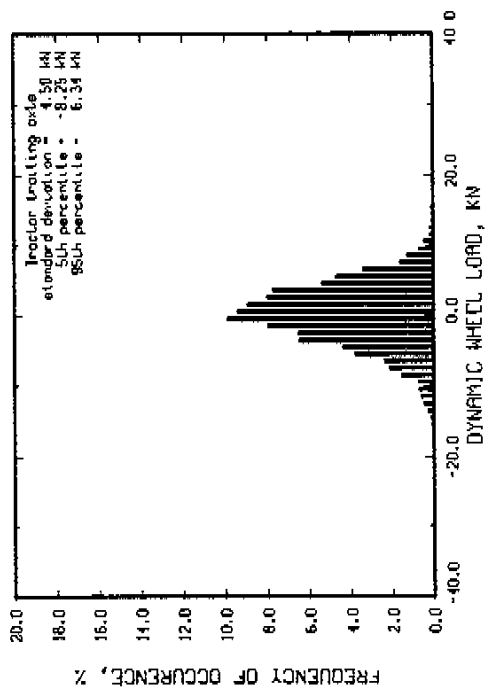
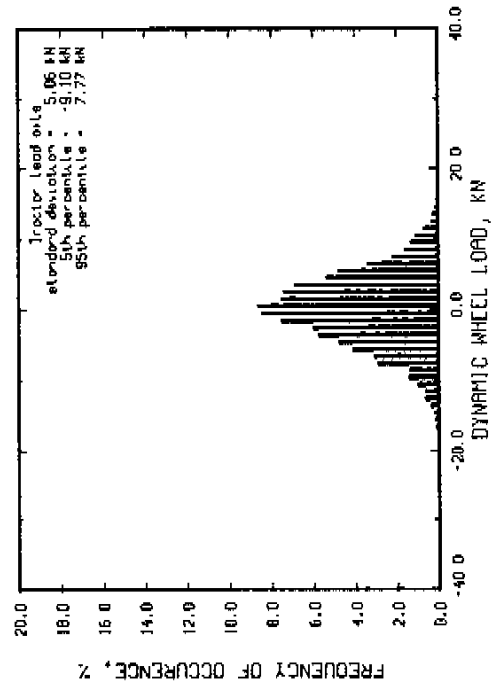
Run # 216 Part 3 Speed = 80 km/hr
 Moys roughness = 217 IPM Trailer axle spread = 1.83 m
 Tractor suspension : spring suspended walking beam
 Trailer suspension : air bags
 Tractor suspension : air bags
 Air suspension lift axle up



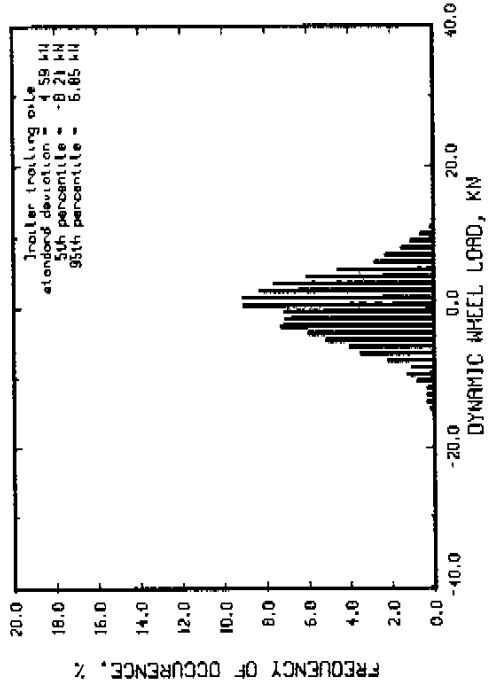
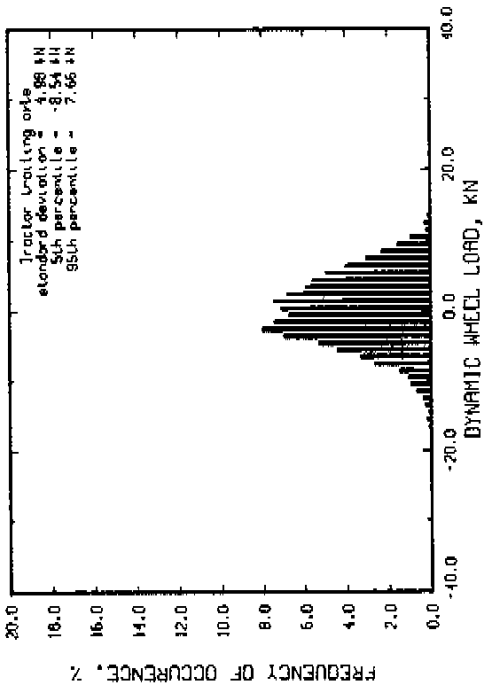
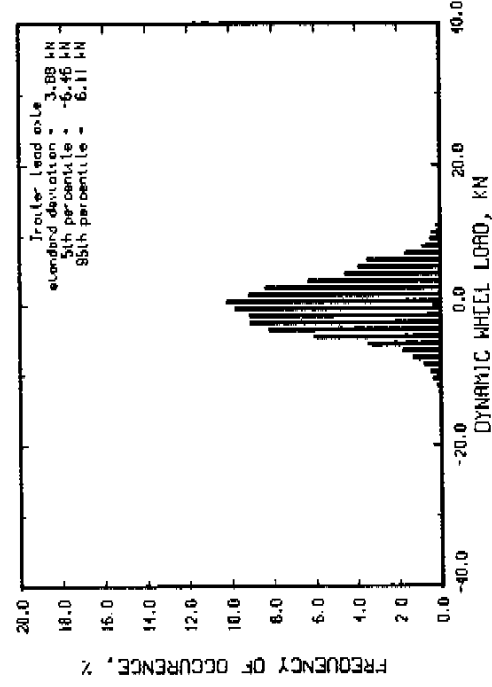
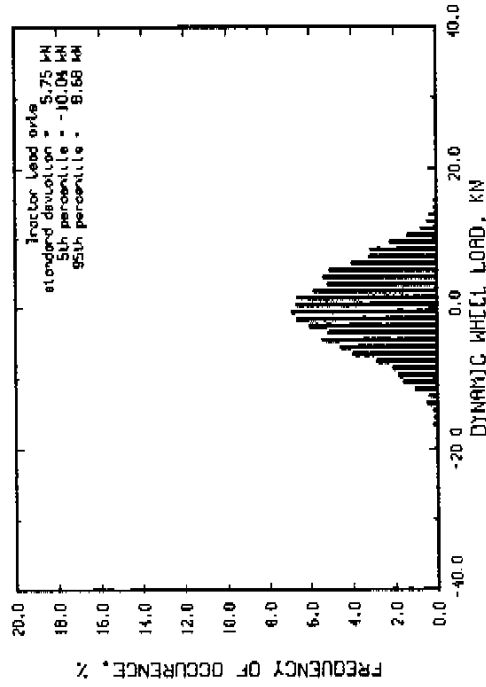
Run # 213
 Speed = 40 km/hr
 Hoys roughness = 73 1PK
 Tractor axle spread = 1.83 m
 Tractor suspension : spring suspended walking beam
 Trailer suspension : air bags
 Air suspension lift axle down



Run # 201 Part 1
 Speed = 40 km/hr
 Hoys roughness = 254 IPM
 Tractor axle spread = 1.63 m
 Tractor suspension : spring suspended walking beam
 Tractor suspension : air bogs
 Tractor suspension lift axle down

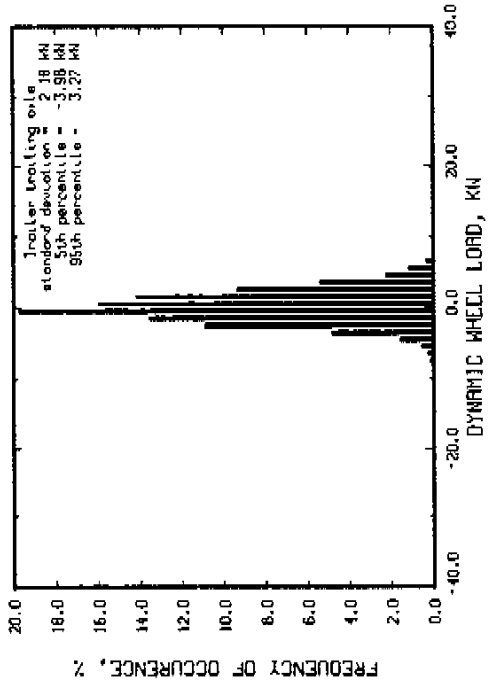
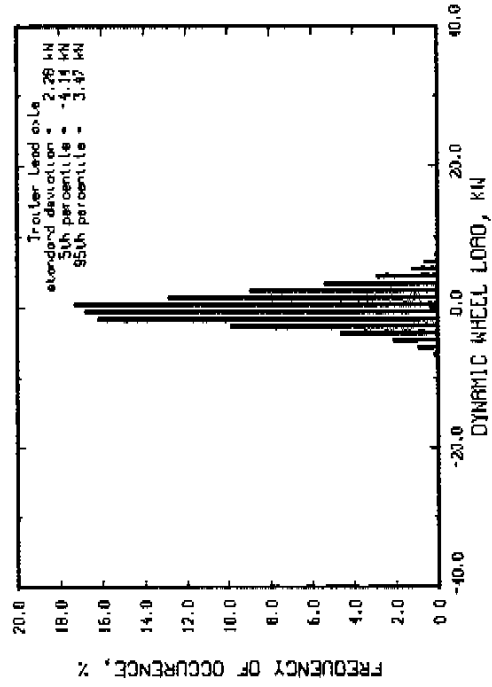
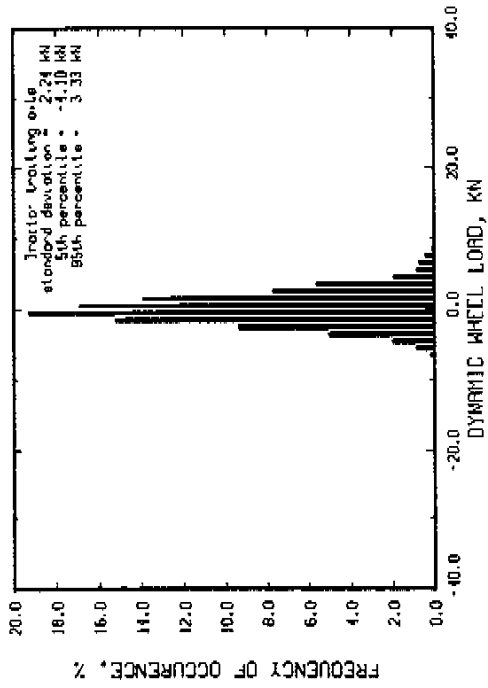
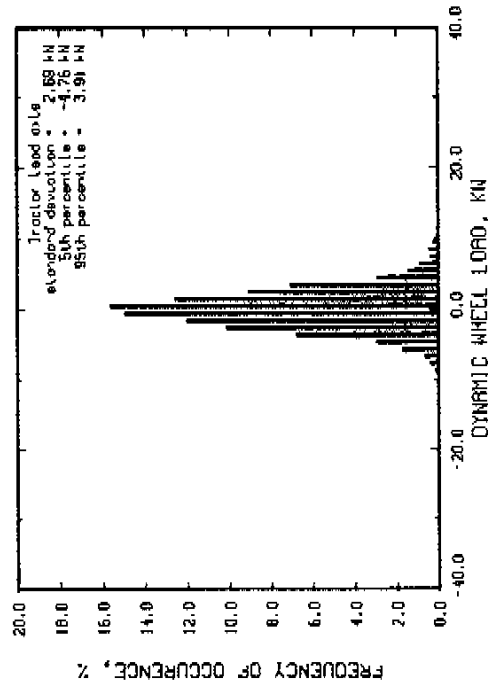


Run # 201 Part 2 Speed = 40 km/hr
 Moys roughness = 424 IPM Trailer axle spread = 1.83 m
 Tractor suspension : spring suspended walking beam
 Trailer suspension : air bags
 Air suspension lift axle down

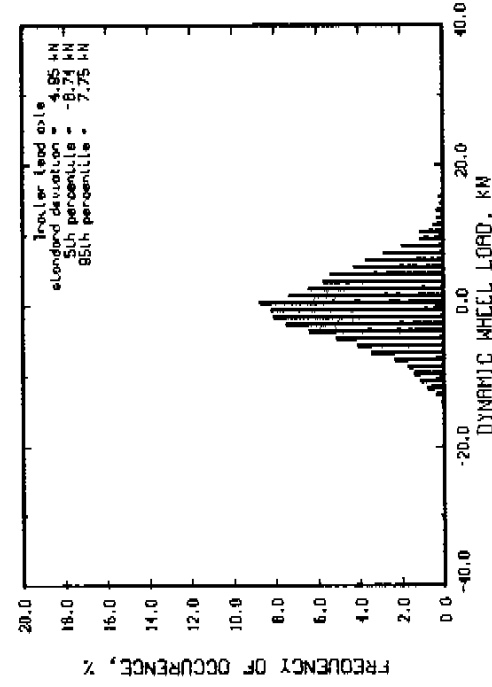
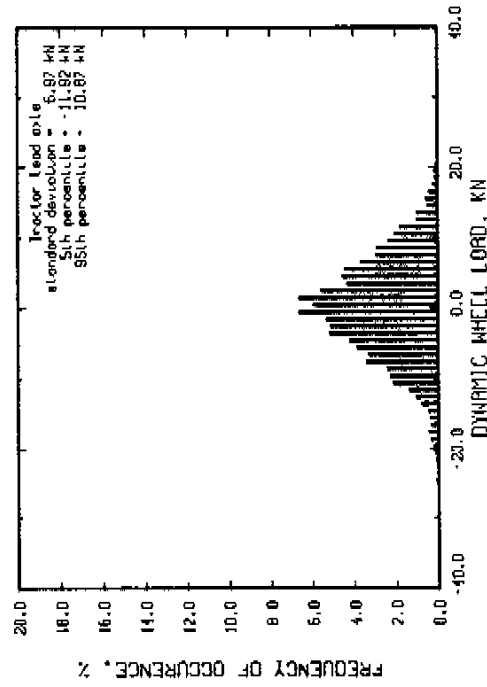
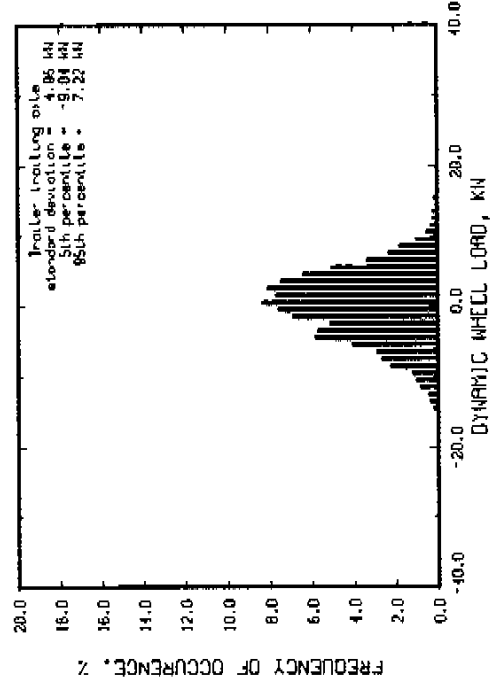
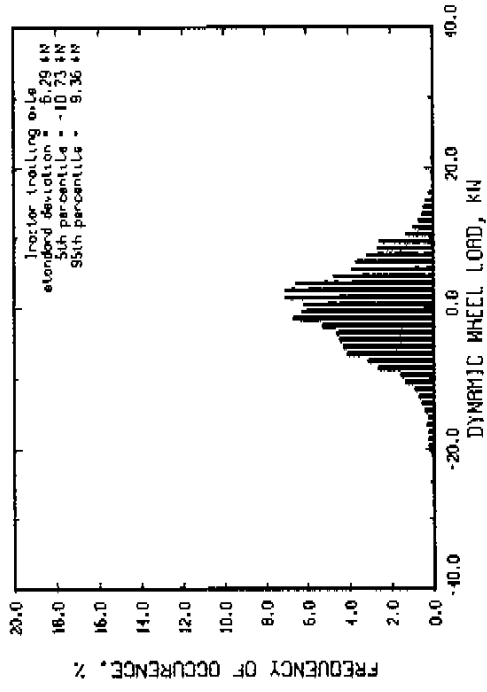


F65

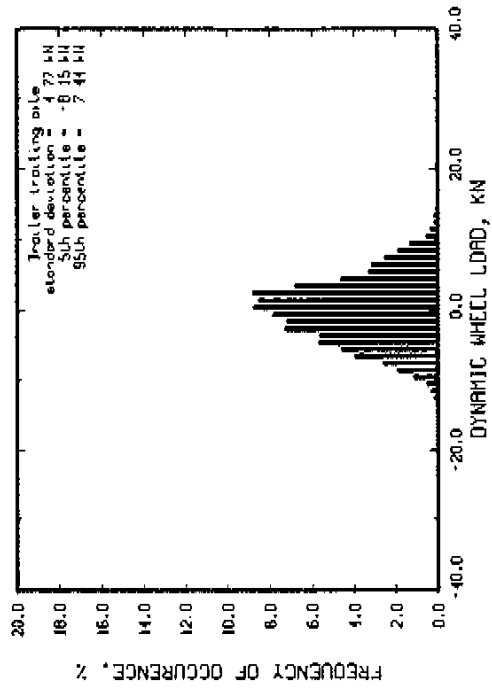
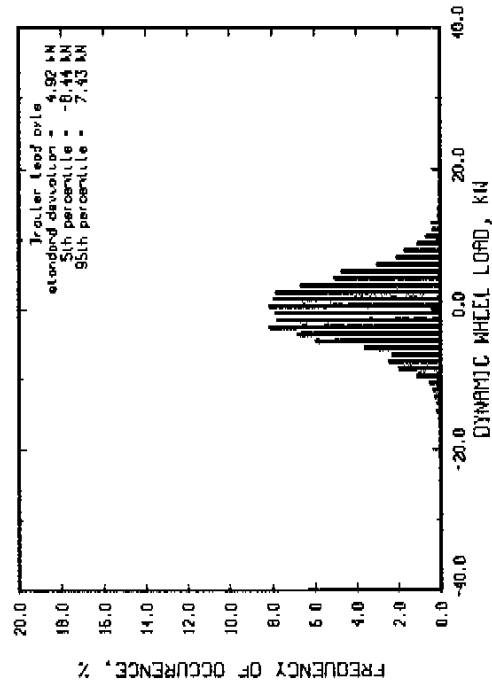
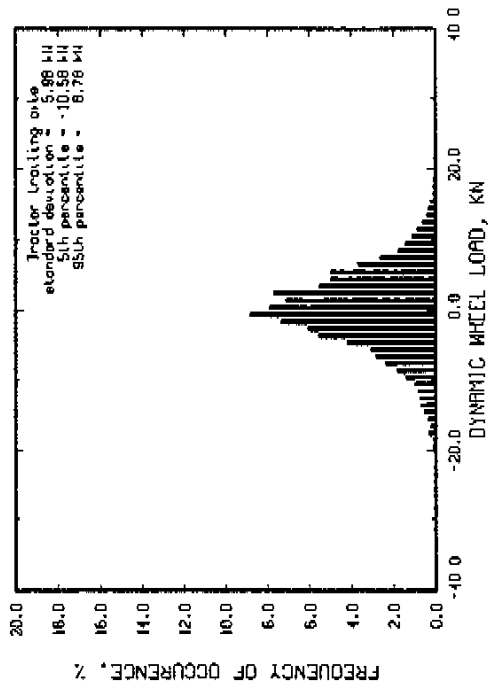
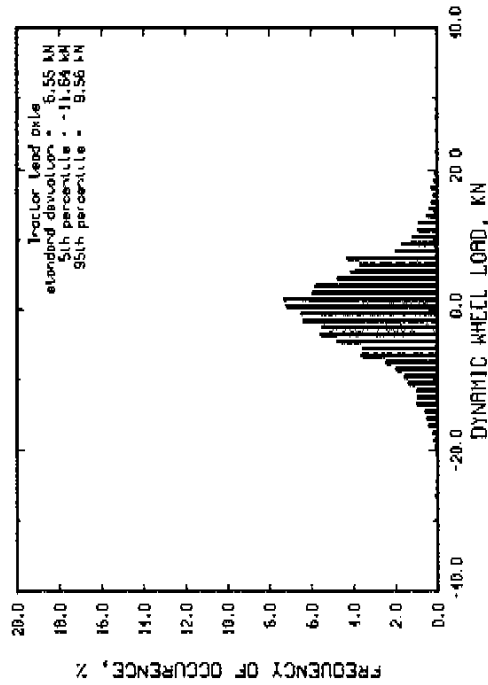
Run # 211 Speed = 60 km/hr
 Moys roughness = 73 IPI Trailer axle spread = 1.83 m
 tractor suspension : spring suspended walking beam
 trailer suspension : air bags
 air suspension lift axle down



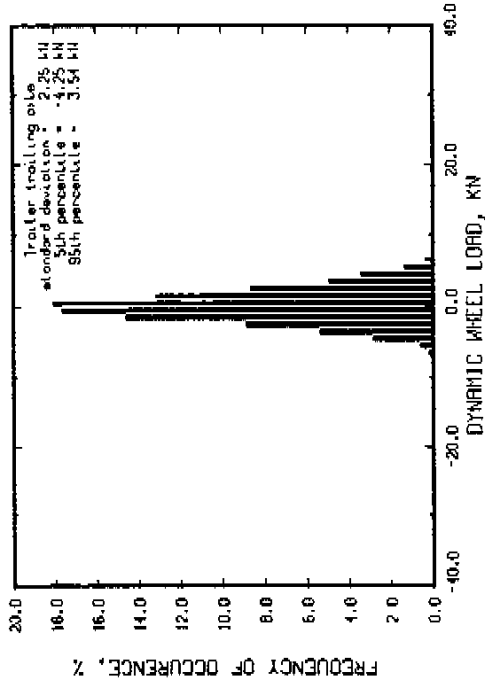
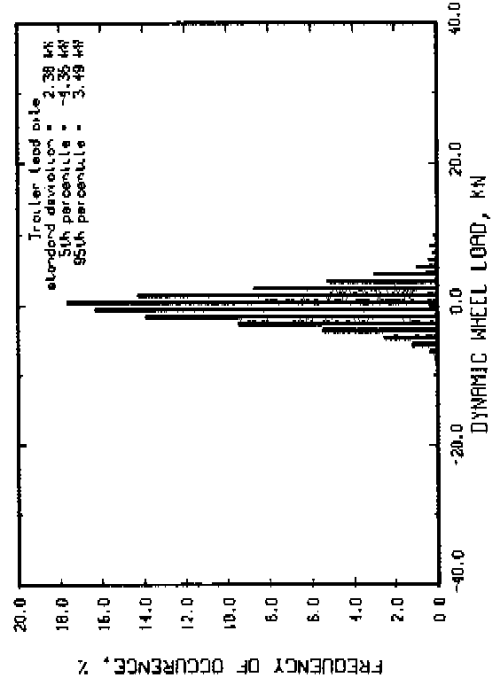
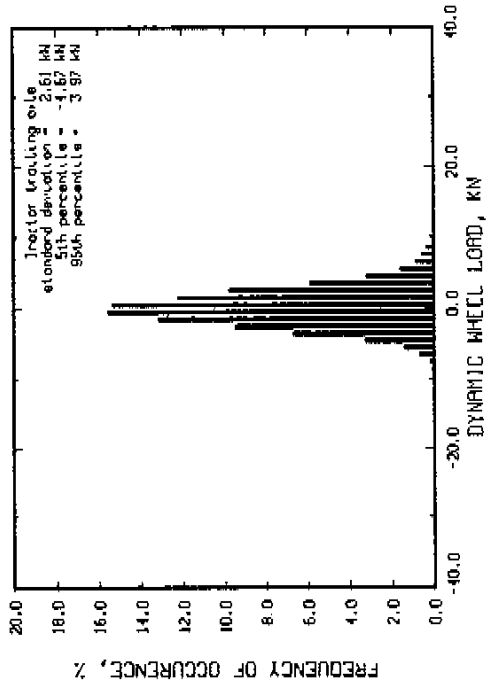
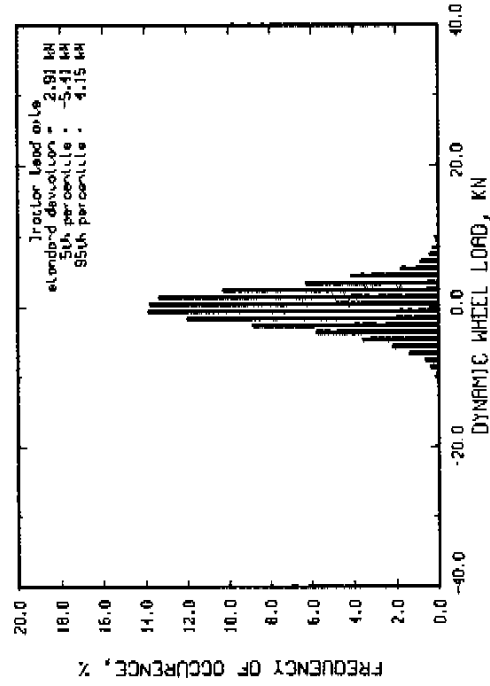
Run # 204 Part 1
 Speed = 60 km/hr
 Mags roughness = 254 JPM
 Trailer axle spread = 1.83 m
 Tractor suspension : spring suspended walking beam
 Trailer suspension : air bags
 Flr suspension lift axle down



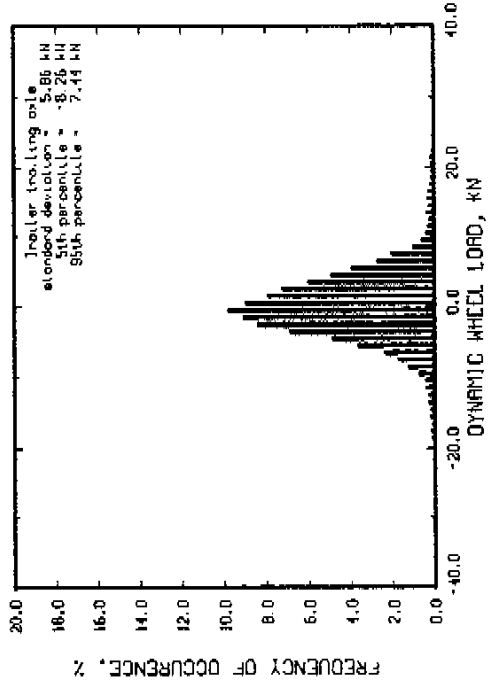
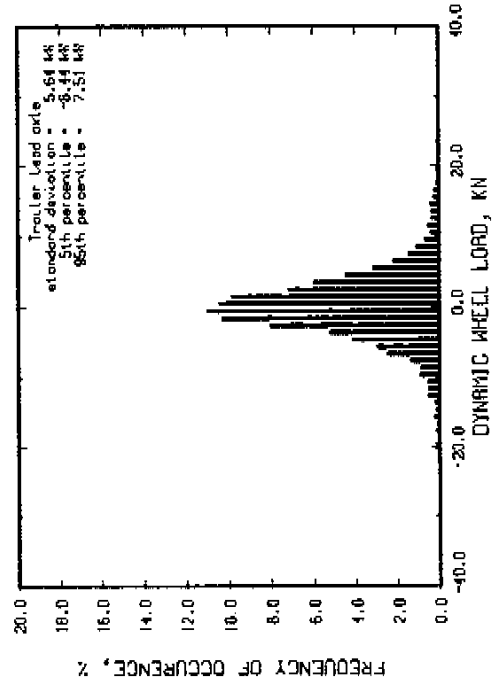
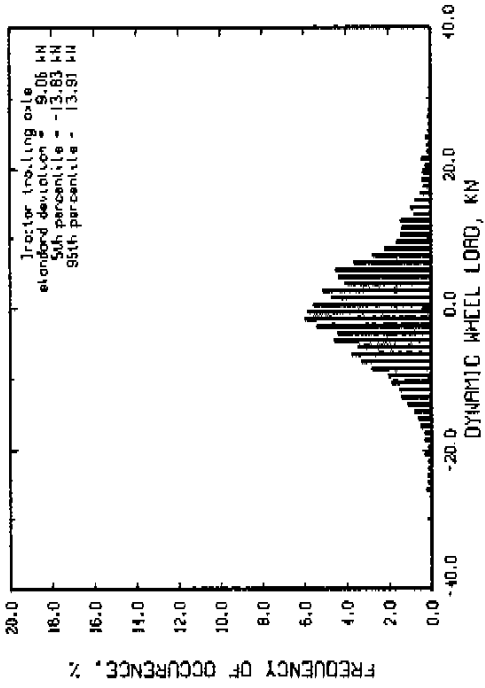
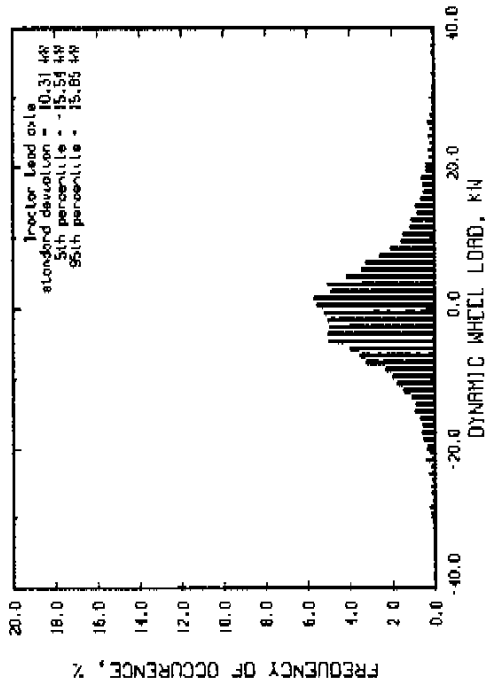
Run # 204 Part 2 Speed = 60 km/hr
 Moys roughness = 424 ipm Tractor axle spread = 1.83 m
 Tractor suspension : spring suspended walking beam
 Tractor suspension : air bags
 R/R suspension lift axle down



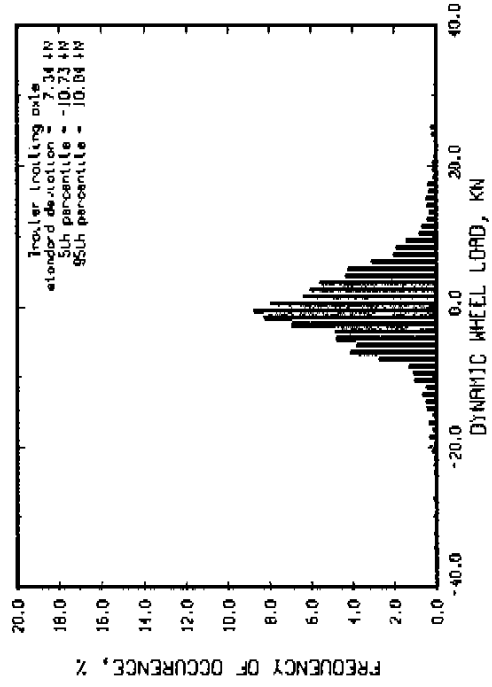
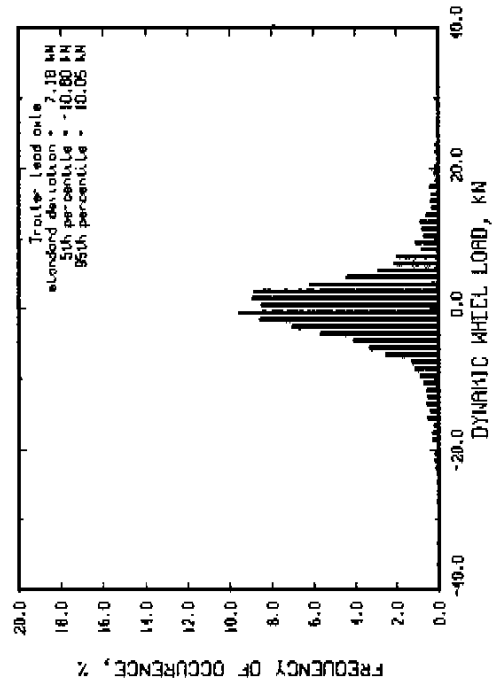
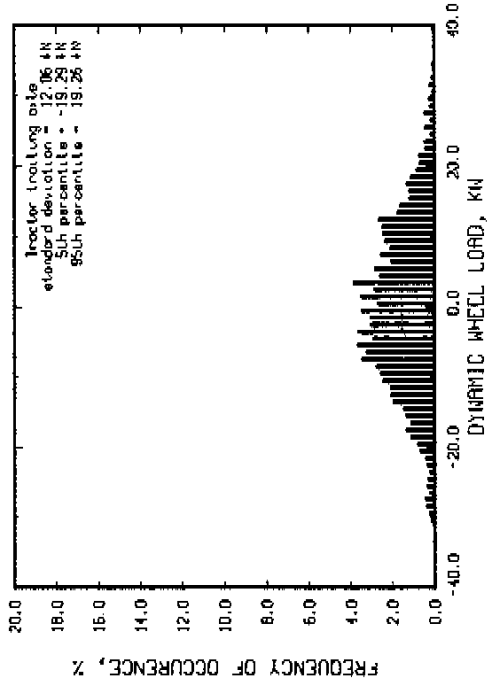
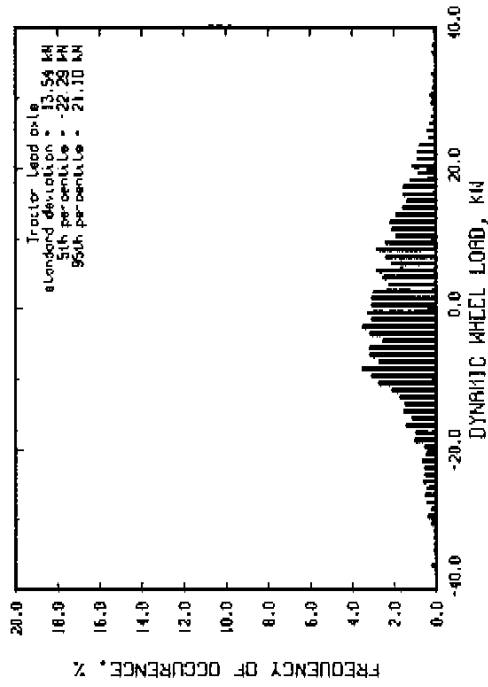
Run # 214 Part 2
 Speed = 60 km/hr
 Hoys roughness = 59 [PH]
 Tractor axle spread = 1.83 m
 Tractor suspension : spring suspended walking beam
 Trailer suspension : air bags
 Air suspension lift axle down



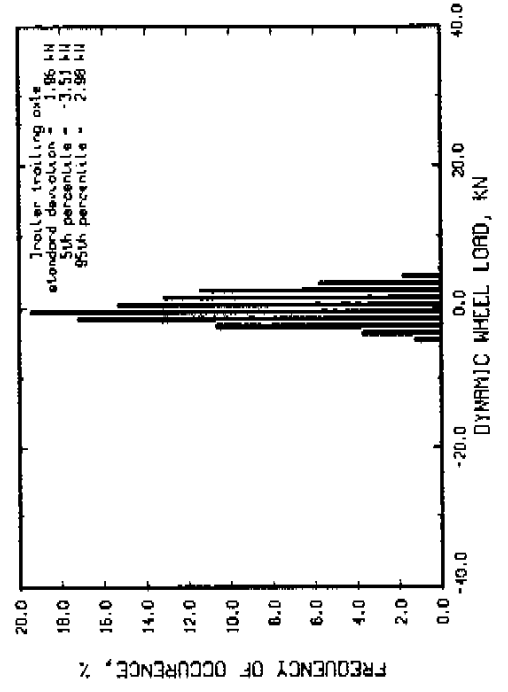
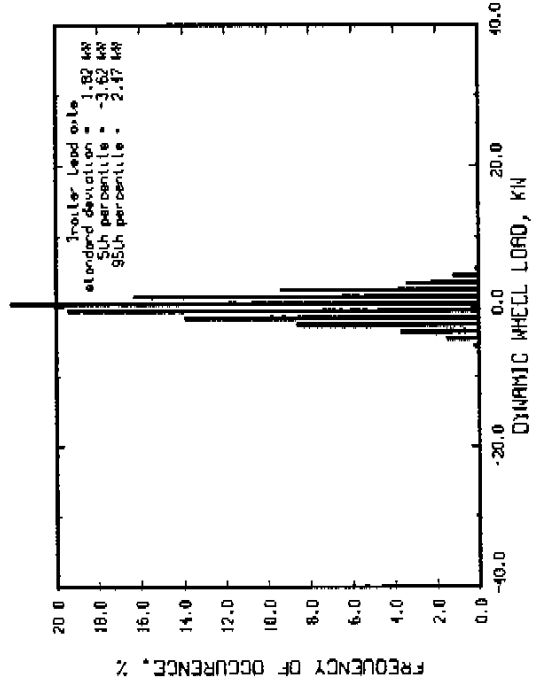
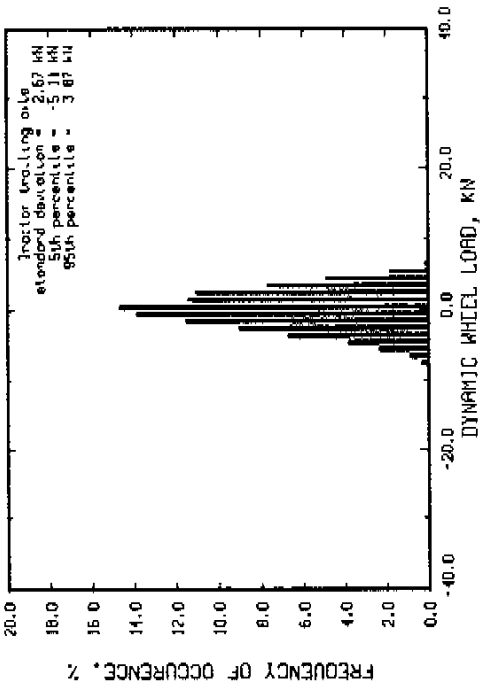
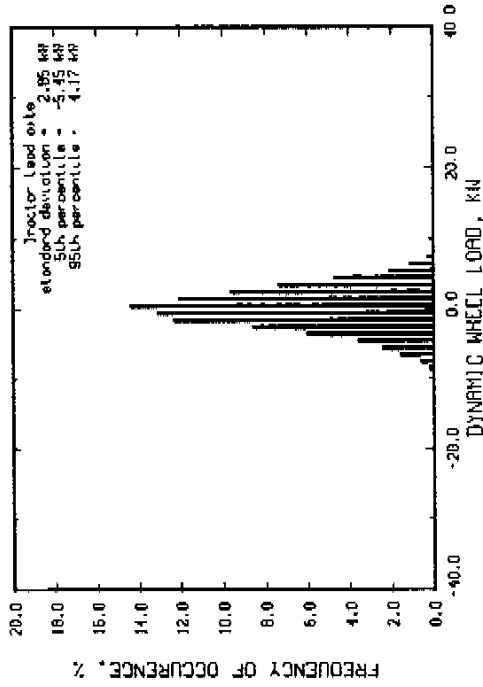
Run # 214 Part 1
 Speed = 80 km/hr
 Moys roughness = 165 jPH
 Tractor axle spread = 1.83 m
 Tractor suspension : spring suspended walking beam
 Tractor suspension : air bags
 Tractor suspension lift axle down



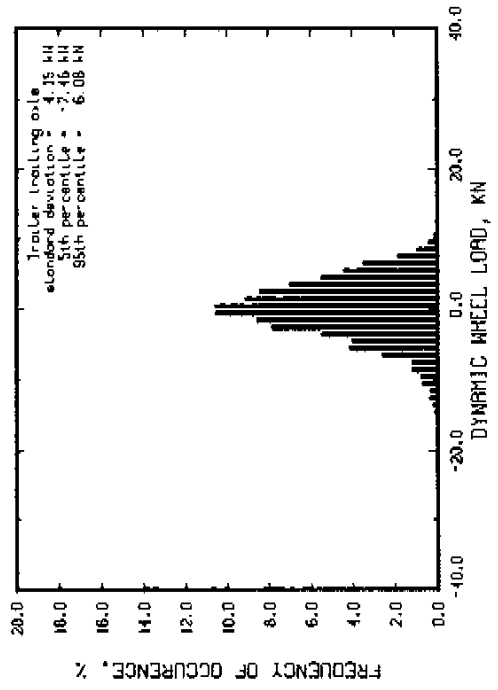
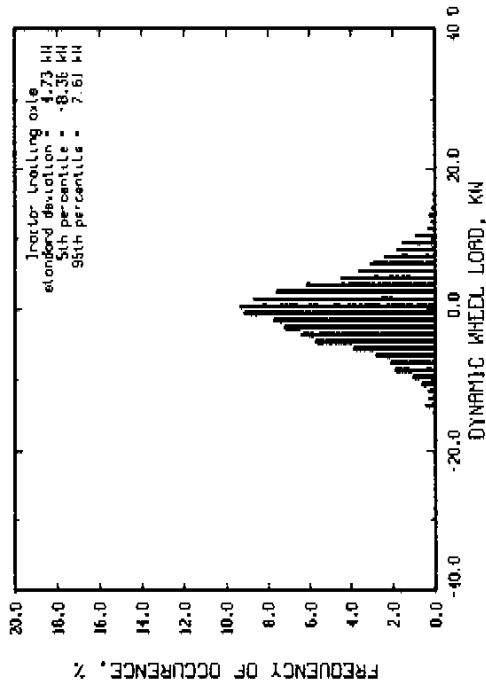
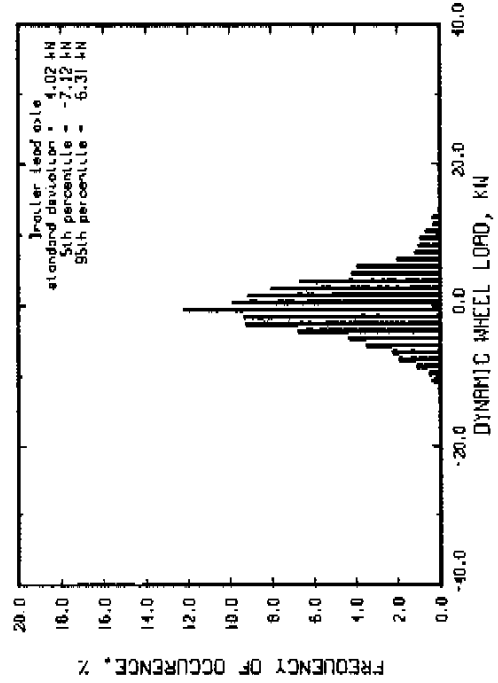
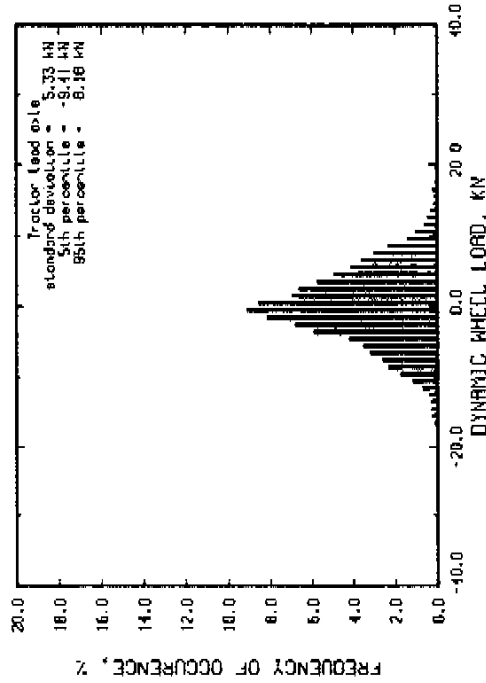
Run # 214 Part 3 Speed = 80 km/hr
 Mays roughness = 217 JPH Tractor axle spread = 1.83 m
 Tractor suspension : sprung suspended walking beam
 Tractor suspension : air bags
 Air suspension lift axle down



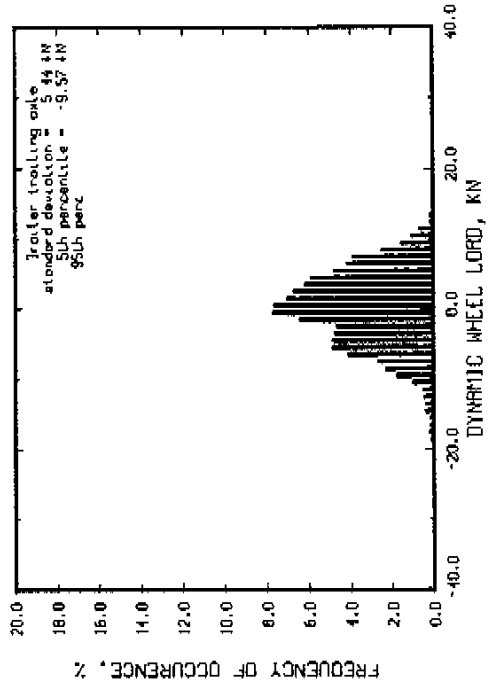
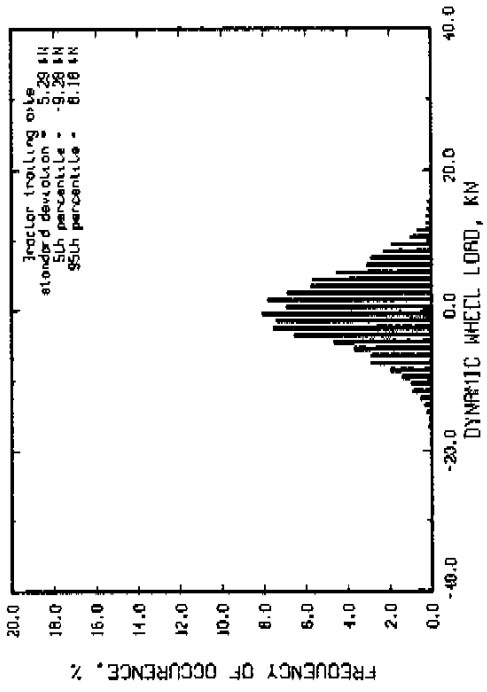
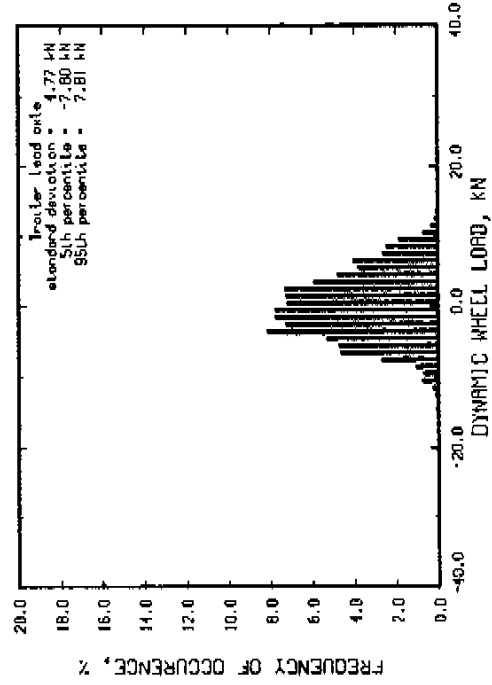
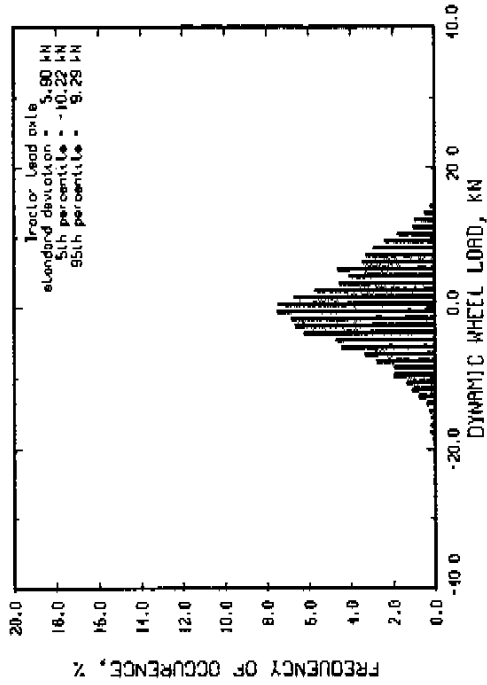
Run # 253 Speed = 40 km/hr
 Moys roughness = 73 IPH Tractor axle spread = 2.44 m
 Tractor suspension : spring suspended walking beam
 Tractor suspension : air bags
 Rlr suspension lift axle up



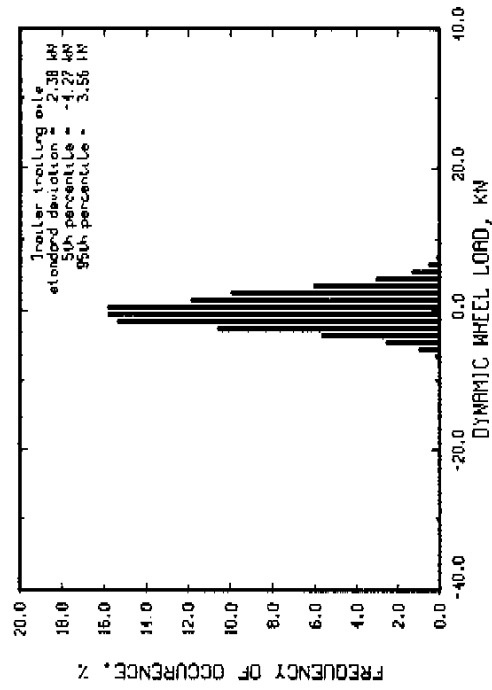
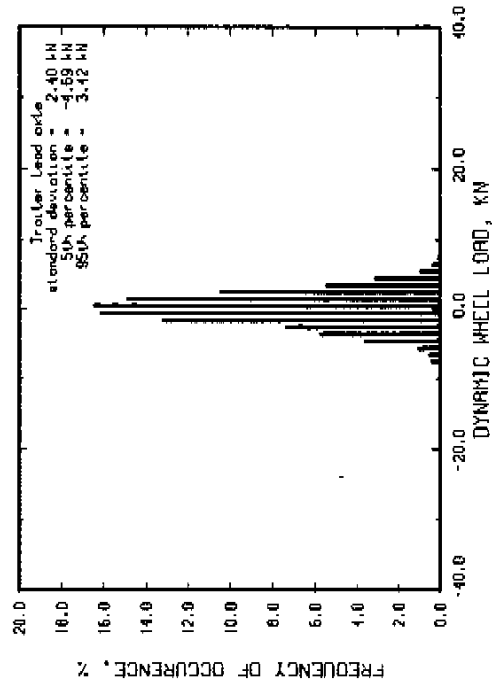
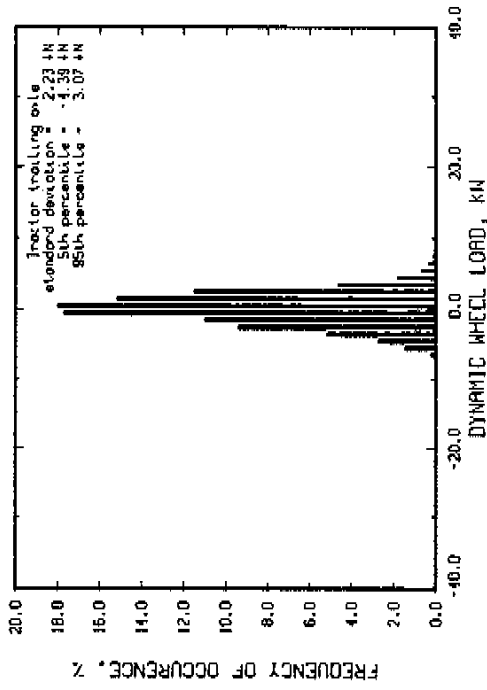
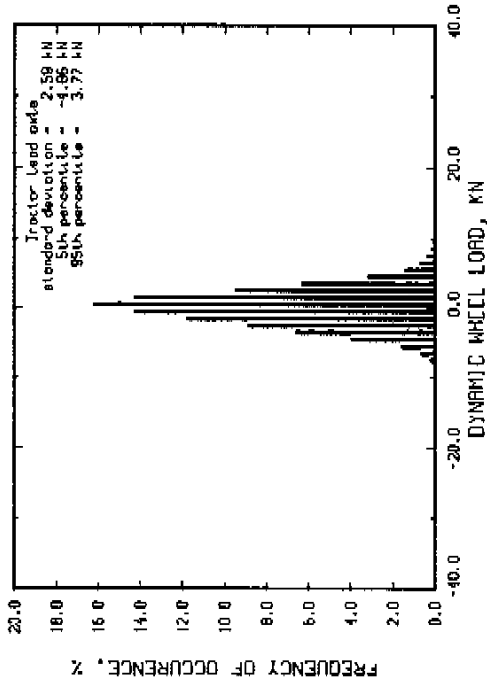
Run # 260 Part 1
 Speed = 40 km/hr
 Max roughness = 254 JPH
 Tractor axle spread = 2.44 m
 Tractor suspension : spring suspended walking beam
 Trailer suspension : air bags
 RLR suspension lift axle up



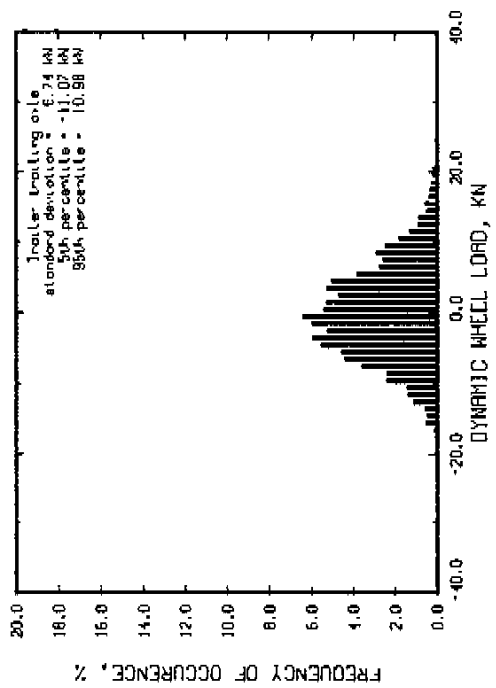
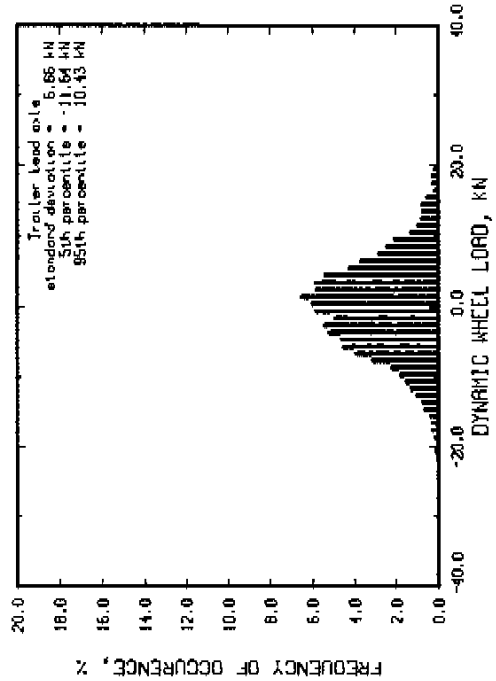
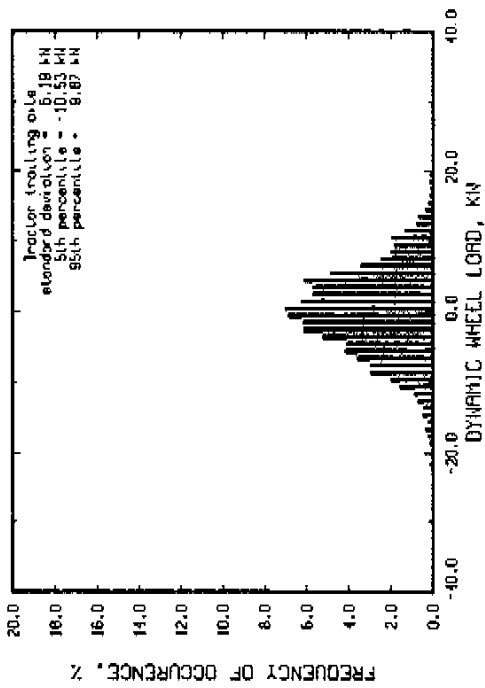
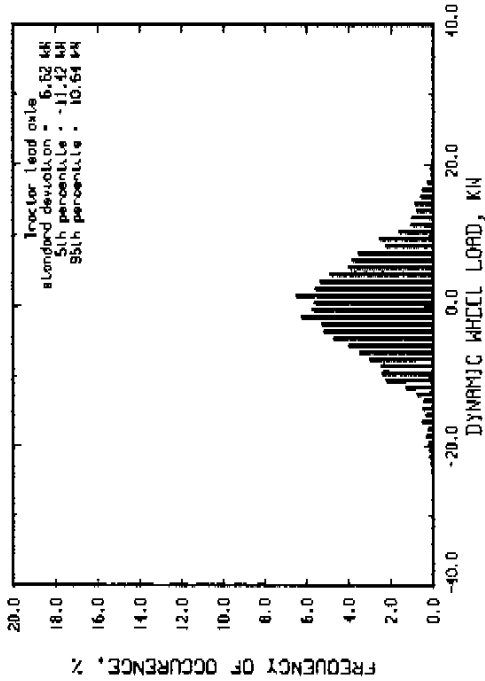
Run # 250 Part 2 Speed = 40 km/hr
 Moys roughness = 424 IPM Trailer axle spread = 2.44 m
 Tractor suspension : spring suspended walking beam
 Trailer suspension : air bags
 Rtr suspension lift axle up



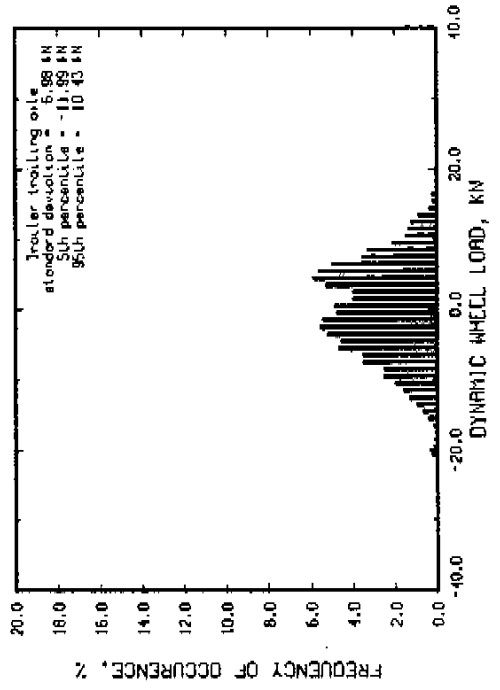
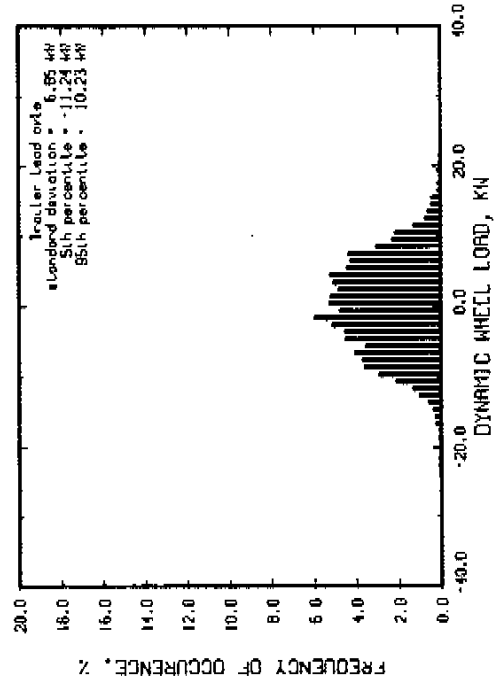
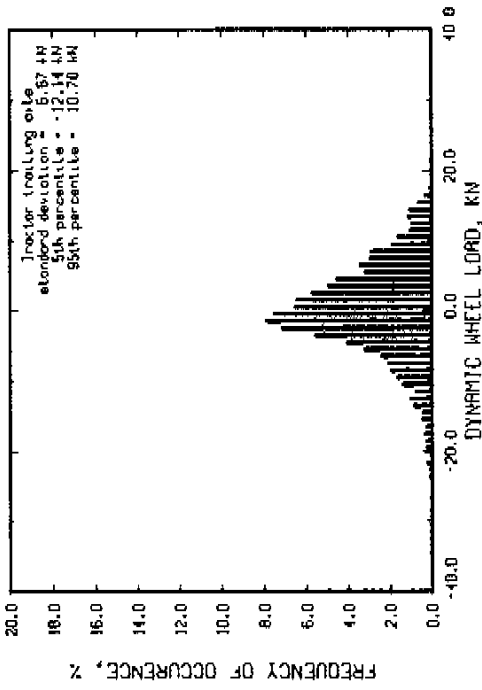
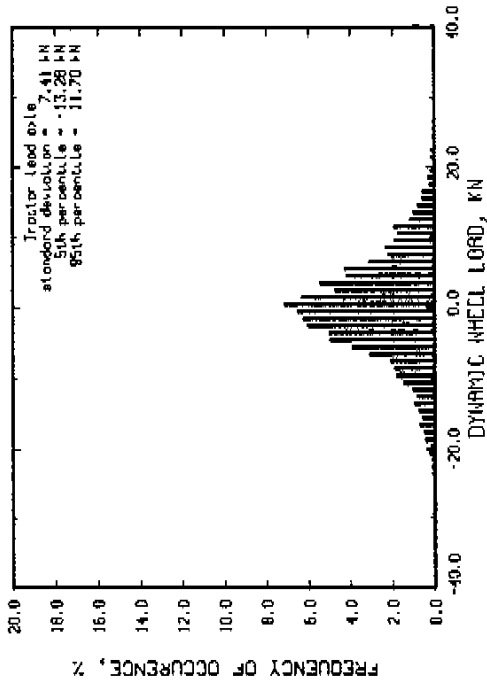
Run # 251 Speed = 50 km/hr
 Mays roughness = 73 IPM Trailer axle spread = 2.44 m
 Tractor suspension : spring suspended walking beam
 Trailer suspension : air bags
 Air suspension lift axle up



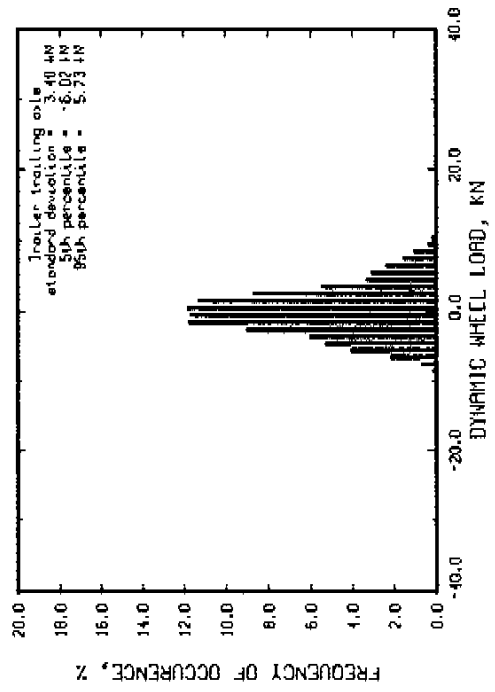
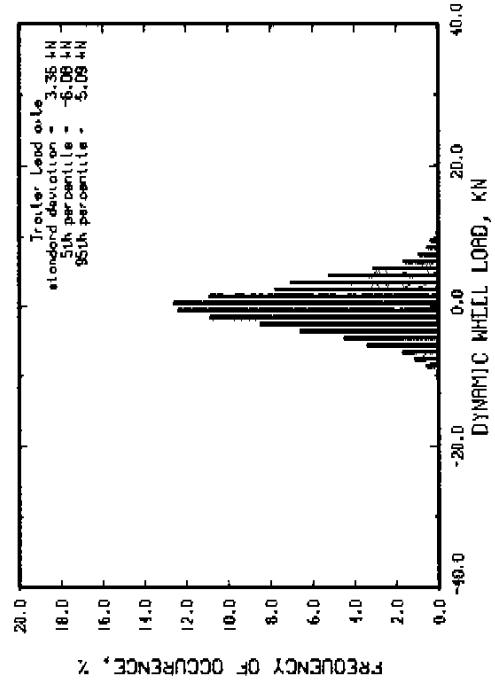
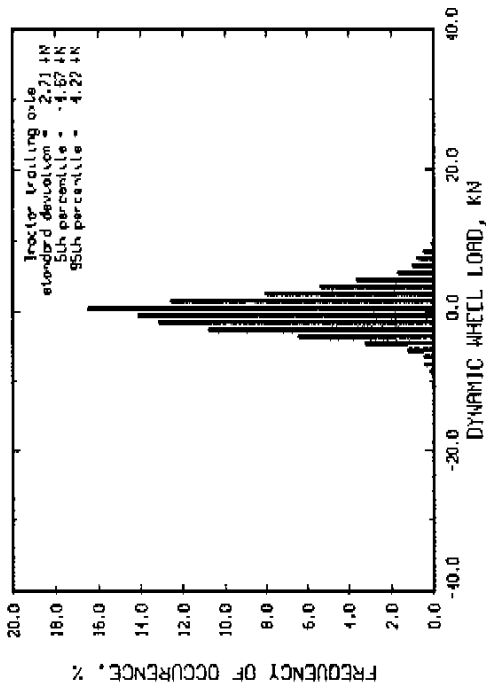
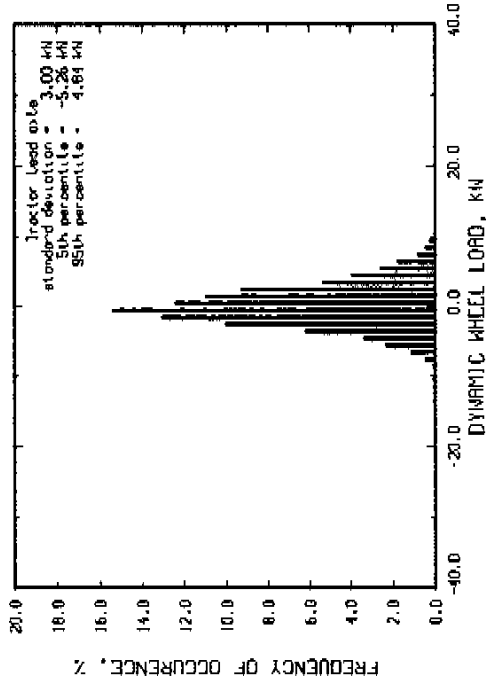
Run # 263 Part 1
 Moys roughness = 254 JPH
 Tractor suspension : spring suspended walking boom
 Tractor suspension : air bags
 Tractor suspension : lift axle up
 Speed = 50 km/hr
 Tractor axle spread = 2.44 m



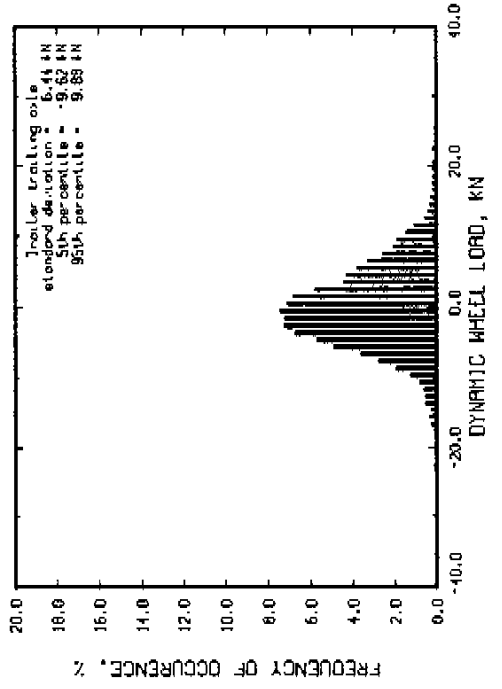
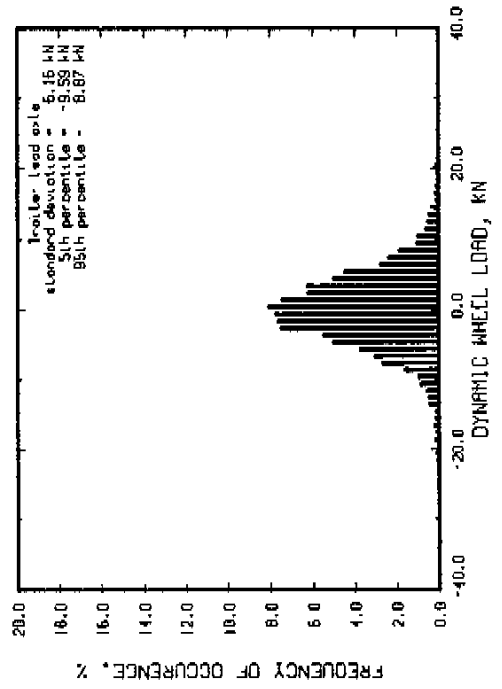
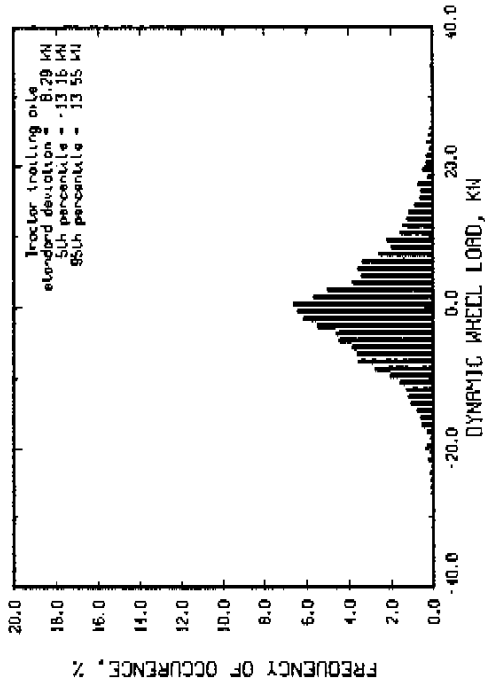
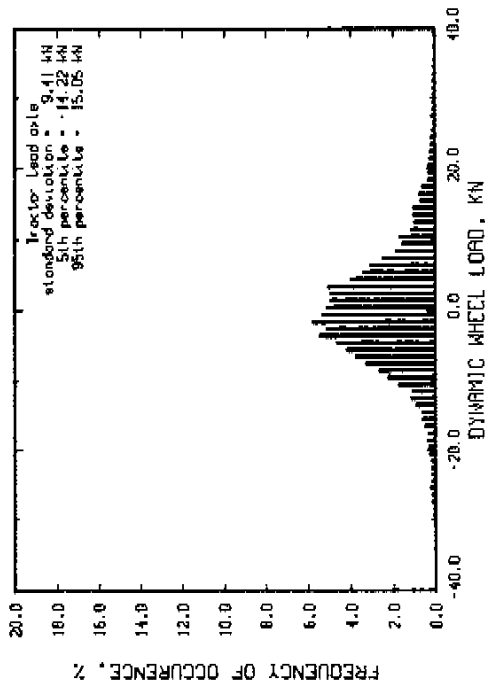
Run # 263 Fort 2 Speed = 60 km/hr
 Moys roughness = 424 IPM Trailer axle spread = 2.44 m
 Tractor suspension : spring suspended walking beam
 Trailer suspension : air bags
 RLR suspension lift axle up



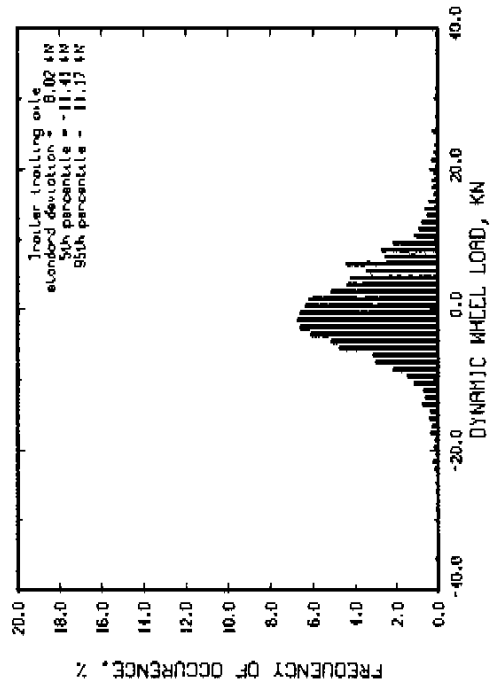
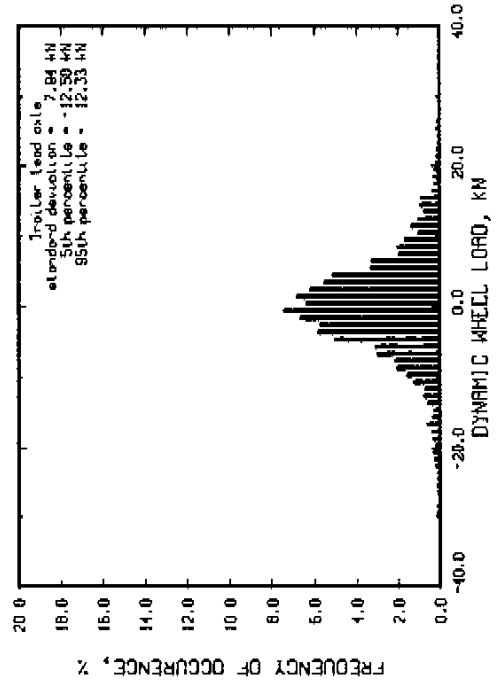
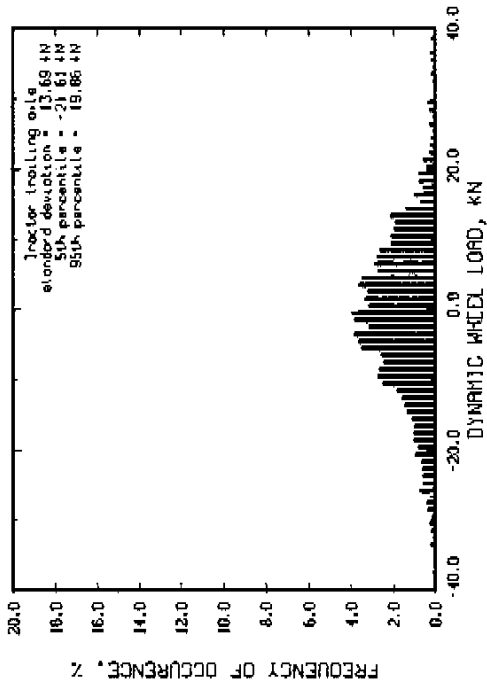
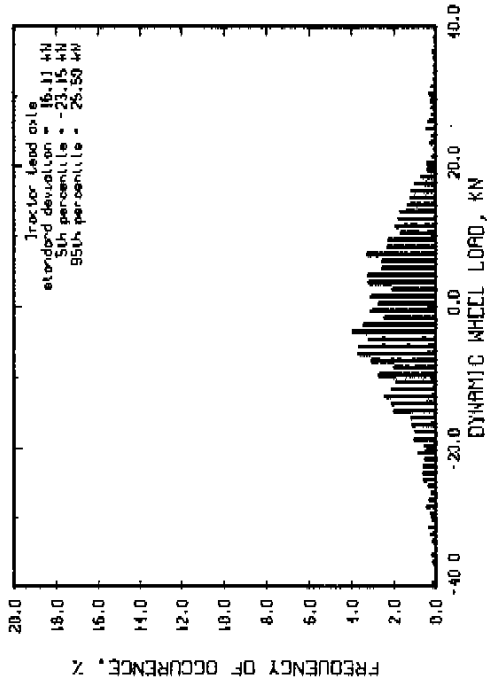
Run # 259 Part 2 Speed = 80 km/hr
 Moys roughness = 59 JPH Trailer axle spread = 2.44 m
 Tractor suspension : sprung suspended walking beam
 Trailer suspension : air bags
 R/R suspension lift axle up



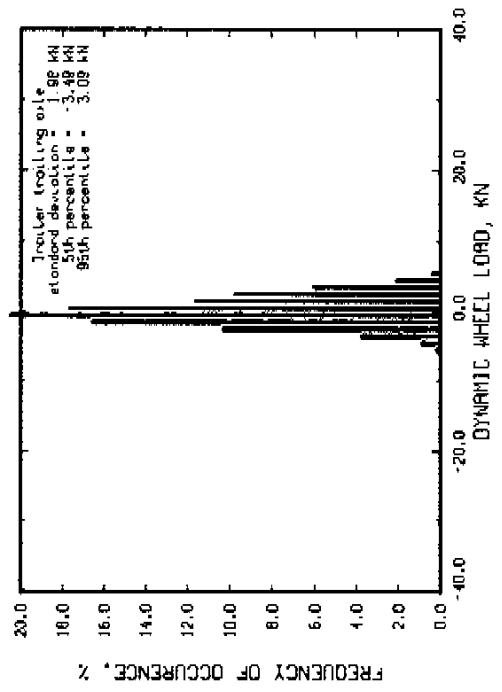
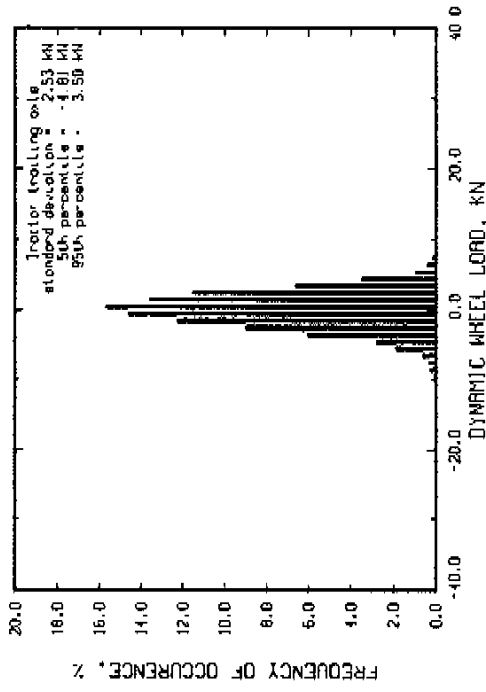
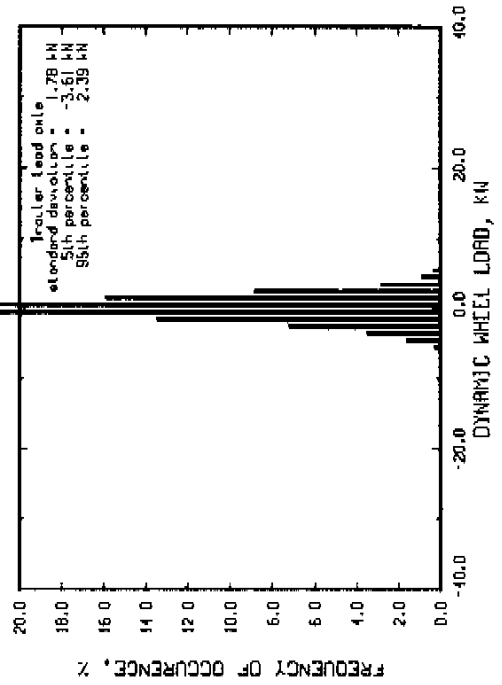
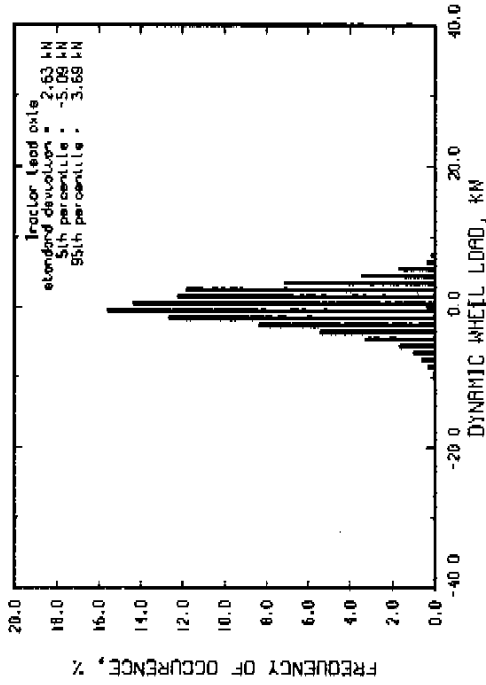
Run # 259 Part 1 Speed = 80 km/hr
 Hays roughness = 165 μ m Tractor axle spread = 2.44 m
 Tractor suspension : spring suspended walking beam
 Tractor suspension : air bags
 Tractor suspension lift axle up



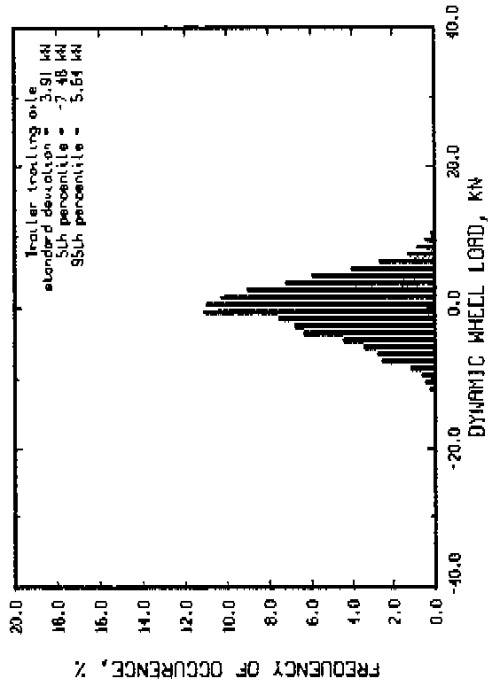
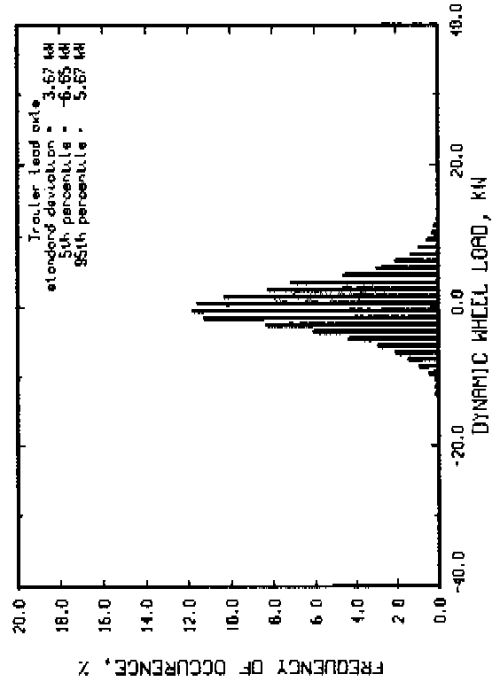
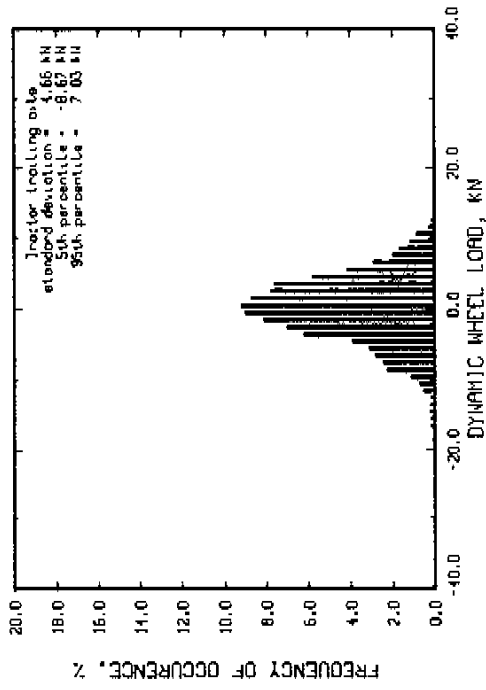
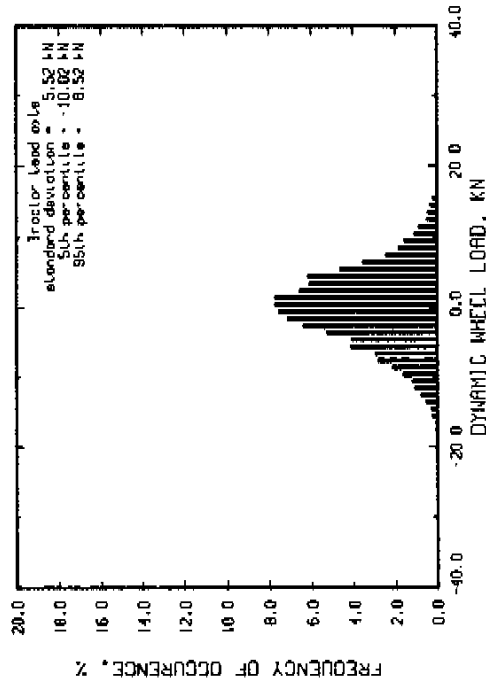
Run # 259 Part 3 Speed = 80 km/hr
 Max. roughness = 217 IPM Trailer axle spread = 2.44 m
 Tractor suspension : spring suspended walking beam
 Trailer suspension : air bags
 Tractor suspension : air bags
 Air suspension lift axle up



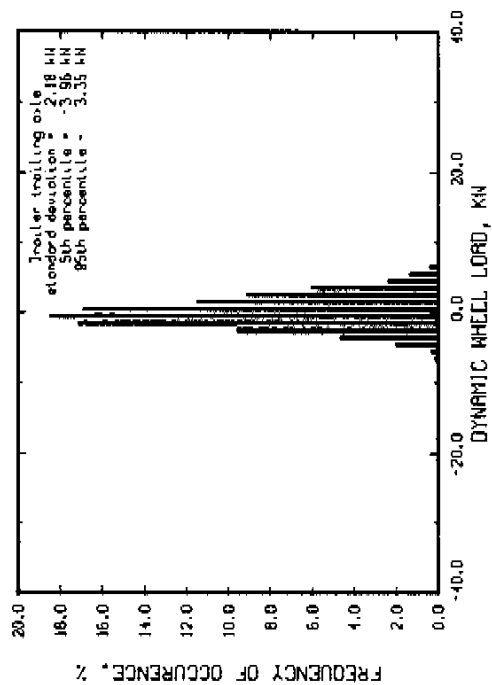
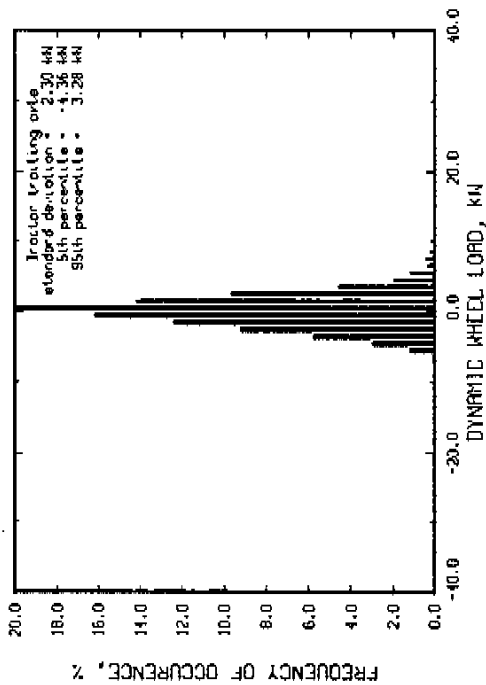
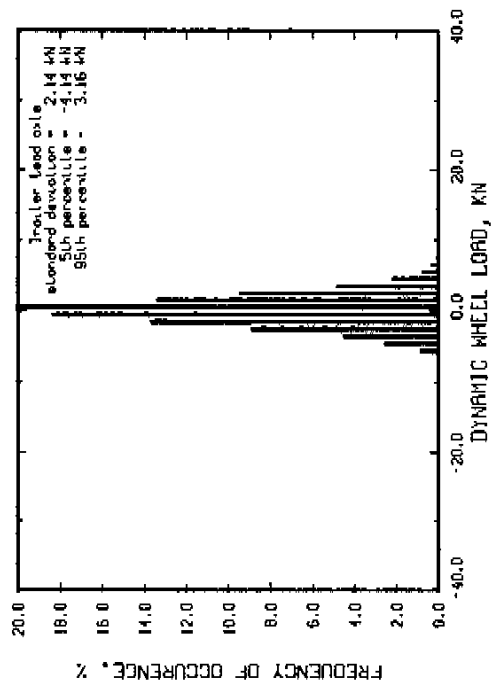
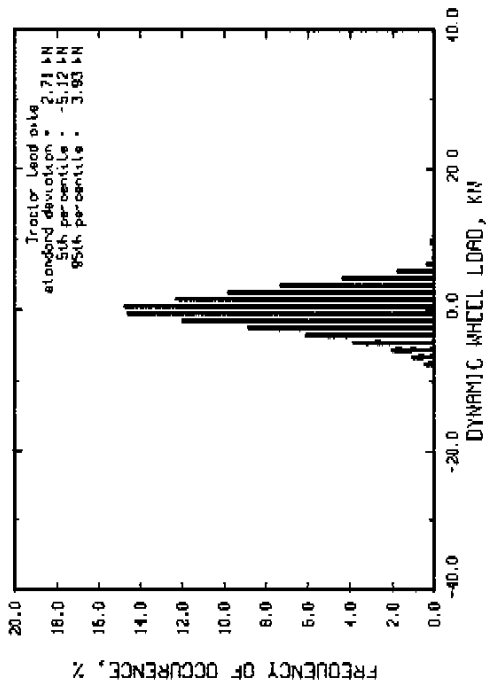
Run # 257 Speed = 40 km/hr
 Max roughness = 73 ipm Trailer axle spread = 2.44 m
 Tractor suspension : spring suspended walking beam
 Trailer suspension : air bags
 Air suspension lift axle down



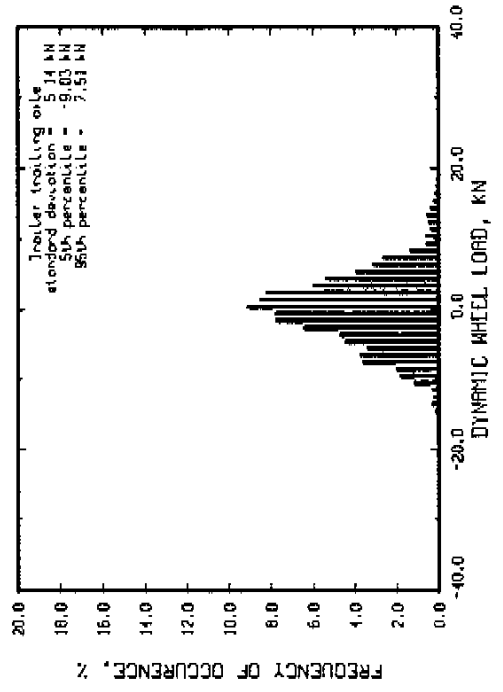
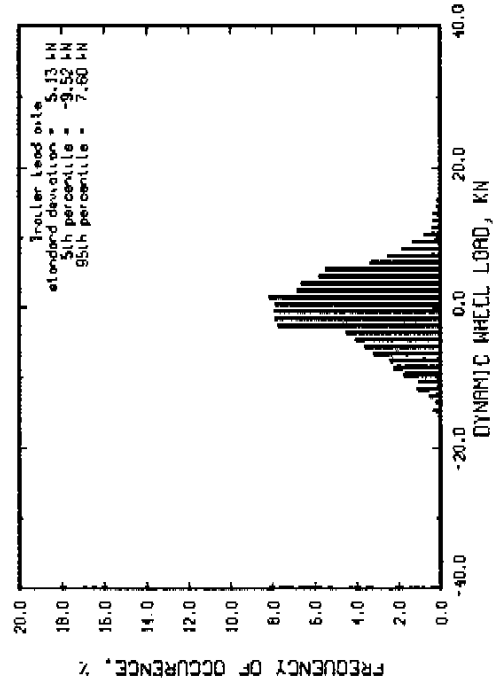
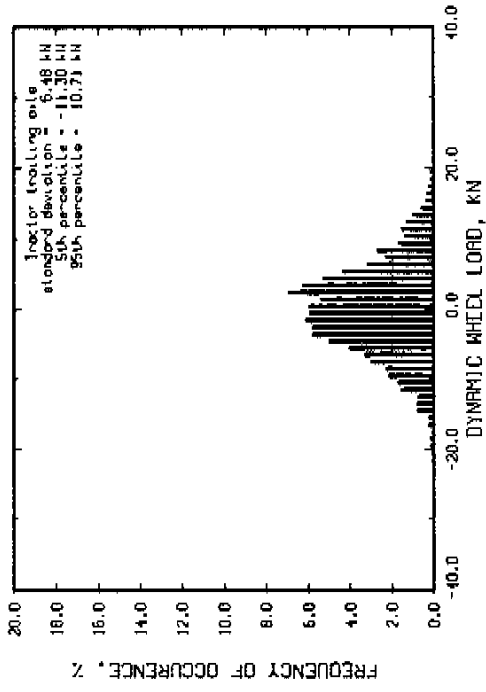
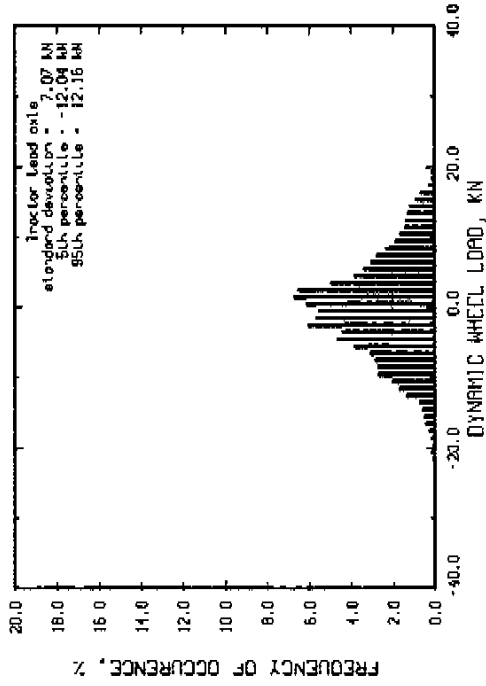
Run # 259 Part 1
 Speed = 40 km/hr
 Major roughness = 254 jPH
 Trolley axle spread = 2.44 m
 Trolley suspension : sprung suspended walking beam
 Trolley suspension : air bags
 Air suspension lift axle down



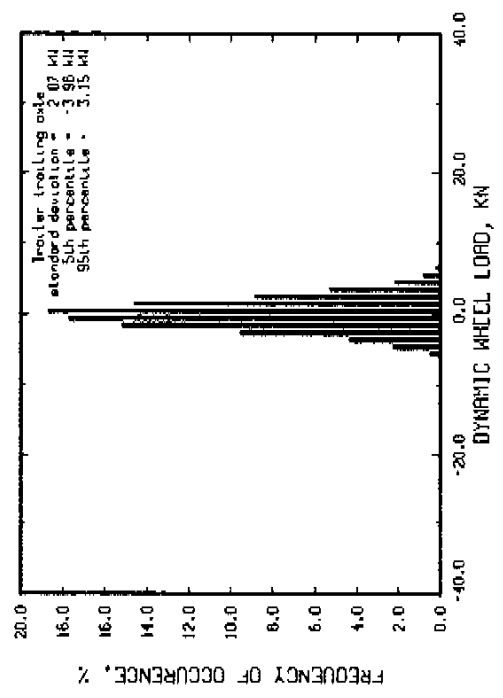
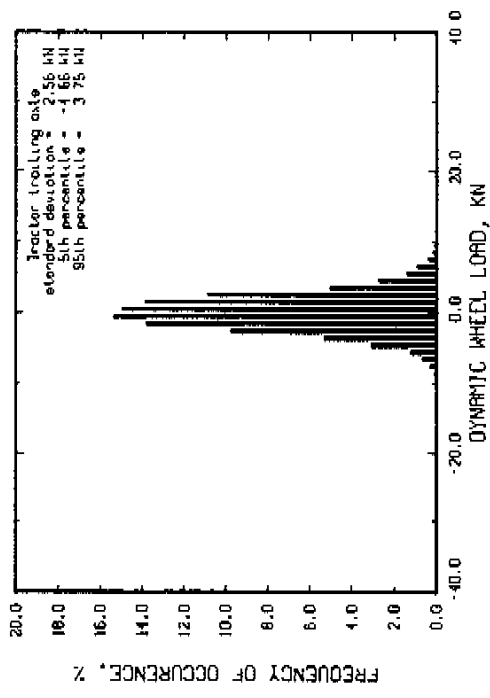
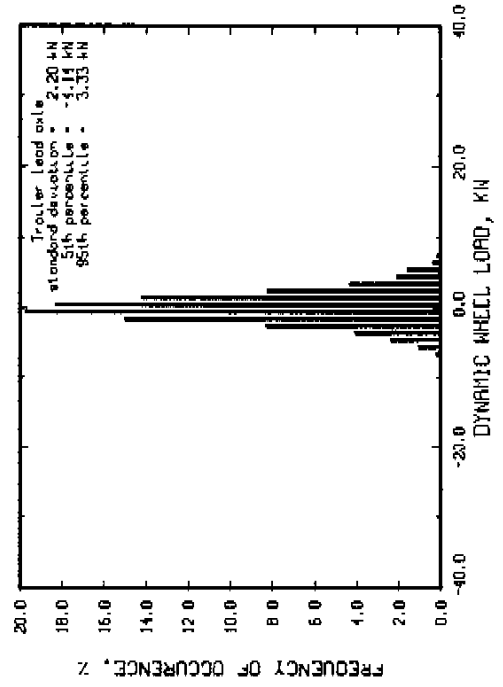
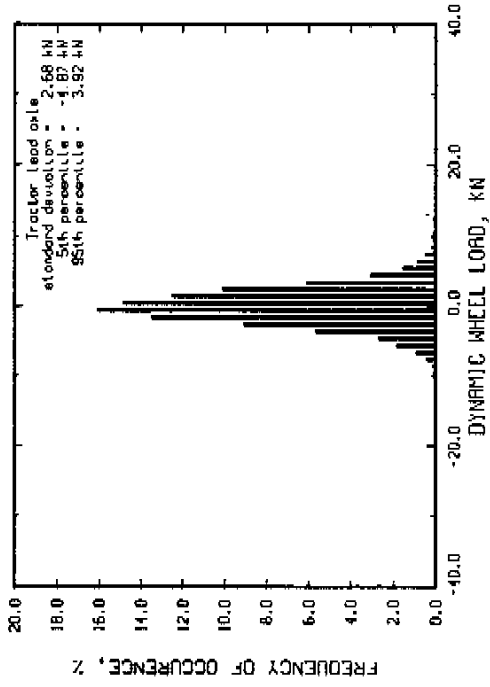
Run # 256 Speed = 60 km/hr
 Moys roughness = 73 JPH Tractor axle spread = 2.44 m
 Tractor suspension : spring suspended walking boom
 Tractor suspension : air bags
 Air suspension lift axle down



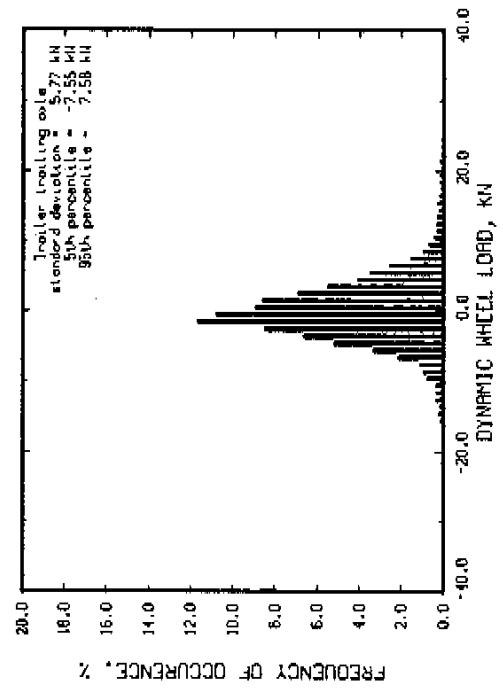
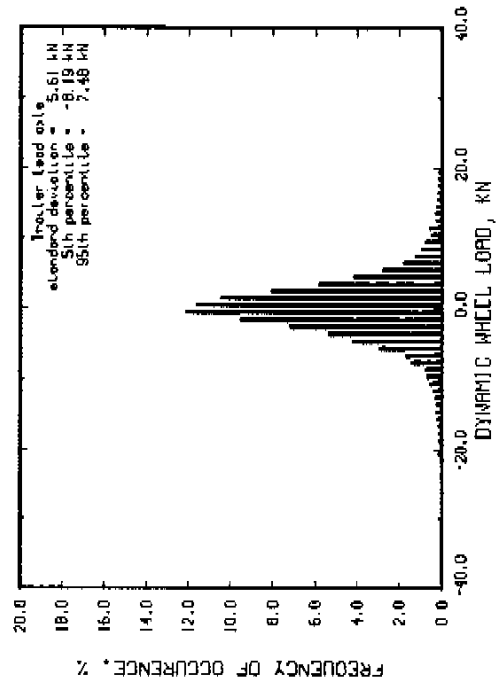
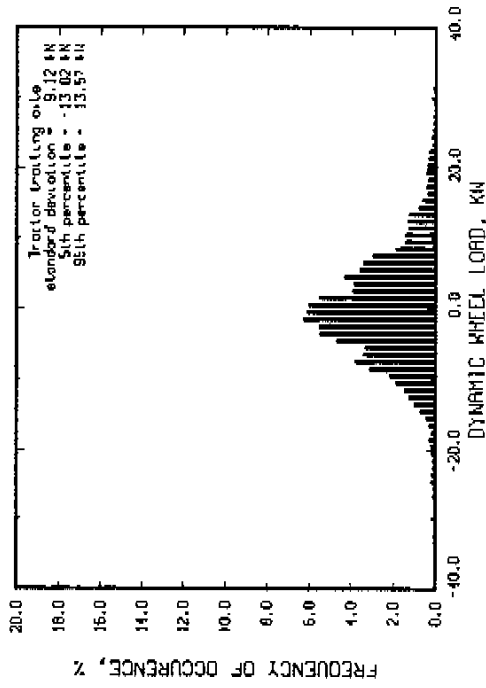
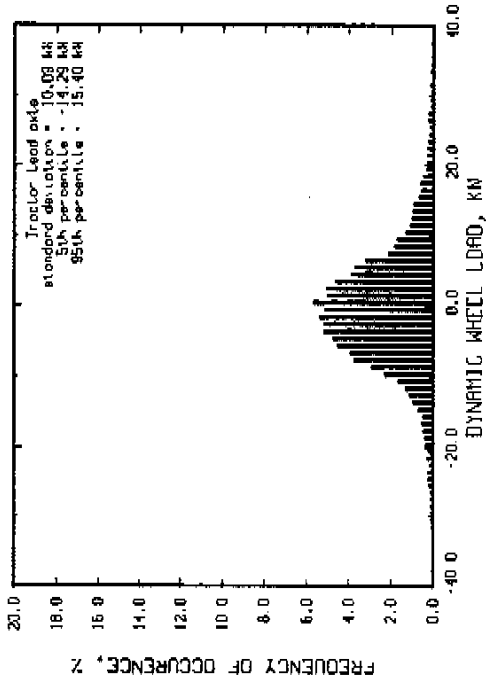
Run # 268 Part 1
 Speed = 60 km/hr
 Moys roughness = 254 jpm
 Trailer axle spread = 2.44 m
 Trailer suspension : sprung suspended walking beam
 Trailer suspension : air bags
 Air suspension lift axle down



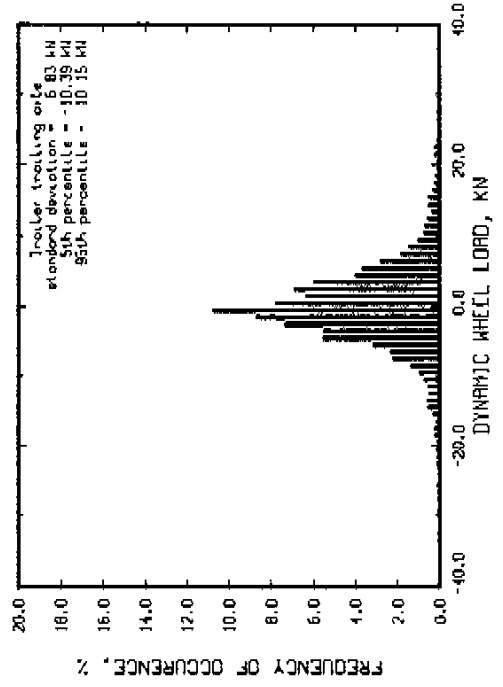
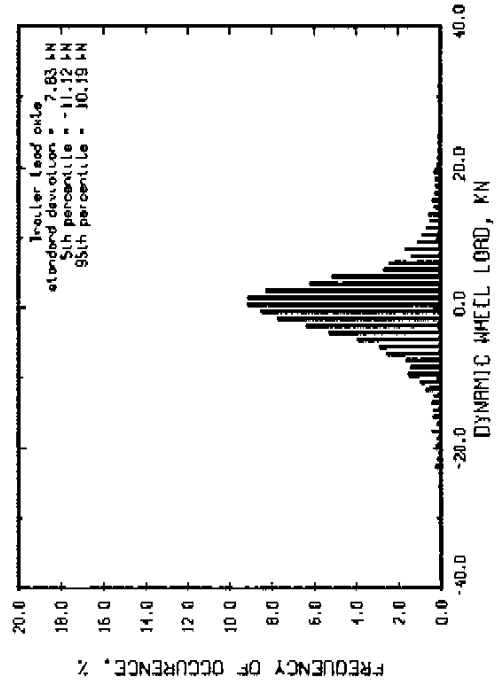
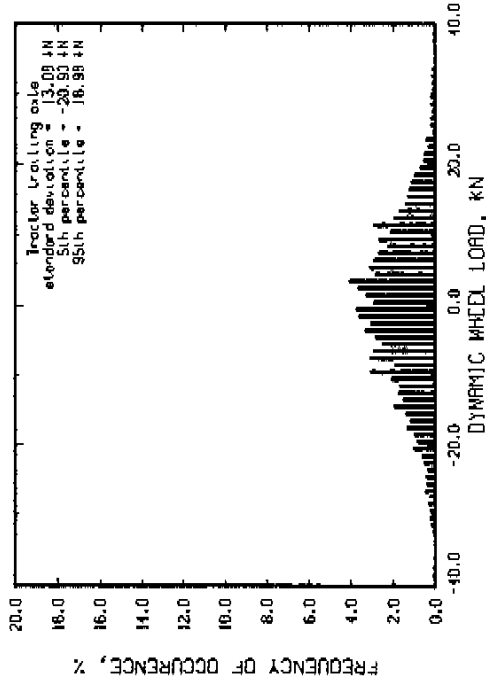
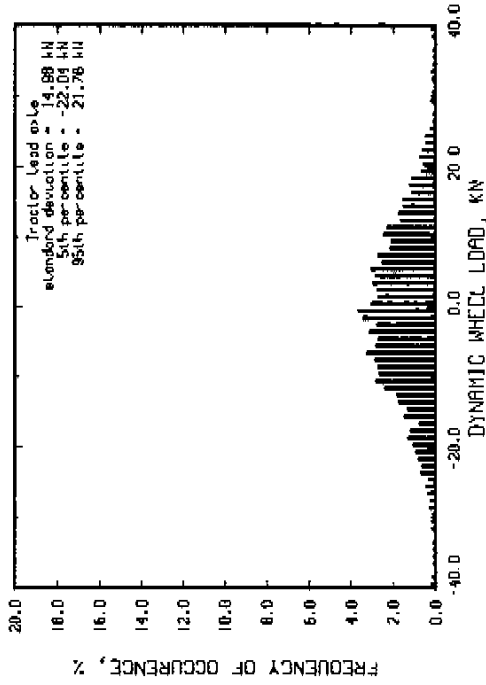
Run # 258 Part 2 Speed = 80 km/hr
 Moys roughness = 59 IPM Tractor axle spread = 2.44 m
 Tractor suspension : sprung suspended walking bear
 trailer suspension : air bags
 lift suspension lift axle down



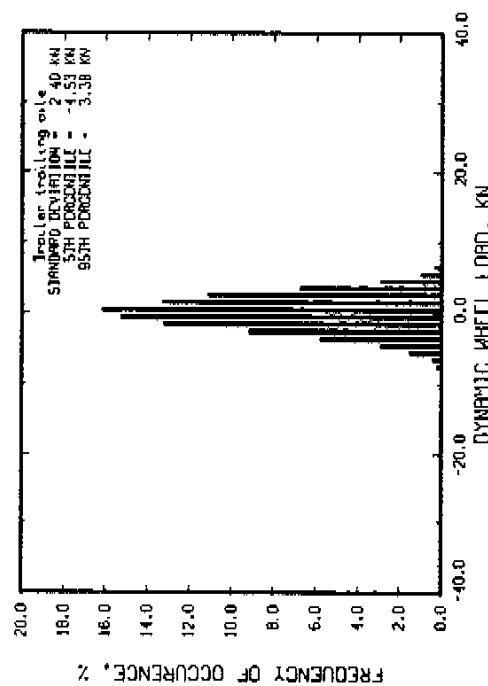
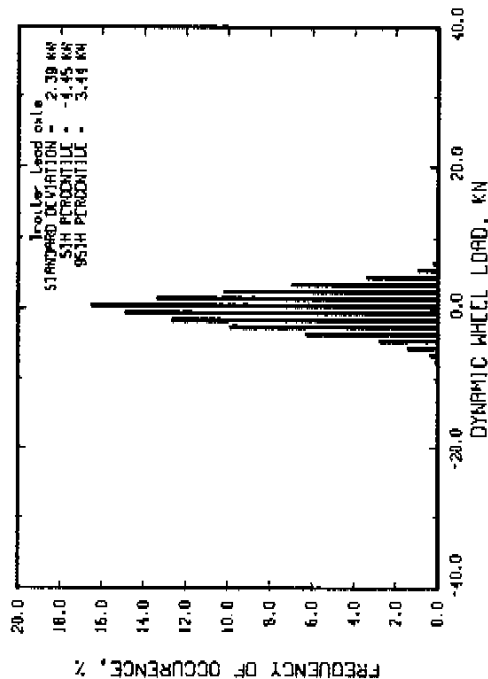
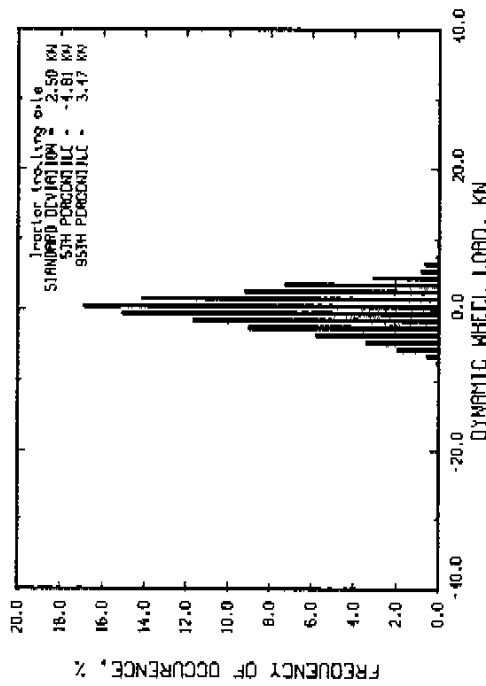
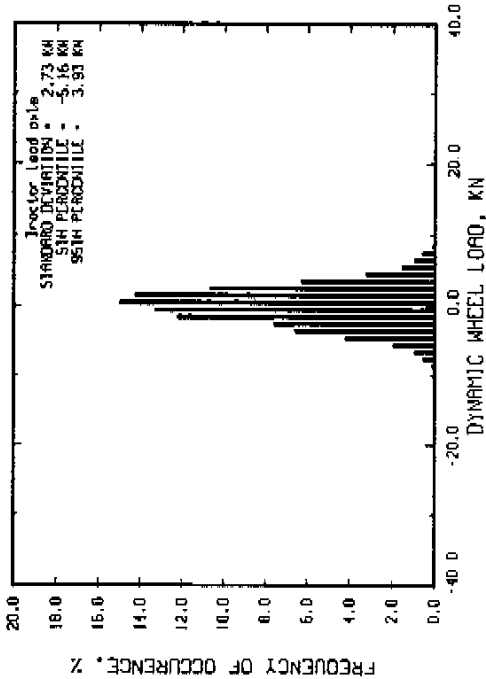
Run # 258 Part 1
 Speed = 80 km/hr
 Moys roughness = 165 IPM
 Trailer axle spread = 2.44 m
 Tractor suspension : spring suspended walking beam
 Trailer suspension : air bags
 Air suspension lift axle down



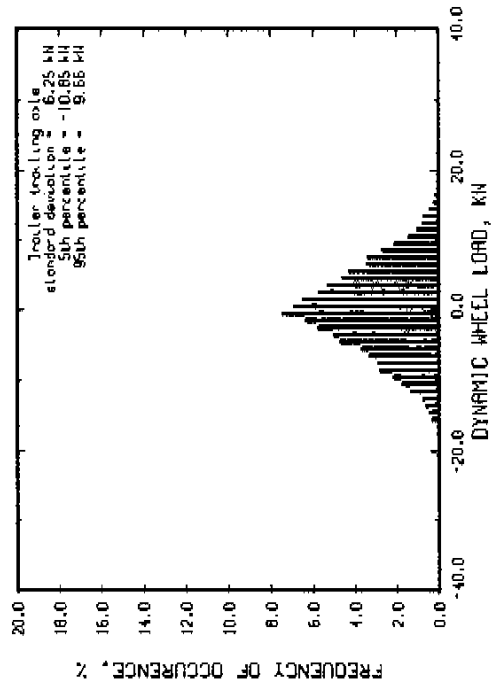
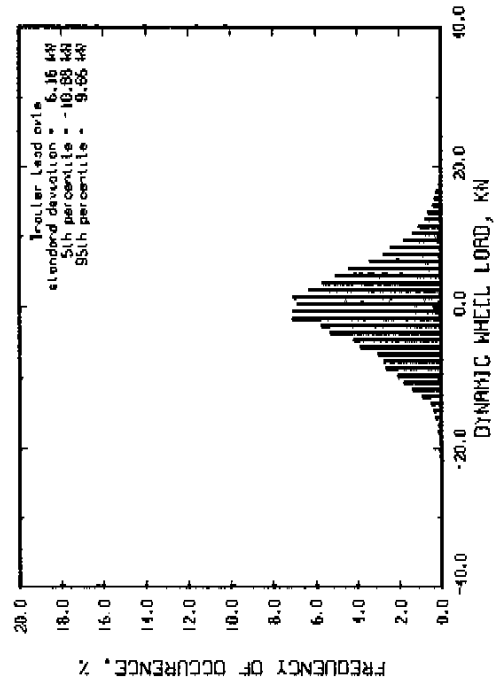
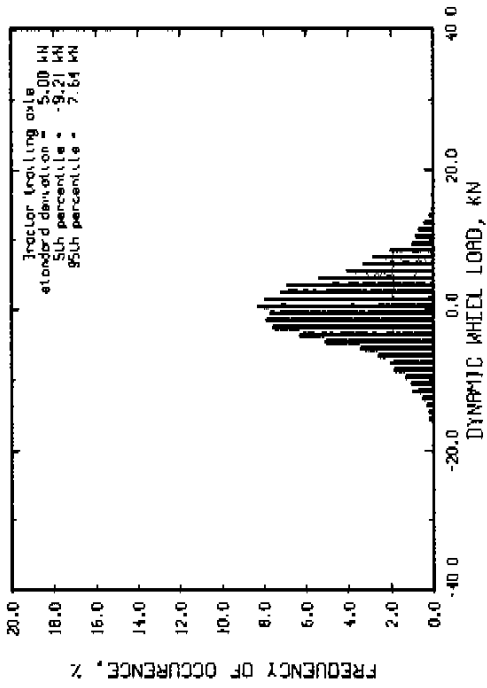
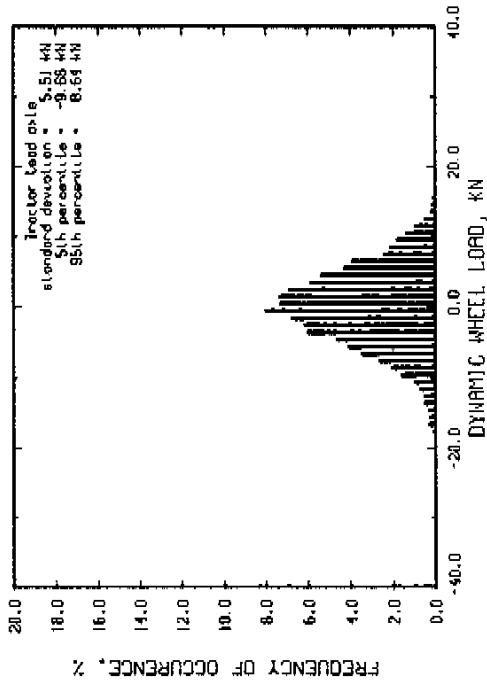
Run # 258 Part 3 Speed = 60 km/hr
 Hoys roughness = 217 IPM Trailer axle spread = 2.44 m
 Tractor suspension : spring suspended walking base
 Trailer suspension : air bags
 R/R suspension : full axle down



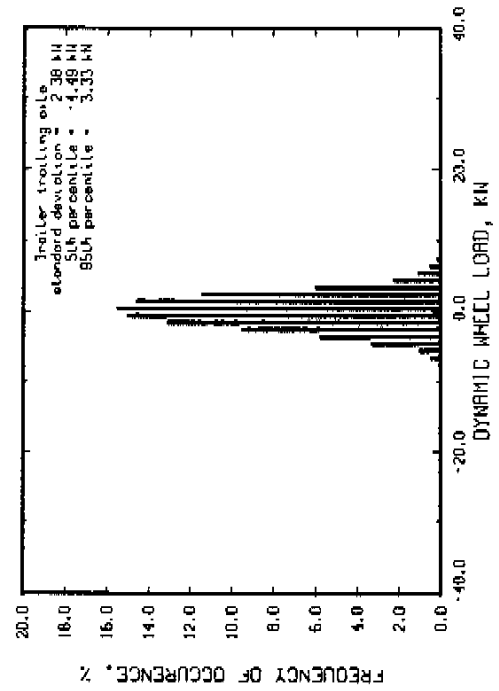
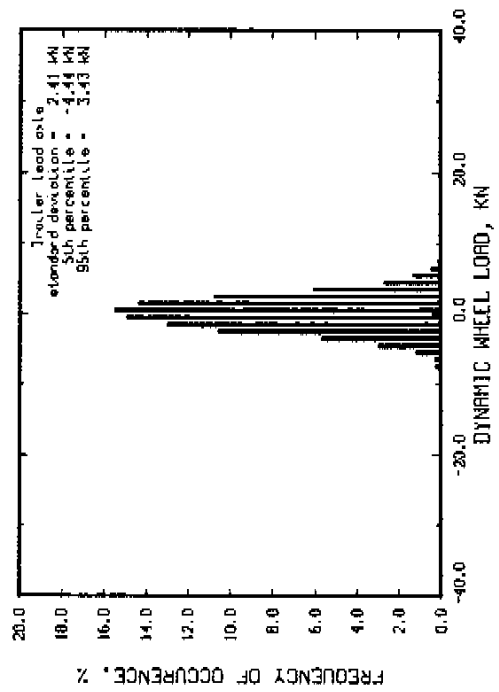
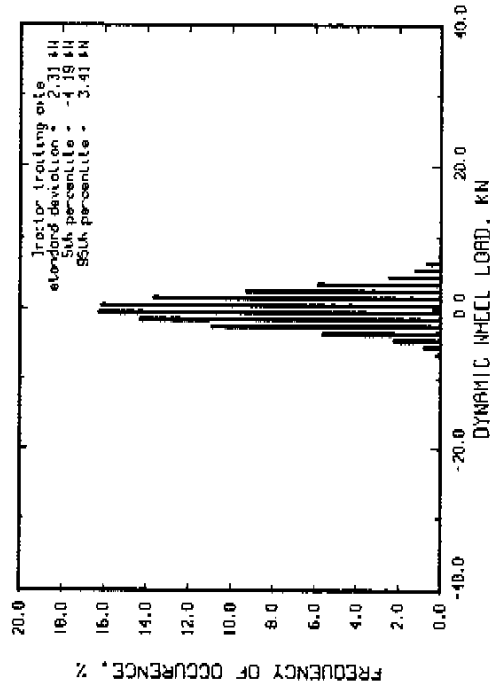
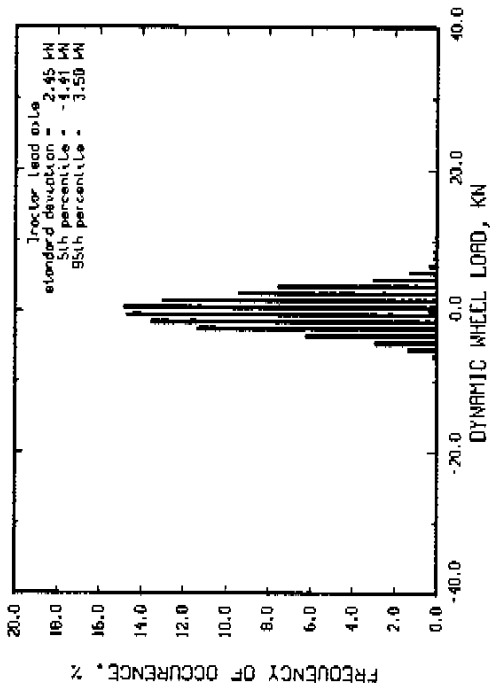
Run # 274
 Speed = 40 km/hr
 Hoys roughness = 73 IPIH
 Trolley axle spread = 1.37 m
 Trolley suspension : spring suspended walking beam
 Trolley suspension : rubber suspended walking beam
 for suspension lift axle up



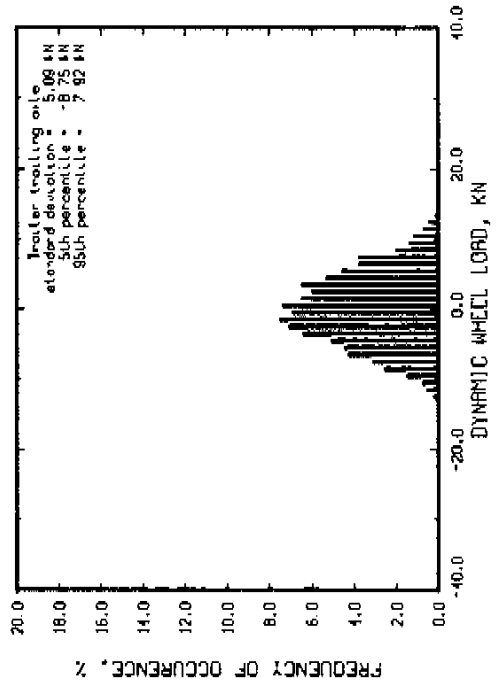
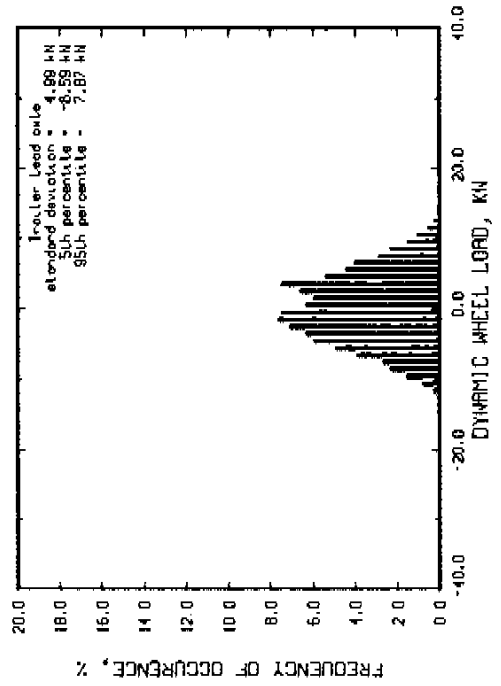
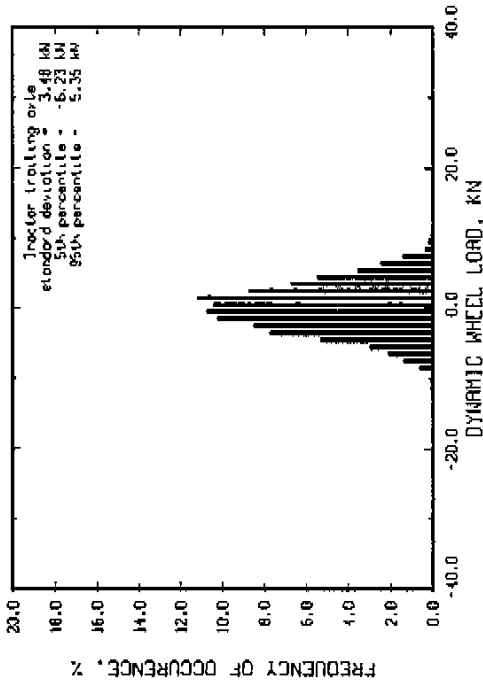
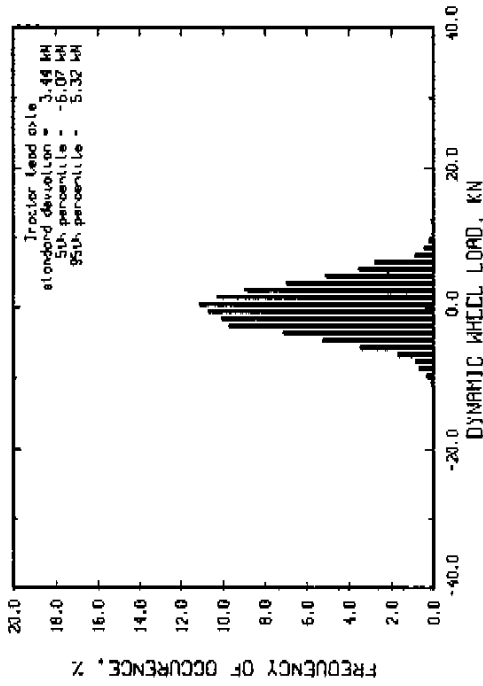
Run # 280 Part 1
 Speed = 40 km/hr
 Moys roughness = 254 IPM
 Tractor axle spread = 1.37 m
 Tractor suspension : spring suspended walking beam
 Tractor suspension : rubber suspended walking beam
 Tractor suspension lift axle up



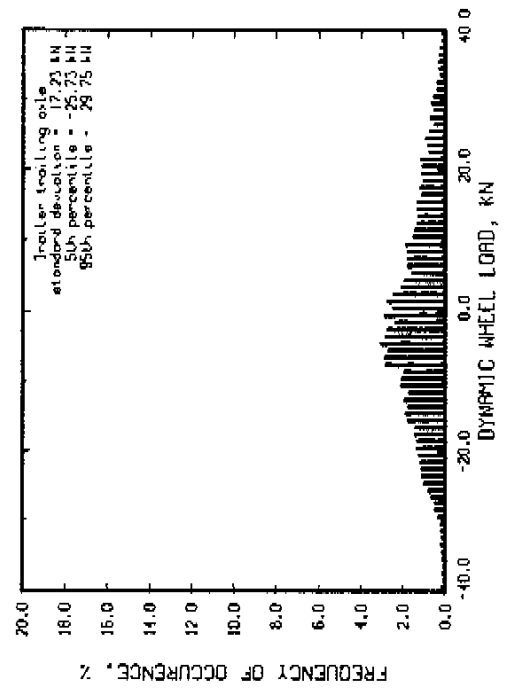
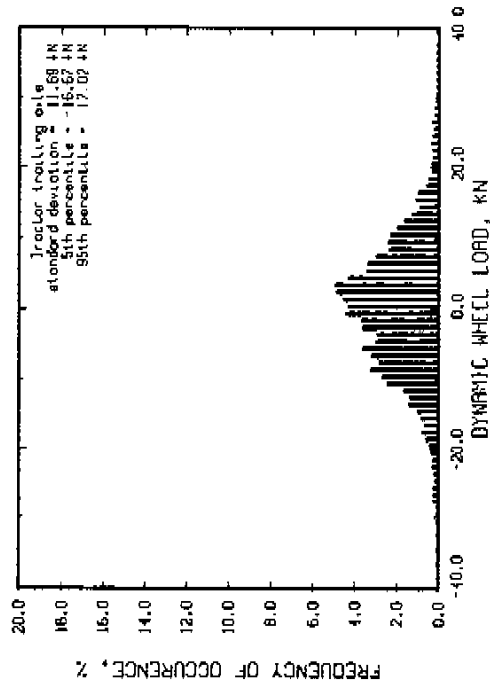
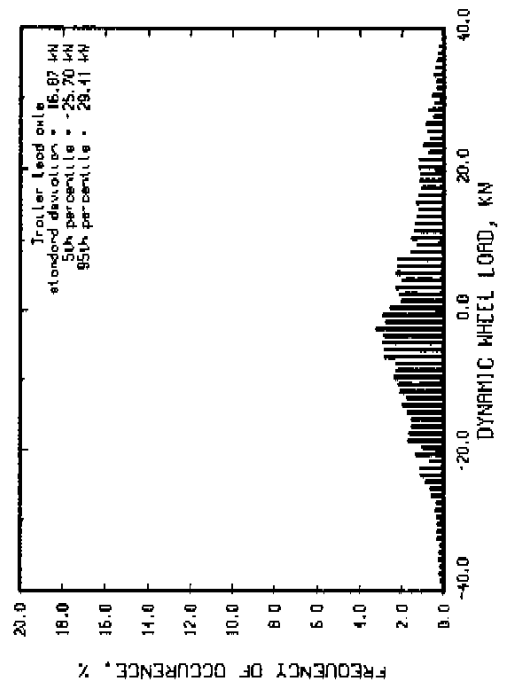
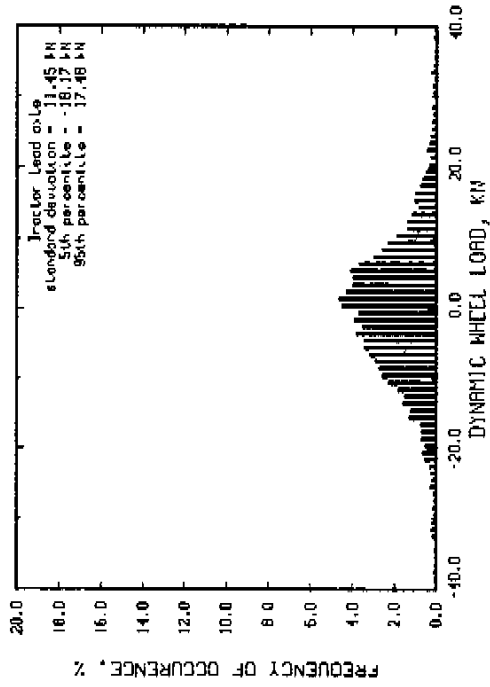
Run # 272 Speed = 60 km/hr
 Mays roughness = 73 JPM Tractor axle spread = 1.37 m
 Tractor suspension : spring suspended walking beam
 Tractor suspension : rubber suspended walking beam
 Tractor suspension lift axle up



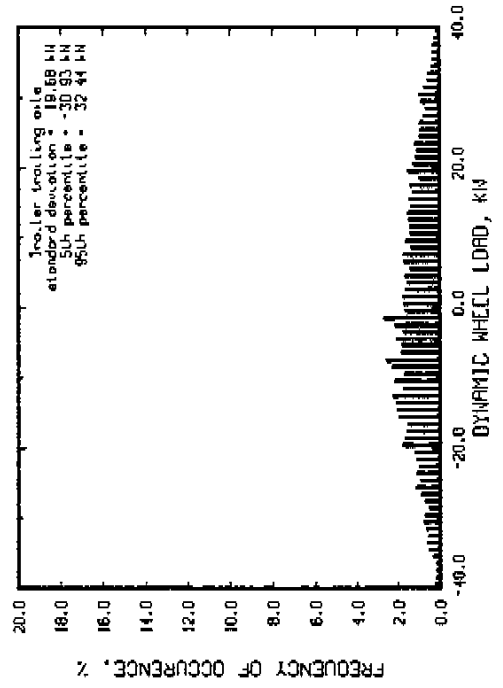
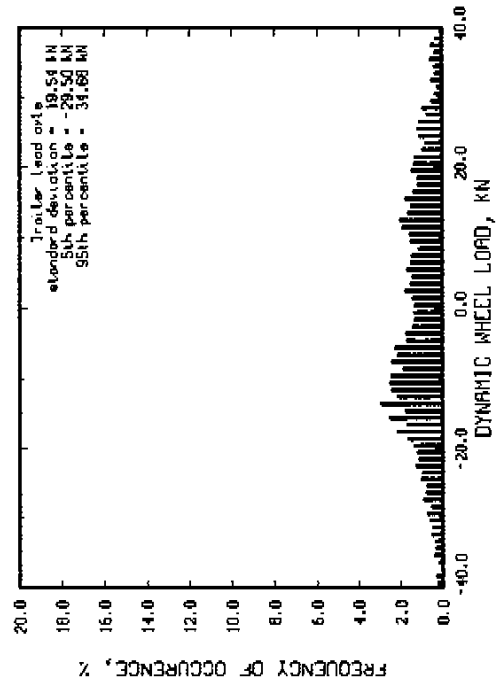
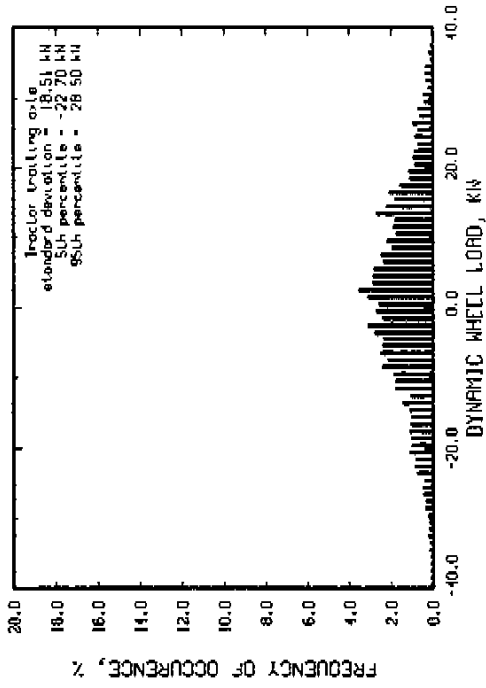
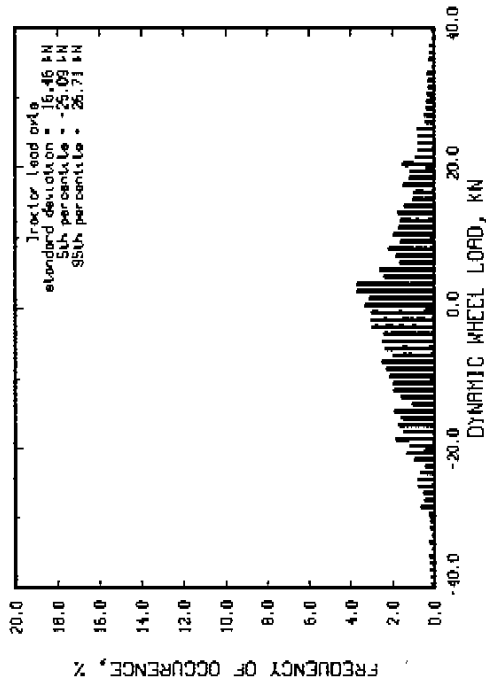
Run # 279 Part 2 Speed = 80 Km/hr
Moys roughness = 59 JPM Trailer axle spread = 1.37 m
Tractor suspension : spring suspended walking beam
Trailer suspension : rubber suspended walking beam
Rlr suspension lift axle up



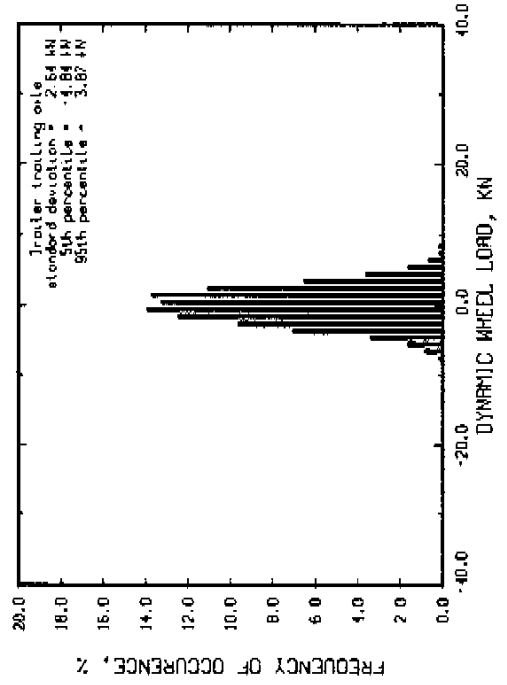
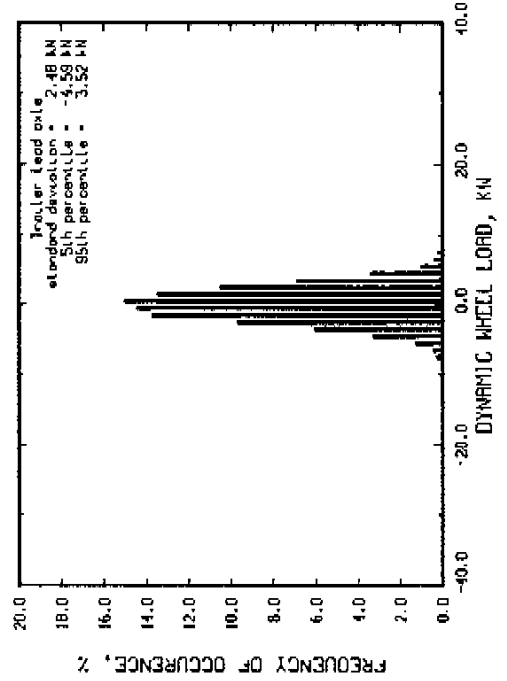
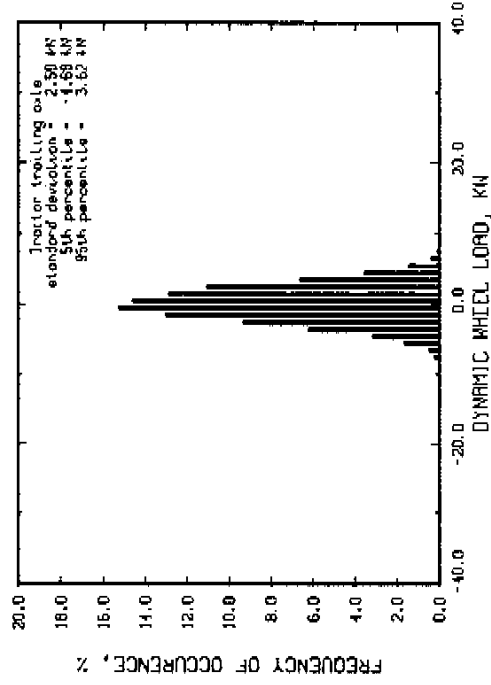
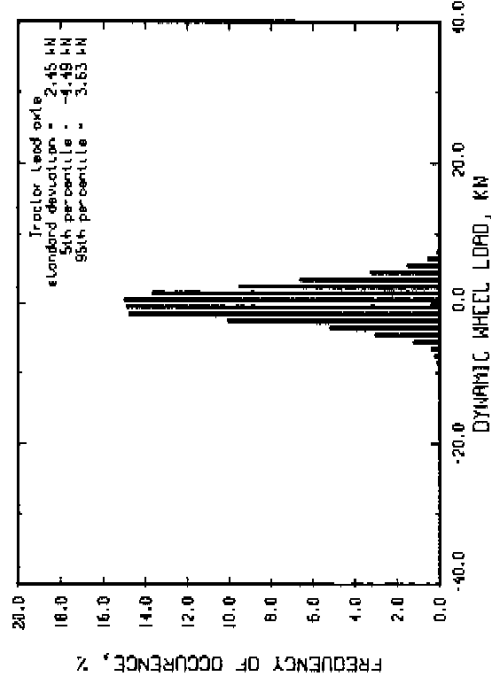
Run # 279 Part 1
 Speed = 80 km/hr
 Tractor axle spread = 1.37 m
 Tractor suspension : spring suspended walking beam
 Tractor suspension : rubber suspended walking beam
 Air suspension lift axle up



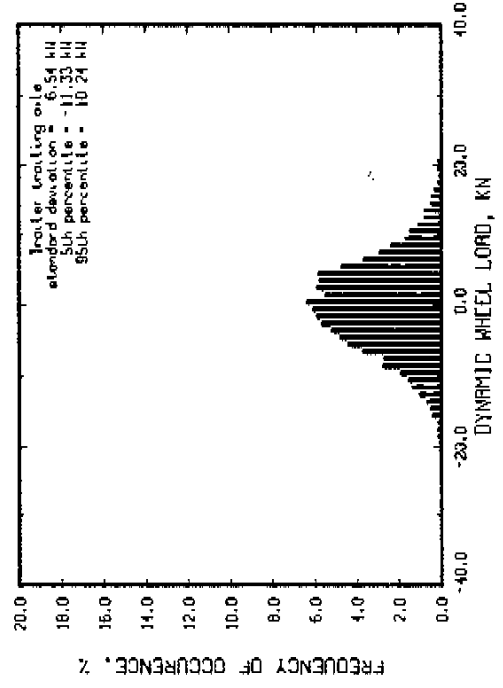
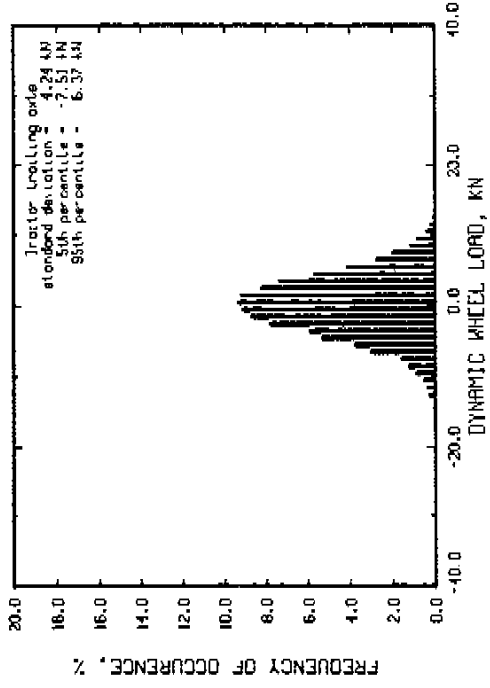
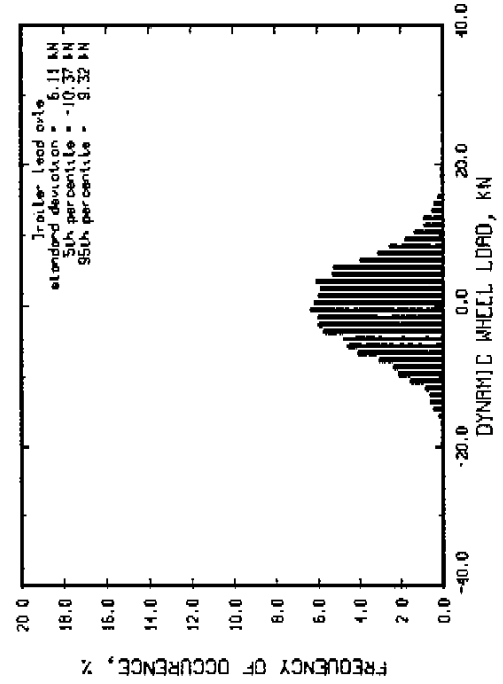
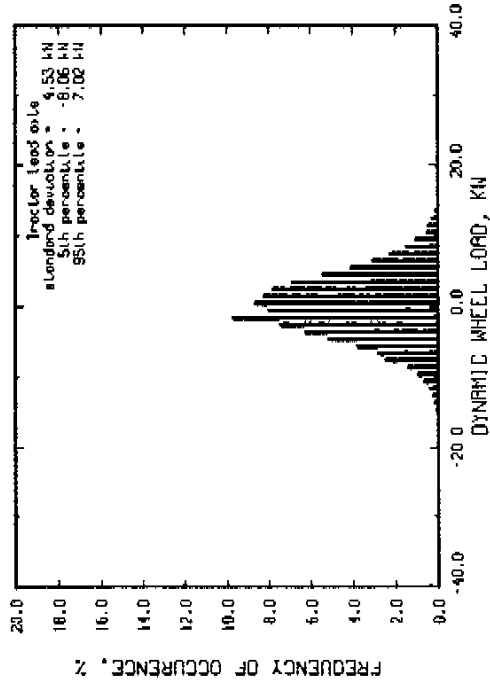
Run # 279 Part 3 Speed = 80 km/hr
 Mays roughness = 217 IPM Tractor axle spread = 1.37 m
 Tractor suspension : spring suspended walking beam
 Tractor suspension : rubber suspended walking beam
 Tractor suspension lift axle up



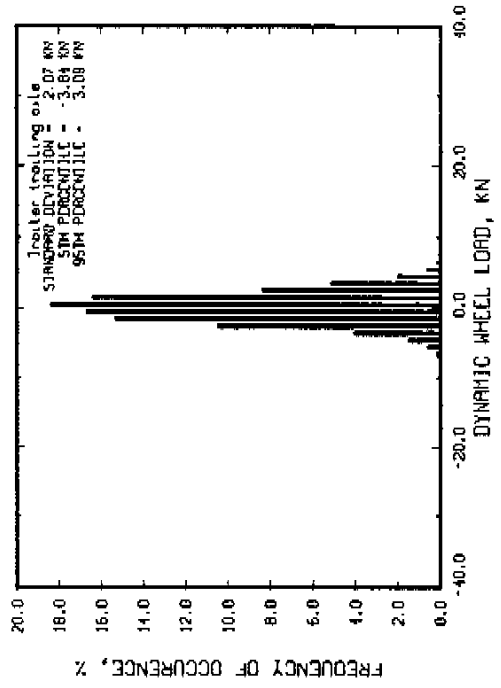
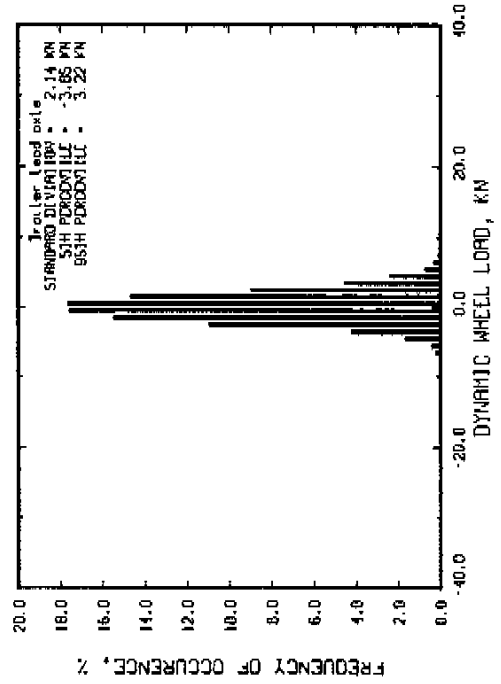
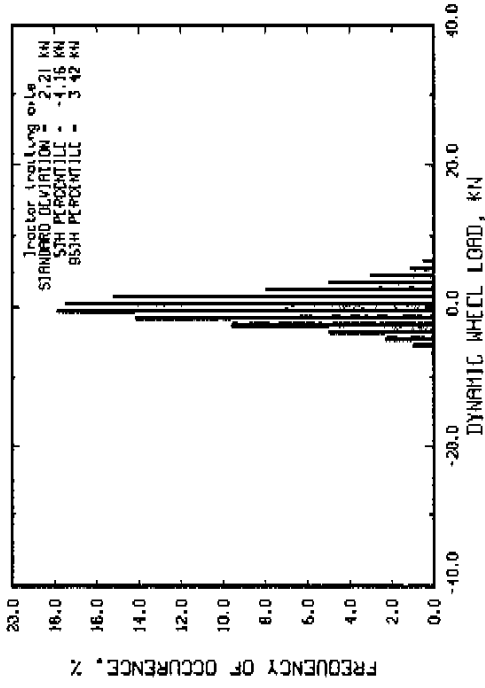
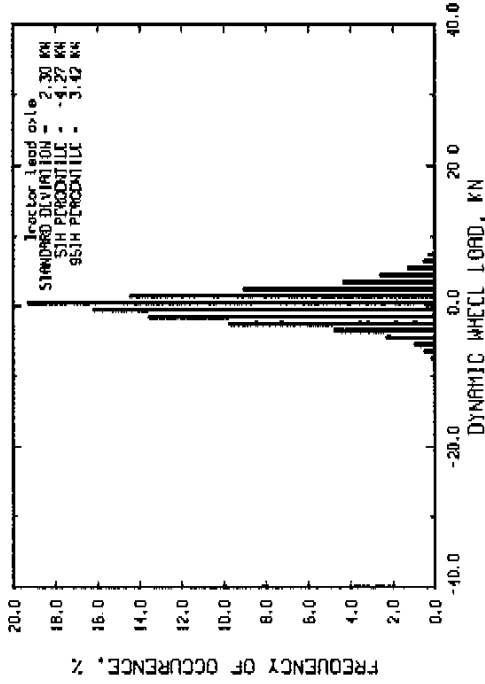
Run # 277 Speed = 40 km/hr
 Moys roughness = 73 IPM Tractor axle spread = 1.37 m
 Tractor suspension : spring suspended walking beam
 Tractor suspension : rubber suspended walking beam
 Tractor suspension lift axle down



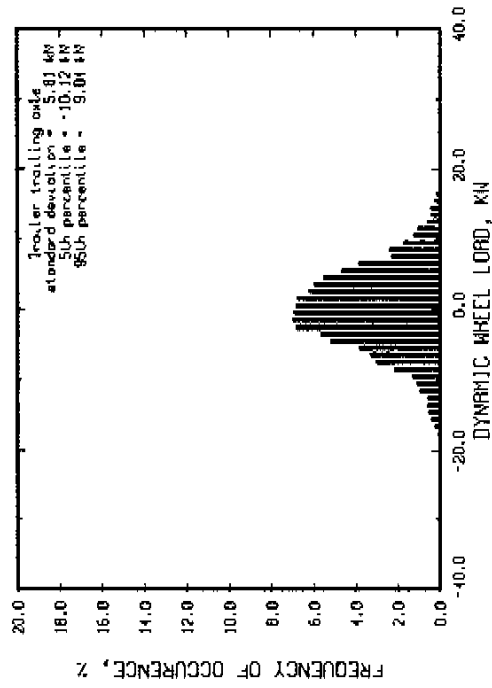
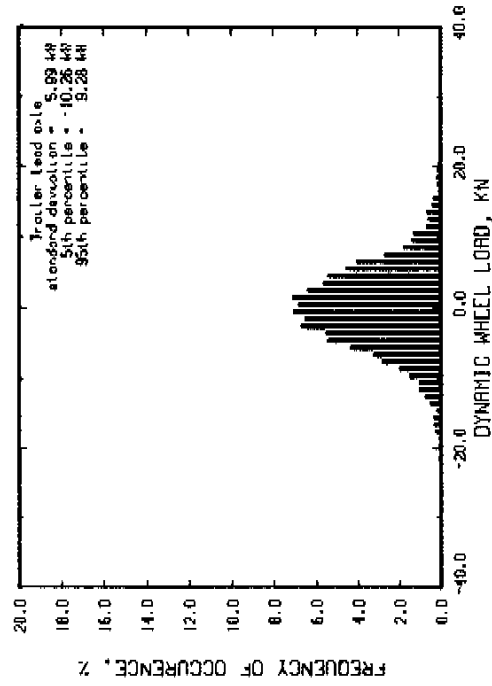
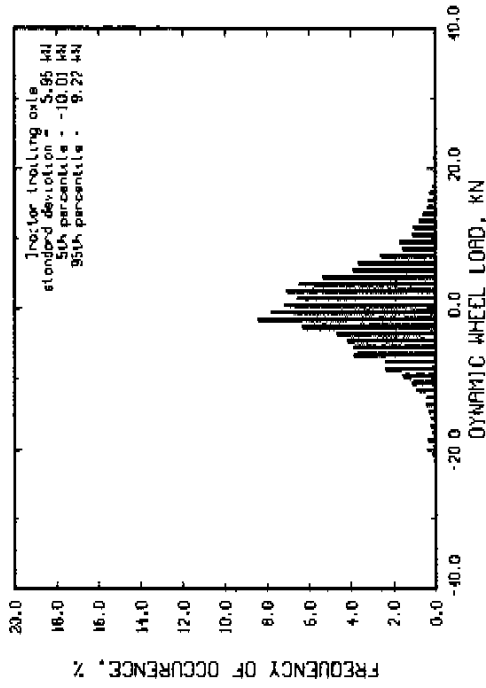
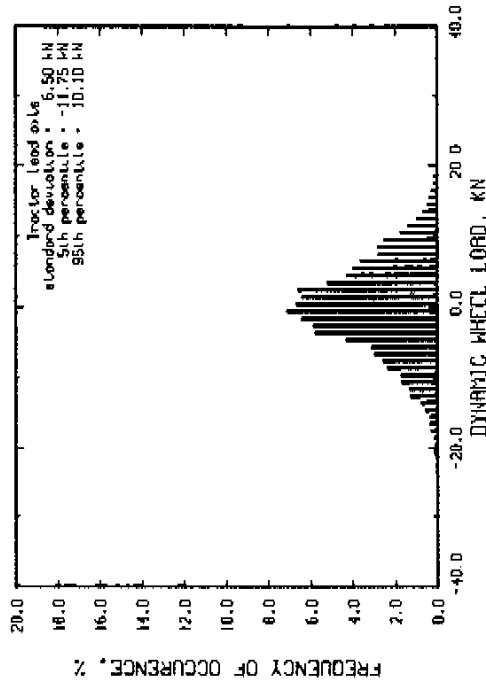
Run # 283 Part 1
 Moys roughness = 254 JPH
 Speed = 40 km/hr
 Tractor axle spread = 1.37 m
 Tractor suspension : spring suspended walking beam
 Tractor suspension : rubber suspended walking beam
 flr suspension lift axle down



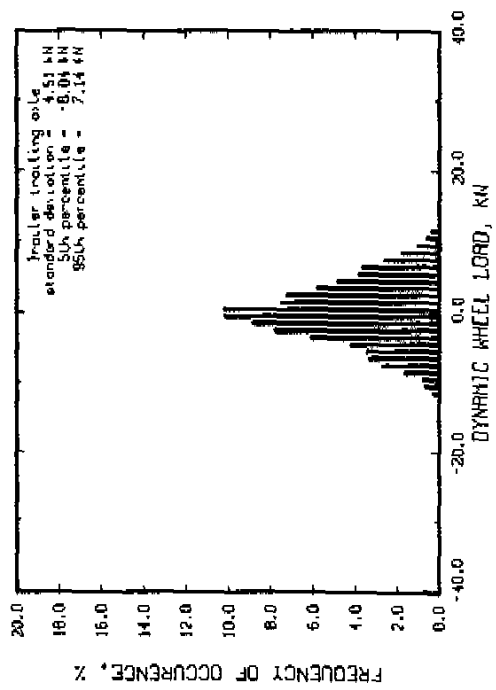
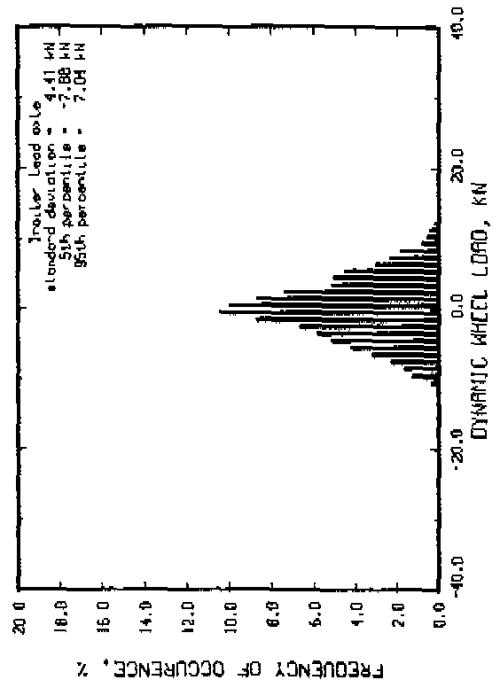
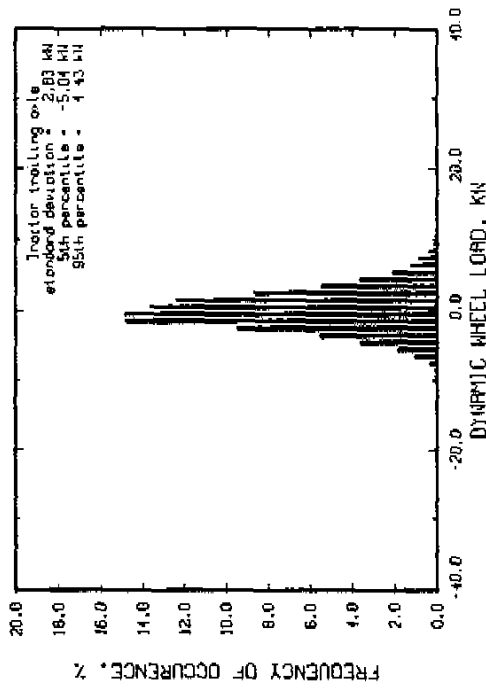
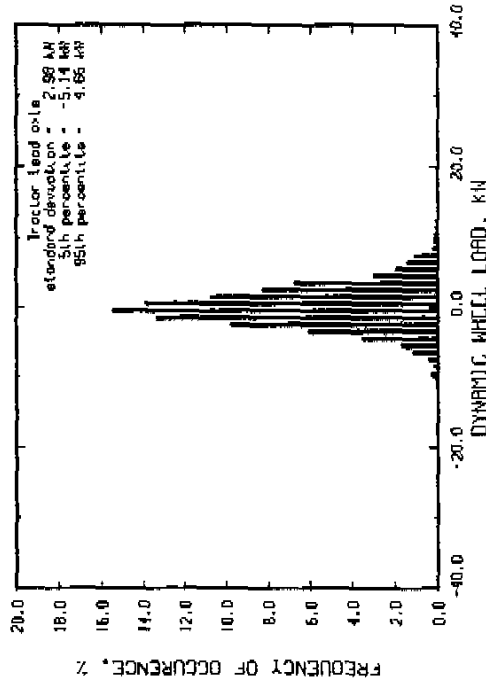
Run # 275
 Speed - 60 km/hr
 Moys roughness = 73 JPM
 Tractor axle spread = 1.37 m
 Tractor suspension : spring suspended walking beam
 Tractor suspension : rubber suspended walking beam
 Hlr suspension lift axle down



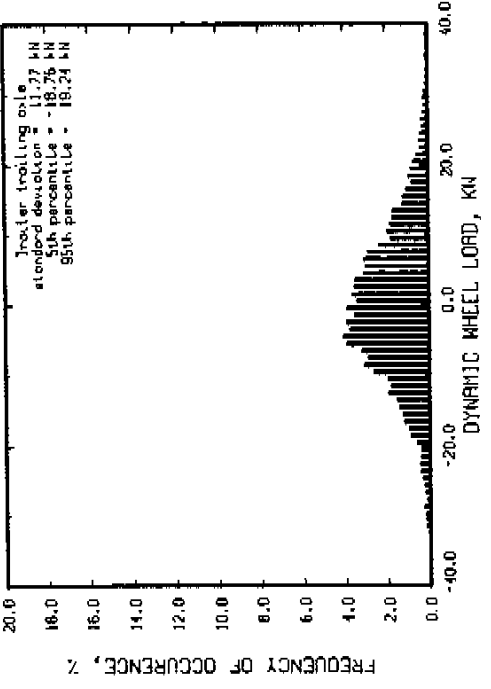
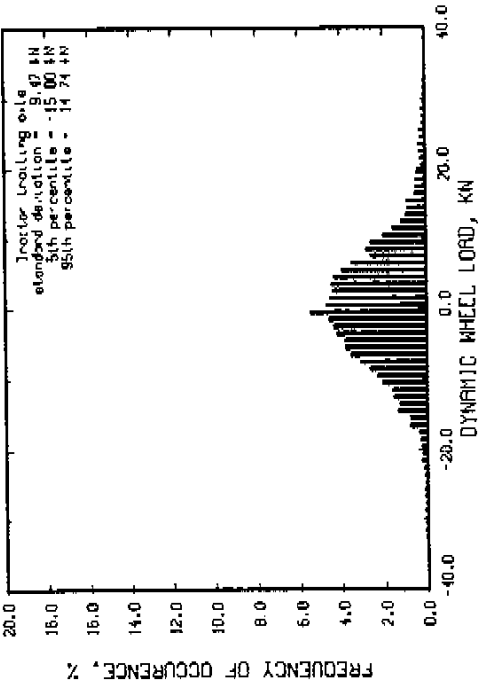
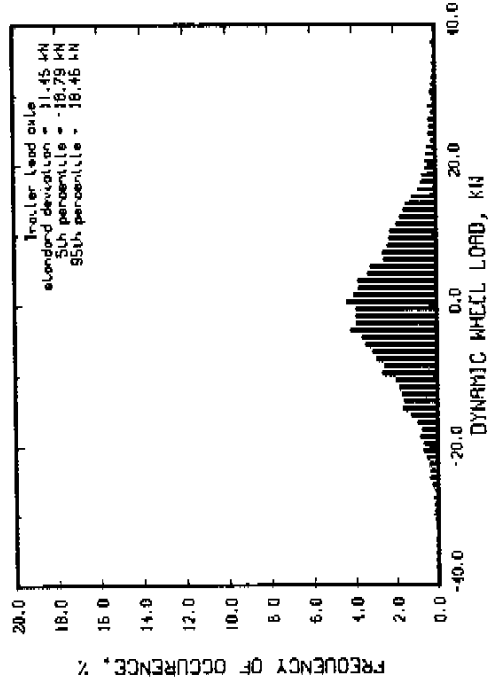
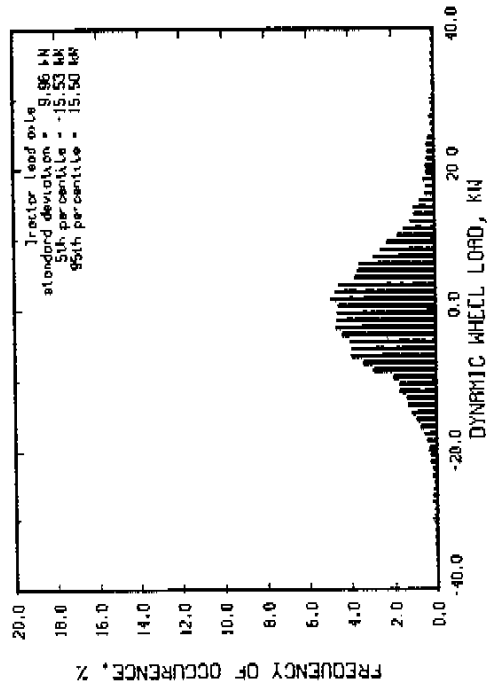
Run # 284 Part 1
 Speed = 60 km/hr
 Moys roughness = 254 IPH
 Tractor axle spread = 1.37 m
 Tractor suspension : spring suspended walking beam
 Tractor suspension : rubber suspended walking beam
 Rlr suspension lift axle down



Run # 278 Part 2 Speed = 80 km/hr
 Moys roughness = 59 JPH Tractor axle spread = 1.37 m
 Tractor suspension : spring suspended walking beam
 Tractor suspension : rubber suspended walking beam
 Tractor suspension (left axle down



Run # 278 Part 1
 Moys roughness = 165 IPM
 Speed = 80 km/hr
 Tractor axle spread = 1.37 m
 Tractor suspension : spring suspended walking beam
 Tractor suspension : rubber suspended walking beam
 Tractor suspension lift axle down



Run # 278 Part 3 Speed = 80 km/hr
 Hoys roughness = 217 IPM Trolley axle spread = 1.37 m
 Trolley suspension : spring suspended walking beam
 Trolley suspension : rubber suspended walking beam
 Air suspension t.t.l axle down

